



Universidad de Valladolid

ESCUELA DE INGENIERÍAS INDUSTRIALES

DPTO. INGENIERÍA ENERGÉTICA Y FLUIDOMECÁNICA

PhD THESIS:

**A COMPARATIVE STUDY OF TRADITIONAL AND
NOVEL HUMIDITY SENSING TECHNOLOGIES IN
NATURAL GAS**

Submitted by
JAIME GARCÍA GALLEGOS

For the Partial Fulfilment of a Doctorate in Philosophy by the
University of Valladolid

Directed by:
Dr. JOSÉ JUAN SEGOVIA PURAS

Dr. ROBERT BENYON PUIG

Valladolid, May 2017

ACKNOWLEDGMENTS

Firstly, I want to thank my tutor, Dr. Robert Benyon Puig, for the opportunity to start working in the world of metrology, and for the enormous time and effort he has given me.

My most sincere thanks also to my tutor Dr. José Juan Segovia Puras, for his complete disposition, patience and support, and for his always wise and useful advice during the guidance and writing of the thesis.

Of course, I am completely grateful to all my LabTH colleagues. For their welcome, support and teachings in many fields, their collaboration and various facets of the thesis, and for their patience and extra effort to allow me to dedicate enough time to my thesis.

To all Enagás staff in Zaragoza: Angel Maria, Jorge and Eva. But especially to Dr. Susana Ávila, a key person in the close cooperation with INTA, allowing access and use Enagás facilities, help me technically both in experimental phase and subsequent data processing. Thanks also to Alberto Martínez and M. Pilar for the access to the UGS of Serrablo, facilitating our work always.

Thanks to Roberto Gavioso and the rest of INRiM staff not only for the two joint publications resulting from the great collaboration performed in Zaragoza, but for the good times spent with such good people.

I thank Dr. Volker Ebert for allowing me to make my stay abroad in his department in the PTB, giving me all the facilities to carry it out. As well as to Dr. Norbert Bosse and Dr. Regina Klüß for his great kindness and support during my stay.

I would like to express my gratitude to INTA and the Spanish Ministry of Defense for participating in access programs for young researchers, such as the FPI fellowships which are unique opportunity for our future and, at the same time, a key element to ensure the future of science in our country.

Acknowledgments also to the entire staff of Michell Ltd., represented by Andy Benton, Andrew Stokes and Michael Summers, and from GE represented by César Muñoz and Gerard Mc Keogh. Thanks for close communication and for the interest they showed at the end of the first part of this thesis, because it was essential to continue research one step further.

And finally, but in a very special way, thanks to my family. Because I will always be forever grateful to my parents, because everything I have been, I am and I will be I owe it to them and their effort. Thank you.

TABLE OF CONTENT

1	INTRODUCTION.....	3
1.1	METROLOGY.....	3
1.1.1	INTRODUCTION	3
1.1.2	METROLOGY IN SPAIN. CEM AND CSM.....	4
1.1.3	METROLOGY IN DEFENSE. INTA.....	7
1.1.3.1	Metrology and calibration center	9
1.1.3.2	Temperature and Humidity laboratory (LabTH)	10
1.2	THE HUMIDITY.....	12
1.2.1	DEFINITIONS	13
1.2.2	HUMIDITY MEASUREMENTS AND RELATIONSHIPS.....	14
1.2.3	BRIEF HISTORICAL EVOLUTION OF EQUATION MODELS.....	16
1.2.3.1	Vapour pressure equations.....	16
1.2.3.2	Enhancement factor equations	18
1.3	NATURAL GAS.....	21
1.3.1	INTRODUCTION	21
1.3.1.1	Definition and history	21
1.3.1.2	Composition and properties	24
1.3.1.3	Applications	28
1.3.2	INDUSTRIAL INFRASTRUCTURE.....	28
1.3.2.1	Natural gas processing steps	28
1.3.2.2	Worldwide	30
1.3.2.3	Europe.....	36
1.3.2.4	Spain	38
1.3.2.4.1	Enagás.....	43
1.3.3	THE HUMIDITY. KEY PARAMETER IN NG PROCESSING	43
1.3.3.1	Definitions and concepts.....	44
1.3.3.2	Condensation and hydrates	47
1.3.3.3	Humidity measurement in natural gas	54
1.3.4	CORRELATION BETWEEN WC AND WDP: THE GERG MODEL.....	56
1.3.5	CHALLENGES OF HUMIDITY MEASURING IN NG INDUSTRY.....	60
2	OBJETIVES	65
3	HUMIDITY SENSING TECHNIQUES.....	67

3.1 HUMIDITY SENSING TECHNIQUES STUDIED	67
3.1.1 TRADITIONAL TECHNIQUES	67
3.1.1.1 Electrical impedance	67
3.1.1.2 Electrolytic	71
3.1.1.3 Condensation Hygrometers	74
3.1.2 NOVEL TECHNIQUES	77
3.1.2.1 Absorption spectroscopy	77
3.1.2.2 Resonance by microwaves	85
3.1.3 OTHER HUMIDITY SENSING TECHNIQUES USED IN GASES	89
3.1.3.1 Karl-Fischer Titration	89
3.1.3.2 Gravimetric hygrometers	89
3.2 HUMIDITY SENSING INSTRUMENTS STUDIED	90
3.2.1 ELECTRICAL IMPEDANCE SENSOR	91
3.2.1.1 Aluminum oxide	91
3.2.1.1.1 Michell's Instruments	91
3.2.1.1.1.1 Easidew PRO I.S.	92
3.2.1.1.1.2 Easidew Transmitter	92
3.2.1.1.1.3 Condumax II (WDP Channel)	93
3.2.1.1.2 General Electric Instruments	95
3.2.1.1.2.1 HygroPro	95
3.2.1.1.2.2 MIS-II (Panametrics)	95
3.2.1.1.3 Shaw Instruments	96
3.2.1.1.3.1 SDT Dew Point Transmitter	97
3.2.1.1.3.2 Superdew 3	97
3.2.1.1.4 Alpha Instrument- Alpha	97
3.2.1.1.4.1 DS-2000	97
3.2.1.2 Polymeric sensor	98
3.2.1.2.1 E+E Instruments – EE371	98
3.2.2 ELECTROLYTIC INSTRUMENT	100
3.2.2.1 Mecco Instruments – Accupoint LP2	100
3.2.3 CONDENSATION HYGROMETERS	102
3.2.3.1 MBW – DP 3D	103
3.2.3.2 Michell Instrument – Condumax II	104
3.2.4 SPECTROSCOPIC (TDLAS)	106
3.2.4.1 General Electrical Instrument – Aurora	107
3.2.4.2 Michell Instrument – OptiPEAK TDL600	108

3.2.5	MICROWAVE RESONATOR	110
4	EXPERIMENTAL SETUP AND PROCEDURES	115
4.1	SEMI-INDUSTRIAL CONDITIONS.....	115
4.1.1	LOCATION AND DESCRIPTION OF THE FACILITIES	116
4.1.2	HUMIDITY SENSORS STUDIED	118
4.1.3	EXPERIMENTAL SETUP	119
4.1.3.1	Introduction.....	120
4.1.3.2	Description and diagram.....	123
4.1.3.3	Process variables. Measurement and control.....	131
4.1.3.3.1	Properties of the natural gas inlet	131
4.1.3.3.1.1	Water and hydrocarbon dew point.....	132
4.1.3.3.1.2	Composition.....	132
4.1.3.3.2	Pressure.....	133
4.1.3.3.3	Humidity	136
4.1.3.3.4	Flow	143
4.1.3.3.5	Room conditions	145
4.1.3.4	Data acquisition system	146
4.1.3.5	Measuring protocols	147
4.1.3.5.1	Variable humidity tests	148
4.1.3.5.2	Pressure changes test	151
4.1.3.6	Other protocols	153
4.1.3.6.1	Start up and shutdown.....	153
4.1.3.6.2	Leak tests	155
4.1.3.6.3	Set the output pressure of the reducing pressure valves	156
4.1.3.6.4	Maintenance and Cleaning.....	157
4.1.3.6.5	Safety	158
4.2	MICROWAVE RESONATOR.....	162
4.2.1	THEORETICAL FOUNDATIONS	162
4.2.1.1	Method valid in binary systems	163
4.2.1.2	New approximation valid for multi-component mixtures	164
4.2.2	PHYSICAL DESCRIPTION.....	166
4.2.2.1	Experimental setup	166
4.2.2.2	Data acquisition system	170
4.2.3	PRELIMINARY TESTS	172
4.2.3.1	Dimensional characterization of QSR	172
4.2.3.2	Initial tests with pure substances	174

4.2.3.3	QSR performance in moist methane.....	175
4.2.3.3.1	Vapor phase measurements in humid methane.....	176
4.2.3.3.2	Condensation tests and determination of f–factor for methane .	177
4.2.4	MEASURING PROTOCOL USING THE QSR.....	178
4.3	INDUSTRIAL CONDITIONS.....	180
4.3.1	LOCATION AND DESCRIPTION OF THE FACILITIES.....	181
4.3.2	HUMIDITY SENSORS STUDIED.....	184
4.3.3	INITIAL INSTALLATION.....	186
4.3.3.1	Introduction.....	186
4.3.3.2	Description and diagram.....	187
4.3.3.3	Data acquisition system.....	190
4.3.4	NEW SAMPLING SYSTEM IMPROVED.....	191
4.3.4.1	Backgrounds.....	191
4.3.4.2	Targets.....	195
4.3.4.3	Description and diagram.....	196
4.3.4.3.1	New sampling point.....	197
4.3.4.3.2	New sampling system.....	198
4.3.4.4	Process variables. Measurement and control.....	205
4.3.4.4.1	Pressure.....	205
4.3.4.4.2	Temperature.....	207
4.3.4.4.3	Composition.....	208
4.3.4.4.4	Flow.....	208
4.3.4.5	Data acquisition system improved.....	208
4.3.5	MEASURING PROTOCOLS.....	210
4.3.5.1	Online recording of all readings.....	212
4.3.5.2	Checks of analyzer performance.....	212
4.3.5.3	Methanol influence.....	213
4.3.6	OTHER PROTOCOLS.....	213
4.3.6.1	Start up and shutdown.....	214
4.3.6.2	Leak tests.....	215
4.3.6.3	Set the output pressure of the reducing pressure valves.....	215
4.3.6.4	Maintenance and Cleaning.....	216
4.3.6.5	Safety.....	216
5	RESULTS.....	219
5.1	RESULTS UNDER SEMI-INDUSTRIAL CONDITIONS	219
5.1.1	PREVIOUSLY ACTIVITIES.....	220

TABLE OF CONTENTS

5.1.1.1	Previous calibrations.....	220
5.1.1.1.1	Complementary instrumentation for humidity measurements....	220
5.1.1.1.2	Hygrometers.....	222
5.1.1.2	Characterization of humidity generator	225
5.1.2	GENERAL CONDITIONS	226
5.1.2.1	Gas natural inlet properties	226
5.1.2.2	Room conditions	230
5.1.3	VARIABLE HUMIDITY TESTS	231
5.1.3.1	Work schedule	231
5.1.3.2	Response time	234
5.1.3.2.1	Raw data	235
5.1.3.2.2	Analogue versus digital output signals	239
5.1.3.2.3	Dynamic behavior.....	242
5.1.3.2.4	Summary of response time tests	249
5.1.3.3	Drift short-term	254
5.1.3.3.1	Spectroscopic instrument used as reference	255
5.1.3.3.2	Conclusion summary of drift study	259
5.1.3.4	Hysteresis study	264
5.1.4	RESPONSE TO PRESSURE CHANGES	267
5.1.5	HYGROMETERS CHECKING AFTER SEMI-INDUSTRIAL TESTS .	268
5.1.6	CONDENSATION HYGROMETERS	272
5.1.7	UNCERTAINTY BUDGET.....	277
5.2	RESULTS OF MICROWAVE RESONATOR.....	282
5.2.1	PRELIMINARY TESTS	282
5.2.1.1	Vapor phase measurements in moist methane.....	283
5.2.1.2	Condensation tests and determination of <i>f-factor</i> for methane.....	286
5.2.2	MEASUREMENTS IN MOIST NATURAL GAS.....	289
5.2.3	UNCERTAINTY BUDGET.....	294
5.2.3.1	Water content.....	294
5.2.3.2	Methane enhancement factor	297
5.3.	RESULTS UNDER INDUSTRIAL CONDITIONS.....	298
5.3.1.	INTRODUCTION	298
5.3.2.	PERFORMANCE UNDER STABLE CONDITIONS	303
5.3.2.1.	Extraction.....	303
5.3.2.2.	Shutdown	311
5.3.2.3.	Injection	319

5.3.2.4. Summary and discussion	324
5.3.3. BEHAVIOUR DURING TRANSITIONAL CONDITIONS	329
5.3.3.1. Amplitude study.....	330
5.3.3.2. Period study	332
5.3.4. INTERMEDIATE CHECK WITH STANDARD SAMPLE.....	334
5.3.5. LONG-TERM STABILITY STUDY.....	336
5.3.6. INFLUENCE OF METHANOL	338
6 CONCLUSIONS	339
7 REFERENCES.....	341
8 ANNEXES.....	363
8.1 DRIFT SHORT-TERM.....	363
8.1.1 ELECTROLYTIC INSTRUMENT USED AS A REFERENCE	363
8.1.2 ELECTRICAL IMPEDANCE INSTRUMENT USED AS A REFERENCE	365
8.2 PUBLICATIONS	369
8.2.1 MEASURING HUMIDITY IN METHANE AND NATURAL GAS WITH A MICROWAVE TECHNIQUE	369
8.2.2 AN INVESTIGATION OF THE COMPARATIVE PERFORMANCE OF DIVERSE HUMIDITY SENSING TECHNIQUES IN NATURAL GAS	371
8.2.3 EXPERIMENTAL EVALUATION OF THE PERFORMANCE OF HUMIDITY ANALYZERS IN NATURAL GAS UNDER INDUSTRIAL CONDITIONS.....	373

LIST OF SIMBOLS

ABBREVIATIONS

ATEX	European directives to work inside Explosives Atmospheres
bcm	Billion cubic meters, 10 ⁹
BCS	British Computer Society
BIMP	Bureau International des Poids et Mesures
CCT	Consultative Committee on Thermometry
CEHIPAR	Canal de Experiencias Hidrodinámicas de El Pardo
CEM	Centro Español de Metrología
CEN	European Committee for Standardization
CGPM	Conférence Générale des Poids et Mesures
CIPM	Comité International des Poids et Mesures
CMC	Measurement and Calibration Capabilities
CMyC	Metrology and Calibration Centre of INTA
CMH	Chilled mirror hygrometer
DI	Designed Institutes
EASEE-gas	European Association for the Streamlining of Energy Exchange - gas
EMRP	European Metrology Research Programme
ENG01-Gas	JRP titled <i>Characterisation of Energy Gases</i> , whose code is ENG01-Gas.
EoS	Equation of state
EURAMET	European Association of National Metrology Institutes
E+E	E + E Elektronik Ges.mbH
F	Filter
FI	Flow rate indicator
FIC	Flow rate indicator and controller
GE	General Electric Company

GERG	Groupe Européen de Recherche Gazières
GH	Gas hydrates
GUM	Guide to the Expression of Uncertainty in Measurement
HCDP	Hydrocarbon dew point
HCV	Higher calorific value
HP	High pressure
IAPWS	International Association for the Properties of Water and Steam
IMEKO	International Measurement Confederation
INRiM	Instituto Nazionale di Ricerca Metrologica
INTA	Instituto Nacional de Técnica Aeroespacial
IPTS	International Practical Temperature Scale
ISO	International Organization for Standardization
ITM	Instituto Tecnológico “La Marañosa”
ITS	International Temperature Scale
JCGM	Joint Committee for Guides in Metrology
JRP	Joint Research Project
LABINGE	Laboratorio de Ingenieros del Ejército “General Marvá”
LCV	Lower calorific value
LabTH	Laboratory of temperature and humidity of INTA.
LEL	Lower explosive limit
LNG	Liquified natural gas
LC	Low cost
LP	Low pressure
MW	Microwave
MBW	MBW Calibration Ltd.
Michell	Michell Instruments Ltd.
NAMAS	National Measurement Accreditation Service

NG	Natural gas
NI	National Institute
NIST	National Institute of Standards and Technology
NMI	National Metrology Institute
NPL	National Physical Laboratory
NRV	Non-return valve
OIML	International Organization of Legal Metrology
PCV	Pressure control valve
PHLC	High performance liquid chromatography
PI	Pressure indicator
PPE	Personal protection equipment
PR	Peng-Robinson
PRV	Pressure relief valve
PT	Pressure transmitter
PTB	Physikalisch-Technische Bundesanstalt
PTFE	Polytetrafluoroethylene
PRT	Platinum Resistance Thermometer
P&I	Pipe and instrument diagram
QSR	Quasispherical resonator
RELE	Red Española de Laboratorios de Ensayo
RKS	Redlich-Kwong-Soave
RV	Reducing valve
S	Saturator
SCCM	Standard cubic centimeter per minute
SCFH	Standard cubic feet per hour
SLPH	Standard Liter per hour
SLPM	Standard Liter per minute

SPRT	Standard Platinum Resistance Thermometer
STP	Standard Temperature and Pressure conditions (298.15 K at 1 atm)
tcm	Trillion cubic meters, 10^{12}
THT	Tetrahydrothiophene
TDLAS	Tuneable diode laser absorption spectroscopy
TI	Temperature indicator
TT	Temperature transmitter
UEL	Upper explosive limit
UGS	Underground gas storages
UKAS	United Kingdom Accreditation Service
V	Valve
VdW	Van der Waals
VIM	International Vocabulary of Metrology
VLE	Vapor – liquid equilibria
VSL	Van Swinden Laboratory (Dutch Metrology Institute)
VNA	Vector Network Analyzer
WC	Water content
WDP	Water dew point
WELMEC	European Legal Metrology
WMO	World Meteorological Organization
WP	Workpackage

SYMBOLS

a	Resonator Internal Radius, m
A	Debye's constant
A_0	First Acoustic Virial Equation Coefficient, $\text{m}^2 \cdot \text{s}^{-2}$
A_1	Second Acoustic Virial Equation Coefficient, $\text{m}^2 \cdot \text{s}^{-2} \text{Pa}^{-1}$
A_2	Third Acoustic Virial Equation Coefficient, $\text{m}^2 \cdot \text{s}^{-2} \text{Pa}^{-2}$

B	Debye's constant
	Second Virial coefficient.
c	Correction
C	Third Virial Coefficient
C_{6+}, C_{12+}	Group of all compounds present in natural gas which have more than 6 (or 12) carbon atoms
D	Diameter
e_{is}	Saturated water vapour pressure over ice, Pa
e_s	Saturated vapour pressure, Pa
e_w	Water vapour pressure, Pa
e_{ws}	Saturated water vapour pressure over liquid water, Pa
f	Enhancement factor, dimensionless
	Fugacity, Pa
f_0	Resonance frequency in vacuum, Hz
f_p	Resonance frequency at p pressure, Hz
$\langle g \rangle$	Average half width of triply-degenerate
H	Hydrogen
	Humidity
	Enthalpy
k_B	Boltzmann's constant, $J \cdot K^{-1}$
k_T	Isothermal compressibility constant of a material, Pa^{-1}
M	Molar Mass, $kg \cdot mol^{-1}$
m	Mass, Kg
n	Resonance mode indicator, dimensionless
N_A	Avogadro's Number, mol^{-1}
O	Oxygen
P	Phosphorous

p	Pressure, Pa
R	Ideal gas constant, $\text{J}\cdot\text{k}^{-1}\text{mol}^{-1}$
r	Reference
RH	Relative humidity, %
t	Time, sec
T	Thermodynamic Temperature, °C
T_{sat}	Saturation temperature, °C
TM_{In}	Transverse magnetic propagation degenerate mode of an electromagnetic signal
TE_{In}	Transverse electric propagation degenerate mode of an electromagnetic signal
$U(x)$	Expanded uncertainty of magnitude x
$u(x)$	Standard uncertainty of magnitude x
$u_r(x)$	Relative standard uncertainty of magnitude x
v	Gas velocity, $\text{m}\cdot\text{s}^{-1}$
x_w	Water molar fraction in gas phase, $\text{mol}\cdot\text{mol}^{-1}$ Water content in gas phase, ppm_v
x_{eq}	Water content in gas phase at thermodynamic equilibrium, ppm_v

GREEK SYMBOLS

α_{th}	Thermal expansion fitting coefficient, K^{-1}
β_{th}	Thermal expansion fitting coefficient, K^{-2}
γ	Adiabatic coefficient, dimensionless Activity coefficient, dimensionless
ϕ	Fugacity coefficient, dimensionless
ϵ_0	Electric permittivity in vacuum, $\text{F}\cdot\text{m}^{-1}$
ϵ_r	Relative electric permittivity, dimensionless
ϵ_{dry}	Relative electric permittivity of dry mixture, dimensionless

ε_{mix}	Relative electric permittivity of moist mixture, dimensionless
κ	Thermal Conductivity, $W \cdot m^{-1}k^{-1}$
\wp	Molar polarizability
μ	Dynamic viscosity, $Pa \cdot s$
μ_0	Magnetic permittivity in vacuum, $N \cdot A^{-2}$
μ_r	Relative permeability magnetic of the gas, $N \cdot A^{-2}$
π	Pi number, dimensionless
ρ	Density, $kg \cdot m^{-3}$ or $mol \cdot m^{-3}$

SUBSCRIPTS

<i>dry</i>	Relating to dry mixture
<i>dp</i>	Dew point
<i>fp</i>	Frost point
<i>mix</i>	Relating to moist mixture
<i>ref</i>	Standard conditions
	Reference instrument

1 INTRODUCTION

1.1 METROLOGY

1.1.1 INTRODUCTION

Metrology is the science of measurement, and covers three main activities: definition of the internationally accepted units of measurement; realization of these units by scientific methods; and establishment of the metrological traceability chains, determining and documenting the value and uncertainty of a measurement and dissemination of this knowledge.

Metrology is generally considered to be divided into three categories: *scientific (or fundamental) metrology*, is the highest level and it is concerned with the organization and development of measurement standards and their maintenance; secondly, *industrial metrology* to ensure the proper functioning of measurement instruments used in industry and in production and verification processes; and lastly, *legal metrology* that deals with those measures that influence the transparency of economic transactions, health and safety of citizens.

Metrology is essential in scientific research, which in turn is the basis of the development of metrology itself. Science always tries to enlarge the limits of knowledge and fundamental metrology deals with the metrological aspects of these new discoveries, allowing researchers to continue their discoveries. On the other hand, industrial and legal metrology must also be developed in order to answer to the needs of industry and society.

In the middle of 19th century, the need for a universal decimal metric system was evident. For that in 1875, in the Metre Convention in Paris, 17 governments, including Spain, decided to create and finance a permanent Scientific Institution, the International Bureau of Weights and Measures (BIPM).

The BIPM is an intergovernmental organization under the authority of the General Conference on Weights and Measures (CGPM) and the supervision of the International Committee for Weights and Measures (CIPM). The CGPM discusses and examines the work done by the National Metrology Institutes (INM). Whilst the CIPM is in charge of appointing presidents of Consultative Committees (CCs), develop the Mutual Recognition Agreement (MRA) [MRA99], and cooperate with another international metrological organizations, such as: ISO, OIML, WELMEC, and IMEKO.

Nowadays, the BIPM is made up by 58 countries [BIPM], and some of their main duties are: the development and maintenance the national standards, collaboration in R+D projects, and participation in national and international comparisons. These key comparisons ensure the international equivalence of the national standards, essential for the metrological traceability in the calibration hierarchy. The BIPM Key Comparison Database (KCDB) [KCDB] contains the results of key and supplemental comparisons, supporting the Measurement and Calibration Capabilities (CMCs) of National Metrology Institutes (NMIs).

Finally, NMIs worldwide are arranged in six Regional Metrology Organizations (RMOs). In Europe the RMO is EURAMET (formerly EUROMET), established as EURAMET e.V., a non-profit association under German law. It has two categories of membership: members and associates. Only one NMI per member state of the European Union and of the European Free Trade Association (EFTA) can be a member of EURAMET. Designated Institutes from states with a member (A-DI) and NMIs applying for membership (A-CA) can become Associates.

Scientific metrology is classified in nine technical fields by the BIPM: Mass, Electricity, Length, Time and Frequency, Thermometry, Ionizing Radiation and Radioactivity, Photometry and Radiometry, Acoustics and Quantity of Substance. According to EUROMET there are two additional technical fields: Flow and Interdisciplinary Metrology. The thermometry field includes temperature, humidity and thermophysical properties.

1.1.2 METROLOGY IN SPAIN. CEM AND CSM.

The Spanish metrological infrastructure consists of *Centro Español de Metrología* (CEM) and the Laboratories Associated with it (currently Real Instituto y *Observatorio de la Armada* (ROA), *Instituto de Óptica-CSIC* (I. Óptica-CSIC), *Instituto Nacional de Técnica Aeroespacial* (INTA), *Laboratorio de Metrología de Radiaciones Ionizantes del Centro de Investigaciones Energéticas, Medioambientales y Tecnológicas* (LMRI-CIEMAT), *Laboratorio Central Oficial de Electrotecnia* (LCOE) and *Instituto de Salud Carlos III* (ISCIII). Together, they constitute the cusp of the national metrological pyramid, where the primary standards of the units of measurement corresponding to the International System of Units (SI System) are established and maintained, as defined in [BOE14b] and [BOE16].

CEM is the highest technical body in metrology field in Spain. It was initially constituted as Subdirección General by R.D. 415/1985 [BOE85] and configured as an Independent Organization of a commercial and industrial nature by the Law 31/1990 of 27th of December [BOE90], in where the main metrological goals and its competences are defined.

The Spanish Metrology Infrastructure is coordinated by the Higher Council of Metrology, *Consejo Superior de Metrología* (CSM), created by article 11 of Law 3/1985 of March 18, of Metrology. It is the highest advisory and coordination body of the State in the field of scientific, technical, historical and legal metrology. It is part of the General Secretariat of Industry and the Small and Medium Enterprise of the Ministry of Industry, Energy and Tourism. It cannot be strictly attributed the status of a body comparable to an interministerial commission, since it coordinates the activities of the ministerial departments related to metrology. However, its function is oriented towards fulfilling this objective, taking into account the great impact that measurements have on day to day activities, informing and proposing to the Ministry of Industry, Energy and Tourism and through this to the Government, as the case may be, the actions for a coordinated national measurement system.

According to the R.D. 648/1994 [BOE94], CEM is the holder of national standards of the basic units of mass, length, electric current and thermodynamic temperature (see Fig. 1.1.a). It also is responsible for the national standards of the derived units as specified in Ministerial Order ITC / 2581/2006, of 28 July [BOE06]. The technical structure of CEM has traditionally been organized in seven areas inside which are included a huge diversity of derived physical quantities and legal metrology [CEM]. This is currently in the process of being re-structured to provide an efficient use of resources, and aligned with the strategic lines of research in Europe.

DIs usually are appointed by the NMIs, in accordance with the metrology strategy established for the different quantities and in accordance with the country's metrological policy. In Spain, they are appointed by the Government at the proposal of the CSM. The laboratories associated to CEM, holders of the national standards as detailed in the following table, constitute together with CEM, the cusp of the Spanish metrological system (see Fig. 1.1.a).

Inside of the metrological traceability pyramid in the second level are the calibration and testing laboratories, and R+D centers regardless their metrological activity in which they are involved. These laboratories usually must be third-party accredited to recognize their technical competence, quality system and impartiality. Accreditation is voluntary, but some international, European and national authorities to guarantee the quality of within their area of competence, request an accreditation.

Table 1.1.a Spanish Designed Institutes by the CEM and quantities of which have the national standards.

Designed Institutes	Quantity
Real Instituto y Observatorio de la Armada (ROA)	Time & Frequency
Instituto de Física Aplicada (IFA-CSIC)	Light Intensity
Laboratorio de Metrología de Radiaciones Ionizantes, del Centro de Investigaciones Energéticas, Medioambientales y Tecnológicas (LMRI-CIEMAT)	Ionizing radiation
Instituto Nacional de Técnica Aeroespacial (INTA)	Humidity, Power, Impedance, electrical attenuation and Noise at High Frequency
Laboratorio Central Oficial de Electrotécnica (LCOE)	High Voltage Electrical
Centro Nacional de Sanidad Ambiental (Instituto de Salud Carlos III)	Ozone concentration

In Spain, the national accreditation body is *Entidad Nacional de Acreditación* (ENAC) is a private, independent and non-profit entity that coordinates and directs national accreditation system. ENAC is the only entity responsible for accrediting calibration and testing laboratories, as well as certification bodies, environmental verifiers, inspection bodies and testing bodies [ENAC]. Accreditations are usually based on international standards, such as: ISO/IEC 17025:2005 “General requirements for the competence of calibration and testing laboratories” [ISO05].

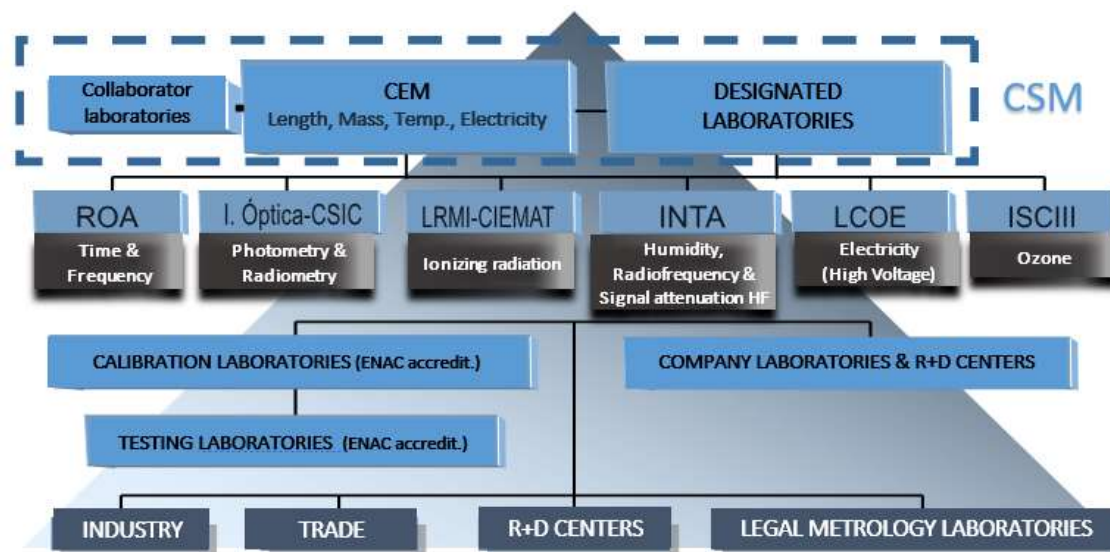


Fig. 1.1.a Scheme of the entire Spanish metrological infrastructure which ensures the traceability in all levels [Vic13].

1.1.3 METROLOGY IN DEFENSE. INTA

The fast evolution of weapons and telecommunications systems and, in general, all the means used by the modern armies, make essential to create an infrastructure of tools, instruments and equipment for assembly, adjustment, verification and periodic control, which requires to carry out exhaustive and continuous measures in a wide variety of magnitudes. For that, the calibration is absolutely necessary to ensure operability of all equipment, systems and facilities.

The high maintenance costs of first level standards in many measuring fields, needs of intercomparisons and periodic calibration, and requirements of their handling and conservation, turn all these activities in key issues of continuous improvement. For that, a calibration system, managed by the armed forces, able to establish a calibration hierarchy that allows to maintain operative, with a minimum cost and maximum efficiency possible, ensuring the highest existing metrological level, is absolutely essential to achieve world-class armed forces.

In that sense, the Technical Commission for Metrology and Calibration of Defense (CTAMCD) was created by Ministerial Order 112/2000, 14th April. [SGTC08], where its composition and functions are defined. INTA was a key player in the creation of this Commission, and after the recent integration process of military technological centers reported later on, INTA assumes the presidency and secretariat of this Commission, with the vice-presidency of ROA. This new structure has been approved by the involved

parties and is in the final stages before publication in the *Boletín Oficial de Defensa* (BOD).

INTA was founded in 1942 and designed as Public Research Institute (OPI) specializing in aerospace technology research and development in Spain, according to the *Ley de Ciencia* in 1986 [BOE86]. Besides, INTA is in charge of the R & D areas in the land and naval areas of the Defense. Among its main functions are included [BOE11, BOE14 and INTA]:

- The acquisition, maintenance and continuous improvement of all those technologies of application in the aerospace field.
- Leading all types of tests to verify and certify materials, components, equipment, subsystems and application systems in the aerospace field.
- Technical advice and the provision of services to official bodies and agencies, as well as industrial companies or technologies.
- Act as technological center of the Ministry of Defense.

INTA is equipped with a large infrastructure of facilities of research, development, measurement and testing laboratories, some of which are unique in Europe, and contribute to the development of R & D & I in Spain.

Practically from its beginnings, INTA was closely linked to space programs. In 1960, began collaboration with the NASA, participating in prestigious programs such as: Mercury Project, the first US space program for manned flights, as well as the Apollo program, with which the man arrived on the Moon.

Another major INTA milestone was its satellite development program, initiated by INTASAT, and followed by other small satellites generations, such as the Minisat, Nanosat and, the recent picosatellites, i.e. the Optos.

INTA also participates in Earth observation projects, monitoring and control of space vehicles, observation and study of the solar system and deep space and astrobiology.

Inside of aeronautic area, INTA is involved in development programs such as Milano, Diana and Siva, and also in European programs such as the European fighter

EF2000 Eurofighter, in testing tests of Rolls-Royce's engine, the EJ200, and during the development of the modern military transport plane, the A400M of Airbus.

In 2014, the integration of INTA, ITM, CEHIPAR and LABINGE took place, which meant the beginning of a new and more complete technological body implies in much more development areas.

1.1.3.1 Metrology and calibration center

The Metrology and Calibration Center of INTA, henceforth CMyC by its acronym in Spanish, is included to the *Subdirección General de Coordinación y Planes*, according to the current internal organization manual.

Metrological activity in INTA started since the foundation of the Institute. CMyC obtained its first accreditation by the British Calibration Service (BCS, now UKAS) in April 1972 in the area of Electricity DC-Low Frequency (Cal. N° 58). Since then it has always been accredited by either the accreditation bodies of the United Kingdom (NAMAS, subsequently UKAS) or Spain (RELE, subsequently ENAC).

Once ENAC became a signatory of the international mutual recognition agreement (ILAC-MRA), the UKAS accreditation was voluntarily terminated. Since 1998, INTA has been accredited by ENAC and currently has accreditation to the requirements of UNE-EN ISO/IEC 17025 [ISO05] for calibrations in the areas of: Dimensional Metrology, Temperature and Humidity, Pressure and Vacuum, Mass, Time and Frequency, DC Electricity and Low Frequency, High Frequency Electricity, Flow, Density and Viscosity. The calibration activities accredited by ENAC are summarized in Technical Annex Ed. 8 Accreditation n° 16 / LC 10.007 [ENAC]. In addition, as it has been explained above, the CMyC has, by the CEM designation, the national standards in Humidity [BOE01], Power, Impedance, Attenuation and Noise at High Frequency (See Table 5.1.f) [BOE04].

CMyC has at its disposal the most advanced measurement and calibration equipment, state-of-the-art technologies and highly qualified staff, which allows to offer and provide one of the most advanced and complete worldwide calibration services, with a great international recognition both industrial and scientific.

All the above together with the adhesion of new calibration and testing centers and facilities, belonging also to the army, allow it to give traceability in the most of quantities

required by the armed forces, being a key piece inside of Ministry of Defense, together with ROA in the field of time and frequency.

1.1.3.2 Temperature and Humidity laboratory (LabTH)

LabTH is physically divided in two technical sections, temperature and humidity, both inside of the CMyC of INTA, which was specifically built to avoid vibrations and radio interference from other nearby buildings. Besides, it is equipped with an advanced system of air conditioning, which allows a rigorous control of temperature and humidity 24 h and 365 d per year.

The INTA activities in the field of humidity started in 1992, with the acquisition of four state chilled mirror transfer standards that covered the range of frost/dew-point temperature from $-75\text{ }^{\circ}\text{C}$ to $+82\text{ }^{\circ}\text{C}$, with an overlap in the range $-10\text{ }^{\circ}\text{C}$ to $+20\text{ }^{\circ}\text{C}$. This enabled two instruments to be used as externally calibrated transfer standards and two nominally identical units to be used as working standards. A hybrid two-pressure/two-temperature/flow-mixing generator was designed and built at INTA, and used together with the chilled mirror hygrometers and precision thermometers to calibrate chilled mirror hygrometers, relative humidity sensors and air temperature sensors. Initially, traceability was obtained from the National Physical Laboratory (NPL), *Physikalische-technische Bundesanstalt* (PTB) and National Institute of Standards and Technology (NIST). After the development of the necessary skills and operational procedures, the first accreditation in humidity in Spain was obtained from NAMAS in October 1993. This covered the complete frost/dew-point temperature range and the corresponding relative humidity at temperatures from $10\text{ }^{\circ}\text{C}$ to $85\text{ }^{\circ}\text{C}$. This milestone served as the basis for establishing technical competence and the basis for designating INTA as an associate laboratory of CEM [BOE01] and holder of the national humidity standards, and therefore the Spanish DI for the field of humidity [BOE06].

This implies several responsibilities and requirements which must be met according to the CIPM-MRA [MRA99], such as: maintenance and development the national standards, participation and compliance with the international agreements and affiliated organizations, promotion and participation in R&D programs both national and international, participation in national and international comparison which ensure the quality and traceability, and more.

LabTH had participated in several R&D programs managed by the European Metrology Research Programme (EMRP). In this sense, INTA has taken part in projects such as:

- The MeteoMet project “Metrology for Meteorology”, in which were involved 18 European NMIs besides of three universities and 35 stakeholders. INTA, by means of direction and efforts of LabTH mainly, carried out the assembling and characterization of several models of outdoor weather stations, by means of the study of temperature and humidity and how these quantities were affected by factors as: solar radiation influence, speed of wind and its orientation, inner homogeneity, response time or daily light cycles.
- Characterization of Energy Gases “ENG01-Gas” (2009-2013), which has been widely explained thought this thesis.

With regard to the national research activities, LabTH support several departments of INTA involved in several fields (i.e.: atmospheric research, aerodynamic tests, turbojets, testing benches of fuel cells) by means of metrology and calibration activities, besides providing advice and consultancy in its field of competence.

In addition, INTA has collaborated directly with Universities, such as the ETSI *Agrónomos of Universidad Politecnica de Madrid*, in the characterization of the temperature and humidity in underground wine cellars [Cañ13].

The scope of ENAC accreditation of LabTH is completely detailed in Technical Annex Ed. 8 Accreditation nº 16 / LC 10.007 [TAA16] and a simple summary is explained more in advance (Section 1.2.3). However, the Capabilities of Measurement and Calibrations (CMCs) by means of the national humidity standards [KCDM] are summarized in the below table:

Table 1.1.b CMCs of the Spanish humidity standards, carry out by LabTH of INTA [KCDB].

Measurement Instrument	Calibration Method	Measured Range, °C		Measurement conditions *		Expanded Uncertainty, °C
		Minimum value	Maximum value	Parameter	Specifications	
Dew-point hygrometer	Measurement against humidity generator	-75	< -70	Ambient Temperature	(23 ± 1) °C	0.15
		-70	< -60			0.10
		-60	< -10			0.05
		-10	60	Test Chamber Temperature	0 °C to 100 °C	0.05
		> 60	70			0.10
		> 70	75			0.15
		0	95	Continuous gas flow	< 5 l·min ⁻¹	0.05

* In any case, measurement room conditions in humidity are always below 60 %rh.

On the other hand, LabTH has been continuously participating in bilateral and key comparisons in the entire range. INTA took part in the very first European comparison of national humidity standards, under the first framework programme MAT1-CT940017 [Act98] and compared bilaterally the first national humidity standards with leading NMIs and DIs [Mac98, Ben98, Ben07]. The Spanish national humidity standards have also been compared in the CCT key comparisons CCT-K6 and CCT-K8 and EURAMET key comparisons EURAMET-T.K6 and EURAMET-T.K8. Information on these comparisons can be found in [KCDB].

1.2 THE HUMIDITY

Humidity word is used is to refer to the presence of water, regardless the state of the matter in which it is (solid, liquid or gaseous). When it is in gaseous way often it is said the water vapour, whilst to refer to the water content in solids, commonly it is used the moisture expression.

Wherever there is water, either as liquid or ice, there will be water vapour in the surrounding air. The extent at which a gas absorbs water vapour depends on several factors, but the most important is the temperature. Usually, the higher is the temperature of a gas, the more water vapour it can hold.

Traditionally, the humidity has been closely linked to water content in air, but this term can be extrapolated to any material. The Psychometry is a branch of science dedicated to the study of the thermodynamic properties of humid air and the effect of

atmospheric humidity on materials and the human comfort. The well-known psychrometric charts are very useful to relate quickly several properties of moist air, from temperature and water content values.

The humidity is a key quantity in many fields and applications, such as: air conditioning; aerodynamics, drying industrial processes; maintenance storage and packaging of food; drug manufacturing processes; metrology; explosive atmospheres; environments in computer or electrical devices rooms; clean rooms; and a wide range of industries (e.g.: chemical, textile, food, paper, oil and petroleum, etc.).

1.2.1 DEFINITIONS

Historically, in metrology the moist air has been always used as a reference, being considered as a binary mixture of water and air, so the vapour mole fraction of a parcel of moist gas containing n_w and n_a moles of water and dry gas respectively, is defined as:

$$x = \frac{n_w}{(n_w + n_a)} \quad \text{Eq. 1.2.a}$$

According to the Dalton's law (Eq. 1.2.b), total pressure of a mixture of gases, which no react chemically each other, is equal to the sum of the *partial pressures*, p_i .

$$p_{Tot} = \sum_{i=1}^n p_i = \sum_{i=1}^n x_i \cdot p_{Tot} \quad \text{Eq. 1.2.b}$$

In hygrometry, at any particular pressure and temperature conditions water partial pressure is commonly called *water vapour pressures*, and is denoted as e . Beyond, a gas is saturated when contains its full capacity of water vapour, in that particular case it is said the *saturation vapour pressure*, denoted as e_s , and in pressure units too.

The water vapour amount present of any gas per unit volume a given temperature and pressure, is denominated the *absolute humidity*, expressed in mass units.

Applying Dalton's law, the water vapour mole fraction is also equal to the ratio of the *partial water vapour pressure*, p_w , to the total pressure and for a gas saturated at temperature t_s and pressure p_s , the *vapour mole fraction*, x_s , is calculated using the following equation:

$$x_w = \frac{p_w}{P} = \frac{e_s(T) \cdot f(T, P)}{P} \quad \text{Eq. 1.2.c}$$

where: x_w is the mole fraction of water vapor in the saturated mixture.

e_s is the pure phase saturation vapor pressure of water substance at the temperature of saturation.

P is the total pressure above the surface on the condensed phase (water or ice), in the same units as e_s .

f is the water vapour-pressure *enhancement-factor*.

The water vapor content of real gases saturated under known conditions of pressure and temperature, is not predicted adequately by ideal gas laws, and it is not generally the same as that for pure water vapor.

This difference from the ideality is mainly due to two factors: molecular interactions between the same and different species due to attractive and repulsive forces; and to neglect the molecular volume of every species present. Other influential effects are [B&B01]: the chemical potential of the condensed substance is increased because of the rise in the applied pressure, called Poynting effect; and if the gas is soluble in the condensed substance then the chemical potential of the solution is different from that of the pure solvent, the Raoult effect.

For that, to achieve an accuracy and reliable description of water content in gases, especially at higher pressures, it is necessary to consider the deviation of the equilibrium moisture content from that given by an ideal calculation based only on the vapor pressure of water. Therefore, the water vapor *enhancement factor* was created to allow quantify this non-ideality of moist mixtures, so for pure substances, $x_w = 1$, when P approaches e_s , the enhancement factors, f , is the unity.

1.2.2 HUMIDITY MEASUREMENTS AND RELATIONSHIPS

Humidity influences a vast range of physical, chemical and biological processes, and many different techniques of measurement have been developed. Because of this wide interest and the multiplicity of measurement principles, humidity is expressed in and measured in several ways.

One of the ways most used to express the humidity of a gas is the *relative humidity*, denoted by *% rh*, and indicates how fully saturated a gas is with water vapour. It is calculated by means of the ratio between the actual vapour pressure, e , and the saturation vapour pressure, e_s , at the same temperature and expressed as a percentage.

$$\% rh = \frac{e}{e_s} \cdot 100 \quad \text{Eq. 1.2.d}$$

The relative humidity is mainly used for moist air systems, so is frequently used in meteorology, climatology, air conditioning rooms, air conditions facilities or equipment.

Another of the most famous ways to express the humidity measurement is the *dewpoint*, or temperature at which condensation starts to happen when a gas is cooling at constant pressure. Depending on the nature of the condensate it can be said dew or *frost point*, if gas is saturated with respect water or ice, respectively. This humidity measurement is expressed in temperature units, commonly in °C.

By the other hand, the volumes of constituents are often used to express humidity as a ratio of volumes on parts per million, ppm_v . This expression can be also achieved from the partial pressures of constituents, according to the Boyle's Law.

$$ppm_v = \frac{V_{water\ vapour}}{V_{dry\ gas}} \cdot 10^6 = \frac{P_{water\ vapour}}{P_{dry\ gas}} \cdot 10^6 \quad \text{Eq. 1.2.e}$$

Also the mass of water vapour per unit mass of dry gas can be used, and it is known as *mixing ratio*, r , and it can be expressed in parts per million by weight, ppm_w .

If the above equation is combined with Eq. 1.2.c an equation which related water vapour pressure at dew point temperature is obtained:

$$ppm_v = \frac{f(P, T_i) \cdot e_i(T_i)}{P_{dry\ air} - f(P, T_i) \cdot e_i(T_i)} \cdot 10^6 \quad \text{Eq. 1.2.f}$$

being T_i the system temperature, e_i , the water vapour pressure at the same temperature. If such temperature is the saturation temperature, ergo dew/frost temperature, $e_i = e_s$.

1.2.3 BRIEF HISTORICAL EVOLUTION OF EQUATION MODELS

In the following two chapters the evolution of equation used to determine the saturated water vapour pressure, e_s , and the enhancement factor, f , for air-water system was briefly explained, mentioning the most influence equations and models for each case.

By means of this chapter, the author wishes to show the correlation between models traditionally used in hygrometry and those used to estimate and evaluate the phase behaviour of non-conventional gases, and which were explained below and used in this thesis.

1.2.3.1 Vapour pressure equations

First equation was given by Clausius-Clapeyron who related saturation vapor pressure and temperature in a system in which two phases of any substance are in equilibrium [Cla37]. This equation is usually given in exponential and logarithmic form.

$$e_{sx} = 10^{[c+(b/T)]T^a} \quad \text{Eq. 1.2.g}$$

$$\log e_{sx} = a \log T + \frac{b}{T} + c \quad \text{Eq. 1.2.h}$$

Parameters a , b and c are specific of each substance, x , and are obtained experimentally.

In 1844, Magnus provided a very good approximation of the water vapour pressure between -7 °C and 105 °C, derived from form originally proposed by August and Roche in 1828 [Mok12]:

$$e_s(T) = 6.1094 \cdot \exp\left(\frac{17.625 \cdot T}{243.04 + T}\right) = a \cdot \exp\left(\frac{b \cdot T}{c + T}\right) \quad \text{Eq. 1.2.i}$$

It is one of the most convenient forms because it allows easily convert between temperature and saturation vapor pressure in either direction. The explicit form for temperature is written below with its coefficients

$$T = \frac{c \cdot z}{b - z} \quad \text{Eq. 1.2.j}$$

$$z = \ln(e/a) \quad \text{Eq. 1.2.k}$$

Goff and Gratch developed a completely novel model to describe the water vapor pressure over water and ice. Their first set of equations was reported in 1945 and increased the current accurate largely. It is denoted commonly in the literature like *GG45* [G&G45]. *GG45* was soon modified by *GG46* for temperature range from 0 to 100 °C. In 1966, World Meteorological Organization (WMO) recommended its use in meteorological calculations and it is still in use in many countries [A&E96]. Besides, *GG46* model have had a huge impact during more than four decades, period in which many empirical equations used this formulation as a standard for comparison, e.g.: *Murray (1967)*, *Richards (1971)*, *Tabata (1973)*, *Lowe (1977)*, *Rasmusen (1978)* [Buc81]. Although the *GG46* was internationally accepted, it was not easy for computation. For this reason, Murray modified it by means of simple operations which are valid for water and ice vapour pressure.

Initially, Wexler and Greenspan formulated their equation to calculate the saturation vapor pressure of water in the IPTS-48 in the temperature range of 0 °C to 100 °C [W&G71]. Then, adapted the coefficients at the new temperature scale, IPTS-68, and later enlarged the work range over ice [Wex77]. Vapour pressure formulation, denoted commonly as *WEX76* [W&G76] has the next form:

$$e_s(T) = \left(\sum_{i=1}^6 a_i \cdot T^{i-2} + a_7 \ln T \right) \quad \text{Eq. 1.2.1}$$

Wexler and his co-worker Hyland redefined two new equations over water and ice in the range of 0.01 °C to 200 °C and -100 °C to 0.01 °C, respectively [W&H83]. Equation that gained the largest international recognition, so its coefficients were updated to ITS-90 by Sonntag (1990) [Son90] and Hardy (1998) [Har98], for water and ice, keeping with the same form in both cases.

Saul and Wagner (1987) [S&W87] developed a new formulation for saturation water vapor pressure which were based on the experiments carried out by Osborne *et al.* during 1930 to 1939 [Nie03]. For vapour pressure above water had this aspect:

$$e_{ws} = P_c \exp \left[\frac{T_c}{T} \cdot \left(\begin{array}{c} a_1 \tau + a_2 \tau^{1.5} + \dots \\ \dots + a_3 \tau^3 + a_4 \tau^{3.5} + a_5 \tau^4 + a_6 \tau^{7.5} \end{array} \right) \right] \quad \text{Eq. 1.2.m}$$

where P_c and T_c are the critical pressure and temperature of water, respectively, and $\tau = 1 - T/T_c$.

A few years later Wagner and Pruß (1993, 1994) updated the a_i coefficients for saturate vapour pressure equation above water [W&P93], and later increased the range above ice, but with a completely different equation form regarding to over water [Wag94]:

$$e_{is} = P_t \cdot \exp[a_1(1 - \theta^{-1.5}) + a_2(1 - \theta^{-1.25})] \quad \text{Eq. 1.2.n}$$

where P_t and T_t are the pressure and temperature in the water triple point respectively), and $\theta = T/T_t$

Being both equations in both ranges ratified and supported by the International Association for the Properties of Water and Steam (IAPWS).

There are many others equations but the most of them are based in some model cited above. Several surveys have been published where a detailed literature review is given, for example Nielsen & Lovell-Smith [Nie03, Lov09] or doctoral dissertations such as Chapoy [Cha04] and Mokdad [Mok12], from which has been collected all this summary and where more information is given including: coefficients values, correlations between different temperature scales, uncertainty assessment of the different models, etc.

1.2.3.2 Enhancement factor equations

It is very probably the most usual form of *EoS* used for real gases, such as the NG, was the Virial Equation, developed by Kamerling Onnes in 1902 [Onn02]. The first virial equation had the form of a development of the compressibility factor as an infinite inverse power series in the *molar volume*, v , but also can be expressed as a power series in pressure.

$$Z = \frac{Pv}{RT} = 1 + \frac{B(T)}{v} + \frac{C(T)}{v^2} + \frac{D(T)}{v^3} + \dots = 1 + B'P + C'P^2 + \dots \quad \text{Eq. 1.2.o}$$

where Z is the compressibility isothermal factor, R is the gas constant, B and B' are second virial coefficients, and C and C' are the third virial coefficients. The second virial coefficient may be considered to express the effects of interactions between two molecules, the third virial coefficients among three molecules, and successively [H&W73]. The second term is significantly large, while the third term is small, and subsequent terms generally considered negligible at moderate pressures and temperatures.

That has sense from the point of view interactions between two molecules are more common than interactions simultaneously involving three or more molecules.

If the gas under consideration is a mixture, as the case of the NG, then the coefficients B, C, B', C' , etc., become *mixture virial coefficients*: B_{mix}, C_{mix} , etc., and they can be written in terms of the mole fractions of the pure components, the virial coefficients of the pure components, and quantities called interaction (cross) virial coefficients [H&W73]. For a two-component gas mixture, and in particular for water vapor-air mixtures, statistical mechanics shows that [Hir54]:

$$B_{mix} = x_a^2 B_{aa} + x_w^2 B_{ww} + 2x_a x_w B_{aw} \quad \text{Eq. 1.2.p}$$

$$C_{mix} = x_a^3 C_{aaa} + x_w^3 C_{www} + 3x_a x_w^2 C_{aww} + 3x_a^2 x_w C_{aaw} \quad \text{Eq. 1.2.q}$$

where: x_a and x_w are the mole fractions of air and water vapor B_{aa} and B_{ww} are the second virial coefficients for pure air and pure water vapor

C_{aaa} and C_{www} are the third virial coefficients for pure air and pure water vapor.

B_{aw} is the cross-second virial coefficient expressing the effects of interaction between an air molecule and a water molecule.

C_{aaw} is the cross-third virial coefficient expressing the effects of interaction between two air molecules and one water molecule.

In the particular case of air-water interactions, non-ideality can typically be approximated accurately at the level of the second virial coefficient, which is the first-order correction to the ideal gas law. Therefore, the key parameter is the *cross-second virial coefficient*, B_{aw} , many works have been reported to evaluate but the most important were performed by Hyland and Wexler [H&W73, Hyl75].

Historically in the most of thermodynamic studies of air-water equilibrium, the air was always considered like a pure substance. However, some researchers calculated the second virial coefficient for water with air with an accuracy superior by means of combining the individual studies of pairs of substance: water–nitrogen, water–oxygen, and water–argon [H&H07].

The correlation between cross-second virial coefficient and the enhancement factor for the system air-water was given by Hyland and Wexler [H&W73] and has the following look:

$$B_{aw} = -\frac{\phi}{2\epsilon} - \frac{1}{2} \left[\left(\frac{\phi}{\epsilon} \right)^2 - \frac{4}{\epsilon} (\gamma - RT \ln f) \right]^{1/2} \quad \text{Eq. 1.2.r}$$

The coefficients γ , ϕ and ϵ of β are complex equations which are function of several quantities, as a B_{aa} , C_{aa} , B_{aaa} , C_{www} , C_{aaw} , C_{aww} , e_s , P , T , x_a . The equations which describe such coefficients were also developed in detail by Hyland and Wexler [H&W73].

Eq. 1.2.r can be rewritten in such a way the enhancement factor is the specific quantity, which is more useful expression in the field of the metrology applied to the measurement of humidity in gases:

$$RT \ln f = \gamma + \phi B_{aw} + \epsilon B_{aw}^2 \quad \text{Eq. 1.2.s}$$

In 1976, Greenspan [GRE76] utilized the data and Hyland's correlations [Hyl75] to fit the enhancement factor to a more simplified equation, whose form is due to Goff [Gof49] given as:

$$f = \exp \left[\alpha(t) \left(1 - \frac{e_s}{P} \right) + \beta(t) \left(\frac{P}{e_s} - 1 \right) \right] \quad \text{Eq. 1.2.t}$$

Being:

$$\alpha(t) = \sum_{i=0}^3 A_i t^i \quad \text{Eq. 1.2.u}$$

$$\beta(t) = \exp \left[\sum_{i=0}^3 B_i \cdot t^i \right] \quad \text{Eq. 1.2.v}$$

where the coefficients A_i and B_i depend in the temperature range. This model is covered for a temperature range from -100 °C to 100 °C, and pressures from 0.1 MPa to 2 MPa. At present, Greenspan's formulation is still considered and usually accepted like the most accurate for achieving the enhancement factors [Nie03].

Hardy [HARD98] updated the coefficients to ITS-90, although use of Greenspan's original coefficients (based on IPTS-68) gives values for the enhancement factor well within Greenspan's original uncertainty.

1.3 NATURAL GAS

1.3.1 INTRODUCTION

1.3.1.1 Definition and history

The natural gas (NG) is a fossil fuel formed millions of years ago that, like oil and coal, releases a lot of energy in its combustion process. Fossil fuels formation is linked with the deposition of microscopic organic matter dead (phyto and zooplankton) in seabed, estuaries and marshes which are buried with sands and clays forming different compact layers getting deeper. These remains afford increasing pressures and temperatures, even to degrade the original organic material generates hundreds of compounds derived carbon (C) and hydrogen (H) by heat and pressure effects.

Once formed oil and gas, as any fluid, they tend to flow toward the surface, looking for lower pressure areas. These movements are performed through permeable rock layers through their tiny pores. However, they usually found with intermediate layers of impermeable rock that avoid their movement continue, therefore they start to accumulate and saturate the pores and fissures of the rocks in which they are, forming a new reservoir.

The fossil fuels reservoirs are spread around the planet and not necessarily in submerged areas close to the coast due to the huge transformations that the Earth's surface has suffered because of the tectonic forces, the formation of continents and immersion/emersion of land areas.

There are two types of gas depending on the reservoir: when the gas is alone is called *free gas* or *unassociated*, and when coexist with oil or coal deposits, in that case called *associated gas*. Every time oil is found there will be associated gas, because as methane (CH₄) is its main component and the most volatile hydrocarbons too.

The first discoveries of natural gas (NG) deposits were made in ancient Persia, now Iran, between 6000 and 2000 B.C. conquests by Plutarch described, in Alexander the Great's memories, a natural source of fire found in Ekbatana [Igl09]. These gas fields probably were firstly fired by a lightning.

Greek and Roman civilizations also knew of its existence. In Greece the oil was discovered in the Caspian Sea because of the large flames originated by the associated gas, Pliny described the existence of a gas which burned when torches were approached. On the other hand, it refers to emanations of gas discovered by a shepherd because of the strange behavior of his flock in the vicinity of Mount Parnassus. The ancient Greeks said that these vapors were the breath of the god Apollo, so a temple was erected in his honor at the current Delphi, becoming it one of the religious centers of ancient Greece [Har02]. However, it seems that none of these civilizations (Greek, Roman or Persian) realized the potential of the gas, as there are only references to him as the "eternal fire" or "sacred fire", considered as divine phenomenon by fire worshipers [INN].

In China, first mentions of NG applications are dated around 900 B.C., and there is evidence of the first NG drilled well in 211 B.C., which reached 150 meters deep. Chinese drilled their wells with bamboo sticks and they even built canalizations made with this material to transport it to heat and light homes [Igl09].

NG was unknown in Europe until its discovery in England in 1659, but their use was not widespread. The first use of NG in North America was in Fredonia (New York) in 1821 [INN], where gas was distributed through a lead pipe for cooking and lighting homes.

Unquestionably, the development of NG knowledge has always been closely linked to oil development. The beginning of oil industry date in 1859 with the famous Edwin L. Drake's well in Pennsylvania (USA) [F&M96], considered the first modern well because it was first drilled, not dug, reaching 21 m deep with a steam engine, which marked the beginning of a great expansion [Chow87]. Since then, its exploitation has changed the world and, the style of life of the XX century has been largely due to the use of the fossil fuels. However, in the early stages of the exploitation of oil, NG was only considered a byproduct and a drawback because the drilling had to be stopped until it was completely released.

Until the late XIX century, the use of NG did not spread beyond the extraction points due to the difficulties of transport it over long distances. For this reason, the coal and oil were most developed to the detriment of NG. It was at the end of the second decade of the XX century, thanks to technological advances in conducting gases, such as leak proof seals, when transport over long distances became possible.

During the last quarter of XX century, huge engineering projects dealing with NG distribution have been performed as, Northern Lights grid with a length of 5470 km, which crosses the Ural Mountains joining the Eastern Europe with the gas fields of Siberia in the Arctic Circle; or the pipeline extending from Algeria to Sicily through the Mediterranean Sea, with stretches built at more than 600 meters deep [INN].

The current global energy dependence on fossil fuels is evident. Currently, oil accounts for 40 % of primary energy consumption worldwide, while coal and NG account for 25 % each. Therefore, 90 % of world energy consumption in 2009, comes from fossil fuels [Igl9]. In addition, the dependence on oil in the transport sector is much higher, 90 %.

To understand this dependence on fossil fuels and, especially on oil and its derivatives, it is mandatory to mention the invention of the automobile in 1896 by Daimler and Benz in Germany. This milestone involved the creation of a new market for oil, then threatened by the discovery of the light bulb by Thomas Edison in 1892 [Igl09]. However, it was in 1922 when there was the final impulse to the automotive industry thanks to Henry Ford and his famous "T" model. That year there were 18 million cars, fifteen years later 40 million, 100 million in 1956 and over 170 million by 1964 [Chow87]. In this way, and very closely linked to the growth of the automotive industry, global oil consumption has increased exponentially until today.

Like any other product, the fossil fuels price is also under control of supply and demand law. However, given its global importance, its price has experienced wide fluctuations due to historical events closely related to the control of extraction areas, for example, Yon Kippur War (1973), the Iranian Revolution led by Ayatollah Khomeini and the subsequent war between Iran and Iraq (1979), the invasion of Kuwait and the Gulf War (1997), and many other examples that would result in a complex historical analysis [Igl09].

Because of this huge worldwide dependence with fossil fuels, particularly with oil, prices fluctuations have enormous consequences at all levels, both national and international economies. For example, Brent barrel variations will have repercussions, for example: in the Global National Product (GNP), which is famous macroeconomic index defines producing capacity of goods and services for a country; or over income transfer rate from consumers to producers countries. For all of that, global regulation of fossil fuel

prices is extremely complex and there are involve many international organizations and groups, such as the Organization of the Petroleum Exporting Countries (OPEC) and the Organisation for Economic Cooperation and Development (OECD), the Gas Exporting Countries Forum (GECF), and a long etc.

1.3.1.2 Composition and properties

NG formation, from the degradation of the original organic material by heat and pressure besides methane, as the main component, generates a mixture of other light hydrocarbons such as ethane, propane, butanes and pentanes. In addition, there are also present various compounds such as carbon dioxide (CO₂), nitrogen (N₂), water (H₂O), mercaptans and heavy hydrocarbons traces, commonly called the heavy fraction and which usually use the C₆₊ nomenclature to refer to those hydrocarbon species with more than six carbon atoms.

Gas composition varies depending on the kind of reservoir, pressure and temperature conditions at which it was formed, and the depth, location and geological conditions of the area, besides of whether is talking about free or associated gas, processed gas, regasified, and many other factors. For all of that, even common NG composition ranges can be quite different in literature. Below table shows an example of usual composition ranges of NG ready to be marketed.

Table 1.3.a Common composition ranges of the most important chemical substance present in NG, data according to NG commercialized in Spain [UNION]. --- Legend used to components present at trace level.

COMPONENTS	Typical value, % mol/mol	RANGE, % mol/mol
Methane	95.0	87.0 – 97.0
Ethane	3.2	1.5 – 7.0
Propane	0.2	0.1 – 1.5
Butane	< 0.7	< 0.7
Nitrogen	1.0	0.2 – 5.5
Carbon dioxide	< 0.5	< 1.0
Heavy fraction of hydrocarbons	---	---
Others (water, derived from sulfur)	---	---
Mercaptans	---	---
Nobel gases	---	---

Compared with other fossil fuels NG has low level emissions of CO₂, the main responsible for the gases emitted to the atmosphere causing of the greenhouse effect, and therefore the global warming. NG combustion emits between 25 % and 30 % less CO₂ per unit of energy produced than oil products and from 40 % to 50 % less than coal [GND].

In addition, NG is substantially free of sulfur, element highly corrosive and whose combustion generates sulfur dioxide (SO₂) that combined with atmospheric steam produces sulfuric acid (H₂SO₄), which is highly corrosive and can precipitate with rainwater producing acid rain. This phenomenon has serious consequences on the environment as ruining crop lands, increasing global deforestation and acidifying of drinking waters [PRTR-S].

Another advantage of the NG is the low concentrations of nitrogen oxides in its emissions (NO_x), compared to coal or petroleum. These compounds are highly soluble in water, with which combines resulting nitric acid (HNO₃), according to the reaction: $3 \text{NO}_2 + \text{H}_2\text{O} \rightarrow 2 \text{HNO}_3 + \text{NO}$. The nitric acid is a strong oxidant, reacts violently with combustible and reducing materials, degrades metals in the presence of water and also produces acid rain [PRTR-S]. Furthermore, NO₂ can release an atom of highly reactive oxygen by irradiating, resulting formation of tropospheric ozone in the presence of non-

methane volatile organic compounds (NMVOC) causing of *photochemical smog*, which is dense and dark fog generated in urban areas with high traffic, warm and sunny weather, and with little movement of air masses. Furthermore, the presence of CO₂ and SO₂ have a negative impact on the heat capacity of NG [Zam10].

In summary, the NG despite being a non-renewable energy source has a large global support and a good public opinion due to the low emissions of the three compounds above mentioned (CO₂, NO_x and SO_x), non-emissions solid particulate, and low emissions of other polluting gases causing of the greenhouse effect. Therefore, within fossil fuels, it is considered the cleanest and respectful with the environment energy source. That is why promote its use to detriment of other fossil fuels to help reduce all environmental problems mentioned, besides of lots of health problems on living beings.

This gas is colorless, odorless, and tasteless, besides it is lighter than air so its presence may cause asphyxia in confined space if oxygen concentration in air decreases below the minimal value needed for the human being. For all before and in order to avoid potential risk situations, mercaptans or another kind of odorant are added to NG in order to detect quickly any possible gas leaks. By the other hand, NG is not corrosive, toxic and poisonous, so risks caused by direct contact are null.

In addition, in spite of it is explosive, it has numerous properties that make it a relatively safe fossil fuel, such as: combustion temperature in air is relatively high, close to 1900 °C [Bru87], auto-ignition temperature range is high too, between 650 °C and 750 °C [Bru87], and it has a narrow flammability range.

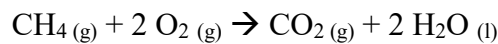
One of the most important features that must be taken into account to compare fuel energy efficiency is the *calorific* or *heating value*. This property expresses the amount of heat produced or released by complete combustion of a specified quantity of fuel, so it is measured as a unit of energy per unit mass or volume of substance (e.g., kcal/kg, kJ/kg, J/mol and Btu/m³). There are two types of heating values:

- *Higher heating value (HHV)*, also known as *gross* or *upper heating value*, defined as heat released once combustion is done and the products have returned to the original pre-combustion temperature. During combustion process, temperature reaches values upper than water vaporization temperature, hence water generated is vaporized. HHV takes into account the latent heat of vaporization of water when combustion products come back to initial temperature state, hence water molecules are condensed to liquid.

The sensible heat of water vapor from the exhaust gas temperature until condensation temperature of water, and sensible heat from this latest to the original pre-combustion temperature are also taken into account.

- *Lower heating value (LHV)*, or net calorific value of a fuel, is defined as the amount of heat released by combusting a specified quantity of fuel, assuming the latent heat of vaporization of water ($\Delta H^\circ = -44 \text{ KJ} \cdot \text{mol}^{-1}$ at standard T and p (STP): 298.15 K at 1 atm [NIST]) in the reaction products is not recovered. This parameter is more frequently used in boiler combustion plants or any industrial process in which a minimal temperature must be hold inside of combustion chambers to get an optimal yield of stage, or directly water vapor is released together with other combustion gases by chimneys.

Difference between the two heating values depends on the chemical composition of fuel, and mainly hydrogen content, which determines amount of final water vapor generated during combustion. According to, value table of the LHV and HHV gas, liquid and solid fuels performed by Argonne [Arg10], the HHV of hydrogen is 18.2 % above its LHV, whilst for gasoline and diesel the differences between heating values are about 10 % and 7 % respectively, and for natural gas about 11 %. This is particularly relevant for the NG, because the high hydrogen content produces hence much water. Supposing an ideal composition of NG completely constituted by methane, the simplest reaction would be as follows:



That means for each methane molecules two water molecules are formed, so difference between HHV and LHV is $-88 \text{ KJ} \cdot \text{mol}^{-1}$, which would be a value quite close for a real gas. The heat combustion of above reaction at STP is, $\Delta H_c^\circ = 891.33 \text{ KJ} \cdot \text{mol}^{-1}$ [NIST]. These quantities can be empirically measured using calorimeters or calculated from fuel composition, which in the case of NG it will be apply the European Standard ISO 6976:2005 [ISO05].

Another important information extracted in Argonne's table [Arg10], besides of the amazing superiority of hydrogen as a fuel, is that the NG calorific value is one of the highest among all energy source, so is considered an energy source highly efficient.

Summarizing, the NG is an economic energy and highly effective performance, a safe and versatile alternative able to meet energy demand in domestic, commercial and industrial sectors, providing significant energy savings [ENG, GND].

1.3.1.3 Applications

Natural gas has many applications but the most important uses are:

- *Power Generation*, is its most important application, by means of electricity generation in combined cycle and co-generation plants. It is the fuel most used because its high efficiency improves the performance of electricity generation, while reducing the environmental impact caused by other fossil fuels.

- *Domestic Sector*, was initially its only use addressed to streetlights, but soon it spread to households for cooking, lighting, heating water and heating, greatly improving the quality of life of households. The gas is distributed in homes and local businesses by secondary supply networks.

- *Industrial Sector*, NG can be used directly as a fuel to generate heat in boilers, highlighting its use in ceramic, cement and glass industries. In drying process, as in paper industry, or heating thermostatic baths, as in food industry. But, it can also be used directly as raw material of the process, as for example: in the steel industry NG is used as a reducing coke instead, in chemical and petrochemical industry to produce fertilizers and methanol, among others.

- *Transports*, its use is starring mainly to bus fleets, which is intended for urban public transport to reduce the pollution, especially in large cities. Despite it is estimated a slight increase of its use in this sector for 2017, that was lower than 4 bcm in 2011 [FUN13] in Europe, making evident its low participation in sector.

Demand share of each of this application groups in Europe in 2013 can be seen in Fig. 1.3.e.

1.3.2 INDUSTRIAL INFRASTRUCTURE

1.3.2.1 Natural gas processing steps

Infrastructure associated with NG industry depends directly on the life cycle of the gas, namely, each stage of gas processing from it is discovered until is delivered to final consumer. The steps of the natural gas cycle are:

- *Exploration*, location starts with a series of explorations consisting conduct drilling in areas where its existence is presupposed. It is said that a reserve of gas is proven when through various drilling one oil field is located and analyzed to determine the quality and quantity of NG that contains. Perforations are made constantly to find

new deposits, although not all of them are analyzed later, because of high costs (about 15,000 \$·km⁻² for three-dimensional seismic survey at sea analyzed [Igl09 - P. 124]). This is the reason by which not all deposits become proven reserves.

- *Extraction*, NG extraction process is very similar to oil extraction. Pressurized NG is extracted from the wells by mere pressure difference and NG is transported to processing plant, which should be located close to the extraction areas.
- *Processing*, NG just extracted is completely saturated with water and comes with a great variety of undesirable compounds, as impurities and pollutants, which must be removed to achieve the quality standards of the final product. Some activities performed in this sense are: condensate removal and drying, removal of several compounds (CO₂, N₂, Hg), and H₂S removal and recovering of sulfur. Once all these substances are removed NG is called *sweet gas* [Per03].
- *Transportation*, the most important worldwide method to transport NG method keeps being the pipeline grids. However, transport of liquefied natural gas (LNG) is becoming more and more important because NG condensation reduces its volume in 1:600 that means, 600 m³ gas turn into 1 m³ of LNG. Condensed NG is transported by ships equipped with refrigerated tanks able to maintain the temperature below -160 °C, temperature at which the phase change occurs. By contrast, work with LNG requires a set of processes and infrastructures extras which leads to more complex processes and higher installation costs to carry out next activities:
 - Transport by means of pipelines from extraction points to distribution ports, which must be equipped with liquefaction plants.
 - To remove any kind of impurities and pollutants and minimizing the water content before being condensed.
 - To condensate NG and fill up the cooled vessels, which must be able to keep the gas temperature below – 161 °C. Condensation temperature of NG is one of weak point of this energy source, because relative costs to hold it in liquid state are elevated because of:
 1. LNG is pumped into the vessels of the ships, which must be refrigerated too.

-
2. Download LNG in ports equipped with regasification plants.
 3. Pumping stations to inject NG to the main transmission lines.
- *Provisioning*, both LNG and in its gaseous phase must be stored until energetic demand required it. For the first case, LNG is directly stored in cooled tanks in facilities associated with reception ports, whilst NG which came directly by pipelines must be injected in underground gas storages (UGS) which usually are old extraction wells or naturally cavities or caves. This provisioning allows face to variations in the demand of NG because of seasonality of any energetic resource during the colder months, and any unpredictable demand peaks.
 - *Commercialization*, NG is distributed throughout the entire territory of a country by the main pipelines grids, but then secondary distribution networks are responsible for delivering NG to all kind of customers, as: households, local business, etc. These secondary networks work at pressure which no exceed 2 MPa, so diameters and walls thickness of the pipes are smaller.

1.3.2.2 Worldwide

To understand well everything surrounding the NG industry at global level, it is important to know and analyze certain indicators to obtain a right idea about its evolution and what are its future perspectives for the coming decades. Firstly, it is going to explain what are proven reserves of NG on the world, later evolution between production and consumption of NG, which are the mayor trade agreements around the world, and lastly, what are the outlooks for this industrial sector.

Proven reserves of NG have had an uninterrupted growth since there are records. According to the annual reports elaborated by *BP p.l.c.*, proven reserves were 150.2 tcm¹ in 2000, 181.9 tcm in 2008, 185.7 in 2013, and global reserves has increased 0.2 % in 2014 regarding the year before [BP15].

The main global reserves are located in the Middle East (39.9 %) and Eastern Europe, commonly also called Eurasia, (31.8%), while Western Europe has only 2.9 % of world reserves [ENG]. The global distribution of proven reserves of NG is more detailed in Fig. 1.3.a, in which can be appreciate constant increase of known reserves in

¹ Along all this section abbreviations *bcm* means billions of cubic meters, using billion as the British culture, namely 10⁹. In the same sense, *tcm* means trillions of cubic meters, namely, 10¹² m³.

all regions of the planet and unequal distribution of extraction areas, highlighting the exporting potential of the Middle East.

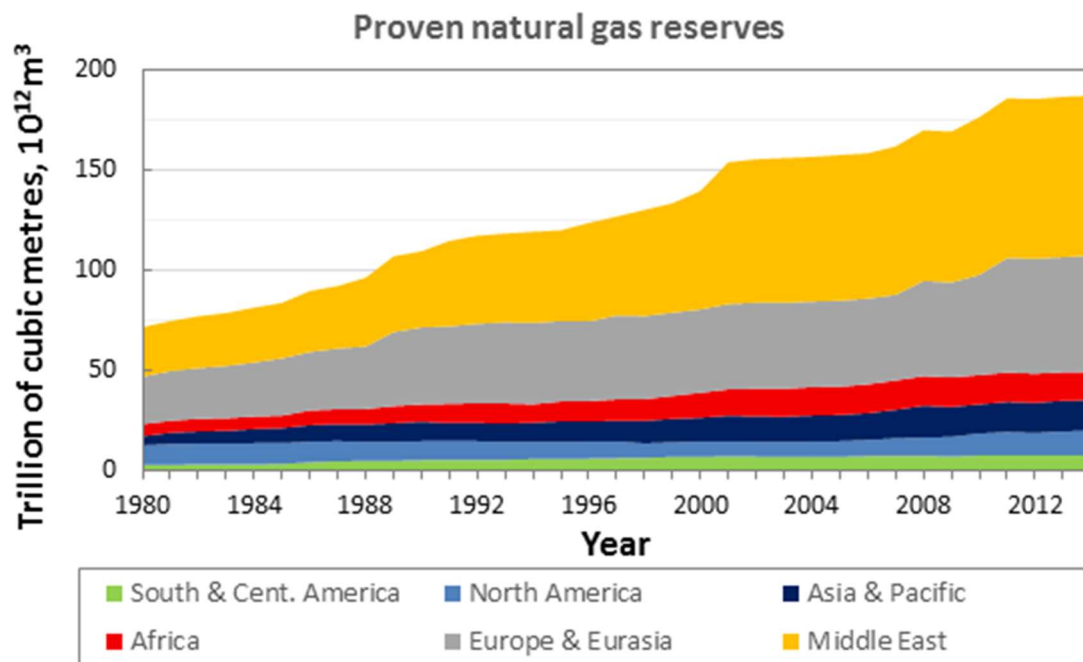


Fig. 1.3.a Evolution of global proven reserves of natural gas since 1980 until 2014 according to annual reports of world energy performed by BP company [BP15].

NG production was duplicate between 1975 and 2000, from (1.2 to 2.4) tcm·y⁻¹. In 2000, USA had 22.9 % of world production and the Russian Federation 22.5 %, covering almost the half world production [BP15].

Regarding with data collected about world consumption of NG, in 2002 it became the second energy source with 25 % share, at the same level than the carbon but with a much higher growth rate, so NG outlook already were very promising.

Today there are two trends that endorse NG consumption: first, developed countries tend to increase their NG consumption for both domestic and industrial use and for electricity generation; and second, producing countries support their self-supplying, as in the case of the Russian Federation and former members of the USSR as, Algeria or Iran.

Fig. 1.3.b. shows evolution rates of NG consumption during the last decades and classified by regions. It can be seen as nowadays Europe together with Russia have the same consumption rate than North America, around 1 tcm per year, whilst South America and Africa are lowest consumers, below 0.2 tcm per year.

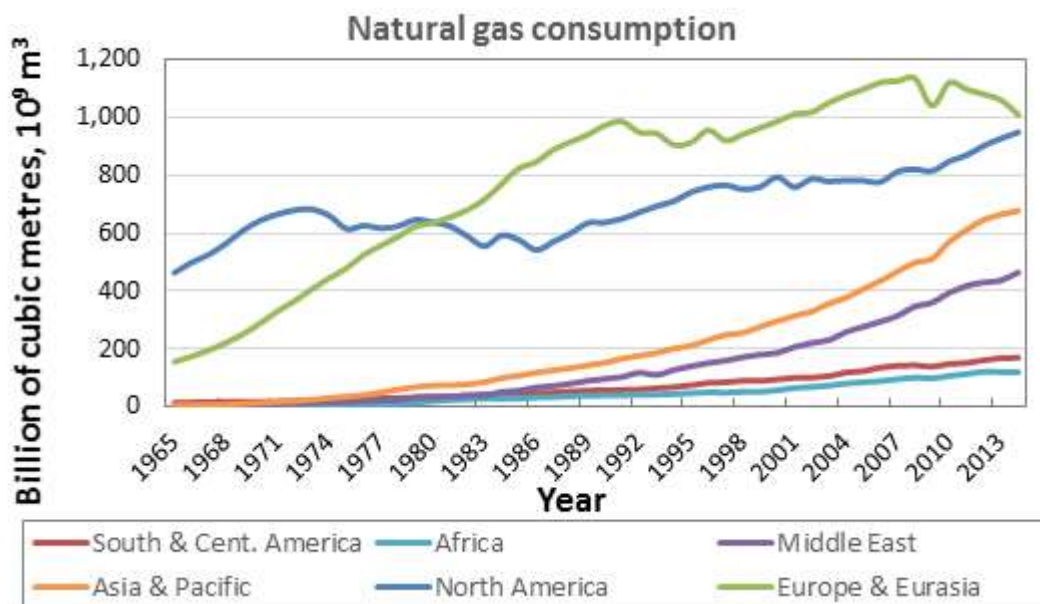


Fig. 1.3.b Global evolution of natural gas consumption since 1965 until 2014 [BP15].

Also, it can be appreciated as all regions increased consumption share during the last 5 years, except Europe together with Eurasia, mainly due to economic recession that hit more strongly in Europe and affected severely to its industrial sector, so NG requirements for power generation and the industry in general fell.

Fig. 1.3.c shows rates of each concepts previously analyzed (proven reserves, production and consumption) classified by regions. From that, essential information can be extracted such as: the Middle East has the 40 % of the global proven reserves, followed by Eurasia, which is also the biggest exporter; North America consumes the same amount that produces; the Western Europe is quite dependent energetically, so also from the point of view the NG; Central and South America, and Africa have not industrial economy very dependent on NG despite of they would have enough reserves in comparison with their consumption rates.



Fig. 1.3.c Graphical summary about the global percentages of reserves, consumption and production of NG in 2008 classified by geographical regions [ENG].

Once the exporter and importer regions of NG are known, the next step must be to know the main international trade agreements among these regions. Table 1.3.b shows total volumes of NG commercialized among these regions during 2014 distinguishing between NG transported by pipelines or in LNG ships.

Table 1.3.b Natural gas trade movements in function of the continents in 2014, including exportations inside and outside of geographic limits established [BP15].

	NG BY PIPELINE, bcm	LNG, bcm
North America	116.9	11.6
S. & Cent. America	17.8	21.4
Europe	361.9	52.1
Former Soviet Union	73.8	
Middle East	27.2	5.4
Africa	8.5	
Asia & Pacific	57.8	242.7
Total exports	663.9	333.3

As above table shows, Europe is responsible for the largest volume of NG commercialized in the world, being responsible of more than half world volume of NG exchanged by pipelines. NG commercialized by methane ships is equivalent to the half of NG volume managed by pipelines. However, in Asia and Pacific region this trend is reversed, because the volume of LNG commercialized is six times higher than NG transported by pipelines. Information content in Table 1.3.b is complimented with Fig. 1.3.d, which detail direction, volume transported and via of the most important global trade movements of NG.

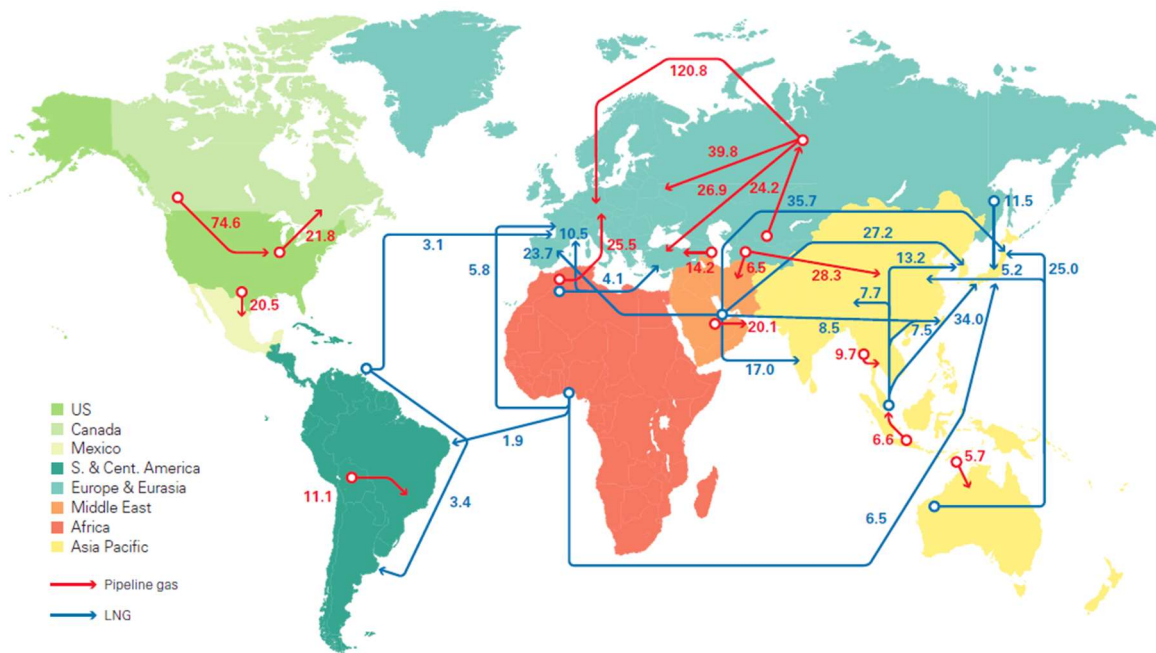


Fig. 1.3.d Major worldwide trade flows of natural gas in 2014. Units expressed in billion cubic meters (bcm) [BP15].

An important indicator about the remaining lifespan of a natural resource is *R/P ratio*, or *RPR*, relationship between proven reserves and their consumption, expressed in terms of years and is used in forecasting the availability of any resource.

According with proven reserves and production rate of its corresponding year, in 2001 *R/P ratio* would represent 61 years of global supply secured. In 2007, the world *R/P ratio* of NG remained constant, 60.3 years, while the oil was already 41.6 years, so situation was already more favorable for NG [Zam10]. In accordance with *BP* [BP15], proven reserves at the end of 2013 would be enough to maintain the current global production for 55 years.

The most positive outlooks for energy demand estimate that global demand for NG will be 5.1 tcm in 2035, which means 1.8 tcm more than today. That implies share of NG in the global energy mix will increase from 21 % to 25 % in such period, overtaking coal as the second world energy source by 2030 [IEA11]. The most important reason of this growth is the development in Asian region that will account for almost half of this rise in global gas demand, largely because imports of this regions will increase 75%, and the main actors of this growth will be Asia and India to supply energy requirements derived to construction of new infrastructures and more than 600 mill of new electricity consumer because of expanding middle class [IEA15a].

Predictions also must be taking into account unconventional NG resources, which includes shale and tight gas, coal bed methane (CBD), and methane hydrates, are now estimated to be as large as conventional resources. Important projects are being developing now as in Australia and in in countries with an emerging industry like China, India or Indonesia [IEA11].

However, not all existing factors will stimulate use of NG, by contrast some of them will influence negatively on global demand of this resource in the coming years. Some of this factors will be:

- Since 2010, there is a global oversupply of NG due to, among other reasons, low demand caused by low (or negative) economic growth caused by economical regression. Thus, NG production and prices fell during these last years. A current example of this phenomena is happening because of Chinese economic slowdown, so its imports of liquefied natural gas (LNG) decreases, producing excess global supply. Therefore, during this last year prices in Japan and Korea, the main importers of LNG in the Pacific region have fallen by half, from about 15 to about 7 US \$/MMBTU [Hsu15].

- Coal will keep being a strong competitor among fossil despite of its lower efficiency and higher pollutant emissions. This situation is partially favored by low price of CO₂ emission rates and penalties when the particular goals assigned for signatory countries of the Kyoto Protocol are not achieved. For this reason, replace the use of coal by another more respectful energy source to reduce emissions of greenhouse gases is not being really favored.

- In addition, NG also must face to the strong competition from renewables, which are driven by continued policy support to electricity power generation that will account for half of additional global electrical generation forecasted for 2040 [IEA15a].

1.3.2.3 Europe

Nowadays NG represents 24 % of European energy consumption and its supply is performed by means of two ways: pipeline grids and LNG transported by ships. There are three main routes of pipeline grids [SEDI]:

- *The East Route*, which supplies to Germany, France, Belgium, Italy and Eastern Europe. Russian gas is the main supplier, representing over 50 % (142 bcm in 2011) of total imports from Europe. Another important input occurs through Turkey from Middle Eastern countries as: Iran (9 bcm), Azerbaijan (4 bcm) or Turkmenistan.

- *Northern Sea Route*, transports gas from the Norwegian offshore fields to Belgium from where is distributed to center Europe.

- *The South Route*, vital for countries like Spain and Italy, whose main producers are Algeria and Libya with 33 bcm and 2 bcm, respectively. However, conflicts in some exporting countries has like a consequence instability in the NG supply and therefore, vulnerability is an added risk. This is not the case of Spain thanks to its energy strategy, based on diversifying gas buyers in a multitude of markets, guarantees stability and supply of the national gas system (see Table 1.3.c).

Traditionally in Europe, trade contracts of NG have been of the long-term kind, usually 20-25 years, directly linked to oil prices and restrictive clauses, which forced to buy a fix rate of NG independently of energy demand.

European regulation has played a very important role in the cross-border trade for an internal gas and electricity market. A legislative package, known as “*Third Energy Package*”, constituted by two Directives and three Regulations, among which the Regulation 2009/715/CE [EPR09a] and the Directive 2009/73/CE [EPR09b] are directly focused on NG. Thanks to this legislative package were established two international bodies: Agency for the Cooperation of Energy Regulators (ACER) and the European Network of Transmission System Operators for Gas (ENTSO-G). The most important European NG transporters are integrated in these entities, and whose duties were perfectly defined in such documents, highlighting the following [FUN13]: ensure a free market

among all European citizens, promote a transparent and cross-border trade in order to achieve efficiency gains, competitive prices and increase the quality and competitiveness of the service, and to contribute to security of supply and sustainability. As a result of this politic, NG suppliers transferred the pressure to the main European producers, such as Gazprom and Statoil.

Finally, a structural radical change was produced in European NG market: old monopolies are disappearing and with them the contractual limitations and high and fixed NG prices directly linked with price of oil. This is leading to free market more efficient, economic and competitive. As a representative example, 67 % of NG supply were indexed to the price of oil in 2009, whilst this quantity was decreased down to 50 % in 2012 [FUN13]. Despite all these improvements, there are currently still remains restrictive long-term oil-indexed contracts, because they were signed in the past.

European NG demand in 2011 was 520 bcm and according with forecasts of International Energy Agency (IEA) that will increase slightly up to 561 bcm in 2017, so it will not recover level of 2010 yet [IEA12]. At this weak growth in demand is joined a drop of NG production (273 bcm in 2011), which is expected to maintain a declining profile over the coming years to reach 256 bcm in 2017, increasing accordingly import requirements above 300 bcm [FUN13]. Fig. 1.3.e specifies share of NG demand according to application sectors.

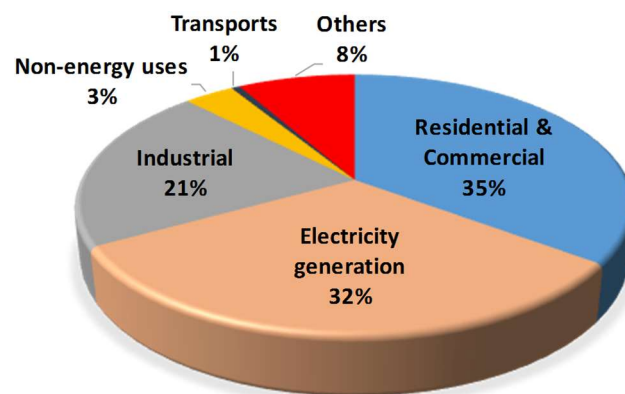


Fig. 1.3.e European energy consumption of natural gas in 2013 classified by applications [SEDIc].

Above figure shows as the major consumption (35 %) of NG in Europa is directed to meet the requirement of homes and local business. Practically at the same consumption level (32 %) is dedicated to electricity generation and thanks to combined cycles and co-generation plants, followed by its countless industrial applications with a 21 %. By

contrast, its low impact as power source in transports with only 1 % must be emphasized too.

By the other hand, it is mandatory mentioning a current situation is occurring since 2015 to which European gas market is facing, the escalating conflict between Russia and Ukraine. That stands for a geopolitical conflict because Russia is the Europe's largest gas exporter and Ukraine is the most important transit country in this exchange. For that, and while Russian's desire to bypass Ukraine as a transit country remains, Turkey will play a very important role, as the most important alternative to Gazprom, the Russian gas leader company, to commercialize with Europe [IEA15b]. To sum up, political scene is quite complex and Europe's strategy is forced to diversify gas supply, finding alternatives that ensure European increasing gas demand.

1.3.2.4 Spain

In the first third of the XIX century in Spain begins gas production from coal manufacturing, being Barcelona the first major city with public lighting based on NG, followed by Madrid. Later, in the mid XX century, liquefied petroleum gas (LPG) began to be used, as propane and butane, and its use was spread in businesses and homes, and even for the first industrial applications.

The first importation of NG was in 1969 by means of LNG in the port of Barcelona. The absence of NG reserves in Spain implies that 99 % of its consumption is imported [SEDI]. Therefore, to develop a national distribution network with receiving and regasification terminals of LNG was essential.

Later, in 1996 NG supply system suffered a great increase by building the Maghreb pipeline (1996) to import NG directly in gaseous state. Before that year, more than 80 % of NG importations in Spain were as LNG, however after implementation there was a significant change in this situation, increasing the percentage of gas received directly by pipeline to reach 51 % of total supplies in 1999.

This diversification in the NG supply provided great advantages in order to guarantee its supply and decrease costs directly linked with LNG processing. However, not all were advantages because in LNG is unusual there are hydrocarbons with more than six carbon atoms, whilst NG that comes directly is more often to find heavy hydrocarbons up to twelve carbon atoms and with higher water contents. For that,

condensation risks (as it can be seen in Section 1.3.3) increased and it had to be included new treatment and drying processes to reduce the high impurities and water concentrations.

The current Spanish NG system consists in the following facilities [SEDI, ENG]:

- Regasification plants, currently there are seven plants (Barcelona, Huelva, Cartagena, Sagunto, Bilbao a Coruña and Gijón) and two more under construction in the Canary Islands. Spain ranks the first position in EU as receiving country of LNG and it had a share 37.5 % [SEDIc] of European regasification capacity in 2013, with a total of 22 regasification plants [SEDIb].

- International connections, understanding as such each of interaction points between the Spanish national transmission grid and any other pipeline network belonging to another country. There are three exchange areas with two connection points each of them:

- NG coming from Africa:

- *Magreb pipeline*, operating since October 1996, comes to the peninsula by Tarifa and later communicates with the Al Andalus pipeline that is key to Portugal to acquire Argelian NG through Spain's pipeline.

- *Medgaz pipeline*, was put into operation during the second half of 2009, receiving terminal is located in Almeria, and it was a great improvement to guarantee NG supply not only in Spain but also in the rest of Europe.

- Connection with Central Europe by France:

- *Larrau pipeline*, operating since 1993, was the first point that connected with European NG grid. Today, it is able to operate with a total $5.2 \text{ bcm}\cdot\text{y}^{-1}$ in both senses.

- *Guipuzcoa pipeline*, connects Spanish national grid with European in Irún. Currently, this connection pipeline is being enlarged to reach a total capacity of $7.1 \text{ bcm}\cdot\text{y}^{-1}$.

- NG exchange with Portugal, in Badajoz and Tui (Pontevedra), which started to operate in 1996 and 1998, respectively.

- Main transmission line, by means of which NG is transported at high pressures (between 4 and 8 MPa). In 2012, length of the main pipeline grid was 12,815 km.

- Distribution grids, work at pressures below 1.6 MPa and communicate with the end consumers. In 2012 was operating 67,282 Km.

- Pumping plants, to give the pressure necessary to NG to achieve wanted destination. They are necessary to compensate the effect of pressure drops because of the frictional forces.

- Storages, whose function is double: strategic importance to guarantee the NG supply in the case to there had been supply problems, and to cover specific demand peaks of gas during especially cold days during winter seasons.

- Underground storages located in Serrablo (Huesca), Yela (Guadalajara) and Marismas (Huelva).

- Two underground storages offshore: Gaviota (Vizcaya) and Castor (Castellón).



Fig. 1.3.f Scheme of the Spanish NG transmission line together with the most important facilities associated that includes: international exchange points, regasification plans and reception ports, underground storages and pumping plants [ENG].

As it has been discussing, Spanish supply strategy of NG is based on diversification not only relative to exporting countries but also in the way the NG is received (liquefied or gaseous).

According with supervision reports elaborated by National Commission Markets and Competition (CNMC) LNG importations represented 47 % of national total supply in 2013, and participation share of the supplying countries for such year (heavily extrapolated to the present) had the following properties [CNMC16]:

- The main supplying country is Algeria with an increasing share, around 42 % in 2012, whilst raised up to 53 % in 2013. Algeria is responsible for 80 % of NG importations by pipelines.
- The second supplying country is Norway, which has a market share of 11.6%, by pipeline and LNG ways.
- The third source of supply is the Emirate of Qatar in the Middle East, which has decreased its LNG exports to Spain slightly, looking for other markets such as Asia, reaching 11 % of rate supply in 2013.

Regarding with the provenance of supplies according to geographic areas, it should be noted that more than 52 % came from Middle East and North Africa countries. In Table 1.3.c, it can be seen that, share of each importing countries of NG in 2014 kept the same behavior than previous years [BP15], but demand fell 8.1 % and importations was reduced 6.8 % [CNMC16].

Table 1.3.c International NG trade movements in Spain in 2014, taking into account NG supplied both by pipeline and LNG through ships [BP15].

COUNTRY	Natural gas imports in Spain during 2014, bcm	
	By pipeline	As LNG
Algeria	11.1	4.9
Norway	3.1	1.2
Qatar		3.0
Nigeria		2.7
Trinidad & Tobago		2.0
Peru		1.2
Oman		0.2
Other Europe	1.1	0.2
TOTAL	15.4	15.5

One of the most remarkable evolutions of NG importations in Spain during last years was increasing supplies by pipeline, from 40 % in 2012 to 53 % next year [CNMC16]. This effect is due to combination of two factors: reduction of energetic demand of NG because of global economic recession and the kind of NG purchase contract with Algeria that forces to receive a constant quantity of NG per year until the end of the contract.

This situation leads to a logistic problem for the Spanish gas system because it is receiving more gas than it is being consumed, so it has been forced to increase its storage capacity, reason by which the new underground storage of Yela has had to be enabled.

By contrast and because of conflict between Russia and Ukraine, Spain has become key piece to meet the energy needs of Centre Europe countries, thanks to its privileged geostrategic position and the fact of having first level gas infrastructure, like the greatest potential regasification.

1.3.2.4.1 *Enagás*

Due to the significant growth of energy consumption and its forecasts in Spain and in order to extend the HG use throughout the entire national territory. In 1972, the National Gas Company (Enagás. S.A.) was founded [BOE72]. Later, 23rd June of 2000, Enagás was appointed by Royal Decree as Technical System Operator [BOE00], and their functions were defined among which stands ensure the continuity and safety of natural gas supply and proper coordination between access points, storages, transport and distribution processes.

Some years later, Enagás acquired certification by the European Union as Transmission System Operator (TSO), resolution also approved by the Spanish National Energy Commission [BOE12]. This certification guarantees the independence of the Spanish transport network with respect to gas producers and traders of NG, and in addition, it is also an essential requirement in order to participate fully in the ENTSO-G.

Enagás is also responsible for the construction, expansion and modernization of its infrastructure with the highest quality standards and techniques available, in a constant effort in innovation. This effort is also aimed at optimizing energy efficiency through the use of waste energy from their processes or increased efficiency in equipment and facilities [ENG]. A large part of facilities cited in the previously section are owned by Enagás as, the main transmission line, several UGS and regasification plants.

Besides, Enagás has been involved actively in international joint R&D projects directly related with the NG, among which is included part of the work developed in this thesis.

1.3.3 THE HUMIDITY. KEY PARAMETER IN NG PROCESSING

Moisture content in NG are extremely important from a technical perspective to ensure and control adequately gas properties in all processing steps, especially during its transport through to the transmission and distribution pipelines.

Moreover, humidity is essential for a properly characterization of final features of product which will be delivered to consumers, in order to ensure properly gas properties during its transport and for subsequent applications. In this sense, contractual specifications with customers and in international exchange points of the national grids must be met [K&P].

For that, moisture removal is one of the key stage of NG processing and its efficiency, because of the large NG volumes handled, is important to reduce associated operating cost. Reason by which to know reliably and accurately final humidity after drying processes is a key point that will allow to have under control this feature along the entire gas system.

The presence of water together with complex hydrocarbons mixtures implies changes in some properties and even variations of the behavior which must be taken into account because can lead to operating problems causing even hazardous situations. For this reasons, many current researches and efforts are focused to characterize influence of water in these gaseous systems to prevent undesired situations [Mok06, Car09].

Below sections explain those concepts, properties and phenomena that must be known to understanding what are phenomena derived from the presence of water in NG, its implications and how to avoid undesirable situations.

1.3.3.1 Definitions and concepts

For a multicomponent system, as the case of natural gas, if its equilibria diagram is depicted on p - T plane, it can be seen some differences from the diagram belonging to pure fluids. Saturated vapor curve, or *dew point curve* (DPC), is different from saturated liquid curve, or *bubble point curve* (BPC). First curve depicts those conditions under which it is produced the first drop, whilst the second indicates the appearance of the first NG bubble. These two curves meet at the *critical point* (CP) where the properties of two phases vanish and they become identical. All together build the *phase envelope* that, in the particular case of pure fluid, both curves overlap forming an increasing curve until to reach its critical point. The inner area contained by the phase envelope is the two-phase region, where coexist hydrocarbons both in liquid and vapor phase.

Hereinafter, the saturated vapor curve for the natural gas will be named *hydrocarbon dew point* (HCDP) *curve*, whilst for water it will be named *water dew point* (WDP) *curve*. These curves have been depicted in the same diagram in Fig. 1.3.i, HCDP is the solid black line, whilst WDP curves for different water content are colored.

Another difference between multicomponent systems and pure fluids is that can exist temperatures and/or pressures higher than those given at the critical point. The highest pressure and temperature defined by this phase envelope are known as

cricondenbar y *cricondentherm*, respectively. Location of all these points only depends on the composition of mixture. Fig. 1.3.g shows qualitatively the phase envelope of any multicomponent mixture, together with all curves and particular points described.

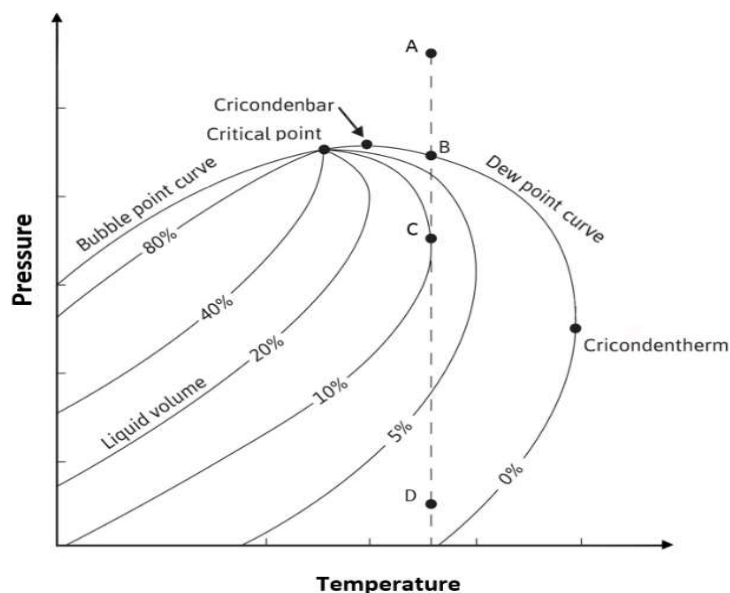


Fig. 1.3.g Vapor-liquid equilibria (VLE) of a multicomponent mixture depicted on p - T plane. It can be seen as bubble and dew point curves are not overlap, they meet in the critical region, making up the phase envelope. Cricondenbar and cricondentherm have been also depicted, in addition to several lines of constant liquid volume percentage.

One of the most important consequences of these differences between the equilibria diagram of mixtures and pure fluids is a phenomenon known as *retrograde condensation*. This name was given by Kuenen in 1892 [K&K40] and makes reference to those condensations occurs in reverse way to the normal situation for pure substances. There are two types of retrograde condensation:

- The *isothermal retrograde condensation* is produced by pressure reduction, using dotted line of Fig. 1.3.g, from A to D . Starting at one temperature fixed higher than the critical temperature, point A . Hydrocarbons condensation will start in point B and liquid amount will increase to reach point C , which is the maxima condensation can be occur at such fixed temperature. Liquid forming produced between B and C is known as *retrograde condensation*. If the pressure keeps decreasing until reaching C point, liquid previously condensed will start to evaporate until reaching again the HCDP curve.

- By the other hand, keeping at constant and higher pressure than in the critical point, if reduction temperature process happens from A point to D , it will appear the first drop of condensate in B . The liquid amount will increase until reaching the maxima in C point,

but later it will start to evaporate until reaching the HC DP in *D*, where all hydrocarbon will be in vapor phase. Vaporization produced by cooling between *C* and *D* point is known as *isobaric retrograde condensation*.

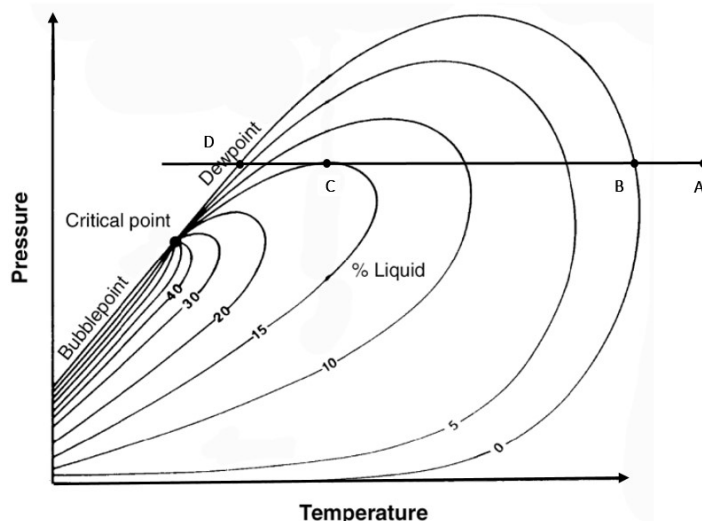


Fig. 1.3.h Qualitative depict of an isobaric retrograde condensation on and VLE diagram of a multicomponent mixture depicted on *p-T* plane.

For the case of wet natural gas, if the VLE diagram is depicted on the *p-T* plane, there will be two kind of curves depending on composition of dry gas and water concentration, as it can see in Fig. 1.3.i. In later sections of this chapter, methods used to calculate both HC and WDP curves are explained in detail.

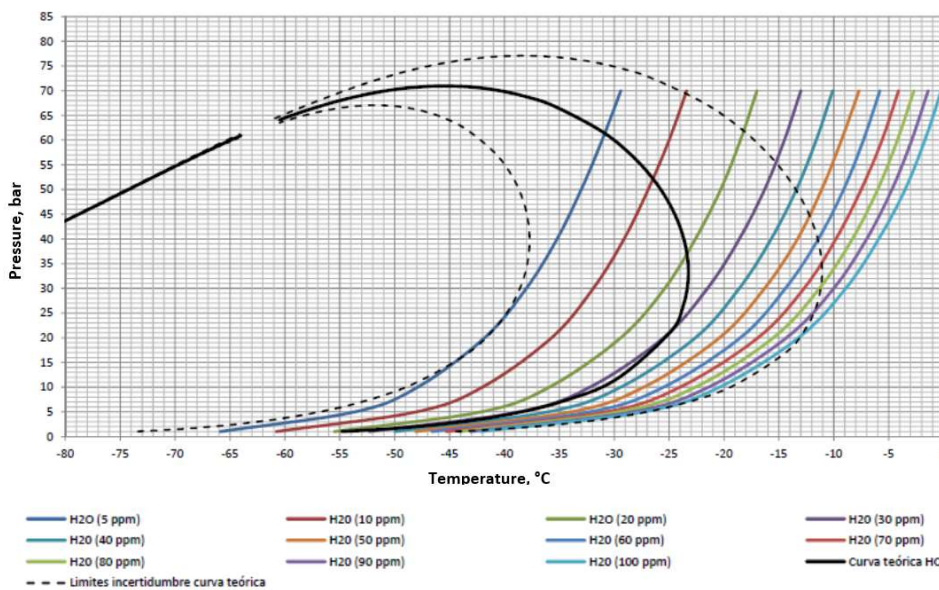


Fig. 1.3.i Phase envelope from NG analyzed one of the tests days performed during this thesis. NG phase envelope is depicted by solid black line, the right side section, separated by the critical region, is the hydrocarbon dew point (HC DP) curve, whilst left section is the bubble point

curve. The dotted black lines depict the uncertainty limits of HCDP curve, theoretically calculated from NG composition obtained by chromatography [ISO03]. Colored curves represent depict water vapor pressure curves at different concentrations, namely, WDP curves.

Looking at Fig. 1.3.i, for such HCDP curve if NG was cooled down at a fixed pressure, two possible situations could happen depending on the WC level. Below these two situations are explained with an example at a steady pressure level close to the cricondentherm, that is, around 3.5 MPa and for two water concentration levels:

- For a water concentration of 50 ppm_v or higher, and an initial NG temperature of -5 °C. When temperature starts to fall, it will not occur anything up to reaching, approximately, -20 °C, time in which the first water drop will appear because the WDP curve was achieved. If temperature continues decreasing the amount of condensate will continue increasing and it will be constituted only by pure water. When the temperature falls up to -23 °C, when HCDP is reached, the heaviest hydrocarbons will start to condensate. From this point and whether NG keeps being cooled, condensate phase will be richer in hydrocarbons as temperature is lower.

- In the opposite situation, if water concentration is relatively low, for example 5 ppm_v, when the temperature starts to fall, the first drop of condensate will be constituted by the heaviest hydrocarbons, because HCDP curve is more to the right than WDP line at 3.5 MPa. If temperature goes down, the lower it is, the lighter will be the hydrocarbons that start to condensate. When temperature is -35 °C, water condensation will start because WDP curve has been already reached.

Summarizing, the nature of the first condensates can be water or a mixture of the heaviest hydrocarbons depending on: composition and moisture content of NG, which determine relative position of HCDP and WDP curves in the phase envelope diagram, and the system pressure and temperature conditions.

1.3.3.2 Condensation and hydrates

Hydrocarbon condensation may create problems with capacity of transport or disabling compression and measurement devices, even affecting the average life expectancy of the pipelines and its components [Myc02, Slo10].

When NG is transported through transmission lines, it is very often that gas is cooled due to many factors, between which the most often is by Joule-Thomson effect during pressure reduction processes. For every 100 psig drop in pressure, there can be 6 or 7 °C drop in temperature [Myc02]. Another reason by which gas cooling can occur is due to interaction between pipeline system and surrounding, which are cooler than the soil temperature [R&Z12], i.e., in a stretch of aerial pipe, or in a section of soil with underground watercourse, whose effect is more remarkable during snowmelt times [P&A86].

Another typical cooling effect happens during the shutdown times, because NG is confined within the inner space of the plant (i.e., tanks, pipes, clarifiers, dehydration towers, etc.), and if industrial facility is placed in cold weather region, NG is cooled too. Initially, pressure increases and the flowline cools at a point that the system may enter to the hydrate formation region. As a consequence, it is important to control the NG thermal condition to avoid the hydrate formation during the shutdown time, to avoid potential problems during the re-start times [Ort08].

Because of all these kinds of cooling effects over gaseous matrix, it might lead to different phase formation as water liquid, condensates and other solid materials, named hydrates. Gas hydrates (GH) are crystalline solids formed when water traps small molecules such as: methane, ethane, propane, carbon dioxide and hydrogen sulfide. Usually, water molecules are linked to each other by hydrogen bonds that in solid state form a regular molecular network with hexagonal shape in which oxygen atoms are located in all vertices. However, presence of these guest molecules makes hydrogen boundary are reoriented surrounding them and forming a cage of water molecules, known as crystal unit. When this crystal unit is repeated one next to the other, shearing water molecules, cages are formed, which in turn are repeated and grouping themselves forming what is called a crystal structure.

In Fig. 1.3.j it can be seen the three types of crystal structures depending on the kind of forming host water cages and their spatial position each other. The kind of structure generated depends on the size of guest molecule, and the pressure and temperature conditions during their formation. In oil and NG, the most often are I and II structure types [Slo10].

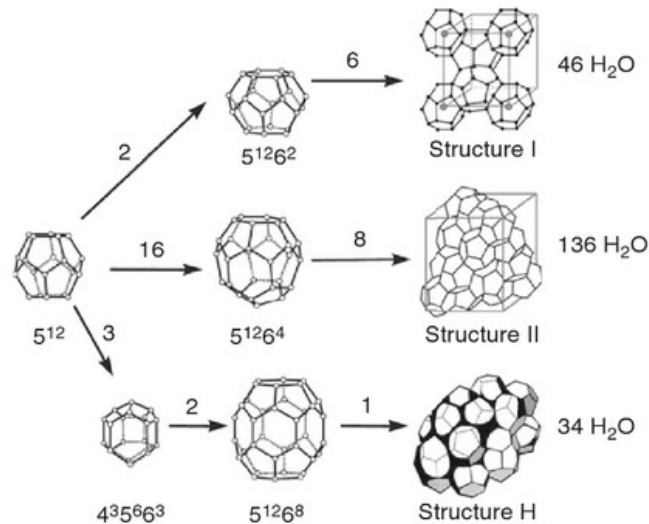


Fig. 1.3.j Three hydrate unit crystal structures which are repeated itself in space [Slo10]. The meaning of $5^{12}6^4$ cage is a 3D configuration composed by 12 pentagonal faces and 4 hexagonal faces. Such that for example, *structure I* is constituted by 6 cages $5^{12}6^4$ [Slo10].

Inner space of *structure I* allows to host methane, ethane and carbon dioxide molecules, *structure II* is enough big to allow larger guest molecules, such as propane and iso- and neo-butane, whilst structure H is able to host iso-pentane and relatively large, branched-chain hydrocarbon [Cha04, Slo10, Ati12, Gam14]. As hydrate crystalline structure is similar to solid water, its macroscopic look is similar to the ice, as can be seen in the below examples.



Fig. 1.3.k Real cases of natural gas pipes blocked by hydrate formation. Left, the similar look between hydrates of NG and ice can be appreciate [Gam14]. Right: A large gas hydrate plug formed in a subsea hydrocarbon pipeline. Source from Petrobras, Brazil [IPE].

NG content per unit volume of hydrates is very high because for each cubic meter of dissociated hydrate at atmospheric conditions are released 164 m³ of gas and 0.8 m³ of liquid water. For that, it is fossil fuel with the highest energy density, $6.2 \cdot 10^6$ KJ·m⁻³. In

addition, the worldwide hydrate reserves are estimated to be $21 \cdot 10^{15} \text{ m}^3$, more than the half of global carbon reserves. Besides, its combustion process has an emission rate very low, 30 times lower than gasoline and 60 times lower than carbon [Delg13]. Because of all of these factors, it is presupposed that gas hydrates will become one of the most important energy sources in the near future.

However, despite of strong energy potential of hydrates, its presence is not desired in the NG industry because it is directly associated with a great amount of problems and hazardous situations. Below are cited the most important drawbacks:

- Their presence is especially critical to instruments equipped with mobile components in contact with NG, such as turbines and compressors whose vanes are seriously damaged by small droplets.

- Water combined with salts or impurities present in NG, namely H_2S and CO_2 , can form potentially corrosive acid chemical substances which stimulate corrosion effects in pipelines and components. This phenomenon can lead to leaks in small cracks [Myc02].

- Corrosion effects are also involved with drastic shortening of life expectancy of pipelines, measurement sensors and any instrument directly in contact with NG. Long term costs and maintenance tasks will rise notably if hydrate condensation is not taken into account. Therefore, number and time spent for the shutdowns by maintenance will be higher, so efficiency of production processes will fall down unavoidably.

- Hydrate formation and deposition leads to a reduction of the inner diameter of pipelines. Looking at any calculation model, such as Darcy and Weisbach equation [Sot99], the inner diameter of the pipe is in the denominator so, the smaller is, due to the depositions, the higher is the drop pressure because of friction effects. Thus, hydrate accumulation will rise pumping costs to counteract the increasing pressure drop.

- When hydrate formation is critical may even block up pipe sections, resulting in severe safety problems, such as blowouts in NG pipelines at high pressure, and which in turn may lead to more dangerous situations like fires or explosions. This problem is especially critical during the extraction step, because the saturated NG stored in the wells at very high pressures, suffer a heavy depressurization that could lead to hydrate formation.

- As is has been explained in Section 1.3.1.2, calorific or heating value is a parameter used to measure the potential of an energy source, directly depend on NG composition. That also involves the WC because the higher is, the lower is the energy released by combustion, reducing the real efficiency of NG, and therefore its quality.

Some estimations about the prevention of hydrates indicates that requires substantial investments up to 10 % to 15 % of the production cost [Ati12]. However, despite of all problems consequence of condensed in NG and forming hydrates, a number of requirements must be met for forming hydrates are necessary as: high pressures, low temperatures, presence of hydrocarbons or another non-polar compounds, and water. If any of these conditions are not met, hydrates formation will not stable and will not take place. Other factors that favor hydrates formation can be listed as high fluid velocities, agitation, pulsations (or any source of fluid turbulence) [Car03]. All of these main conditions are gathered in seabeds, where sea temperature is around 3 °C condition at which only pressures higher than 0.7 MPa are required to form stable hydrates, which is a value amply reached at depths exceeding 100 m. For that, the most of known reserves of GH are located in seas and it is a great challenge for oil and NG industry, particularly during the extraction step of in offshore wells.

For the case of hydrates formation in NG transmission lines or any other is mandatory the prior condensation of water. When NG molecules cross sections with condensed water, and the properly pressure and temperature conditions are, probably hydrates formation and their subsequent accumulation progressive downstream will happen.

Condensates removing is complicate because maintenance and cleaning tasks cannot be performed only in those points where they were originated, because condensates are dragged at different extent depending on gas velocity. That means, the higher is gas velocity, the higher will be distance traveled by condensates before falling at the bottom of the pipeline. This happens because when the drops are travelling, at the same speed than gas flow, they are growing and clustering each other at the same time until their surface tension equal to their kinetic energy.

Different methods are currently in use for reducing hydrate problems in hydrocarbon transfer lines and NG process facilities. Practical methods can be classified in three main blocs which are:

-
- Removing water content directly, by means of dehydration or drying processes. These methods can be performed by classical chemical engineering processes such as, membrane filters and clarifiers.
 - Avoiding to work in those areas where combination of pressure and temperature conditions may lead to hydrates formation. Watching the phase diagram in p-T plans, there are two ways to work:
 - At fixed pressure, operating at temperatures above the hydrates formation temperature, by means of insulation or heating equipment. However, it is completely unworkable isolating or heating completely the entire national transmission networks.
 - At fixed temperature, operating at low pressures, however the most part of the time during NG life cycle, the pressures are quite high.
 - Chemical inhibition of hydrates formation conditions using chemicals additives to prevent, reduce or delay their formation. They can be classified as follow [Delg13]:
 - *Thermodynamics*, introduce disorder in the hydrogen bounds located between the water molecules, increasing the entropy of the system. Inhibition capability of these substances is measured as the decreasing of dew point or subcooling capacity.

Polar compounds like alcohols and glycols are used for this purpose because they also form hydrogen bounds with water molecules preventing properly formation of crystal structures (see Fig. 1.3.j). The most typical inhibitors are: methanol, and mono-, di- or triethylene glycol (TEG). This kind of substance usually is recovered by means of separation processes to be able to be used again.

There are also salts which can be used for this purpose, as NaCl, KCl, CaCl₂ [Bapt07] or MgCl₂, but currently they are being retired because their use causes corrosion problems.

- *Low-dosage hydrates inhibitors* (LDHI's), used to reduce cost related to recovery steps of the previously group, because they do not require separation steps. This kind not prevent hydrate formation but avoiding

their association and so, their agglomeration and final plugging of lines. There are two kinds:

- *Kinetic inhibitors (KI)*, which are the most often inhibitors and commonly are polymers with low molecular weight (polyethylene, polyvinyl) which are in charge of surrounding the hydrates reducing, this way, formation and growing rate of crystals.
- *Anti-agglomerants (AA)*, also known as anticoagulant, the most important are the soluble surfactants.

Knowing and controlling HC and WDP parameters accurately and reliably is not only for safety reasons or to have every processing steps well-controlled. In addition, these parameters are key to guarantee the quality requirements which must be met. For example, in the European Union the current contractual NG specifications in international exchange points have been defined by the European Association for the Streamlining of Energy Exchange - gas (EASEE-gas) and they are as follows [EAS05]:

- HCDP has to be lower than $-2\text{ }^{\circ}\text{C}$ at any pressure between 0.1 MPa and 7 MPa (or at the maximum pressure line).
- The maximum WDP for cross border points is $-8\text{ }^{\circ}\text{C}$ at 7 MPa (or at the maximum pressure line)².

These quality criteria have to be strictly met in international connections, because otherwise national NG suppliers run the risk of being shut out of the pipeline transportation and distribution network [Sol09] and the ENTSO-G association too. However it is not mandatory these standards must be achieved within national borders where legislation can be more permissive. For example, internal specification to transport NG within the Spanish national grid is less restrictive as the WDP of the final product developed to dealers and final consumers cannot exceed $+2\text{ }^{\circ}\text{C}$ [PREN15]. Therefore, to prevent condensations and hydrate formation, gas transmission lines must be operated at temperatures above the HCDP.

² In the USA, the standard for the maximum absolute humidity in interstate pipeline NG is $112\text{ mg}\cdot\text{m}^{-3}$ [Sol09].

1.3.3.3 Humidity measurement in natural gas

HC and WDP can be quantified by two ways: empirically using adequate measuring instruments or theoretically applying predicting calculation models. Thus, there are two potential development lines that will have a strong and direct impact in NG industry and on its profits generated: develop thermodynamic models able to describe more accurate the phase behavior of NG, or creating new sensing humidity technologies (or improving those available) useful for complex mixtures with no standard and fix composition.

Regarding to forecast correctly the phase equilibria and thermodynamic properties of fluids by means of calculation methods, there have been a huge historical evolution in order to select the most accurate for each particular case. Different models can be taken into account, but the most of them include activity models and equations of state (EoS), being this latest essentials in modeling of vapour-liquid equilibrium (VLE).

There are mainly two different approaches to model phase equilibrium, but both of them are based on the fact that at thermodynamic equilibrium, fugacity values are equal in both vapour and liquid phases, under the same pressure and temperature conditions, as below equation shows.

$$\hat{f}_i^v(P, T) = \hat{f}_i^l(P, T) \quad \text{Eq. 1.3.a}$$

The first approach, the $\gamma - \phi$ approach, is based on activity model for the liquid phase and one EoS for the vapour phase. The above equilibrium equation can be rewritten as follows:

$$\phi_i^v y_i P = \gamma_i x_i f_i \quad \text{Eq. 1.3.b}$$

where: f_i is the *fugacity* of the pure compound i in the liquid phase.

ϕ_i^v is the *fugacity coefficient* of the pure compound i in the vapour phase.

$$\phi_i = \frac{f_i}{P} \quad \text{Eq. 1.3.c}$$

γ_i is the *activity coefficient*, which measures degree of divergence of the substance i with respect to the ideal behavior.

By the other hand, the second approach, the $\Phi - \Phi$, uses one EoS for each phase of the system. Thus the thermodynamic equilibrium can be written:

$$y_i \cdot \hat{\phi}_i^v(T, P, y_i) = x_i \hat{\phi}_i^l(T, P, x_i) \quad \text{Eq. 1.3.d}$$

Therefore, regardless what approach type is chosen, at least one EoS will be absolutely necessary.

Many calculation models and correlations are available to predict the phase equilibria and thermodynamic properties in water and hydrocarbon systems, and they are able to model liquid, ice and gas hydrates phases [M&R08]. Many models and approach have been developed including activity models and equations of state (EoS), being this latest essentials in modeling of vapour - liquid equilibria (*VLE*).

The world of EoS is really vast, and a huge number of models have been developed along the history, with very different pros and cons. However, inside of this diversity of possibilities, there are a group methods, denominated symmetric, which are preferred because allow to describe regions both one and two phases with only one EoS. At the same time, inside of the symmetric methods there are two classifications more: those that apply *mixing rules*, and those that use *excess functions*. These last are used to predict those systems which far away from ideality, but the first kind have been traditionally more used in the study phase equilibriums of complex mixtures such as, the natural gas.

In literature there are a lot of EoS and models to predict the phase equilibria and thermodynamic properties, and many bibliographic review surveys [Avi99, Cha04], but the most known and used among them are: Van der Waals (VdW), Redlich-Kwong and its improvement introduced by Soave (RKS) [Soa72], Peng-Robinson (PR) [P&A86], and Virial.

All these models are based on different parameters which depending on some thermos-physical properties of substances (i.e.: critical pressure and temperature, acentric factor). However, for gaseous mixtures cases, calculation of such parameters must be extended taking into account the influence of each pure compound presents and their interactions between them. By this reason, the *mixing rules* were defined. There are several reports discussing the utility and accuracy of different mixing rules depending on the system applied, some interesting works were performed by Orbey and Sandler [C&L07, O&S98]. All these EoS models and mixing rules had had to be validated by comparing many sets of *VLE*.

HCDP determination and search of theoretical models which describe better this feature from pressure, temperature and NG composition of is one of the actual challenge of NG industry. Hence, a large literature is focused in this researching line [Geo05, Her11 and G&B14].

Once composition is well known by chromatography, the most commonly EoS accepted to calculate the HCDP are PR and RKS EoS [Bull11, Her11 and Hal13] because they have demonstrated to be suitable to predict accurately the condensation properties of NG mixtures [Nasr05]. The RKS-EoS is a modification of VdW-EoS but adding a temperature-dependent attractive term (to enable the accurate calculation of pure component vapor pressures) and binary interaction parameters (to give accurate phase behavior for multicomponent mixtures of nonpolar compounds) [Brow09]. In this sense, Enagás used RKS-EoS to describe the HCDP saturation curve, whilst for the WDP used the PR-EoS.

1.3.4 CORRELATION BETWEEN WC AND WDP: THE GERG MODEL

During all this thesis, two way to express the water concentration in the NG have been used: water content (WC) and water dew point (WDP). Both expressions are widely extended, and conversion between them is very often. In the particular case of this thesis, conversion is essential because some instruments gave WC readings and other WDP, so to carry out the comparative performance of the different technologies was mandatory to be able to convert all results to the same expression.

For this propose was approved the International Standard ISO 18453:2005 [ISO04] that establishes the method to convert humidity units in NG. It was defined by the European Gas Research Group (GERG), which in turn is based on the model developed by Oellrich and Althaus in 2001 [O&A01]. The GERG model was experimentally obtained from water concentration measurements to water and six different natural gases, and for pressures included within the range from 0.5 to 10 MPa, and for a temperature range from 258.15 to 278.15 K. From such experimental values, it was decided to fit them to a model based on Peng Robinson's equation (*PR-EoS*) [P&R76]:

$$P = \frac{RT}{v - b} - \frac{a(T, \omega)}{(v^2 + 2bv - b^2)} \quad \text{Eq. 1.3.e}$$

where: a and b are parameters both depending on critical conditions of p and T .

ω is the Pitzer's acentric factor. This parameter gives an idea about the sphericity of a molecule, being 0 when is perfectly spherical and close to 1 when not. It is defined by next equation [Smi97]:

$$\omega = -\log_{10}(P_r^{sat}) - 1 \text{ at } T_r = 0.7 \quad \text{Eq. 1.3.f}$$

This equation was proposed in 1976 as a new version of Soave-Redlich Kwong's equation (*SRK-EoS*) [SOA72] through a modification of the attractive parameter (the second term) and a new dependence of the parameter a regarding to the acentric parameter. This equation gives better estimations than the *SRK-EoS* for polar compounds and light hydrocarbons, even for heavy hydrocarbons through a modification of the α -function. Nevertheless, as happened with *SRK-EoS*, it must not be used below atmospheric pressures and substances with more than ten carbon atoms, and near to the critical point because commits important errors.

GERG model is the most amply used inside of the NG field, mainly because of its great ratio between simplicity and accuracy and gives good results for extended ranges for pressure and temperature: from 0.5 to 30 MPa, and from 223.15 to 313.15 K [Avi99].

The parameters a and b are defined in the critical point of every substance and their expressions are the followings:

$$a(T_c) = 0.45724 \frac{(RT_c)^2}{p_c} \quad \text{Eq. 1.3.g}$$

$$b(T_c) = 0.07780 \frac{RT_c}{p_c} \quad \text{Eq. 1.3.h}$$

For different temperatures that the critical, b parameter is the same, but a is recalculated as follows:

$$a(T) = a(T_c) \cdot \alpha(T_r, \omega) \quad \text{Eq. 1.3.i}$$

The α -function is dependent to the *reduced temperature*, T_r , and the *acentric factor*, ω . From experimental vapour pressure values available in literature, Peng and Robinson found an expression to α function, which is dimensionless and valid for hydrocarbons and other nonpolar compounds, but is not sufficiently accurate for polar substance, as the water. The general α -function is:

$$\alpha^{1/2} = 1 + \kappa(1 - T_r^{1/2}) \quad \text{Eq. 1.3.j}$$

κ is a constant characteristic of every substance and is function of ω as shown the below equation. Thus, α function is lineal regarding the temperature.

$$\kappa = 0.374640 + 1.54226\omega - 0.26992\omega^2 \quad \text{Eq. 1.3.k}$$

All previously equations are valid for all compounds present in the NG except to water, for which an own equation of the α -function was defined by Mathias-Copeman and depicted below [M&C83]:

$$\alpha^{1/2} = A_0 + A_1(1 - T_r^{1/2}) + A_2(1 - T_r^{1/2})^2 + A_3(1 - T_r^{1/2})^3 \quad \text{Eq. 1.3.l}$$

The coefficients of the α -function for water are different when it is wanted to calculate the vapour pressure over water or ice. In below table are shown the values of each coefficient calculated both water and ice.

Table 1.3.d Coefficients of α function for water depending on the temperature range [Avi99].

Coefficients	223.15 K < T < 273.15 K	273.15 K < T < 313.15 K
A_0	0.77404	1
A_1	1.58484	0.90544
A_2	0	-0.21378
A_3	-2.28241	0.26

When it is worked with mixtures, the parameter a and b of each pure substance which compound it are related by means of the mixing rules.

$$a = \sum_i^n \sum_j^n x_i x_j a_{ij} \quad \text{Eq. 1.3.m}$$

$$b = \sum_i^n x_i b_i \quad \text{Eq. 1.3.n}$$

$$a_{ij} = \sqrt{a_i a_j} (1 - k_{ij}) \quad \text{Eq. 1.3.o}$$

1. INTRODUCTION

where k_{ij} is the binary interaction parameter, frequently obtained from experimental data of vapor-liquid equilibria of binary mixtures. These parameters have the following peculiarities: $k_{ij} = k_{ji}$, and $k_{ii} = k_{jj} = 0$.

Below table shows the binary interaction parameters for all species present in the NG below to the C_{6+} hydrocarbons fraction, because the GERG model has not taken in count hydrocarbons formed with more than six carbon atoms. This table was taken from Avila's doctoral thesis [Avi99], in which is specified the bibliography source of all data.

Table 1.3.e Binary interaction parameters for all species present in the NG below to the C_{6+} hydrocarbons fraction [Avi99].

	N ₂	H ₂ O	CO ₂	CH ₄	C ₂ H ₆	C ₃ H ₈	C ₄ H ₁₀		C ₅ H ₁₂		C ₆ H ₁₄
							iso	neo	iso	neo	neo
N ₂	0										
H ₂ O	0.4800	0									
CO ₂	-0.0170	0.1840	0								
CH ₄	0.0311	0.6510	0.0919	0							
C ₂ H ₆	0.0515	0.6350	0.1322	-0.0026	0						
C ₃ H ₈	0.0852	0.5300	0.1241	0.0140	0.0011	0					
i-C ₄ H ₁₀	0.1033	0.6900	0.1200	0.0256	-0.0067	-0.0078	0				
n-C ₄ H ₁₀	0.0800	0.6900	0.1333	0.0133	0.0096	0.0033	-0.0004	0			
i-C ₅ H ₁₂	0.0922	0.5000	0.1219	-0.0056	0.0160	0.0111	-	-	0		
n-C ₅ H ₁₂	0.1000	0.5000	0.1222	0.0230	0.0078	0.0267	-	0.0174	0.06	0	
n-C ₆ H ₁₄	0.1496	0.5000	0.1100	0.0422	-0.0100	0.0007	-	-0.0056	-	-	0

Because of the α -function of water was defined by means of a different equation (Eq. 5.1.a), its interaction binary parameter must be adapted by using next equation:

$$k_{ij}(T) = k_{ij,0} + k_{ij,1} \left(\frac{T}{273.15} - 1 \right) \quad \text{Eq. 1.3.p}$$

where: $k_{ij,0}$ is the binary interaction parameter previously described and which is not temperature dependent.

$k_{ij,1}$ is a new binary interaction parameter which introduces the water temperature dependence.

Among all substance present in the NG only water interactions with carbon dioxide, methane and ethane, require to use this new parameter, $k_{ij,1}$, to adjust correctly with the experimental values. Table 1.3.f summarizes such parameters for the three substances when interact with water.

Table 1.3.f Temperature dependent binary interaction parameters for water with carbon dioxide, methane and ethane [O&A01].

$k_{ij,1}$	CO ₂	CH ₄	C ₂ H ₆
H ₂ O	0.2360	-1.3850	-0.9300

1.3.5 CHALLENGES OF HUMIDITY MEASURING IN NG INDUSTRY

The main problem of thermodynamic models is their dependent on gas composition, temperature and pressure, so substantial extrapolations need to be done when they are being used out of working conditions range by which they were previously proven. In addition, because there are not a standard NG composition, which is constantly changing in real industrial processes, these extrapolations may well lead to deviations in WDP obtained of up to 10 °C [Pan09], when an accuracy of 1 °C to 3 °C is actually required in industrial applications.

For that, predictive calculation methods have suffered a continuous historical evolution to our days, in order to select the most accurate tool to estimate such properties for each particular case. Currently, there are large list of reports and publications in literature that try to find the best thermodynamic models which is able to describe more accurately thermo-physical properties, including the phase behavior for hydrocarbon mixtures, water and even the typical additives added to NG such as: methanol, glycols, odorants, etc. These researches are focused to enlarge application ranges for operation conditions, improving at the same time the accuracy in the broader range, and/or simplifying their complexity by reducing the number of parameters required.

Consequently with all explained before, extremely accurate and reliable methods of measuring WDP and HCDP are of vital importance for the global NG industry. Not only from the point of view of safety, avoiding condensations and hydrate formation or to ensuring the final quality of NG which is supplied to final consumer or exchanged in international points, but also to design and control all engineering processes during NG handling, improving this way the economic viability of each production step.

By the other hand, the other way to know the WC of a NG is directly using humidity measuring instruments. However, alternatively pressure-reducing sampling lines are applied when using humidity analyzers based on detecting water vapour condensation because they can only operate at low pressure. As a result of the effects of heat transfer, condensation and the optical properties of gases, on-site conditions may significantly affect the measurement results obtained with this kind of instruments. This phenomena is very important because some humidity measuring technologies are based in condensation methods, such as *chilled mirror hygrometers* (see Section 3.1.1.3), and depending on relative position between both curves, they could give wrong humidity measurements which in turn may lead to severe problems in humidity control of drying plants or even forming hydrates in different NG processing steps.

By the other hand, the kind of probe traditionally used as a hygrometer in the worldwide NG industry, is the capacitive sensors based on metallic oxides. However, this kind of probes suffers strong downward drift effects, which are well known to the users and metrology laboratories from measurements performed in nitrogen and other gases [Bel04], and also confirmed over NG by means of another research performed by Løkken, which was simultaneously developed during the experimental part of this thesis [Løk12]. However, current practice for such moisture measurements is for the devices to be calibrated at atmospheric pressure and in nitrogen or air as the matrix gas, conditions that vary significantly from those present in the actual industrial process.

Lastly, another reason is the need to establish standards accepted by producers, distributors and consumers that allow the easy, accuracy and reliable determination of humidity in NG, and thus really know the quality of the product.

For all of that, metrology can play an important role in providing support in order to overcome some of the current challenges of this energy sector by avoiding inaccurate water vapor monitoring in order to maximize the performance of its processes, and in particular of non-renewable resources. The main targets, a short and medium term, of the European humidity metrology are clearly defined in the EUROMET roadmap for humidity and moisture measurement [Bel08, Fer12].

As can be seen below (Fig. 1.3.1), among many other goals marked on one of the last roadmaps, the following action lines should be highlighted : to evolve new humidity instruments, such as spectroscopic and condensation, and develop emerging new

laboratory techniques (resonators); to develop new and improved transfer standard and methods, especially at trace level; to enlarge range of national standards to give traceability to instruments which work at high pressures and/or temperatures and even in non-conventional gases; and finally, to improve the precision and humidity control in industrial processes.

All these targets will contribute to fight against worldwide goals such as the global warming and reduction of contaminant emitted. Thus, in this sense there is an especial interest to maximize the efficiency in all industrial process step, especially fossil fuels combustions, which are going to be substitute for more clean and environmental friendly, such as the NG or even for other non-conventional and renewable gaseous fuels (e.g. biogas, coal bed methane, coal mine methane and hydrogen enriched with NG) [ENG01].

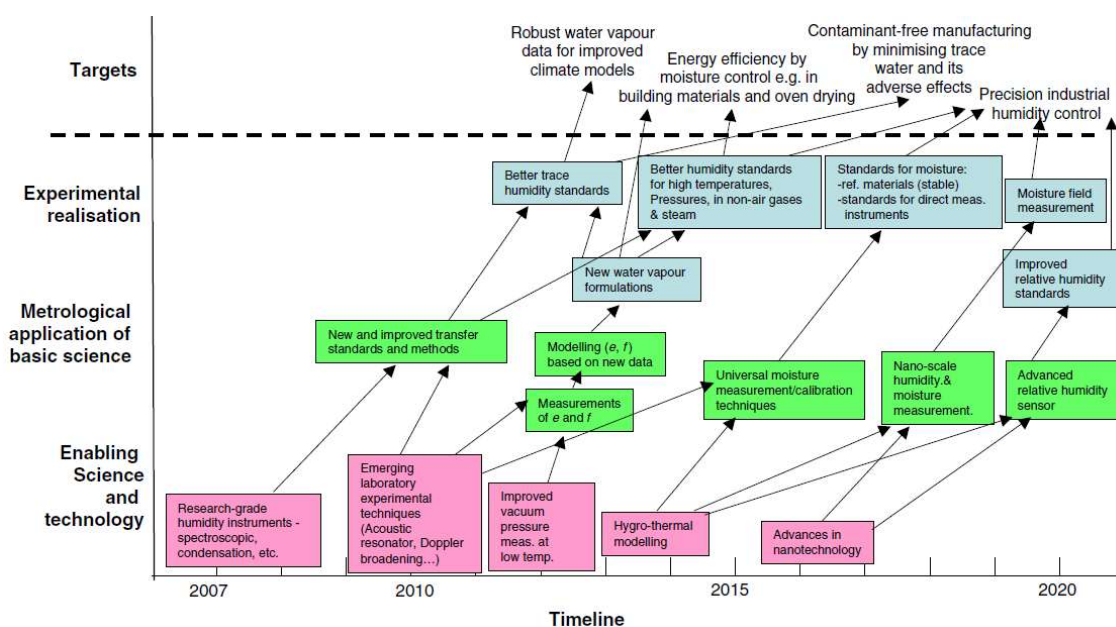


Fig. 1.3.1 Roadmap for Humidity and Moisture Measurement, vertical axis shows increasing specialization of technology towards the final targets, whilst horizontal axis shows approximate timescale [Bel08].

For all of that, this thesis was focused on this second way to measure the humidity in the NG, that is to say: the experimental measurement. That implies, providing the necessary metrological support, by means of development and validation highly accurate measuring methods to achieve the uncertainty required for overcoming the current challenges of NG industry as well as the contractual requirements established by EASEE-gas for the physical properties of gases injected into the European national networks,

according to the metrological strategic lines established in the two last European humidity roadmaps [Bel08, Fer12].

2 **OBJETIVES**

Before anything else, it is important to explain some issues to fully understand what the objectives of this thesis were. This thesis was performed within the LabTH of INTA, the Spanish DI in the field of humidity [BOE01]. Among many other duties of DIs is to take part in national and international research projects [CLA09].

As a part of such participation in research projects, it is essential to emphasize that the first part of this thesis was completely developed inside of the framework of the joint research project “ENG01-Gas. Characterization of Energy Gases” which running under the European Metrology Research Program (EMRP) ENG01-Gas [ENG01]. Thus, this thesis shares the majority of those goals fixed in the workpackages in which LabTH had tasks assigned.

In addition, according with the last European roadmaps for humidity measurements [Bel08, Fer12]. One of the main targets for the last fifteen years (until 2020) was to constitute the European metrology infrastructure necessary to support those industrial processes that do not work with conventional gases. In this sense, this also was one of the main objectives of the EMRP "ENG01-Gas", but in this particular case directly focused on energy gases, and in this thesis more concretely on the natural gas.

Thus, taking into account all the above and as a result of all surrounding conditions, the inherent objective of this thesis was also to provide the metrological support required by the natural gas industry in the hygrometry field, in order to overcome current real challenges. For that and in this line, the specific objectives of this thesis are enumerated as follows:

- To develop and validate new highly accurate measurement methods to achieve the uncertainty required by the European Association for the Streamlining of Energy Exchange – Gas (EASEE-gas) [EAS05] for the humidity measurements of natural gas injected into the European supply network. That includes, to participate in the development of humidity measuring prototypes based on new and promising sensing technologies such as, the microwave resonance and the absorption spectroscopy.

- Draw up new measuring methods and protocols for comparing the most humidity sensors commonly used in industrial natural gas monitoring conditions, against these novel sensing technologies previously developed here.

- To design and assemble the required facilities to obtain new empirical data that allow compare the behaviour of different sensing humidity techniques in natural gas and under real industrial conditions.

- To assess the dynamic behaviour of sensing humidity technologies studied here, characterizing their response against to variations of some process variables, as for example: line pressure, water content and natural gas composition, because of interactions between water and other gas molecules.

- To give technical support to improve the validity and reliability of humidity measurement during sampling, and to develop methods to harmonize the industrial calibration processes. Increasing in this way, accurate humidity control in the natural gas industry.

- To validate the performance of all available humidity sensing techniques for their use in diverse natural gas process stages, by means of the validation of hygrometers representative of these.

- Lastly and as a part of development of the European metrology infrastructure, it should be given traceability to humidity sensors studied, through the new humidity standards for high temperatures and pressures in non-air gases and steam, whose development was carried out by other NMIs inside of EMRP "ENG01-Gas" project, during the course of this thesis.

3 HUMIDITY SENSING TECHNIQUES

Along the history many techniques have been developed to measure the humidity in gases. These techniques are based on different measurement principles and because of that, the humidity can be expressed in absolute quantities such as: water content in mass or volume (ppm_w and ppm_v , respectively) and water dew/frost point; or relative quantity as percentage of relative humidity, % rh.

In this research only those humidity sensing methods that really were evaluated over NG have been really describes in depth. By the other hand, it was considered important to give an overall vision about all humidity sensing techniques exist nowadays, so those techniques that were not compared here were briefly cited and explained. Reason by which there is a chapter titled "other humidity sensing techniques used in gases" (Section 3.1.3).

For each sort of technology the most important techniques were described taking into account issues such as: measuring principles, physical description, types, characteristics and properties, and the most important advantages and drawbacks prior founded in literature.

3.1 HUMIDITY SENSING TECHNIQUES STUDIED

In this section were described all those technologies which were evaluated in this thesis through the all humidity instruments available along this thesis.

3.1.1 TRADITIONAL TECNQUES

In this first group were included those humidity techniques which have been commonly applied in the natural gas industry. Their use is more or less spread in such industrial activity and in some cases, primary techniques have been evolved towards more complex and accuracy methods, but always based in the same measuring principle.

3.1.1.1 Electrical impedance

Measuring principle

This kind of sensors is fabricated from a hygroscopic material that will absorb or desorb water depending on the water vapor partial pressure in the atmosphere around it. Humidity variations lead to hygroscopic materials change their electrical properties,

specifically the impedance, which is translated to variations in the capacitance, the resistance or a combination of both. The relationship between the water vapor partial pressure and the electrical properties of sensor is given by the following equation [K&S11]:

$$Z^{-1} = Ae^{BP_w} + C \quad \text{Eq. 3.1.a}$$

where: Z is the impedance of the sensor.

P_w is the partial pressure of water vapor.

A, B, C are constants characteristic of the each sensor.

The conductivity of the hygroscopic material changes with the amount of water absorbed, creating fluctuations in the impedance of sensors. A zero-centered AC voltage is used to measure the conductivity to prevent polarization of the sensor. The resulting current flow is then converted to a DC value by the signal-conditioning circuits of the sensor.

This kind of moisture sensing technique is the most widely used in the NG industry. The active part of these sensors is often made of metallic oxides (e.g.: Titanium [He10], Zinc [WAN09], Vanadium [ANB12]) but very especially of aluminum oxide (Al_2O_3) and silica-base material, being the first of them the most used in the vast majority of NG facilities. Nowadays, new sensors built on polymeric materials are also being developed for this application [Son02, Li12].

Physical description

The common look of this instrument is a small wand-shaped probe connected by a cable (or directly attached) to the main body of instrument. Electrical impedance hygrometers usually are compact and small, so they usually are useful to portable applications, as checking on site. These probes are often equipped with a temperature sensor and a filter to protect it against pollutants, which by contrast usually increases the response time.

The majority of modern impedance sensors use *thin-film* technology, where two thin layers of noble metal (gold, platinum, etc.) work like electrodes (see Fig. 3.1.a). One of them is located on a ceramic substrate and over such electrode is positioned the

3. HUMIDITY SENSING TECHNIQUES

hygroscopic material layer. And the other, it will be the external porous layer which is positioned over the hygroscopic material.

The hygroscopic mean also appears as a porous matrix forming a configuration of many parallel pores connected between both layers, which is visible at microscopic level. This distribution of porous layers allows that water molecules to be able to cross the first metallic layer and be absorbed or released inside of hygroscopic material (see Fig. 3.1.a). Each pore works as a micro-capacitor and like they are in a parallel arrangement, the total capacitance will be total the addition of all pores.

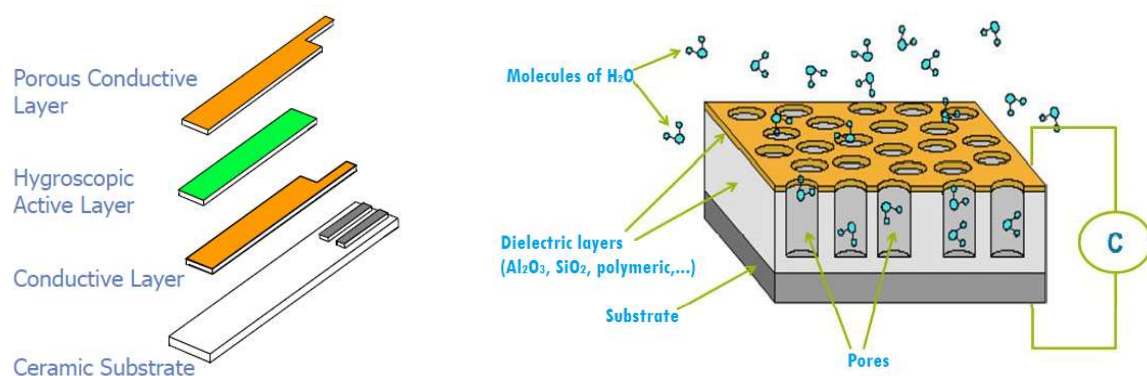


Fig. 3.1.a Application of the thin-film technology for the impedance sensors. Left: Position of each layer which conform the usual impedance sensor [Ben10]. Right: Microporous structure of external electrode and hygroscopic means.

Types

The electrical impedance sensor can be divided in three types:

- *Capacitive sensors* respond most closely to relative humidity, rather than dew point, with a best linearity at low relative humidities. In general capacitive sensors are not damaged by condensation, however potential drift effect could happened, so the consequent calibration should have be performed.
- *Resistive sensors* also respond most closely to relative humidity, rather than to the dew point. Linearity of resistive sensors is best at high humidities. Most resistive sensors cannot tolerate condensation. However, some are "saturation guarded" with automatic heating to prevent these situations that would damage the instrument. In the Fig. 3.1.b, it can be seen the usual spatial layers distribution for these first shorts of sensors.

- *Dew-point sensors* are a special case of impedance hygrometer that are used to measure in absolute units rather than relative humidity. Commonly the signal is converted to other absolute units, as dew point or parts per million by volume. These sensors can have wide measurement range, including very dry gases even below than $-85\text{ }^{\circ}\text{C}$ of WDP, so they are used in applications in which humidity must be controlled at trace levels.

A very good comprehensive review about all these kinds of sensors was performed by Farahani *et al.* [Far14], in which they can be seen many examples all these groups of sensors and the *thin-film* technology applied.

Sometime these sensors are referred as *electrolytic* because they have a polyelectrolyte material as hygroscopic element of the sensors. They must not confuse with *electrolytic sensors*, which use electrolysis as the sensing mechanism and they were also described later in this chapter.

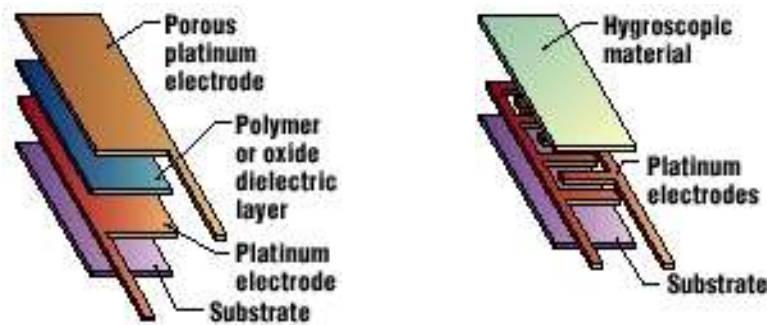


Fig. 3.1.b Comparison of the usual layer spatial configuration between the capacitive (Left) and resistive (Right) impedance sensors [Coc].

Characteristics and Properties

By general, the impedance sensors provide excellent response against to moisture changes in the dry to wet direction. However, they require significant response times in the wet to dry direction. They usually are affected by drift and hysteresis over time, but this kind of problem can be managed by applying the properly recalibration schedule.

These sensors are economical and frequently used during maintain tasks, as a spare probe, maintaining always in-service at least one sensor within its recommended recalibration interval, which is typically a year.

In addition, they can endure high pressures of up to 45 MPa, but these sensors are seldom installed directly in the pipeline process located in field, but they need a sampling

3. HUMIDITY SENSING TECHNIQUES

system associated with them to regulate the pressure, flow rate and erase any water drop or solid particles dragged by the gas stream.

The measurement range of the electrical capacitive hygrometer is from 0 to 100 % rh, and in the dew/frost scale a common working range would be from -85 °C to 110 °C.

Its accuracy is around 2 % rh, but it can be improved by calibration with standard hygrometers, reaching typical error of 1 % rh or less in the range from 0 to 90 % rh and error of 2 % rh or less in the range from 90 to 100 % rh [JMA].

This kind of sensors has temperature dependence of about 0.1 % rh·°C⁻¹ for the temperature range from 5 to 30 °C; and 0.2 % rh·°C⁻¹ for the temperature range from -30 to 0 °C. For that, it is very often a temperature sensor is installed together with the humidity sensor to compensate this dependency, which should be properly calibrated too [JMA].

The sensor of the electrical hygrometer can be separated from display and/or recording units. Besides, new communication technologies allow download data recorded without a physical connection with a PC, both Bluetooth and Wi-Fi via.

3.1.1.2 Electrolytic

Measuring principle

This humidity sensing technique consists on a film of powerful desiccant such as, the phosphorous pentoxide (P₂O₅), which strongly absorb the water vapor from the surrounding gas. Such hygroscopic material cover two closely spaced electrodes and when an electrical potential (voltage) is applied on them, the water molecules previously absorbed are dissociated in its constituents, hydrogen and oxide, hence the electrolysis is taking place and a finite current is being generated, which is precise and linear function to the amount of water absorbed, according to Faraday's law:

$$m = \frac{Q}{F} \cdot \frac{M}{z} \quad \text{Eq. 3.1.b}$$

where: m is the mass of the substance generated in an electrode, in g.

Q is the total electric charge passed through the substance, which is equal to the product of the current, I , by the time, t .

F is the Faraday constant and is equal to 96.485 C/mol.

M is the molar mass of the substance, g/mol.

z is the valence number of ions of the substance (electrons transferred per ion).

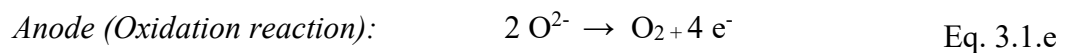
Hence, using an amperemeter to measure the current generated and through above equation, it can be known the water content of the stream which crosses the cell. For convenience, a flow of 100 mL/min (measured at 25 °C and 1 atm) is generally used for ideal gaseous samples. At these conditions, the electrolysis current is 13.2 μ A per 1 ppmv. In accordance with Faraday's law electrolysis of 0.5 mol of water requires 96.485 coulombs [Kei95].

The global process consist on one molecule of water is absorbed by one molecule of phosphorus pentoxide, generating as by-product two molecules of phosphoric acid ionic in the matrix placed between electrodes. When the electrolytic process occurs, this sub-product is divided in its basic components of water and phosphorus pentoxide molecule is regenerated:



As it can see in Eq. 3.1.c and Eq. 3.1.d, this process has a net consumption of phosphorus pentoxide null, because each molecules used to absorb one of water it is subsequently regenerated when is electrolyzed. Therefore, the P_2O_5 is always present in the cell, ensuring a complete removal of the water in the sample gas.

Because of the high resistivity of anhydrous phosphorus pentoxide, a potential between the two electrodes must be applied to accelerate ionic diffusion and subsequent electrolysis of the absorbed water [Col59], converting it to oxygen and hydrogen at the anode and cathode, Eq. 3.1.e and Eq. 3.1.f, respectively. Below are described the main reaction and those semi-reactions which take place in both electrodes:



These sensors are able to measure very low humidity levels, even lower than 1 ppm_v, but they require a steady (and very well known) flow rate of gas. These instruments

measure the water concentration by unit of volume, thus humidity is measured directly in an absolute quantity.

Physical description

The first electrolytic hygrometer was described by Taylor in 1956 [C&D59]. An electrolytic hygrometer consists on a tube inside which there are two interlaced but separate spiral electrodes of fine wire. These electrodes are covered with a thin layer of phosphorus pentoxide (P_2O_5).

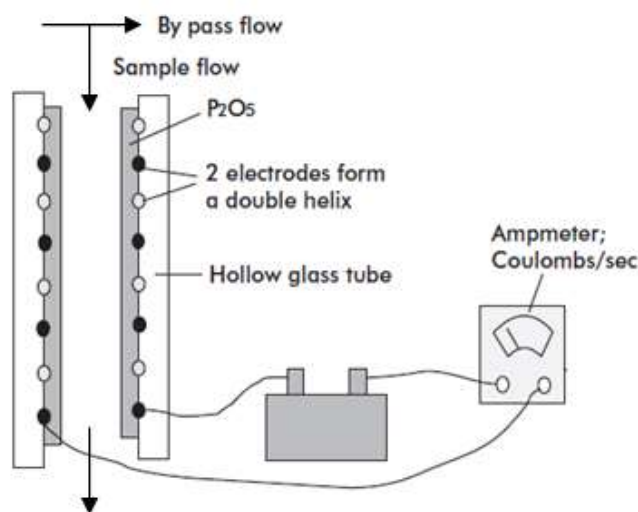


Fig. 3.1.c Basic scheme of an electrolytic cell where it can be seen the spiral form of both electrodes and how they are covered by the thin film of phosphorous pentoxide [MEE05].

Characteristics and Properties

This sensing technique is able to measure the moisture of organic compounds streams even when are in liquid state, as it demonstrated Cole *et al.* in 1959 [Col59]. They used a stripping tower, located up stream respect to the electrolytic cell, to evaporate the inlet stream by means of an inert and dry gas stream, e.g. liquid nitrogen. They obtained accurate analyses at moisture levels down to 1 ppm_v. However, this technique is not adequate to measure the humidity in hydrogen or oxygen.

One of the most important feature of this technique is its high sensitivity, which can be even lower than 1 ppm_v for a wide measuring range, between 1 and 5000 ppm_v [MEE05]. This low detection limit defined as absolute quantity, it would be equivalent to -80 °C of WDP, approximately. Besides, this technique does not require to be calibrated for each new gas, just the flow must be checked periodically, especially in applications where composition is not steady.

By contrast, the main disadvantage is that this technique is very sensitive to pressure and flow changes, so both quantities must be very well controlled and steady. Besides, this kind of technology do not endure pressures higher than 0.7 MPa. For that, in applications with pressure values higher than such limit, a pressure regulator system must be mounted upstream of the hygrometer.

By other hand, it must be taken into account some maintenance criteria to extend the lifetime of the P_2O_5 , such as: avoid certain acids, amines and ammonia, because they could react with it; it is suitable periodic challenges with high moisture content gas to avoid that outer layer of P_2O_5 becomes “hardened” and sensor loses sensitivity.

3.1.1.3 Condensation Hygrometers

Measuring principle

Measuring principle of these instruments is quite simple: to measure the humidity of gas by cooling until condensation starts to appear in a surface. The stable temperature at which this phenomenon occurs is measured and reported as dew or frost point. Hence they humidity measure is reported in absolute units directly. Although, knowing the temperature of the gas stream, it is possible calculate its relative humidity too.

Physical description

Conventional condensation hygrometers are the well-known *optical chilled-mirror hygrometers*. Their usual format consist on a surface on which condensation appears, coupled to an optical detection system used as feedback to control the mirror temperature. In an optical hygrometer, the condensation is sensed by detecting changes in how the mirror reflects or scatters light. When the mass of condensate on the mirror is in equilibrium with the surrounding gas sample, the mirror temperature is by definition equal to dew/frost point temperature.

Chilled mirror technology can also be used to determine the HCDP. In those mixtures that contain heavy hydrocarbons and because of the partial pressure of hydrocarbons is enough high, the first drops which appears on the mirror are constituted for the heaviest components present in the hydrocarbon mixture.

Types

The chilled mirror hygrometers or condensation hygrometers, which will be called of both ways and without distinction through this thesis, can be classified into two basic categories, manually or automatically operated:

- *Manual chilled mirror*: typically use the expansion high-pressure gas as the coolant. When high-pressure gases, such as methane, natural gas or CO₂, are decompressed at the same time they are cooled due to the Joule-Thomson effect. The user observes the onset of condensation via a view port while the mirror surface is cooling. One of the most important aspect of these instruments is the rate of cooling, because it must not be too fast because condensation will happen prior to get thermal stability [K&S11].

The manual chilled mirror apparatus is described in ASTM-1142, where a working procedure is recommended [AST95]. In the Fig. 3.1.d, it can be seen the different parts of a typical manual chilled-mirror. They are traditionally used for spot-checks but not in key points of the process where humidity readings must be taken continuously and online.

The dew/frost reading using these instruments are subjective because depend on of each operator and its ability to recognize the nature of the condensate: dew, frost or hydrocarbon dew points.

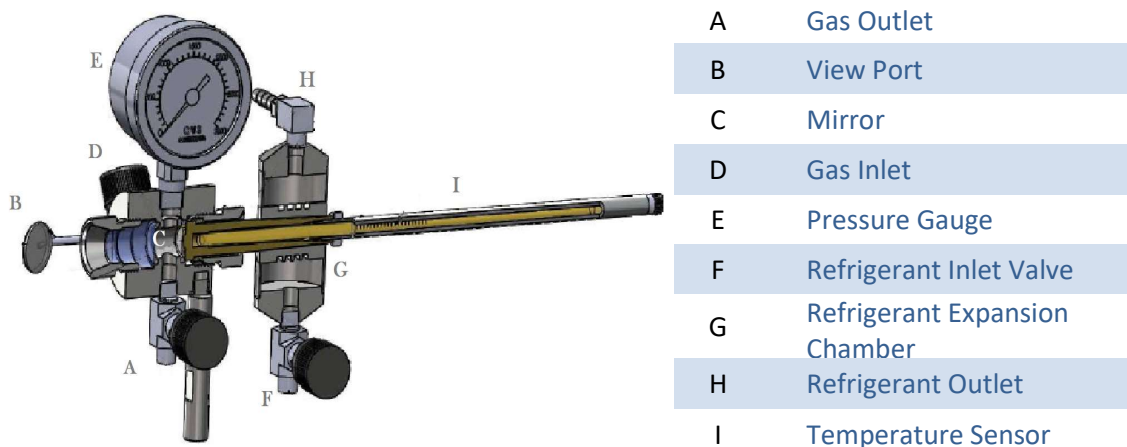


Fig. 3.1.d Appearance of a traditional manual chilled mirror and brief description of the most important parts in which it is composed [CVS10].

– *Automated chilled mirrors*: utilize a thermoelectric module, denominated peltier, coupled to the mirror and used to control its temperature. Condensation conditions are monitored using a photo-detector with the reflection of a light-emitting diode (LED) on the mirror. Light received by the photodetector decreases due to both absorption and scattering effects of the incident light when condensation is present. When that occurs, the signal from the photodetector is utilized in a feedback control loop to maintain a constant mass. If the polarity of the current which crosses the peltier is reversed, the mirror will be heated and the condensate layer will disappear, which is used to clean the mirrors and generate a new condensate layer.

The measurement range of this apparatus go from $-95\text{ }^{\circ}\text{C}$ to $+95\text{ }^{\circ}\text{C}$, achieving high precisions thanks to a PRT (Platinum Resistance Temperature) that measures the mirror temperature. This sort of hygrometers offer an excellent precision, close to $\pm 0.035\text{ }^{\circ}\text{C}$ (as can be demonstrated by the CMCs of many NIs: NPL, PTB, INTA, etc.) [KCDB] and minimal long-term drift, thus they are widely used as laboratory reference standards for calibration and metrology applications. For keeping a high precision using these instruments the mirror surface must be kept clean, because any different substance to water, even inert contaminants, will change the reflective properties of the light and will increase the dew/frost point temperature.

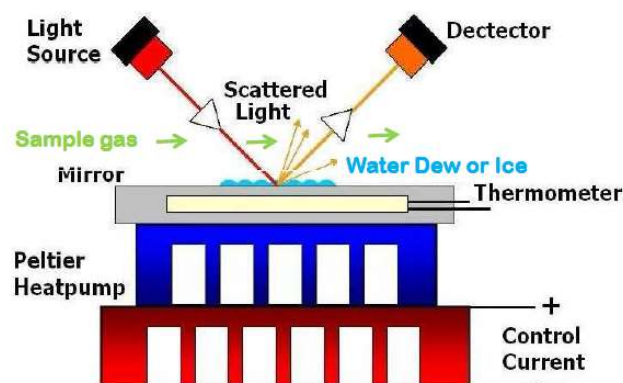


Fig. 3.1.e Basic scheme of cooling/ heating system of mirror and the optical signal detection system [Ben10].

An important variant which includes these instruments is a cyclical operation mode, that consists on the condensed is not maintained constant, if not that they have a system of regeneration of a new condensate layer by means of programmable thermal cycles which increase and decrease the mirror temperature depending on if it is going to create

3. HUMIDITY SENSING TECHNIQUES

or delete the layer. The cooling ramp is sufficiently slowed. Cycling chilled mirrors are generally not as precise as constant mass units [K&S11].

Some of the main problems of this technology are: the presence of contaminants previously explained and the uncertainty produced at dew point lower than 0 °C, because it must be sure if condensate is dew or frost to apply the correct formula in relative humidity calculation.

3.1.2 NOVEL TECHNIQUES

3.1.2.1 Absorption spectroscopy

Measuring principles

The absorption spectroscopy is based on the Beer–Lambert Law which says when a radiation source impacts on a molecule, a fraction is absorbed by such substance, and the rest is emitted. For a gaseous medium, this law is described by the following equation:

$$A = \ln\left(\frac{I_0}{I}\right) = \alpha \cdot l = \varepsilon \cdot c \cdot l \quad \text{Eq. 3.1.g}$$

where A is the *absorbance*, which is dimensionless and is equal to $-\log T$, being T the transmittance, which is another way to express this law.

I is the *light intensity transmitted* through the measuring cell which is collected by the detector.

I_0 is the *light intensity incident* on the gas cell, emitted by the source.

α is the *absorption coefficient* of the sample (typically with units of cm^{-1}).

It is the product of the gas concentration, c , and the *specific absorptivity* of the gas, ε .

l is the cell's *optical path length*.

According with the above equation, the ratio between the light intensity emitted and transmitted on a gaseous medium depends on to the concentration of such gas, and in the case of a mixture, the partial pressure of the target molecule. Therefore, this technology detects selective and quantitative way the presence of the target molecule. However, concentration in gaseous phase is usually given in pressure units and to convert to more typical units such as ppm_v , temperatures and pressure measurements must be made and used in the ideal gas equation (or any other more accurate EoS) $PV = Nk_B T$, where V is

the volume of a closed cell, k_B is the *Boltzmann constant* and N is the number of molecules in the cell. The Beer–Lambert Law can also be extrapolated to liquid phase samples, modifying slightly Eq. XX using base 1, so α values will be 2.3 times smaller.

An absorption spectrum is a plot of α or ε as a function of wavelength (e.g. in μm) or its reciprocal, wavenumber (in cm^{-1}). Gas phase absorption spectra exhibit narrow lines due to electronic transitions and/or vibrations and rotations molecular movements. The absorption lines or bands are specific to each species, for that are commonly also called fingerprint, and this forms the basis for their detection and measurement. Example of absorption spectrums for the methane and water were depicted below (Fig. 3.1.g and Fig. 3.1.h).

Other fundamental of this technique is based on many chemical species exhibit strong absorption in the UV/visible, near and mid infrared (NIR and MIR) regions of the electromagnetic spectrum, so many chemical species can be detected and quantified by means of this technology.

There are several public-domain databases which are a compilation of spectroscopic parameter of many substances, the most known are: the HITRAN, acronym for high-resolution transmission molecular absorption [HITRAN]; and another digital base containing the vapor-phase infrared spectra of pure chemicals, which was created jointly between the National Institute of Standards and Technology (NIST) and the Pacific Northwest National Laboratory (PNNL).

The width and shape of each absorption line depend on temperature and pressure because of different broadening mechanisms [Ert04]. This dependence is usually classified into three pressure ranges [Sch93]:

- At pressures below 10 Torr, *Doppler broadening*, caused by the random thermal motion of the molecules. The spectral lines have Gaussian shape and their width is proportional to the square root of the absolute temperature.
- For pressures above 100 Torr, the line shape is determined by *collision or pressure broadening*, produced when a molecule undergoes a collision during the radiation process, perturbing the phase of the emitted wave train. The resulting shape is defined by a Lorentzian function.

3. HUMIDITY SENSING TECHNIQUES

- Intermediate region is known as Voigt regimen where the absorption line profile can be described as a convolution between Doppler and Lorentzian broadening. This fitting is being very used in atmospheric applications, even for NG [Nwa14].

Below an example of the characterization of the absorption lines is shown, being dominant in this case the pressure broadening effect and therefore, matching to a Lorentzian profile [H&T13]:

$$\alpha = C_{mol} \cdot S \cdot \frac{\gamma}{\pi(\gamma^2 + (\nu - \nu_0)^2)} \quad \text{Eq. 3.1.h}$$

where: C_{mol} is the gas concentration in units of molecules·cm⁻³.

S is the *line intensity* (cm⁻¹, molecule·cm⁻²).

γ is the line halfwidth at half maximum (HWHM), cm⁻¹.

ν is the *wavenumber*, cm⁻¹.

ν_0 is the position of the line center.

The linewidths vary with the pressure and the temperature, so-called ‘self-broadening’ parameters. Thus, their effect must be quantified, especially for gases that can have strong interactions with their neighbors, for example via H-bonding, as the case of water molecules. In those cases, in which the interaction among difference molecular species is high, the parameter γ must be corrected and for the simplest case, a binary mixture, will have the following expression:

$$\gamma = \gamma_1 \cdot (p - p_1) + \gamma_{self} \cdot p_1 \quad \text{Eq. 3.1.i}$$

where p , is the total pressure, p_1 is partial pressure of substance 1, and γ_{self} , is the self-broadening parameter. All these parameters can be founded in databases mentioned above. By the other hand, to apply this law it must be assumed that there are no chemical reactions in the sample.

Below is shown an example of the three adjustments methods for the same absorption peak.

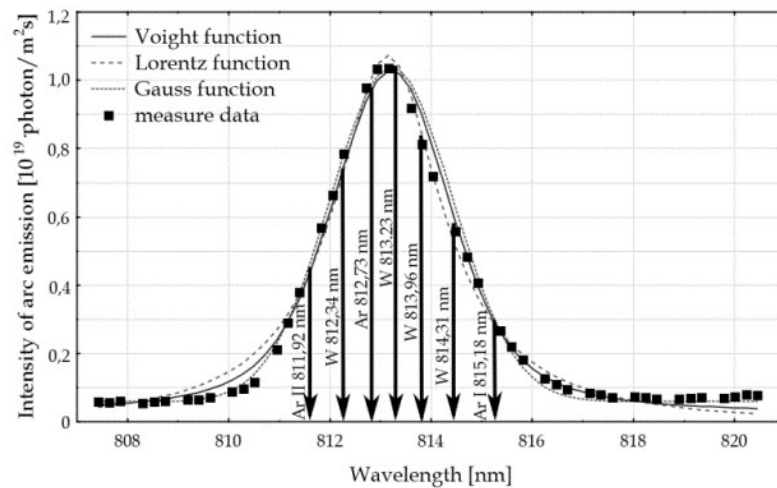


Fig. 3.1.f An example of peak obtained from several experimental data at different wavelength, and matched for Gaussian, Lorentz and Voigt function [Weg12].

In any case, regardless the fitting method to determine the shape of the absorption line, the integrated area under the curve is proportional to the number density of molecules present.

For particular case of humidity measurement in NG, one of the most important parameter to use this technology is to choose properly the wavelength(s) to quantify the water concentration in the sample. Because of the complex composition of the NG, many components should have to be considered in this sense, to avoid potential errors could happen both the self-broadening and contributions of neighboring absorption lines are neglected, which can result in over and underestimation, respectively [Ert04]. Below are shown the absorption spectrums of water and methane (as a major component of NG) within which the best choices of wavelengths must be found.

3. HUMIDITY SENSING TECHNIQUES

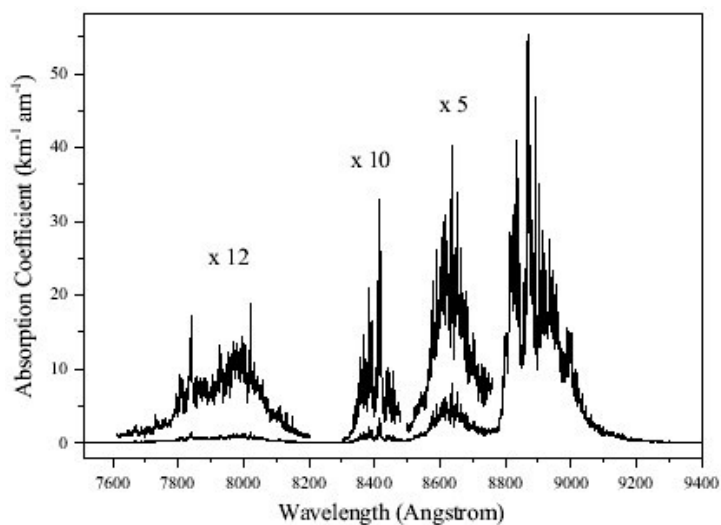


Fig. 3.1.g Methane absorption coefficients at 296 K for the wavelength range from 750 nm to 940 nm, ergo, within the NIR region [B&C02].

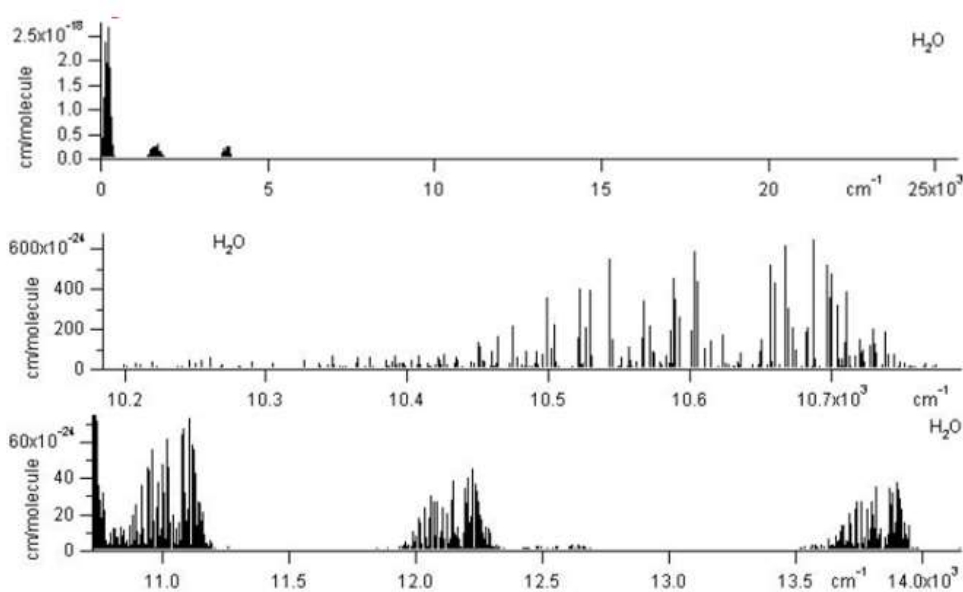


Fig. 3.1.h Water absorption spectrum expressed in wavenumber vs. $\text{cm}\cdot\text{molecule}^{-1}$ within the NIR region. Images collected from HITRAN 2004 database [HIT04].

The first graph of Fig. 3.1.h shows a very large region of absorption spectrum of the water, whilst the other two graphs depict the equivalent spectral area to the methane spectrum shown in Fig. 3.1.g.

Physical description

Despite of the great diversity of configurations available within the field of the optical sensing techniques, and particularly to the absorption spectroscopy. There are a

series of common elements in all of them, whose peculiarities are the basis of the different sensing methods. Below are cited the most important compounds in any optical sensing technique:

- *Radiation source*, which must be monochromatic when light sources is broader than the absorption lines chosen for each application. Besides the light source must meet other features such as: stability, addressability, continuous spectral energy distribution and long life. The most common examples of sources are diodes and lamps mainly made of Tungsten, Xenon or Deuterium.

- *Monochromator*, in charge of isolating the radiations of desired wavelength, to obtain monochromatic light for those cases in which the light source has very large spectral broadband. A monochromator can be composed by several elements but not always all of them must be present. Some components are: entrance and output slits, multiple sorts of lens, optical filters, beam splitters, etc.

- *Collimator*, is a device which receives the divergent beam emitted by the source, constituted by rays that move in all directions, and turns it into a set of parallel rays with the same properties. This element is also used to replicate a target focused at infinity, to minimize parallax problems, and even to calibrate other optical devices.

- *Sample or measuring cell*, is the cavity inside of which the beam coming from the source and that it has been already treated interacts with the sample which contents the target substance. It can be either open or closed, depending on the experimental setting up developed for each application.

- *Detection system*, is responsible for collecting the resulting beam after crossing the target sample, so it must be designed according to the nature of the signal (photon beam, heating or electromagnetic radiation, optical). Inside of this function is very often the used of electrical amplifiers and transformers.

- *Registration and control system*, in charges of converting the physical phenomenon in numerical values representatives of the concentration of the target substance in the sample, storing them and sending the orders to the control loops of the sensing instrument to correct or adjust any specific control parameters.

3. HUMIDITY SENSING TECHNIQUES

The path length is a quite important factor because the higher is, the higher is the magnitude of the signal received, the measurement accuracy and the low detection limits decrease. All of this is achieved because ratio between noise and signal is minimized.

Due to the multiple advantages associated with higher path lengths, it is very often to employ multipass cells, that is, the incident light beam is reflected several times within of the same measuring cell, thereby increasing the path length.

Regardless with method used to increase the path length by multipass, there are several configurations and the most common are: the Herriott type, the cell of Chening, and Ofner system [H&T13].

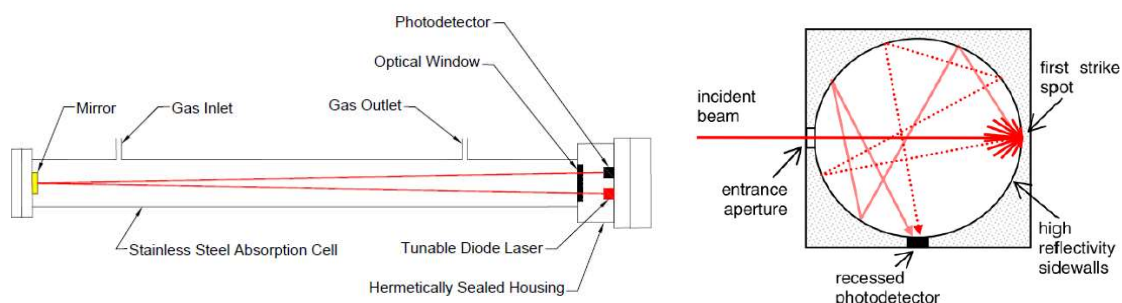


Fig. 3.1.i Example of two typical configurations of optical sensing technologies. Left: basic scheme of double-pass laser absorption cell used for one of the instrument studied [GE11]. Right: scheme of random reflection suffered by the collimated beam inside of a spherical cavity [H&T13].

Types

There several detection and measurement techniques of gas concentration using the optical absorption characteristics depending on the different approaches applied during their designs. An extensive and detailed bibliographic review was performed by Hodgkinson and Tatam and a little example of such diversity is given in Table 3 of their compilation [H&T13].

Some of most important groups are: non-dispersive infrared (NDIR), tuneable diode laser spectroscopy (TDLAS), quantum cascade laser absorption spectroscopy (QCLAS) [Wei08], cavity ring down spectroscopy (CRDS) and all its variants [Laj08] (cavity enhanced absorption spectroscopy-CEAS [T&Y08], phase shift CRDS and Fourier transform), photoacoustic spectroscopy (PAS) and Noise-Immune Cavity-Enhanced Optical-Heterodyne Molecular Spectroscopy (NICE-OHMS).

Other classification can be given depending on the kind of signal processing, where two techniques are commonly used for TDLS: one directly works the spectroscopic scan, and another that uses a wavelength modulation spectroscopy (WMS). The most important example of this second type are the FTIR (Fourier Transform Infrared Spectroscopy), which are based on the second harmonic of Fourier transform and an endless of scientific reports evidence their useful [Esl00, Cha09].

By the other hand it can be given a lot several classifications depending on the feature compared, for example: open or closed measuring cell; single or multiple pass; one or more measuring cell within which some of them can be used to measure the blank, or to carry on a simultaneously analysis of several substances, and much more.

Characteristics and Properties:

Optical absorption offer multiple advantages such as:

- They have been proven to be very high resolutions gas detectors, due to their high sensitivity and specificity [W&S09], with zero cross-response to other gases as long as their design is carefully considered [H&T13]. All of that is possible thanks to a high signal to noise ratios resulting from fully resolved gas lines as long as a region can be found for which the narrow individual absorption line of the target has no overlap with other potential interference lines.

- Their fast response allows to measure in real time, so this feature turns this technology into a very attractive option that may play a very important role in the process control system for countless industrial applications.

- Another of the most important advantages of the optical sensing techniques is that they measure contactless, which means that not disturb the gas sample, adding this way potential measurement errors.

- In addition, if an optical measuring cell is combined with the optical fiber technology more several advantages can be achieved. The first is to reduce the high costs of the light sources, by sharing only one analyzer to several sample point. The second, like an alternative when it is desired apply this technology in explosives areas where it is mandatory all instrumentation meet safety requirements, such as ATEX directive in the NG industry [H&T13]. This way, it is simpler and safer to transport the sample to the place where the optical instrumentation was assembled inside of an intrinsically safe area.

3. HUMIDITY SENSING TECHNIQUES

- This technology could be an alternative to traditional, expensive and laborious laboratory methods, such as, mass spectroscopy (MS) and gas chromatography (GC).

This spectra region, in which TDLAS instruments works, is particularly interesting for the atmospheric science field where almost all species of interest have strong fundamental absorptions while the major constituents, nitrogen and oxygen do not [Sch93]. In that sense, this technology is considered as an excellent and very useful method in the current greenhouse gases researches [Laj09].

For all the above and the In addition, gas detection by means of this technology has an impact across a wide range of applications, such as: the petrochemical or any other industrial process, to ensure safety (e.g. via detection of toxic or flammable gases) and to monitor and measure key species during the processes and in the final product [H&T13]; or in human breath diagnostics to detect potential markers for diseases [Cur07].

However, despite of the large number of advantages, like the other technologies, it has also weak points or issues that can be improved. In this sense, and as it has been explained that the absorption spectrum shape is absolutely dependent on the temperature and pressure, and over time, fluctuations in temperature and/or vibrations of the cavity cause the interference to shift in wavelength. For that and due to operate at reduced pressure improves the limit of detection, both quantities must be very well controlled, so a pressure reducing and a thermostatic system must be implemented, together with the optical part of the measuring device, when it is going to be used in situ under industrial conditions.

Gas absorption linewidths are narrow, so requires lasers with narrower emission linewidths, which means that interference effects are unavoidable for such high-resolution spectroscopy [H&T13].

By the other hand, the presence of dust or dirt could also cause interference because of reflections and/or light scattering problems. The same happens if condensed water vapour reaches the measuring cell. Thereby, very careful sample conditioning must be included.

3.1.2.2 Resonance by microwaves

The bipolar structure of molecules of water is one of most important characteristics, as well as the asymmetric electric charge distribution that is responsible for many of its

properties, such as: very high dielectric constant, high solubility, formation of hydrogen bonds, high surface tension, and many others.

Measuring principle

By the other hand, another key feature of the water is its molecular capability to interact within an electric field, absorbing energy from microwaves and turning it into oscillating and/or vibrating molecular movements. The measuring principle of this techniques is just based on this last characteristic and hence, in the attenuation of the microwave signal that passes through the sample measured and which is directly related to the moisture content. Thus, the energetic losses of the microwaves that cross the wet sample will increase with the amount of water contained by such material.

This experimental technique is based on the study of the microwave resonance frequencies over a cavity, which contents small concentrations of water, because they are particularly sensitive as a result of the high polarizability of this substance. Thus, by means of the characterization of the resonance frequencies when the moist gaseous sample is crossing the cavity, it is able to determine the water content of such sample. Theoretical foundations of this technology were deeply explained in Section 4.2.1.

Types

The water molecules do not only absorb energy but also reflect it. To calculate the moisture content, both factors need to be taken into account together with geometrical factors, such as the position between emitter and detector, the cavity geometry where the sample analyzed is placed, etc.

In order to maintain the resonance at one operating frequency and for an efficient energy transfer into the resonant cavity, the inductance and capacitance must be reduced. The re-entrant cavities are specially designed to meet this requirement, besides of reducing and preventing radiation losses by means of a self-shielding enclosure [Bag09]. All of that allows energy emitted by microwaves is extremely low, avoiding time that the temperature of the sample may increase at the same. An example of application of this kind of cavities was performed by Goodwin *et al.* [Goo96], who used it to detect phase separation processes in gaseous mixtures.

One of the most common configurations used are the re-entrant cavities, and inside of this group a number of co-axial cavities have been specially developed (see Fig. 3.1.j).

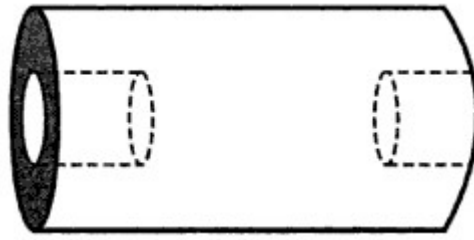


Fig. 3.1.j Scheme of co-axial re-entrant cavity [Bag09].

Nowadays, the classical co-axial re-entrant cavities have been substituted by the quasi-spherical resonator (QSR), which early demonstrated their high and accurate performances to measure the water vapor mole fraction of moist nitrogen or air mixtures within the temperature range between 241 K and 291 K at atmosphere pressure [Cuc12, Und12]. May *et al.* [May08] also worked with this kind of cavity to measure the relative dielectric permittivity of O₂ between 273 K and 323 K and pressures up to 6.5 MPa. They demonstrated that the uncertainty of this new cavity for getting relative magnetic permeability data is lower than 1% at pressures above 2 MPa.

Characteristics and Properties

Some of the potential advantages of microwave resonator for moisture sensing are:

- One of the most important properties of this technique is that it is a contactless measurement that allows no abrasion of the sensors and no sticking of material. Besides, microwaves are not sensitive to pH and conductivity properties of the material under which is going to be analyzed. To sum up, it is a technique with no interference with the process and may not suffer contamination problems.
- This technique allows to measure the total moisture content, which includes the surface water as well as the internal or inherent water. This way, the moist content of any sample in solid state could be measured and therefore, it could lead to an essential measuring technology very useful in countless industrial processes.
- Its high accuracy in the measurement of resonance frequencies and the fact that microwave hygrometers do not need to be calibrated suggest that this technique could be used as a primary humidity standard if it was combined with a suitable humidity generator, which may solve some of the biggest metrological challenges [Veg12].

-
- QSR is a powerful experimental tool not only in hygrometric field, also for applications in acoustic thermometry, determination of the Boltzmann constant, resonance acoustic, etc. [Meh09].
 - The measurement gives instantaneous results, in real time, and can be utilized for industrial control processes.
 - Its design simple, rugged and robust makes of this kind of hygrometers a technique potentially applicable over extended pressure and temperature ranges. These qualities make things about this instrument could be used as a portable humidity standards, which would be ideal to calibrate on-site and under real industrial conditions.

Microwave resonators performance has been largely demonstrated in several hygrometric applications, for example, Rouleau *et al.* [Rou00] used a single cylindrical cavity to measure trace moisture levels in SF₆, which is a gas very widely used as a insulation in electricity distribution systems, especially in high voltage systems, reason by which the water content must be minimized to avoid high risk conditions. Its use is remarkable in the manufacture of electrical compounds, integrated circuits or industrial iron-steel processes.

Potential of this technique has been also notorious for hydrocarbon mixtures determining electrical and thermophysical properties, including the dielectric constants and polarizabilities [M&M02], and phase behaviors (e.g. dew points, liquid volume, cricondentherm), respectively [May03]. In all previously surveys, the upper pressure values achieved were around 10 MPa for temperature work ranges between 20 and 40 °C.

Inside of the framework of the European project Characterization of Energy gases. ENG-01 Gas [ENG01], studies with humid methane mixtures were performed by INRiM using a QSR cavity. Afterwards, one step further was carried on checking the performance of such QSR cavity measuring the moist content of real natural gas mixtures under semi-industrial conditions. This last aim was achieved thanks to the cooperation among INRiM, ENAGAS and INTA and it is one of the tasks which is included in this thesis [Gav14].

3.1.3 OTHER HUMIDITY SENSING TECHNIQUES USED IN GASES

3.1.3.1 Karl-Fischer Titration

This method is based on a chemical reaction between water and the *Karl Fischer Reagent*, which is typically a mixture formed by sulfur dioxide, iodine, pyridine, and methanol. For many years, this method was limited to laboratory applications because of the equipment and chemical agents required to carry out the determination turned into a laborious and complex method very hard to extrapolate to applications on field.

The Karl Fischer titration can be divided into two basic analytic groups with respect to the method to use the iodine [Cha04]:

- *Volumetric titration*, in which the water-containing sample is solved in alcoholic solvent and is titrated with a Karl Fischer solution. Volumetric titration is applied for amounts of water within the range from 1 ppm_w to 100 ppm_w.
- *Coulometric titration*, the iodine is not dosed but is directly used in an iodine containing solution. It is a method highly accuracy, thus it is used to determine extremely low amounts of water (10 ppb_w to 50 ppm_w). For this reason, this method is less useful than volumetric for water content measuring of gases on field conditions.

Methods to determinate water concentration in a natural gas are described in ISO 10101:1993, titration in part 2 and coulometric in part 3 [ISO93]. Recently, the newest Karl Fischer methods are faster and more convenient than conventional, especially for measuring water in hydrocarbons mixtures.

3.1.3.2 Gravimetric hygrometers

This technology provides an absolute humidity measurement weighing the water molecules absorbed from an incoming gas whose flow must be controlled very accurately.

This technique can be applied for gases that contain light components (e.g. methane and ethane), because the condensation temperatures for these hydrocarbons are lower than water. However, when intermediate or heavy hydrocarbons are present in the gas stream a previous separation stage must be included, because they tend to condense together with water, which could decrease the accuracy of method.

By means of this method and according with the ISO 6570:2001, the *potential hydrocarbon liquid content* (PHLC) for a natural gas can be determined. This parameter describes the amount of hydrocarbon condensate which can be formed at a pressure and temperature fixed [ISO01]. That parameter is important for the NG industry because knowing WDP and HCDP give information about when condensation starts, but not providing further information about the amount of condensate generated under certain operation conditions. This information is very useful to developing calculation models which estimate fluid buildup in NG pipelines and NG processing plants, and to be able to schedule maintenance tasks as, drainage and purging pipes.

This method has been developed as primary standard in NIs like the NPL, as a result of a PhD work [Bel98], nevertheless it is not running currently.

Associated at this technology auxiliary measurements of the weight, temperature, pressure and volume must be performed with extreme precision, so its implementation on-site and even outdoor applications are pretty far to be a reality, so only in this kind of laboratories, equipped with the most advanced measurement technologies, gravimetric hygrometry can be developed. In addition, for low water content ranges it may require up to a couple of days per calibrate one point. Therefore and due to all these reasons, the gravimetric technology is not useful for industrial measurements.

3.2 HUMIDITY SENSING INSTRUMENTS STUDIED

In this section, all humidity measurement instruments studied in this thesis were described. They were classified according to the sensing technology they were based on, which were previously described just in section before.

The humidity measurement quantity, the range and the accuracy will be indicated for each equipment. In addition, other properties that influence in the humidity measuring were specified when the manufacturers did it in the handbooks such as: temperature, pressure and flow ranges.

The pressure was one the most important factors that had to be taken into account from the point of view of safety both sensor and the own measurement process, because if the upper pressure limit was overtaken, it could lead on diverse hazardous situations.

3. HUMIDITY SENSING TECHNIQUES

All manufacturers must provide optimal operation ranges that warranty both accuracy and reliable of measurement as well as a safe handling.

All hygrometers compared here were borrowed by the manufacturers, who participated in the EMRP ENG01-GAS project as stakeholders [ENG01]. During the two years prior to the activity performed in this thesis, the most of them were previously used in other NIs, mainly NPL, where they had been tested in nitrogen and methane up to 3 MPa [Bel13, Car13a], to check the performance of the new humidity calibration facility for pressurized gases, which had been recently developed inside of that European project.

3.2.1 ELECTRICAL IMPEDANCE SENSOR

As it was said before, this kind of sensors is the most widely used in the worldwide natural gas industry, because they can endure large humidity and pressure ranges, covering practically all treatment processes of NG. In addition, they have an acceptable accuracy and they are quite economical. For these reasons, a huge volume of this sensors is currently spread around the world, so the majority of manufacturer have one or several probe models based on this technology.

3.2.1.1 Aluminum oxide

Inside of the wide variety of electrical impedance sensors in the most of this instruments their hygroscopic material is usually made of different metallic oxides, highlighting above all those made of aluminium oxide, Al_2O_3 , which are the most widely used and for this reason, at this group belongs the most number of sensors evaluated here and described below.

3.2.1.1.1 *Michell's Instruments*

Michell Instruments Ltd. is one of the most important European manufacturer of all short of humidity measurement instruments based on wide range of detection technologies. They lend several probes of different models through diverse tasks included in the EMRP project. Below, were described the models used, summarizing their main features too.

3.2.1.1.1.1 Easidew PRO I.S.

The *Easidew PRO I.S.* is a dew point transmitter for trace moisture measurement in gases and non-polar liquids. Humidity is measured as moist content in volume or weight, ppm_v or ppm_w, or as dew point in °C if the sample gas pressure is known.

It has numerous certifications for use in hazardous area locations, for that the meaning of acronym of intrinsically safe, I.S., used in its name. Besides, it is easy to install and operate in any situation due to its simple and rugged design.

3.2.1.1.1.2 Easidew Transmitter

The *Easidew Transmitter* also is a dew-point transmitter with a really simple design, but in this case it has not got any certificate as intrinsically safe, thus it is not allow to be used inside of areas classified as hazardous. It was developed before than the probe model previously described, and for dew points higher than -60 °C it has two times the accuracy of its improved version.



Fig. 3.2.a Actual look of Michell 's electrical impedance humidity probes fitted with aluminum oxide sensor. Left: Easidew PRO I.S. [MIC12b]. Right: Easidew Transmitter [MIC12a].

All instruments based in these models were shipped from NPL to INTA directly, after being measured in methane up to 3 MPa. That means they were not adjusted before and it is unknown if they have suffered some kind of drift effect, contamination, or anything else. In the following table, the most important properties of Michell's instruments were summarized:

3. HUMIDITY SENSING TECHNIQUES

Table 3.2.a Summary of the most important properties of Michell's humidity probes based on aluminum oxide [MIC12a & MIC12b].

	<i>EASIDEW PRO I.S.</i>	<i>EASIDEW TRANSMITTER</i>
Performance		
Measurement Range, °C	-100 to 20	-100 to 20
Accuracy, °C	± 2 for -100 to -60 ± 1 for -59.9 to +20	± 2 for -100 to 20
Response time, min	5 for 95 %step (dry to wet)	5 for 95 %step (dry to wet)
Repeatability, °C	± 0.5	± 0.5
Operating conditions		
Humidity, %rh	0 - 100	---
Temperature, °C	-40 to +60	-40 to +60
Pressure, MPa	45	45
Flow range, NL/min	1 to 5	1 to 5
Hazardous areas certificates	Yes	No

3.2.1.1.1.3 Condumax II (WDP Channel)

Nowadays, Condumax II is one of the most advanced Michell's instrument to work with NG, because it is able to measure the WDP and the HCDP at the same time and independently. That is possible because of it combine two sensing technologies: electrical impedance to measure the WDP and condensation chilled mirror to the HCDP, which will be explained in Section 3.2.3.2. Humidity is continuously measured by means of an *Easidew PRO I.S.* probe, which was previously described and it is housed inside the black enclosure (see Fig. 3.2.b).

This device is certified in several categories to be set up inside of hazardous areas, and it is also fitted with a complex sampling system prior to both sensors which allows the *Condumax* to be mounted in any stage of NG processing such us, extraction, drying, distribution or regasification. The sampling system was designed to be mounted on-site and outdoor, and it is constituted by the following components [MIC11]:

- One coalescing filter that is in charge of removes both water and solid particles which are suspended in the gas stream.

- A pressure regulator system that consists on: one heated regulator to sure a line pressure prior lower than 2.7 MPa in the HCDP line, because the sensor cell only endures up to such value. Two pressure regulators positioned upstream of the flowmeters set up in the WDP line and by-pass line to reduce the pressure close to atmospheric pressure before being vented.

- Flowmeters set up at the end of the all measurement lines, to control flow that crosses each sensor.

- The inner volume of stainless steel box, which covers and protects the whole sampling system, is heated by means of a thermoelectric resistance to keep the inner temperature above of a set point that guarantees there will not be condensation problems in any place.



Fig. 3.2.b Look of Condumax II. Left: Black enclosure where WDP and HCDP sensors are confined. Right: Sampling gas panel associated with the Condumax II and required to adequate the gas stream at the optimal conditions for each measuring sensor. The entire facility is mounted within stainless steel box to be positioned outdoor and inside of ATEX areas.

The *Condumax II* came directly from factory, so it was delivered together with its calibration certificates for WDP and HCDP sensor, as well as the calibration certificates of the pressure transmitters used in both measuring lines. Such certificates can be seen in the Section 5.1.1.1.2.

3.2.1.1.2 *General Electric Instruments*

3.2.1.1.2.1 HygroPro

It is one of the most advanced GE's moisture transmitter based on an aluminum oxide sensor which is able to measure over gas or liquid stream. It is compact, intrinsically safe and has the two communication routes: an analogue output 4-20 mA loop powered, meaning and the two-wire supply lines are also the signal lines; and analogue and digital RS485 communications, because it allows longer distances and higher speeds than RS232, and offers the possibility of a multi-drop network, which are ideal features in industrial facilities.

Besides, one temperature thermistor and one pressure transducer are built-in to calculate correlations among the different forms in which the humidity can be defined, as: dew/frost point, water content expressed as relation in volume, ppm_v, or weight, ppm_w, and relative humidity.

The *HygroPro* transmitter can be installed into a sample system or directly into the process, although it is more convenient set it up with a sampling system to protect the sensor. In Fig. 3.2.c it can be seen the look of this sensors and in its main features.

3.2.1.1.2.2 MIS-II (Panametrics)

The *MIS-II* model was designed by Panametrics, but nowadays it is one of analyzers manufactured and commercialized by GE. This instrument is often used on-site, in fact Enagás has one in its facilities of Serrablo, as humidity indicator of NG that is extracted from the underground wells and is subsequently dried with glycols. For that, this instrument was used in this comparative study but directly under real industrial conditions (Section 0). In right picture of Fig. 3.2.c, it can be seen the look of the *MIS-II* probe and in Table 3.2.b its main features.



Fig. 3.2.c Actual look of electrical impedance humidity probes fitted with aluminum oxide sensors commercialized by General Electric and which have been compared in this work. Left: *HygroPro*. [GE07]; Right: the *MIS-2* probe [GE-2].

Table 3.2.b Summary of the most important properties of General Electric's humidity probes based on aluminum oxide [GE-2 & GE07].

	HYGROPRO	MIS-II
Performance		
Measurement Range, °C	-80 to 20	-110 to 60
Accuracy, °C	± 3 for -80 to -66 ± 2 for -65.9 to +10	± 3 for -80 to -66 ± 2 for -65.9 to 10
Response time, sec	1 to 10 for 63.2 %step	---
Repeatability, °C	± 1.8 for -80 to -66 ± 0.9 for -65.9 to +10	± 1.0 for -80 to -66 ± 0.5 for -65.9 to +10
Operating conditions		
Humidity, %rh	---	---
Temperature, °C	-30 to +70 / ± 0.5	-30 to +70 / ± 0.5
Pressure, MPa	0.4 to 3.5 / ± 1 %F.S	34.5
Flow range, NL/min	1 to 2	1 to 5
Hazardous areas certificates	Yes (ATEX, IEC Ex)	Yes (ATEX, IEC Ex)

3.2.1.1.3 Shaw Instruments

Two electrical impedance sensors manufactured by Shaw were compared here.

3. HUMIDITY SENSING TECHNIQUES

3.2.1.1.3.1 SDT Dew Point Transmitter

It is a compact dew point transmitter with analogue output connection of 2 wire and 4-20 Ma. This unit is be self-contained within a robust housing providing weatherproof protection that join with its lightweight is ideal to be directly connected to pipeline.

3.2.1.1.3.2 Superdew 3

Electrical impedance probe, capacitive type to be more precise, designed to measure the dew point in dry air or any other compressed gas. The main external body is made of plated steel and a stainless-steel filter guard protects the sensing element within it. It is possible to connect with it through analogue output 4-20 Ma and digital RS-485 communications, thanks to this latest the sensor can be up to one kilometer away from the dew point meter.

Manufacturer recommends that the sample should not contain particulate matter, oil or other heavy hydrocarbon condensate, warning that if the measuring sensor is affected by contamination, the response time will be lengthened, although the sensor calibration will not be effected. So, it will be interesting try to check this affirmation.



Fig. 3.2.d Appearance of electrical impedance humidity probes based on aluminum oxide commercialized by Shaw and they have been compared in this work. Top: *SDT Dew point Transmitter* [SHAW1]; Right: the *Superdew 3*. [SHAW2]

3.2.1.1.4 *Alpha Instrument- Alpha*

3.2.1.1.4.1 DS-2000

Alpha's humidity probe was exactly the same sensor than *Superdew 3* sold by *Shaw Moisture Meters*, which has just been described just above. Alpha Moisture Systems commercializes such sensor with the name of *DS-2000*. Its differences are both in the electronic part inside the junction box and in the panel display.

For instance, its features are practically equals, except small differences given by manufacturers in technical datasheets and operating manuals.

Table 3.2.c Summary of the most important properties of Shaw [SHAW1 & SHAW 2] and Alpha's [ALP04] humidity probes based on aluminum oxide.

	<i>SDT DP Transmitter</i>	<i>SUPERDEW 3</i>	<i>DS2000</i>
Performance			
Measurement Range, °C	-100 to 20	-100 to 20	-100 to 20
Accuracy, °C	± 2	± 2	± 2
Response time, sec	20 to 120	20 to 120	20 to 120
Repeatability, °C	± 0.3	± 0.3	± 0.3
Resolution, °C	0.1	0.1	0.1
Operating conditions			
Humidity, %rh	< 95 %	< 95 %	< 95 %
Temperature, °C	---	-20 to +60	-20 to +60
Pressure, MPa	0 to 35	0 to 35	0 to 35
Flow range, NL/min	2 to 5	2 to 5	2 to 5
Hazardous areas certificates	No	No	No

3.2.1.2 Polymeric sensor

The active part of a sensor that is to say, the hygroscopic material, does not need be made of metallic oxide, but the development of new polymeric material is also being determinant in this field. For that, it was mandatory to have a representation of this kind of sensors.

3.2.1.2.1 *E+E Instruments – EE371*

The core of the *EE371* is the monolithic measurement cell type HMC01, polymeric sensor manufactured in thin-film technology by E+E Elektronik [EE371]. The design of the HMC01 consists on over the same thin glass substrate the temperature sensor and directly above the humidity sensor are located. Combination of humidity and temperature sensors usually consists of two substrates glued together, each with one sensor, so the thermal connection between both elements is loosed, which affects to the accuracy. This sensor arrangement allows that the temperature sensor can be operated as a heating

3. HUMIDITY SENSING TECHNIQUES

element to keep the relative humidity close to a set point, reducing potential drift effect due at high humidity conditions.

By the other hand, this measuring devices contains a special autocalibration method that is used to compensate usual drift effects, resulting in high-precision measurements even at the lowest dew point temperatures. Autocalibration is performed every 30 minutes and takes approximately 3 minutes in which one heating cycle is carried out to dry the sensor and delate some impurities may have been deposited on. During the autocalibration, the analogue outputs are frozen at the last measuring value, but this attribute was turned off by the manufacturer to get the actual values at all time in this work.

This borrowed sensor was shipped to us from manufacturer directly, so it did come calibrated for water dew point within the range from $-57\text{ }^{\circ}\text{C}$ to $-10\text{ }^{\circ}\text{C}$ by the own manufacturer, because it also is the Austrian Calibration Body for humidity, temperature and air. The results of its certificate are attached in Section 5.1.1.1.2.



Fig. 3.2.e Look of the *EE37*, electrical impedance humidity probes fitted with a polymeric sensor. Left: external look of sensor with electrical and junction box. Right: polymeric sensor is housed inside of microporous stainless steel sintered filter, which protect it for contamination [EE317].

The communications of this instruments are: two analogue outputs 4 to 20 Ma, and RS232 for digital mode. In the following table are summarized other features of such sensor.

Table 3.2.d Summary of the most important properties of the humidity sensing instrument EE371, impedance electric sensor based on a polymeric material [EE317].

EE371	
Performance	
Measurement Range, °C	-80 to 60
Accuracy, °C	± 2
Response time, sec	---
Repeatability, °C	---
Resolution, °C	0.1
Operating conditions	
Humidity, %rh	---
Temperature, °C	-40 to 60
Pressure, MPa	0 to 10
Flow range, NL/min	1
Hazardous Areas certificates	No

3.2.2 ELECTROLYTIC INSTRUMENT

Other kind of sensors, very useful in applications where high accurate is for very low water contents, are those based on the humidity measurement by means of electrolytic process. By applying an electrical potential (voltage) to the electrodes, each absorbed water molecule is electrolyzed, generating a finite current what is proportional to the amount of absorbed water.

3.2.2.1 Mecco Instruments – Accupoint LP2

Mecco Inc. has a long tradition using electrolytic techniques in its humidity sensors, using phosphorous pentoxide (P_2O_5) as active material always. It has several models belong this group as, the *Waterboy* and the *Accupoint*, for high and low pressure applications. These instrument is directly able to detect the molecules of water present in a gas stream, thus theirs measured quantity will be the water content, which is commonly expressed as fraction in volume, ppm_v.

In this survey, the low-pressure version of Accupoint 2 was borrowed for this purpose, being its upper pressure limit of 0.69 MPa. For that, in the most of NG processing steps, it will necessary to set up a regulator for reducing the pressure below of this limit.

3. HUMIDITY SENSING TECHNIQUES

The Accupoint LP2 functions as a standard 24 VDC, two-wire loop powered transmitter. RS-232 output signal in three-wire mode is also available for this analyzer. Furthermore, this instrument is housed in an enclosure box to be directly mounted at the sample point (whether indoors or out).



Fig. 3.2.f Look of *Accupoint LP2*, electrolytic humidity sensor manufactured by Meeco Inc [MEE05].

The *Accupoint* used did not come with updated calibration certificate, but this technology, based on Faraday's law, is absolute. This feature allows checking if the unit has working well, doing flow changes several times and checking that the moisture readings change proportionally, for one sample standard with a water content constant and well-known. After checking the right function of the unit, the true sample flow rate had to be set to achieve 0.1 L/min, because the flow had to be properly corrected to be used with NG.

Table 3.2.e Summary of the most important properties of the humidity sensing instrument *Accupoint 2 LP*, electrolytic sensor (P₂O₅) [MEE05].

Accupoint 2 LP	
Performance	
Measurement Range, ppm _v	-0 to1000
Accuracy, ppm _v	± 0.4 (or 5% of reading)
Response time, sec	---
Repeatability, ppm _v	---
Resolution, ppm _v	0.1
Lower detection limit, ppm _v	1
Operating conditions	
Humidity, %rh	---
Temperature, °C	-20 to 60
Pressure, MPa	0.69
Flow range, NL/min	0.1
By-pass flow	1
Hazardous areas certificates	Yes (ATEX)

3.2.3 CONDENSATION HYGROMETERS

The condensation chilled mirror hygrometers are instruments very well-known because they usually are used as standards, due to their high accuracy, very good long term stability and the opportunity to handle the condensate nature to make dew or frost point as it is wanted, when the condensate temperature is close to – 10 °C.

This technology is used mainly with air or nitrogen in national metrology laboratories, as it is the case of Temperature and Humidity laboratory of INTA, who gives traceability to the first level calibration laboratories in Spain, besides to participate in intercomparisons among other countries around the world. For all of that, it looks logical try to apply the knowledges in this technique but in this case given one step more and checking its performance in non-conventional gases, as methane or natural gas.

Despite of being a technology that requires a high training to distinguish between dew or frost even in conventional gases, its applications is also spread in the NG industry, where *manual chilled mirror* are usually used in field to make occasional measurements, whilst *automatic chilled mirror* are assemble in fix points in key points in the national

3. HUMIDITY SENSING TECHNIQUES

gas network, or as a standard instrument to calibrate the rest of second order humidity probes which do not need high specifications but are essential too. Two condensation hygrometers were included in this research.

3.2.3.1 MBW – DP 3D

Model manufactured by MBW Calibration Ltd., it is an automatic condensation hygrometer, belongs to Enagás and borrowed to INTA to compare its performance again the rest. The same instrument was used in a couple of thesis carried out in the old humidity laboratory which is located in the Research and Development building of Enagás in Zaragoza. In those works, influence of hydrocarbons condensation to determine water frost/dew point, phase diagrams of hydrocarbons or comparative among several theoretical and experimental calculate models of the saturation curves, are some matters evaluated [AVI99]. Thus, despite of complexity of this technology to be implemented in mixtures, keeps on having great interest in the NG industry.

This instrument was calibrated by INTA using air and close to atmospheric pressure levels. The calibration range for dew point was from $-75\text{ }^{\circ}\text{C}$ to $-10\text{ }^{\circ}\text{C}$, and results are indicated in Section 5.1.1.1.2.

In this model, the sensor head housing was modified to be able to afford pressures up to 10 MPa. The look of this picture can be seen in the following picture, in which also is appreciated its cooling unit in the lower part, needs to chill the surface of the mirror until reaching the condensation points. Table 3.2.f shows the most important features of all chilled mirror studied included the MBW's instrument.



Fig. 3.2.g Enagás' chilled mirror hygrometer manufactured by MBW and used in this thesis.

3.2.3.2 Michell Instrument – Condumax II

As it was commented before in the section, this instrument is also equipped with chilled mirror technology, but in this case only applied to detect first hydrocarbon condensates, namely, the hydrocarbon dew point (HCDP). In Fig. 3.2.b it can be seen the look of such instrument, fitted with its sampling system used to be mounted in-site and inside of hazardous areas.

This humidity meter is equipped with an automatic optical condensation measurement principle, to give an on-line measurement of hydrocarbon dew point that is reproducible and free from operator bias. That is possible thanks to detection technique patented by Michell, known as *Dark Spot* [Her11], which is based on the principle of that surface tension of water is very high, whilst of hydrocarbons is very low. The WDP sensors can be easily detected on a small mirror, which consists on well-polished surface. However, for improving the HCDP detection, it should be used a rough surface to counter such problem.

Dark Spot technique consist on modify and etched surface on which condensation is produced in a conical, to increase its roughness. Due to this conical surface and the orientation and position of the emitter and detector among them. When a hydrocarbon layer appears, then a dark spot is clearly identified by the detector, and this is the reason which gives the name to this novel technique.

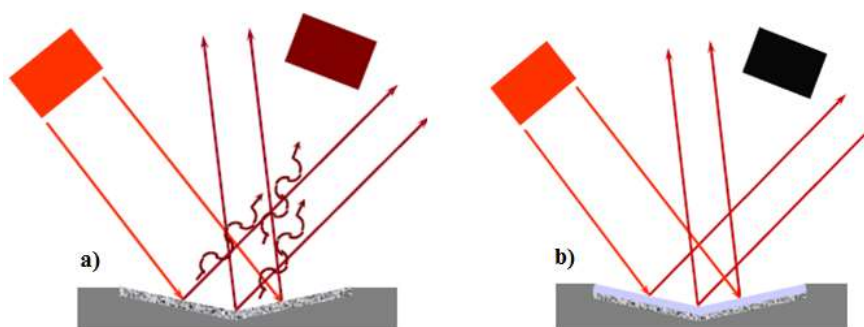


Fig. 3.2.h Light rays reflected from the conical surface to the detector: a) without hydrocarbons condensed, b) with a layer of hydrocarbons [Ben10].

If a study about the light signal received on the detector was made, evolution of results would be the next. Initially, there is not a layer of hydrocarbons condensed, so the light uniformly reflected go to the detector, where it can be seen a smooth circle. (Fig.

3. HUMIDITY SENSING TECHNIQUES

3.2.i.a) When condensation of hydrocarbons occurs, reflected light is not uniformly reflected but it is focused on the perimeter of the circle now, generating a dark spot in its center. (Fig. 3.2.i.b) The more condensate is generated, the stronger will be the collected light (Fig. 3.2.i.c), until the darkness of the circle is invaded (Fig. 3.2.i.d).

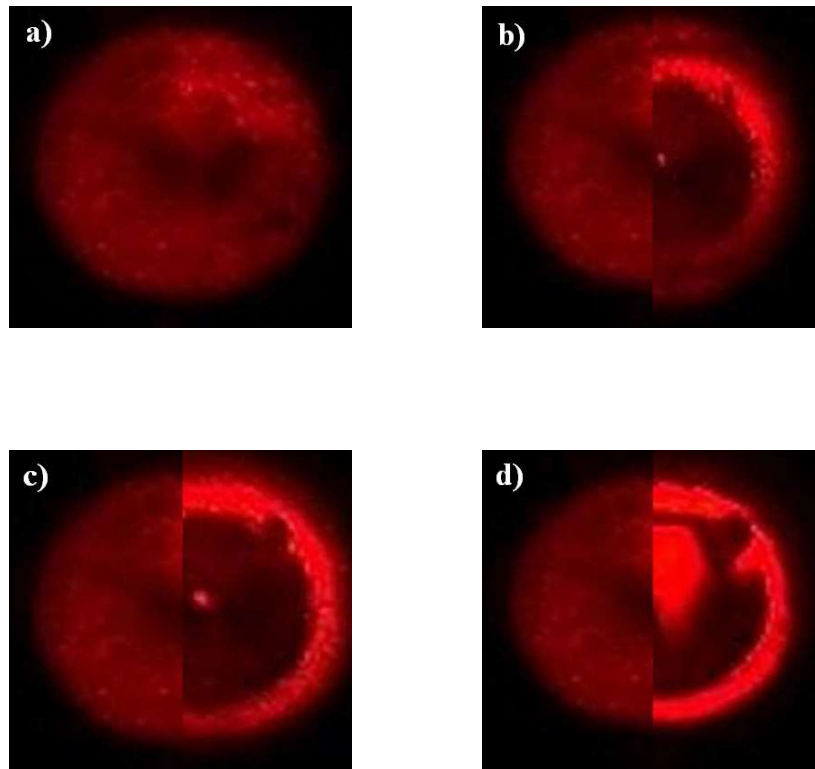


Fig. 3.2.i Look of collected light on the detector while condensate of hydrocarbons is occurring: a) Dry optical surface, b) some condensate beginning to form, c) more condensate forming, this temperature will be equivalent to the HCDP, d) excess of condensate, so temperature will be below HCDP [Ben10, Her11].

While the measurement of the WDP is continuous and the gas sample flow is uninterrupted, the measurement of HCDP is cyclical and discontinuous. This last consists in trapping a gas sample in the sensor cell, where the controlled cooling of the optical surface takes place until the optical system reaches a user-set trip point. Then the temperature of the optical surface is recorded as the HCDP after which the sample gas flow is restored and the optical surface is heated to ensure that any hydrocarbon residue may affect the next measurement cycle. The minimum cycle time is 10 minutes

At the beginning of a measurement cycle, the sample solenoid valve is closed to trap a gas sample in the hydrocarbon sensor cell for analysis and. When the scattered light intensity measured by the optical measurement system reaches a user-set trip point, the temperature of the optical surface is recorded as the hydrocarbon dew point, after which the sample gas flow is restored and the optical surface is heated to the temperature set-point. The heating of the optical surface to an elevated temperature to avoid residue build-up on the optical surface which may affect the next measurement cycle.

In the following table are summarized the most important properties of all instruments equipped with condensation technique as humidity sensing system.

Table 3.2.f Summary of the most relevant properties of the chilled mirror hygrometers tested in this work [MIC11].

	<i>MBW DP 3D</i>	<i>CONDUMAX II HCDP</i>
Performance		
Measurement Range, °C	-100 to 20	for $T_{\text{sample}} > 50$ at 2.7 MPa
Accuracy, °C	± 0.1	± 0.5
Repeatability, °C	± 0.05	---
Resolution, °C	0.1	0.1
Operating conditions		
Humidity, %rh	< 90 %	---
Temperature, °C	-10 to 50	-20 to 60
Pressure, MPa	≤ 10	≤ 10
Flow range, NL/min	0 to 1	0.5 to 1
By-pass flow, NL/min	---	1
Hazardous areas certificates	No	Yes (ATEX)

3.2.4 SPECTROSCOPIC (TDLAS)

The detection technology of water content in a gas stream by means of absorption spectroscopy is one of the most growing currently, because it can be used in wide range of applications both industrial and laboratory. This is possible thanks to non-steady compositions of a mix stream should not affect to humidity measurement, an exception of just few substances which could be present in the mixture and have absorption peaks very close from the water.

3. HUMIDITY SENSING TECHNIQUES

Besides the advantage to offer because it is not a contact technology and hence, it does not alter any gas property, it must be taken in count the ability of technique to measure concentrations of diverse substance at the same time with only one sensor, as O₂ o CO₂, convert this detection method in an alternative so promising.

Below the most relevant features of two spectroscopic sensors tested in this work have been detailed.

3.2.4.1 General Electrical Instrument – Aurora

It is one of the moisture spectroscopic analyzers of GE that is able to measure the water content, in ppm_v, of a hydrocarbons gaseous stream and can be mounted in-site in real industrial process even in explosive areas.

Although this unit has its own sampling system which can reduce the gas pressure to atmospheric levels, before coming in the spectroscopic sensor cell. It must be used another reducing valve upstream to decrease the pressure below to 1.3 MPa [GE11]. Also, there is a first filter stage, one flow regulator after the sensor cell, one by-pass line and another drain line. Furthermore, there is and PRT-100 inside the sample box, whose temperature readings are used as temperature of gas stream, and a heating system is also assembled to avoid freezing processes.

In the Fig. 3.2.j, both internal and external views of Aurora are shown of the sampling system and its more relevant properties are cited in Table 3.2.g.



Fig. 3.2.j Pictures of Aurora. Left: External appearance of the sampling system box and on top of this are located the display and keypad unit, and wiring terminal block. Right: Gas sampling system and spectroscopic sensor cell.

3.2.4.2 Michell Instrument – OptiPEAK TDL600

The OptiPEAK TDL600 is the first instrument of Michell based on absorption spectroscopy for automatic online measurement of moisture in variable compositions gas stream, and specially designed for application in natural gas and methane industry.

When this analyzer began to be part of this comparative of sensing humidity techniques, it was still in a β -version, which means it was still a prototype or a pre-commercial version when this research was made. In fact, the TDL600 tested here was one of the first units manufactured by Michell, which were distributed around the world in different industrial processes to evaluate its performance under whatever weather condition and for gas compositions quite different.

Such analyzer was thought to be mounted on-site because of that, it is fully hazardous areas certified. Thus, and taking advantage of this feature, this instrument was set up in the facilities of underground NG storage and drying plant of Serrablo, described in Section 4.3.

The measuring principles are the same than Aurora but there are differences between both sampling systems [MIC15]:

3. HUMIDITY SENSING TECHNIQUES

- *TDL600* is fitted with two stages pressure reducing system, to decrease the process pressure up to the atmospheric levels required for this technique in the sensor cell. The two reducing stages allow gradual pressure decrease to ensure that condensation does not origin from anywhere. The maximum pressure of inlet natural gas stream which this system can hand, it is 13.8 MPa. Thus, it is not necessary to have to add another reducing valve before the sampling box, as in the case of *Aurora*.

- The borrowed prototype had two thermostats to keep the temperature of measurement system within work range. This way freezing or condensation process are avoid as well as temperature gradients are minimized.

As the same than the *Aurora* analyzer, filtering system has been set up before reducing valves, and flow regulators were positioned at the end of the main and by-pass lines.

Regarding to communications with this instrument, it had two ordinary analog signals 4 to 20 mA, and digital communication were carried on by means of RS-485 Modbus RTU transmission protocol, because was the most properly to longer distances, higher speeds than the RS-232 and the possibility of a true multi-drop network, which were ideal features for industrial facilities.

In the below figure, a real view of the prototype of *TDL600* is shown join its sampling system. The most relevant properties are summarized in Table 3.2.g.



Fig. 3.2.k Real pictures about Michell's spectroscopic humidity analyzer, prototype of the OptiPeak TDL600 assembled in real industrial facilities.

Table 3.2.g Summary of the most important properties of the two humidity sensing instruments based on absorption spectroscopic technology, the Aurora TDLA [GE11] and the OptiPeak TDL600.

	<i>Aurora TDLAS</i>	<i>OptiPEAK TDL600</i> ³
Performance		
Measurement Range	-65.5 to -2.6 °C 5 to 5000 ppm _v	1 to 1000 ppm _v
Accuracy	± 4 ppm _v or 2% of reading ± 2 °C	± 1-2 ppm _v ± 2 °C
Optical response time, s	---	0.2
Repeatability, ppm _v	---	< 1
Limit detection, ppm _v	---	1
Resolution, ppm _v	0.1	0.1
Operating conditions		
Temperature, °C	-20 to 65	-20 to 55
Pressure, MPa	≤ 1.3	≤ 13.8
Flow range, NL/min	0.2 to 1	1
By-pass flow, NL/min	> 5 x Q _{cell}	1 to 5
Hazardous areas certificates	Yes (ATEX, IEC Ex)	Yes (ATEX, IEC Ex)

3.2.5 MICROWAVE RESONATOR

The cavity used in this thesis had been designed and manufactured by NIST, [Hua06], whose Process Measurement Division loaned to INRiM years later to keep researching the possibility to use a microwave resonator as a standard hygrometer [Cuc12]. The first tests done in this field were aimed to use this cavity to measure the water vapor fraction in air and nitrogen mixtures over a limited pressure and temperature range. Its performance was demonstrated by comparison with a calibrated chilled mirror hygrometer used as a standard by NPL [Und12].

In this work the resonator used was a QSR maraging-steel triaxial ellipsoidal cavity with an internal volume about 69 cm³, which was equivalent to a nominal average radius

³ All values indicates here for *TDL600* were those provided by the manufacturer during the test time of this thesis, thus there could be difference respect to the final and commercial version already available [MIC15].

3. HUMIDITY SENSING TECHNIQUES

$a = 2.54$ cm. The inner cavity surface was plated with a $10\ \mu\text{m}$ thick layer of gold, which enhanced the resonance quality factors and increased its chemical inertness [Cuc12].

The cavity was drilled four times, originating four inner holes with a diameter of 2.3 mm which were used to mount two microwave cables whose central conductor was terminated in two loop microwave probes for excitation and detection of both classes of TM and TE modes which belonged to the electromagnetic field transmitted through the cavity. The other two holes provided mechanical support for the inlet tube of the flowing gas sample and outlet vent within the containing vessel.

Copper plates externally joined to top and bottom of the cavity had two fold function: determining the temperature of the cavity, mounting capsule platinum resistance thermometers (PRTs); and the incoming wet gas. The cavity was contained into a vacuum and pressure vessel equipped with microwave and electrical feedthroughs.

INRiM continued studying the performance of this techniques in non- conventional gases inside of the framework of the European project ENG-01 Gas [ENG01]. For this propose, they have implemented minor modifications as the mechanical support of the QSR and its hydraulic connections to match the features and dimensions of the thermostat and the pressure vessel.

In Fig. 3.2.1, the external and internal views of the improved QSR were depicted [Und12]; and in the Fig. 3.2.m the new bigger container that houses the pressure vessel, inside which QSR was assembled, was also shown.

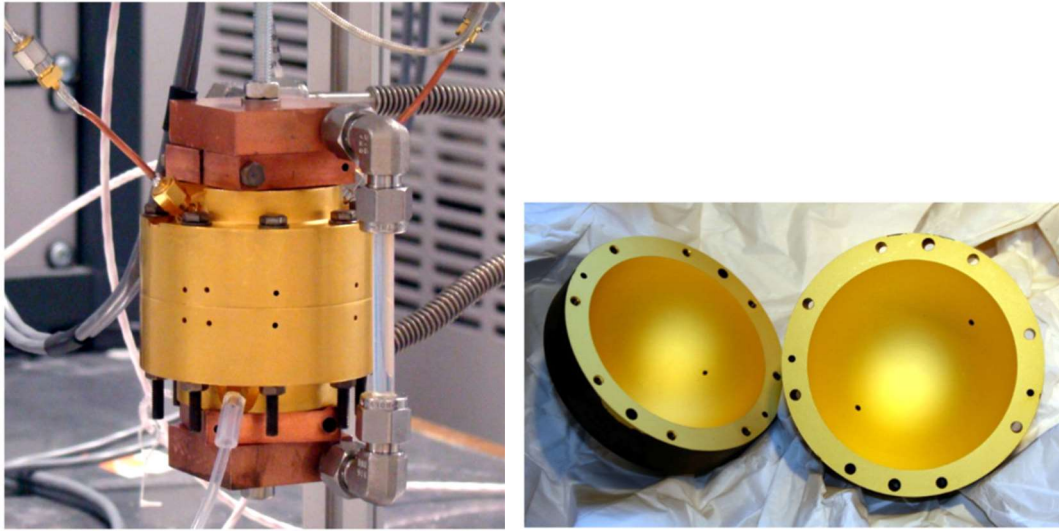


Fig. 3.2.1 Left: the external QSR view, in which it can be seen the wet gas inlet line (in the bottom) and the two PRTs on both sides of the top. In the right side of the picture, it is also shown the recirculation loop through which ethanol liquid flowed from the thermostatic bath. Right: the two quasi-hemispheres of gold-plated triaxial ellipsoidal that comprising the resonance cavity [Und12].



Fig. 3.2.m Left: the external QSR view, in which it can be seen the thermostatic loop filled with ethanol, and the two TRPs. Right: the new larger container which houses the pressure vessel before depicted in the left picture.

This instrument was a prototype still in development phase and the test done in this thesis were the first performed under real industrial conditions and measured directly from a process pipe. For that, it was not possible to describe its performance in natural gas for the most important features, as it has been done for the rest of instrument before, but this was one of the great challenges of this part of the thesis. By the other hand, and due to the development phase in which was this prototype, it has not been taken into

3. *HUMIDITY SENSING TECHNIQUES*

account its adaptation to be used in hazardous areas yet, so this instrument only can be tested in semi-industrial conditions tests.

4 EXPERIMENTAL SETUP AND PROCEDURES

In this chapter, it is going to explain all experimental setups designed and manufactured to achieve the target previously marked.

The experimental work of this thesis is divided in two big subsections (semi-industrial and industrial conditions) which are clearly separated each other, but nevertheless both are key to thoroughly characterize the performance of different humidity sensing techniques in natural gas.

Also, it must be noted that the majority of experiments performed in this thesis were carried out in Enagás facilities as stakeholder in the JRP ENG01-Gas [ENG01]. For that, we had to adjust to the facilities in which we were allowed to work and all requirements imposed by them (before and during the tests time), which were diverse nature, such as: legal, safety, knowledge and fitting to internal procedures/protocols, etc. All issues related with mutual cooperation between Enagás and INTA were detailed and signed by appropriate legal capacity persons in both parts by means of two private agreements [E&I13a, E&I13b].

Furthermore, and due to peculiarity and complexity of the microwave resonator still in development phase, a full chapter was developed to explain in detail all experiments carried out with this prototype to check its potential in hygrometric applications and concretely for natural gas. Because of this analyzer is still a prototype, it could not be tested under real industrial conditions yet, so it was assembled and compared together with the rest of sensors which were setup under semi-industrial conditions.

4.1 SEMI-INDUSTRIAL CONDITIONS

Complexity and challenges related with humidity measurements in natural gas have been already exposed the introduction. This fact, together with the great quantity of sensors compared and their individual peculiarities and characteristics, justified that the main experimental bench was mounted under semi-industrial conditions. Besides, all sensors had not certificates to be mounted and used either in hazardous areas or even outdoor simply, so it was not possible to make all experimental part in only one industrial location.

4.1.1 LOCATION AND DESCRIPTION OF THE FACILITIES

Finally, it is decided that one part of the experimental setup created for this thesis was mounted in Enagás facilities in Zaragoza, concretely inside of their Research and Development Center. This decision was taken mainly because in such building had been operating the old hygrometry laboratory of Enagás which was closed by then. This way, Dr. Angel Maria Benito and Dr. Susana Ávila, who had worked and managed such laboratory, were Enagás staff responsible for overseeing our labor in Zaragoza, besides of supporting and helping us in all issues concerning to humidity measurement in natural gas. Another reason for which this facility was chosen, was that it receives NG from regasification plants of liquefied natural gas (LNG) and from international exchanges via the national grid. Thus, the water content of NG must be very closely controlled at these points to be able to reduce the humidity locally in the case of a problem being detected at any point of the grid.

It was a privilege that Enagás allowed us to access to their facilities and take all natural gas we required for this research. Besides, location facilities in Zaragoza were ideal because if it is looked at the map of the Spanish national grid of natural gas supply (Fig. 1.3.f), it can be noted as Zaragoza is a key point in the strategic supply of natural gas in the northeastern of Spain. There, the source of natural gas can be very diverse: gas extracted and dried from the underground storages in Serrablo (close to the Pyrenees Mountains); LNG shipped by ships from around the world, stored in tanks and regasified in Barcelona; and that gas coming from France by means of the international connections of Larrau and Irún. That might lead to checking the performance of the sensors with quite diverse compositions of natural gas, depending on geographical distribution of energetic demand, which is very interesting but at the same time supposes one challenge more to this study. In the below figure it can be seen sampling point in the national grid and the rack pipe through which the natural gas is driven to the test laboratory.

4. EXPERIMENTAL SETUP & PROCEDURES

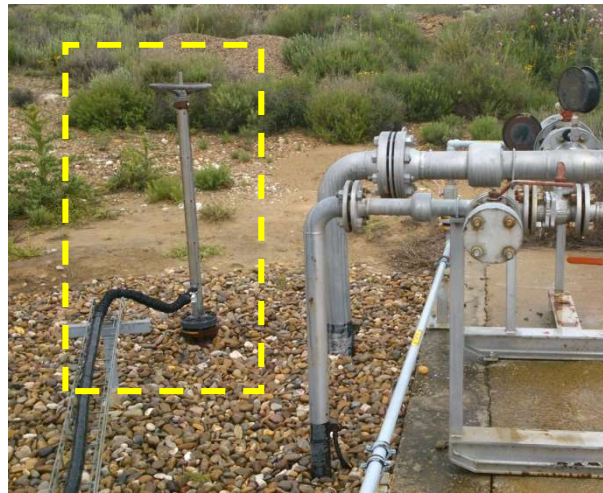


Fig. 4.1.a Top: sampling point from the main national grid of natural gas on its ways through Zaragoza. Bottom: inlet pipe rack goes from the sampling point to laboratory enabled to carry out the sensor study under semi-industrial conditions.

One of the most important advantages of this semi-industrial facilities was that the laboratory has been assigned for these tasks, it was equipped with all safety systems to guarantee the safety of people and the rest of around facilities. The safety system consisted of detectors of gas concentration in the air, protective and firefighting equipment, common vent manifold, and automatic cut-off systems both electrical power and gas inlet supply, and isolating inlet manifold. As it can see in the right picture of Fig. 4.1.b, the latest system was used as isolating system and also like first two-steps pressure regulation system, by means which the natural gas also can be depressurized up to atmospheric values, and after that to be bypassed and removed by the common vent manifold.



Fig. 4.1.b Left: the cut-off solenoid valve in a heated box which is positioned outdoor just before of gas inlet in the laboratory. Right: isolating inlet manifold and first regulation system.

This first pressure reduction system was a fix element mounted by Enagás which only was used in the first setup steps while the leak tests were carried out in the different plant sections. Once the whole experimental system had been checked the needle valve, placed in this inlet manifold, was kept fully opened.

4.1.2 HUMIDITY SENSORS STUDIED

The main target of this thesis is to evaluate and compare the performance of the traditional humidity sensing technique each other and also between the new emerging technologies currently. In the study under semi-industrial conditions of the most of instruments described in Section 3.2 were assembled and after that tested in Zaragoza facilities. Below table shows a summary of all of instruments which participated in these tests:

4. EXPERIMENTAL SETUP & PROCEDURES

Table 4.1.a General information about the instruments were studied under semi-industrial conditions in Zaragoza.

Manufacturer	Model	Sensing technology	Quantity	NPL
Michell	Condumax II HCDP	Condensation / dark spot	1	No
	Condumax II WDP	Al ₂ O ₃	1 ⁴	No
	Easidew Transmitter	Al ₂ O ₃	2	Yes
	Easidew Pro I.S.	Al ₂ O ₃	1	Yes
GE	HygroPro	Al ₂ O ₃	1	Yes
	Aurora	TDLAS	1	Yes
Alpha	DS2000	Al ₂ O ₃	1	Yes
Shaw	SDT DP Transmitter	Al ₂ O ₃	1	Yes
	Superdew 3	Al ₂ O ₃	1	Yes
Meeco	Accupoint 2 LP	P ₂ O ₅	1	Yes
E+E	EE371	Polymeric	1	No
MBW	DP3D	Condensation	1	No
INRiM	QSR	Microwave resonance	1	No

In addition, those instruments which were previously studied in NPL with nitrogen and methane at low pressure ranges were identified too. This task was performed by means of a new mix flow humidity generator which was developed in the same JRP of EMRP in the previously WP. NPL facilitated us the information about calibrations of the most of these sensors before being manipulated by us with natural gas, and they also sent us the results of checks carried out by them after the tests in Zaragoza. That way, the likely effects due to flow natural gas through these sensors may be analyzed and quantified comparing both datasets. In Section 5.1, such results have been shown, compared and analyzed.

4.1.3 EXPERIMENTAL SETUP

This section will explain in detail everything related with humidity measurements made on sensors listed above in Enagás facilities in Zaragoza. It will be described and justified all components fitted in the experimental setup created for this occasion. Besides,

⁴ The Condumax II is fitted with two sensors which detect WDP and HCDP, simultaneously. Thus, only one Condumax II unit was used.

it will be explained all process variables taken in count in this experimental stage and how they were controlled, recorded or only fitted depending on the kind of test performed. In addition, all measuring procedures carried to achieve the goals proposed in this part of thesis will be reported, together with those "secondary" procedures which are absolutely necessary to get accuracy and reliable measurements from all instruments analyzed.

4.1.3.1 Introduction

Prior to describe experimental setup built for semi-industrial tests, it is very important to know the main requirement which was used to distribute all sensors listed in Table 4.1.a within the whole experimental rig.

Due to the great number of sensor analyzed here, 14 concretely, and the large variety of sensing technologies employed, 6, some features of these sensors may be quite different among them. However, beyond any property there is one especially important: the work pressure range. Such property is key not only to safety of sensors but the staff who manipulate this experimental test bench as well. In the following table, the pressure ranges of all tested sensors are shown and also depicted in the following graph (Fig. 4.1.c).

Table 4.1.b Summary of work pressure ranges of all devices handled.

DEVICES	LIMITS, MPa	
	Lower	Upper
<u>HUMIDITY MEASUREMENTS</u>		
<i>Condumax II HCDP</i>	0.0	10.0
<i>Condumax II WDP</i>	0.0	13.9
<i>Easidew Pro I.S.</i>	0.0	45.0
<i>Easidew transmitter</i>	0.0	35.0
<i>Cong Prima 10</i>	0.1	10.1
<i>Aurora</i>	0.0	1.4
<i>HygroPro</i>	0.5	3.6
<i>Accupoint LP 2</i>	0.1	0.8
<i>SDT DP Transmitter</i>	0.1	35.0
<i>Superdew 3</i>	0.1	35.0
<i>DS2000</i>	0.0	3.0
<i>DP3D</i>	0.0	10.0
<i>EE371</i>	0.0	10.0
<i>QSR</i>	0.0	1.5
<u>PRESSURE TRANSMITTERS</u>		
<i>PTX 510</i>	0.0	20.0
<i>PTX610</i>	0.4	20.0

4. EXPERIMENTAL SETUP & PROCEDURES

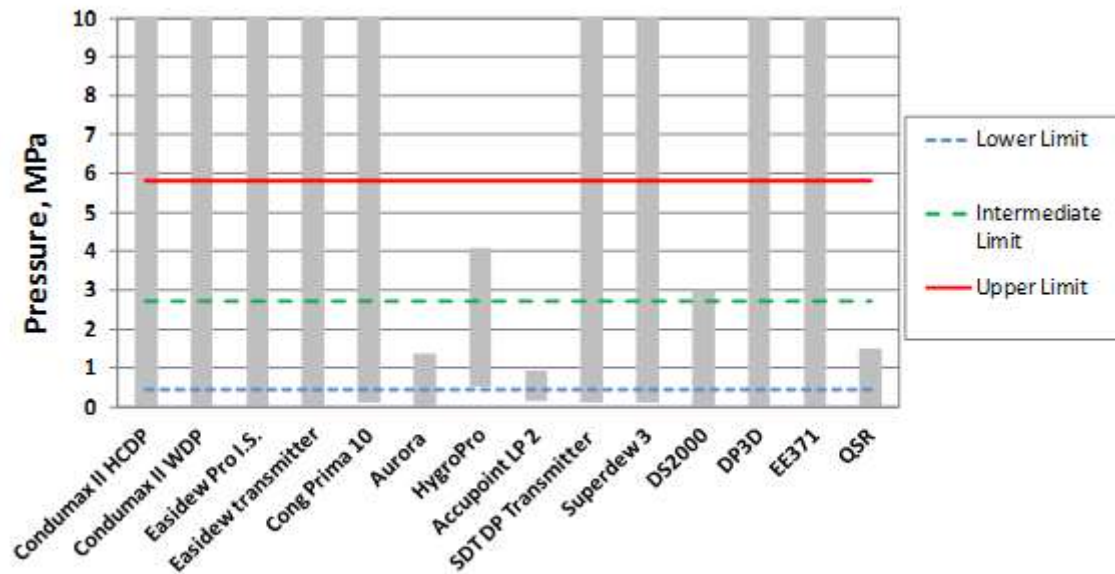


Fig. 4.1.c Summary of the work pressure ranges of analyzed sensors and the work pressure limit chosen to carry out the tests under semi-industrial conditions.

As it can see in the above graph, three nominal pressure values were chosen to be able to measure all instruments at least at one pressure level. The pressure levels selected were next:

- Lower level, at a nominal absolute pressure equal to 0.55 MPa. This way Aurora and Accupoint could be compared.

- Medium level, at a nominal absolute pressure equal to 2.8 MPa, to measure as high as possible within the range of HygroPro and DS200. Besides, this pressure level should be close to the cricondentherm of the natural gas which means that, the maximum value of HCDP could be achieved at this pressure level. For that, this pressure level is quite interesting from industrial point of view.

- Upper level, to be able to compare the instruments at the maximum line pressure given by the pipe which come from sampling point shown in Fig. 4.1.a. This value was approximately 5.8 MPa. Measure under this conditions is especially important to natural gas industry, because according to the current specifications in the transmission of natural gas within Europe, the WDP must be measured at 7 MPa or the maximum pressure line [EAS05].

Some components that were used in the experimental setup built for this occasion, were loan by Enagás from their old hygrometry laboratory and their test bench designed by Ávila [Avi99], e.g. the reducing pressure valves equipped with self-heating or the saturator which will be explained below. Because of those components had not been used during years, hydrocarbon residues were present in wet parts of them, even blocking completely the gas flow, as it can be seen in Fig. 4.1.d.

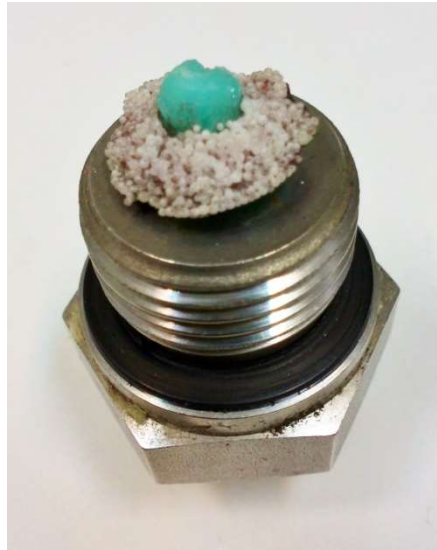


Fig. 4.1.d Real picture taken of fitting which was mounted at the bottom of the saturator (see Fig. 4.1.m), and that it had been previously built and used in the bench test of old hygrometry laboratory of Enagás. Here, it can be seen a clear example of a pipe totally blocked by hydrate formation. Besides, two different ways to crystallize can be appreciated: whitish structure made of white small spheres similar to ice, and another bluish green compact and uniform crystalline structure.

For that, all items which were reused suffered a thorough cleaning system to erase any impurity which might affect the results given in this thesis. The cleaning protocol consisted of immersing those components into a thermostated ultrasonic bath which contented aqueous mixture with industrial cleaning products at 40 °C. The cleaning process lasted 10 min and it was repeated but changing the water and adding cleaning product again, until the water was not exhibited turbidity that evidences still the presence of contaminants. In the Fig. 4.1.e it can be seen the cleaning process described above over some elements that were reused.

4. EXPERIMENTAL SETUP & PROCEDURES



Fig. 4.1.e Cleaning process of all elements that belonged to the old hygrometry laboratory of Enagás, by means of ultrasonic bath with industrial cleaning products mixed with water.

4.1.3.2 Description and diagram

The test rig was designed in order to be able to perform all the measurements in one system, needing only to modify the valve configuration in order to control the pressure, flow-rate and direction of flow of the natural gas sample. All the components of the sampling system in contact with the gas were high-quality electro-polished stainless steel and polytetrafluoroethylene (PTFE) in the sampling system and the low-pressure vents, respectively.

The design and mounting of the experimental bench of this section were carried out in compliance with the recognized good practice applicable to the installation of pressurized natural gas sampling systems [G&B08, ISO97a and ISO97b].

First of all and to understand more easily the running of the experimental setup and each of sections in which was divided, this has been simplified in a schematic block diagram of the whole installation by means which can be compared the behavior of the most of humidity measurements at the same time.

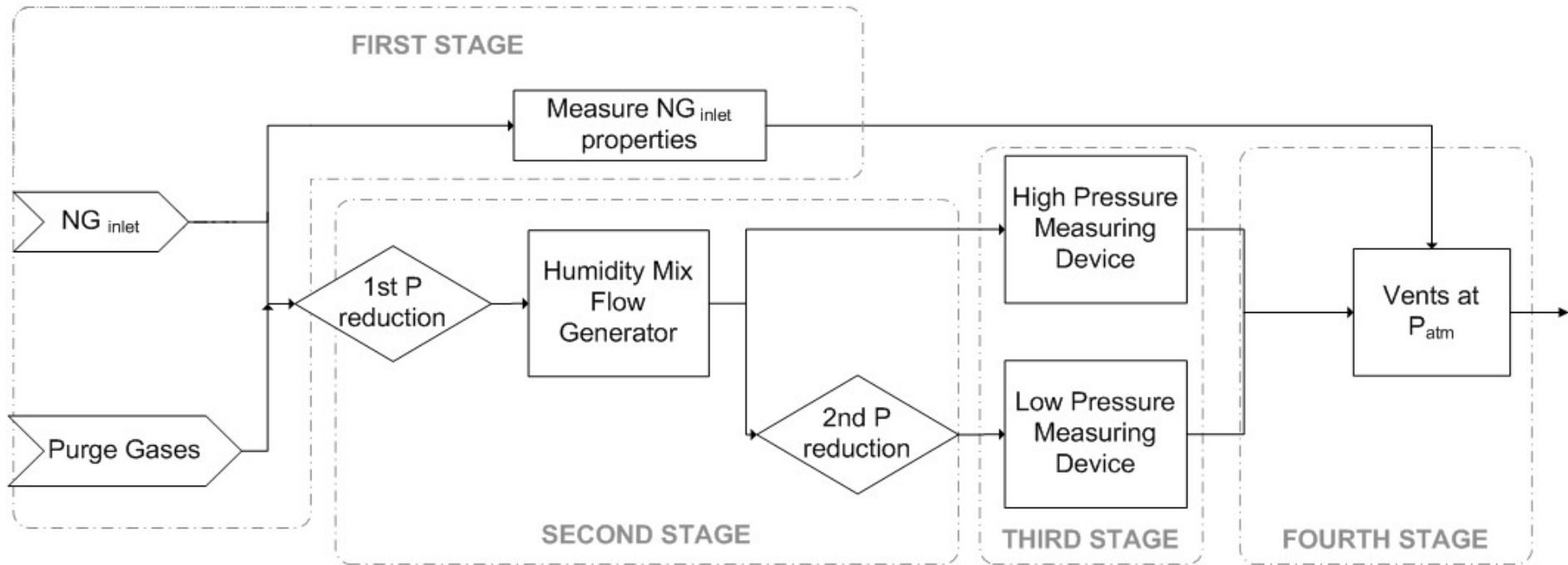


Fig. 4.1.f Schematic block diagram of the experimental setup built to carry out the comparative study of the diverse humidity sensing techniques under semi-industrial conditions.

4. EXPERIMENTAL SETUP & PROCEDURES

Fig. 4.1.j shows the complete installation which can be divided in four main sections as it is explained as follows:

- Section 1: input section constitutes the first part of the plant which includes all input lines of those substances (gases or liquids) which were needed during the test time and the other secondary tasks were also needed as: leak tests, saturator fill up, etc. All substances used in this experimental setup, besides of the natural gas, were:

- *Nitrogen* was used for two reasons: safety and cleaning element, being this latest very important to keeping clean the humidity sensors. As safety element, nitrogen had two missions: as purging element to displace the natural gas after having performed tests with it (decreasing the concentration of fuel and oxidant which are essential to produce any combustion or flame process) and as leak detector using soap solution.
- *Helium* was also used as leak detector too but in this case it was necessary a helium detector (See Section 0).
- *Water* was used to fill up the humidity saturator, which is necessary to vary the water content of natural gas to check the behavior of sensors within an interesting range for the industry.

This section also includes measuring and recording the natural gas properties when goes into the laboratory. This target was subdivided in two tasks:

- Measure and record the humidity of natural gas which arrived to the experimental rig. Besides, the line pressure should be recorded to convert the humidity in water dew point units. This task had to be done by one of the humidity sensors loaded for this study. The explanation about the choice taken has been developed in the Section 4.1.3.3.1.1
- Measure the composition of NG according to the European Standard ISO 6974:2003 [ISO03]. This activity has been described more in detail below in the Section 4.1.3.3.1.2.

- Section 2: in this phase the natural gas properties are adjusted according to the set point chosen for each single test. This section guarantees that gas properties, before entering in any humidity sensing studied, are optimal and within of their work ranges.

The quantities controlled and fitted here were pressure, flow and humidity; such regulator systems are explained more in detail in next section.

It must be indicated that this phase includes one last filtering system with a coalescing filter, also named *membrane filter* because is constituted by several membranes parallel to each other and perpendicular to the gas flow direction. Thanks to this system, if some water droplet is dropped after crossing the saturator, it will be adsorbed when crosses the filter [ISO97a and b].



Fig. 4.1.g Membrane filter model Avenger 38M assembled just downstream of the humidity generator.

- Section 3 involves all sensors under study in this work. The main problem of this section was the great quantity of instruments analyzed and that the best way to compare all of them simultaneously, it would be assembling them in parallel branches to minimize the interaction each other, that would affects directly final reliability of measurement. However, this fact would imply to multiply enormously the equipment required for this task and complexity of the experimental setup and its handling. For that, it was looked for the best balance between both effects and the decision finally taken was a hybrid system in which the humidity sensors will be distributed in parallel branches and at the same time in such branches there will be sensors assembled in series.

Firstly, the sensors were grouped according to the pressure ranges defined, after this criteria they were paired by their optimal nominal flow. From this first criteria the humidity meters were classified in two groups: *low pressure* and *high pressure* measuring device (see Fig. 4.1.c). First group only contains the Aurora and the Accupoint 2 LP, *line 2* and *line 3*; while the second group, constituted by six lines, has the rest of humidity detectors. Numbering lines can be seen in Fig. 4.1.j.

In concordance with the first criteria, HygroPro and DS200 were assembled in the same line because they cannot afford the maximum pressure line that was close to 6 MPa (see Table 4.1.b and Fig. 4.1.c). Regarding to the second criteria, Michell's sensors were

4. EXPERIMENTAL SETUP & PROCEDURES

grouped in the same pipe and the same happened with Shaw's probes. However, EE371 and condensation hygrometer of MBW (DP3D) were mounted alone in different lines.

The quasi-spherical microwave resonator was assembled completely in parallel with the rest of instruments integrated within of the *high pressure* group. This way and due to this instrument developed by INRiM had much more complexity, it was not affected by the rest of analyzers.

In this third area, it is important to explain another two issues more: firstly, in all lines upstream to the first humidity instrument, one valve was placed to isolate the sensors from several reason (safety, leak tests, these device do not afford the maximum pressure level and they must be bypassed, etc...) [ISO97a and b]; secondly, one pressure transmitter must be mounted in the line where a condensation hygrometer (e.g.: DP3D) has been set up with the aim of being able to exchange WDP measurements in water content units, or vice versa [ISO04].

All details explained here can be seen in Fig. 4.1.j in which the whole P&I diagram of the experimental setup built in Enagás facilities in Zaragoza has been depicted.

- Section 4, makes reference to the outputs from all humidity measuring systems. Such outputs went to a collector pipe depressurized which vents to the atmosphere. All lines which went out from any sensor must contain the following sequence of components: a needle valve to reduce the pressure down to atmospheric pressure levels, after a flowmeter in charge of regulating and controlling flow which crosses the instrument, and finally, one non-return valve to avoid potential interference among lines because of small back pressure effects. Fig. 4.1.h shows the classic scheme of a sampling system associated with any humidity analyzer used in natural gas [ISO97a and b]:

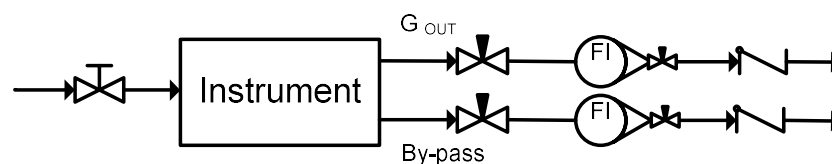


Fig. 4.1.h Scheme of flow and pressure control system applicable to all instruments. The by-pass line is not always mandatory.

Thanks to the needle valves positioned downstream of any humidity measuring instrument, the flowmeters mounted do not need to be specially built to endure high

pressures, because the pressure is decreased down to atmospheric levels by such valves. This way, the regulating valves associated with the flowmeters will only fit the flow in the line in which they have been positioned.

Alphabetic code used in all P&I diagrams depicted in this thesis to name all devices assembled in the experimental setup has been explained in nomenclature and it agrees with the American National Standard ANSI/ISA-5.1 [ISA84].



4. EXPERIMENTAL SETUP & PROCEDURES



Fig. 4.1.i Photograph of the test rig. Top: on the left, the two low-pressure devices (spectroscopic and electrolytic P_2O_5), can be seen at the back and center with the two chilled mirror instruments at the front. The rest of the sensors are connected behind these. Bottom: On the top left is the data acquisition system and the electronic displays and power supplies of the different analyzers and just below is the control panel with the three sampling lines. On the right is the instrument used to monitor the gas inlet conditions (HCDP and WDP).

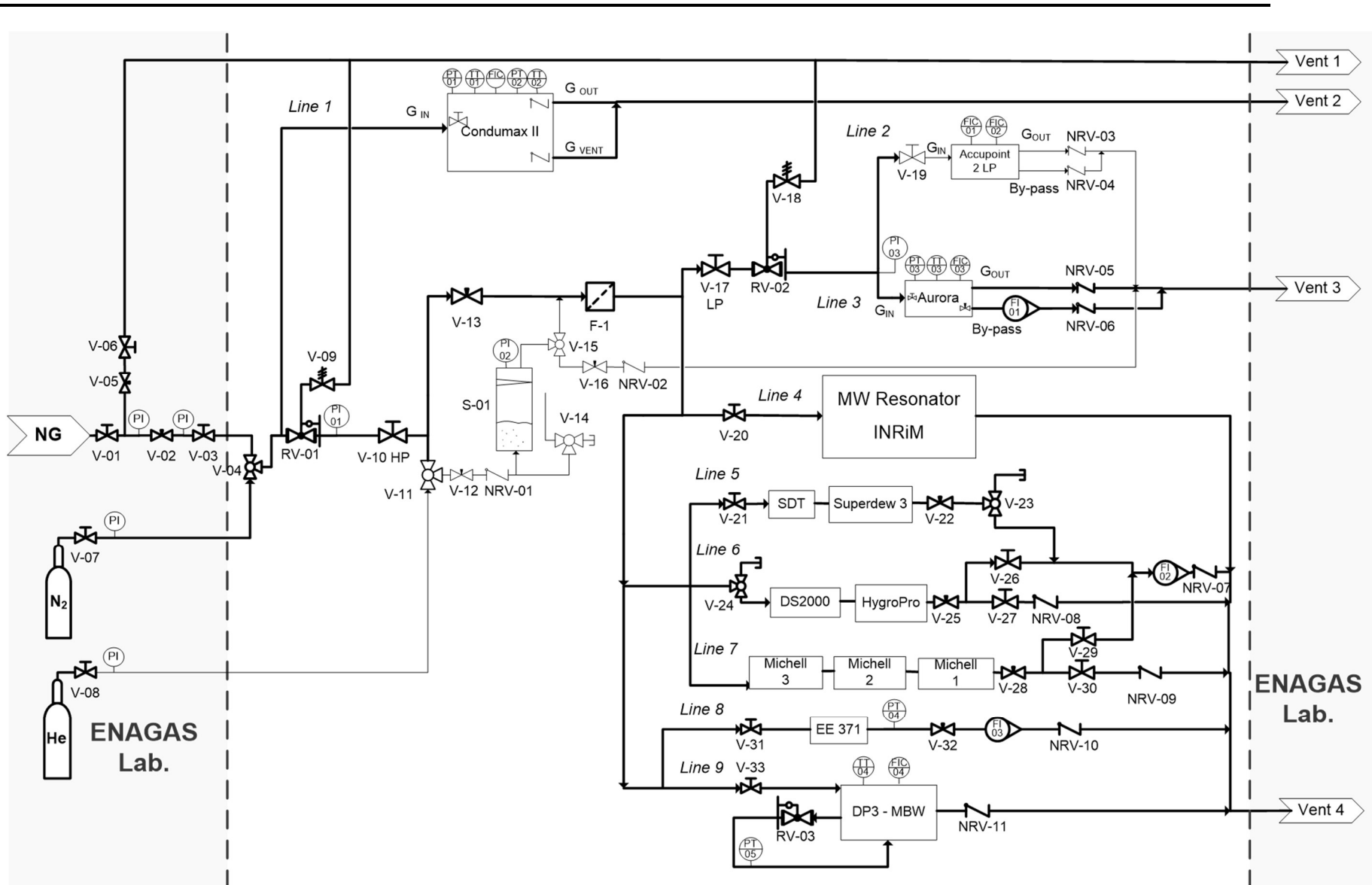


Fig. 4.1.j P&I diagram of the whole experimental setup built in Zaragoza to carry out the study of behaviour of all sensors under semi-industrial conditions. The fine lines depict the pipes with nominal diameter equal to 1/8", while the thick lines shows the pipe section built with nominal diameter equal to 1/4".

4.1.3.3 Process variables. Measurement and control.

To know the process variables of this experimental rig is absolutely necessary to have full control of the plant and thereby, to be able to study the behaviour of all humidity sensors under the desired conditions.

Three types of control instruments were used depending on purpose desired:

- *Indicators*, which simply inform the current values of the measured quantity. In this case, pressure gauges, named PI in the P&I diagrams (Fig. 4.1.j and Fig. 4.1.s) [ISA84].

- *Transmitters*, charged with recording the values of the quantities measured as a function of time, so that afterwards all data recorded can be processed.

- *Controllers or regulators* are all those devices that are able to measure and also change the quantity measured at the same time. Some examples of this kind of instruments are: the regulator pressure valves (denoted as RV) and the flowmeters fitted with their own needle valves.

In this section, all process variables which were controlled have been described because they may affect to the humidity measurements in natural gas under semi-industrial conditions. Also, it will be explained how these quantities were recorded and controlled.

All control and monitoring devices used to record the process variables (e.g. gauge pressure transmitters, flowmeters, platinum resistance thermometers, data loggers, etc.) were calibrated at INTA prior to the assembling and the necessary corrections applied were included in the subsequent data analysis.

4.1.3.3.1 *Properties of the natural gas inlet*

Measure and record the water content of NG, which arrived to the facility where experimental setup was located, was essential because the inlet of natural gas directly came from the national grid of Enagás in its way through Zaragoza. That means the composition, water content and any other NG property were constantly changed. Thus, to evaluate correctly the behaviour of the humidity sensors, it was mandatory to know fluctuations of such quantities in the inlet, to evaluate potential disagrees among analyzers.

The source of these disturbances depends on the origin of the gas which was being flowed in that time by Zaragoza (e.g.: from underground storages, drying plants LPG regasified or gas from Russian or Maghreb line). By the other hand, it cannot be forgotten inherent industrial nature at this process, so any change in process variable due to maintenance tasks or any trouble which implies manipulate whatever parameter of the network, it will affect directly to the gas properties, including composition and definitely the water content.

4.1.3.3.1.1 Water and hydrocarbon dew point

The current specifications that must be met in the NG transmission grids within Europe were defined by the European Association for the Streamlining of Energy Exchange - gas (EASEE-gas). In the case of hydrocarbon dew point (HCDP) it must be lower than $-2\text{ }^{\circ}\text{C}$ at any pressure between 0.1 MPa and 7 MPa. For water dew point (WDP) it must be lower than $-8\text{ }^{\circ}\text{C}$ at 7 MPa [EAS05]. These criteria must be met in international connections but it is not mandatory they must be achieved within the national borders of any country. In this sense, the internal specification to transport ng in the Spanish national grid is less restrictive. Enagás establishes that the WDP of the final product which arrives to the customer cannot exceed $+2\text{ }^{\circ}\text{C}$.

Such activity had to be performed by one of humidity sensors loaned for this project. The Condumax II was chosen as the best choice available, because of it was the most qualified instrument according to following points: its own sampling system which allow to be assembled directly in the high pressure line without not requiring anything more because it is equipped with its own filtering system, pressure regulators and drain and by-pass lines. In addition, the Condumax II is able to measure the water content as WDP at the actual line pressure, as well as the HCDP. For all of that, this instrument was the best choice to get a full record of the HCDP, WDP and line pressure of the natural gas inlet during the whole test time.

4.1.3.3.1.2 Composition

In order to perform the necessary unit conversion between the different ways to express the humidity in a gaseous matrix of NG, as WC or WDP, gas composition was necessary [ISO04]. This was essential because the gas sampled from the main transmission pipeline was not a standard mixture with steady and known composition,

4. EXPERIMENTAL SETUP & PROCEDURES

but a system under continuous change depending on the demand and origin of the NG transported.

For that, headquarter laboratory of Enagás provided us the results of daily gas composition analysis throughout the entire test time. Composition studies was performed using gas chromatography (GC), providing the content of N₂, CO₂ and hydrocarbons since methane to hydrocarbon fractions constitute by twelve carbon atoms, C₁₂.

Measures of NG composition were made according to the European Standard ISO 6974:2003 [ISO03], which establishes how calculate composition and associated uncertainty for each component presents within gaseous matrix. This task was carried out by means of gas chromatography HP-6890 model.

From these composition analyses, many others physical and chemical properties could be determined. Applying the European Standard ISO 6976:2005 [ISO05b], it was obtained the following properties: *lower and higher heating values* (LHV and HHV, respectively), *relative density*, *compressibility factor* and *Wobbe index*. By the other hand, if the European Standard ISO 15403:2006 [ISO06] was applied, it would get a parameter called *Methane number*, which gives an idea about the quality of NG.

4.1.3.3.2 Pressure

The pressure played a very important role in the hygrometry field, especially when the humidity was expressed as dew point temperature, and it also was an essential quantity for correlating with other ways to express the humidity in gases, as the water content (WC) [ISO04]. Therefore, this quantity had to be measured and controlled very well during all tests made on the humidity probes to make the properly correlations between the different humidity units given by the great diversity of sensors. The maxima pressure data in the whole experimental setup were those recorded by the pressure transmitter assembled inside of the own sampling system of the Condumax II, because no gas pumping system was used.

As it has been already explained, besides of the named *maximum pressure level*, another two more levels were configured by means of two pressure reducing regulators, also called *reducing valves* and denoted by the acronym RV. These two pressure reducing steps were performed by two heated regulator models, which decreased the pressure down to an adjustable set point.

The first two pressure reducing steps were carried out by two heated regulators belonging to *AVR-2* series (RV-01 and RV-02). It was essential to use this kind of heated regulators to avoid potential condensation problems originated by the cooling effects, which usually occurred in strong expansion processes of a gas stream due to the well-known Joule-Thompson effect. Another reason more by which these pressure reductions were one of the most critical point of the rig, it was due to its relatively large inner surface area, namely the internal volume, that would play a role similar to a condensate trap, so it would work like a gas humidifier. The first regulator decreased the pressure down to 2.70 MP and the second fitted the output pressure at 0.45 MPa (see Fig. 4.1.j and Fig. 4.1.k).

In addition, another reducing valve (RV-03) was fitted together with the chilled mirror hygrometer *DP3D*. The goal of this valve was to reduce the pressure in the measured cell at atmospheric values, avoiding having to recalculate the dew points measured later. The *IR401S* model was used in this case, whose main feature was that it was not equipped with heating system. In the three cases the reducing valves were manufactured by Veriflo Corporation and their main properties can be seen in Table 4.1.c and their look is shown in Fig. 4.1.k.

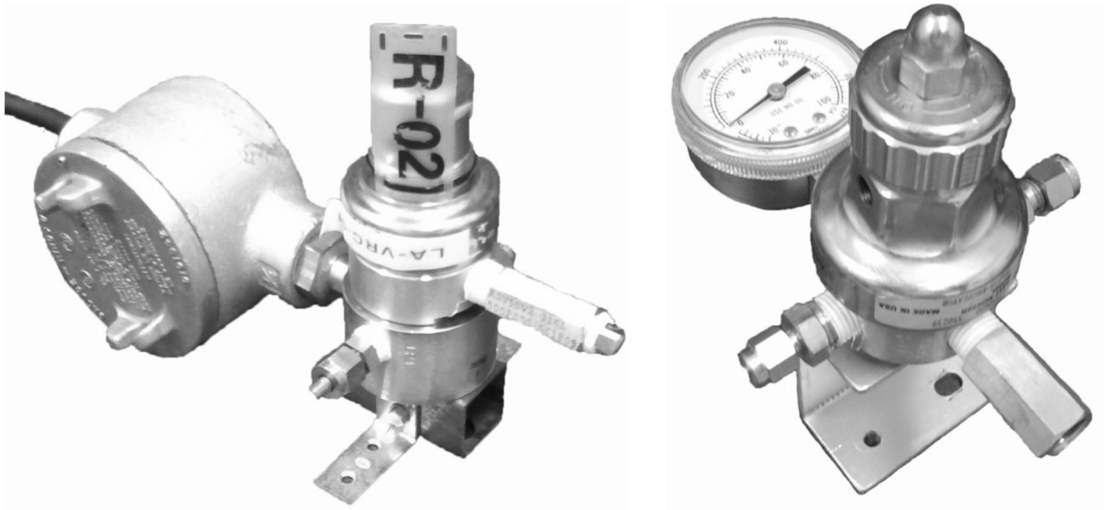


Fig. 4.1.k Real pictures of pressure reducing regulators setup in Zaragoza facilities. Left: heated regulator RV-01 and RV-02 used in the first and second reduction stage, respectively. Right: the RV-03 assembled just before the inlet to the measured cell of the chilled mirror hygrometer.

4. EXPERIMENTAL SETUP & PROCEDURES

Table 4.1.c The main features of the pressure reducing valves used in the experimental facilities built to tests under semi-industrial conditions.

Numbering Code	RV-01	RV-02	RV-03
Model	AVR2-S-K-5	AVR2-S-K-4	IR401-S
Max. Inlet Pressure, MPa		24.1	27.6
Outlet Pressure Range, MPa	0 to 3.45	0 to 1.72	0.01 to 0.7
Flow Capacity (c_v)		0.06	0.13
Gas temperature, °C	- 40 to 260		- 40 to 66
Heater	Yes	Yes	No

By the other hand and as it can see in the P&I plant scheme (Fig. 4.1.j) and in the pictures of the pressure reducing regulators (Fig. 4.1.k), one relief valve was associated with each heated regulator and they were positioned in one outputs of such regulators. Its numbering codes are V-09 and V-18, respectively. They were responsible for ensuring that the pressure in the outputs of the regulators did not exceed a maximum value set. This way, the integrity of the humidity sensors was kept all the time and any potential risk situation was also avoided. The relief valves were set at 2.8 MPa and 0.55 MPa, that is to say 0.1 MPa over the pressure set points established in the tests.

Two kind of pressure transmitters were used to record the pressure data during the tests: barometric and atmospheric pressure transmitters. The first instruments measure the relative pressure of the NG that was flowing, while the second kind measures the atmospheric pressure because of the air that involves the laboratory in which this experimental section was set up. Thus, the total pressure in any point of the experimental rig could be known adding both quantities. Position of the relative pressure transmitter should be closely linked to the three pressure reducing regulators to be able to know the total pressure in all lines in which humidity analyzers were assembled (see the plant diagram Fig. 4.1.j.).



Fig. 4.1.1 Left: relative pressure transmitter PTX-610 model (PTX-510 has the same external look). Right: Digital pressure indicator DPI-265 model with remote transducer used to record the atmospheric pressure.

The relative pressure transmitters used in this section were manufactured by Druck and two models were used: *PTX-510* and *610*. Regarding to the atmospheric pressure the model used was the *DPI-265*, also manufactured by Druck. These models are depicted in Fig. 4.1.1., and their main features are summarized in Table 4.1.d. Besides, it is important to denote that all these pressure sensors were calibrated previously in INTA.

Table 4.1.d The main features of the pressure meters used in the semi-industrial experimental section.

	PTX-510	PTX-610
Measure Range, MPa	0 to 20	0.4 to 20
Accuracy, % FS	± 0.15	± 0.08
Long term stability, % FS· y⁻¹		0.1
Gas temperature, °C	- 29 to +121	
Power supply, V DC	9 to 30	
Outputs, mA	4 to 20 (Analogue)	

4.1.3.3.3 Humidity

The humidity evidently is the key parameter when it wants to study the behaviour of different humidity sensing techniques. For that, the need to generate multiple humidity levels to evaluate the analyzers within interesting range for the NG industry was a requirement absolutely essential when the experimental setup was being designed. Thus, a humidifying system had to be implemented within the whole experimental rig.

By the other hand, for a couple of days after starting to run the experimental setup in Zaragoza, it was checked that the NG which came into the laboratory was very dry and

4. EXPERIMENTAL SETUP & PROCEDURES

the WC readings were not higher than 6 ppm_v which, making a rough approximation, would amount to a WDP lower than -30 °C at a usual maximum pressure line of 5.5 MPa. This value was well below from the European specification which must be met in international connections, -8 °C at 7 MPa [EAS05]. Besides, these values were very close to the lower detection limit of the most of instruments, so it was imperative to get the capacity to increase, and decrease, the humidity of the natural gas controlled manner.

In this chapter, it is going to explain everything related with the mechanism to generate and modify the water content of the natural gas which was arriving to the experimental facility. That includes a deep description of the humidity generator used and its associated installation, besides of all protocols related with it.

Humidity generator. Description and diagrams

The core of the humidity generator is the saturator. This specific component was designed and built by Enagás, to be used in its old hygrometry laboratory, and besides was used by Dr. Susana Ávila in her PhD thesis to create countless humidity measurements on synthetic wet NG with and without methanol [Avi99]. This saturator was loaded to INTA to meet the aims targeted for this work.

The saturator scheme, presented in Fig. 4.1.m, was built according to the drawings developed by ITTK (Institut für Technische Thermodynamik und Kältetechnik) at the University of Karlsruhe in the development of an experimental dew point generation plant [Noë95].

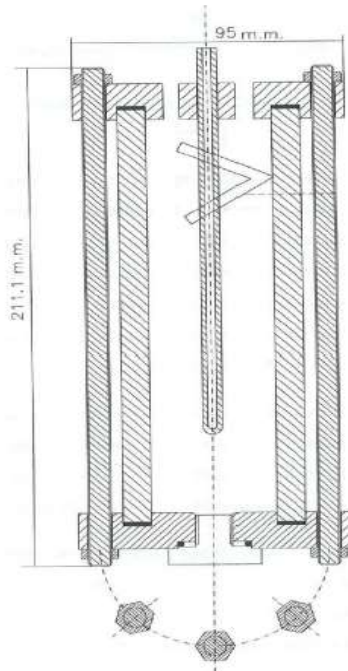


Fig. 4.1.m Look of the saturator used as the main element of the humidity generator. Left: drawing used by Enagás to build the saturator [Avi99]. Right: Real picture of the saturator.

As it can see in the sketch depicted in Fig. 4.1.m, the saturator is a vertical cylinder with two covers positioned in the top and bottom, which have thickness slightly higher than the own cylinder. The saturator input is in the central axis of the bottom, while in the top there are two outputs with the same diameter and equally separated from the center. This element was designed to endure pressures higher than 9 MPa, including the corresponding safety factor. The covers were fitted between themselves thanks to eight threaded rods located around the outside of the cylinder. All elements of the saturator were made of stainless steel. Inside of the cylinder in the upper part just before to one of the outputs, and horizontal V-shape mist separator was assembled to avoid any water droplets can be dragged by the NG, reaching even the measurement cells of humidity sensors.

Once the saturator has been characterized as the key component of the section of the plant responsible for humidifying the gas, it must be explained how it works. For this occasion a mix flow humidity generator was chosen as the easiest way to control the humidity of the NG. This kind of generator is based in two lines, *dry line* and *wet line*. The dry line is the main stream and the most part of the NG flow crosses it. The wet line

4. EXPERIMENTAL SETUP & PROCEDURES

receives this name because the saturator is positioned there, so it is where the gas wetting process takes place. The wet line comes from the dry line and once the gas crosses the saturator returns to join with the main gas stream. Therefore, the mechanism of this kind of the humidity generators is based on the next idea: when the flow ratio between both lines changes, the resulting water fraction will vary too. This way, if the NG flow that crosses the saturator increases, the final WC when the NG leaves this section of the plant will grow too.

In both lines one needle valve was assembled to get an accuracy flow control and therefore an accuracy humidity generation skill. One non-return valve was assembled just before the inlet to the saturator to avoid water droplets were transported in reverse sense to the normal gas flow, even reaching the dry line. Besides of all of this, the membrane filter (see Fig. 4.1.g), was mounted right downstream to the junction between lines, avoiding this way that any water drop can arrive to the humidity sensors, which may damage some of them or in the best case give false humidity readings. All these component, and another more related with the saturator, can be seen in the following diagram (Fig. 4.1.n), which shows more in detail this section of the plant and in Fig. 4.1.o it can be seen the final actual look.

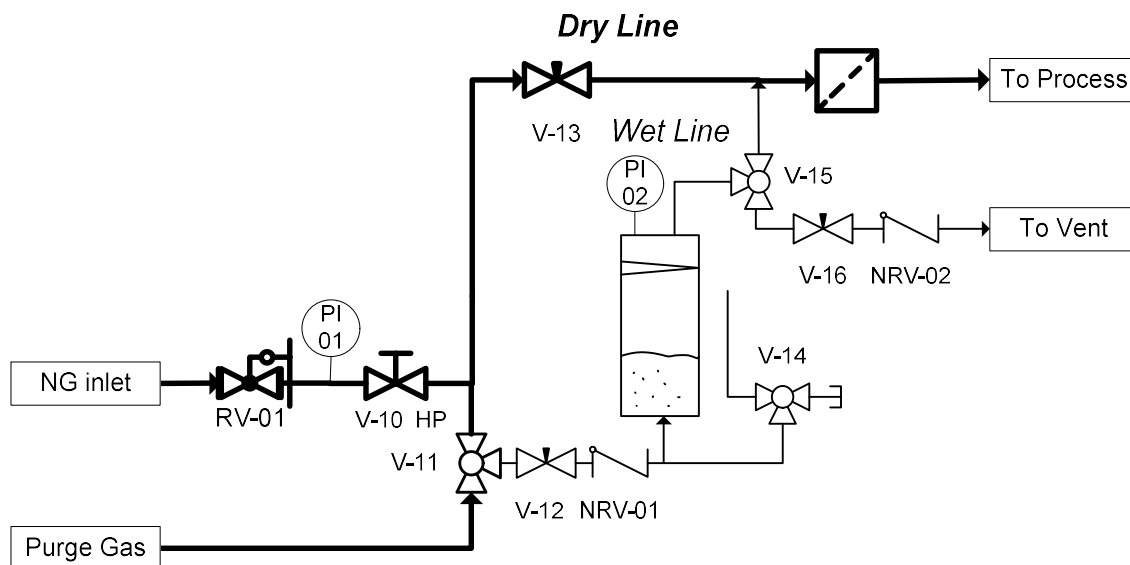


Fig. 4.1.n Scheme that includes the first pressure reduction step and the mix flow humidity generator, necessary to wet the NG. This configuration allows humidify the gas, besides of filling and purging the saturator.

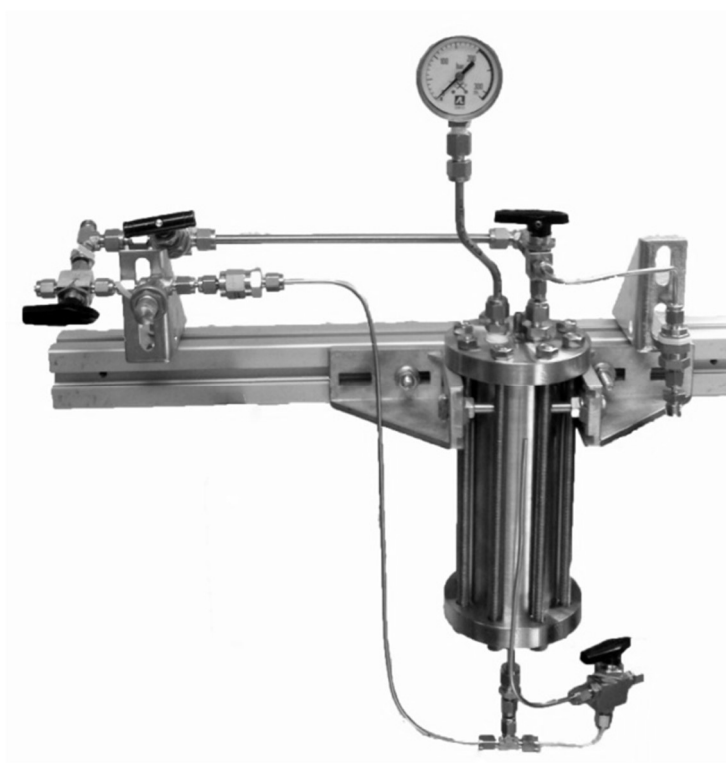


Fig. 4.1.o Real picture of the section of the experimental setup responsible for humidity changes in the natural gas.

Humidity generator. Characterization test

Mix flow generator was the chosen option to generate different humidity levels. As it has been explained before, the mix flow ratio, between *dry and wet* lines, determines the final water content in the NG. Therefore, known mix flow ratios will lead to desired humidity values, called hereinafter *nominal humidity values*. This statement will be right only when the following assumptions are met:

- Firstly, it is supposed that the water content that arrives to the laboratory is relatively steady. That statement is based on the water content of the NG that comes from the national grid is so low that small disturbances will affect very little in the final water content achieved in the outlet of the humidity generator. Besides, these disturbances in the WC in the inlet NG were recorded by the Condumax II during the whole test time, so its effect can be evaluated later. This error source could have been removed implementing a powerful drying system at the beginning of the experimental rig, but it would be lost the initial idea of compare all instruments under semi-industrial conditions, with every problems that entails.

4. EXPERIMENTAL SETUP & PROCEDURES

- Secondly, it is supposed that the temperature into the laboratory is stable enough in comparison with a real outdoor process. For that, the temperature at which the phase equilibrium was produced was not controlled. However, the room conditions in the laboratory did were recorded, if it was necessary include these factors in the study of the behaviour of the different humidity sensing techniques in NG.

The way to change the mix flow ratios between both lines were varying the opening of the needle valves assembled in such lines. To simplify the protocol to change the nominal humidity value generated, the needle valve of the dry line (V-13) was completely open, while the needle valve in the wet line (V-12) was actually the only valve handled. The protocol to characterize the humidity generator consisted on increasing the opening of V-12 gradual and controlled way, measuring the humidity recorded by the analyzers once the signals were steady. Three instrument based on three different measurement technologies were used for that: Aurora, Accupoint and HygroPro based on spectroscopic, P₂O₅ electrolytic cell and Al₂O₃ capacitive sensor, respectively. Finally, the final humidity values were recorded according to the opening of V-12.

In the case that, the humidity values would had been too low regarding to the interesting range for the NG industry, it should have been repeated the same protocol but now in the first place, the needle valve positioned in the dry line (V-13) must be closed slightly.

Humidity generator. Protocols filling and emptying

This protocol describe the method used to fill up the saturator when the NG is being fluidized through it, ergo, the pressure inside the saturator is the same that the wanted process pressure. Next, the saturator filling protocol is describe in detail, while for the emptying protocol only have to do until the 8 point, inclusive.

1. Connect the pressurized cylinder with N₂ and its own pressure regulator in *purge gas* line.
2. Close the valve V-16 completely.
3. Change the valve V-15 to *vent*.

-
4. Adjust outlet pressure in the pressurized cylinder of N₂ slightly higher than the operation pressure, to avoid strong changes in the plant because of difference pressure levels.
 5. Modify position of V-11 to *purge* gas, where N₂ bottle is connected. Now the saturator section is completely isolated.
 6. Open slowly the valve V-16 to flush the remaining NG inside the saturator. V-16 must be slightly open to reduce the pressure of stream which is flowing to vent at atmospheric levels. Continue flushing with nitrogen for 5 min.
 7. Close the nitrogen supply coming from the pressurized cylinder, and waiting until the saturator pressure decreases below to 0.5 bar.
 8. Place a glass beaker in the drain point and open the valve V-14 to empty from the saturator. Measure the collected water, to know the water that has been used during the previous tests.
 9. Turn the valve V-14 towards the cup and waiting until decreasing to zero the pressure inside the saturator, shown by the manometer PI-02.
 10. Open the saturator by the place where the pressure gauge is setting up and that will be used to fill up the saturator now.
 11. Fit the funnel in such point and addict 100 mL of deionized water. To easy filling it may be necessary flowing N₂ at 1.5 bar to help out the air inside the saturator.
 12. Fit again the manometer PI-02 in the same point.
 13. Slowly increase the pressure of N₂ to achieve close level than the process pressure set. At the same, the air is being dragged by the vent line, avoiding a potentially explosive mixture when the NG starts to flow through the saturator.
 14. Carry out the leak test with soapy water in these point which had been modified in this section of the plant. (Protocol describe in Section 0).
 15. Slowly change the position valve V-11 and slightly open the needle valves V-12 and V-16 to delete the remaining wet nitrogen inside the saturator line.

4. EXPERIMENTAL SETUP & PROCEDURES

Now, the nitrogen dragged by the NG will be by means of the vent line.

Only during 5 min.

16. Progressively decrease the nitrogen pressure and close the outlet of the pressurized cylinder.

17. Leak test with the NG detector. (Protocol describe in Section 0).

18. Close the valves V-12 and 16 to minimize the natural gas which flows through the saturator.

19. Change again the valve V-15 to *process line*.

4.1.3.3.4 Flow

In order to have a good control of this quantity in the whole experimental rig, two tasks must be taken in count: the flow direction and the flow amount in those lines where some humidity sensor has been setup. Regarding this point, during the design phase of the experimental setup it was carefully studied the minimum number of (2 and/or 3 ways) ball valves and where they would be positioned. The final result (Fig. 4.1.j) makes possible to isolate any section of the plant or measurement humidity device, and to carry out the different modes of work: *measurement phase, purge, start up* and *shut down*.

Due to the different flow ranges required by the humidity analyzers, the NG flow must be measured and controlled in all lines where humidity sensors were positioned. Thus, flowmeters fitted with its own needle valve at the inlet was placed just after the measurement devices to obtain a suitable flow control. Only by means of this kind of flow control structure, already depicted in Fig. 4.1.h, it could be obtained accuracy and reliable measurements in all humidity analyzers.

Besides of that typical flow control structure, there was special flow control loop which could regulate the flow of three lines with only one flowmeter and its own needle valve. This special flow control structure can be seen in Fig. 4.1.p.

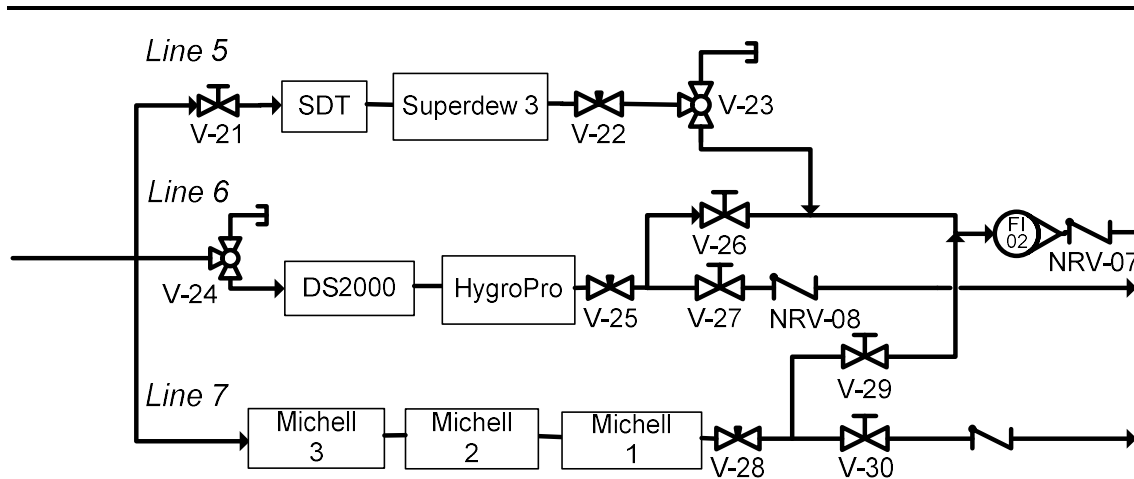


Fig. 4.1.p Special flow control loop to the sample lines 5, 6 and 7 in which humidity sensors were fitted.

The procedure performed to fit the flow in these three lines is detailed below:

1. Starting with all valves closed and the valves V-23 and 24 turned towards the cups⁵.
2. Turn V-23 towards the flowmeter (FI-02) and after that, open V-21. Turn lightly the valve V-22 until reading 60 SLPH.
3. Open V-26 and after turning V-24 towards the humidity sensors. Adjust the flow of *line 6* opening V-25 until the flowmeter reads 120 SLPH, the total flow of *lines 5 and 6*.
4. Open V-29, and after adjust the needle valve V-28 until the flowmeter reads 180 SLPH, that is the total flow of the three lines.
5. Check the flow in *line 5*. Firstly, open V-30 and after that close V-29, then the flowmeter should measure 120 SLPH again.
6. Secondly, open V-27 and after that close V-26, then the flowmeter should measure 60 SLPH again.
7. Keep this last position in all valves during the test time.

If it is going to work at the maximum line pressure (see Section 4.1.3.5.2), line 6 should be completely closed, so the valves V-25, 26 and 27 must be closed and the valve V-24 to be turned toward the cup. Besides, valve V-20 must keep also closed, isolating

⁵ The V-23 and V-24 3-ways ball valves should have been simply 2-ways valves,. However this kind of valves were not available, so it had to use this resource isolating one of outputs with cups.

4. EXPERIMENTAL SETUP & PROCEDURES

the section of the MW resonator. Previously procedure would be simplified quite as it is shown below:

1. Initially, all valves of this section must be closed, then turn V-23 towards the flowmeter (FI-02) and after that, open V-21.
2. Turn lightly valve V-22 until reading 60 SLPH.
3. Open V-29, and after adjust needle valve V-28 until the flowmeter reads 120 SLPH.

4.1.3.3.5 Room conditions

Room conditions must be known and recorded because the environmental conditions under which the measurement humidity instruments are subjected during the tests could change the behaviour of analyzers affecting their performance. Any conclusion obtained from the results of this report should be associated with the ambient conditions during the test time.

Three quantities were recorded to know the room conditions during the test time: atmospheric pressure, air temperature and relative humidity. The first was recorded by *DPI-265*, as it has already explained in the Section 4.1.3.3.2. The other two quantities were recorded by means of one datalogger *I71-2* (Fig. 4.1.q) equipped with an internal humidity and temperature sensor and large memory. Table 4.1.e summarizes the most important properties of this instrument, both temperature and humidity.

Table 4.1.e Summary of the most important features of datalogger *I71-2* given by the manufacturer (Testo).

	Temperature, °C	Relative humidity, %rh
Measure Range	-20 to 70	0 to 100
Resolution	0.1	0.1
Accuracy	± 0.4 (-10 to 50)	± 2 (2 to 98)

This instrument can calculate the dew point and record up to 55.000 readings, so it was the ideal for the activity developed here, because it was taking temperature and humidity readings during the whole test time, so the data size was considerable. For

security, data were downloaded and the files saved every week, avoiding to lost information.



Fig. 4.1.q Datalogger *171-2* of Testo used to record the room conditions (relative humidity and temperature) during the test time.

4.1.3.4 Data acquisition system

All information about the process variables and measured quantities should be read and recorded for the subsequent data analysis. Because of the great number of humidity sensors analyzed, even having some of them several analog outputs, the need to measure the humidity as a function of the time to know their behaviour, there will be a huge data volume to being recorded and processed. In addition, the readings from the three pressure transmitters must be recorded too.

For all of that, there were enough reasons to justify the need to use a unit of data acquisition system. All analog outputs were logged using an Agilent *34970A* data acquisition/data logger switch unit, together with three 20 channel multiplexer (2/4 wires) Agilent *94901A* (Fig. 4.1.r). Thanks to this configuration, all process variables and analog outputs could be registered on-line.



Fig. 4.1.r Left: the data acquisition / data logger switch unit. Right, the appearance of 20 channel multiplexer (2/4 wires) *94901A*.

4. EXPERIMENTAL SETUP & PROCEDURES

The 4 mA to 20 mA current outputs were transformed to voltage by means of precision film resistors of 100 Ω with a low temperature coefficient (1 ppm \cdot °C⁻¹) and high long-term stability that were installed in all inputs to the scanner which needed to be converted. Resistor model chosen for this purpose was the *VFP-3* equipped with Bulk Metal[®] Foil technology [Vish].

By the other hand, some of the instrument that were studied had digital outputs, so they were recorded both by means of this way and their corresponding data acquisition software developed by the manufacturer. This was the case of the Aurora, Condumax II and HygroPro. The first instrument was recorded by the standard communication protocol RS-232 while the other two by means of RS-485, whose use is theoretically more recommended for industrial conditions.

Through the digital outputs much more information could be collected from the instruments, and not only one parameter associated with the NG humidity. If such instrument were fitted temperature and pressure probes, they would give a lot information, for example, temperature and pressure of the NG, the WC and the WDP calculated by several methods from the first three parameters, etc.

4.1.3.5 Measuring protocols

In this section, it is going to explain the kind of tests that was performed and what features of the humidity sensors could be extracted. According to the process variable manipulated, there were two kind of test: variable humidity test and pressure change test.

Other variables, such as the dependence on the gas temperature or flow-rate through the sensors were not evaluated but were set in order not to affect the results. The gas flow through each sensor was maintained constant and within the particular specifications given by each manufacturer. Regarding the temperature, the two pressure reducing valves were heated to avoid condensation and the gas temperature was kept close to the room temperature in the laboratory.

In the following sections, the measuring protocols for the two studied variables are explained in detail.

4.1.3.5.1 Variable humidity tests

Natural gas coming from Enagás network was very dry, approximately between (4 and 6) ppmv, so a humidifying system was implemented. From results of generator characterization (Section 5.1.1.2), the humidity range for this section of thesis was established. The minimum nominal WC was approximately 13 ppm_v, while the maximum nominal WC value reached was 250 ppm_v. These limits describe very well the range of interest to the natural gas community.

By the other hand, to be able to compare different humidity sensing techniques within of this useful range. Several nominal humidity levels must be reproduced many times to be able to evaluate the capability to generate the humidity wanted in the NG, and to getting a good characterization of the most important features of each humidity sensor. The humidity values generated were eleven: (13, 30, 45, 55, 70, 85, 100, 125, 160, 200 and 250) ppm_v. During this big block of tests, the gas pressure was always kept constant downwards to the two reducing pressure.

Below it is described the procedure that must be completely performed when a serial of variable humidity test it is wanted to do:

1. Carry out the Start-up protocol described in the Section 4.1.3.6.1.
2. Adjust the position of needle valve V-12, fitted in the denominated *wet line* (Fig. 4.1.n), depending on the nominal water content desired for each test.
3. Set up the flow that crosses every sensors:
 - a. Open the isolating inlet valve of the Condumax II and carry out the specific protocol described by the manufacturer for both channels (HCDP and WDP).

Table 4.1.f Summary of flows that must be set in the Condumax II.

	HCDP line	WDP line	Bypass line
ACCUPOINT 2	1 SLPM	3 SLPM	3 SLPM

- b. Open the isolating inlet valve of the Accupoint 2 (V-19) and Aurora and adjust the flows of their main and by-pass lines according to their manual.

4. EXPERIMENTAL SETUP & PROCEDURES

Table 4.1.g Summary of flows that must be set in the Aurora and the Accupoint both main line (where sensor is fitted) and bypass line. The flows are expressed in the same units given by the corresponding flowmeter fitted.

	Main line	Bypass line LP
AURORA	0.5 SLPM	1.5 SLPM
ACCUPOINT 2	8 SCCM	1 SCFH

- c. Perform the particular protocol to fitting the flows in lines 5, 6 and 7 at 60 SLPH in each line (see Section 4.1.3.3.4).
 - d. Open V-31 and adjust the flow in line 8 at 0.85 SLPM by means of the flowmeter FI-03.
 - e. Open V-33 and fit the flow of DP3D at 0.5 SLPM with its internal flowmeter. After that, carry out the internal protocol of INTA to calibrate chilled mirror hygrometers.
4. Record all data outputs during the whole test time. Generate a new file every day for each one of the following data recording system:
- a. Start to record the atmospheric pressure with its RS-232 and initialize recording of room conditions by means of the datalogger 171-2 of Testo (Fig. 4.1.q).
 - b. Start software of Agilent 34970A to record all analogue outputs.
 - c. Start software of Michell to record all information sent by the Condumax II.
 - d. Start software of Aurora to record all its information.
 - e. Start software of HygroPro to record all its information.
 - f. Wait a couple of full scans to check that all readings are being recorded correctly.
5. Wait until achieving relative stable humidity readings from all instrument during at least half an hour.
6. If the test is considered successful then, generate the next nominal humidity level predetermined fitting the position of needle valve V-12 (Step 2 of this procedure).

-
7. Check that the flows in all lines are correct (Step 3).
 8. NOTE: Not create new data files, keep activated the recording files during the whole working day.
 9. Perform the shutdown protocol (Section 4.1.3.6.1) when no other set point of nominal water content that wanted to be studied.
-
-

Below are detailed all properties studied during the *humidity variable tests*, and that tests were necessary to evaluate such features.

Response time tests

Instruments response facing humidity changes in NG sampled, was evaluated in order to determine stabilization times required by all instruments analyzed with the final goal to find out if there were some kind of correlation between sensing technology and their response times.

Hysteresis study

This kind of tests were performed to check if at a nominal humidity set point, some hygrometers could give different readings depending on humidity of NG came from drier or wetter humidity values, by last if some instruments suffered hysteresis, it would be analyzed if this effect could be linked with sensing technology.

Evaluation of drift

During the whole test period, analyzers were measured on several occasions at many nominal humidity levels. Their behavior throughout the test period was evaluated comparing results with respect to the three measurement technologies, each of them represented by one instrument: Aurora, Accupoint and HygroPro for spectroscopic, electrolytic and Al₂O₃ technologies, respectively. This features was evaluated by this relative way from three reference instruments, because there were no instruments with the properly features to be considered as standard measuring instrument for being used in natural gas with variable composition.

The fact that, there were not a standard reference humidity instrument was one of the most problems, nevertheless proposing some of technology studied here as a potentially valid for non-standard complex gas mixtures was one of the main targets in this thesis.

4. EXPERIMENTAL SETUP & PROCEDURES

4.1.3.5.2 Pressure changes test

As it was said, the second group of tests performed under semi-industrial conditions was evaluate the response of analyzers to pressure changes. This time, the humidity level was maintained constant at the nominal value of 100 ppm_v.

Only one test was made in this sense, that consisted of subjecting those instruments with the permissible operating pressure range, to the maximum line pressure (around to 5.8 MPa) for four days, and then decreasing the gas pressure at the initial pressure level around 2.8 MPa. This way, it could be evaluate the effect of strong pressure changes on some of the different humidity sensing techniques.

The effect was expressed as the difference between corrections of readings obtained at the intermediate pressure level, before and after subjecting the humidity instruments to the high-pressure soak. Again, one instrument had to be considered as reference to remove those difference between two measurements given by each instrument, because the NG inlet is not a standard sample with constant properties, not even the humidity content.

This test was done only for those probes that could endure the maximum line pressure, according to the work pressure ranges given by the manufacturer. For this reason, the HygroPro could not be analyzed, so the line 6 was bypassed, closing the valves V-24 to V-27. Besides, the QS microwave resonator did not participate in this test because it had already come back to INRiM. By other hand, the experimental rig had to be reconfigured bypassing the first pressure reduction, RV-01, but keeping activated the section of the saturator to fix the humidity at the nominal value selected of 100 ppm_v.

The sensors assembled downstream of the second pressure reduction RV-02, the Aurora and Accupoint, could be measuring but their behavior on the high-pressure soak could not be analyzed because the gas pressure was always constant at 0.45 MPa. However, one of them was used as reference to remove the effect of humidity variations in the NG during those four days.

The final configuration of the experimental setup assembled for the *pressure change test* can be seen in Fig. 4.1.s, where the new pipe sections built were depicted in green and the dotted lines shows those sections that were not used. Thanks to these changes, the measuring protocol was the same independently of the kind of test performed.

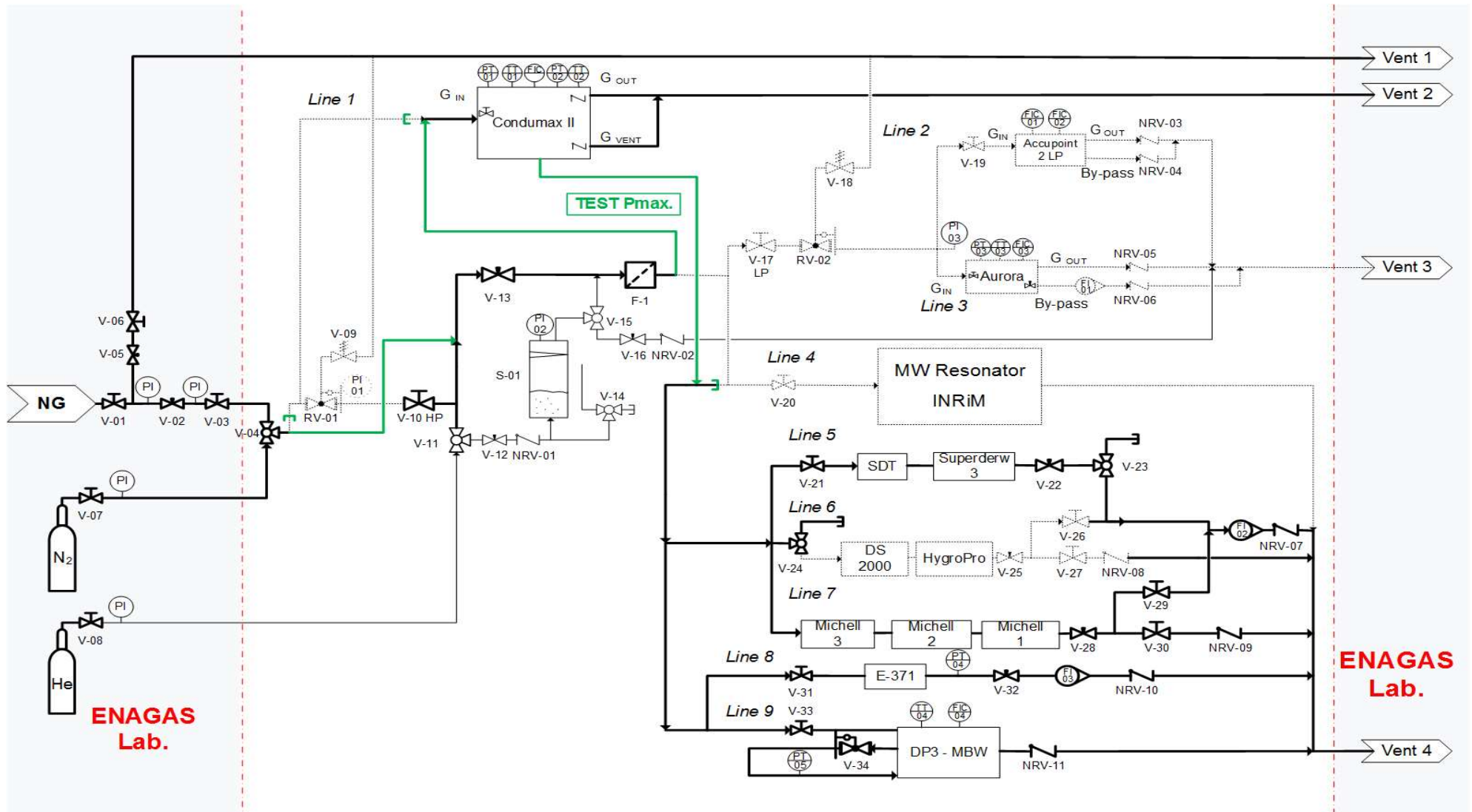


Fig. 4.1.s P&I diagram modified for the pressure change test. The green lines show the new pipe sections built for this time, the dotted lines shows the sections were not used during the *pressure change test*. The fine and thick lines depict the pipes with nominal diameter equal to 1/8" and 1/4", respectively.

4.1.3.6 Other protocols

In this section all protocols used with the experimental rig built in Zaragoza have been thoroughly described. That includes the start-up and shutdown protocols, leak tests procedures, maintenance test, etc.

4.1.3.6.1 *Start up and shutdown*

START-UP PROTOCOL

Depending on the short of test (*Variable humidity tests* or *Pressure change test*) and two different plant configurations were required. For the first case, the experimental setup should be agreed with the scheme depicted in Fig. 4.1.j, while the second case by Fig. 4.1.s. In addition, before starting any test it must be checked all electrical connections are correctly wired and that all valves are closed.

By the other hand, the reducing valves and their associated relief valves should had been fitted with nitrogen at their corresponding pressure level during the leak test, according to the kind of test is going to perform.

Once these tasks have been completed, the start-up procedure could be carried out as follow:

1. Open the valves V-01 and V-03, and the isolating inlet valve of the Condumax.
2. Change the position of three ways ball valve V-04 to allow the NG flows into the experimental rig.
3. Open progressively V-02 up to reach the maximum pressure (approx. to 5.8 MPa).
4. Check that the pressure in the WDP line of the Condumax is around such value. Later, check also the pressure shown by the pressure gauge, PI-01, agrees with the value fitted for the output pressure of the first reducing valve, RV-01 (see section - Section 4.1.3.6.3).
5. Perform the properly measurement protocol according to if it is going to perform *variable humidity tests* or *pressure change test* (Sections 4.1.3.5.1 and 4.1.3.5.2, respectively).

SHUT DOWN PROTOCOL

At the end of one test series and/or the most of working days in Enagás' facilities of Zaragoza, the NG supply should be completely close, all sections of the plant should be fully depressurized and all electrical instruments switch off. This way, the risk that any problem happens during the shutdown of the plant is minimal. Shut down protocol is described below:

1. Close the gas inlet valve (V-01).
2. When the first two manometers show there is no pressure, then close V-02 and V-03 to cut off the NG supply.
3. Continue closing valves when the pressure shows by the diverse pressure instruments distributed along the plant was zero. Then, close their corresponding valves to each section:
 - a. When PI-01 and PI-02 read zero, then close the valves V-10 to V-17, namely, the saturator section.
 - b. When there is no pressure in PI-03, then close V-19 and the isolating valve of Aurora, namely, the low pressure section.
 - c. If the pressure transmitters PT-03 and PT-04 are recording null values, then close V-31 and V-33, respectively.
 - d. By means of the flowmeter FI-02 check there is no flow in the lines 5, 5 and 7. Then, close all valves that are this section.
4. When the whole plant is depressurized, stop the data acquisition system and switch off the power supplies of all analyzed humidity sensors.
5. Unplug the electrical connections.

4. EXPERIMENTAL SETUP & PROCEDURES

4.1.3.6.2 Leak tests

The leak test is one of the mandatory step that must be done before starting to flow NG along the experimental setup. That is one the most important actions to ensure and preserve the safety of the experimental facility as well as the staff is going to use it.

As in any kind of leak test, every section of the plant must be checked at the maximum pressure at which the working fluid could cross it, adding to such levels a safety factor that guarantees the integrity in the whole installation in any case of overpressure regardless of the reason. In this case, the coverage factor used was at least 30 %. That means, for example, if the maximum expected NG inlet pressure was 5.8 MPa, the overpressure at which some sections of the plant had to be tested was of 7.5 MPa at least.

Three kinds of leak tests were performed depending on the substance used like detector: nitrogen, helium and natural gas. The tests were made in this order for safety and economy reasons.

The soap solution method was used to detect bubbles formation that indicates where there is a leak. This method was only used with nitrogen, while for the other two substances particular detectors were necessary. Thanks to this first method the majority of leaks were detected and the responsible fitting was correctly tight.

The leak test with helium is one of the most widely used because this element is one of the most inert gas and its small molecular size enables the highest sensitivity to detecting smaller leaks than the previously method. The detector gases housing inside of pressurized cylinders were connected to the experimental rig in the points shown by Fig. 4.1.j. Both cylinders must be fitted with their own pressure regulator. Finally, the NG was flowed and another leak test was made but this time using a NG detector.

The search of leaks was performed progressively opening new pipe sections with the ball vales assembled when the upstream sections were verified. The division of sections made was as follow:

- The main line until the first reducing pressure valve (RV-01). That means the group of valves from V-01 to V-06 and the Condumax II (inlet, outlets and its internal sampling system). The maximum pressure in this section was 7.5 MPa.
- The saturator section until the isolation inlet valves of all lines where humidity analyzers were assembled. This section was independently checked with

nitrogen before to be assembled inside of the rest of plant. The entire assembly of the saturator was tested up to a maximum pressure of 3.5 MPa.

- Low pressure measuring device (see Fig. 4.1.f), namely, the second pressure regulator (RV-02) and the sample lines 2 and 3, corresponding to Aurora and Accupoint 2 (inlet, outlets and its internal sampling system). This region was checked up to 0.6 MPa, because it was the maximum pressure endure by the pressure gauge PI-03.
- Individual check of the rest of lines where humidity analyzers were assembled. Check a new line only when the previously had been completely verified, which means inlet, outlet and the humidity analyzer. Much care was taken not to overcome the pressure limits of the analyzers, particularly in the line 6 where the maximum pressure during the leak test was 3.0 MPa. In the case of the configuration plant for the *variable humidity test*, there was not this problem because the output pressure of RV-01 had already been fitted at 2.8 MPa (Protocol described in Section 4.1.3.6.3).

The leak test protocol was made orderly fashion according to the kind of detector and the four regions of the plant. When the whole plant were checked at a certain pressure level, so all sections were closed, the pressure of the gas detector is increased and all process is repeated again. This way up to reach the maximum pressure levels desired, or as the case of the helium up to the maximum pressure given by the cylinder which housed it.

Another way to check leaks in those section where a pressure transmitter were assembled, was monitoring the pressure readings during 5 - 10 min, until checking that there was not pressure drops.

When any change was introduced in the plant or in any connecting point or fitting was manipulated, a leak check had be done at least on those points or sections modified.

4.1.3.6.3 *Set the output pressure of the reducing pressure valves*

The set points of the output pressure in the reducing pressure valves and their relief valves associated should be fitted with nitrogen. This procedure had to be done only once, because when the configuration of the plant was changed to performing the pressure

4. EXPERIMENTAL SETUP & PROCEDURES

change test, the reducing pressure valves RV-01 and 02 were bypassed (see Fig. 4.1.s). This procedure was done just before to the leak test with nitrogen.

1. Adjust the output pressure from the cylinder houses the nitrogen at 3.0 MPa by means of its own pressure reducer.
 2. Open the isolating valve between the bottle and the reducing valve RV-01, and fit the outputs at 2.7 MPa.
 3. The relief valve associated at the first reducing pressure valve, V-09, was fitted at 2.8 MPa.
 4. Repeat the same process with RV-02. Fit the output at 0.45 MPa.
 5. The relief valve associated at the second reducing pressure valve, V-18, was fitted at 0.55 MPa.
-

4.1.3.6.4 Maintenance and Cleaning

Contamination effects were expected because the NG is not a clean and pure gas, but rather a complex mixture consisting of variable fraction of heavy components that can be condensate due to diverse cause, such as: water composition too high, cold spots in the installation, etc. For that, it was suspected that some of sensors could suffer contamination problems ever, so in this case it should be made the following cleaning procedure:

1. Close the isolating valve upstream of the analyzers that has contamination problems.
2. Check the sensor are depressurized and there is no flow through in the affected line.
3. Procedure to performed the cleaning protocol described by the manufacturer in its manual:
 - Condumax II, chapter 4, page 28.
 - Aurora, chapter 6.3 "Cleaning the mirror", page 89.
 - Accupoint 2 LP, section 6 " Maintenance and Troubleshooting ", page 31.
 - HygroPro, section "Maintenance ", page 27.

-
- EE371, section 6 "Maintenance", page 28.
 - DS2000, section 6 "Maintenance and Troubleshooting", page 20.
 - DP3D, carry out the internal cleaning procedure for chilled mirror hygrometers developed by INTA.
4. If some fitting had been manipulated, a simple leak test with the NG detector should be done.
5. Check that the readings of the contaminated analyzer are coherent with the water content which was being flowed.
-
-

4.1.3.6.5 *Safety*

The safety was one of the most important factor that was taken in count during all stages of development of this thesis. It is very important to have very clear what are the risks of working with pressurized natural gas. The importance of the safety is not only for legal reasons and the regulatory compliance, but mainly for the safety of all those people relate to the activity or those that can be affected for our tasks, including living beings and the environment. In this sense, the most important properties of the NG described in its safety sheets are:

- In its natural state, natural gas is odorless, colorless and tasteless, but to notice its presence in case of leakage odorous substances (mercaptans) are added and they are responsible for the characteristic odor of rotten eggs.

- Despite of its high flammability and explosiveness, it requires a source of ignition, spark, flame or heat for combustion.

- Its relative density it lighter than air (0.61), so leaks or emissions dissipate quickly in the upper layers of the atmosphere hindering the formation of explosive mixtures in the air. It should avoid handling of natural gas in confined spaces because it displaces oxygen available for breathing.

- Noncorrosive.

Another way to avoid risks and hazardous situations was using the appropriate personal protection equipments (PPEs), such as: safety shoes because some of humidity

4. EXPERIMENTAL SETUP & PROCEDURES

instruments were very heavy, safety goggles when it was worked with pressurized gases or during the mounting, and laboratory coat.

By the other hand, when it is handled flammable or explosive substances, as the natural gas, it is important to be clear the well-known fire triangle, which is a simple model for understanding the three elements that a fire needs to ignite: heat, fuel, and an oxidizing agent (usually oxygen). A fire naturally occurs when these elements are present and combined in the right mixture. In contrast, a fire can be prevented or extinguished by removing any one of these three elements. Other model slightly more complex is the fire tetrahedron (see Fig. 4.1.t), that represents the addition of a component, the chemical chain reaction, to the three already present in the fire triangle. Once a fire has started, the resulting exothermic chain reaction, very common in combustion reactions, sustains the fire and allows it to continue until or at least one of the fire elements is blocked.



Fig. 4.1.t Basic schemes about the fire triangle and tetrahedron.

Regarding with the right mixture between the fuel and an oxidizing agent, two concepts more must be defined:

- *Lower explosive limit (LEL)* is the lowest concentration (percentage) of a gas or a vapour in air capable of producing a flash of fire in presence of an ignition source
- *Upper explosive limit (UEL)* is the highest concentration (percentage) of a gas or a vapour in air capable of producing a flash of fire in presence of an ignition source.

In the case of ideals and homogeneous mixtures of natural gas in air, the explosive area is limited by natural gas concentrations between 4.5 %, as LEL, and 14.5 % as UEL. That means when the air mixtures with less than 4.5 % and more than 14.5 % of natural gas will not explode, while in the explosive area only will be necessary an ignition source to trigger an explosion (see Fig. 4.1.u).

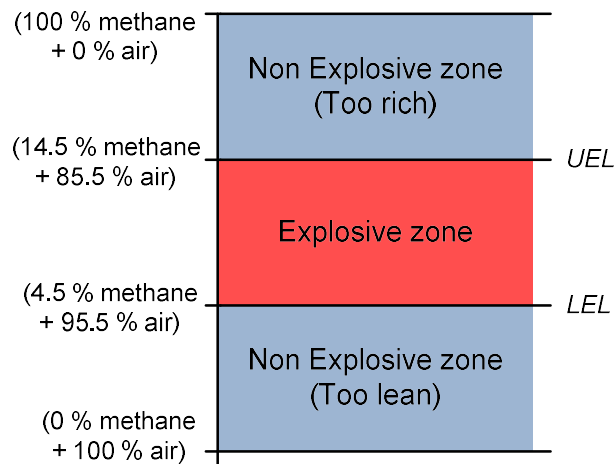


Fig. 4.1.u Diagram shows the lower and upper explosive limits and the explosive zone of the natural gas, expressed as concentration of methane in volume.

To ensure a safety atmosphere in the laboratory of Zaragoza, Enagás installed explosimeters specifically designed and calibrated for the usual natural gas composition given there. This kind of explosimeters work as alarm and actuator at the same time, control variable is the percentage of the relative concentration of methane (as major component in the NG) in air remaining to reach the LEL. Therefore, when the lower explosive mixture (LEL) is reaching the signal given by the explosimeters will be 100 % (see Fig. 4.1.u). As internal procedure of Enagás and to increasing the safety margin, the explosimeters were set to operate in the case of 18 % of LEL was reached. As it can be seen the safety margin used was really large. Once one explosimeter exceed this set point, the emergency protocol would be activate.

In the case of an alarm was triggered, the following events would occurs consecutively:

1. Power outage in the laboratory and the surrounding area by thermal magnetic circuit breakers.
2. Automatic interruption of the natural gas supply in the laboratory by means of the electrovalve depicted in Fig. 4.1.b and previously described.
3. Switch on the ATEX extractor fan and emergency lighting automatically.

If the alarm has been activated, the following actions must be performed:

- Leave the room.

4. EXPERIMENTAL SETUP & PROCEDURES

- Close the door. In the case of the power supply has not been automatically switched off, after closing the door it must be switch off manually using the emergency stop bottom located right in the next room.
 - Go to the meeting point that is located in a safety area outdoor.
 - Warn the safety person in charge.
 - Wait instructions from emergency staff of Enagás.
-
-

Besides of this specific safety protocol, every protocol performed during this thesis was meticulously designed taking very much into account the safety issues that involved the activity made, and being that one of the a key goal present all time.

In this sense, every user's manuals of the tested sensors takes into account safety both the user and the instrument. In fact, they are full of warning messages, advices, proper ways to work, maintenance periods, etc.; that try to avoid no one be injured and/or damage the own instrument or any other equipment that surrounds it.

4.2 MICROWAVE RESONATOR

As it was commented in the previously chapter because of the great peculiarity of the QSR microwave resonator and the development phase in which this prototype was, it was necessary dedicate an individual experimental chapter only for this hygrometer based on this technology. Microwave resonator was depicted in Fig. 3.2.1, to get a global idea about the whole installation built for the test under semi-industrial conditions, but characterization tests performed over it were completely different than the rest of humidity meters.

In this section, it was explained those particular tests done to evaluate the performance of the QSR to detect the water content in pressurized NG, but the first of all it was to explain the theoretical foundation in which is based this sensing humidity technology

4.2.1 THEORETICAL FOUNDATIONS

The *electric permittivity*, ϵ , also called *dielectric constant*, is a physical constant that describes how an electric field affects and is affected by a material. The permittivity is determined by the tendency of a material to be polarized by an electric field, being the own electric field reduced at the same time. This is directly related to electric susceptibility. The electric permittivity in the vacuum, ϵ_0 , is a constant value equal to $8,8541878176 \cdot 10^{-12} \text{ F}\cdot\text{m}^{-1}$ [COD14]. However, the *relative electric permittivity* of a mixture, ϵ_{mix} , may be experimentally obtained, assuming that the mixture constituents are non-magnetic, from the following squared ratio:

$$\epsilon_{mix} = \left(\frac{f_0}{f_p} \right)^2 \quad \text{Eq. 4.2.a}$$

where f_0 and f_p are the *resonance frequencies* of the cavity alternatively evacuated or filled with the sample mixture at the same temperature and at a total pressure. The relative electric permittivity of the mixture is related with the *molar polarizability* and density of the mixture, and it can be approximated as [Hua06]:

$$\epsilon_{mix} = \frac{2 \rho_{mix} \wp_{mix} + 1}{1 - \rho_{mix} \wp_{mix}} \quad \text{Eq. 4.2.b}$$

4. EXPERIMENTAL SETUP & PROCEDURES

where: \wp is the *molar polarizability* and it may be assumed independent of density with the exception to vapor of water, which is temperature dependent. The polarizability is expressed as: $\wp = A + B/T$, being A and B the Debye 's constants which have been empirically achieved [Aki06].

$\rho_{mix} = \rho_0/(1 + B_{mix}\rho_0)$, and $\rho_0 = p/RT$. B_{mix} is the second density virial coefficient [Onn02], which is function of the water vapor mole fraction, x_w , and for a binary mixture has the same form:

$$B_{mix} = x_w^2 B_{ww} + x_d^2 B_{dd} + 2x_w x_d B_{wd} \quad \text{Eq. 4.2.c}$$

From Eq. 4.2.a and Eq. 4.2.b, and the relation between ρ_{mix} and B_{mix} , which is also dependent on water fraction, it is possible to find out the water content of the sample gas analyzed by means of undergone changes in resonance frequencies selected when the cavity is empty or filled by the sample gas.

4.2.1.1 Method valid in binary systems

Initially, the problem was simplified as much as possible. Cuccaro *et al.* [Cuc12] combined the above equations to develop a method that obtained the water vapor mole fraction, x_w , in binary mixtures, as the only physically possible solution of this polynomial equation: $a_2 x_w^2 + a_1 x_w + a_0 = 0$, where a_i parameters are given below:

$$a_2 = k(B_w - 2B_{wd} + B_d) \quad \text{Eq. 4.2.d}$$

$$a_1 = 2k(B_{wd} + B_d) - \wp_w + \wp_d \quad \text{Eq. 4.2.e}$$

$$a_0 = k(B_d + B_d^{-1}) - \wp_d \quad \text{Eq. 4.2.f}$$

where $k = (\varepsilon_{mix} - 1) / (\varepsilon_{mix} + 2)$

B_w and B_d are the second virial coefficients of water and dry substance.

B_{wd} is the cross-second virial coefficient.

ε_{mix} is known from frequency recorded and applying Eq. 4.2.a.

Polarizabilities, \wp , can be known from Debye's constants.

However, this simple method was not useful for the case of NG, or what is the same, a complex mixture forming by many compound in variable compositions, so a new analysis method had be developed for this particular case.

4.2.1.2 New approximation valid for multi-component mixtures

The electromagnetic resonance is characterized using two types of propagation degenerate modes in microwave resonances: transverse magnetic mode (TM mode) and transverse electric mode (TE mode). In TM mode, magnetic field lines are entirely transverse to the direction of electromagnetic wave and the electric field has a component in that direction. The same occurs for the case of TE mode [Bag09]. Both modes are designed by two subscripts which indicates the number of half wave variations of electrical/magnetic field in the wide and narrow dimension of the waveguide, respectively. As it has been explained above, the energy emitted by microwaves must be as low as possible to avoid heating the sample gas. For that, it is used to choose the vacuum frequencies of the four lowest frequency modes TM_{11} to TE_{12} , which includes TM_{11} , TM_{12} , TE_{11} and TE_{12} . In order to know the overall performance of this kind of apparatus, it is necessary characterize very well frequencies in the chosen propagation modes and at different pressure and temperature values and for a single mixtures.

Degenerate modes are commonly depicted as triplets what means they have three peaks of resonance that only can appear when resonating cavity is not a perfect sphere. This is the reason by what is often use quasi-spherical or even ellipsoidal cavity for this purpose. The variations on the cavity surface do not affect acoustic resonance, but it has some effect on the width of the peak, enlarging them which has a negative effect on uncertainty determination, therefore it is important to induce a very small misalignment but enough to measure the triplets. For that, the relative electric permittivity of a pure gas or a gaseous mixture must be determined more complex way than Eq. 4.2.a. The following squared ratio was described by Gavioso *et al.* [Gav 14]:

$$\varepsilon_r = \frac{1}{\mu_r} \left(\frac{\langle f_{ln}^\sigma + g_{ln}^\sigma \rangle_0}{\langle f_{ln}^\sigma + g_{ln}^\sigma \rangle_p (1 - k_T^p/3)} \right)^2 \quad \text{Eq. 4.2.g}$$

where: $\langle f \rangle$ is the average frequency.

 4. EXPERIMENTAL SETUP & PROCEDURES

$\langle g \rangle$ is the average halfwidth of triply-degenerate and (with single components identified by the set of indexes l, n, σ) microwave mode of QSR cavity measured at the same temperature T both in vacuum (subscript 0) and at pressure p .

μ_r is the relative magnetic permeability of the gas. In the previously equation, it is usually a good approximation to assume to be equal than 1, with the clear exception of the oxygen. The magnetic permittivity in vacuum, μ_0 , is $1.2566 \cdot 10^{-6} \text{ N} \cdot \text{A}^{-2}$ [COD14].

k_T is the isothermal compressibility factor of metal is made the resonator, accounts for pressure induced changes of the cavity dimensions.

σ , this superscript is used to distinguish the two classes of mode whilst l and n subscripts defining the function [Und12].

For the procedure discussed just above, new working equations were considered and evaluated to determine x_w , which were reported by Gavioso *et al.* [Gav14] and used to measure humidity in this thesis. In this case, the expression of permittivity of the mixture was given as follow:

$$\varepsilon_{mix}(p, T) = \varepsilon_{dry}(p, T) \left(\frac{f_{dry}(p, T)}{f_{mix}(p, T)} \right)^2 \quad \text{Eq. 4.2.h}$$

The humid and dry fractions of the mixture have densities (ρ_{mix} and ρ_{dry} , respectively) and polarizabilities (\wp_{mix} and \wp_{dry} , respectively). If polarizability is isolated in one side of Eq. 4.2.b the results for both polarizabilities will be the next:

$$\wp_{mix}(p, T) = \frac{1}{\rho_{mix}} \frac{\varepsilon_{mix} - 1}{\varepsilon_{mix} + 2} \quad \text{Eq. 4.2.i}$$

$$\wp_{dry}(p, T) = \frac{1}{\rho_{dry}} \frac{\varepsilon_{dry} - 1}{\varepsilon_{dry} + 2} \quad \text{Eq. 4.2.j}$$

Hence, the ratio of the polarizabilities will have the following form:

$$\frac{\wp_{mix}}{\wp_{dry}} = \frac{\rho_{dry}}{\rho_{mix}} \left(\frac{\varepsilon_{mix} - 1}{\varepsilon_{mix} + 2} \frac{\varepsilon_{dry} + 2}{\varepsilon_{dry} - 1} \right) \quad \text{Eq. 4.2.k}$$

Assuming that when the water content in the mixture is very low ($x_w \ll 1$) then it could be say that $\rho_{dry} = \rho_{mix}$, and using the below expression to link all polarizabilities (Eq. 4.2.1), the water mol fraction, x_w , can be finally defined by Eq. 4.2.m:

$$\wp_{mix} = \wp_w x_w + (1 - x_w) \wp_{dry} \quad \text{Eq. 4.2.1}$$

$$x_w = \frac{\left(\frac{\epsilon_{mix} - 1}{\epsilon_{mix} + 2} \frac{\epsilon_{dry} + 2}{\epsilon_{dry} - 1} \right) - 1}{\wp_w / \wp_{dry} - 1} \quad \text{Eq. 4.2.m}$$

This last expression is a quite simpler method to find out the water mol fraction by means microwave resonance that solve the quadratic polynomial defined by Cuccaro *et al.* [Cuc12], and select those solutions with real physical meaning, as was explained by binary mixtures.

4.2.2 PHYSICAL DESCRIPTION

Throughout this sub-section, the features of resonant cavity used were described and characterized in order to have nice control over the resonance frequencies. For such target temperature, pressure and flow were process variables which had to be accurately and reliably defined and controlled.

In this section were described the different components of the QSR cavity, the process diagram in which resonator was embedded to control and handle the critical variables, and finally, corresponding data acquisition system to record such variables and resonances frequencies.

4.2.2.1 Experimental setup

The manifold associated to the microwave QSR had to have at least one control unit for each measuring variable associated such as: pressure, flow and temperature. Due to the measuring methods applied here, which will be explained hereinafter, it is necessary design and implement a drying system to know the resonant frequencies from dry gas matrix and this way to achieve the electric permittivity of dry mixture, ϵ_{dry} . All equipment associated with the control of all process variables in microwave hygrometry were described in detail below:

4. EXPERIMENTAL SETUP & PROCEDURES

- Temperature control, was carried out by means of two systems simultaneously working. First of them was responsible for keeping the QSR cavity temperature close to the set point chosen by flowing ethanol from an external circulating thermostat. This system gave a coarse control temperature that allowed to bring near to the gas temperature to the nominal value required for each test, but it was necessary another system more which guaranteed a finer control of the gas temperature just before to the cavity inlet. This more accuracy second system consists on a PID temperature control provided by a low power electrical heater in contact with the inlet connection to the thermostat. As it was said in Section 3.2, two PRTs, in contact with the shell of resonator, were embedded to know gas temperature as well as its uniformity inside the cavity.

- Mass-flow and pressure controls, were positioned on the inlet stream to the QSR and together with PID electro-actuated valve on the outlet vent, the pressure was maintained steady within ± 10 Pa around the pressure value selected as set-point. Flow rates had to be inside the range of 0.1 to 0.3 L/min, because if the flow was too high it would prejudice the precision of the pressure control, by cons flow rates below such minimum would only cause that the required time to refresh the whole gas contained within the inlet manifold and cavity would be higher. The estimated inner volume of this plant section was lower than 200 cm³, which means that any perturbation in the sampled gas could be detected in one minute proximately.

- Humidity control, must be mounted if it was wanted to evaluate the performance of resonator at different humidity levels. How it can be seen in the process diagram depicted in Fig. 4.2.a, the plant section called "generator & driers" was responsible for controlling the water content present in the gaseous matrix. Humidity control had two goals: remove completely all water molecules present in the inlet gas stream and by cons, humidify the gas.

For the first case, two hermetic tubes, made of stainless steel plated with nickel to prevent corrosion, were filled with desiccant substances. These tubes had an internal volume of 100 cm³ and they were able to endure up to 10 MP. They were positioned in vertical and flow direction was downward, so the gas inlet was in the top. Both top and bottom of each tube were assembled metal filters with a grid size of 2 μ m to prevent the desiccants were dragged by the gas stream. The first tube

contained 30 g of anhydrous magnesium perchlorate, $\text{Mg}(\text{ClO}_4)_2$, and the second was filled with 30 g of anhydrous phosphorous pentoxide, P_2O_5 . The first tube collected the vast majority of the water, while the second tube collected the remaining fraction to verify that all water in the gas has been removed. The reason by which these desiccants were arranged this way was that according with a previous report, the NIST had already been implemented this drying system in hygrometry applications, but in that case in gravimetric hygrometers [Mey10].

By the other hand, two humidifying systems were used: one simple bubbler for the previously test performed in INRiM facilities (Section from 4.2.3.1 to 4.2.3.3), and the humidifying system, which has been already described in Section 4.1.3.3.3 for the test performed under semi industrial conditions with real NG.

Diagram drawn in Fig. 4.2.a shows all installation associated with the microwave hygrometer, but some sections were only used in laboratory for tests with moist methane, and another for on-site measurement in NG. All control system explained before can be seen in this figure.

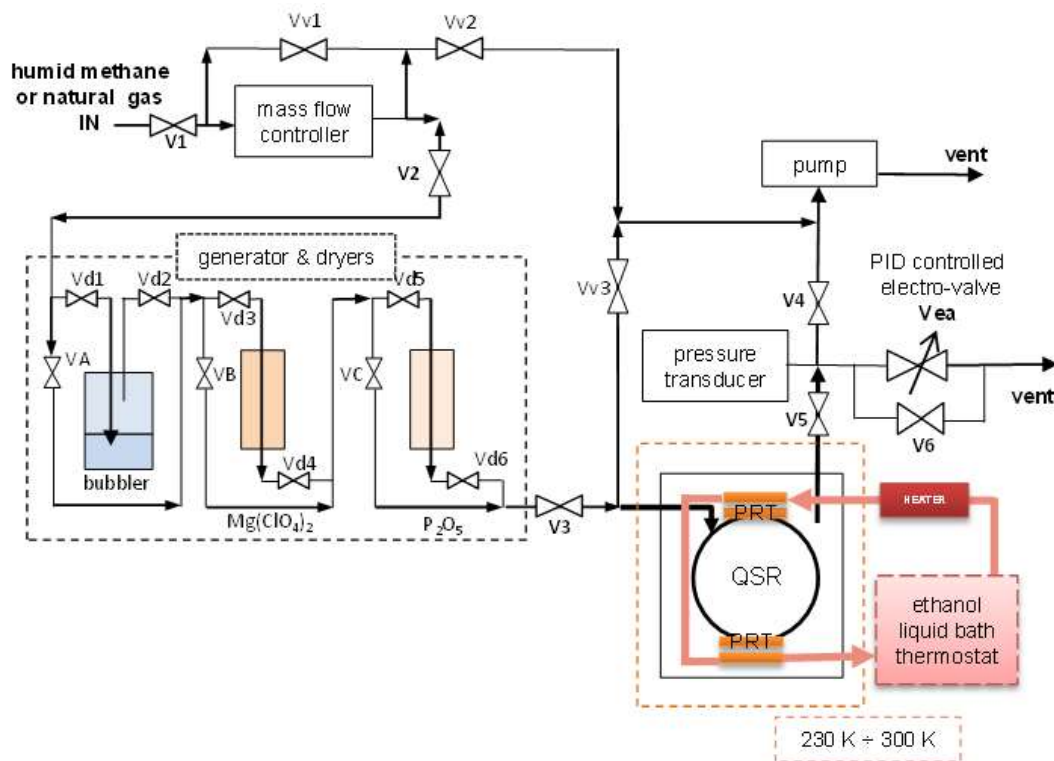


Fig. 4.2.a Schematic diagram of the gas manifold used for humidity measurements with the microwave resonator for the tests with moist methane and natural gas [Gav14].

4. EXPERIMENTAL SETUP & PROCEDURES

For laboratory applications in which the bubbler was used, the initial scheme included a pumping system together with a filtering and deionization system of the sample. Therefore, both bubbler, pumping and water treatment systems were not assembled for test with NG, but nevertheless they have been keeping in this figure, because they have been used during previously tasks.

Particularly designed for field applications with NG, the pressure vessel that housing the resonator was inserted in a larger stainless steel container. The intermediate space between both containers was maintained empty during the course of the measurements to cushion the thermal gradients between the resonant cavity and environmental temperature. This way, any external temperature change produced due to daily cycles or any other factor, it would influence the temperature control described before in lesser extent. Fig. 4.2.b shows the final look of the section plant of the microwave resonator which was implanted in-situ, together with its whole manifold associated.



Fig. 4.2.b Real look of the larger container especially manufactured to the measurements performed on-site for NG inside of which the vacuum and pressure vessel was inserted with the QSR resonator housed within of this last at the same time. Besides, it can be seen practically the whole gas manifold depicted in the schematic diagram (Fig. 4.2.a), especially the two desiccant tubes in the central position of the picture.

4.2.2.2 Data acquisition system

This section describes the practical implementation of the measuring procedure for on-site tests at Enagás, in which was tested a new electronic device for the acquisition of microwave frequency data which had been developed by Politecnico di Torino within the course of the ENG-01 GAS project [ENG01].

This prototype was create as alternative to those ordinary instruments used to excite and detect the microwave resonances, and they are commonly called Vector Network Analyzers (VNAs). Nowadays, these analyzers are frequently too bulky so are not very useful to field applications, even VNAs have unnecessary capabilities for hygrometric applications, so their costs are considerably high. For this reason, those requirements associated with the portability (e.g.: limiting the power consumption, weight, and dimensions) and a final low-cost (LC) product were two key parameters when designing this alternative analyzer [C&G13]. Of course, another required specifications with regard to the operating frequency range, frequency resolution, dynamic range, and noise background were also taken into account during characterization and development of this prototype [C&G13]. The final look of this prototype developed by INRiM and which was used in this thesis to generate and collect the microwaves frequencies from QSR cavity which was used as hygrometer to check its performance in on-site application with natural gas, can be seen in Fig. 4.2.c.

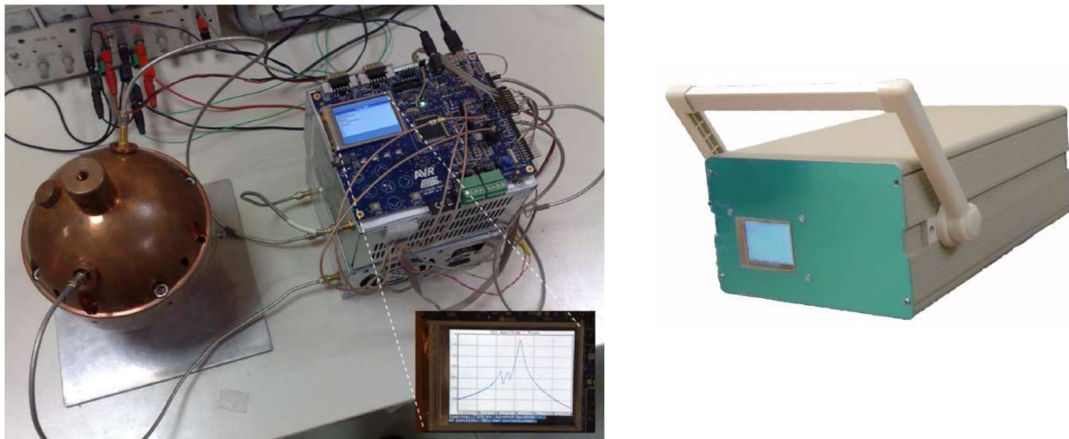


Fig. 4.2.c Left: Photograph of the prototype during a measurement with a QSR in which resonance is shown in real time on the graphical LC [C&G13]. Right: Final look of potable prototype for the acquisition of microwave frequency data.

4. EXPERIMENTAL SETUP & PROCEDURES

Corbellini and Gavioso [C&G13] evaluated the performance of their prototype in two different QSR cavities: the first one 6 cm of inner radius made of copper with which resonance frequencies of the modes TM_{11} and TE_{12} were measured in air at ambient conditions; the second was the same cavity used in this project but under a moderate vacuum (lower than $1 \cdot 10^{-2}$ mbar) and at 9 °C, but this time flowing helium at 120 mL/min to determinate its permittivity near 100 kPa and 273.16 K.

For the first comparison, data were repeatedly recorded as a function of time, first with the designed instrument and successively with the reference VNA, model *HP8510C*. Such comparison did not show evidence of systematic errors, and the scatter of the residuals for the prototype was lower than 30 ppb, whilst for the second cavity, the VNA reference model was an *Agilent E5071C*, which was also used in this work to check the performance of the prototype. The relative differences between both were well below the 50 ppb level, which have been taken as the initial required specification. Therefore, it has been demonstrated that the performance of LC prototype, whose overall cost was less than 2000 \$, would satisfy the accuracy requirements of industrial applications, as well as in many other scientific application [C&G13]. VNAs used as reference to determine the behaviour of new designed analyzer can be seen in Fig. 4.2.d.



Fig. 4.2.d Network analyzers. Left: *Hewlett-Packard-8510C*. Right: *Agilent (Keysight) Technologies-E5071C*.

According with these previous comparisons, fitting allowed to determine the frequency and halfwidth of TM_{11} mode had to meet a relative uncertainty of 50 ppb as maximum, so frequency determination was not expected to represent a major source of uncertainty in humidity determination in NG by microwave hygrometry. However, the measured frequencies vary if temperature and pressure vary, because these changes affect dimensions of resonator and the density dependence of the refractive index of the gas.

The limited frequency range of this prototype (1 GHz to 6.9 GHz) allowed to measure with just one triply-degenerate cavity mode (TM_{11} at 5.14 GHz). To determine the frequencies and half-widths (f and g , respectively, defined in Eq. 4.2.g) of such triplet, the prototype was set to sweep through 201 frequencies, spanning approximately 16 MHz and centered approximately at the average triplet frequency.

4.2.3 PRELIMINARY TESTS

In this section those previously tasks that had to be performed before comparing the performance of QSR cavity as a humidity measuring instrument were explained. A chronological summary of all those steps that were carried out during the development of this technology in the hygrometry field, allows us understand much better how works and how not only was reached the state of art of this technology, but it was overcoming in this thesis.

Initially, the resonator cavity had to be characterized. Then, the behavior of QSR against gaseous substances was analyzed, firstly using well-known pure substances as nitrogen. Next step complicated a little bit the problem by adding water to nitrogen and air, considering in both cases binary mixtures [Cuc12, Und12]. The following action was to know its performance with moist methane, as an intermediate step to face the final aim of using it with complex mixtures as NG, and even under close similar industrial conditions.

All these tasks were performed by INRiM before checking the performance of the QSR under semi-industrial conditions and over real natural gas. For that, in this section are briefly explained

4.2.3.1 Dimensional characterization of QSR

The QSR must be very well dimensionally characterized as a function dependence of the temperature and pressure variables, because the resonance frequencies vary due to such quantities.

According to Eq. 4.2.a, the relative electric permittivity, ϵ , for any pure compounds or mixture is given by the square of ratio of frequencies when the cavity is empty or filled by a sample. Thus, defining the vacuum resonance frequency, f_0 , of the cavity had to be the first task performed. In addition, f_0 must be very well defined because any mistake

4. EXPERIMENTAL SETUP & PROCEDURES

committed in this stage would affect on humidity determination deeply for transmitting a systematic error.

To evaluate how resonance frequencies vary against dimensional changes caused by thermal variations. One of the first test carried out with this resonator was measure the eigenfrequencies of the four lowest frequency modes TM_{11} to TE_{12} in the vacuum between 250 K and 300 K. An interpolation of the vacuum frequencies as a quadratic function of temperature leads to an accuracy empirical determination of the *thermal expansion coefficient*, α_{th} , of the resonator [Gav14]:

$$\langle f_{ln}^{\sigma} \rangle_0(T) = \langle f_{ln}^{\sigma} \rangle_0^{T_{ref}} - \alpha_{th}(T - T_{ref}) - \beta_{th}(T - T_{ref})^2 \quad \text{Eq. 4.2.n}$$

where $T_{ref} = 273.15$ K and the empirical parameters achieved by means of this fitting were: $\alpha_{th} = -9.71 \pm 0.02 \cdot 10^{-6} \text{ K}^{-1}$ and $\beta_{th} = -4.72 \cdot 10^{-9} \text{ K}^{-2}$. The value used here for α_{th} was enough in consonance with these obtained by Cuccaro *et al.* [Cuc12] a couple of years before within the temperature range between 320 K and 460 K.

In Eq. 4.2.g it can be assume that the relative magnetic permeability, μ_r , on any gas is equal to 1, except for the oxygen. However, to determine the *isothermal compressibility*, k_T , of the metal with which was made the shell of resonator, for taking into account its elastic properties.

For the dimensional characterization of resonance cavities, helium gas is frequently used, because determination of dielectric constant in mixtures requires an estimate of density and the dielectric virial coefficients of the pure components. For the particular case of He, these quantities are quite well known empirically, so its use will give accurate calculations from theory. Thus, helium has become a reference substance for the dimensional characterization of resonators, as can be seen in previously works reported [Sch07].

The final value obtained for such cavity was $k_T = 6.27 \pm 0.26) \times 10^{-12} \text{ Pa}^{-1}$, achieved flowing helium at 210 °C in a pressure range between 0.1 MPa and 1.9 MPa [Cuc12, Gav14].

4.2.3.2 Initial tests with pure substances

Before verifying the resonator performance in hygrometry applications, it was necessary to know its behavior on pure substances. For that, INRiM researchers determined the relative permittivity, ϵ_r , of pure N_2 and CH_4 measuring the four triplets TM_{11} to TE_{12} applying Eq. 4.2.g.

Both gases were supplied by pressurized cylinders that contented the standard samples allowed, this way, measuring at different pressure levels. For N_2 , the initial pressure was set at 500 kPa and was increased up to 1.5 MPa and then, it was gradually reduced down to 200 kPa. However, for test with methane, the initial pressure started at 300 kPa and raised up to 1 MPa, and later, was reduced to 150 kPa. The results of both tests are shown in Fig. 4.2.e and commented below:

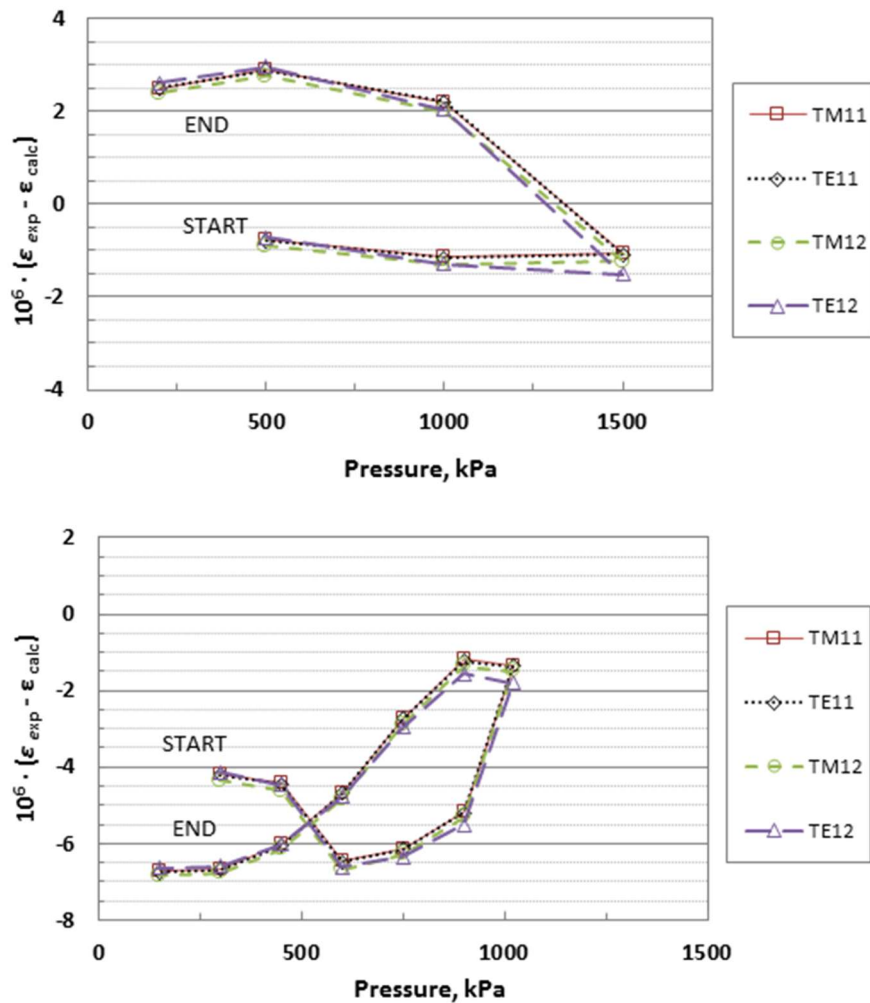


Fig. 4.2.e Deviations (ppm) between experimental determination of the dielectric constants both N_2 (top) and CH_4 (bottom) and their calculated values theoretically [Gav14].

4. EXPERIMENTAL SETUP & PROCEDURES

Looking at these results it can be said that there were very nice correlations between all collected data set, independently of which were the resonance frequency modes compared and the substance tested. Thanks to this conclusion, the volume of experimental data that had to be performed in the future could be reduced, because studying one or two resonance frequency modes would be enough. Linked with this last, another example of that great correlation among modes was also justified by the extremely low standard deviations of the TM_{11}/TE_{11} ratio in different propagation means and measurement conditions, summarized in the Table 4.2.a [Gav14].

By the other hand, a couple of more issues can be extracted from Fig. 4.2.e:

- Firstly, it can be seen in both gases a hysteric effect over the relative deviation happened. Later, it was detected that this behaviour could be due to the capacitive pressure transducer of INRiM, because its historical calibration showed similar hysteric trend, with typical deviations up to ± 200 Pa. Therefore, it looked quite probably that these hysteresis behaviors may be due to the pressure transmitter chosen in this tests, and not to disagreements between the theoretical model and relative permittivity experimental.
- Secondly, nitrogen deviation was within of a range of ± 2.5 ppm for all data set which was quite satisfactory. However, methane data shown a negative mean deviation from the baseline of about 5 ppm. As a possible explanation of this effect, it could be the presence of impurities in the methane standard sample which had 99.995 % of purity.

4.2.3.3 QSR performance in moist methane

In order to apply the microwave technology to measuring the humidity in NG, it was advisable to carry out a previously test to evaluate the behaviour of QSR with moist methane at several water content levels. These tests in binary mixtures (methane + water) were very interesting because greatly simplified the final aim of this chapter. This way, the measuring procedures used could be evaluated to detect any deficiency or potential improvement coming from the variable control systems, before facing the complexity of measuring in NG.

INRiM staff considered two operation methods to determine the water content, x_w , from measurements in vapor phase, or alternatively the dew/frost point temperature,

working close to saturation conditions. These methods were explained more in detail in the following two sections but they are based on the following measuring principles:

- Vapor phase method, directly estimates the water mol fraction, x_w , of the humid mixture from a single microwave frequency measurement in the mixture maintained in vapor phase. This method is available always that pressure and temperature inside the cavity are away from saturation conditions.

- Condensation method, which is like the operating method of chilled mirror hygrometers, when it is working with a moist mixture under away conditions from saturation, the ratio of any two mode eigenvalues of the microwave cavity is expected to be a stable property which depends on the cavity geometrical shape and it should be independent of the gas composition and density. This disturbance in such ratio can be interpreted as the beginning of a condensate layer on the internal surface of the resonator [Und12]. For this operating method, a stable cavity temperature control is required to keep the dew (or frost) point.

4.2.3.3.1 *Vapor phase measurements in humid methane*

Measurement principle implied a steady flow of humid mixture and of its dry fraction through the microwave cavity, reason by which was necessary to add a humidifying / drying section, because if the initial sample was enough dry, it had to be sent to the wetting section, while if the water content was high, it had to be dried by means of the tubes filled with hygroscopic materials to determine the resonance frequency taken as reference when the sample was completely dried.

These tests were made by INRiM staff supplying pure methane (99.995 % of purity), so in this case the sample had to be humidified by the bubbler, and the chemical drying section isolated, both assembling parts were already described in the previously sections and depicted in Fig. 4.2.a.

Temperature inside the generator was kept approximately constant at about (4.0 ± 0.5) °C within a refrigerated container while the temperature of the QSR was maintained close to 20 °C by immersing within the liquid containing in a thermostatic bath. Absolute pressure inside the saturator and QSR was initially increased from 150 kPa up to 1 MPa, and subsequently decreased to the initial value, measuring at twelve different set points.

4. EXPERIMENTAL SETUP & PROCEDURES

Finally, the frequencies readings of four modes TM_{11} to TE_{12} were taken at twelve different pressure levels for approximately one hour for each pressure level. Frequencies were read and recorded by *Agilent E5071C* and the results were exhibited and evaluated in Section 5.2.2.

4.2.3.3.2 *Condensation tests and determination of f -factor for methane*

As it was mentioned above, any change in the ratio of any two mode eigenvalues of the microwave cavity can be interpreted as the beginning of a condensate layer. However, it must be noted that thermal expansions and elastic deformations of the cavity may happen when temperature and/or pressure vary. It could happen that both effects have opposite senses and canceled each other, so before starting condensation tests, this statement was verified for the ratio TM_{11}/TE_{11} for all fluids and measurement conditions carried out.

Table 4.2.a Repeatability of the TM_{11}/TE_{11} ration at different measurement conditions.

Fluid	Measurement conditions		TM_{11}/TE_{11} ratio	
	Temperature, K	Pressure, KPa	Mean value	Standard dev.
vacuum	300 to 350		0.610 598 015	0.000 000 071
dry N_2	294	200 to 1500	0.610 598 009	0.000 000 032
dry CH_4	293	150 to 1000	0.610 598 008	0.000 000 011
$CH_4 + H_2O$	293	150 to 1000	0.610 598 007	0.000 000 084

From the results shown in Table 4.2.a, in the last three cases in which the temperature was similar, the mean values of the ratio TM_{11}/TE_{11} were the same regardless which were flowing through the resonator. At vacuum and temperatures slightly above than those three cases the ratio was a bit higher, but looking at all standard deviations can be seen the good agreement among all of them.

The experimental procedure to determine the dew-point temperature, T_{dp} , of a moist mixture consisted of decreasing the QSR temperature until a decrease of the otherwise constant TM_{11}/TE_{11} mode ratio was detected. When this condition was met, resonator temperature was controlled at such T_{dp} to maintain equilibrium between evaporation and condensation of the surface layer and the magnitude of the deviation of the TM_{11}/TE_{11} ratio from its reference value was proportional to the thickness of the condensate.

Two tests were performed in INRiM with humid methane mixtures at 273.15 K and at two absolute pressures (150 kPa and 750 kPa), which were flown through the QSR at a rate of 50 mL·min⁻¹ and 300 mL·min⁻¹, respectively [Gav14]. These tests were performed directly by INRiM staff but they have been included in this thesis as an essential step before checking the performance of the QSR as hygrometer in NG.

4.2.4 MEASURING PROTOCOL USING THE QSR

The usefulness QSR cavity to determine several physical and thermodynamics properties of simple gases has been greatly demonstrated in a wide pressure range and at moderate temperatures, but always under laboratory conditions. However, one step further in the development of microwaves in the hygrometry field has been carried on in this thesis.

Nowadays, the first commercial humidity measurers based on microwave resonance have been developed. Such analyzers presume to be able to compete again the rest of sensing humidity technologies even in industrial applications. For that, it was essential to equate the development of INRiM resonator with the newest instrument which were being already commercialized. This section is framed as one of scheduled research activities of the Characterization of Energy Gases (GAS) project [ENG01] included in its final stage, in which one of its targets was the validation of new humidity sensing methods and its comparison with traditional humidity sensors used in industrial gas. For that, to compare QSR performance with the rest of technologies industrially available would contribute to improve characterization of such microwave resonator and to know better which was its relative potential regarding to the rest of technologies compared.

This task was made available thanks to Enagás enabled to access at their industrial facilities in Zaragoza (Spain) to INRiM and INTA staff, besides of providing us all natural gas requirements during the whole test period completely unselfish way. The QSR was assembled into the experimental rig described in Section 4.1.

Regarding to the own manifold related with the resonator, a few modifications were incorporated for this task and were included in Fig. 4.2.a. These included the substitution of the mass-flow controller, not rated to work leak-proof above 800 kPa, with a manual flow regulating needle valve and the addition of a second PID controlled electro-valve located just before the resonator for keeping within specification the pressure drop inside.

4. EXPERIMENTAL SETUP & PROCEDURES

In the other hand, humidifying and drying section was quite modified: the bubbler was not brought from Turin, because the experimental rig built up in Serrablo already included a humidity generator; and the cartridge of $\text{Mg}(\text{ClO}_4)_2$ was by-passed, because according with its safety data sheet if this substance is used as a desiccant of an organic compound, it could generate an organic perchlorate substance which has explosion risk in reducing atmosphere. Hence, such desiccant was not used during natural gas tests to avoid any risky situation.

Despite of the QSR cavity and its manifold had been tested for pressures beyond 3 MPa, tests with natural gas were limited at a maximum working pressure of 750 kPa. That was due to the time available for testing the QSR only was one week because of the great delay accumulated by the previously activities performed inside of the ENG01-Gas project [ENG01]. By then, it was the first test week in the semi-industrial facilities with NG and it should be go forward carefully meeting all safety requirements and protocols previously designed. Because the thermostatic bath associated to the QSR did not work well and another choice had to be found and implemented, the leak test for the whole experimental rig only could be performed up to 750 kPa, being therefore the pressure set point to check the performance of QSR with NG.

The instrument used as generator and receptor of microwaves was the low-cost prototype, described above in Section 4.2.2.2. Only TM_{11} resonance mode data was recorded, because it was considered enough according to the conclusions extracted in all previously tests performed. All data were stored in a laptop for successive analysis.

In NG tests, the humidity generator was configured to supply initially a nominal intermediate water content value. Once all process variables were well controlled, NG line flow was modified upstream the resonator, in such way the humidity generator was bypassed and gas stream was redirect to the P_2O_5 cartridge, to be completely dried. This way, dry NG went across resonator the enough time to get a steady signal and a number values of TM_{11} , allowing determine the f_{dry} , which was needed to calculate the permittivity of the mixture. After that, the drying manifold was then by-passed returning to the initial nominal humidity level to check its repeatability, and TM_{11} data were recorded for one hour more to know the f_{mix} .

Finally, one last test was carried out to know the dynamic behaviour and response rate of QSR against humidity changes in gas line. For that, the humidity generator was fitted to generate a lower nominal water content.

Like was performed in the previously experimental section, and with the main goal to know the relative performance of the microwave technology to estimate the x_w regarding with the rest of technology studied. Four commercial instruments built by different manufacturers and based on diverse sensing techniques, were simultaneously measuring. In addition, the detailed and accurate daily chromatographic analysis of NG, which was being flown, was also provided by Enagás, like during the section before.

4.3 INDUSTRIAL CONDITIONS

This experimental section was the continuation of the extensive comparison of the most relevant humidity sensing technologies in natural gas performed in controlled laboratory conditions using natural gas, as part of the EMRP project “Characterization of Energy Gases” [ENG01].

Inside of the context of such project and thanks that we had duplicate the same instruments equipped with the novel technology of absorption spectroscopy. It was decided testing one of them in semi-industrial conditions (laboratory of Enagás in Zaragoza described in Section and the other under real industrial conditions.

Initially, this chapter was thought as a simple milestone inside of the framework of the EMRP project to compare the performance of this new promising technology against the aluminum oxide probes, traditionally used in the worldwide NG industry. However, due to the growing interest shown throughout the study by the three parts (Enagás, INTA and manufacturers) and certain events happened and will be explained below in detail, there were a second phase of the study more complex with specific scores and more elaborated.

All this evolution in the development of the tests under industrial condition, facility where was made and the experimental set up needed to carry it out is deeply detailed in this section.

4.3.1 LOCATION AND DESCRIPTION OF THE FACILITIES

In this second experimental block, Enagás continued its cooperation together with LabTH. In this sense, Enagás allowed access to INTA staff to one of its industrial facility to give another step more in the comparative of different humidity sensing technologies. According to the interest and profit for both parts, it is decided that the best option were a storage plant of NG.

The function of this kind of plants is twofold: firstly, constitute a strategic reserve for possible failures on NG supply; and secondly, it is an important tool of the national gas modulation system to deal with increases in energy demand in short-term peaks, bringing flexibility to the seasonal and daily variations in supply and demand. The gas is stored during the months of lower demand and is consumed during winter periods mainly to satisfy heating demand, completing this way its annual cycle.

The most advantageous option for storing large volumes of gas are the underground gas storages (UGS) [N&D12]. In this particular case, the industrial facility chosen to carry out this second experimental part of this thesis was the Enagás UGS of Serrablo, which is located in the province of Huesca, between the towns of Jaca and Sabiñánigo and very close to the Pyrenees. Serrablo was the first gas field reconverted to UGS in Spain at the end of its exploitation in 1989, so the ground properties were ideal for reuse as a strategic storage. Currently, there are six productive wells connected to two independent reservoirs, which are located at 1.5 km and 2.7 km underground, and they have a total volume of 1.1 NGm³ [Ena10]. Fig. 4.3.a shows a simple scheme where it can be seen the distribution of wells in both deposits.

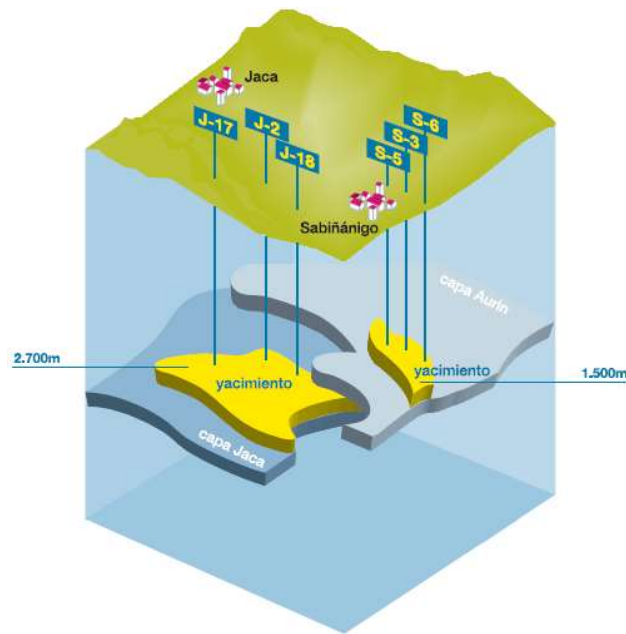


Fig. 4.3.a Simple scheme that shows the distribution of the six operative wells distributed between both deposits [Ena10].

It is interesting explain that the total volume of the UGS does not mean that all this gas can be used to produce energy but only a fraction of such volume, because the soil properties must be kept stable enough to avoid potential effect as geological change in the surroundings or reduction of storage capability of the wells. Agree with this matter, the useful gas of each well can be seen in the Table 4.3.a.

Table 4.3.a Storage capability wells in NMm^3 [Ena10].

	AURÍN	JACA	TOTAL
Operative gas	160	520	680
Mattress gas	135	285	420
TOTAL	295	815	1100

The pressure inside the storages increases as the gas is being injected, up to values close to 19 MPa, however the usual pressure values inside of the main lines of the national distribution grid are around to 7 MPa. Thus, this kind of facility must be also associated with a pumping system to inject the gas into the wells, and an expansion system when the gas is extracted. By other hand, the extracted NG is fully saturated of water and it must be subjected to drying process. Fig. 4.3.b shows the Enagás' facilities associated with the UGS of Serrablo, where it is included pumping system and dehydration process.

4. EXPERIMENTAL SETUP & PROCEDURES



Fig. 4.3.b Aerial view of Enagás' facilities associated with the UGS of Serrablo [Ena10].

As it has been said above, the NG dehydration is closely linked to its storage, so the industrial facility chosen in this thesis is equipped with its own NG dehydration plant with a daily treatment capacity up to $7.5 \text{ NMm}^3 \cdot \text{d}^{-1}$ [Ena10].

The drying process of Serrablo has one first physical step in which the most water content is deleted from the NG by horizontal separators, and another second chemical step where the triethylenglycol (TEG) is used as dehydration method (see Fig. 4.3.c). This system has gained nearly universal acceptance as the most cost effective of the glycols due to many factors as: superior dew point depression, lower operating cost and reliability [Pol09]; TEG exhibits ease of regeneration and operation, minimal losses of drying agent during operation, high affinity for water, chemical stability, high hygroscopicity and low vapour pressure at the contact temperature [Any14]. For these and many other reasons, TEG dehydration is the most used worldwide compared to other methods such as activated alumina, silica gel or zeolites molecular sieves [Moh09].

TEG is regenerated later by distillation to separate it from water (see Fig. 4.3.c). Subsequently, the gas is odorized with tetrahydrothiophene (THT), passes through the unit of measure and finally is incorporated into the national grid. In the measurement section is where the humidity sensors studied here were installed, just after the pressure and flow meters.



Fig. 4.3.c Some examples of essential elements in gas drying process. Left: horizontal separators used in the first drying step. Right: recovering of TEG, which is essential in the dehydration process of the NG, by means of a distillation tower [Ena10].

The UGS of Serrablo and its associated dehydration plant is a key point to control NG humidity in the northeast section of the Spanish grid (see Fig. 1.3.f). During the extraction time the NG humidity reaches the final customers will depend on mainly of the right operation of this plant. Besides, the water content of NG must be very closely controlled to be able to reduce the humidity locally in the case of a problem being detected at any point of the grid.

For all of that, Serrablo facilities were the perfect place where testing the performance of the behavior of spectroscopic humidity analyzers under completely real industrial conditions.

4.3.2 HUMIDITY SENSORS STUDIED

As mentioned in the introduction of Section 4.3, the main target was comparing the performance of two kind of humidity sensing techniques: Al_2O_3 capacitive transmitters and absorption spectroscopy analyzers. The first is used globally in the natural gas industry, and the latter is an extension of a promising technology used in countless sensing laboratory applications in other gases.

The Al_2O_3 capacitive sensor evaluated was a Panametrics-MIS II, manufactured and sold by General Electric (GE). This sensor was used by Enagás to know the final humidity of the NG which was going to be sent into the national grid, in other words, it

4. EXPERIMENTAL SETUP & PROCEDURES

was one of the control items to certificate the final quality of the NG so its role is especially important for Enagás. The MIS-II probe was positioned inside of a heated sampling box that includes the simple glass bead filter. The sensor has a built-in pressure sensor to express the humidity in WDP directly. Enagás' logging system records one value every hour throughout the year.

The spectroscopic analyzer was the Aurora, exactly the same model as these instrument whose performance had already been evaluated successfully in semi-industrial conditions (see Section 4.1 and 5.1). This instrument was loaned to INTA by GE and came directly from the manufactory.

Because of the duplication of one of the instruments based on one of the new technologies, absorption spectroscopic, and so successful was obtained in semi-industrial conditions. It was decided to study the relative behavior of Aurora under real industrial condition.

In the second phase of this study one more spectroscopic instrument was added at this comparative of technologies. The third instrument was an OptiPEAK TDL600, manufactured and provided by Michell Instruments Ltd. When the study was started, this sensor was still in a pre-commercial phase, so tests performed here were key to the manufacturer to checking the performance of its instrument under real industrial conditions after in-house tests performed at their facilities in England. Currently, this analyzer is already fully commercialized with an improved version with respect to the instrument evaluated here, thanks in part to the work carried out in this thesis and the conclusions extracted.

Both spectroscopic analyzers were supplied ready for on-site outdoor use, regardless of weather conditions. Each analyzer had its own integral sampling system, designed by each manufacturer and located in the same enclosure as the laser cell. The sampling systems of the three instruments have small differences, but follow the same overall scheme: isolating valves in all input and output lines, filtering system, pressure reducing system, flowmeters positioned downstream of the measuring cell and a heating system to avoid water condensation effects in any point.

All analyzers had the applicable ATEX certification for use in hazardous areas, according to the European Directive 94/9/EC [EUD94], approved in Spain by the Real

Decreto 400/1996, 1st of March [BOE96]. Table 4.3.b summarizes the principal features of the humidity instruments studied in this section. More details of these three hygrometers were cited in the Section 3.2.

Table 4.3.b Summary of the most important properties of all humidity instruments evaluated.

	MIS-II	AURORA	OPTIPEAK TDL 600*
Manufacturer	General Electric	General Electric	Michell Instruments
Model	MIS-II	Aurora	OptiPEAK TDL 600
Principle of measuring	Al ₂ O ₃ capacitive sensor	Absorption Spectroscopy	Absorption Spectroscopy
Range	-65 °C to 10 °C	5 to 5000ppm -65 °C to 2 °C	5(1) to 5000ppm -65(-76) °C to 2 °C
Accuracy	± 2 °C	± 4 ppm _v or 2 % of reading ± 2 °C	± 2 (1) ppm _v (2% of reading) ± 2 °C

* Information contained within the parentheses corresponds with the final properties of the instrument already commercialized but these values were not used in this report.

4.3.3 INITIAL INSTALLATION

4.3.3.1 Introduction

This chapter initially was thought as a simple milestone inside of the framework of the EMRP project [ENG01]. The main reason for having had to take this measure was the great delay inside of the working group in which the target given to INTA to compare different sensing technologies (had to be performed in the last period of the project. Because of both factors, the lack of time to INTA to performing its goals was evident.

For all above, the time spent in this task was only two months and the scored target was as simple as possible: install the Aurora in Serrablo, as close as possible to MIS-II and compare the readings taken by both instruments, extracting much information as possible.

4. EXPERIMENTAL SETUP & PROCEDURES

This task was developed during the months of May and June in 2013, and one of the most important premise taken by INTA was to carry out our tasks with the minimal impact upon the facilities and activities of Enagás.

4.3.3.2 Description and diagram

Once the industrial facility of Serrablo was chosen as place to carry out the study, the particular point where Aurora was going to be mounted should be specified. The MIS-II, used by Enagás as the humidity measurer of NG, is located in the measurement area that, at the same time, is located in the last stage of the drying process to know all final properties (pressure, flow, composition, water content, etc.) of the NG before being sent to the national grid. The position of the MIS-II was next to the cabin that houses the whole chromatographic system (see Fig. 4.3.e).

The inlet pressure in the chromatographic system must be lower than 0.2 MPa, while the NG pressure in the main line is around 6 MPa, so a reducing pressure system was necessary. Fig. 4.3.d shows the outdoor box that houses the reducing valve and its associated manometer that displays the output pressure, besides of a simple safety system based on two isolating valves at the inlet and outlet, one relief valve and a coalescing filter.



Fig. 4.3.d Look of the reducing pressure system used by Enagás and located up stream to the chromatograph.

In Fig. 4.3.e it can be seen the particular position of the MIS-II sampling system box and the box that houses the reducing pressure system regarding to the chromatographic room. This position was where it was decided to set up the Aurora.



Fig. 4.3.e The outdoor sampling box that housed the MIS-II was located in left side of the chromatographic room (the biggest cabin), while the box housed the reducing pressure valve was in the right side.

The sampling system of the MIS-II inside of its outdoor box has been depicted in the first scheme shown by Fig. 4.3.f. To choose the position where install the Aurora, two aspects were taken into account: provoke the minimum impact upon the original facilities of Enagás, and set the Aurora as close as possible from MIS-II for the properties of the NG arrives the analyzers were practically the same.

According with these both premises, it was decide to use the purge line like the inlet to the Aurora. This way, only changing the flowmeter located in this line by a reducing pressure valve, together with its respective manometer, the Aurora would be operative and the properties of the NG reached both hygrometers should be the same because were taken from the same point. The reducing pressure valve was essential because the maximum pressure in the inlet of the Aurora must be 1.3 MPa and the usual process pressure was around 6 MPa. The second scheme of Fig. 4.3.f. shows the final look of the sampling system of MIS-II once the reducing valve was fitted.

4. EXPERIMENTAL SETUP & PROCEDURES

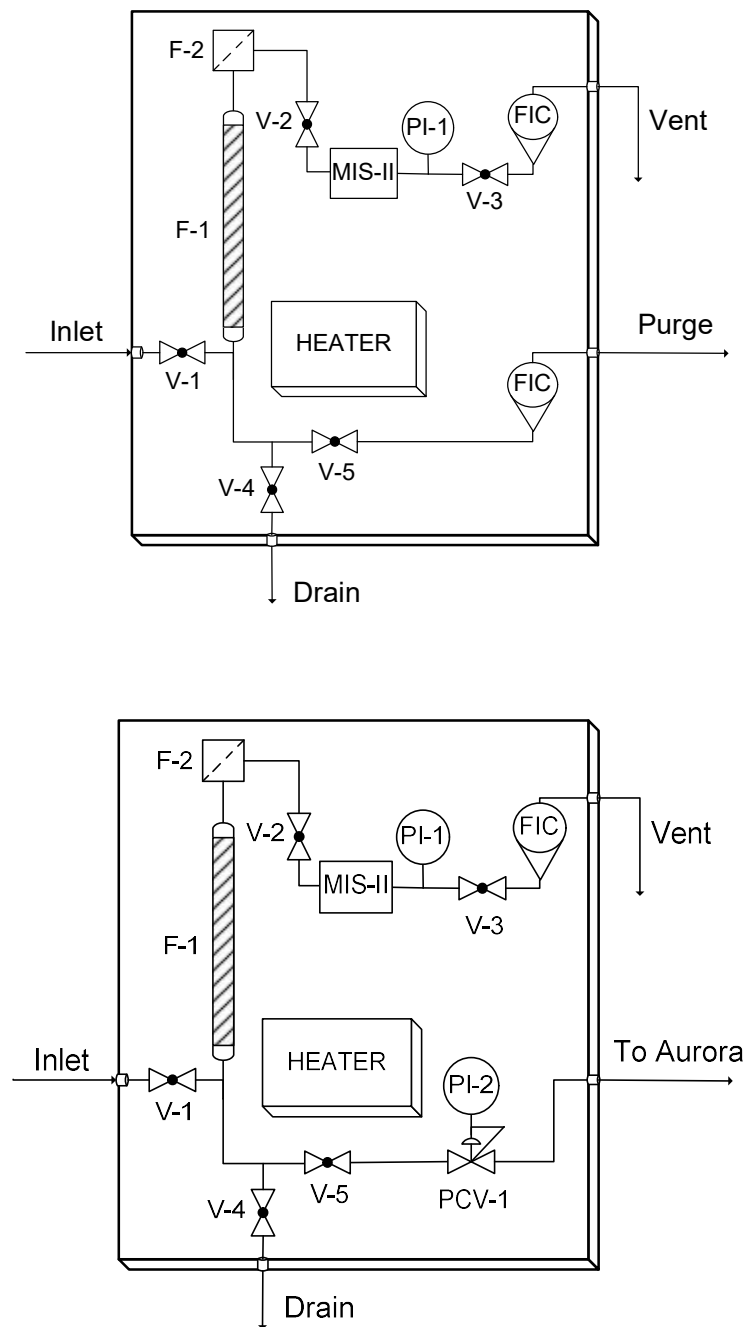


Fig. 4.3.f Differences between the original sampling system of the MIS-II (top), and the new scheme used to connect also the Aurora on it (bottom).

The sampling system of the MIS-II had all necessary elements: isolating V-1 to V-3 valves to protect the sensor; filtering system based on two steps: firstly, simple vertical glass bed filter (F-1) holds back potential condensed water have not been removed yet; and secondly, a particle filter (F-2) to hold back solid particles with sizes higher than 5 μm ; manometer to indicate the pressure is being endured by the humidity sensor;

atmospheric flowmeter, which needs a valve upstream to reduce the pressure down to the atmospheric levels.

There were a vent was going directly to the atmosphere because the low flow that crosses the sensor (1 SLPM) is negligible and it is not need to be collected. By other hand, there was also a drain line to remove condensed water held back by F-1. In addition, a heating system was responsible for preventing condensation phenomena inside the sampling enclosure.

The Aurora's sampling system already came fitted with all this elements to handle the NG.



Fig. 4.3.g Final look of the sampling system of MIS-II after changing the flowmeter for a reducing pressure valve and its manometer associated, both necessary in the input line of the Aurora, placed in the right side of the picture.

4.3.3.3 Data acquisition system

Enagás provided us humidity data from its MIS-II together with pressure and gas temperature data. These values were recorded each hour throughout the whole test period. However, a new recording system should be implemented to be able to measure both digital and analogue outputs from the new spectroscopic instrument. For this reason, we installed a laptop in the control room of the plant, located 100 m away approximately

4. EXPERIMENTAL SETUP & PROCEDURES

from the position where the hygrometers had been installed. INTA staff had remote access at this laptop to overview and download data files generated daily.

Digital outputs were recorded using specific data recording software supplied by the manufacturer. In contrast with test performed under semi-industrial conditions, the standard communication protocol was MODBUS RS-485 instead of RS-232 because its effectiveness over long distances and in electrically noisy environments, as industrial facilities, is higher. Analogue outputs were obtained by means of the data acquisition and recording unit, model 34970A, manufactured by Agilent and already described in Section 4.1.3.4.

4.3.4 NEW SAMPLING SYSTEM IMPROVED

4.3.4.1 Backgrounds

As it has been already explained, initial installation was used only to compare readings of two humidity instruments during the summer season of 2013, having simultaneously the least possible impact on facilities and activities of Enagás.

During that time, the UGS of Serrablo was in injection stage which means that NG coming from the national grid was pumped inside the wells. This processing stage happens when energetic demand decreases which usually is associated with the good weather mainly. All results of that initial comparison have been depicted below:

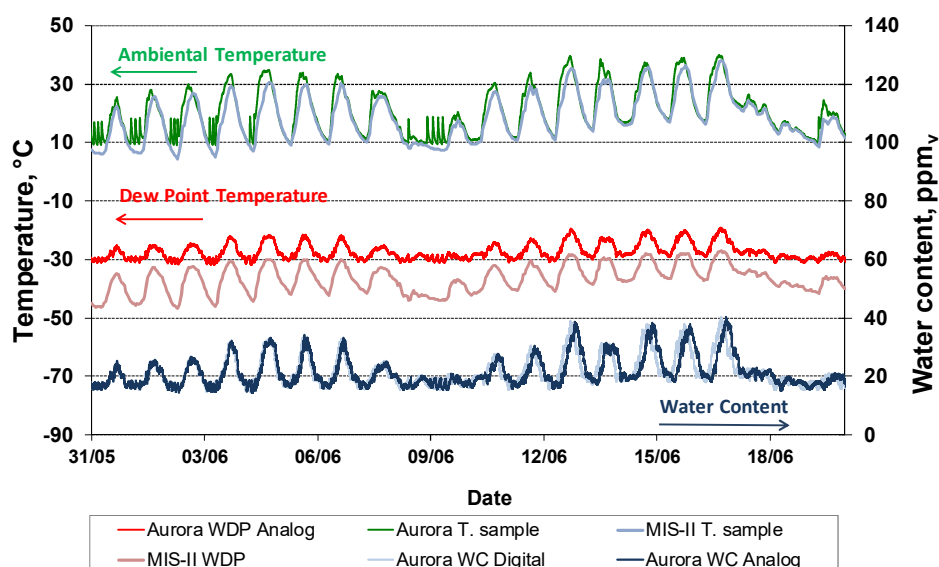


Fig. 4.3.h Data collected from both humidity measurers which were mounted under real industrial conditions. The first Y axis

This first comparative of instruments under industrial conditions allowed us to discover a series of knowledges:

- Firstly, the most remarkable thing was the oscillatory way of absolutely all signals collected, which apparently seem to be quite synchronized with temperature of the NG.
- Humidity levels of the NG were really low, so NG coming from the national grid was very dry. This fact can be seen in WDP signals, because during the whole test time, recorded values were very below that the legal limits to be commercialized in Spain, and even to be deal in international trades.
- Despite of both instruments gave very low humidities, there were a great different offset between both instruments. MIS-II always read much lower than the spectroscopy instrument, being the highest differences around 15 °C. Thus, clearly there was a great difference of performance between them.

In injection phase, humidity of the NG level is not determinants, so it is not parameter controlled by the drying plant and it is simply recorded by the MIS-II.

For this reason, it was decided to carry out a more complex study to evaluate the behavior of humidity instruments during the three production stages of Serrablo: injection, shut down, and particularly during the extraction because is the most critical phase in which humidity of the NG must be really well controlled and measured.

In addition, one of the most important European manufacturer of humidity sensors wanted to participate in this study to compare and evaluate the performance of its new spectroscopic humidity analyzer: the OptiPEAK TDL 600. However, the initial installation, which had been obtained by a simply change in the original sampling box of MIS-II, could not admit another independent sampling line for another humidity sensor more (see Fig. 4.3.f). For that, another new sampling system had to be designed and built for this new score.

By the other hand, few days later of the beginning of the extraction stage (14th November 2013) for the new production season 2013/2014, there was a determinant fact to design and built a new installation. By then, two installed instruments were the Aurora and MIS-II and thanks to the reading from both instruments it was demonstrated the presence of a real and big problem in the drying plant of Serrablo. In the following picture

4. EXPERIMENTAL SETUP & PROCEDURES

(Fig. 4.3.i), it can be seen as the humidity readings given by the Aurora (the same happened with the MIS-II) were extremely high and were quite above from the upper limit allowed to exchange NG within Europe, which according to the European Association for the Streamlining of Energy Exchange-gas (EASEE-gas) for WDP must be lower than $-8\text{ }^{\circ}\text{C}$ at 7 MPa [EAS05]. Readings of WDP shown in Fig. 4.3.i were even higher than the Spanish limit to distribute NG inside of the national borders. This problem was not more transcendent because thanks of the hygrometry section this kind of problem are detected and corrected in other points of the national grid, but anyway is an evidence that there was a problem in the drying process of the plant.

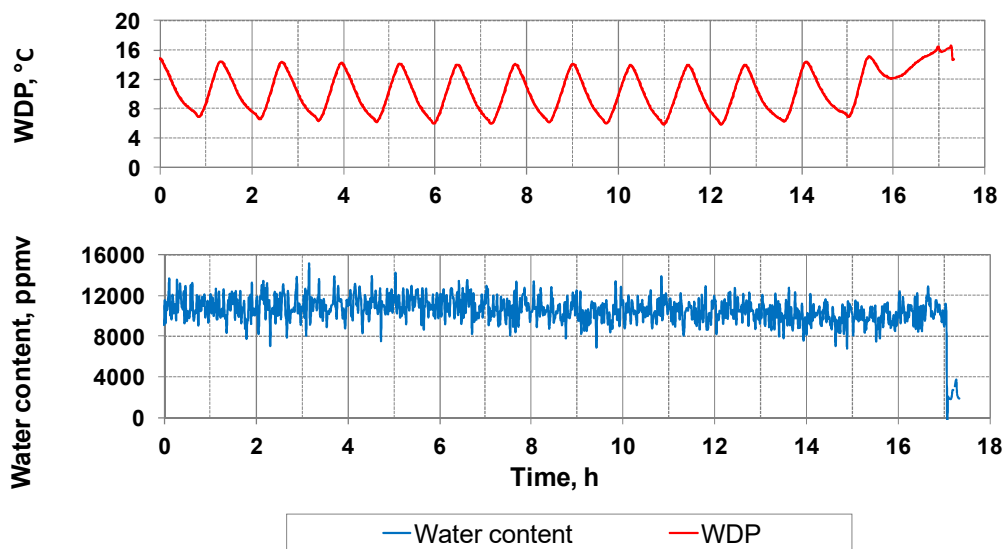


Fig. 4.3.i Example of extremely high readings taken by Aurora few days later to start the extraction phase of the new production year.

As a results of these readings given by the Aurora, also backed by those taken by the MIS-II, Enagás checked all parameters of its drying process and finally, they decided to modify some of them with the aim to achieve an extra drying of the NG. Once introduced these changes it was not seen any reduction in humidity levels of the NG, so the source of problem lay elsewhere. Enagás asked counseling to INTA, and through joint collaboration it was decided that the sampling system shared by both hygrometers were completely flooded, so both instruments were reading well above. Besides, condensed water joined to low temperatures below $0\text{ }^{\circ}\text{C}$, which is very often in this region during those dates, is a hazardous mix that could trigger hydrates formatting effects both the

sampling system and the hygrometers themselves, resulting hazardous situation both the plant, the analyzers and Enagás' staff.

Because of this important setback, Enagás and INTA jointly decided carrying out two action lines: first of them focused to starting up again the analyzers and their sampling system, because the humidity of the NG that was being sent into the national grid is one of the critical features have to be very well controlled at all time; and secondly, research and find what was the underlying problem to avoid this situation can be repeated again.

Inside of this first action line, staff from LabTH travelled immediately to Serrablo. It was confirmed the sampling system was flooded, reason by which no hygrometer was able to detect any change when drying parameters were fitted. Besides, the sampling cells of both instruments had evidence of condensates inside them, because the coalescing filters was not able to hold back the huge quantities of water dragged by the gas. The actions made by INTA and Enagás to start up again the whole humidity measurement section of Serrablo were:

- Dry the shared sampling system, from the sampling point until the inlet of both analyzers, by dragging the condensed water with dry N₂.
- Make the proper maintenance of both hygrometers according to their handbooks that include: dry their individual sampling system with N₂ opening drains, check filters and dry sensors and measuring cells. A depth maintenance of Aurora, due to its complexity, had to be done. The membrane filter had to be changed for another new, because exhibited hydrocarbons residues. Fig. 4.3.j shows the status of the spectroscopic messed mirror by condensed solution of water and hydrocarbons.

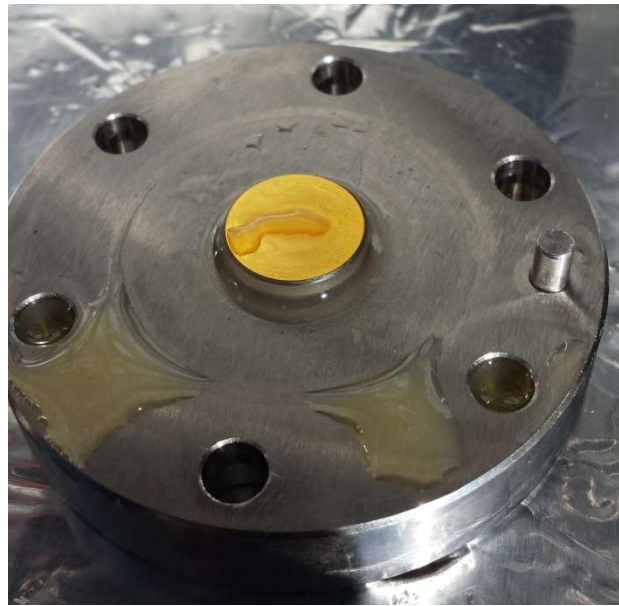


Fig. 4.3.j Aspect of the mirror assembled inside of the measuring cell of the Aurora when there were measurement problems caused by presence of solution of water and hydrocarbon that can be appreciated easily in this picture.

Once the above maintenance tasks had been completely performed and the NG flow had been returned to cross the hygrometry section, the Aurora detected a sharp fall of WC, as can be seen in Fig. 4.3.i at 17 h time. However, humidity levels, around 2000 ppm_v, remained quite high, although they started to decrease softly and continuously way during following days. For this reason, performing the second action line was absolutely critical to find the root of the problem.

4.3.4.2 Targets

After a thorough study we conclude, the whole sampling system used in Serrablo in hygrometry section had to be completely redesigned and renovated to avoid the appearance and accumulation of condensates in any point of this section, because the original sampling system were enough simple and it had neither any trace-heated lines nor heated reducing pressure valve in the input to the chromatograph (see Fig. 4.3.d). For all of that, future condensation problems may happen and humidity readings would be useless independently of the sensing technology used. This situation would have serious consequences over the control of the final quality of the NG goes to the national grid and this lack of knowledge is unacceptable by Enagás, who cannot be assume that happen

this. Therefore, Enagás considered essential INTA propose to install a new sampling system for the hygrometry section in the facilities of Serrablo.

According with this, staff of INTA, with the support of the R&D department of Enagás and Michell Instruments Ltd., was responsible for designing and building the new sampling system including: the new sampling point, the new sampling box and all its input and output lines.

By the other hand, the three parts involved in this project (INTA, Enagás and manufacturers) decided enlarge the aim of the initial comparative between the newest humidity sensing techniques, absorption spectroscopy, with respect to the aluminum oxide sensors both installed in field. That was consistent with the further work suggested at the conclusion of the EMRP project [ENG01] and in view of to the good results shown by spectroscopy instruments [Gal15], statement justified by the results shown in Section 5.1 of this thesis and their corresponding conclusions.

For all of that, it was extended the comparative study of the performance on field for both kind of the hygrometers, spectroscopic and aluminium oxide capacitive, the latest traditionally used in the NG industry. In this sense, the new study was performed during almost the whole season 2013 - 2014, in order to study the performance of both technologies during the three production stages of the plant: extraction, injection and shutdown.

4.3.4.3 Description and diagram

The main requirements had to be met by the new sampling system were:

- Provide service to both the chromatography system and those hygrometers were wished to study and compare under real industrial conditions.
- Guarantee the imperturbability both water content and composition of the NG while the rest of properties are fitted according to the measuring systems associated. This way, chromatograph and hygrometers will give readings that faithfully represent the properties of the gas is being injected into the national grid.
- Guarantee accurate and reliable humidity measurements at all time, even when some problem might arise on the plant upstream of the analyzers. Hence, Enagás will always have online and live knowledge of the actual humidity of the NG.

4. EXPERIMENTAL SETUP & PROCEDURES

- Ensure safety of the analyzers preventing condensation effects in any place, reducing at the same time cleaning and maintenance costs and extending the lifetime of the analyzers.
- Allow and facilitate maintenance tasks in all sections of the sampling system by means of drains, vents and purge systems.

4.3.4.3.1 *New sampling point*

Location of the new sampling point was in the same process pipe just 2 m downstream from the original point. Therefore, if there had been meaningful change in the historical humidity or chromatograph after and before installing the new sampling point, it would not be able to be justified by the new position of the sampling point.

The new sampling point was designed according to the sampling guideline for NG, given by the International Standard ISO 10715:1997 [ISO97a]. For this reason, the position of the new sampling point was on the top of the pipe, in contrast to the old point that was positioned at half height of the pipe. This way, if there were condensate phase in this section of pipe, denser than the gas phase, it would be very difficult some drops could be dragged through the vertical sampling point. Below differences between both sampling points can be seen.



Fig. 4.3.k Difference between the original (left) and new (right) sampling point.

As it can see in both above pictures, both options were based on the same scheme: firstly, an isolating needle valve, and later a three-ways valve through which a purge gas can be connected to be used in cleaning or maintenance tasks, for example, purging with

dry N₂ to dry this section and/or remove remaining oxygen before restarting the NG flow through this section.

4.3.4.3.2 *New sampling system*

The sampling enclosure was designed and purpose built for the comparison humidity measurement instruments, including supply to the chromatography system that is essential to express humidity as the WDP, in °C, instead of the WC, in ppm_v [ISO04]. Although this latter quantity is absolute it is less used in the NG industry, because it is a less intuitive quantity and laws regulating the humidity in the NG are expressed as WDP. For that, in this work humidity values have been expressed in both ways, so the not only the gas composition is required for giving WDP measurers but also the line pressure values.

The most important features of the new sampling system will be explained coming up next, doing emphasis in those novelties introduced respect the original installation:

- The two spectroscopic analyzers were assembled in the same position that the MIS-II used by Enagás. Therefore, the new sampling system box was designed to serve up to three hygrometers, regardless of the kind of sensing technology used, besides of the associated chromatography system, used by Enagás to give the daily NG composition. The whole experimental set-up built in Serrablo is depicted in Fig. 4.3.1.

- One of the most important novelty added in the new design was including the reducing pressure system together with the rest of the sampling system, thereby removing its corresponding outdoor cabin, shown in Fig. 4.3.d. This way, the reducing pressure valve will be supported by the heating system of the sampling box, besides of its own embedded heating, avoiding potential condensation problems caused by Joule Thomson cooling effect. In addition, the new reducing pressure valve will give service both chromatographic section and any other hygrometer whose pressure range is lower than the usual process pressure of the plant, which usually is around 6 MPa.

- The whole experimental section can be isolated from the rest of plant by means of a gate valve located right after the sampling point, as it was explained in the previous chapter. As it can be seen in the block diagram (Fig. 4.3.1.), as well as the three sampling system boxes, corresponding to the three hygrometers that were compared, were fitted with auxiliary lines as: drains and purges for removing condensates, vents for

4. EXPERIMENTAL SETUP & PROCEDURES

depressurizing or controlling the pressure in a section of pipes, and finally, by-pass lines for controlling the flow crosses the measuring cell. The new sampling system box was also designed with two drains and one vent, all of them explained later.

- The new sampling box was made of 304 stainless steel because has a high resistance to rust that will withstand long-term exposure to the environment. Dimensions of the enclosure were 800 x 800 x 300 mm of width, height and length, respectively. Base and laterals were thermally isolated by fiberglass layer 6 mm thick, whilst it has a double bottom, also made of 304 SS, to fix all components of the sampling system on the internal panel avoiding vibration and potential risk situations.

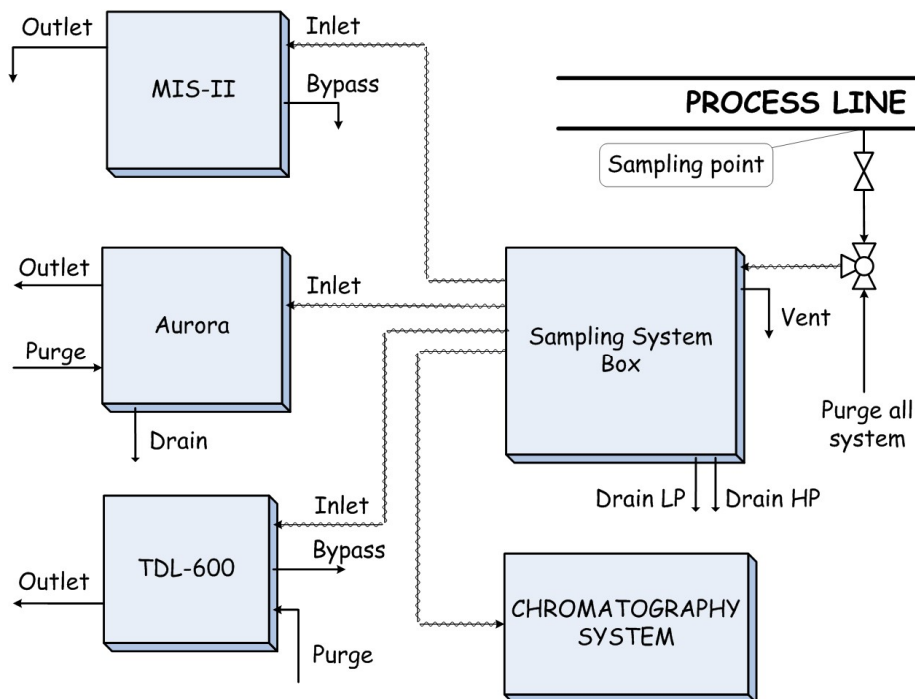


Fig. 4.3.1 Block diagram of the whole humidity measurement setup used in this work. Note that all pipe sections upstream of the four measurement systems were trace heated by means of electric trace system.

- Just like the sampling system enclosure of the MIS-II (Fig. 4.3.f), the new model also had internal electric heater to avoid condensation effects and even freezing problems when the WDP is lower than 0 °C, according to the recognized guidelines and good practices applicable to the installation of pressurized natural gas sampling systems [ISO97a and ISO97b]. The model used was a Multitherm TS 230 V and 100 W equipped with thermostat, commercialized by Intertec and according to the ATEX certification [EUD94].

- Another more important feature of the new experimental set up was that all inputs to any sampling box were heated by means of self-regulating insulated trace-heated lines (see Fig. 4.3.1), to keep the sampled gas above the water and hydrocarbon dew-point, according to the recognized guidelines [ISO97a and ISO97b] and with the same goals mentioned in the before paragraph. The sampling lines used were designed by O'Brien Corporation and equipped with TRACEPAK® technology consisting on: tubing bundle which contents the process pipe in contact with electric traced system (see the bottom image of

- Fig. 4.3.m), all of that wrapped by two external slayers to isolate from the temperature and humidity of the surrounding atmosphere (see the top image of

- Fig. 4.3.m). The process pipe is made of 316 SS, 6 MM of nominal diameter and 1 mm of thickness. The entire assembly can be easily formable by hand to be fitted to the different geometry of the process. The heating system used required 240 V power supply, gave 15 W/m electric power and fulfilled the requirements of 1 and 2 category to work under explosive atmospheres [EUD94].

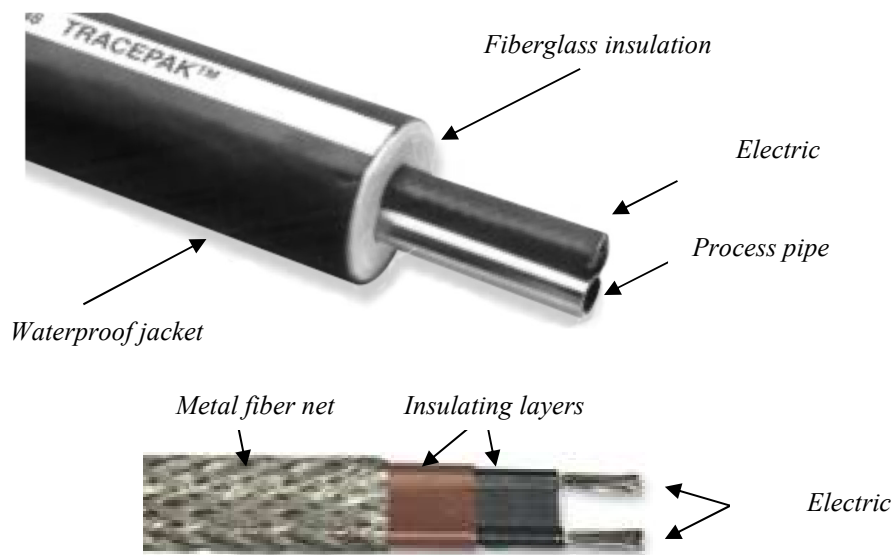


Fig. 4.3.m Look of the trace heated tubing bundle used in the sampling lines assembled to work under industrial conditions and hazardous areas. Top: look of the entire assembly. Bottom: detail of the different parts that shape the electric traced system.

All self-regulating insulated trace-heated lines should be connected by one their ends to the proper power supply, while in the other end the electric traced shown above

4. EXPERIMENTAL SETUP & PROCEDURES

should be right isolated using termination kit that avoid electric contact between both cables and the environmental humidity goes into and rots the fiberglass, thereby decreasing a lot the useful life of the traced lines. The electric connections scheme belonging to the sampling lines were explained below and it can be seen in Fig. 4.3.p, while one of the steps of the insulating treatment given in the other end can be seen in Fig. 4.3.n.



Fig. 4.3.n Termination kit used to cover the electric traced end that is not connected to electric supply. After this step, an adhesive tape will wrap the entire end from the waterproof jacket until the process pipe but leaving a couple of centimeters to assemble the pipe fitting, thereby this end was completely protected from the environmental humidity.

To fulfill ATEX requirements of the sampling enclosure, another two more essential targets should be taken into account to both all inputs and outputs of the process lines and any kind of cables (power supply or data): firstly, ensure the tightness inside of the sampling enclosure from the surrounding atmosphere; and secondly, isolating the whole electric installation from the pipe process through which NG is flowed. Regarding these two issues, the following actions were made:

- All inputs and outputs process lines were not equipped with trace heated system were connected to the sampling enclosure by means of bulkhead union tube fitting. According to Fig. 4.3.p, these bulkheads were fitted in two drains and vent line.
- Two electric junction box, name *Box 1 and 2*, with ATEX certificates and manual cutting switch, were necessary to safely connect the most of assembly component that required power supply. Each box had eight connection holes that were used as follows:
 - Five were occupied by all trace heated lines by means of five cable glands made of brass M20 size and equipped with Ex protections and ATEX/IEC certificates. This kind of flat and grey cable can be seen Fig. 4.3.o.

- Another five cable glands, made of black nylon M20 size and Ex protections, were used for these proposes:
 - i. Two more were used to connect the heating systems belonging to the reducing pressure valve and the own heating system of the enclosure. Red and black cables on the top of Fig. 4.3.o.
 - ii. One port connection of the Box 1, which is positioned on the right, was occupied by the main cable that was connected to the electric source for energizing the entire system. It is the black cable located at the bottom of Fig. 4.3.o.
 - iii. Other two holes were used to interconnect both electric junction boxes. Therefore, they were interconnected in serial, in such way the Box 2 could only be energized if the Box 1 was too.
- The other six ports were not used so they were closed with ATEX caps made of nylon.



Fig. 4.3.o Look of the entire electric installation associated with the new sampling system. In this picture can be seen both inside and outside look of the two electric junction boxes, and all kind of cables, glands and caps used. On the left side, the internal heating of the sampling enclosure and its thermostat were positioned.

Distribution of electric connections were thought in such way that, all electric connections belongs to those instruments were not owned by Enagás, such as, Aurora and

4. EXPERIMENTAL SETUP & PROCEDURES

TDL600, could be removed after the project completion without any modification in the rest of installation. Just manually turning off the Box 2, chromatograph and hygrometer of Enagás would be kept on service and the rest of installation would be deenergized. For this reason, the Box 2 was only connected to the electric heating lines of Aurora and TDL600.

By the other hand, all cables had their own ground wire and in both electric junction box all ground wires were linked among themselves and with the back panel at the same time. In addition, such panel had a bus bar where some ground wires came from particular components were connected to the back panel too. Finally, the whole sampling enclosure was connected to mass by means of the ground wire belonged to the main cable that supplied the whole installation. The rest of instruments and their outdoor enclosures were equally operated, resulting that the entire facility was completely equipotentialised.

The schematic diagram of the new sampling system is depicted in Fig. 4.3.p and its real final look can be seen in Fig. 4.3.q.

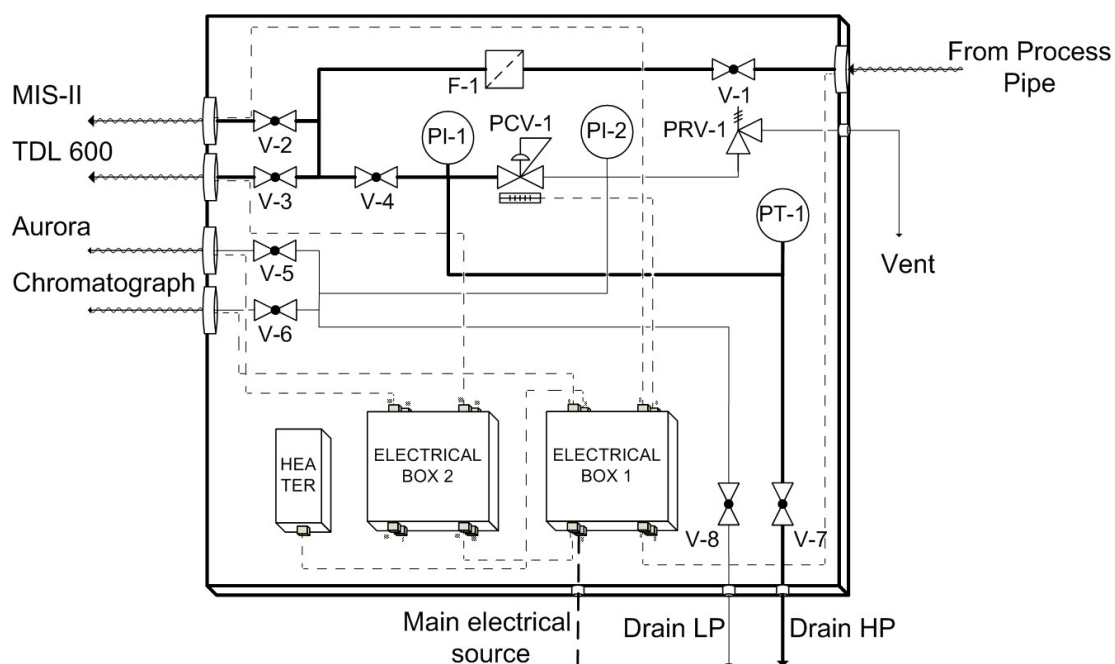


Fig. 4.3.p Pipe and Instrument (P&I) diagram showing the new sampling system box designed and built for these tests. Thick lines denote pipe sections where the NG is at the maximum pressure line (HP), whilst the thin lines indicate those areas where the NG had been undergone to the pressure reduction step (LP). Dashed lines show electric cables, both by those used by the trace heated lines and by the own heater positioned inside the box.



Fig. 4.3.q Final look of the new sampling system designed and built for providing service to the chromatography section and the three hygrometers studied in this section of the thesis.

As it can see in Fig. 4.3.q, all pipe sections were strategically fixed to the back panel by means of clamps, avoiding movements or vibrations of any element forming the system while pressurized NG was flowing.

The final look of the entire experimental set-up built in Serrablo, which includes the new sampling system, the three sampling enclosures for the three hygrometers studied and the outdoor room of the chromatography system, can be seen in Fig. 4.3.r.



Fig. 4.3.r View of the whole experimental facility assembled for the comparative study of two sensing humidity techniques under real industrial conditions. On the left, it is the sampling box housing the capacitive sensor, the MIS-II. The common sampling system box (with its four trace heated output lines) is positioned between the two spectroscopic analyzers, on the left Aurora and on the right the TDL600.

4.3.4.4 Process variables. Measurement and control.

As it has been commented several times, certain properties are essentials both measuring the humidity in a gas and doing conversions between the different ways to express it, either WDP or WC. Such magnitudes are: pressure, temperature, flow rate and gas composition. For that, the functions of every variable and how they were controlled were explained in the following chapters.

4.3.4.4.1 Pressure

Relevance of pressure to measure and compare the absolute and relative humidity quantities between themselves has been explained several times in previously chapters (see Section 1.2 and Section 4.1.3.3.2). The sampling system designed to Serrablo had the peculiarity of being able to work simultaneously at two pressure levels: high (HP) and low pressure (LP), up or downstream of the heated pressure regulator, respectively. This was a mandatory feature required because the Aurora and the chromatographic system could not measure at the maximum pressure line directly. The upper pressure limits at the inlets of both instruments were limited to 1.3 MPa for the Aurora, and 0.3 MPa for the

chromatograph. The output pressure of the heated reducing pressure valve was set at 0.14 MPa, in such way this set point could give service to both measuring systems. As additional safety element, a relief valve was assembled in the LP zone. Its working range for the relative pressure was since 0.068 MPa to 1.55 MPa and it was set at 0.2 MPa.

In addition, two pressure gauges were fitted just on both sides of the reducing pressure valve, so any operator can handle the panel safely. According to scheme depicted by Fig. 4.3.p, PI-1 shown the actual process pressure, while PI-2 would have to be always fixed at the set point chosen, namely, 0.14 MPa and should never be higher than 0.2 MPa. If latest happens, it would means the relief valve is not working well and may damage the chromatograph section. The relative pressure ranges of these gauges were (0 to 10) MPa to PI-1 and (0 to 1) MPa to PI-2.

Pressure measurements are essential to convert WDP to WC and vice versa. For this reason, each hygrometer analyzed had its own pressure transmitter, thereby the comparative would be as accurate and reliable as possible. Initially, both spectroscopic instrument borrowed had not integrated a pressure transmitter, so they had to be added before.

Pressure transmitter of TDL600 was directly positioned inside of its own sampling panel, but the Aurora had not enough space inside its sampling panel to mount one pressure transmitter, so it had to find the best position possible. For this reason, pressure transmitter of Aurora was assembled just before of pressure reduction step to give WDP measurements converted at the actual process pressure. Fig. 4.3.q shows like the position of such transmitter was in the upper right corner, so the measuring point was the same than the PI-1 gauge.

The pressure transmitter used by Aurora was UNIK-5000 model, whilst TDL600 used HYDAC HD 47 which was commercialized by the own GE. Below can be seen their look in Fig. 4.3.s and the most important features are summarized in Table 4.3.c:

4. EXPERIMENTAL SETUP & PROCEDURES



Fig. 4.3.s Pressure transmitters of spectroscopic analyzers: UNIK-5000 used by Aurora (left) and HYDAC HD 47 used by TDL600 (right).

Table 4.3.c Summary of the most important properties of pressure transmitter associated with the Aurora.

	UNIK5000	HYDAC HDA 47
Relative pressure range	(1 to 10) MPa	(-1 to 10) MPa
Accuracy	± 0.2 % FS *	± 0.25 % FS
Hysteresis	---	± 0.1 % FS
Repeatability	---	± 0.05 % FS
Non-linearity	---	± 0.3 % FS
Long term drift	± 0.05 % FS / year	± 0.05 % FS / year
Operating temperature	(-40 to 125) °C	(-40 to 60) °C
Temperature effects	(-20 to +80) °C ± 1.0 % FS	± 0.008 % FS / °C
Hazardous area	Intrinsically safe [EUD94]	Intrinsically safe [EUD94]

* Combined effects of non-linearity, hysteresis and repeatability.

4.3.4.4.2 Temperature

Temperature is another of the most important parameter must be well controlled and accurate measured inside of the hygrometry field. According to the European standard ISO 18453:2004 [ISO04], the temperature of the NG is necessary to perform the unit conversion between WC and WDP. For that, it was another parameter had to be into account in this experimental section. Each of three hygrometers studied had an individual temperature probe integrated inside of its own sampling system, however in both

spectroscopic instruments a peculiarity there were: temperature probes were not in contact with the NG but it is located inside of the sampling enclosure, so these instruments are based on there are a thermal equilibrium inside the box, simplifying the inner temperature like the NG temperature.

4.3.4.4.3 *Composition*

That is the last of three parameters that must be measured to convert WC and WDP units and vice versa [ISO04]. The NG composition was provided by Enagás by means of the chromatography section cited throughout this chapter like part of the facility supported by the new sampling system built.

Daily NG compositions were supplied to INTA staff for further analysis during the whole test time. Reports received had the information about the concentration of next chemical species: methane, ethane, propane iso- and neo- butane and pentane, nitrogen, carbon dioxide and C₆₊ fraction, which groups those hydrocarbon constituted by six or more carbon atoms.

Just like Section 4.1.3.3.1.2, from these composition analyses it can be determine many others physical and chemical properties [ISO05]. Parameters reported in this case were: the relative density, lower and higher heating values (LHV and HHV) and Wobbe index.

4.3.4.4.4 *Flow*

In this case the flow control was much easier than the experimental rig described in section of semi-industrial tests. Because both measuring techniques studied in this block were not dependent on the flow crossing the measuring cell, only it had to be kept within the working range described by the manufacturers, so this parameter was only controlled by the flowmeter directly associated with each instrument. Flow crossed sensors of the three instruments was relatively stable during the whole test time, except in specific times because of some kind of handling in the process and/or sampling line. Flows was around 60 SLPH both spectroscopic and capacitive Al₂O₃ sensors.

4.3.4.5 *Data acquisition system improved*

For the new installation two new wires had to be mounted for transmitting the measuring data coming from the two spectroscopic instruments and energize them. These wires should connect the sampling zone where the hygrometers were installed with the

4. EXPERIMENTAL SETUP & PROCEDURES

control room, which was approximately at 100 m away in a safety area. Such wires should be installed 1 m underground, support medium voltage range and had to be shielded for protecting from outdoor humidity and rodents. The features of wires chosen were as follow: for the power supply cable consisting of 2-wires copper 1.5 mm² of section and all that wrapped by one steel grid; for the other cable used to data transmission was formed by six twisted-pair cables 1.5 mm² section with strand shielding each pair and the entire assembly.

Inside of the control room it had to adjust the expansion of the of the hygrometry section in the main control center of the plant by means of one differential relay Merlin Gerin II 40 A 30 mA model and a pia Merlin Gerin I+N 10A. Thanks to this installation any hygrometer could be switched on/off at any time from the control room.

By the other hand, the laptop previously mounted for the initial tests was connected to an uninterruptible power supply (UPS), to protect the recording system from small micro-cuts in the power supply because of the often storms that happens in this areas or by maintenance tasks associated to the plant that imply cut the power supply in different areas. The UPS used was the SPS 1000+ SOHO manufactured by *SALICRU*, which was able to keep operative up to three electrical systems.



Fig. 4.3.t Uninterruptible power supply (UPS) installed in Serrablo to keep operative the whole recording data system both analogue and digital output.

Recording scheme was the same explained in Section 4.1.3.4 both analogue and digital outputs, there were only two small differences:

- Data recording software of TDL600, also supported by Michell, was installed in the same laptop. This software, like the instrument, was still in a beta version when this study was performed, so its capabilities were limited during the whole test time.

Initially, this software only recorded the WC, then TDL600 received a firmware and software update, so three parameters could be recorded at the same time: WC, WDP and pressure. Nowadays, software included together with the final version of this instrument has far greater potential.

- By the other hand, one new analogue output was configured in the data acquisition / data logger switch unit, manufactured by Agilent and it was already described in Section 4.1.3.4. This new channel read the WC measured by the last spectroscopic instrument installed. Enagás continued providing us humidity data from its MIS-II together with pressure and gas temperature data.

Fig. 4.3.u shown the entire data acquisition unit installed in the control room of the plant of Serrablo. In this picture can be seen, the UPS unit, the data logger switch unit for the analogue outputs at the lower left corner, the laptop where were set up the two data logger software of the spectroscopic instruments and Agilent unit. Also it can be seen a junction box where the three analogue outputs (WC and WDP measured by Aurora, and WC of TDL-600) and the other two digitals outputs came. Digital outputs signals should be converted from RS-485 to USB by means of particular converters that were positioned inside of this electrical function box.



Fig. 4.3.u Entire data acquisition system used in Serrablo to record both analogue and digital outputs of three instruments evaluated in this section of thesis.

4.3.5 MEASURING PROTOCOLS

The main target of this experimental section was evaluate and understand the performance of the promising humidity sensing technique, the absorption spectroscopy,

4. EXPERIMENTAL SETUP & PROCEDURES

versus the most commonly technique used inside of the NG field under real industrial conditions. As a result of the preliminary test performed during the injection time (see results shown in Fig. 4.3.h), it was decided study the behavior of both technologies during all kind of process stages occur at the UGS and drying plant of Serrablo. In this kind of facility there are two production stages, *injection* and *extraction*, which are interspersed by *shutdown* times. Below is explained the activity carried out during each of this production step:

- Injection time is the step during which NG is coming from the national grid to be stored inside of the underground wells. NG arrives at pressure levels around 6 MPa and it must be pressurized through pumping stations up to the usual pressure levels inside the wells, which can be around 20 MPa depending on the surrounding soil properties. During these periods the drying section of the plant is not operational because the NG comes dry from the grid and it will be saturated inside the wells.

- Extraction times are those periods during which the plant is withdrawing the NG stored in the wells to be introduced into the national grid and this way, fulfill the energy requirements of every consumer. It is in this step when the drying plants are working because the NG coming from the wells is completely saturated with water, so is now when humidity of the NG must be accuracy controlled because that directly affect properties of the final product which will be sent to the customers. Therefore, it is the key time in which the humidity must be perfectly measured and the hygrometers must demonstrate their measuring capabilities. Extraction process occurs during the cold months because the high energy demand requires the use of these strategic storages. The most critical moment for the UGS it during extraction when the saturated NG from the wells is being dried and condensation effects and hydrate formation need to be avoided in the extreme low temperatures commonly experienced in these months.

- Shutdown times are those periods when NG is not flowing across the plant, so the NG is stopped and confined by the inner volume of all elements forming the plant. During this time, staff plant carries out maintenance and/or repair tasks, including calibration of all instrumentation.

Thus, study the performance of both technologies under real industrial conditions will have to take into account the behavior of instruments under these three production steps to find out, or discard, different behaviors between process productions of Serrablo.

4.3.5.1 Online recording of all readings

The method used to study the behaviour of sensors during the three production processes was recording evolution of humidity in the NG uninterruptedly. This way, not only can be analyzed their behaviour in these three phases of the plant, but also during the transition states produced when one production stage of the plant is changed. Thus, their behaviours could be evaluated both in steady and transitional production phases of the plant. Thus, not only measuring capabilities of hygrometers will be evaluated but also their dynamic behaviour as a response against a change of production process of plant.

4.3.5.2 Checks of analyzer performance

Initial conditions of the three instruments were quite different because of their origin and they were lend for this project in different moments. The initial conditions were as follow: the MIS-II had been in use using the current manufacturer's calibration coefficients obtained using N₂ as the carrier gas; the Aurora had been supplied for use in a previous research project [Gal15] and had been in the field for over a year; and finally, the OptiPEAK TDL600, was a pre-commercial prototype calibrated by the manufacturer in methane. For all of that, it was absolutely mandatory to carry out at least one check point to know the state of hygrometers.

Independently of the verification test performance for this study, manufacturers checked their analyzers on site at least twice during the test period and included improvements in hardware and software to ensure reliable measurements.

Because of the problem of the initial conditions of all sensors, the great difference between their arrival dates and that there was not a common standard procedure to calibrate instrument that was going to be used in complex gaseous matrix, as the NG, even there is not agreement about the gas must be used during calibrations. For all of that, it is impossible and it would be a mistake compare in absolute terms the performance of this analyzers. In this sense the check test was performed with the aim to know the relative conditions of the instruments and to be able to evaluate the relative performance of them.

Check test consisted on a simple calibration with a standard mixture sample of N₂ and H₂O with a water concentration equal to 24 ppm_v ± 4 ppm_v, was used. The test commenced with a critical humidity condition of WDP higher than 15 °C to simulate a high risk situation in which great amounts of condensate may appear inside the sample

4. EXPERIMENTAL SETUP & PROCEDURES

lines. Initially the whole experimental section (see Fig. 4.3.1) was isolated from the NG supply and was dried by flushing dry N₂ at 5 MPa and after that, it was to start to flow standard sample of N₂ and H₂O. The results obtained from this test were described in Section 5.3.4, where each perturbation in the signal of three sensors is justified with each of actions made during the test.

4.3.5.3 Methanol influence

Hydrate inhibition is typically implemented when it is not cost effective to install a full dehydration unit, or when an operating dehydration unit cannot obtain the desired dew point depressions. A known hydrate inhibitor is introduced upstream of the location where solids formation is predicted to occur. The inhibitor provides some dehydration, but its primary function is to act as an "antifreeze" agent in suppressing the formation of solid hydrates [K&R85]. Methanol injection, proposed by Hammerschmidt in 1939 [Ham39], is one of the options available to control hydrate formation but is not regenerated in the gas processing systems, unlike other choices such as TEG [K&R85].

However, it has been reported that Al₂O₃ capacitive probes, commonly used by the NG industry, tend to increase the measurement uncertainty in the presence of methanol, through increased drift speed or shifts in the moisture readings [Løk12b and Løk13]. A basic methanol injection test was performed during the injection phase by adding 25 L of methanol to the test section during 45 minutes in order to ascertain whether the new spectroscopic sensors are also influenced by this inhibitor. During the test, the mean NG flowrate was 46 Nkm³·h⁻¹. This yields an approximate methanol concentration of 7 μmol·mol⁻¹ at the temperature and pressure at the time the test was performed. The results compiled by this test are shown and commented in Section 5.3.6.

4.3.6 OTHER PROTOCOLS

In this section all those protocols associated with the experimental installation mounted in UGS of Serrablo have been thoroughly described. That includes the start-up and shutdown protocols, leak tests procedures, maintenance test, etc.

4.3.6.1 Start up and shutdown

START-UP PROTOCOL

Start-up protocol was thought starting from the initial position of all valves closed, and supposing that the heated reducing pressure valves and their associated relief valves had been fitted with nitrogen at their corresponding pressure level during the leak test. The protocol was as follow:

1. Turn on spectroscopic instruments from the control room.
2. Manually open the valves V-1 to V-3, and check that pressure and humidity readings shown on the screen of TDL600 are coherent.
3. Open the valve V-4 and check the reading given by the pressure gauge PI-1 is agree with the pressure reading shown by Aurora, by means of the pressure transmitter, PT-1.
4. Check the reading given by the pressure gauge PI-2 is agree with the output pressure previously set in the pressure control valve PCV-1, and is never higher than 0.2 MPa.
5. Open the valves V-5 and V-6 and check that pressure and humidity readings shown on the screen of Aurora are coherent.
6. Start Agilent's software to measure the analogue outputs.
7. Start data logger software of TDL600 and Aurora and check that these readings are similar than their corresponding analogue values.

SHUT DOWN PROTOCOL

If for any reason, despite waiting to do a continuous recording of readings during one full season, it had been wanted to shut down and close the new hygrometry section, it would have to do the following protocol:

1. First of all, close the gas inlet valve, V-1.
2. When the gauge pressure PI-1 shows there is no pressure, then close V-2 to V-4.

4. EXPERIMENTAL SETUP & PROCEDURES

3. When the gauge pressure PI-2 shows there is no pressure, then close V-5 and V-6.
4. When the whole plant is depressurized, stop and record log files of analogue and digital outputs.
5. Turn off the power supplies of the entire new hygrometry section:
 - a. Use the switches of both electric function boxes.
 - b. Disconnect also the power supplies coming from the room control.

If it is only wanted let out service some of instruments associated with the new sampling system, then it will have to close the properly gas inlet valve (V-2, 3, 5 or 6, as appropriate).

4.3.6.2 Leak tests

The soap solution method was used to detect leaks by means of bubbles formation. This method was firstly used with nitrogen, and after that, with NG. First step with N₂ up to 9 MPa, which was the maximum pressure given by the cylinder contained the gas, ensuring this way the integrity in the whole installation with a coverage factor even higher than 30 %. After that, the same procedure is repeated but this time flowing NG.

The leak test had to check the whole hygrometry section, namely, not only the new sampling system, if not also connections with the sampling box belonging the three instruments and their individual sampling panel.

The protocol performed is the same that the start-up protocol described before, but connecting previously the pressurized cylinder at the inlet. The pressure level of nitrogen will be increased as the whole sampling section was checked, then it will do the shutdown procedure and it should start again the start-up protocol but increasing at the next pressure level. Sequence of nominal pressure levels of nitrogen was as follow: (0.5, 3, 6 and 9) MPa, whilst with NG was only tested at 3 MPa and 6 MPa.

4.3.6.3 Set the output pressure of the reducing pressure valves

The set points of the output pressure of the reducing pressure valves and its relief valves associated were fitted with nitrogen. This procedure had to be done only once at, just before to the leak test with nitrogen.

-
1. Adjust the output pressure from the cylinder houses the nitrogen at 0.5 MPa by means of its own pressure reducer.
 2. Open the isolating valve between the bottle and the reducing valve RV-1, and fit the outputs at 0.2 MPa.
 3. Then, the relief valve associated was fitted at 0.14 MPa.

4.3.6.4 Maintenance and Cleaning

The NG is not a clean and pure gas, but rather a complex mixture consisting of variable fraction of heavy components that can be condensate due to diverse cause, such as: water composition too high, cold spots in the installation, etc. Then, contamination effects were expected and, in fact, condensation problems of hydrocarbon emulsions happened with the older sampling system (see Fig. 4.3.j).

In case that it is suspected some hygrometer may be suffering contamination effects, which is usually shown by humidity measurements exceptionally high, the instrument affected will have to be isolated, closing the appropriate isolating valve, and to carry out the maintenance protocol described by the manufacturer in their handbooks.

Either high and low pressure drain lines can be used to remove those condensates which may appear inside the sampling box. Thanks to all heating systems installed would be very strange that condensation effects appeared, but drains must be placed anyway because they are useful for several tasks, as: connect dry nitrogen to drag condensates and dry the line, connect a standard sample to calibrate or check the performance of hygrometers.

4.3.6.5 Safety

Besides of those points related with the safety and handled of NG pressurized that were commented in Section 4.1.3.6.5, as for example: NG properties, use of personal protection equipments (PPEs), the fire tetrahedron conception, lower and upper explosive limits (*LEL* and *UEL*). Some more specific concept had to be taken into account before and during the work performed at the industrial facilities.

The most important point was related with the fact that the entire experimental section was located inside of area classified as ATEX. This acronym, coming from the words "explosives atmospheres", which makes reference the European directives for

4. EXPERIMENTAL SETUP & PROCEDURES

working inside of such zones. In this sense, nowadays in Europe there are two kind of laws applied according to the implementation theme:

- The European Directive 94/9/EC [EUD94], denominated ATEX-100 and approved in Spain by the Real Decreto 400/1996, 1st of March [BOE96], which regulates the equipment and protective systems that is intended for use in potentially explosive atmosphere.

- Therefore, had to meet this directive all those components associated with the power supply, as for example: heater inside the sampling enclosure, the electric traced lines, junction box, the pressure transmitter of the Aurora, or the heated reducing pressure valve. In this point, are also included those elements charged with avoiding a potential contact between the NG and any electric component in case of gas leak, as: bulkheads and their correspondent sealing glands, caps, cable glands and caps.

- The European Directive 99/92/EC [EUD99], denominated ATEX-137 and approved in Spain by the Real Decreto 681/2003, 12th of June [BOE03], which regulates the minimum requirements for improving the safety and health protection of workers potentially at risk from explosive atmospheres. This law involved all those tools and materials were needed during the mounting of the whole experimental section, besides of the PPEs that were mandatory wearing during the work in this hazardous area, as safety boots, safety goggles, electrician gloves and winter clothes specially thought to work outdoor at very low temperatures.

5 RESULTS

5.1 RESULTS UNDER SEMI-INDUSTRIAL CONDITIONS

In this section, all experimental data obtained during the tests performed under semi-industrial conditions have been shown. In addition, various analyses and data treatments performed have been thoroughly explained, together with all information and conclusion that can be extracted from them.

First of all, it must be explained nomenclature used by simplify the way to name all humidity instruments compared. In the below table is shown the code used:

Table 5.1.a Nomenclature used along the whole experimental section under semi-industrial conditions to simplify the identification of all humidity instruments in all figures, graphs, and tablets.

HUMIDITY METERS	MANUFACTURER	CODE
<i>Aurora</i>	GE	A
<i>Accupoint LP 2</i>	Meeco	B
<i>DS2000</i>	Shaw	C
<i>Easidew transmitters</i>	Michell	D, E
<i>Easidew Pro I.S.</i>	Michell	F
<i>HygroPro</i>	GE	G
<i>SDT DP Transmitter</i>	Alpha	H
<i>EE371</i>	E+E	I
<i>Superdew 3</i>	Shaw	J
<i>DP3D</i>	MBW	K
<i>Condumax II HCDP</i>	Michell	L1
<i>Condumax II WDP</i>	Michell	L2

Since there were two Easidew transmitters, two letter were used to name them. For the case of the Condumax II, because the same instrument had two channels to measure the WDP and the HCDP at the same time, it was associated to one letter joined with a number 1 or 2, to denote both measurement quantities.

5.1.1 PREVIOUSLY ACTIVITIES

Before starting the study of humidity instruments some tasks, directly linked with the assurance of the quality of the measure, had to be performed. Below were explained the activities previously done.

5.1.1.1 Previous calibrations

In this sense, calibration of all supplementary instrumentation required to measure accurately and reliably the water concentration in NG was mandatory. According to the equations developed in Section 1.2, to measure the water partial pressure in a mixture gas, namely, as a NG, is necessary to know the total pressure and temperature of the mixture. In addition, some humidity sensing technology compared here were also dependent on the flow, so it had to be taken into account.

5.1.1.1.1 Complementary instrumentation for humidity measurements

In this section are shown all those calibrations previously performed and directly linked with the humidity measurement in NG.

Firstly, the relative pressure of NG was measured by three pressure transmitters. Below are shown each of their previously certificates performed by the pressure and mass laboratory of INTA:

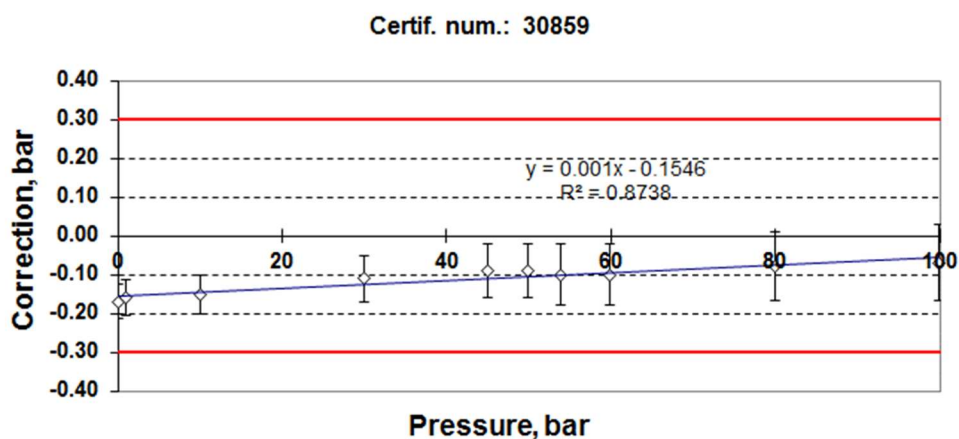


Fig. 5.1.a Calibration certificate of pressure transmitter, model PTX-510.

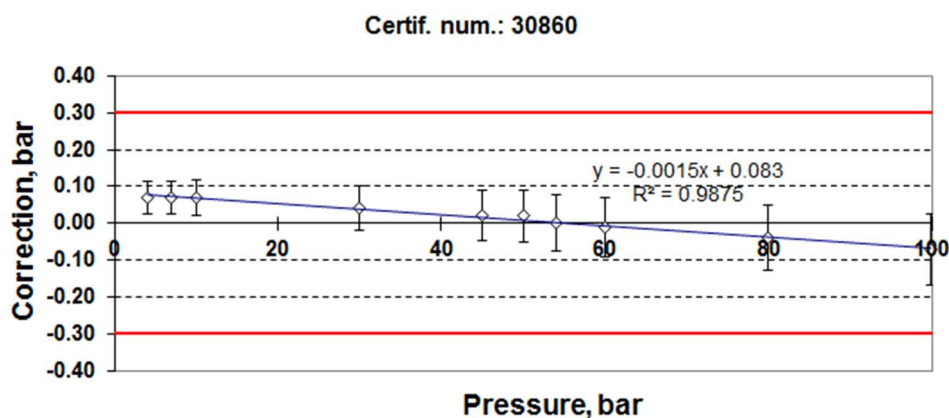


Fig. 5.1.b Calibration certificate of one of the two pressure transmitter, model PTX-610.

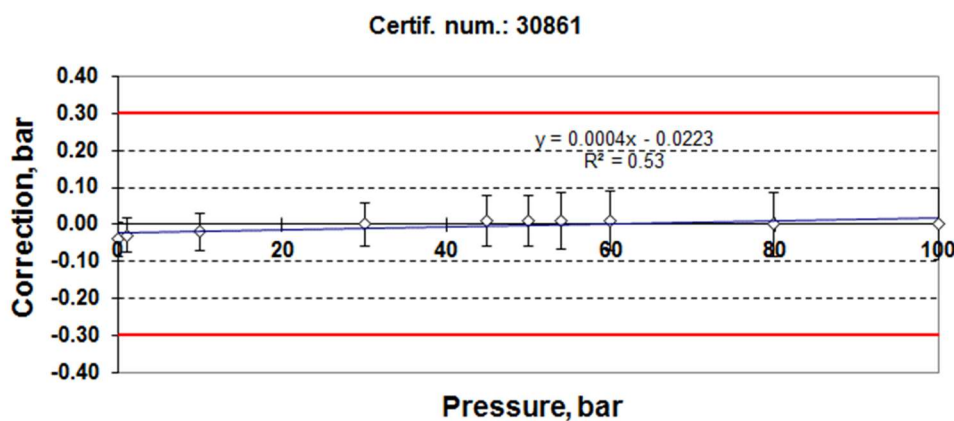


Fig. 5.1.c Calibration certificate of the other pressure transmitter, model PTX-610.

The linear fit equation shown in Fig. 5.1.a to Fig. 5.1.c were used to correct the pressure readings given by such transmitters, including the subsequent conversion to the International System of Units (SI), ergo, in Pa units.

By the other hand, gas flow was another variable that affects the humidity measurement in technologies as the condensation methods, capacitive sensors and polymeric. For that, the flowmeter shown in the P&I diagram, depicted in Fig. 5.1.d, was used as flow controller in those three sampling lines that contained hygrometers under study. Fig. 5.1.e shows the old calibration, which was performed by its owner (Enagás), and the new calibration performed by the flow laboratory of INTA.

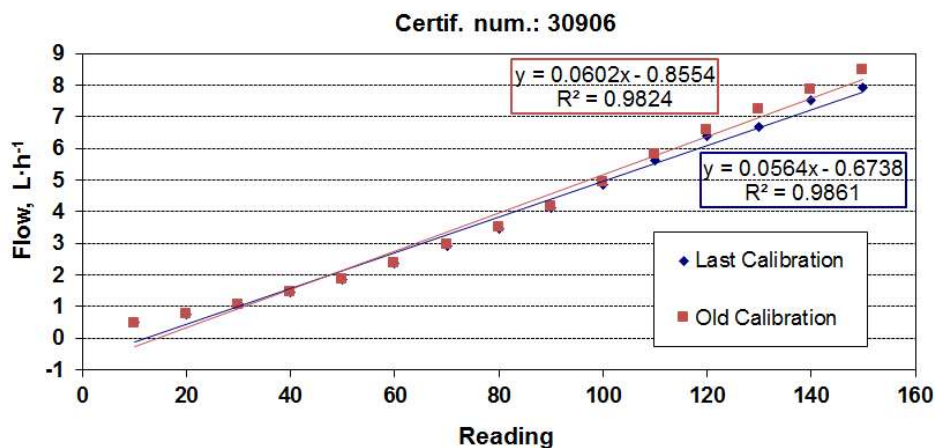


Fig. 5.1.e Calibration certificate of the flowmeter borrowed by Enagás.

For the case of this flowmeter, fitting linear equation was not inserted to correct its readings, just it was used to be sure that the manual adjustment of flow rate was properly performed always before starting any test.

Another calibration performed was with data acquisition unit (see Section 4.1.3.4), which was used to record all analogue outputs. Despite to be a unit specifically purchased for this project, an electrical calibration by simulation was performed to check that was functioning right. Every channel of every multiplexers associated met specifications from manufacturer, so any correction had to be applied for any analogue output measured.

5.1.1.1.2 Hygrometers

As it has been commented along this thesis, the most of humidity instruments did not came directly from the manufacturers recently calibrated and adjusted, but they had been used in diverse tasks previously performed during the EMRP project [ENG01] and they were shipped directly to us. Thus, depending on the origin of the hygrometers there were three possible situations:

- First group it would comprised by those humidity measurers coming directly from manufacturers and with their calibration certificates performed by the own manufacturers. That was the case of the Aurora, the Condumax II and the EE371. The certificates provided by the manufacturers were as follows

- Condumax II came directly from Michell's factory in U.K. and brought its calibration of certificates of both measurement channels (HC and WDP), together with certificate of both pressure transmitters assembled in each channel.

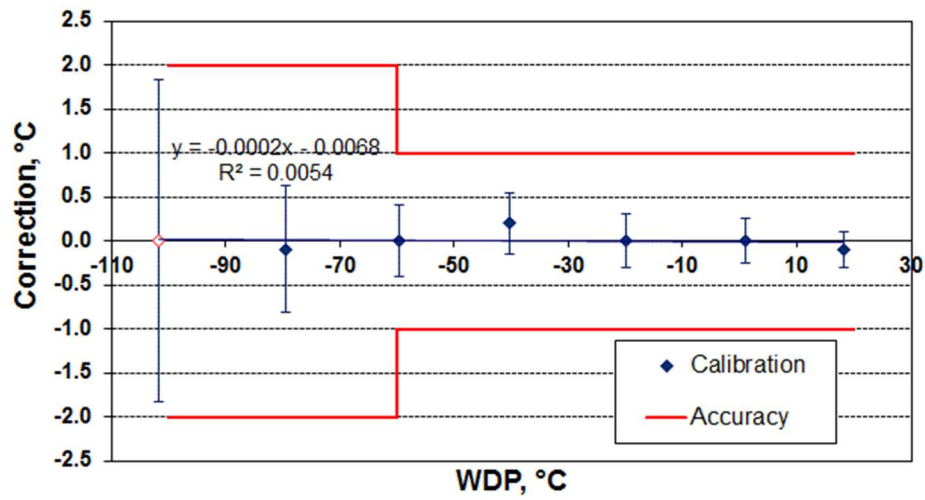


Fig. 5.1.f Calibration certificate of the two pressure transmitters assembled in both measurement channels of Condumax II, provided by Michell.

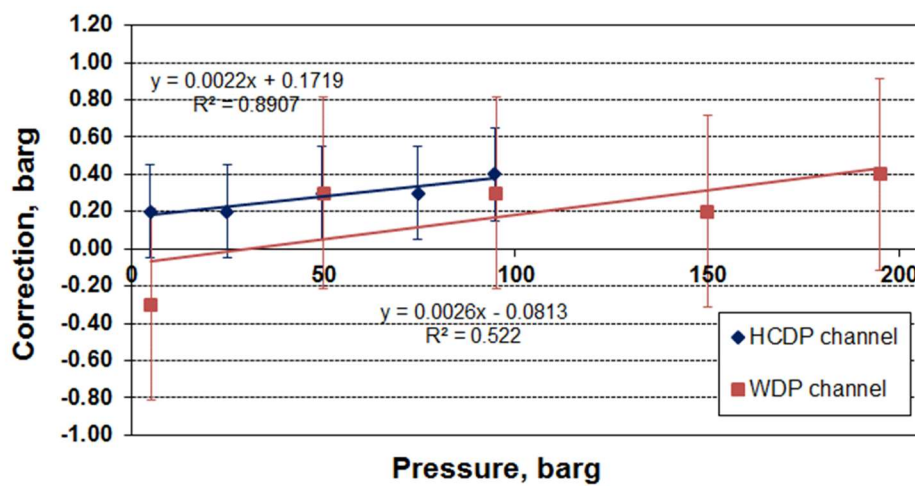


Fig. 5.1.g Calibration certificate of WDP sensor assembled in the Condumax II, which was provided by Michell.

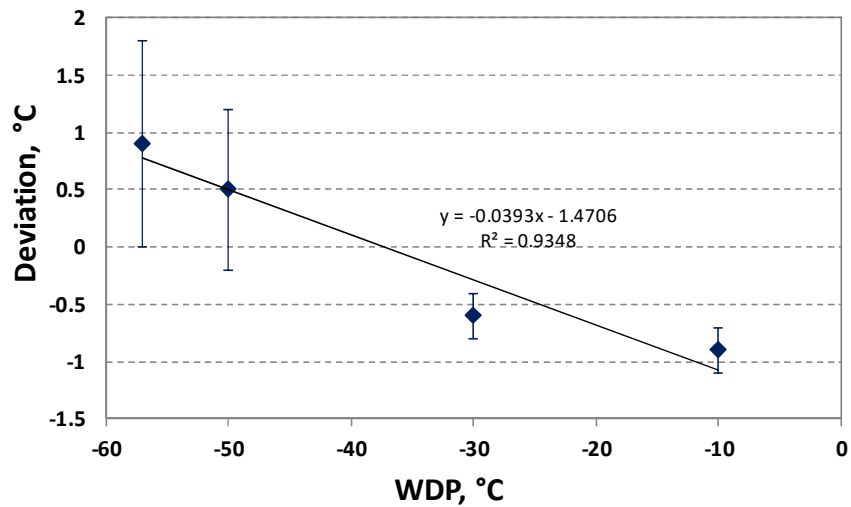


Fig. 5.1.h Calibration certificate of EE371 probe provided by the manufacturer

It must be careful because calibration certificate can be expressed in terms of the correction, as the most certificates, but also as the deviation, as that provided for the EE371 and depicted in the above figure.

- Secondly, the most of instruments coming from NPL such as the case of sensors C, D, E, F, G, H and J (See Table 5.1.a). They were calibrated with methane up to 3 MPa before and after the experimental test performed during this thesis and their results have been shown and analyzed in Section 5.1.5. This way, it can be obtained more information about the drift suffered by these probes during the test performed over real NG.

- And finally, the chilled mirror hygrometer DP3D, which was owned by Enagás and was borrowed to INTA during this research, was calibrated by ourselves in LabTH.

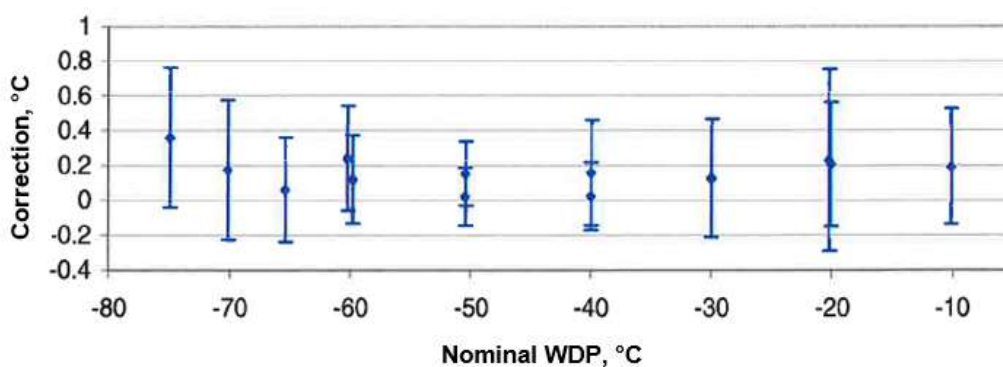


Fig. 5.1.i Correction WDP graph belonging to calibration certificate of DP3D chilled mirror hygrometer owned by Enagás.

5. RESULTS

The only hygrometer that have not been calibrated before being shipped to our facilities was the Accupoint LP 2. The reason of that was this instrument is auto-calibrable by flow adjust, which at the same time is dependent on the gas is flowing across the sensor cell, so it had to be calibrated directly with NG.

5.1.1.2 Characterization of humidity generator

In this section were shown the results obtained during the characterization of the mix flow humidity generator, described in Section 4.1.3.3.3. In the below table were summarized the results given by the three humidity instruments for all combinations of dry and wet NG flows.

Table 5.1.b Characterization of humidity control system taking into account measurements of three instruments based on different sensing technologies.

VALVE TURNS	INSTRUMENT		
	A	B	G
1 3/5	30.0	24.57	15.7
2 3/5	42.5	39.69	21.2
3 3/5	57.9	51.03	29.9
4 3/5	70.0	68.67	38.5
5 3/5	82.5	81.9	43.3
7	98.0	100.17	49.2
8 3/5	123.4	117.81	58.4
10 3/5	161.9	166.32	80.7
12 3/5	195.9	205.38	100.0
14 3/5	243.1	262.71	127.5

Data shown in column of instrument B were data already corrected once its flowrate was fitted at value recommended by manufacturer. Check and adjustment of electrolytic instrument was performed because its humidity reading were being quite higher than the other two instruments which were also being used during the characterization of humidity generator. Procedure carried out to fit the flow that crossed the sensor cell was performed according the procedure explained by the manufacturer in its handbook, “Section 4: Calibrations & Settings”.

If results of Table 3.2.a were shown in a graph (Fig. 5.1.j), it could be seen at a glance that humidity measurements recorded by three instruments had a linear behavior regarding to the opening of the control needle valve, V-12, according to the Fig. 4.1.n.

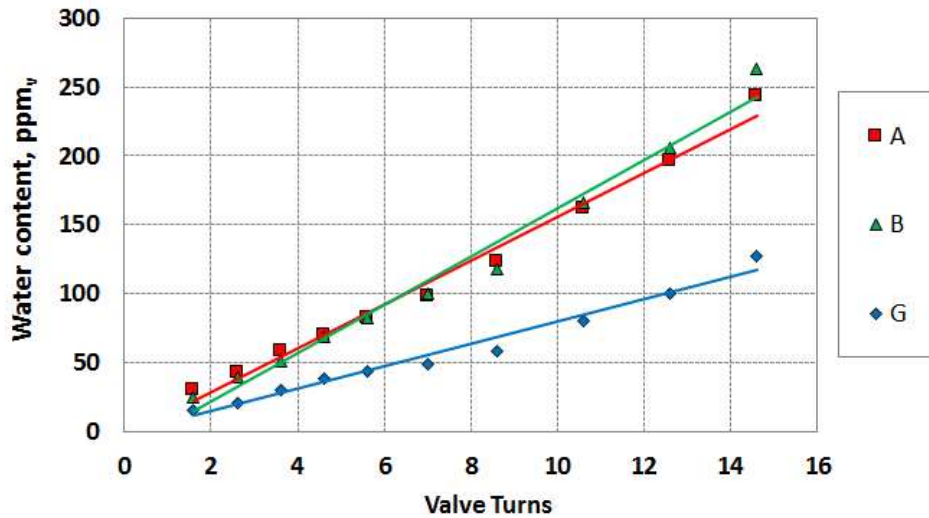


Fig. 5.1.j Readings given by the three hygrometers which were used during the characterization of humidity generator, regarding the opening of flow control valve.

From these data collected, instrument A was chosen as a reference, because its readings were very close to readings of B, but its response rate was much faster. Also this way, nominal humidity values chosen in this study, and expressed in terms of WC, were as follows: (13, 30, 45, 55, 70, 85, 100, 125, 160, 200 and 250) ppm_v. The nominal WC of 13 ppm_v were not depicted in Fig. 5.1.j because corresponded with the valve V-12 completely closed, being the own WC of the NG inlet.

5.1.2 GENERAL CONDITIONS

In this section has been explained which those general properties that were linked with humidity measure of a non-standard and fixed NG mixture and under laboratory conditions, which were taken into a count to carry out this research, such as: laboratory and natural gas inlet conditions.

5.1.2.1 Gas natural inlet properties

Before starting the test time, it was considered essential to record the HC and WDP conditions of NG sampled, in order to obtain continuous readings of such quantities to assist the subsequent interpretation of results, avoiding misinterpretations of the performance of the hygrometers. This was indispensable because NG sampled from the

main transmission pipeline was not a standard mixture with well-known and stable composition, but a system under continuous change depending on the demand and the source of NG transported.

For this reason, Condumax II was the only hygrometer able to record both quantities simultaneously and because of that had to be used as monitor to record NG inlet properties. Fig. 5.1.k depicts all HC and WDP readings given by the Condumax II during the whole experimental test time and at their corresponding pressure levels.

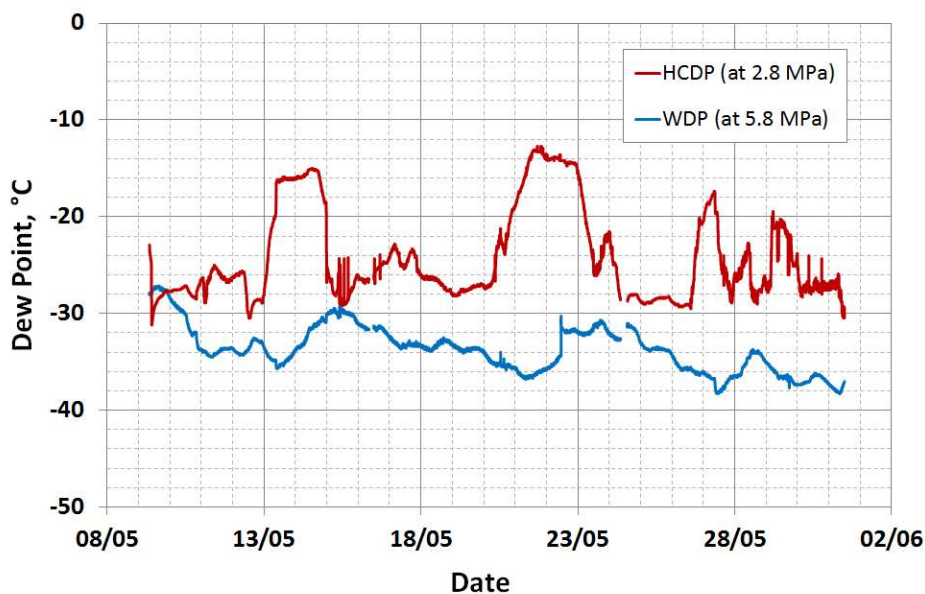


Fig. 5.1.k HCDP and WDP readings of NG inlet during the entire test time.

Looking at Fig. 5.1.k the achieved values were well below the upper limits specified by EEASE-gas, which establishes that HCDP must be lower than $-2\text{ }^{\circ}\text{C}$ at any pressure between 0.1 to 7 MPa, and WDP must be lower than $-8\text{ }^{\circ}\text{C}$ at 7 MPa [EAS05]. For these reasons, HCDP was measured at 2.8 MPa, because such pressure level is close to the cricondentherm or the maximum condensation temperature of hydrocarbons, while WDP was measured at maximum pressure line. The fact that both criteria were widely achieved means that NG quality assurance from the point of view of the humidity was warranted, by contrast it also implied NG was overdried which leads to higher costs during drying stages.

In addition, Fig. 5.1.k also gives information about how big HC and WDP changes were and if there was directly correlation between HC and WDP changes or not. These continuous oscillations in NG inlet together with the fact that there was a standard

hygrometer which could be used as a reference, implies that all measures and results obtained in this work were relative, so it should be very careful if data shown here were used in another context.

By another hand, depending on the sort of instrument, humidity could be expressed either as WC or WDP, so in order to facilitate the comparative study performed here, all values were converted to WDP according to the International Standard ISO 18453:2005 [ISO04]. As it was mentioned in Section 4.1.3.3.1, to carry out this unit conversion, it was necessary to know the gas composition. Below is shown an example of the daily composition analysis of NG provided by Enagás. As can be seen, the chromatography analysis gave a very detailed composition study for the main components of NG and the most important hydrocarbon species constitute for up to twelve carbon atoms, C₁₂. Each particular concentration data were expressed as molar concentration percentage together with its own uncertainty and coverage factor, k, associated.

The GERG model describe in Section 1.3.4 was used to convert WC and WDP units, thanks to a calculation software developed by Enagás and which was loaded to INTA staff to carry out all activities developed along all this thesis.

5. RESULTS

Table 5.1.c Example of detailed report about the daily gas composition tests obtained by means of chromatographic analysis.

		Componente	Concentración % mol/mol	Incertidumbre % mol/mol	k
Componentes Principales		N2	0,846 ±	3,5E-02	2,01
		CO2	0,150 ±	1,2E-02	2,02
		Metano	90,576 ±	1,2E-01	2,01
		Etano	6,468 ±	9,5E-02	2,01
		Propano	1,293 ±	1,9E-02	2,03
		i-Butano	0,217 ±	7,3E-03	2,03
		n-Butano	0,313 ±	8,4E-03	2,03
		i-Pentano	0,047 ±	1,7E-03	2,03
		n-Pentano	0,043 ±	2,0E-03	2,02
Fracción C ₆ + : 467,40 ppm	Fracción C ₆ 284,0 ppm	Cy-Pentano	0,003660 ±	1,4E-03	2,01
		y-C6	0,014386 ±	5,6E-03	
		n-Hexano	0,010309 ±	3,7E-03	
	Fracción C ₇ 140,0 ppm	Me Cy-Pentano	0,004543 ±	1,8E-03	2,02
		Benceno	0,000813 ±	3,5E-04	
		Cy-Hexano	0,004314 ±	1,7E-03	
		y-C7	0,003323 ±	1,3E-03	
	Fracción C ₈ 42,0 ppm	n-Heptano	0,001040 ±	3,3E-04	2,02
		Me Cy-Hexano	0,002693 ±	1,3E-03	
		Tolueno	0,000269 ±	1,4E-04	
	Fracción C ₉ 1,4 ppm	y-C8	0,001130 ±	5,7E-04	2,02
		n-Octano	0,000073 ±	3,6E-05	
p-Xileno		0,000039 ±	1,1E-04		
Fracción C ₁₀	y-C9	0,000090 ±	2,5E-04	2,02	
	n-Nonano	0,000007 ±	1,9E-05		
Fracción C ₁₁	x-C10	N.D.			
Fracción C ₁₂	n-Decano	N.D.			
	n-Undecano	N.D.			
	n-Dodecano	N.D.			

N.D.=No detectado. Concentración inferior al límite de detección

In Section 4.1.3.3.1.2, it was already explained that from all this composition information, many other NG properties can be obtained. For that, some of the most important were directly given together with the certificates provided by Enagás. Below it is shown a table with summarizes such properties.

Table 5.1.d Example of those properties of NG which were obtained from the composition analysis and that were given together with the previously table.

Propiedad	Valor	Incertidumbre	k
Poder calorífico superior (kW.h/m ³ (n)):	11.652 ±	1.5E-02	2.03
Poder calorífico inferior (kW.h/m ³ (n)):	10.500 ±	1.4E-02	
Densidad (kg/m ³ (n)):	0.7829 ±	1.0E-03	
Densidad relativa:	0.6056 ±	8.0E-04	
Factor de compresibilidad:	0.9972		
Índice de Wobbe (kW.h/m ³ (n)):	14.973 ±	2.2E-02	
Peso Molecular (kg/kmol):	17.50 ±	2.3E-02	
Número de Metano:	82.2 ±	1.6E-01	

By other hand, cause NG composition was not a quantity which was going to be in count in this thesis as a variable that may affect the humidity measurements given by the different sensing technologies. It was decided to use an average composition of the main chemical substances to carry out the unit conversion between WC and WDP readings. Table 5.1.e shows those values used for this purpose.

Table 5.1.e Average NG composition which was used as a reference for conversion between humidity units along the whole test time under semi-industrial conditions.

NG composition, % mol/mol			
N₂	0.846	n-C₄	0.313
CO₂	0.15	neo-C₅	0
C₁	90.576	i-C₅	0.047
C₂	6.468	n-C₅	0.043
C₃	1.293	C₆₊	0.047
i-C₄	0.217		

5.1.2.2 Room conditions

It must be known and recorded the room conditions in which the probes were studied, because it is possible that their behaviour could vary depending on ambient conditions, principally by temperature but relative humidity too. Any conclusion obtained from the results of this report should be associated always with the ambient conditions during the test time. Fig. 5.1.j shows temperature and relative humidity room conditions during the entire test time:

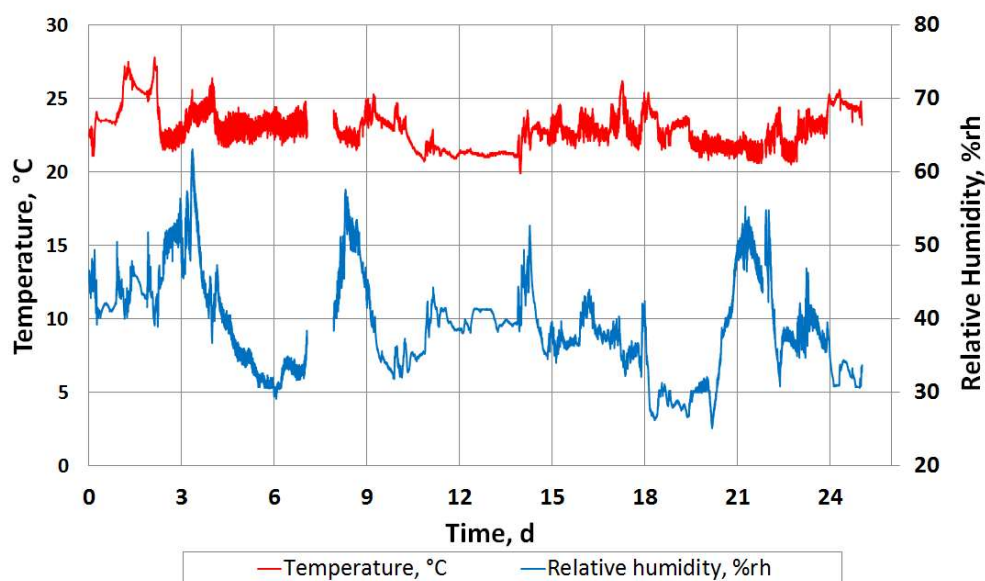


Fig. 5.1.1 Room conditions during the entire test time under semi-industrial conditions.

During the first fourth days, room temperature was higher than the rest of days, which occurs when INRiM staff were researching simultaneously than us. It was due to great quantity of electrical auxiliary instrumentation required by the microwave resonator of INRiM. Because of this, a huge quantity of heat was generated that could not be removed by the air conditioning system of the lab room. Table 5.1.f summarizes temperatures and relative humidity data about laboratory conditions giving their maxima, minima and mean of each week.

Table 5.1.f Summary room conditions during characterization tests of sensing humidity technologies under semi-industrial conditions.

		REL. HUMIDITY, TEMPERATURE,	
		%rh	°C
6 - 13 May	Max.	63.1	27.8
	Min.	29.1	21.1
	Aver.	41.0	23.8
14 - 28 May	Max.	57.6	26.2
	Min.	25.1	19.9
	Aver.	38.2	22.4
28 - 31 May	Max.	54.8	25.6
	Min.	30.6	20.5
	Aver.	36.7	23.4
TOTAL	Max.	63.1	27.8
	Min.	25.1	19.9
	Aver.	38.6	23.2

5.1.3 VARIABLE HUMIDITY TESTS

In this chapter were collected all experimental data performed during all variable humidity tests to know those properties has been already described in Section 4.1.3.5.1, i.e.: response time, hysteresis and drift. As it has been explained, these kind of tests were performed at fixed and steady pressure value, varying only the NG humidity levels. Thus, for those humidity sensors be able to endure at high pressure level the pressure set point was 2.7 MPa, whilst for the rest instruments the low pressure set point was 0.45 MPa.

5.1.3.1 Work schedule

In this sections it is going to explain, the measurement cycles carried out in order to evaluate such properties cited above. The humidity values generated along all variable humidity tests were eleven: (13, 30, 45, 55, 70, 85, 100, 125, 160, 200 and 250) ppm_v; but depending on the property studied not all nominal points were performed.

I. Response test time:

A detailed study of response time implies to know the behavior of hygrometers versus different humidity steps. Response test time study was performed at five humidity set points considered the most representatives of the entire humidity range evaluated, which were: (13; 30; 100; 200 and 250) ppm_v. For each humidity step, enough time was waited until considering that all instruments readings were acceptably stable.

Response test time were performed during several days to have a knowledge about the global behaviour of all instruments along the whole humidity range. However, there were specific steps which had a special interest and had to be performed. Following these special cases are detailed and their schedule is also explained:

- The smallest humidity changes both for upper and lower limits of humidity range studied that implies the following measuring cycles: (250 → 200 → 250 and 13 → 30 → 13) ppm_v, respectively.

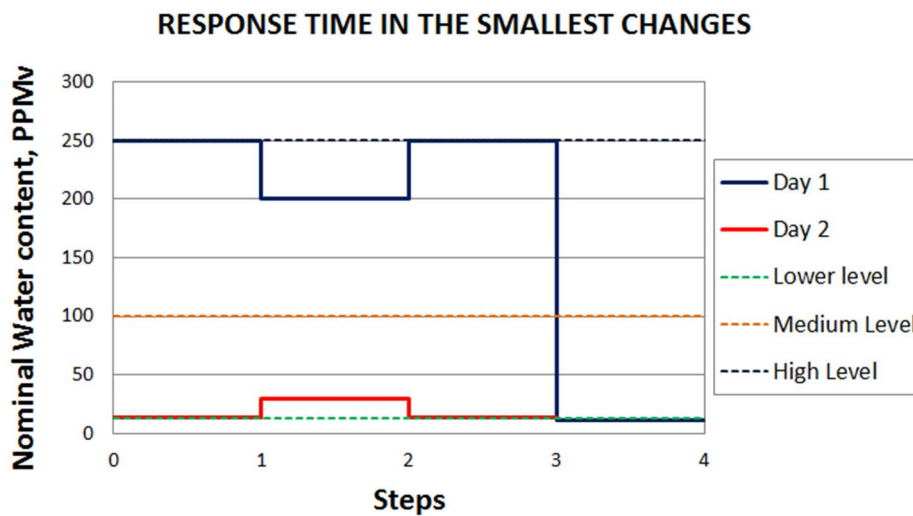


Fig. 5.1.m Scheme of data series used to evaluate the response time of instruments versus the smallest changes in both extremes of the humidity range evaluated.

- The biggest humidity change, so initially measuring cycles performed was (13 → 250 → 13) ppm_v. However, another more measuring cycling was performed from the second drier nominal humidity level, namely (30 → 250 → 30) ppm_v, to get a better control over humidity level generated in which humidity oscillations from NG inlet had the least impact.

- And finally, from the upper and lower ends to one intermediate value of range:
The measuring cycles carried out were: (30 → 100 → 30 and 250 → 100 → 250) ppm_v.

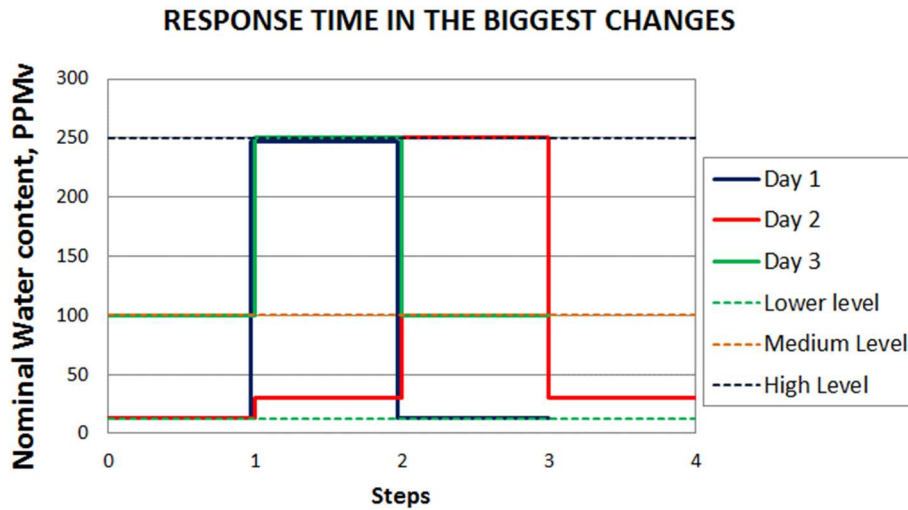


Fig. 5.1.n Scheme of data series used to evaluate the response time of instruments versus the biggest humidity changes evaluated.

II. Hysteresis study:

To check if some instrument under study was suffering some kind of hysteresis and if this effect could be linked with the measuring sensing, hysteresis study had to be done. Such tests consisted on a measuring cycle with eight nominal humidity point that involved the entire humidity range studied. Initially, humidity set points were performed increasing way and next same points were analyzed in descending order as can be seen below:

Increasing: (13 → 30 → 55 → 70 → 85 → 100 → 160 → 250) ppm_v

Decreasing: (250 → 160 → 100 → 85 → 70 → 55 → 30) ppm_v

Hysteresis effect for each humidity meter was calculated as the difference between their readings between the increasing and decreasing cycle. For that, hysteresis effect cannot be evaluated both in the highest and lowest nominal humidity values, and that was the reason for by which the decreasing cycle did not arrive down to 13 ppm_v.

Hysteresis study lasted three days: the first was used to do the most part of increasing cycle, whilst during the second day the highest two nominal points were repeated twice, and lastly, the third day was performed the rest of points of the decreasing cycling. This work methodology was depicted below in Fig. 5.1.o.

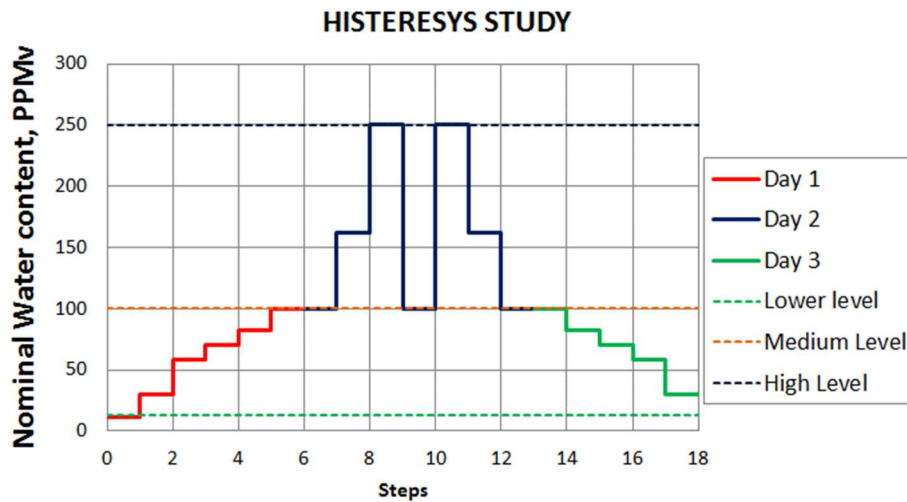


Fig. 5.1.o Scheme of data series used to carry out the hysteresis study for the entire humidity range evaluated.

III. Drift study:

During the course of the whole test time, all nominal humidity points were measured several times. However, to simplify drift study was evaluated at six points considered the most representatives of the entire humidity range evaluated, which were: (13, 30, 70, 100, 200 and 250) ppmv. Such points were generated regardless in increasing and decreasing humidity cycles, drift study include both of them because if some hygrometer could have been experimenting some kind of hysteresis, this effect would have been also included. This way, drift behaviour of the hygrometers would be show more realistically for their ordinary use under real conditions.

5.1.3.2 Response time

This sort of test has been classified in three sections because of the huge quantity of data collected:

- Firstly, all raw data collected during the response time tests were depicted in the following figures, distinguishing among those instruments which gave WC or WDP readings.

- Secondly, it was evaluated the relative behaviour between analogue and digital outputs of those instruments which were able to measure simultaneously by both ways. Thereby, if there had been some difference depending on the kind of data recording system used, it could be checked and demonstrate.

- Coming up next, the response time tests of all humidity steps chosen were shown and analyzed and always both for increasing and decreasing humidity steps.
- And finally, a summary of the most important results is shown together with the main conclusions.

5.1.3.2.1 *Raw data*

In this chapter all those data which were collected during the response time tests has been depicted. This way, it can be already appreciate some differences between the behaviours of some humidity sensors.

All graphs depicted in this section show the raw data of all hygrometers, which means that such data series were not corrected according with their certificates, in the case they had it, and they didn't suffer any kind of handling or mathematical treatment. This last was not necessary because in this section we wanted to evaluate the time required for each instrument to provide stable readings against to a humidity changes, so if they were or not measuring accurately and reliable way, it would not affect to final conclusions extracted in the response times study.

At the same time and for the same reason commented above, all figures were directly represented in the humidity quantity in which instruments were measuring, namely, WC or WDP, by means of two vertical axes. The main vertical axis depicts all WDP datasets, which have been always placed in the top group of readings at the same, whilst the secondary vertical axis shows WC readings, corresponding to bottom dataset group.

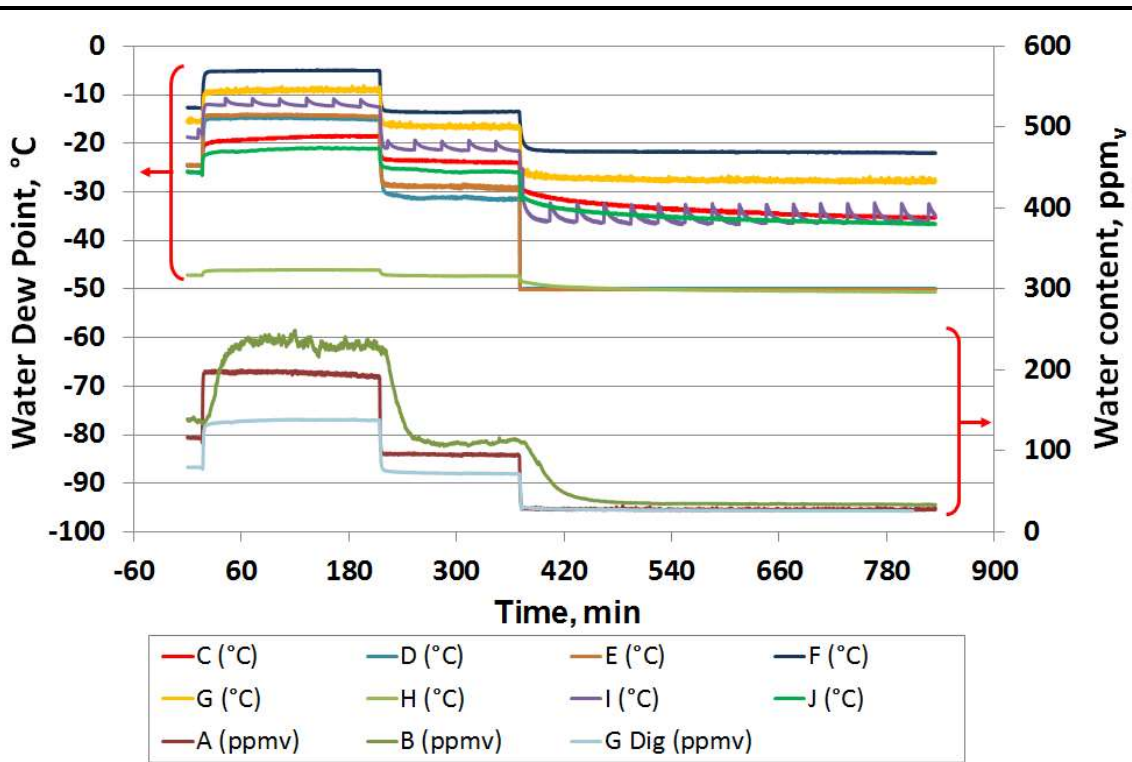


Fig. 5.1.p Data recorded of the first study day of response time tests (13/05/2013).

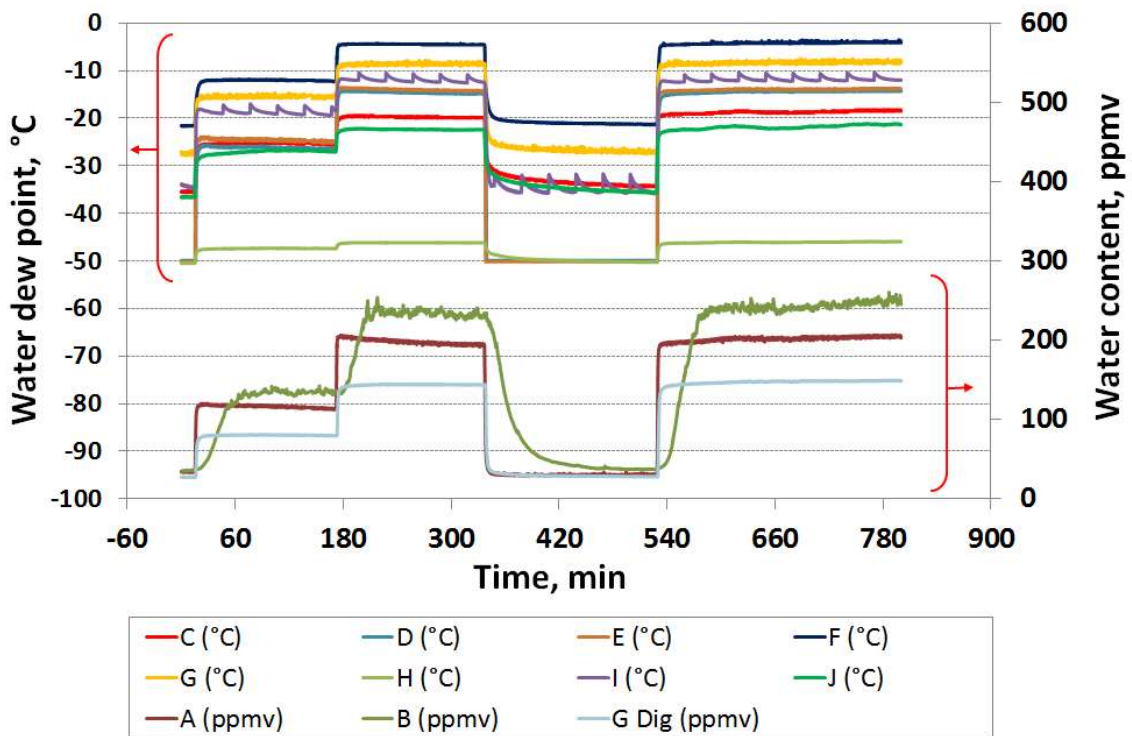


Fig. 5.1.q Data recorded of the second study day of response time tests (14/05/2013).

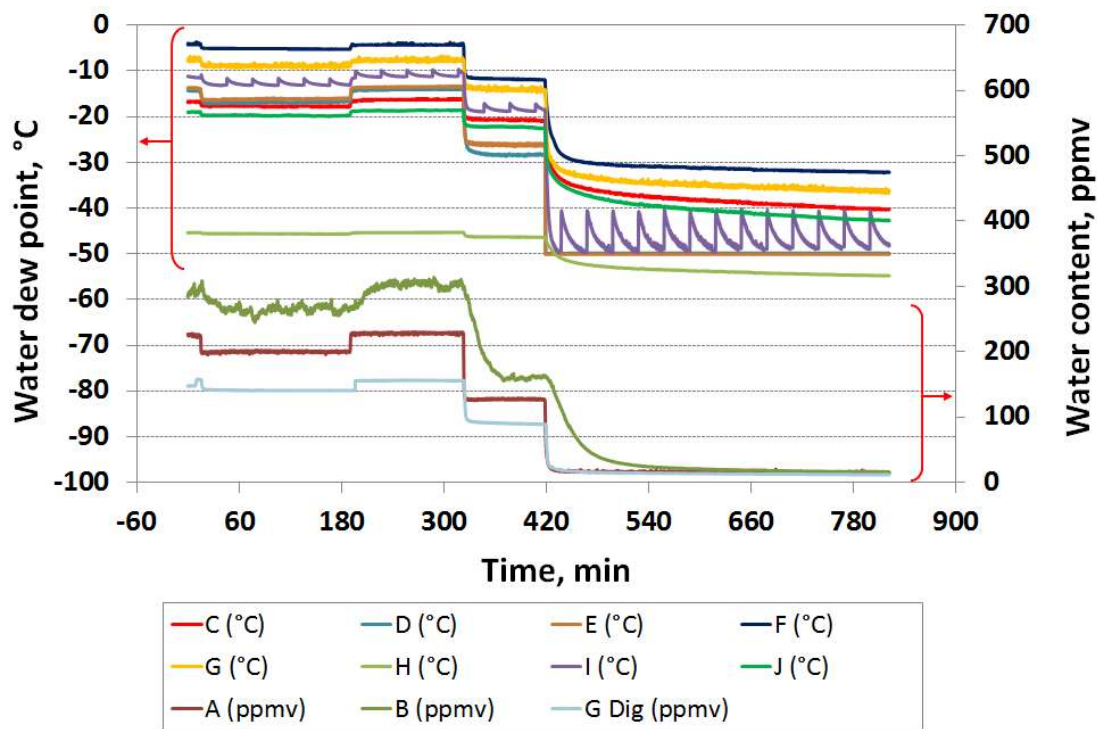


Fig. 5.1.r Data recorded of the second study day of response time tests (15/05/2013).

Fig. 5.1.r depicts the smallest changes in the upper part of the humidity range, i.e., (200 to 250) ppm_v, and vice versa. By the other hand, two of the biggest humidity changes (250 to 100) ppm_v and (100 to 13) ppm_v were also performed the same day.

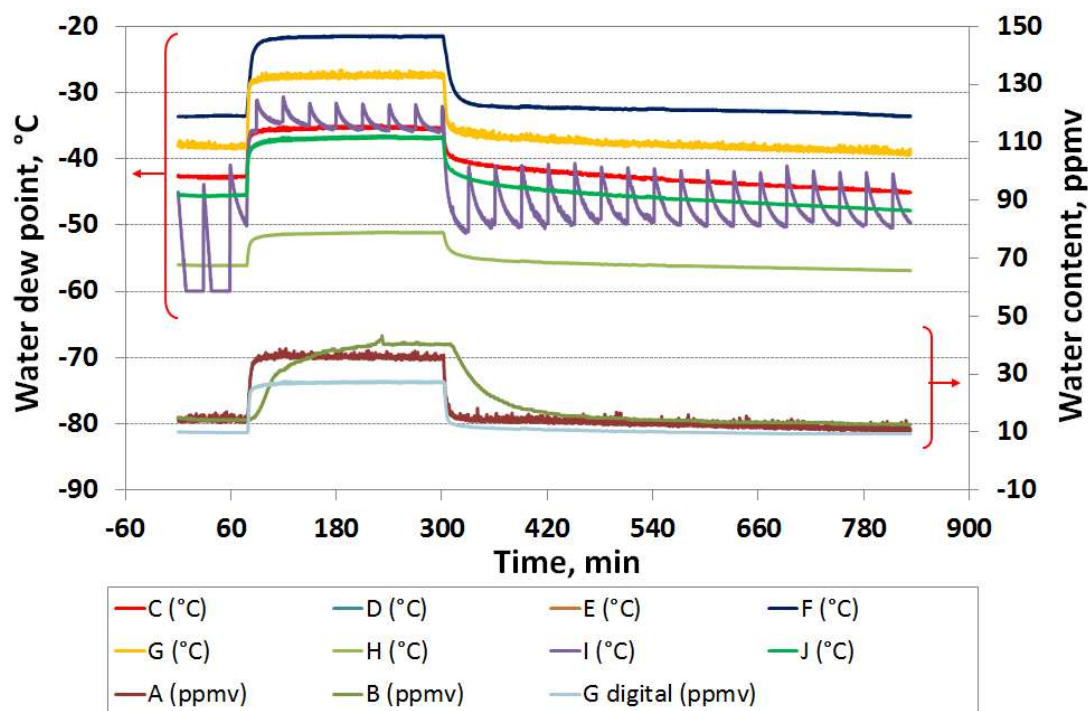


Fig. 5.1.s Data recorded of the fourth study day of response time tests (16/05/2013).

Fig. 5.1.s includes the results of the response time tests for the smallest changes in the lower end of humidity range, i.e., (13 to 30) ppm_v and, vice versa. And lastly, the biggest change (13 to 250) ppm_v and its reverse were included in Fig. 5.1.t.

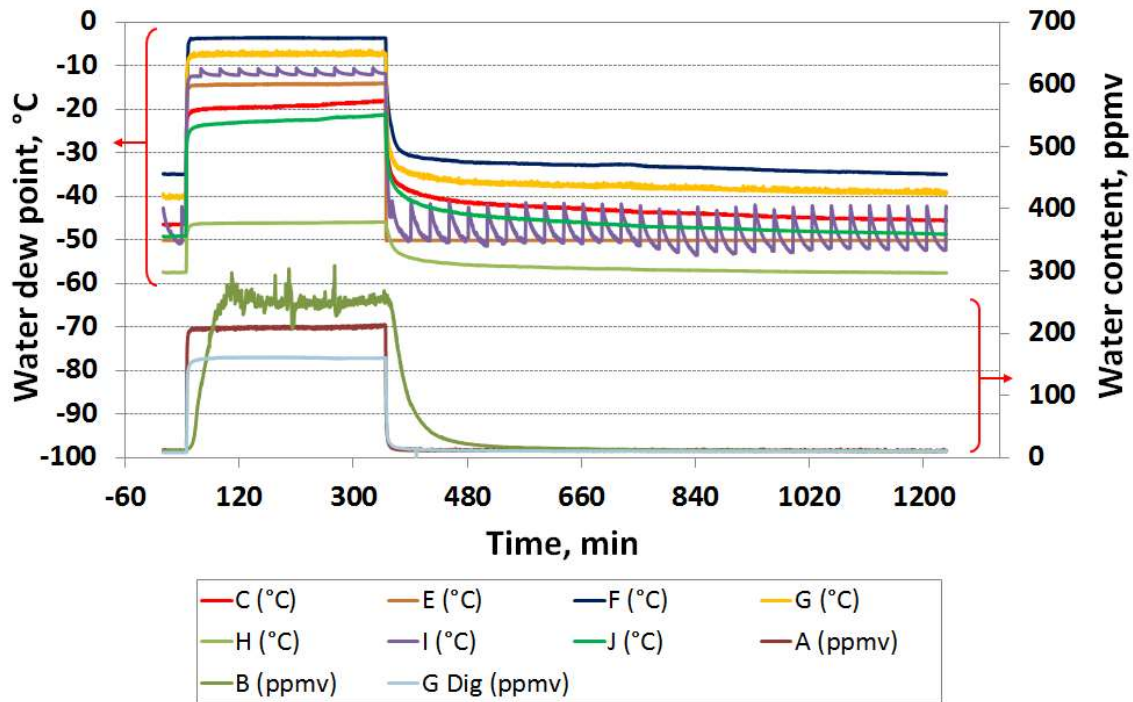


Fig. 5.1.t Data recorded of the fifth study day of response time tests (17/05/2013).

From all of these figures, it can be extract a lot of information about the behaviour of the most of humidity instruments studied. One of the first thing quickly noticeable was the great spread between the readings taken both WC and WDP dataset groups. Besides, there seems to be some sort of order among the series of data that was maintained over all test days, this means that those instruments which were measuring wetter kept doing along of all humidity levels, and the same happened for those instruments which were measuring drier.

An extreme example of this last case was the instrument H that was the device which gave the driest humidity readings throughout all tests by far. Because of the huge differences exhibited compared with the rest of instruments, it was already started to suspect that this instrument could be suffering a great drift before any data analysis.

Another remarkable effect was the cyclic behaviour of polymeric sensor I, the EE371, during the whole test time. Thanks to private conversation with its manufacturer

we knew that such cycles were associated with cleaning tasks by means of thermal sensor treatments to regenerate it. This activity was automatically performed approximately each 30 min, once a series of stable measurements were recorded. Commercial version of the EE371 does not exhibit this behaviour because it is electrically compensated, but the manufacturer allowed us to know more in depth the behaviour of its measurer within the framework of EMRP project [ENG01].

By the other hand, it can be observed at a glance, as the electrolytic sensor B needed more time to reach the steady final value in all humidity changes. In addition, readings of such instrument for the high humidity levels had quite noise and therefore, less stability. So that, it seems that this technology is more sensitive at high humidity levels than the rest.

5.1.3.2.2 *Analogue versus digital output signals*

Before than all collected data were analyzed in depth, the behaviour from those humidity meters that had analogue and digital outputs was studied to check if there could be some difference among them or not. Only the instruments A and G met this criterion because the other instruments were not able to use both kind of signals at the same time, except the Condumax II which was being used to monitor NG humidity inlet in the laboratory.

To facilitate analysis and understanding of the response time performance, it was decided to normalize all data shown in the previously section to initial and final steady values for each of signals belonging to all hygrometers under study. The response time was determined by fitting to Eq. 5.1.a that represents the humidity signal as a function of time, $\Delta H(t)$ [B&H12]:

$$\Delta H(t) = \left(1 - e^{-t/\tau}\right) \Delta H_F \quad \text{Eq. 5.1.a}$$

where ΔH_F was the final steady state humidity level and knowing that for $t = \tau$ a value of 63.2 % of the step was reached and that for $t = 5\tau$ a value of 90 % was obtained.

The value of $t = 0$ was considered as the instant in which a change was detected. It was considered that such change happened when a variation higher than three times the standard deviation of the mean, regarding to those obtained during the initial steady state humidity level, had taken place.

The percentage of the normalized value for humidity as function of time, $H \% (t)$, was calculated as follow:

$$H \% (t) = \frac{(H_t - H_0)}{(H_F - H_0)} \cdot 100 \quad \text{Eq. 5.1.b}$$

where ΔH_F was the actual humidity value collected each timespan, ΔH_F was the initial steady state humidity level ΔH_F was the final steady state humidity level.

ΔH_F and ΔH_F were calculated from an own software developed and validated by LabTH, called *Ptramos*, and which is continuously used during any calibration process. Such software calculates the mean and the standard deviation of any quantity chosen, considered as a standard, finds the most stable period for each step, and finally gives the mean and standard deviation of the all readings for the same period. This calculating tool allowed to calculate all average values and standard deviations of all readings taken throughout all this thesis.

Despite every signal from every instrument had its own reference source of time, for depicting all results was necessary to choose a mutual for all of them. The only criterion to select the properly instrument was it had to be one of the fastest to detect any humidity change. In that sense and as a result of previously section, the spectroscopic instrument, A, was chosen to establish the mutual reference source of time ($t = 0$) in every humidity step depicted below.

In the following graphs, two examples representatives of the smallest and largest step changed studied were depicted.

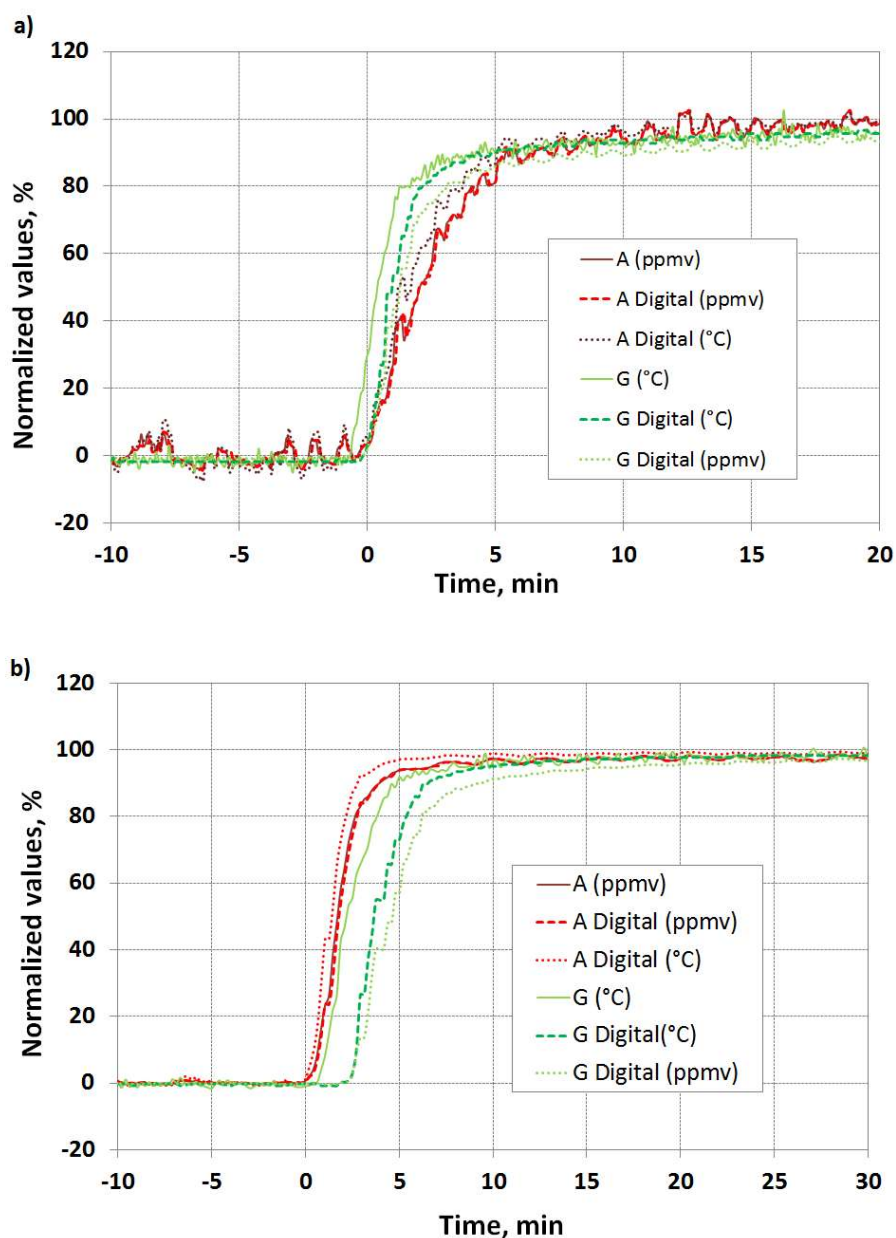


Fig. 5.1.u Example of the comparative study of response times both analogue and digital outputs of A and G instruments. (a) For an increasing humidity step from (13 to 30) ppm_v and (b) from (30 to 250) ppm_v.

In the case of instrument A, both signals overlapped within the range studied. However, for instrument G, analogue signal was always faster. In the smallest humidity changed depicted (first graph of Fig. 5.1.u) differences were less than 20 s, but for the largest step change studied (second image of Fig. 5.1.u), there were differences up to 120 s. Most likely the reason by which digital output of instrument G was delayed regarding its corresponding analogue could be that, the RS-485 is a standard communications

protocol specifically designed to field application where large distances between control rooms and measuring systems are very often. In this case, the length of the communication wire of the HygroPro were approximately 80 m, so such delay in the digital output could be related with this fact.

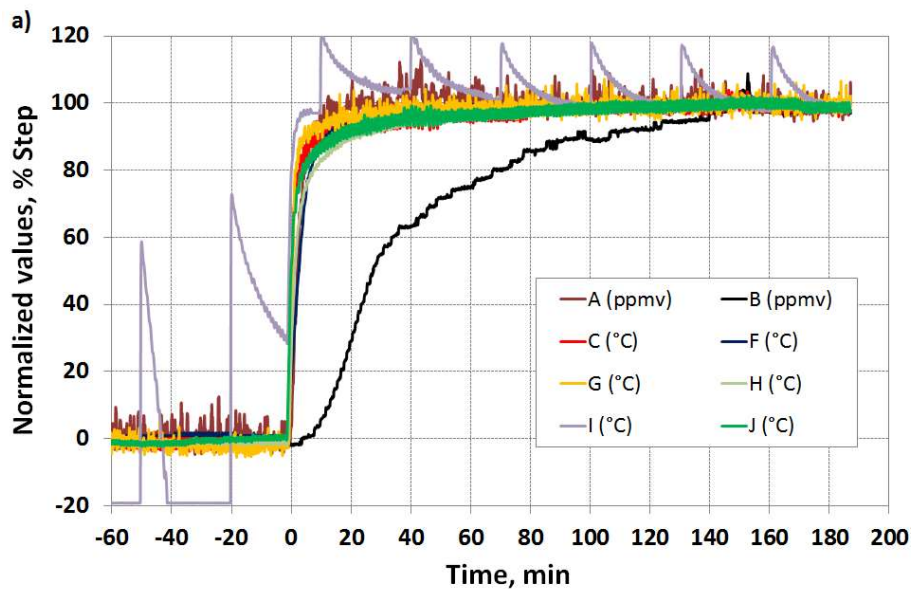
For the rest of the response time tests only analogue signals were compared, as all humidity analyzers shared a mutual data acquisition system that ensured that the readings were highly correlated and reduced the influence of any possible drift at the multimeter used.

5.1.3.2.3 *Dynamic behavior*

In this section, the response time behaviour for each humidity step was analyzed in deep and as happened before, mutual reference source of time for all humidity step was given by the spectroscopic instrument, the Aurora.

Coming up next, those humidity step analyzed were depicted both rising and falling way. The time scale, depicted in horizontal axis, has been given both hours and minutes depending on the performance of the humidity instruments.

STEP (13 – 30) ppm_v



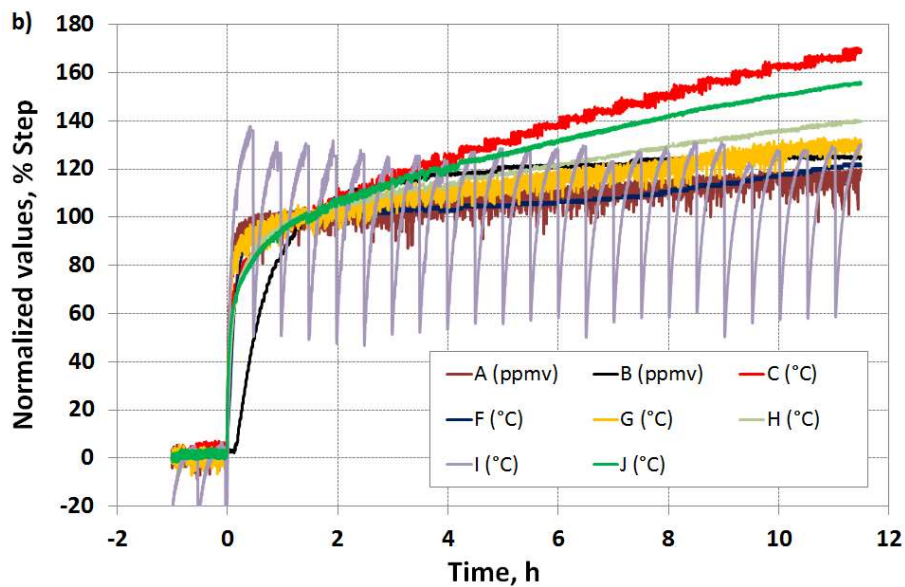


Fig. 5.1.v Summary of response time test for the humidity step (13 - 30) ppm_v: a) increasing and b) decreasing.

In this case, instruments D and E were not depicted because they didn't detect any humidity change, so it was supposed these humidity levels were below of the lower detection limit for these instruments, which were the same model and manufacturer.

By the other hand, it can be seen in the first graph of Fig. 5.1.v as the instrument I could not read at the lowest nominal humidity level, 13 ppm_v, because it reached its lower limit of -60 °C, as can be seen in Fig. 5.1.s.

For the smallest and lowest humidity change, there was another remarkable issue because of it was significant that all instruments exceed 100 % of step which means that all of them read drier until reaching the final steady value. Most of them read around 20 % drier for a nominal humidity variation of 17 ppm_v, but attending to the Aurora accuracy, which is 4 ppm_v, would be equivalent to almost 25 % for the step. Consequently, and extrapolating this survey for the rest of instruments, it can be said that the most of them were under specification at all time.

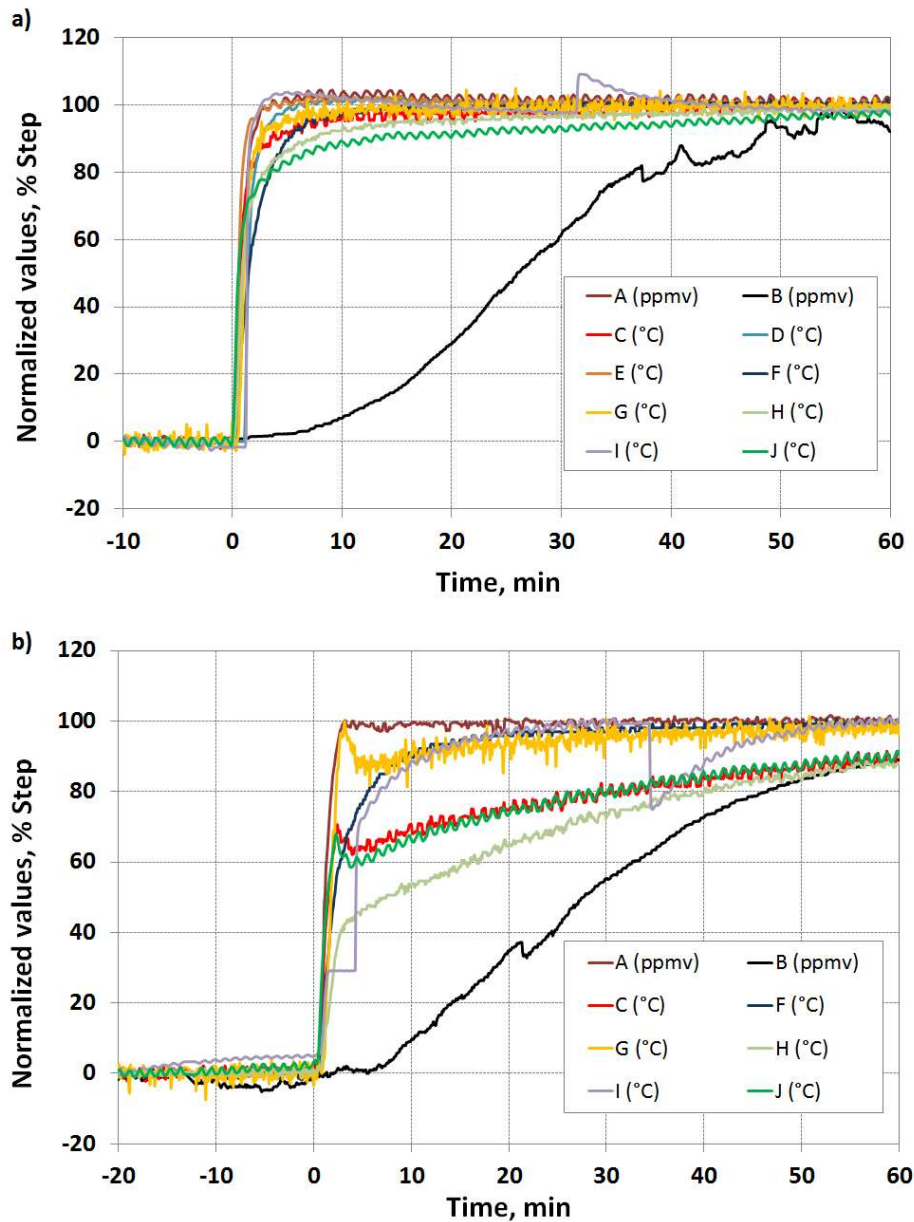
STEP (30 – 100) ppm_v

Fig. 5.1.w Summary response time test for the humidity step (30 – 100) ppm_v: a) increasing and b) decreasing.

In this case, it can be seen as the performance of all instruments for rising step is really good regardless the humidity sensing technology, except to electrolytic instrument, whose response time in both cases is quite slower. However, for decreasing step (second graph of Fig. 5.1.w) there were more heterogeneous results, since despite detecting almost instantly humidity change, there were big differences regarding to the required time to reach the final steady values.

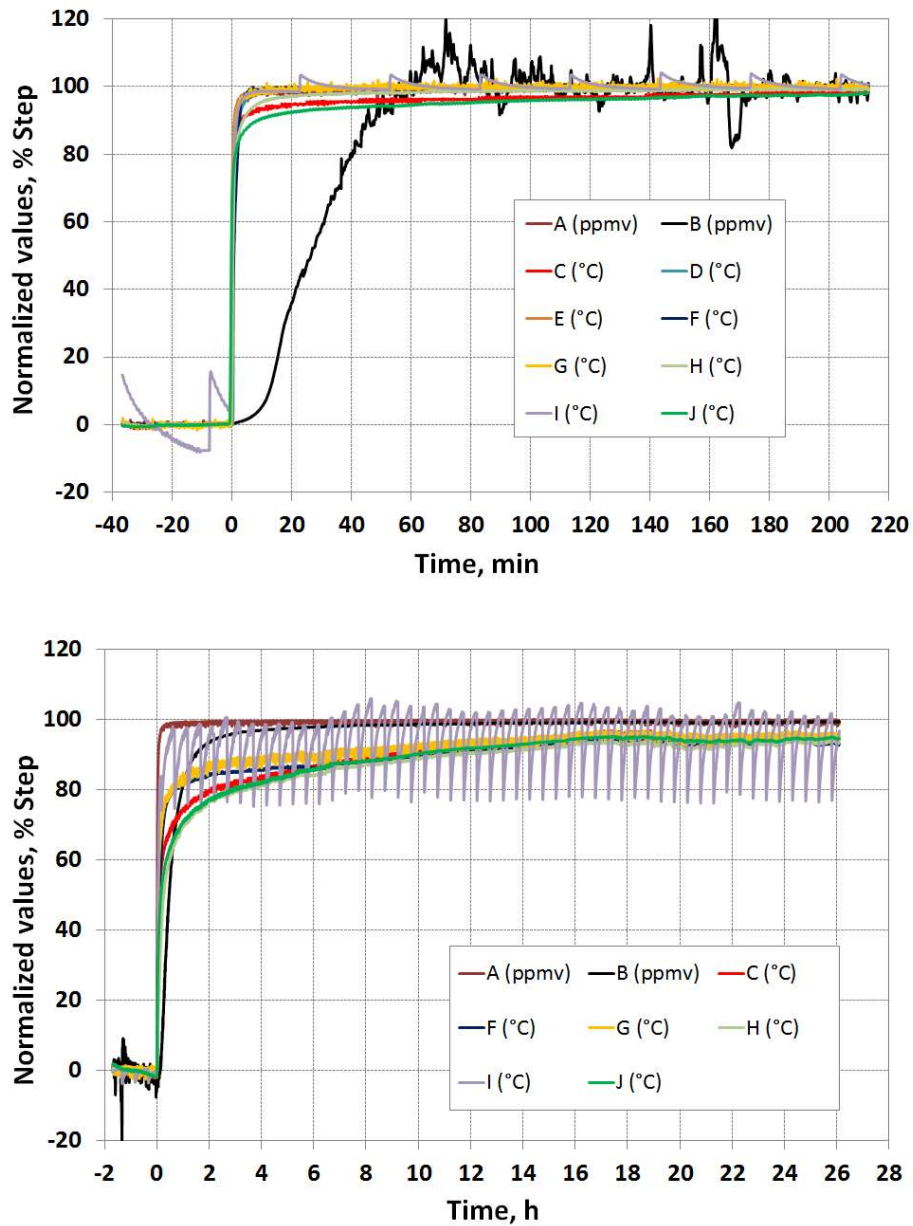
STEP (13 – 250) ppm_v

Fig. 5.1.x Summary response time for the humidity step (13 – 250) ppm_v: a) increasing and b) decreasing.

For the biggest humidity change analyzed, similar results were given for rising humidity change comparing the first 60 min. However, the most of capacitive instruments needed almost around 8 h to reach 90 % of step during the falling test, against to only 20 min required during the increasing humidity step.

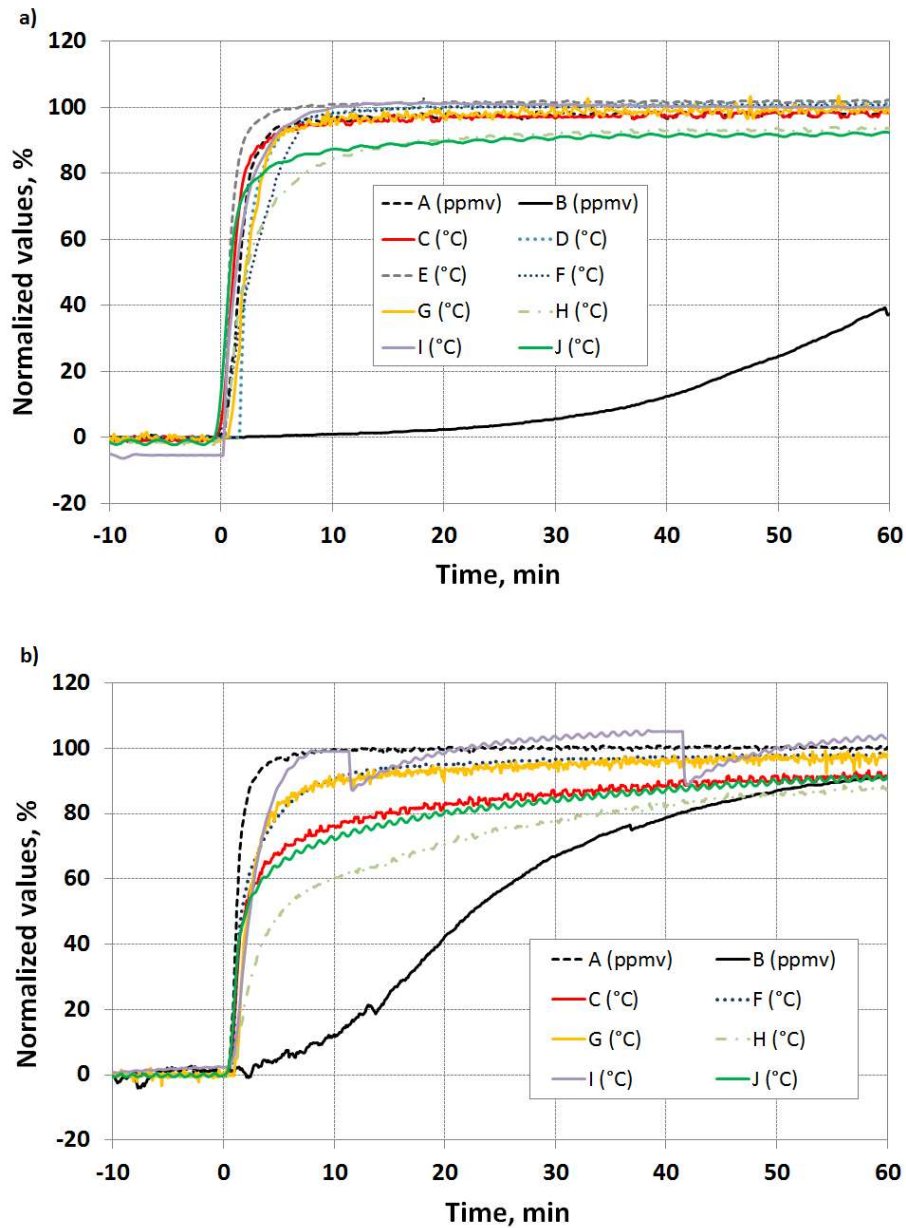
STEP (30 – 250) ppm_v

Fig. 5.1.y Summary response time for the humidity step (30 – 250) ppm_v: a) increasing and b) decreasing.

For this step, the behaviour of the humidity instruments during the rising step was quite similar than the previously cases: in just 5 min the most of them had detected 90 % of the humidity change, except for the electrolytic hygrometer which after 1 h only had reached 40 %. By contrast, during the decreasing step, the performance of such instrument was more heterogeneous among them and the times used were quite higher, expect to the spectroscopic and polymeric instruments, A and I, respectively.

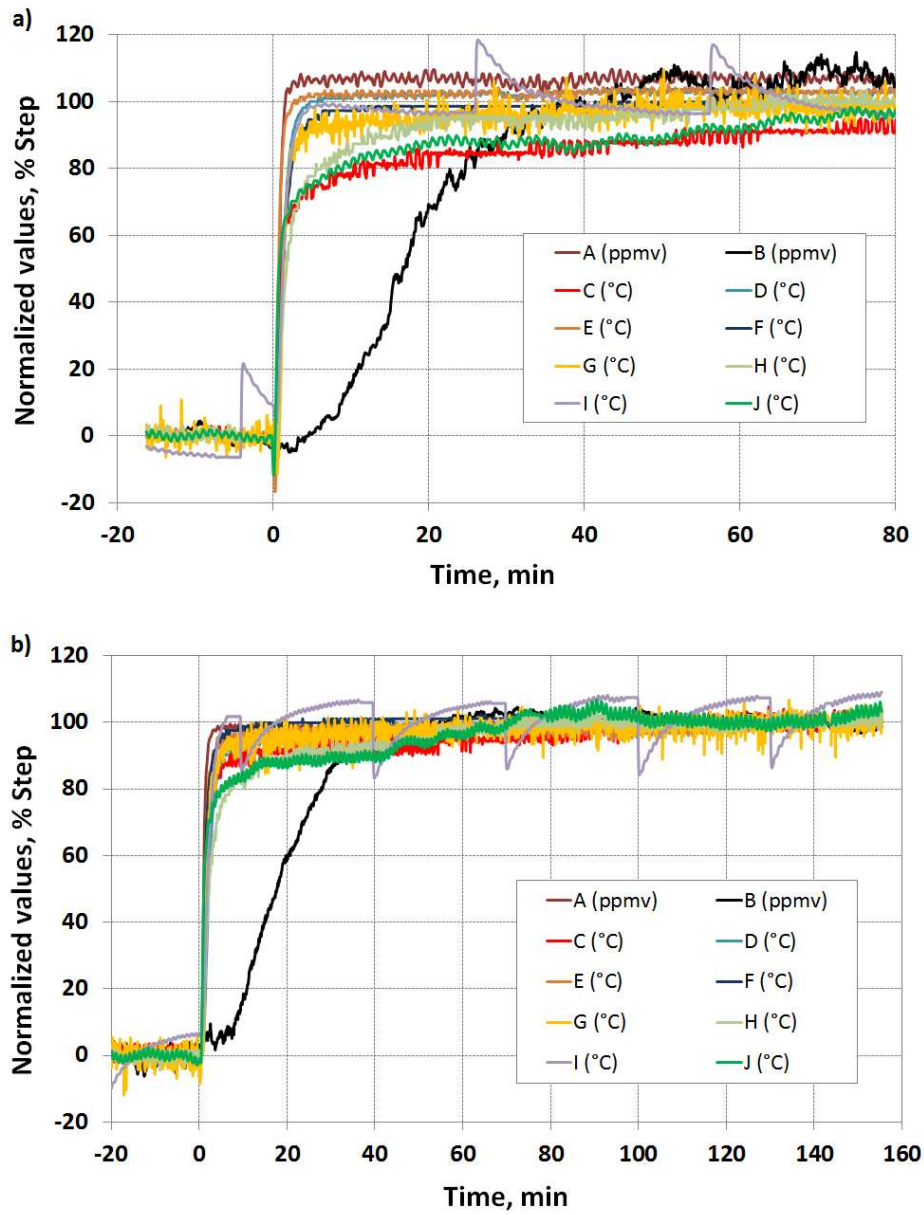
STEP (100 – 250) ppm_v

Fig. 5.1.z Summary response time for the humidity step (100 – 250) ppm_v: a) increasing and b) decreasing.

For this step, really very similar performances were recorded in both cases, becoming even somewhat better during the decreasing step.

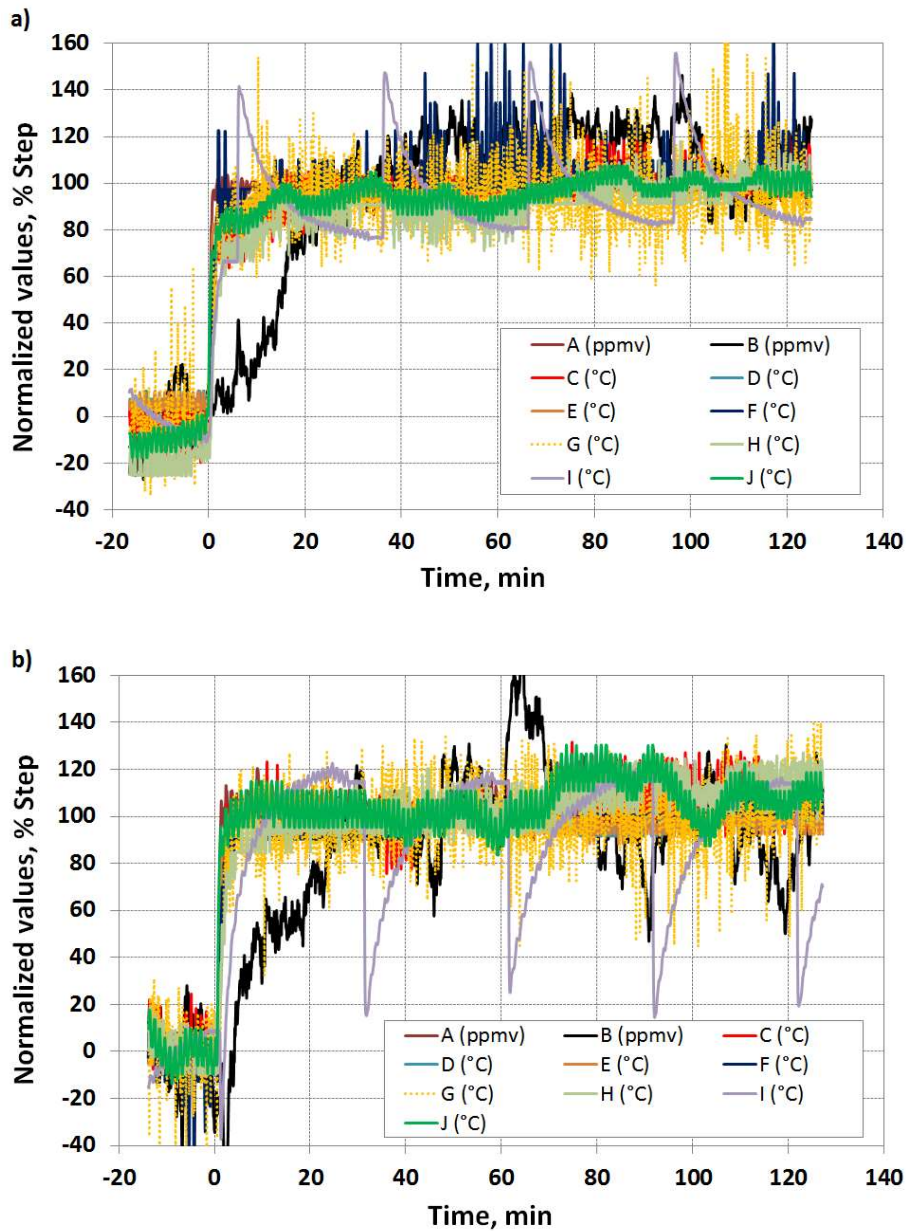
 STEP (200 – 250) ppm_v


Fig. 5.1.aa Summary response time for the humidity step (200 – 250) ppm_v: a) increasing and b) decreasing.

For this last humidity step, which corresponds to the smallest change in the upper humidity range studied, the main feature that can be seen in both graphs is the high instability showed by all instruments, except for the polymeric probe, I. The rest of shown signals had a great noise because of the high sensitivity of all sensing technologies around this humidity range.

Once the huge quantity of data of this section was analyzed in detail, were extracted the following conclusions:

- All instruments detected any humidity change very fast, independently of how long they required to reach the final steady values. All figures also show that the behaviour of instrument pairs C / J and D / E, were identical, as it was expected because both were the same models of probes.
- From all graphs shown in this section, required times by the electrolytic sensor, B, to reach the final humidity values were significantly slower than the rest. It could be thought that this situation was due to the flow-rate that was crossing the measurement cell, was very low (0.1 L/min), whilst the bypass flow for was set at 1 L/min. However, such flow rates values were fixed according to manufacturer's manual, and in addition, electrolytic instrument detected rapidly any sudden humidity change, but another different thing was the time taken to give the actual final value.
- Another conclusion extracted was that instruments equipped with Al₂O₃ capacitive probes behave in a more heterogeneous manner for decreasing water content in the gas, whilst for rising humidity changes their performances were quite similar.
- Another effect that could be evaluated was the noise levels in the output signals. At very low humidity levels, signals noises have quite lower than their respective uncertainties, for that they are a negligible effect. However, at the two highest levels for some probes based on aluminium oxide, as F and G, their signals noises were up to five times bigger than their measured uncertainties. Polymeric probe had the best damping of noise in the whole range study, as can be seen in Fig. 5.1.aa.

5.1.3.2.4 *Summary of response time tests*

For every humidity steps, time employed to reach 63.2 % and 90 % of steady final humidity values both increasing and decreasing way were indicated. For that, first of all was to find out the humidity values at the two particular percentages. This action was carried out by means of below equation, which comes from Eq. 5.1.b but solving ΔH_F .

$$H_{63.2\%} = (H_F - H_0) \frac{63.2}{100} + H_0 \quad \text{Eq. 5.1.c}$$

where ΔH_F was the humidity value measured when 63.2 % of the humidity step had been already performed, ΔH_F and ΔH_F was previously defined. The same equation was used to find humidity values at 90 % of the step.

Once knows all results, they were collected in Table 5.1.g that shows a full summary of the results obtained during the response time tests performed in this section.

First look at the below table allows to prove that electrolytic analyzer, B, was overall the slowest, whilst the aluminium oxide sensors such as instruments D, E and G were the fastest for the most steps evaluated. Spectroscopic, polymeric and rest of aluminium oxide sensors exhibited a very similar behaviour but were slightly slower to reach the 90 % of the final values than the previously group.

By the other hand, in the biggest humidity decreasing step, from 250 ppm_v to 13 ppm_v, can be noticed as practically all aluminium oxide probes (except instruments D and E) were unusually slow and their performance were quite questionable. An explanation of this behaviour change, which only happened in this step, could be that this kind of sensors would have come to be saturated and thereby, they would have needed more time to regenerate the active part of the sensor and to be able to detect humidity change toward drier levels.

5. RESULTS

Table 5.1.g Summary of the response times of all instruments to increasing and decreasing steps. The sampling interval used was 5 s. “—” indicates that instrument readings lie outside the programmed range of the indicator.

		Time, s	A	B	C	D	E	F	G	H	I	J
Increase	13 - 30	τ (63.2%)	160	1715	100	—	—	280	75	195	60	110
		5τ (90.0%)	325	5290	495	—	—	755	270	1275	175	825
Decrease	13 - 30	τ (63.2%)	125	1720	265	—	—	475	165	400	255	445
		5τ (90.0%)	425	3535	2195	—	—	1215	770	2055	780	2610
Increase	30 - 100	τ (63.2%)	70	1910	40	30	15	105	40	50	85	50
		5τ (90.0%)	110	2955	195	90	50	285	105	405	95	710
Decrease	30 - 100	τ (63.2%)	85	1735	95	25	20	145	60	980	265	130
		5τ (90.0%)	135	3360	3255	30	20	540	95	3600	455	3160
Increase	13 - 250	τ (63.2%)	55	1900	45	30	10	85	50	55	50	45
		5τ (90.0%)	120	2690	205	120	55	175	105	250	140	535
Decrease	13 - 250	τ (63.2%)	95	1645	970	75	40	625	300	2105	260	1685
		5τ (90.0%)	235	4735	31870	85	45	35625	15890	38960	1090	35075
Increase	30 - 250	τ (63.2%)	50	1965	40	20	10	90	60	75	45	35
		5τ (90.0%)	95	2670	110	80	40	160	110	470	110	550
Decrease	30 - 250	τ (63.2%)	85	1530	185	100	50	110	105	665	165	230
		5τ (90.0%)	160	3255	2400	115	60	520	490	3895	275	2880
Increase	100 - 250	τ (63.2%)	60	840	65	40	20	60	40	95	105	55
		5τ (90.0%)	80	1515	3075	100	50	170	145	685	205	2635
Decrease	100 - 250	τ (63.2%)	75	1460	45	90	50	40	50	<5	145	55
		5τ (90.0%)	115	2120	375	260	145	140	155	695	245	1360
Increase	200 - 250	τ (63.2%)	395	20	40	25	<5	35	<5	70	355	35
		5τ (90.0%)	1180	80	125	85	105	50	200	270	730	550
Decrease	200 - 250	τ (63.2%)	720	15	40	45	45	<5	<5	10	95	230
		5τ (90.0%)	985	675	135	170	95	295	630	5420	365	2880

Because of the great quantity of data depicted in Table 5.1.g and the difficult to extract information in all of that data matrix, another way to depict the data was thought. By this reason, two bar graphs were built to be able to compare in an easier way the behaviour of all hygrometers analyzed for all humidity steps in both senses. Fig. 5.1.bb shows times required to reach 63.2 % for each individual final value, whilst Fig. 5.1.cc shows the corresponding results to 90 %.

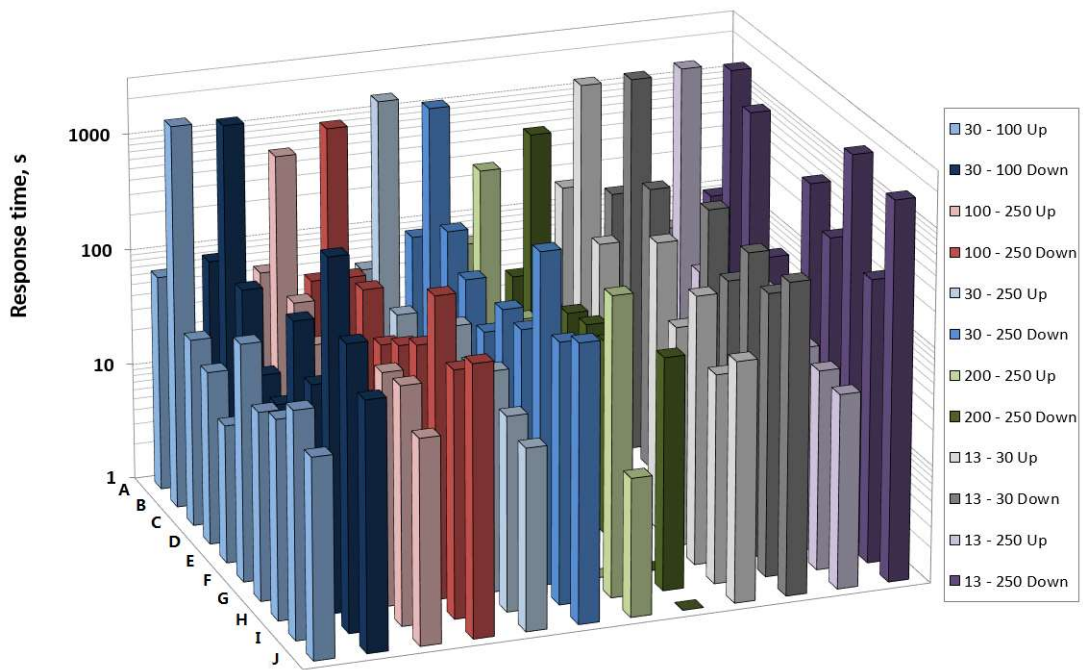


Fig. 5.1.bb Summary results of the entire response time tests against humidity changes. Times required to reach the 63.2% for each singular final value of each instrument were depicted.

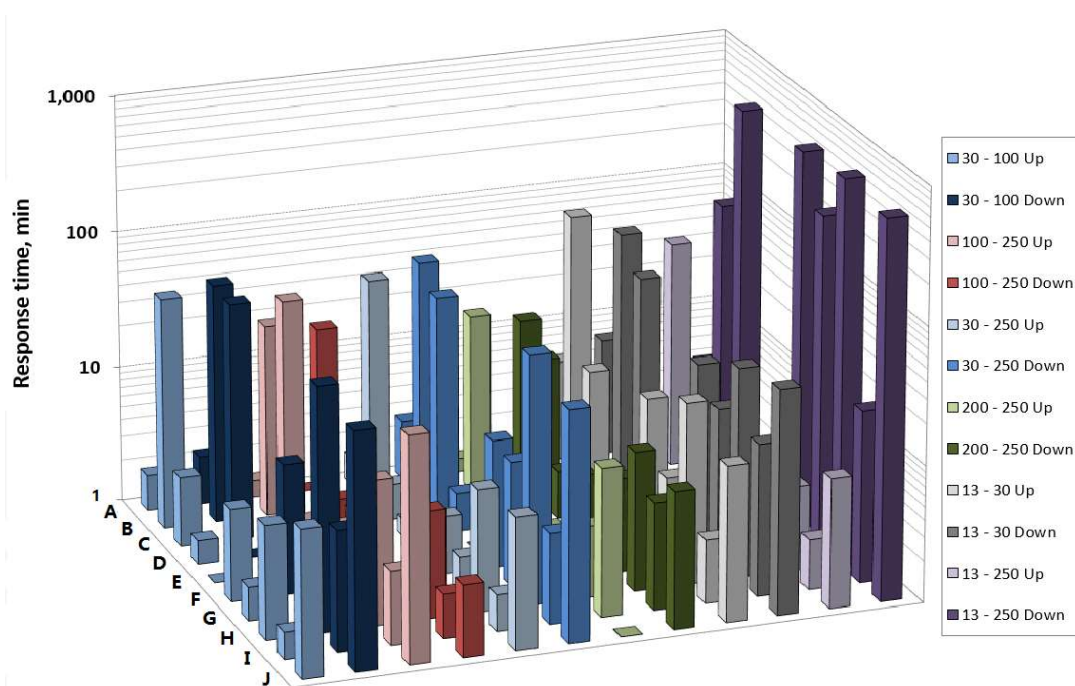


Fig. 5.1.cc Summary results of the entire response time tests against humidity changes. Times required to reach the 90 % for each singular final value of each instrument were depicted.

Light colors bars represent the increasing humidity changes, by contrast dark colors depict decreasing humidity. Besides, it must be warned that the timescale used in Y axis is different in each figure: Fig. 5.1.bb is in seconds and Fig. 5.1.cc in minutes.

By the other hand, two situations must be considered to understand completely well the information that can be extracted from both pictures:

- Firstly, the timespan between readings for the data acquisition system (described in Section 4.1.3.4) was 5 s, so if the required time to reach the 63.2 % was lower than such time, the value showed by Fig. 5.1.bb was zero.

- Secondly, Y axis of Fig. 5.1.cc is logarithmic, thus response times lower than 1 min cannot be depicted, so the height of the bars for such cases will be zero too.

In both figures, it can be also seen that upon increasing humidity, the most critical situation in the handled of NG, and for any time. The number of instruments that reached the 63.2 % or 90 % was always higher than for decreasing humidity situations. Thus, percentage of the final stable value was reached, compared to the case of a drying process where the response was more gradual, possibly due to the desorption effects in the sampling line and regeneration effects principally in the capacitive sensors.

Fig. 5.1.bb and Fig. 5.1.cc demonstrate that the electrolytic analyzer, B, was the slowest in practically all steps tested. By contrast, some of the aluminium oxide probes, such as: instruments D, E and G; were the fastest with response time lower than 5 min. Spectroscopic, polymeric and the rest of aluminium oxide hygrometers exhibited a very similar behaviour and were slightly slower than the group of the fastest. These summary conclusions agreed with those found out by Løkken [Løk12].

5.1.3.3 Drift short-term

In order to evaluate the stability of the instruments during the whole test time, drift of instruments at several nominal humidity levels was evaluated.

Since we were not available any standard hygrometer be able to be used as a monitor and reference over NG, we had to find an instrument whose performance was better to be used as reference, during the drift calculating.

In that sense, three humidity measurers of three different sensing technologies were considered: the spectroscopic (A), electrolytic (B) and as representation of aluminium oxide the HygroPro (G). This last was chosen for its good performance previously detected during the response time tests, besides to be able to measure in the whole humidity range evaluated and both analogically and digitally way.

Because the study of drift behaviour was done by means of corrections respect to one instrument, which had not been calibrated in any system be able to faithfully reproduce the actual measurement conditions and for the particular NG composition which was flowing. Thus, along all this experimental results, it has been told about relative drift, cause the own drift of reference instrument was really unknown.

Drift assessment was done for five nominal humidity values (13, 30, 70, 100 and 250) ppm_v because were performed much more times along the whole test time the rest of nominal humidity values.

The stability was calculated from the variation of the correction of all instrument readings as a function of time. The correction, c , for each reading, j , was obtained as follows, according to its definition given by the VIM [VIM12] and the GUM [GUM08]:

$$c(j) = r(j) - i(j) \quad \text{Eq. 5.1.d}$$

where r and i were the readings of the reference device and instrument, respectively. Thus, a positive correction indicates that the instrument read drier than the reference device.

Finally, the WDP relative drift for each instrument was calculated from the slope of the linear fit of the series of the correction for each humidity level analyzed, but changing symbol.

Due to the similarity of results obtained using the three reference instruments, and to facilitate the visualization and understanding of its conclusions, below have been only shown the results obtained using only the spectroscopic instrument as a reference. However, the same study but with the particular results obtained using the other two reference instruments have been also attached in Annex I, and their final results and conclusion have been included in Section 5.1.3.3.2.

5.1.3.3.1 *Spectroscopic instrument used as reference*

As the spectroscopic instrument directly measured in WC units, all their readings had to be converted to WDP, being those last values that would be used as a reference to calculate the correction of the rest of instruments. This unit exchange was performed according to the International Standard ISO 18453:2004 [ISO04] using the NG composition given by Table 5.1.e, and the pressure values recording by the pressure transmitters assembled.

Variations of corrections over the test time for all hygrometer studied have been depicted in the following graphs, which were divided according to the nominal humidity levels generated.

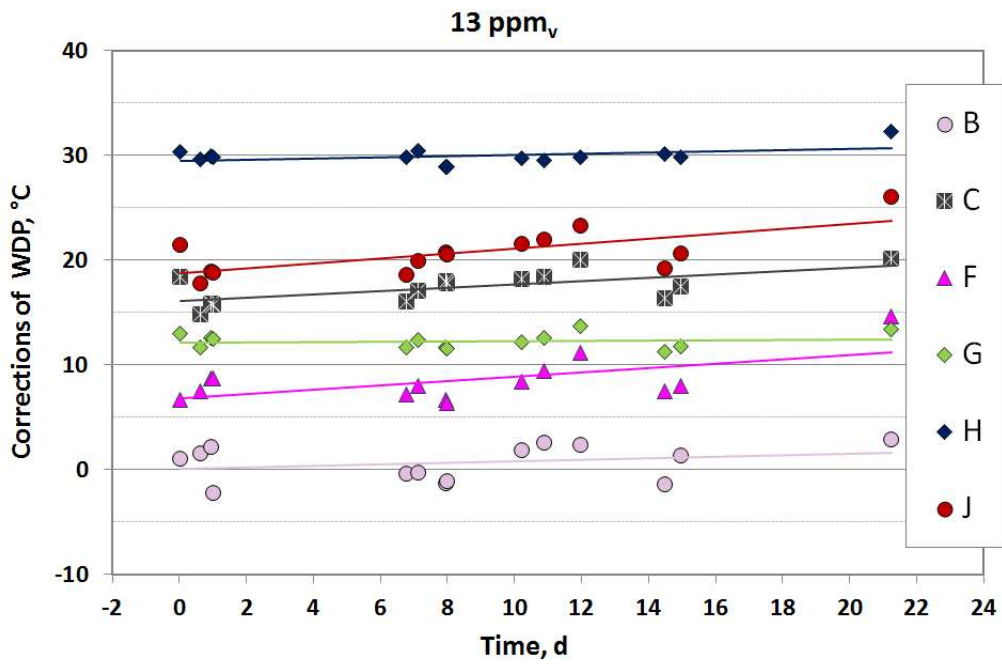


Fig. 5.1.dd Short-term relative drift at nominal water content of 13 ppm_v, using spectroscopy instrument as reference.

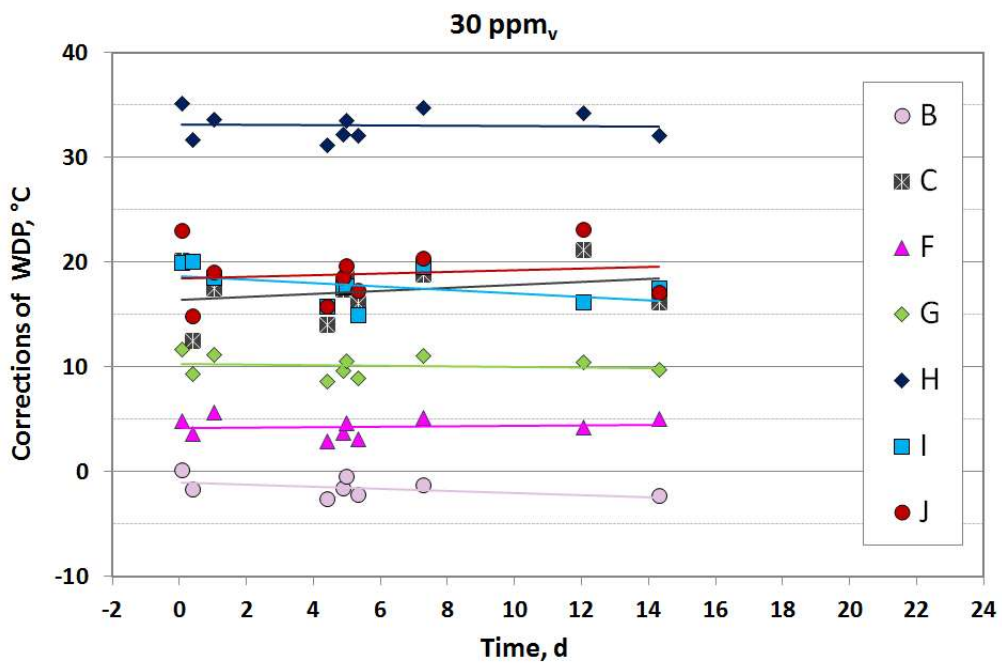


Fig. 5.1.ee Short-term relative drift at nominal water content of 30 ppm_v, using spectroscopy instrument as reference.

5. RESULTS

As the same that happened during the response time test (see Table 5.1.g), hygrometers D and E, which were the same model of capacitive probe, could not measure at the two driest humidity level, so they were not depicted in the two above figures.

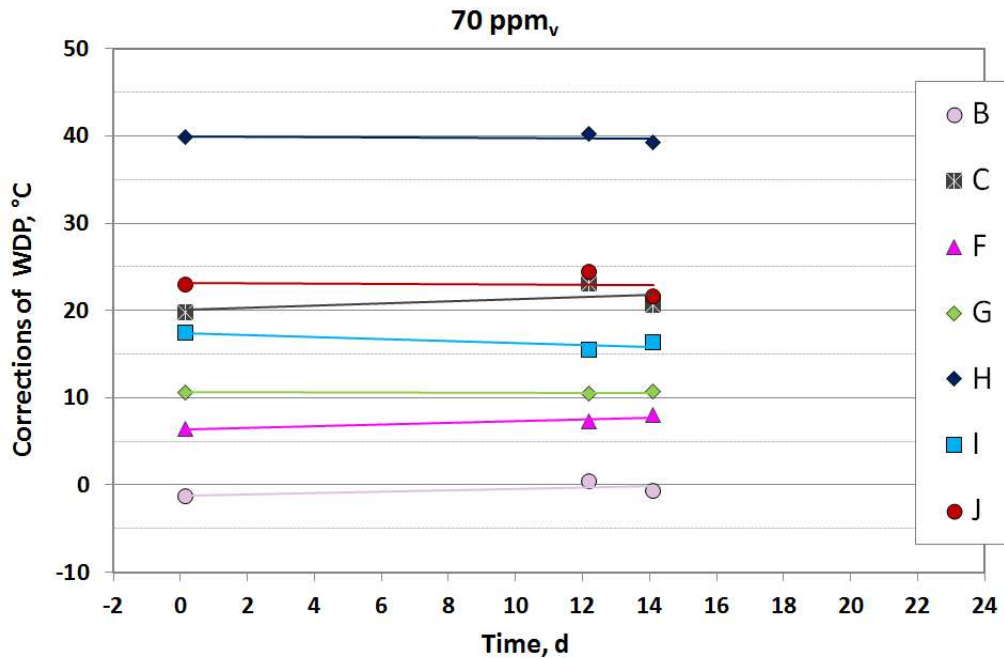


Fig. 5.1.ff Short-term relative drift at nominal water content of 70 ppm_v, using spectroscopy instrument as reference.

Similarly, to the previously humidity levels, hygrometer D and E did not exhibit any read different than their bottom scale, so they have not been shown neither in Fig. 5.1.ff. This effect could not be detected in response tests because this feature was not evaluated at this humidity.

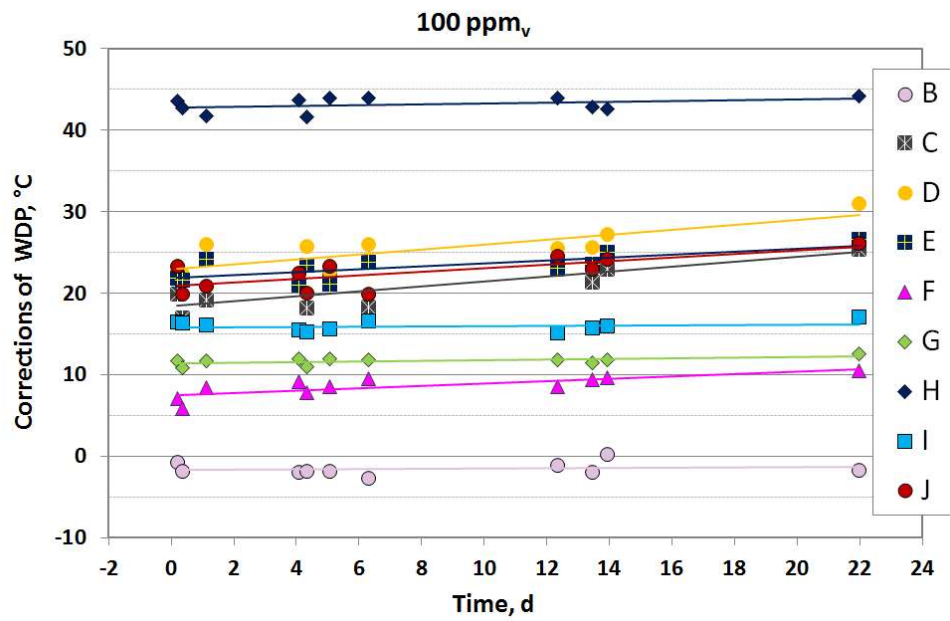


Fig. 5.1.gg Short-term relative drift at nominal water content of 100 ppm_v, using spectroscopy instrument as reference.

As can be seen in the figure above, hygrometers D and E could measure from 100 ppm_v until the upper humidity level.

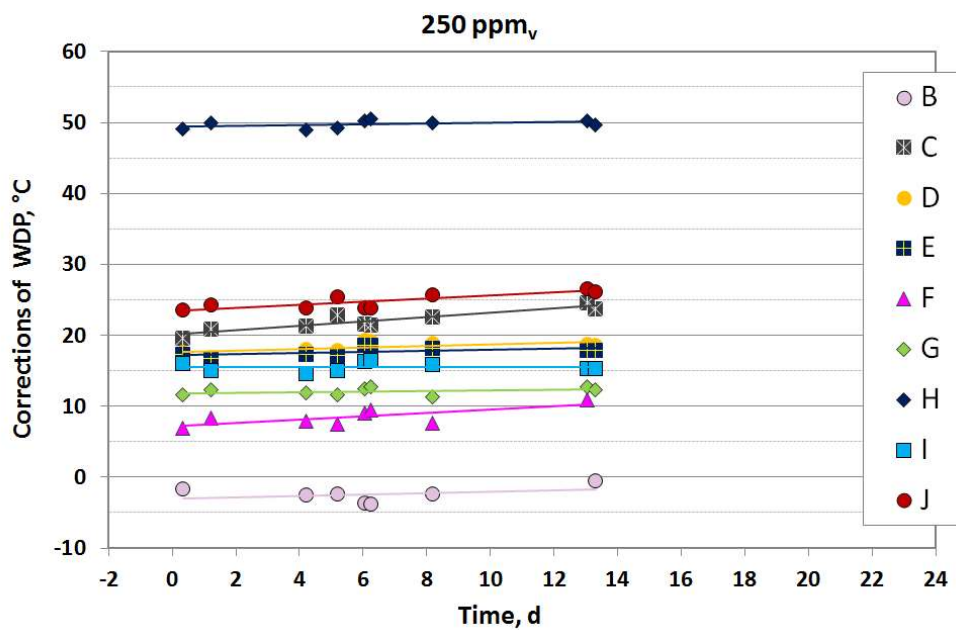


Fig. 5.1.hh Short-term relative drift at nominal water content of 250 ppm_v, using spectroscopy instrument as reference.

5.1.3.3.2 *Conclusion summary of drift study*

Before extracting any final conclusions on the instruments and/or technologies, the following two aspects must be taken into account: (a) the condition of instruments when received and (b) the internal instrument configuration. In the first case, it must be pointed that many of the instruments evaluated had been used previously by other project partners (Section 5.1.5] for up to two years where measurements were made in methane, nitrogen or air without performing any adjustments or specific maintenance, whilst others were supplied directly by the manufacturer shortly before the commencement of the tests. In the second case, some instruments had default parameters that assume a certain gas composition and these could only be adjusted to a certain extent to the actual composition of natural gas flowing in the Enagás line. Despite this, it was observed that the difference between readings were very stable throughout the test period, allowing the relative performance of the instruments was evaluated, even if the actual initial corrections over NG were not known.

The first thing that becomes apparent looking any previously figure was the large dispersion reported between the correction series of all instruments. For example, for the extreme values it is up to 55 °C at a concentration of 250 ppmv and nearly 30 °C at 13 ppmv (see figure Fig. 5.1.dd and Fig. 5.1.hh, respectively). This effect was observed throughout the whole research. An exception to the instrument H, the rest of hygrometers was kept more or less in the same correction range regardless the humidity level measured.

As it has been already demonstrated in the previous study, the behaviour of those instruments which had the same model of measuring sensor was identical throughout the work. It can be seen as since Fig. 5.1.dd until Fig. 5.1.hh, the pairs of series D/E and C/J had very similar behaviour between themselves for all humidity values.

By the other hand, paying attention to the particular scattering in the vertical axis of the experimental values obtained for each instrument at each humidity level. It can be seen that such scatters were close to the reproducibility of the instruments, except in specific cases and to the instruments D/E and C/J. Seen from another point of view, it could be said that the reproducibility of the humidity generation system, which was developed for this project, looks quite acceptable even despite of the own NG variation both composition and water content.

Directly linked with the previously issue, the horizontal behaviour, shown by the most of instruments and depicted by the linear fit of all them, can be translated into a similar relative drift behaviour of such instruments regarding with the reference.

Giving another step more looking for more information from the experimental date, if all data series of all previously graphs were grouped in one only picture that depicted all corrections versus WDP measured by the reference instrument, the resulting figures for the three reference instruments would be as follows:

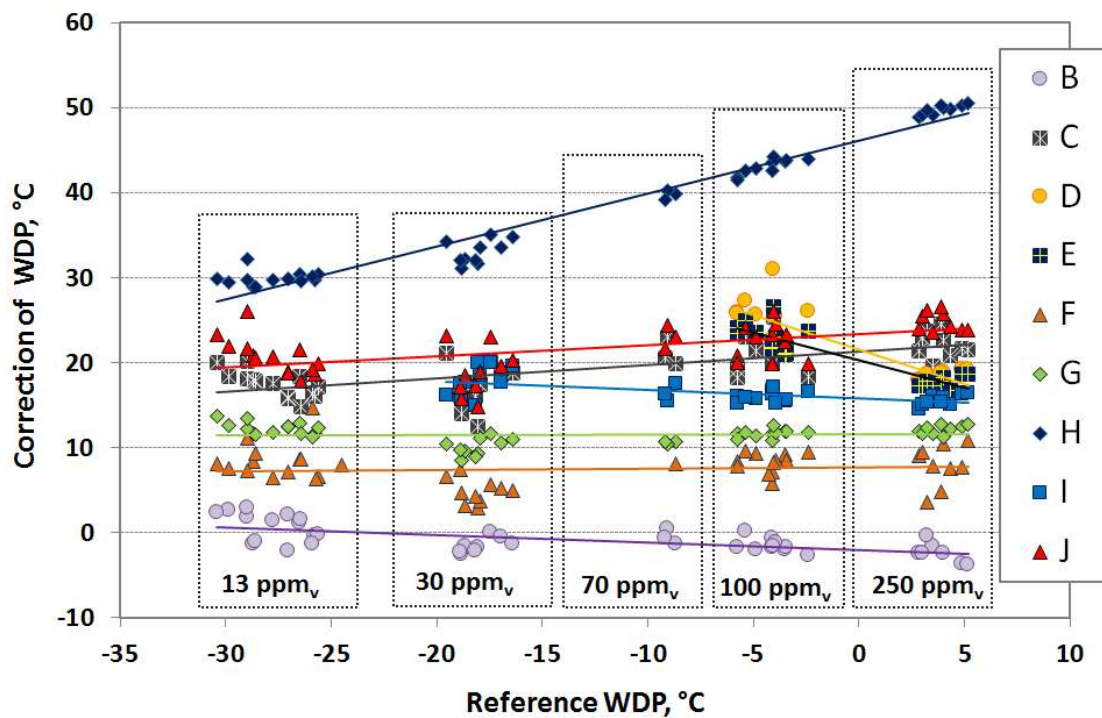


Fig. 5.1.ii Relative corrections of humidity sensors regarding with spectroscopic instrument for five humidity levels generated.

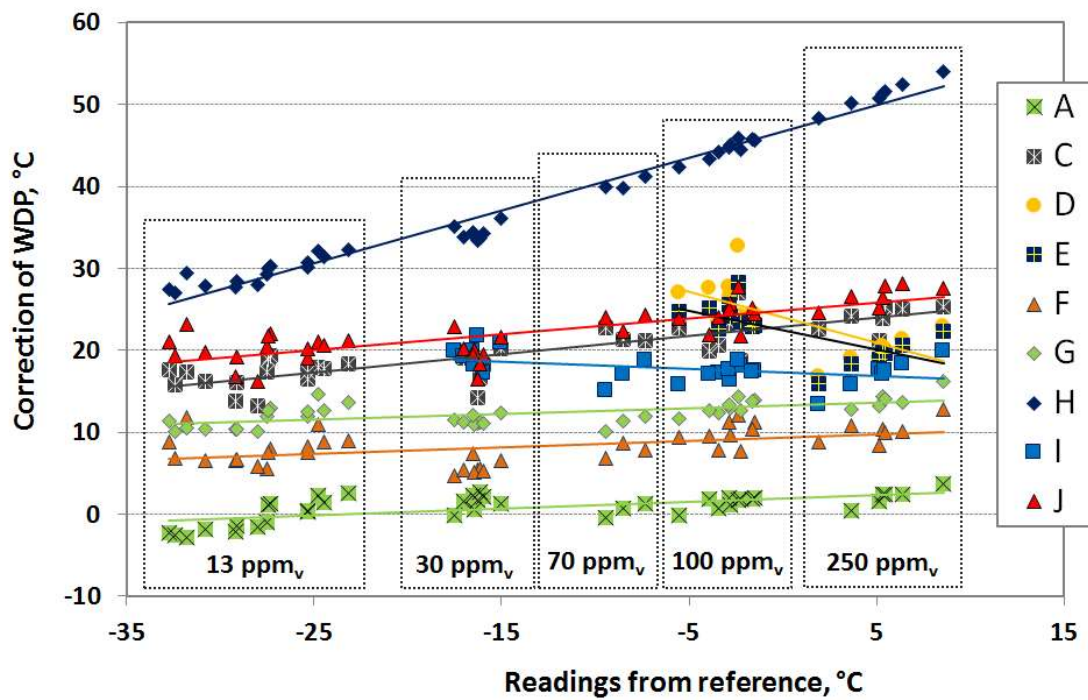


Fig. 5.1.jj Relative corrections of humidity sensors regarding with electrolytic device used as reference for five humidity levels generated.

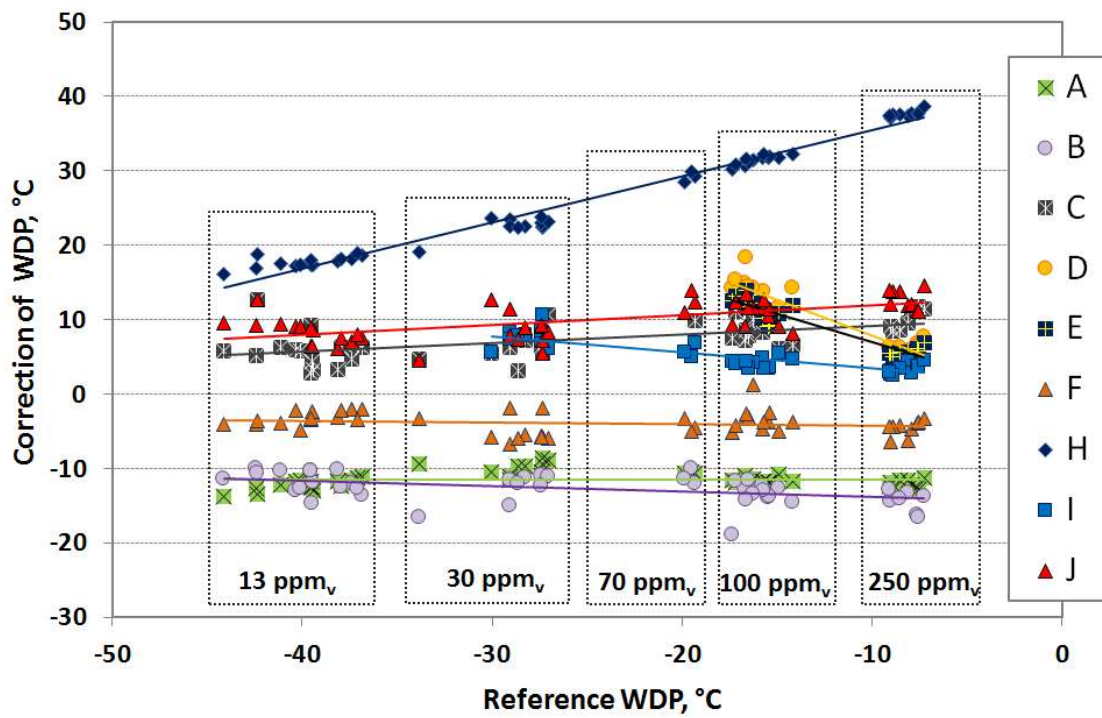


Fig. 5.1.kk Relative corrections of humidity sensors regarding with electrical impedance device chosen as reference for five humidity levels generated.

As can be seen, the look of the last three figures is quite similar and very especially between the first two, where the only difference was the slightly higher scattering shown by the reference WDP given by the second reference hygrometer, the electrolytic, for the two driest humidity levels.

From this kind of figures it can be said that, there were two kind of behaviours of the humidity instruments. The first sort showed a similar drift regardless the humidity level, namely, their corrections kept a horizontal behaviour through the whole humidity range evaluated. While by the other case, drift had a clear dependence on the WC of NG. At this second group would belong the hygrometers D/E, C/J and H, as capacitive probes, and I, as polymeric sensor.

The most remarkable cases of this dependent drifts were starred by the hygrometers H and D/E. For this first probe, the dependence of the drift was evident and looked like to keep a constant slope of drift of the correction, which was positive, so the higher WC there were, the drier were their readings. The second pair of probes, hygrometers D and E, was the most representative case of dependent drift of the WC level with negative slope regarding the correction.

Finally, the drift results obtained for all hygrometers at the five humidity levels, taking as a reference each of three instruments previously chosen, were summarized in Table 5.1.h.

gases, and were confirmed in NG, also. On the other hand, contrary to what has been seen with the rest of technologies, polymeric sensor, I, had a slightly positive drift.

It can also be concluded that all the aluminium oxide sensors except G (that did not show any detectable drift), the drift is negative for the major part of the range studied, tending to successively indicate a dryer gas. This effect is well known to the users and metrology laboratories from measurements performed in nitrogen and other gases, and are confirmed in natural gas, also.

5.1.3.4 Hysteresis study

To assess this property, the pressure line was kept constant at 2.8 MPa and 0.55 MPa for the two sampling zones in which the humidity instruments were classified according to the pressure level that they could endure (see Fig. 4.1.c). This way, potential differences between measures because of pressure changes effects would not affect the hysteresis analysis carried on in this sort of tests.

Due to difficulty of not having a standard hygrometer specifically calibrated to NG, since it was one of the goals scored for this thesis: to find what kind of humidity sensing technology could perform this role. For that, to evaluate the hysteresis of the humidity measurers compared was mandatory evaluating their corrected difference, with regard to one instrument considered as the reference, r . Thus, first of all such reference instrument had to be chosen, and so that is why Fig. 5.1.11 shows the results of the hysteresis study of the spectroscopic analyzer, instrument A.

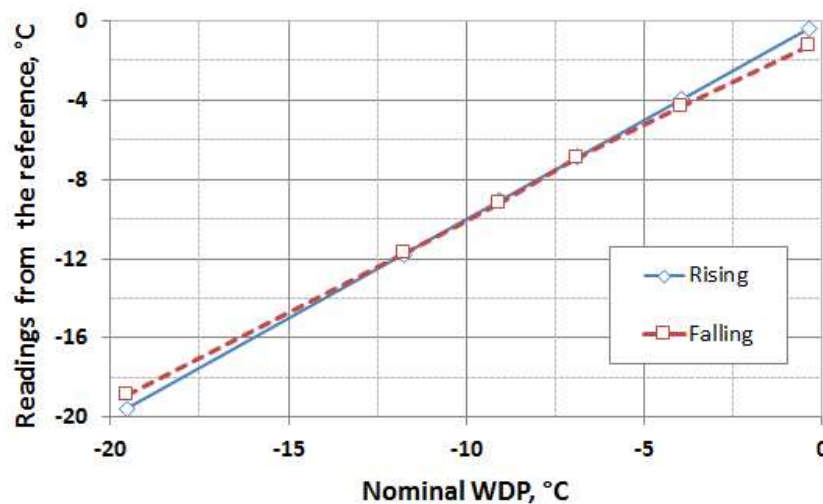


Fig. 5.1.11 Response of the spectroscopic analyzer (instrument A) to rising and falling levels humidity cycles.

Nominal WDP depicted in Fig. 5.1.1l were the equivalent values to the nominal WC, many times cited previously, and applying the International Standard ISO 18453:2004 [ISO04] using the NG composition given by Table 5.1.e.

As can be seen, its performance throughout the whole humidity range studied was consistent regardless of whether readings were taken during the rising or falling humidity cycles. Besides, from above figure it can be conclude that humidity generator system has a reproducibility quite acceptable. So, having been used the spectroscopic instrument as reference for this feature was more than justified.

For the study of such property, the correction was also calculated by Eq. 5.1.d, so a positive correction indicates that the instrument was reading lower than the reference device by contrast, negative corrections denote that was measuring wetter than the reference hygrometer. The results of relative hysteresis study can be seen in Fig. 5.1.mm where both rising and falling humidity levels were represented for each humidity measurer.

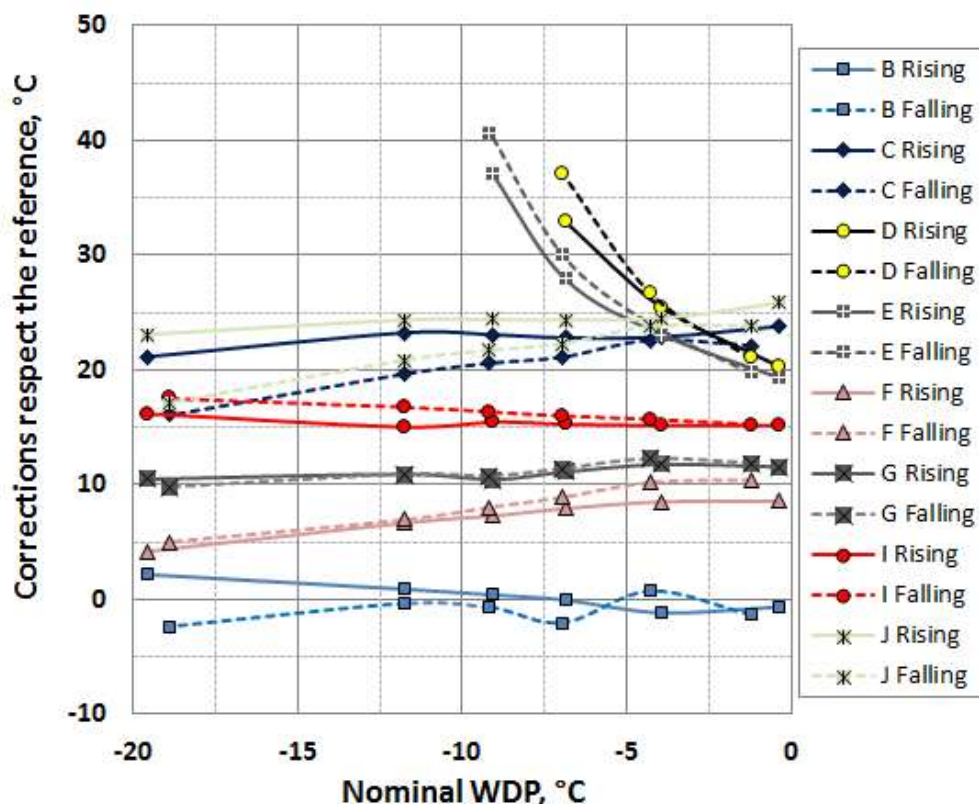


Fig. 5.1.mm Hysteresis of the instruments corrected with respect to the spectroscopic analyzer, A, which was used as a reference. The solid and dashed lines represent rising and falling values, respectively.

From above figure, it can be seen that instruments D and E exhibited a very different behaviour regarding to the rest of devices but were very similar to each other, as expected because they were of the same model of probe. Similarly, instruments C and J shown the same behaviour because although the systems had different electronics, the sensor element was in fact from the same manufacturer.

If stability results, above section of short term drift, are compared with hysteresis tests shown in Fig. 5.1.mm, it can be seen that the readings of instruments A (spectroscopic) and B (electrolytic) were still very similar, resulting in relative values and corrections close to zero. On the other hand, the measurement series that were in the negative range during all drift test study, now they appear as positive due to the definition of the correction. Therefore, it could be concluded that differences observed through the whole drift study were consistent with hysteresis results.

Table 5.1.i summaries all hysteresis corrected values for each nominal values generated. It can be seen from the results of reference instrument, A, as the nominal intermediate values generated were practically identical. However, differences in the extreme nominal values were slightly larger. Despite this, considering the uncertainty with which the European NG industry is currently working with, differences below 1 °C can be considered as practically the same humidity values generated, because was amply covered by the own uncertainty of all instruments.

Table 5.1.i Summary of the results of the hysteresis study. The hysteresis was expressed as the corrected WDP difference (rising - falling), so it was negative when the instrument read dryer in descending humidity.

NOMINAL WDP	INSTRUMENT										
	A	B	C	D	E	F	G	G _{Dig}	H	I	J
°C	°C										
-19.5	-0.7	4.5	5.1	—	—	-0.8	0.7	0.7	2.1	-1.7	6.0
-12.0	0.0	1.2	3.6	—	—	-0.3	0.0	-0.5	1.7	-0.9	3.5
-9.0	0.1	1.1	2.5	—	-3.6	-0.8	-0.3	-0.2	1.1	-0.6	2.7
-7.0	0.1	2.0	1.7	-4.1	-2.1	-1.0	-0.2	-0.3	0.7	-0.5	2.1
-4.0	0.3	-1.9	0.3	-1.2	-1.0	-1.7	-0.5	-0.6	0.6	-0.5	0.7
-0.5	0.9	0.7	1.7	-0.7	-0.5	-1.9	-0.3	-0.3	1.0	-0.2	2.0

5. RESULTS

Looking on the results shown by Fig. 5.1.mm and Table 5.1.i, it can be seen that in the range studied, the majority of instruments did not exhibit appreciable hysteresis irrespective of their technology, with the exception of instruments B (electrolytic P₂O₅), C y J (Al₂O₃ probes) that exhibit a large positive hysteresis for WDP below -12 °C.

5.1.4 RESPONSE TO PRESSURE CHANGES

Changeable conditions of temperature, pressure and composition of NG inlet made difficult to generate the identical WDP after a significant pressure change. In order to minimize the error derived of this uncertainty due to the reproducibility in the WDP generated, all readings were corrected regarding the instrument A cause was a non-pressure dependent instrument. Line pressures for all branch of the sampling system, where instruments under studied were placed, were recorded.

The behaviours against pressure changes was evaluated at a constant humidity level of 100 ppm_v after subjecting those instruments with the permissible operating pressure range, to the maximum line pressure (5.8 MPa) for four days. During this kind of test humidity generation section was bypassed, so humidity of NG was only that coming from the NG inlet stream.

The effect was expressed as the difference between the readings obtained at a pressure of 2.8 MPa, before and after subjecting the instruments to the high-pressure soak, taking instrument A as a reference.

Due to the maximum allowable working pressure range of some instruments, in this tests only the Al₂O₃ and polymeric sensors were compared. In Table 5.1.j the actual value measured were depicted, that is, corrections with respect to instrument A weren't applied yet.

Table 5.1.j Actual data collected after and before the high pressure tests.

	D	E	F	H	I	J	K
	°C						
Before	-30.9	-28.3	-14.5	-47.7	-7.7	-20.0	-28.1
After	-35.0	-30.7	-14.5	-48.3	-9.0	-21.1	-30.1

Correcting the previously values with regards to instrument A, and calculating their difference before and after the pressure change, the following results were obtained:

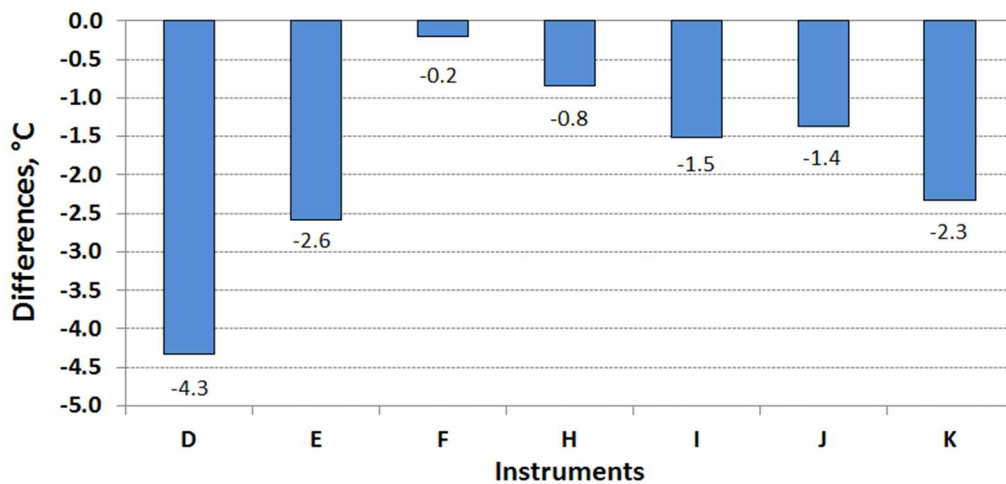


Fig. 5.1.nn Relative differences of measured WDP at 100 ppm_v after having been subjected to the maximum line pressure available.

All negative values shown by Fig. 5.1.nn indicate that all sensors read much dryer after having been subjected to the maximum line pressure. Despite of this, the relative differences of the most instruments analyzed were close to their reproducibility expected (± 2 °C), implying that the changes to line pressure did not significantly affect their performance. The exception were the sensors D and E, which were absolutely identical, and from the results can be inferred that they suffer certain variations due to pressure changes.

5.1.5 HYGROMETERS CHECKING AFTER SEMI-INDUSTRIAL TESTS

According with the last European roadmaps for humidity measurements. One of the main working lines of this first quarter of XXI century was to constitute the European metrology infrastructure necessary to support those industrial processes that do not work with conventional gases, and in particular with non-renewable resources, such as the natural gas [Bel08, Fer12].

For that, inside the 3rd workpackage of the joint research project “ENG01-Gas. Characterization of Energy Gases” [ENG01], one of the tasks carried on was to develop and validate new test facilities for characterization of humidity sensors used in industrial NG as monitoring conditions. That implied to design and built new humidity generators be able to work at pressure ranges well above the atmospheric level and with non-conventional gases.

5. RESULTS

In this sense, NPL built a mix flow humidity generator was able to work with wet methane. Sensors evaluated in such new calibration facilities were calibrated at 3 MPa, with binary mixtures of methane and air at different moisture concentrations [Car13a]. Such pressure set point was ideal because was close to the typical cricondentherm of any NG and besides was also close to the working pressure value fixed in the most of tests which were carried out in this part.

When the available time to INTA to perform these tests expired, the set of capacitive hygrometers, which had been previously shipped and calibrated by NPL, were sent back to check if they had suffered drift effects or they showed any kind of change in their behaviours. Below were depicted the calibration results of such metal oxide probes which were performed by NPL [Bel13, Car13a & Car13b]:

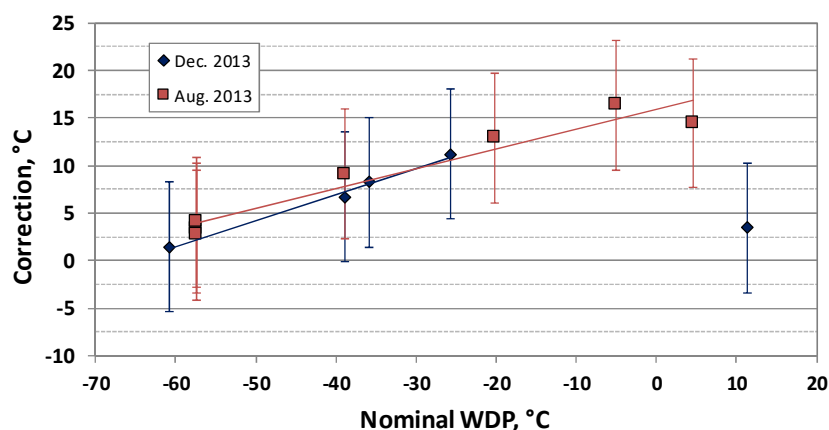


Fig. 5.1.oo Calibrations performed by NPL at 3 MPa before and after the experimental tests doing during this thesis for the DS2000 of Alpha, instrument C [Car13b].

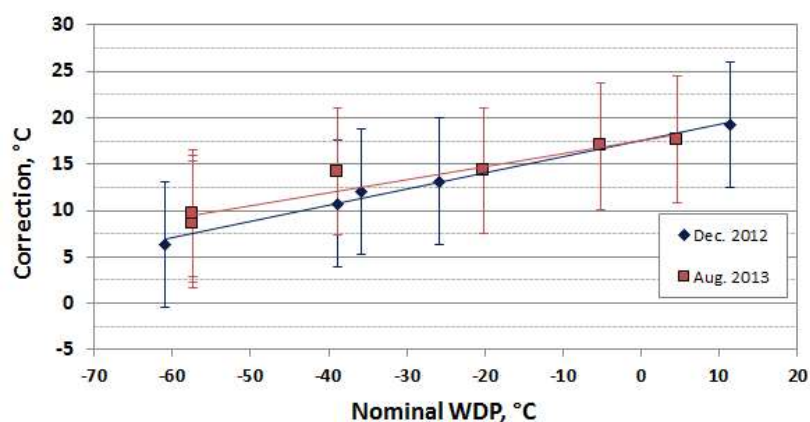


Fig. 5.1.pp Calibrations performed by NPL at 3 MPa before and after the experimental tests doing during this thesis for the Superdew 3 of Shaw, instrument J [Car13b].

Because of instruments C and J were the same probes but with different electrical part, specifically designed by each of manufacturer, was unavoidable to look at simultaneously both figures to try to find similarities between them.

Instrument J exhibited a very similar behaviour for dew points between $-60\text{ }^{\circ}\text{C}$ to $+10\text{ }^{\circ}\text{C}$, range in which both calibrations were practically overlapped. Instrument C would have exhibited the same behavior for both calibrations if it was not for the WDP of $+10\text{ }^{\circ}\text{C}$ in its first calibration, so reliability of such point looked quite questionable and should have been checked again.

Thus, erasing that point, both probes would confirm the same behavior shown in absolutely every tests performed in NG, but with an average difference between both probes lower than $5\text{ }^{\circ}\text{C}$ in all humidity range evaluated and decreasing with the WDP. In addition, it can be seen as corrections obtained during NG test were approximately around $6\text{ }^{\circ}\text{C}$ higher than their calibrations in methane (see Fig. 5.1.ii).

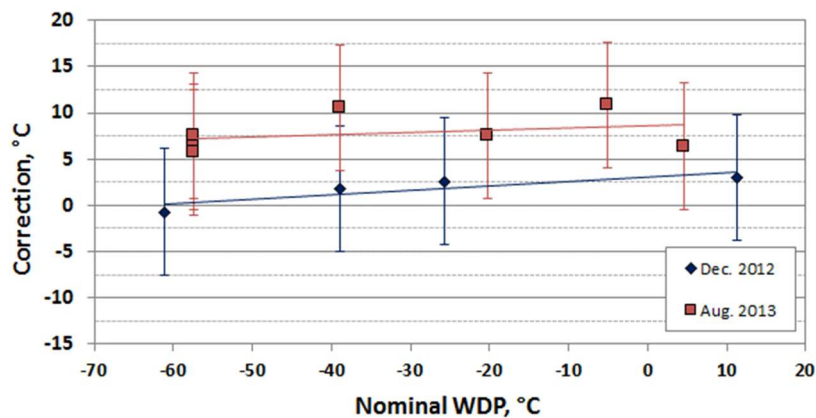


Fig. 5.1.qq Calibrations performed by NPL at 3 MPa before and after the experimental tests doing during this thesis for the Easidew transmitter of Michell, instrument D [Car13b].

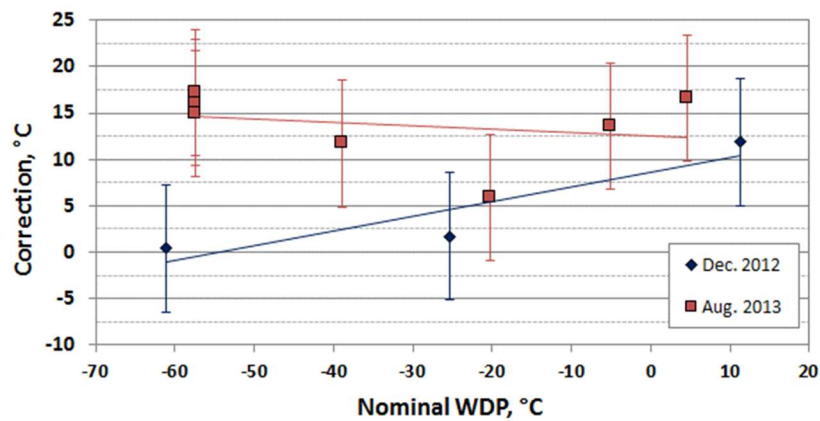


Fig. 5.1.rr Calibrations performed by NPL at 3 MPa before and after the experimental tests doing during this thesis for the Easidew transmitter of Michell, instrument E [Car13b].

Regarding with instrument D and E, both same models Michell (see Table 5.1.a), exhibited very different behaviours. By the first of them, a clear drift effect in all calibration range was shown with a relative steady offset of approximately 6.5 °C, so was measuring drier the second time. The other probe behaved in a very different way in the entire range studied. Thus, it was very difficult to get good conclusions only with this information, except that such model of probe can behave in many different ways.

Comparing the results of these calibrations in methane against their corrections given in NG (see Fig. 5.1.mm), it can be said that both instrument had correction quite higher than those shown in the above figures, nevertheless for the NG readings their behaviors were quite similar in the whole test performed. Thus, for these probes there was a clear discrepancy between methane and NG results.

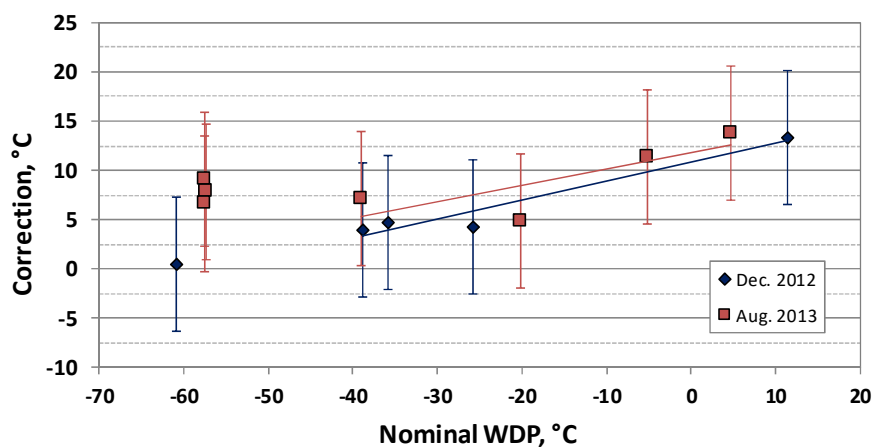


Fig. 5.1.ss Calibrations performed by NPL at 3 MPa before and after the experimental tests doing during this thesis for the Easidew Pro IS of Michell, instrument F [Car13b].

Both calibrations of instrument F in methane seemed quite similar for WDP higher than $-40\text{ }^{\circ}\text{C}$, and its corrections in NG were kept quite steady at approximately $7\text{ }^{\circ}\text{C}$ in the whole humidity range studied. Thus, correlation between both tests was really good and close to the uncertainty of the instrument, the uncertainty calibration given by the NPL and the reproducibility and repeatability of the test carried out in NG.

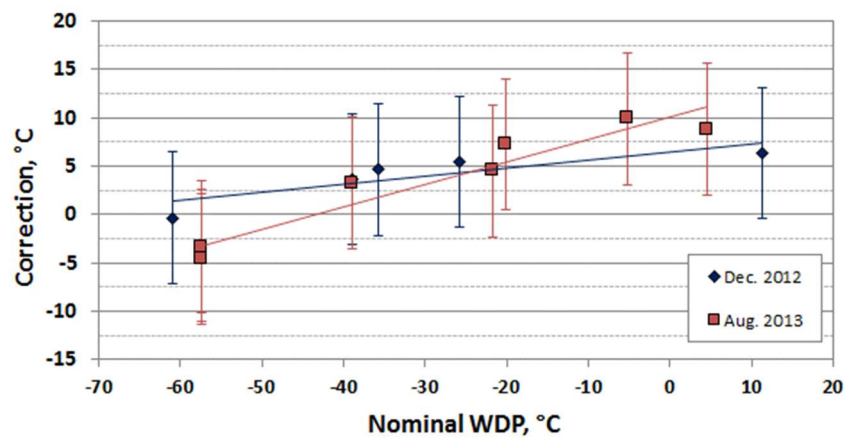


Fig. 5.1.tt Calibrations performed by NPL at 3 MPa before and after the experimental tests doing during this thesis for the HygroPro of GE, instrument G [Car13b].

Hygrometer G had a steady relative correction in NG, regarding the spectroscopy instrument (Fig. 5.1.mm), around $7.5\text{ }^{\circ}\text{C}$ for the WDP range from $-30\text{ }^{\circ}\text{C}$ to $+5\text{ }^{\circ}\text{C}$. These results were quite similar than those shown in its calibration in methane, so it can be said that the HygroPro did not suffer any drift effect.

In summary, all these metal oxide probes exhibited a great heterogeneity between calibrations and very large corrections from $4\text{ }^{\circ}\text{C}$ to $20\text{ }^{\circ}\text{C}$, always in a downward direction. However, these discrepancies were observed throughout all this experimental section, being even larger when the sensors were tested in NG. Thus, this fact suggests such dispersion could not be attributed to the dependence on NG composition but would be more likely to be associated to the different condition under which these humidity probes had been received at the beginning of these semi-industrial tests.

5.1.6 CONDENSATION HYGROMETERS

In Section 3.2, it was already said that two hygrometers based on condensation technology were used in this thesis: the Condumax II which was able to measure the HCDP by means of a conical surface and the Dark Spot technology, patented by Michell; and the DP3D of MBW which was modified to afford up to 10 MPa. The first of them

was used to record the HCDP of the NG inlet stream, whilst the second was studied to check its behaviour using NG under real process conditions.

At any fix pressure value, hygrometers based in this technology works decreasing the temperature of a surface until a thin and steady condensate slayer appears. Keeping in mind the example of phase envelope depicted in Fig. 1.3.i, if the temperature decreases (horizontal leftwards movement in such graph), the nature of the first condensate drops will directly depend on whether the first line reached is HC or WDP curve.

Although the DP3D belongs to the automated chilled mirror type, it was not equipped with an optical instrumentation, such as an endoscopy or any other more complex system, which could recognize or allow to analyze the kind of condensate which was being formed. Consequently, one of the biggest challenges of this experimental semi-industrial section was to obtain accuracy WDP measurement with a relatively large certainty about the nature of the condensate.

For all the above, only two simple tests could be carried out with these hygrometers:

- To evaluate the performance of the DP3D at different nominal humidity levels generated for a fixed pressure value equal to 2.8 MPa, which usually is a pressure level close to the cricondentherm.
- The uninterrupted WDP readings of the NG which came directly from the national supplying grid, were compared with those taken by the DP3D during the four days in which NG was flowing across the experimental rig at the maximum line pressure, as a part of the test to check the behavior of the hygrometers against high pressure changes, whose results were shown in see Section 5.1.4.

Regarding with the first kind of test, in the below graph all WDP readings taken by the automatic chilled mirror were depicted.

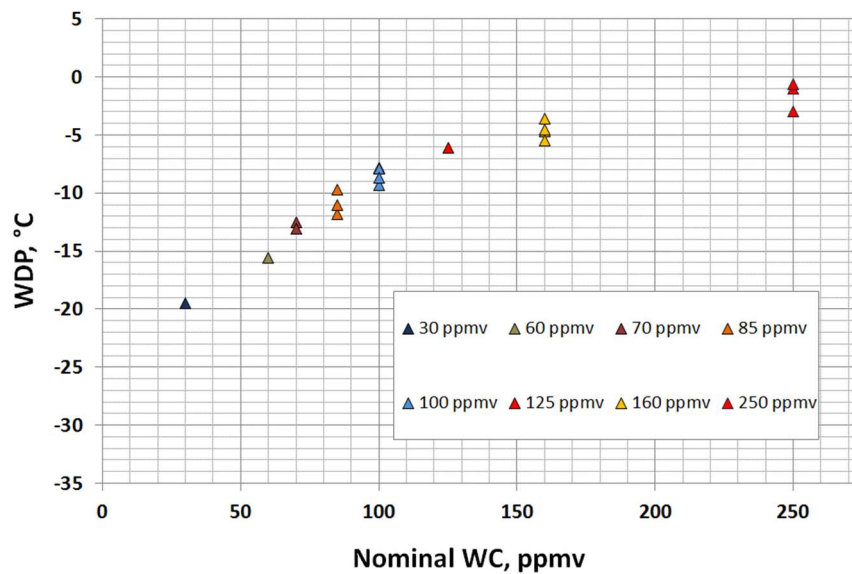


Fig. 5.1.uu All WDP measurements recorded by the DP3D at 2.8 MPa for the whole humidity range evaluated in this thesis.

As can be seen above, the number of experimental values was quite limited because in this graph only were depicted those WDP values whose nature of condensates had been completely confirmed. That was made comparing all values given by the DP3D with the HC and WDP recordings about the NG inlet stream given by the instrument used as monitor, depicted in Fig. 5.1.k. Therefore, if WDP readings given by the CMH were higher than the HCDP at the same time, then these WDP values would be considered reliable and valid. By contrast they would be refused by considering the condensate layer as a mixture of hydrocarbons and water. For this reason, the number of accepted values under 70 ppmv was really low.

Despite of the low number of experimental values accepted, as can be seen in the above figure, the scattering of results for every nominal WC points was inside of ± 2 °C of WDP, and this behaviour looks it was keeping in the entire humidity range evaluated. According to the humidity fluctuations of the NG inlet, shown in Fig. 5.1.k., a scattering below ± 2 °C looks a performance quite promising for condensation hygrometers not equipped with technologies able to detect the nature of the condensates.

By the other hand, exponential WDP decreasing with regard to the proportional reduction of WC adjusted very well to the expected behaviour, according with many theoretical calculation methods based on EOS and used to describe the saturated water

vapour pressure as variable dependent on pressure, temperature and composition of the mixture.

During the second kind of test performed, the humidity generator section was bypassed (see P&I diagram show in Fig. 4.1.s) so, if WDP readings from the Condumax II and the DP3D were compared, both measurements should have been very similar, always that measurements of DP3D were corrected due to the pressure drops suffered by the NG stream until reaching the measuring cell of the CMH.

In the below figure, WDP measurements of both hygrometers were compared together with HCD readings, also measured by the Condumax II but at 2.8 MPa.

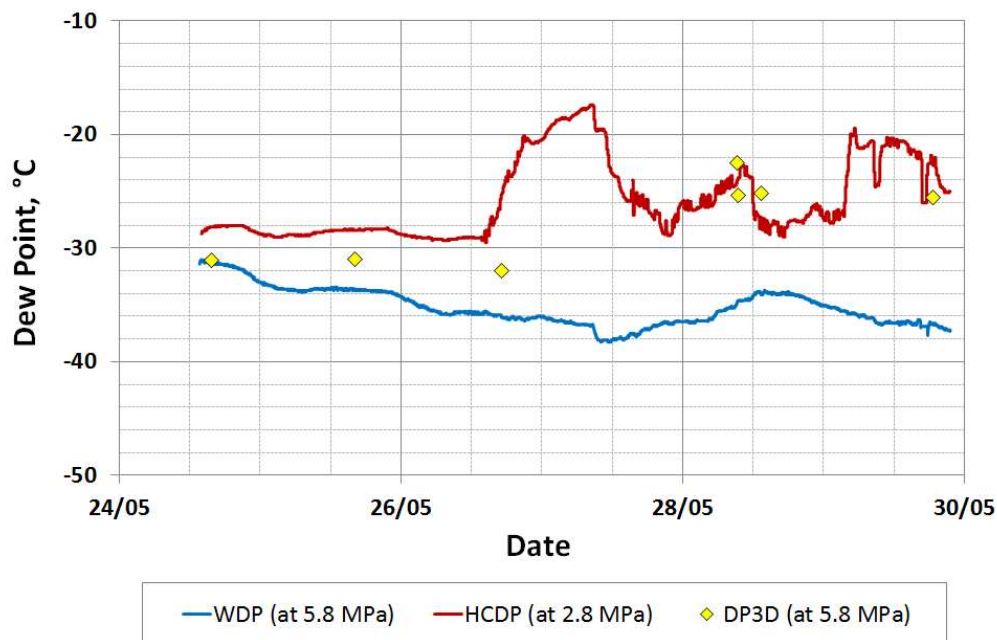


Fig. 5.1.vv Comparative study between WDP recordings given by the instruments used as a monitor, the Condumax II, and those obtained by the DP3D (yellow rhombuses) based on condensate technology at the maximum line pressure.

Comparing both WDP readings, measured at similar pressures values, it can be said that chilled mirror hygrometer always measured wetter than the monitor. This phenomenon cannot be justified by the small pressure drops because in that case, DP3D readings should have been lower not the opposite. Thus, another effect responsible of that situation had to be looked for.

If HCDP values (red line in Fig. 5.1.vv) were recalculated at the same pressure value than the other readings, it would be easier to compare the three data series. In this

sense, going back to have a look at the phase envelope depicted in Fig. 1.3.i, an increasing of pressure of 3 MPa from a region close to the cricondentherm, it would involve a HCDP reduction around 3.5 °C for the average composition used in this section, depicted by the pink series in Fig. 5.1.ww. Thus, including this correction to the previously figure, and assuming a typical uncertainty for the DP3D measurements of ± 2 °C, the results would be the following:

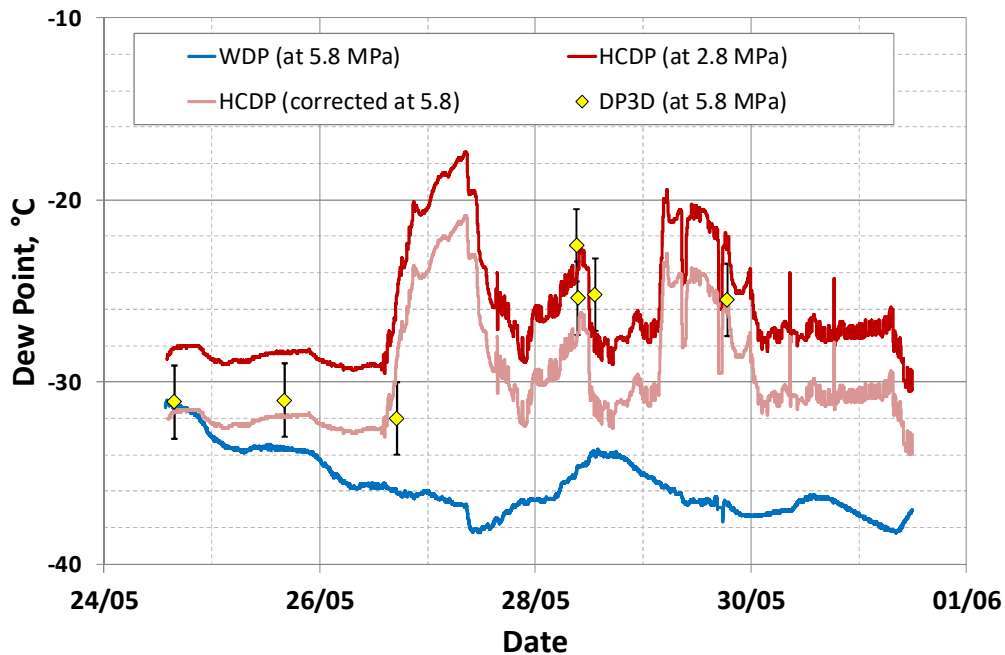


Fig. 5.1.ww Comparative study between HC and WDP readings of the NG inlet stream given by the instruments used as a monitor, and those obtained by the DP3D (yellow rhombuses), being all of them evaluated at the maximum line pressure.

From the above figure, it seems appropriate to say that point measurements given by the DP3D were in good correlation with the wettest kind of DP, regardless of whether their nature. Hence, dew points given by DP3D could be referred both HC and W, depending on which of them were higher.

Therefore, traditional chilled mirror hygrometers are not equipped to select the kind condensate desired. However, novel instruments based in the same measuring principle but more advanced, as the *dark spot* used by the Condumax II, or supplementary equipment such as, modern optical detection technologies, would allow to determine more accuracy and reliable way the condensation properties of complex gaseous mixtures, or what is the same, their HC and WDP, and therefore the gas humidity.

To conclude, chilled mirror hygrometers based on condensation technologies can be used to know NG condensation behaviors but a great experience must be required, besides of a very well knowledge in handling NG, because otherwise would be very difficult to know for sure the nature of the condensates obtained.

5.1.7 UNCERTAINTY BUDGET

Uncertainty assessment study is an essential tool to evaluate the capability of the humidity generation and sampling systems to check the specifications of those instruments whose performance and behavior were evaluated.

According to the indications given in the guide to the expression of uncertainty in measurement, commonly known as the GUM [GUM08], uncertainty assessment was performed applying the uncertainty propagation law, because is currently the internationally agreed method inside of the metrology field and it is essential to estimate the expanded uncertainty of the measurement for results obtained.

For this particular case, the standard uncertainty of measurement coming from any hygrometer evaluated is a combination of three combined standard uncertainties, which are: uncertainty due to the humidity generation system, $u_{generation}$; and those related with the measuring instrument used as reference and instrument which was being calibrated, u_{ref} and u_{inst} respectively. Below equation shows the uncertainty propagation law for this case:

$$u_c(WDP) = \sqrt{\sum_{i=1}^n u_i^2(x_i) \cdot c_i^2} = \sqrt{u_{generation}^2 + u_{ref}^2 + u_{instr.}^2} \quad \text{Eq. 5.1.e}$$

Next step had to be to assess each of these three uncertainty components, which in turn was the result of a combination of several components developed below developed:

Firstly, to estimate the uncertainty by the humidity generation system was resorted to the work reported by Nielsen [Nie03] and used again by Smith [Lov09] regarding to the water vapour obtained by a flow mixing generator, model at which has been equated the saturator used in this section and is given by the following equation:

$$x_{out} = \frac{\phi(x_{sat} - x_{in}) + x_{in}(1 - x_{sat})}{\phi(x_{sat} - x_{in}) + 1 - x_{sat}} \quad \text{Eq. 5.1.f}$$

where: x_{out} , the water vapour content really generated.

x_{in} , the water vapour content in the inlet stream to the saturator.

x_{sat} , the saturated water vapour content at pressure and temperature NG inlet conditions, and for composition of NG which is being flowing across it.

ϕ is the flow mixing ratio and it is calculated as [Nie03]:

$$\phi = \frac{Q_w}{Q_w + Q_{dry}} \quad \text{Eq. 5.1.g}$$

being Q_w the volume (or mass) flow rate entering the saturator, and Q_{dry} the volume (or mass) flow rate of the dry stream.

Table 5.1.k Budget of standard uncertainty of WDP generated, $u_{generation}$.

Uncert. Compont. x_i	Symb.	Units	Stand. Uncert. $u(x_i)$	Sensitivity coeff. c_i	Distrib. / Divisor	Contribution
WC inlet ¹	x_{in}	°C	$u(x_{in})$	$(\partial x_{out} / \partial x_{in})$	Normal / 2	$u(x_{in}) \cdot c_i$
Flow mixing ratio ²	ϕ	---	$u(\phi)$	$(\partial x_{out} / \partial \phi)$	Normal / 1	$u(\phi) \cdot c_i$
Saturated WC ³	x_{sat}	ppm _v	$u(x_s)$	$(\partial x_{out} / \partial x_s)$	Normal / 1	$u(x_{sat}) \cdot c_i$

Below are explained each of uncertainties components previously numbered:

1. WC measured by the Condumax II (hygrometer used as a monitor) for a confidence level of $k = 2$ previously given by the manufacturer in its calibration certificate.
2. Flow mixing ratio uncertainty component, which in turn was also dependent on Q_w and Q_{dry} , so applying the same uncertainty propagation method the $u_c(\phi)$ comes given by:

$$u_c(\phi) = \sqrt{u(Q_w)^2 \cdot \left(\frac{\partial \phi}{\partial Q_w}\right)^2 + u(Q_{dry})^2 \cdot \left(\frac{\partial \phi}{\partial Q_{dry}}\right)^2} \quad \text{Eq. 5.1.h}$$

where sensitivity coefficients are calculated from the partial derivatives regard to Q_w and Q_{dry} . However, cause no rotameter was assembled in any line, a very simple estimation of ϕ could be made from the humidity generator characterization (Section 5.1.1.2) based on opening ratio of valves. Regardless the method used, $u(\phi)$ must be divided by $\sqrt{3}$.

3. Saturated WC must be obtained from an EoS or any other predictive model. Regardless the model chosen, it will be dependent on several quantities, such as: p, T and xi of all components present in the mixture. Each of these variables will have an individual uncertainty associated results of several factor in turn, for example:

- $u(p)$ will be the result by combining several components, such as: calibration of pressure transmitters mounted, and components associated at this kind of instruments (thermal gradient, hysteresis, drift, linearity, etc.), besides of drop pressure corrections.

- $u(T)$, cause the wholes installation had not thermal isolation system, it can be supposed there were a thermal equilibrium between room and NG temperature, so uncertainty components coming from the room conditions datalogger instrument.

- $u(x_i)$, given in the NG composition certificates provided by Enagás, according to the European Standard ISO 6974:2003 [ISO03] (see Table 5.1.c). Complexity of this component is truly huge because some substances affect positively, but another negatively, to the final WDP estimated theoretically. In addition, the endless combinations of composition, in agree with the individual composition ranges of each substances, make of this individual uncertainty, and therefore, its associated uncertainty, $u(x_s)$, a very complex problem which was not a goal in this thesis, so this issue was not addressed here.

By the other hand, depending on the instruments selected as standard and as equipment to calibrate, there will be certain specific components of their standard uncertainty, u_{ref} and u_{inst} respectively. Such components will be different due to manufacturing features or even by the measuring technologies itself, not only by those

quantities required to calculate the humidity, but also by other secondary effects which affect at such quantities. For example, some uncertainty components of chilled mirror hygrometers, which may be considered because affect the final DP temperature obtained, would be contamination or temperature gradients on the mirror; for the electrolytic hygrometer, due to contamination of P_2O_5 electrode; spectroscopic instruments because of the presence of solid particles or substance with absorption peak close to that chosen to measure the WC, etc. A great knowledge of measuring process, based on the experience using each instrument under real working conditions, is key to recognize and estimate all these components

As already has been explained, the DP3D chilled mirror hygrometer initially thought to be the reference instrument, it could not be used as such. For that, three instruments based on different sensing technologies were used as a reference, so individual uncertainty components to calculate u_{ref} were also different in each case.

Below it has been shown a summary table of the most important components required to calculate both u_{ref} and u_{inst} . It could be used as a template but taking in count peculiarities of each instrument for all components, and even to add or delate some of them.

5. RESULTS

Table 5.1.1 List of standard uncertainty components both reference, u_{ref} , and calibrated instrument, u_{inst} .

Uncert. Compont. x_i	Stand. Uncert. $u(x_i)$	Type	Distrib. / Divisor	Explanation
Calibration	$u(x_{cal.})$	B	Normal / k	Calibration certificate, or in case of absence, technical specification of accuracy.
Resolution	$u(x_{res.})$	B	Rect. / $\sqrt{3}$	Specification technical sheet
Stability / Readings.	$u(x_{stab.})$	A	Normal / 1	Average standard deviation from n readings.
Linearity	$u(x_{res.})$	B	Rect. / $\sqrt{3}$	From Fig. 5.1.ii and slopes of each instrument
Long-term drift	$u(x_{drift})$	B	Rect. / $\sqrt{3}$	Specification technical sheet or extrapolating drift sort term results of this thesis.
Hysteresis	$u(x_{hyst.})$	B	Rect. / $\sqrt{3}$	Specification technical sheet or as the maximum difference between rising and falling series shown in Fig. 5.1.mm.
Repeatability	$u(x_{repe.})$	B	Rect. / $\sqrt{3}$	Scattering formed by experimental results obtained from the same nominal value generated.
Reading Instrument	$u(x_{read.})$	B	Normal / 1	Combined standard uncertainty resulting of individual uncertainties because of: calibration, drift, resolution, linearity, thermal coefficient. Applied over those instruments which had not straight reading on measurement units (WDP).

When uncertainty assessment is given in WDP units and if u_{ref} and u_{inst} are based in hygrometers that give WC readings, both they and $u(x_s)$ (in Table 5.1.k) should have to be combined with one more uncertainty component because of conversion between WC and WDP unit [O&A01, ISO04]. This component was called u_{calc} and has the same individual uncertainty components, and therefore, the same complexity already explained above for $u(x_s)$.

The expanded uncertainty of measurement given by NPL calibrations after this experimental section, ± 6.8 °C, (Section 5.1.5) could not be used because it was almost

three times more than the specifications of all hygrometers and so great uncertainty is not useful for the NG industry.

Finally, applying Eq. 5.1.e the combined expanded uncertainty, $u_c(WDP)$, is obtained. And, multiplying it by a coverage factor, k , will get the expanded uncertainty, U :

$$U(WDP) = k \cdot u_c \quad \text{Eq. 5.1.i}$$

where k is obtained from the *effective degrees of freedom*, ν_{eff} , calculated from the Welch–Satterthwaite equation and using the *t-student* probability function for the *confidence level* wanted [Sat46, Wel47].

To sum up, due to the huge complexity to get the resulting standard uncertainty coming from the predictive models used and assess the accuracy or error of such model chosen was not one of the goal established in this thesis, only a small guide was given to explain how it would have to carry out the uncertainty assessment in this kind of experimental tests.

5.2 RESULTS OF MICROWAVE RESONATOR

In this section have been reported those results obtained by INRiM, in which was evaluated the behaviour of the QSR cavity with moist methane as an intermediate and absolutely mandatory step. And of course, the final performance of such technologies in the hygrometry filed applied to the NG industry and under semi-industrial conditions was also reported.

5.2.1 PRELIMINARY TESTS

This part was important to understand well how the two calculating method used to measure the water volume fraction, x_w , from the resonance frequencies worked, besides comparing both results to demonstrate the viability and reliability of the new method, which would be the only available choice that could be applied in complex mixtures as the NG case.

5.2.1.1 Vapor phase measurements in moist methane

Research group of INRiM performed several measured with QSR flowing moist methane at different pressures. They assumed that moist methane was a binary mixture which contains only water and methane, so the water mole fraction can be calculated by means of the procedure described from Eq. 4.2.d to Eq. 4.2.f for each pressure levels generated.

For this procedure, ε_{mix} , was calculated from Eq. 4.2.a, in which $f_0(T)$ was given by Eq. 4.2.n, both obtained experimentally. The density of the mixture, ρ_{mix} , was calculated from Ideal Gas Law: $\rho(p, T) = p/R \cdot T$, where $R = 8.314471 \text{ J} \cdot \text{K}^{-1} \text{ mol}^{-1}$ and the water and methane polarizabilities were evaluated as follows:

- For water, the method described by Birnbaum and Chatterjee was used [B&C52]:

$$\wp_w(T) = A_{\varepsilon_w} + \frac{B_{\varepsilon_w}}{T} \quad \text{Eq. 5.2.a}$$

where: $A_{\varepsilon_w} = (3.96 \pm 0.32) \cdot 10^{-6} \text{ m}^3 \cdot \text{mol}^{-1}$

$$B_{\varepsilon_w} = (2.077 \pm 0.016) \cdot 10^{-6} \cdot 10^4 \text{ m}^3 \cdot \text{mol}^{-1} \cdot \text{K}$$

- For methane, the expression defined by Harvey and Lemon was applied [H&L05]:

$$\wp_{CH_4}(T) = \wp_d(T) = A_{\varepsilon_d}(T) + (1 + b_{\varepsilon_d}(T) + \rho_d(p, T)) \quad \text{Eq. 5.2.b}$$

where:

$$A_{\varepsilon_d}(T) = a_0 + a_1 \left(\frac{T}{273.15} - 1 \right) \cdot 10^{-6} \text{ m}^3 \cdot \text{mol}^{-1} \quad \text{Eq. 5.2.c}$$

$$B_{\varepsilon_d}(T) = b_0 + b_1 \left(\frac{T}{273.15} - 1 \right) \cdot 10^{-6} \text{ m}^6 \cdot \text{mol}^{-2} \quad \text{Eq. 5.2.d}$$

$$b_{\varepsilon_d}(T) = \frac{B_{\varepsilon_d}(T)}{A_{\varepsilon_d}(T)} \quad \text{Eq. 5.2.e}$$

$$\rho_d(p, T) = \frac{\rho(p, T)}{1 + B_d \rho(p, T)} \quad \text{Eq. 5.2.f}$$

Those parameters used to get the first and second dielectric virial coefficients of methane were collected below:

$$\begin{aligned} a_0 &= 6.5443 & b_0 &= 8.4578 \\ a_1 &= 0.0133 & b_1 &= 3.7196 \end{aligned}$$

Finally, regarding the second density virial coefficients used in this method: for water, B_w , was taken from [W&P02]; for methane, B_d , from [S&W91]; and the cross-second virial coefficient, B_{wd} , of the methane-water system from [Aki06].

For this kind of test, the new calculation method was also applied to determine the water content of a mixture. In this case, Eq. 4.2.a was used in first place to determine, ε_{dry} , from the resonance frequency of the dry mixture, f_{dry} . After that, the moist mixture was flowed to collect its resonance frequencies which will be inserted in Eq. 4.2.h, as f_{mix} , obtaining the permittivity of the mixture, ε_{mix} . By last, the water content was determined through Eq. 4.2.m, where polarizabilities were known by means of Eq. 4.2.i and Eq. 4.2.j.

In this section, the water mole fraction in gas stream of methane was evaluated for twelve nominal pressure levels. INRiM generator was kept at a steady temperature around 4.0 ± 0.5 °C and pressure set points were within the range of 150 kPa and 1 MPa. These twelve pressure levels chosen for checking the performance of QSR with moist methane can be clearly looked in both graphs of Fig. 5.2.a:

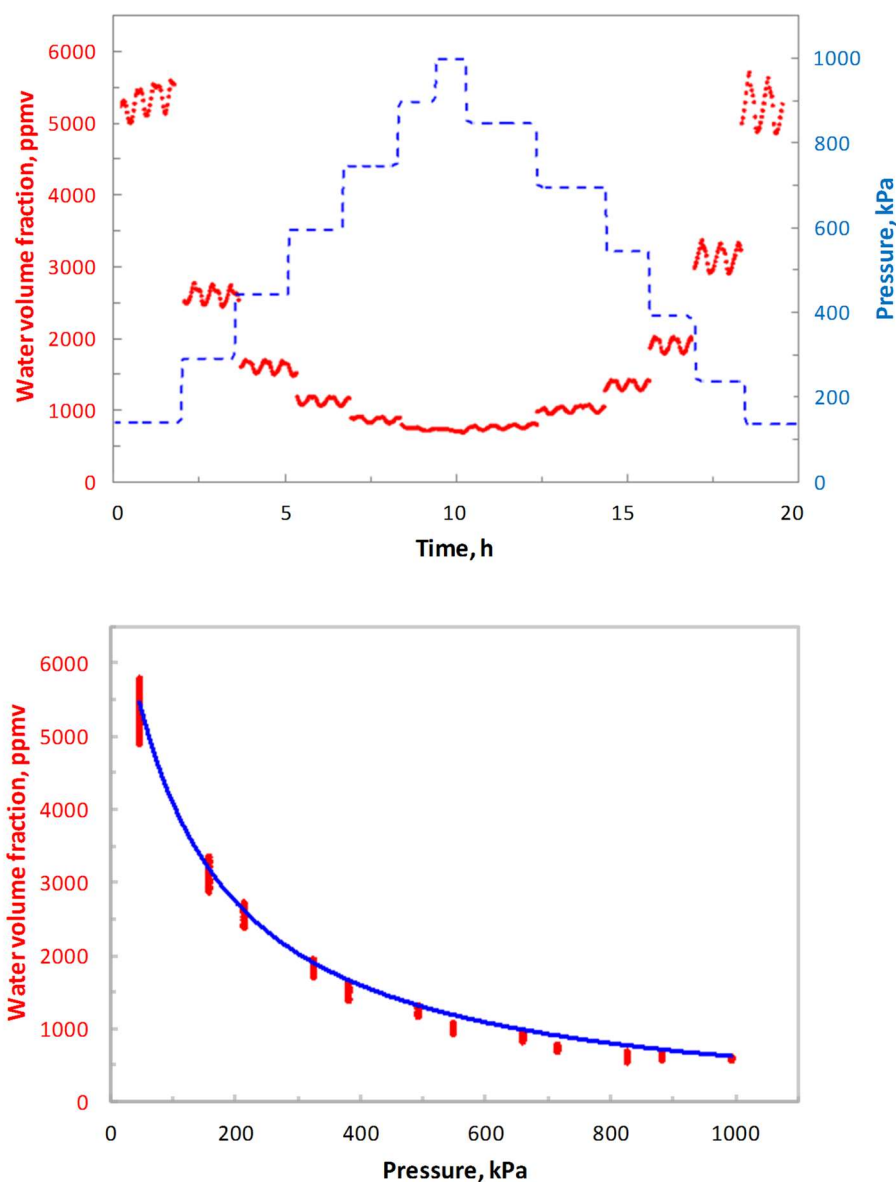


Fig. 5.2.a Red dots show the water volume fraction, x_w , generated by the saturator of INRiM, and determined from microwave measurements in the QSR. Top: blue dashed line indicates the sample pressure. Bottom: blue line depicts the absolute humidity for each pressure level and at the same temperature (4 °C) [Gav14].

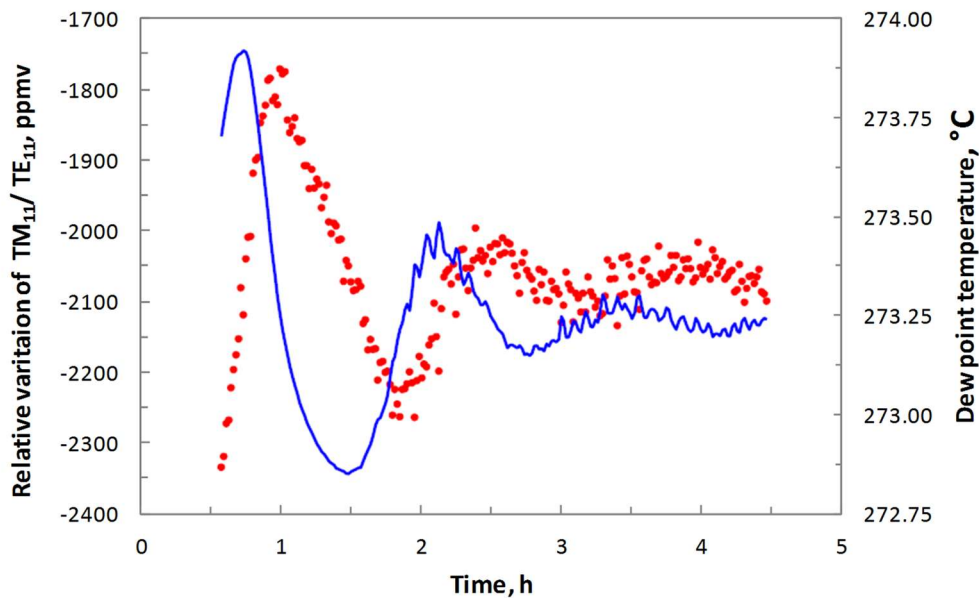
The oscillatory behaviour shown by the water content readings in the top graph of Fig. 5.2.a evidences the weakness in the thermostating system of the saturator. This solubility changes of water in compressed methane are also shown in the bottom picture, but in this case is depicted as the wide of vertical scattering of red dots. In both pictures, it can be noticed this problem was higher as lower was generated pressure in the system.

In the bottom picture of Fig. 5.2.a, the blue line depicts the absolute humidity, what means the maximum water content which can be present in a gas, and it only depends on the pressure and temperature according to Eq. 1.2.c, considering a pure gas.

As it can see in the same graph, the maximum possible water content, given theoretically by such equation, was practically the same to those experimental values obtained which means that methane was going out practically saturated from the humidity generator. The water volume fractions range obtained was between 600 ppm_v and 6000 ppm_v at temperatures between 273 K and 300 K.

5.2.1.2 Condensation tests and determination of *f*-factor for methane

Once confirmed the ratio TM_{11}/TE_{11} was a reference really stable and repeatable (see Table 4.2.a), two tests were performed at INRiM with humid methane mixtures at two absolute pressures. To reduce thermal oscillations effects shown in the previously section, the bubbler was inserted in a dewar in contact with a melting water-ice mixture, keeping approximately constant and slightly above 273.15 K for several days. Both tests were depicted in the two below graphs of Fig. 5.2.b.



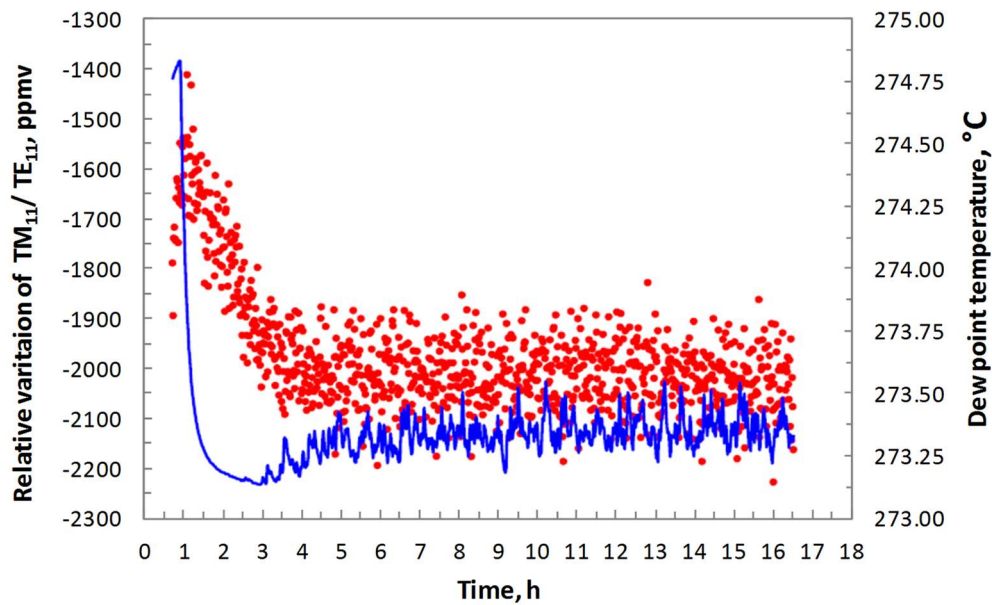


Fig. 5.2.b Condensation tests for humid methane at 150 kPa (top) and at 750 kPa (bottom) [Gav14].

The red spots depicted in Fig. 5.2.b shown the relative variations of the measured ratio TM_{11}/TE_{11} from its reference value. It was established as reference a constant relative variation of -2000 ppb, which corresponded to maintaining a volume of 1.2 mm^3 of condensed water on the resonator surface, with an average layer thickness of 150 nm. By the other hand, the blue lines represent the dew point temperature obtained keeping constant such relative difference of the frequency modes ratio. And, as it has been explained in introduction section from dew point values, water vapour pressures can be recalculated by means of several equation models, which describe the water vapor-liquid equilibrium.

In addition, the *enhancement factor*, f , for the methane was evaluated too, as an indicator of the deviation of such substance regarding with the ideal behaviour of a pure substance because of the effect of molecular interactions. The relative amount of such deviation is a function dependent of temperature and total pressure $f(p, T)$.

Thus, from data recorded during these tests, it could be determined the enhancement factor of the methane/water mixture by means of the Eq. 1.2.c, explicit to f and calculating the saturated water vapor pressure of water at the dew point temperature, $e_w(T_{dp})$, from the IAPWS95 formulation [W&P02].

In the below figures, it has been depicted variation in time of the calculated enhancement factors of moist methane. Area limited by the grey lines indicates the overall uncertainty estimated, $u(f)$, considering the contributions by temperature and pressure measurements, and discrepancies between experimental and calculated permittivity of dry methane (Fig. 5.2.c).

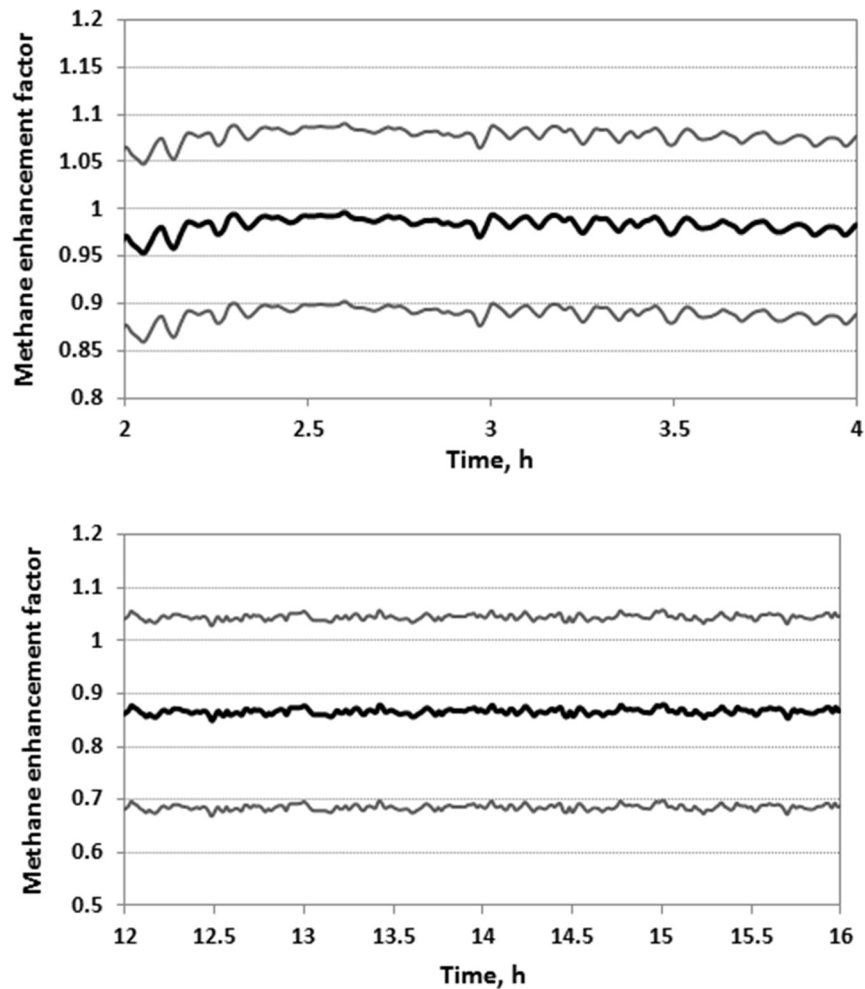


Fig. 5.2.c Enhancement factors of a humid methane mixture at 273.25 K at 150 kPa (top) and 750 kPa (bottom).

The enhancement factors obtained together with their correspondent standard uncertainties with a coverage factor $k = 1$ were:

$$- f(150 \text{ kPa}, 273,25 \text{ K}) = 0.97 \pm 0.09$$

$$- f(750 \text{ kPa}, 273,25 \text{ K}) = 0.90 \pm 0.15$$

During these preliminary methane tests, the maximum pressure value generated was 750 kPa, which theoretically was close to the ideality, so this deviations were not very important and their effect was not evident.

The following picture (Fig. 5.2.d) shows the comparative between data published in literature and the two values of enhancement factors of moist methane which have been obtained by INRiM during the prior characterization steps to flow natural gas through the QSR:

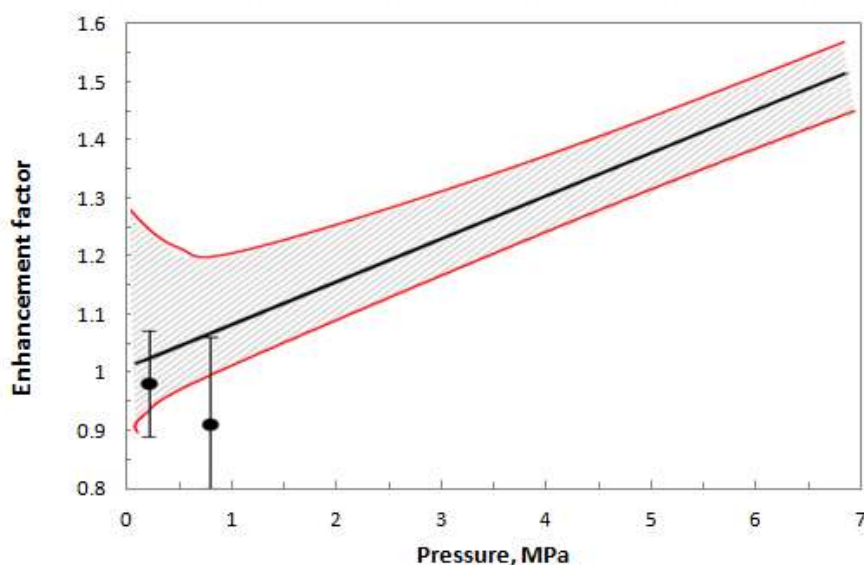


Fig. 5.2.d Comparison of the enhancement factor of humid methane determined in this work [Gav14] with data published in literature [Buk55 and Fat07].

Looking at the above figure, it was demonstrated that those enhancement factors calculated here did not have very good consistence with those previously published about the methane/water systems. In fact, the trend of the enhancement factors obtained here for methane decreased with the pressure in contrast with several reports published [S&H14a and b].

5.2.2 MEASUREMENTS IN MOIST NATURAL GAS

The study of the behaviour of QSR in moist natural gas was integrated inside of the comparative of several humidity measuring instruments based on diverse sensing technique. For that, the performance of microwave resonator will be shown as a relative comparison from the achieved outcomes by the other instruments.

The mechanism carried out in this test have been already explained in detail in Section 4. During the whole test time, the cavity was maintained stable by suitable PID controls at (297.00 ± 0.01) K, (752.00 ± 0.01) kPa and it was supplied $0.1 \text{ L} \cdot \text{min}^{-1}$ of NG flow.

The resonance frequency mode of TM_{11} was recorded every 70 sec. Fig. 5.2.e shows the variation on time of such frequency during the whole test time and it can be seen time the spent in each of steps. It was considered as frequency reference value that measurement just before starting the drying process.

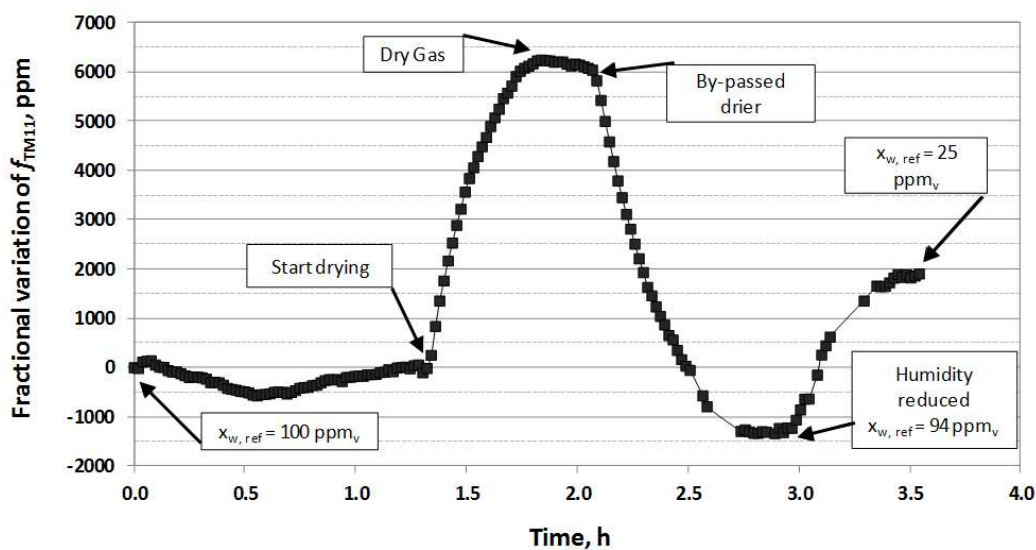


Fig. 5.2.e Relative frequency change recorded for mode TM_{11} during the different phases of the test to determine the water fraction in a NG stream.

Fig. 5.2.e shows that for the first 75 min it was checked that all process variable inside the cavity were steady and all devices associated with data acquisition system were working properly. The frequency readings suffered a change after 30 min, because of the pressure in the humidity generator was slightly fitted again.

Once spent the first 75 min, the drying process started, causing an increasing of the TM_{11} frequency. Only 30 min was needed to complete the drying process, as can be seen watching Fig. 5.2.e where the variation of the TM_{11} frequency became steady and approximately 6000 ppm higher than the initial value. However, the drying step was kept running for 15 min more to get enough data to achieving a reliable reference frequency, f_{dry} , minimizing this way as much as possible a potential mistake obtaining this quantity,

which would have affected to all water vapour pressures calculated later, according to the method already described

After that, the drying system was by-passed and the moist NG readings were collected. Looking at Fig. 5.2.e, it can be noticed as the fractional variation reached negative values beyond -1000 ppm. That could indicate the water content in the NG had really increased respect to the reference value previously considered. Finally, the humidity generator was set to reduce the nominal humidity value generated and observe the dynamic behaviour of the MW resonator.

The quantity f_{dry} was obtained as the average of about 20 successive measurements recorded: $f_{dry} = 5138.4790 \pm 0.0005$ MHz. Then, the permittivity of the dry component, ε_{dry} , can be calculated from the squared ratio $(f_{dry}/f_0)^2$, where $f_0(T)$ was previously interpolated for the test temperature applying Eq. 4.2.n. Resulting value was: $\varepsilon_{dry} = 1.006\ 478$, which was in agreement with $\varepsilon_{dry} = 1.006\ 472$ reported in literature [S&M03].

Now, knowing f_{dry} and ε_{dry} , and having the full record of evolution of f_{mix} along the time, if Eq. 4.2.h is applied, it will get the evolution ε_{mix} through time, and finally the water fraction, x_w , using Eq. 4.2.m.

To be able to compare the performance of microwave resonator in the hygrometry field, all humidity readings given by instruments were recalculated to be expressed as water vapour fraction instead of WDP. For that, readings given by the HygroPro and the EE371m had to be transformed to WC applying the European Standard ISO 18453:2004 [ISO04] and using the pressure transmitters, which had been mounted in all lines where humidity analyzers were located. For this test, the NG composition used for this unit conversion was as follows:

Table 5.2.a Daily average composition of natural gas supplied that day. The results were provided by Enagás by means of gas chromatographic analysis.

Component	Molar fraction, %	Uncertainty (K = 2)
Methane	90.43	± 0.12
Ethane	6.46	± 0.09
Propane	1.32	± 0.02
Nitrogen	0.90	± 0.03
Carbon dioxide	0.30	± 0.01
i-Butane	0.210	± 0.007
n-Butane	0.275	± 0.007
i-Pentane	0.037	± 0.001
n-Pentane	0.031	± 0.001
C ₆₊		< 0.04

Once all readings were expressed at the same quantity, the comparison among all instruments could be performed. Fig. 5.2.f shows the WC calculated by the method described in Section 4.2.1.2 together with those readings given by the other four hygrometers based on four different sensing technologies. From this graph, the performance of the QSR cavity could be compared against the rest of instruments both for the two humidity levels generated and the response rate between both steady final values.

On this occasion, the EE371 was considered the reference instrument because between all instruments chosen for this relative comparison, it was the only that came directly calibrated from the manufacturer, so in theory and without having any information more about the behaviour of the rest of hygrometers, this choice seemed the most reasonable. Once steady readings from EE371 had already been achieved, the two nominal humidity values generated were 100 ppm_v and 25 ppm_v, respectively.

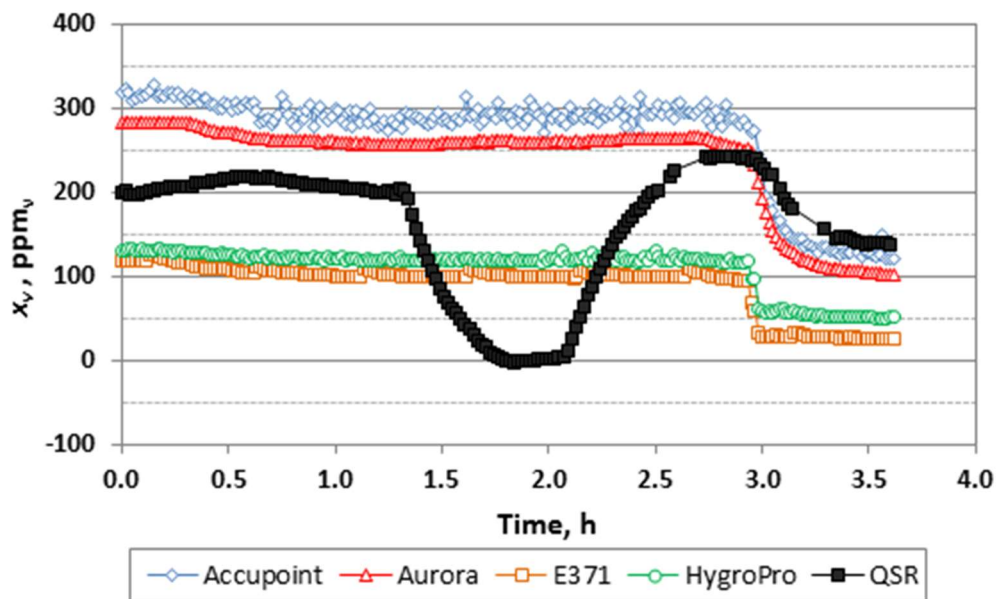


Fig. 5.2.f Comparison of water fraction estimation from the microwave resonator with the readings recorded by other four commercial humidity sensors.

As it can see in the Fig. 5.2.f, the slight increase of pressure in the sampling system produced past 20 min from the beginning of the test, was recorded as small reductions in the water content read by the five instruments compared. Also, it is clearly noticed the particular measuring procedure carried out with the QSR to establish the resonance frequency for the blank, in other words the NG completely dry, f_{dry} .

By the other, Fig. 5.2.f shows the same effect detected throughout all results given in Section 5.1., the huge scattering between all readings collected. The WC readings given by Aurora and Accupoint were quite agree but were higher than the reference values given by EE371, which was also well correlated with HygroPro during the whole test time.

Moreover, the microwave QSR had more complex behaviour than the rest of instruments. Initially, its readings had intermediate values between both signal groups. However, after resonator drying step, at the first nominal humidity level, the water fraction calculated was relatively higher even arriving to reached readings of the Aurora, but in the case of the second humidity level readings from the resonator were the highest. To understand better the relative behaviour of microwave resonator against the rest of instrument compared, the average water vapour fractions given by the five sensors were plotted together with their uncertainties in Fig. 5.2.g.

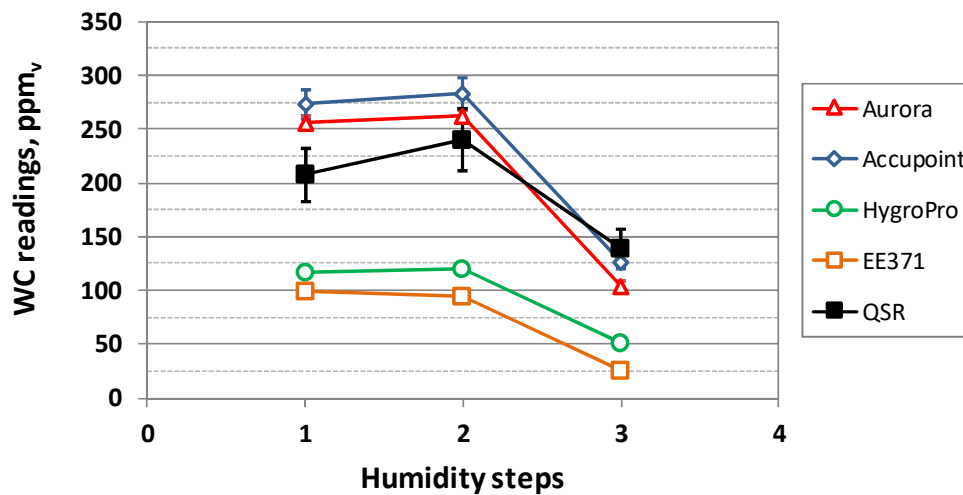


Fig. 5.2.g Readings of water vapour fraction given by the five instruments compared.

The first two steps correspond to the same nominal humidity level, 100 pmm_v, but in the second step the QSR had already measured the frequencies for dried NG and then had come back to the same humidity value. Also can be seen in Fig. 5.2.g that all hygrometers, excluding the EE371, measured slightly higher WC for the second case, being the QSR which suffered the biggest change.

Conclusions extracted from above figure was that, there were two behaviour clearly different, at one group belong the Aurora and the Accupoint, and the other the EE371 and the HygroPro. In accordance with the entire results shown in the previously chapter (Section 5.1), keeping the same relative offset between all of them. Besides, it seems like the QSR resonator behaved more similar than the first group with which had a correlation quite acceptable.

5.2.3 UNCERTAINTY BUDGET

Uncertainty assessment of the QSR was performed by INRiM for determination both of the water vapour fraction and the enhancement factor but only for the case of the methane. This study was reported in literature by *Gavioso et al.* [Gav14] together with the results obtained sampling NG.

5.2.3.1 Water content

From Eq. 4.2.hand replacing ε_{mix} for such expression in Eq. 4.2.m, resulting Eq. 5.2.g. In such equation were specified those thermodynamic variables depending on the pressure and temperature and the frequencies measured, in order to evaluate the

robustness of the new method against systematic errors in both the determination of the pressure and the estimate of ε_{dry} .

$$x_w(p, T) = \frac{\left[\frac{\varepsilon_{dry}(p, T)(f_{dry}/f_{mix})^2 - 1}{\varepsilon_{dry}(p, T)(f_{dry}/f_{mix})^2 + 2} \frac{\varepsilon_{dry}(p, T) + 2}{\varepsilon_{dry}(p, T) - 1} \right] - 1}{\rho_w(p, T)/\rho_{dry}(p, T) - 1} \quad \text{Eq. 5.2.g}$$

First of all is that the term associated with the multiplication by the squared frequency ratios has a negligible effect, because their difference from the unity or the value 2 is extremely small. For example, for the fraction $x_w = 1000$ ppm of water in methane at 275 K and 150 kPa, $(f_{dry}/f_{mix})^2 - 1 = 4.7 \cdot 10^{-6}$ [Gav14] and ε_{dry} for any substances is a value very close to the unit, bearing out this first approximation.

Following, next step should be to assess the variation of $\varepsilon_{dry} = f(p, T)$, which was perfumed through the following expressions:

$$\frac{\partial \varepsilon}{\partial T} = \frac{\varepsilon_T - \varepsilon_{T-\Delta T}}{\varepsilon_T} \quad \text{Eq. 5.2.h}$$

$$\frac{\partial \varepsilon}{\partial p} = \frac{\varepsilon_{p+\Delta p} - \varepsilon_p}{\varepsilon_p} \quad \text{Eq. 5.2.i}$$

In Table 5.2.b were summarized the variation of ε_{dry} of methane because of a change of 1 K and 100 Pa, applying the above equations:

Table 5.2.b Summary the variation suffered by ε_{dry} of methane because of an increase of 1 K or 100 Pa.

	PRESSURE	
	100 kPa	2.7 MPa
$\left. \frac{\partial \varepsilon}{\partial T} \right _{300 K}, \text{ ppb} \cdot \text{mK}^{-1}$	1	10
$\left. \frac{\partial \varepsilon}{\partial p} \right _{300 K}, \text{ ppb} \cdot \text{Pa}^{-1}$	4	4

Concluding that an error in the determination of the pressure of 100 Pa (relatively 0.1 %) or 1 K resulting to the numerator of Eq. 5.1.i changes x_w by only 1 ppm. Thus, the precision of the pressure control, usually lower than 100 kPa, has a negligible variation over water molar fraction determination, x_w .

Another way to know the effect of $\varepsilon_{dry}(p, T)$ may be either determined experimentally the squared ratios $(f_0/f_{dry})^2$ or calculated if the composition is previously known. In both cases, the determination of x_w from Eq. 5.2.g is extremely robust against any systematic error in the measurement of $\varepsilon_{dry}(p, T)$.

Fig. 5.2.h depicts a quantitative comparison of the overall uncertainty budget in determination of x_w for a binary mixture of methane + water applying the two methods describes in Section 4.2.1

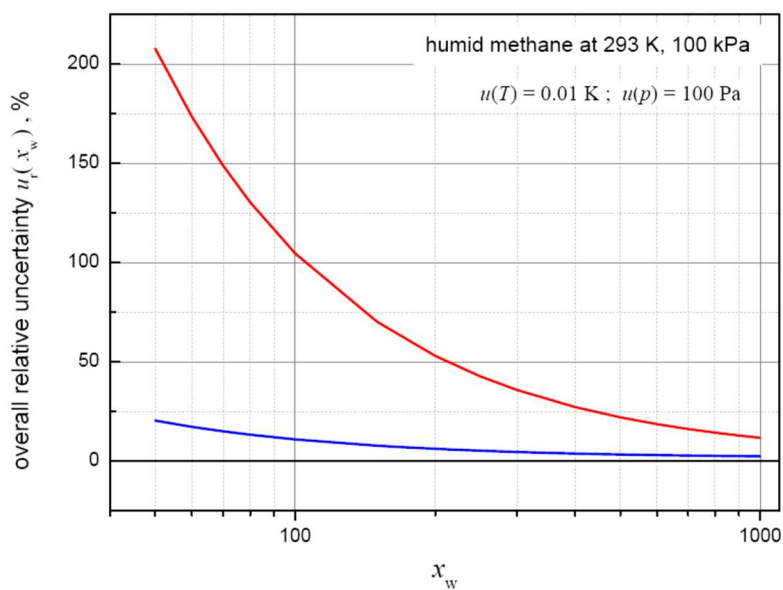


Fig. 5.2.h Comparison of the relative overall uncertainties achievable in the determination of the molar fraction x_w of a humid methane mixture at 293 K, 100 kPa with two different methods used in this work: (red) procedure only useful for binary mixtures (described in Section 4.2.1.1); (blue) relative procedure (described in Section 4.2.1.2) [Gav14].

The uncertainty budget in the above figure were included usual contributions of pressure and temperature measurements: $u(p) = 100$ Pa and $u(T) = 0.01$ K; as well as from reference functions or correlations predicting the thermodynamic and electrical properties of methane and water [Gav14].

From Fig. 5.2.h it can be extracted that, within the common WC range used in NG industry (5 to 100 ppm), the new method improves the sensitivity of the microwave technique since 10 to 5 times, determining the water molar fraction content in a sample of most methane. Also, it can be seen how the lower is the water concentration, the higher is the relative improvement of the new method.

Thanks to this new calculation method and its experimental procedure which implies the consecutive flow through the microwave cavity of the humid mixture and of its dry fraction, it has been avoided to add one relevant uncertainty contribution and laborious to calculate such as the mixture density. Besides, the contribution of the uncertainty associated to frequency measurements can be usually kept so small to be negligible with respect to other sources.

However, there are many other sources that contributes in the overall uncertainty of x_w , including [Gav14]: pressure determination; the composition of the mixture, due to the possible presence of unknown or variable amounts of impurities; the imperfect knowledge of the thermodynamic properties, i.e. the virial coefficients, or the electrical properties, i.e. the polarizability, and belonging this latest group the most predominant uncertainty comes from the Debye constants of water vapor [B&G52]. Finally, regarding with the determination of dew point by means of the microwave resonators, the overall uncertainty of T_{dp} is mainly due to temperature errors,

5.2.3.2 Methane enhancement factor

The uncertainties of the enhancement factors reported in this work were calculated applying the equation that defines this quantity, (See Eq. 1.2.c). Thus, the individual contributions of these three main sources were evaluated and the overall uncertainties have been already plotted as grey lines in graphs of Fig. 5.2.c.

From the point of view of the uncertainty associated to the determination of pressure measurement, mainly due to its typical deviations was estimated as a relative standard uncertainty equal to $u_r(p) = 0.05 \%$.

On the other hand, the uncertainty related with temperature values had a dominant contribution due to the gas temperature gradient which was detected inside the resonator by two PRTs located on the top and bottom. Such difference was since a few mK up to as much as 0.15 K as a function dependent of the temperature. The final weight of the uncertainty associated by the temperature was of 0.15 K for the experimental test performed at 273.25 K

Finally, the uncertainty caused by the permittivity of dry methane was estimated by the systematic deviation between the results of the preliminary measurements and literature references to the same quantity [S&W91]. These deviations should have

allowed to recalculate and correct the experimental data, but because of large hysteresis shown in dry methane data Fig. 4.2.e and caused by the pressure transmitter used, discourage from implementing a correction procedure. Thus, once assembled a suitable pressure transmitter and after repeating the same kind of tests explained in Section 4.2.3.2, that correction could be applied, so this uncertainty source would be reduced.

5.3. RESULTS UNDER INDUSTRIAL CONDITIONS

5.3.1. INTRODUCTION

In this section, the most relevant raw data given by those instruments compared during the three production stages are reported. Readings from the three instruments were taken for 250 days, during which several extraction and injection processes, intercalated by intermediate shutdowns occurred.

During those months, there were situations in which one or more instruments did not provide correct readings or lost communications happened because of several reasons: updating of pre-commercial communications firmware, failures or resets in digital communications due to micro-cuts of the power supply, instruments and/or humidity probes were sent for calibration, etc. For all that, the study of the relative behaviour of the three instruments simultaneously was not always possible as we would have desired. Despite all, enough data were collected to study the hygrometer behaviour during all sort of process steps of the plant.

Data processing methodology used to simplify the great data volume analyzed and facilitate pertinent evaluation for those objectives aimed are discussed in this section. The criteria applied to the comparison and the influence of correlation between the measurements is also presented and discussed.

In the first place, one of the main features that can be noticed was a daily cyclic behavior exhibited by the three humidity meters throughout the whole test time. This sinusoidal behavior was present regardless production state that were being performed (injection, extraction or shut down) and the measuring quantity (WC or WDP). An example of this phenomenon can be seen in Fig. 5.3.a, which shows readings for 10 days during one shutdown.

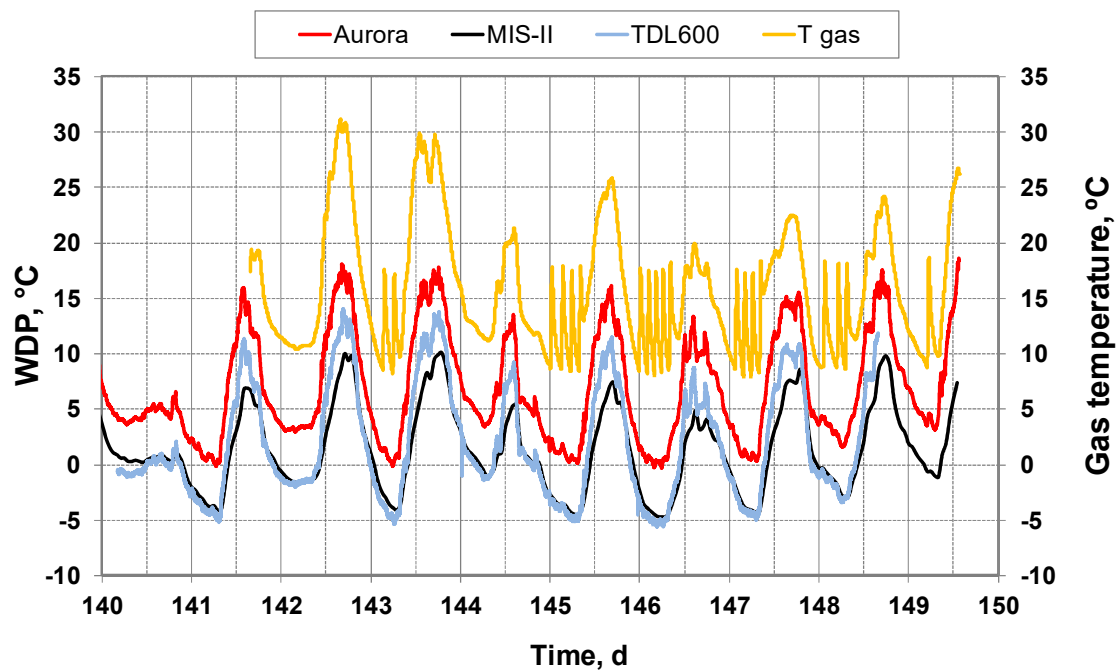


Fig. 5.3.a Representative example of oscillatory behaviour of WDP readings collected by the three hygrometers, compared them with the gas temperature indicated by the PRT of the Aurora and depicted by yellow line.

This kind of behavior is well known in non-insulated and non-thermostated facilities where the oscillations are due to absorption and desorption effects of water molecules that take place between the matrix of NG and the inner walls of any component of plant in contact with the gas.

Studying and understanding the origin and nature of this kind of behavior is very important because it can mean the difference between meet or not national and international safety, commercial or even legal requirements for handling NG. For this reason, sinusoidal signals were analyzed according to two of the most important parameter for this sort of signal such as, the *amplitude* and the *period*:

- *Amplitude*, denoted as A , is defined as the mean value between one maximum and minimum consecutive.

$$A = \frac{V_{max,i} - V_{min,i}}{2} \quad \text{Eq. 5.3.a}$$

- *Period*, denoted by T and expressed by time units, it is the time required by a wave to finish a cycle, that is to say, to reach the same initial point regardless of which was.

$$T = t_{min,i+1} - t_{min,i} \quad \text{Eq. 5.3.b}$$

Looking at the representative example of Fig. 5.3.a, it could be considered that one maximum and minimum happened every day. Due to the effect of the oscillatory readings previously explained and in order to simplify the comparison, it was decided to evaluate the behavior of the humidity instruments at specific points of the cycles, developing a data processing tool be able to identify such daily points and calculate the time elapsed between consecutive maxima and minima and the amplitude. From this study, the dynamic behavior of the industrial facility as well as the humidity measuring instruments would be understood much better, making possible to improve the NG processing stages and the accuracy measure and control of the humidity in the NG.

Once identified all the singular points of the sinusoidal signals by means of the data processing tool we decided work with only one kind of them, these were the possibilities among which we had to decided: use the inflexion points (maxima or minima), or the intermediate section between these (rising or falling). Finally, the minima were considered the best choice for three reasons: firstly, they coincide with the minimum ambient temperature, when the potential risk of condensation effects appearing is highest; secondly, differences among instrument readings are larger at their minima, so if they reach good correlations in the most adverse conditions, better results are ensured during the rest of day; and finally, the minimum values of WC and WDP are more relevant to the optimal operating range found in the NG industry.

The choice of analysing the minima without potential problems of “aliasing” of signals by the instruments is corroborated by analysing the evolution of the differences between instruments as a function of time. A horizontal baseline (constant difference) even in a slowly varying signal as found in the “stable” condition is indicative of high correlation between instrument readings and the fact that they are in equilibrium with the measured quantity. This can be seen from the instrument readings sampled every minute by the TDL sensors and every hour for the MIS-II, during the third injection process depicted in Fig. 5.3.b

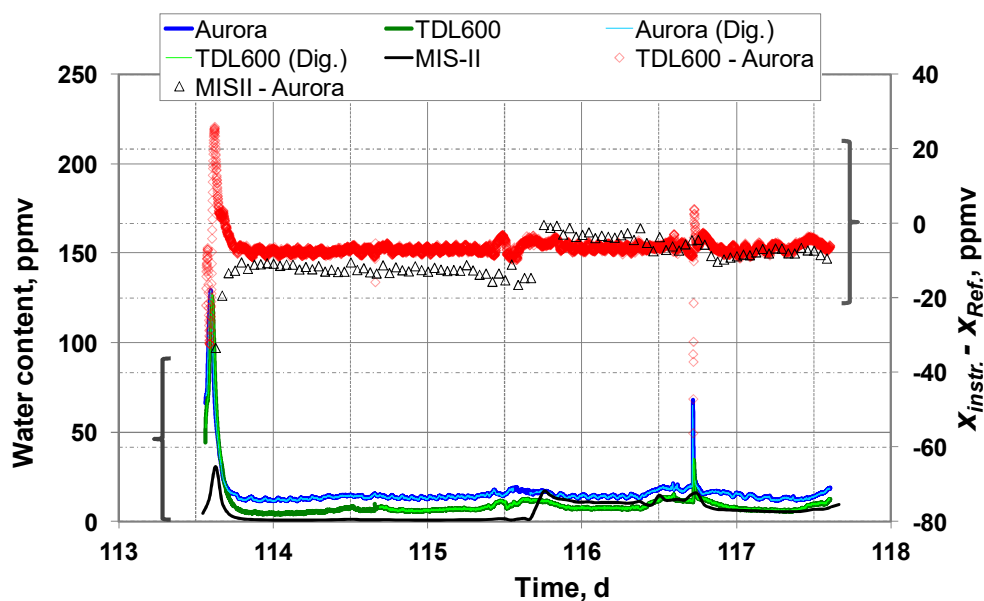


Fig. 5.3.b Instrument readings (lines) during the third injection process, expressed as WC on the left ordinary left, and difference (points) between instrument and reference (Aurora) on the right ordinate axe.

The graph shows the whole process over four days, starting with the change-over from a 10-week shut-down to the injection mode. Within approximately five hours the instruments were stable with respect to each other. Note the MIS-II probe substitution at 4 pm of day 115. The peak around 5 pm the following day, detected by all instruments is due to maintenance on the Aurora.

Besides, the three instruments have been evaluated in two situations: under stable conditions when the humidity levels of NG were relatively stable during several days taking into a count their daily minima, and secondly under transitional conditions, which happened when the production mode of the plant was changed. Both studies were developed in depth in Section 5.3.2 and 5.3.3, respectively.

By the other hand, and as essential element to convert WC to WDP values and vice versa [ISO04], daily composition of NG was analyzed by the chromatographic system described in Section 4.3 during the whole test time. Table 5.1.e shows average composition data, detailed for each of the most relevant production steps which occurred and were analyzed in depth along this chapter. Those periods that were not shown in such table were not considered important because they last few days, so they were not

considered relevant for extracting more information besides of those extracted from the other periods. Each case will be explained below more in detail.

Table 5.3.a Summary of NG average composition data obtained during the whole test time for each most relevant process step studied. In addition, other properties usually used in NG transport and commercial trades, directly linked with the composition, are also shown.

AVERAGE CONCENTRATIONS, % mol/mol							
Chemical Compound	Injection (2013)	Injection (2014)	Extraction 1st time	Extraction 3rd time	Extraction 4th time	Shut down 3rd time	Shut down 4th time
<i>CH₄</i>	89.225	91.193	91.583	91.624	91.756	92.245	91.681
<i>C₂H₆</i>	7.416	5.536	5.562	5.534	5.262	5.098	5.509
<i>C₃H₈</i>	1.551	0.929	0.862	0.900	0.810	0.771	0.897
<i>i-C₄H₁₀</i>	0.186	0.188	0.154	0.155	0.177	0.135	0.155
<i>n-C₄H₁₀</i>	0.273	0.146	0.142	0.153	0.138	0.125	0.153
<i>i-C₅H₁₂</i>	0.034	0.047	0.038	0.038	0.041	0.031	0.038
<i>n-C₅H₁₂</i>	0.026	0.020	0.025	0.026	0.023	0.021	0.022
<i>N₂</i>	0.718	1.097	0.936	0.914	1.014	0.993	0.909
<i>CO₂</i>	0.568	0.830	0.692	0.644	0.762	0.572	0.623
<i>C₆₊</i>	0.003	0.015	0.005	0.011	0.018	0.009	0.013
OTHER PROPERTIES							
REL. DENSITY	0.623	0.610	0.607	0.607	0.606	0.602	0.606
WOBBE INDEX⁶	15.164	14.863	14.917	14.939	14.870	14.900	14.943
HCV	11.968	11.611	11.620	11.638	11.580	11.562	11.637
LCV	10.793	10.463	10.471	10.487	10.434	10.416	10.486

⁶ Wobbe's index (*WI*) is calculated as the ratio between capacity value and the square root of the relative density. It can be expressed as higher or lower *WI* depending on whether *HCV* or *LCV* is used.

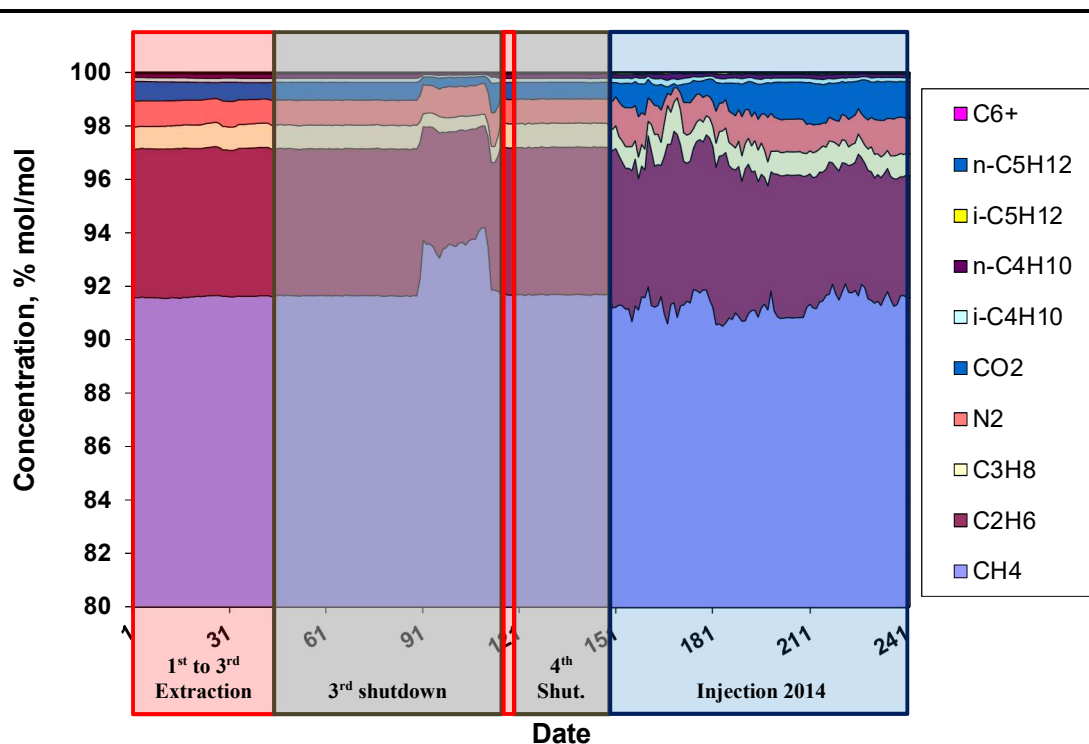


Fig. 5.3.c Variation of daily NG composition along the whole test time. The most relevant periods analyzed in this report have been included according to the production process that was being carried out.

From the Table 5.1.e and Fig. 5.3.c, it can be concluded that methane, ethane, propane, carbon dioxide and nitrogen involved more than the 99 % of total molar composition of NG. Besides having a look to Fig. 5.3.c, it can be quite acceptable to assume that the average compositions for each period studied were values that represent faithfully the actual compositions. Thus, to use those values depicted in Table 5.1.e to simplify conversion process between WC and WDP readings is more than justified.

5.3.2. PERFORMANCE UNDER STABLE CONDITIONS

In this chapter are shown the results obtained for the three hygrometers during the three production stages when readings are relatively steady, that is to say, at the end of any production stage, just before changing the production state of the plant.

5.3.2.1. Extraction

Extraction phase started the 14th of November of 2013, thus starting the new season 2013 - 2014. Since the beginning of extraction process, humidity readings taken by the two instruments mounted were extremely high and quite above of any legal limit (see Fig.

4.3.h). As it was said in Section 4.3.4.1, the old sampling system was completely flooded and both sensors were saturated. For that, we travelled the 1st of December to enable again the whole humidity and chromatography measurement section of Serrablo. This date has been considered in this thesis as our reference time source, and more specifically and to simplify the 01/12/2013 at 00:00:00, because that day we had the certainty to be obtaining real and life humidity readings representative of the NG was being injected in the national distribution grid.

Throughout this comparative study to evaluate the performance of different humidity sensing technologies under real industrial conditions, there were four extraction periods during the season 2013 to 2014 and Table 5.3.b shows the start and end dates of each of them, which were alternated by shut down times.

Table 5.3.b Start and end dates of all extraction periods.

TIME	START DATA		END DATA	
	Data	Day	Data	Day
First	01/12/2013 0:00	0.0	28/12/2013 16:00	27.7
Second	30/12/2013 12:30	29.5	31/12/2013 12:30	30.5
Third	02/01/2014 13:30	32.6	12/01/2014 16:00	42.7
Fourth	24/03/2014 13:30	113.6	28/03/2014 14:30	117.6

a) 1st, 2nd and 3rd time

During the first five days after our startup (see Fig. 5.3.d), there were still humidity levels unusually high, even overtaking the legal limits in the case of international exchanges. That was due to not only the NG sampling line was still being dried by the own NG stream, but also the rest of the plant had not been reached the steady state yet.

During these times, readings belonging to Aurora and MIS-II were taken by hand each 4 h, because of communication parameters were unconfigured and they could not be corrected until our following technical visit, because if we were busy designed and setting up the new sampling system, being this activity much more priority for the productive and safety interests of the Enagás drying plant.

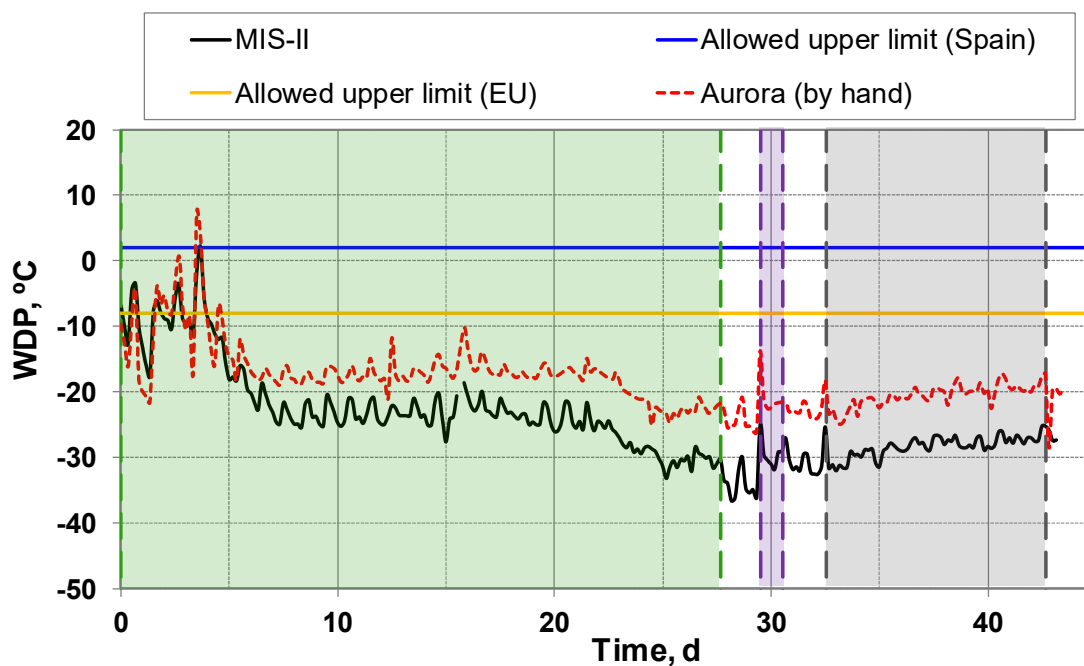


Fig. 5.3.d Real reading taken by hand each 4 h about the first three extraction periods, comparing with the upper limit specified by EEASE-gas for the WDP which establishes that must be lower than -8°C at 7 MPa, or at the maximum line pressure [EAS05].

Fig. 5.3.d shows how after the first five days the humidity levels reached usual and steady humidity levels, never again exceeding the legal limits during the extraction process.

The second extraction period was not studied because spend only one day and it did not add any extra information.

b) 4th time

During the fourth and last extraction time, the three humidity meter had already been mounted and was recording. In Fig. 5.3.f and Fig. 5.3.e can be seen the WDP and WC readings respectively, which were taken using the data acquisition system explained in previously chapters and their respective data acquisition software.

First picture does not show TDL600 readings because initially this humidity analyzer did not came setup from the manufacturer with its own pressure transmitter, so unknowing the real line pressure it was not possible convert WC readings to WDP. By the other hand, the second picture does not show MIS-II readings, because that instruments only read WDP values.

Besides, Michel's recording software was being developed and still was in an initial phase, so it only was able to measure only one variable, in this case the WC. Later, and because of the increasing interest of all parts involved, Michell supplied a software more complex and advanced that was able to measure simultaneously up to three quantities, which usually were WC, WDP and temperature or pressure line.

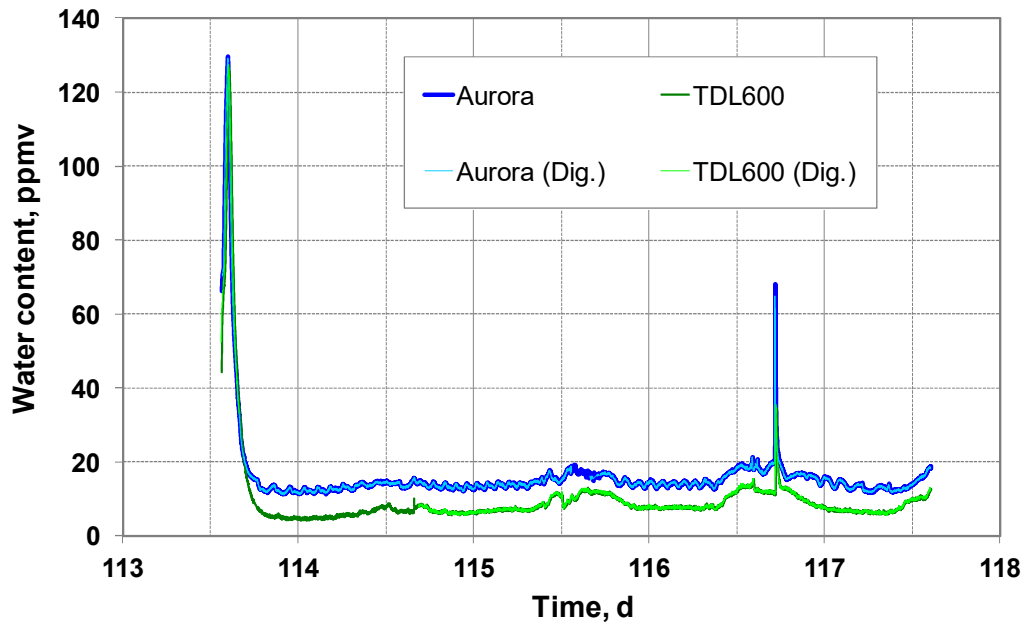


Fig. 5.3.e WC readings given by two spectroscopic humidity analyzers during the last extraction time.

As can be seen in the previously figure, analogue and digital readings are exactly the same for both spectroscopic instruments.

In above figure, it can be seen how humidity levels were initially high but they went down to usual values quickly in less than 6 h. That was a normal behaviour of the plant after any shutdown time.

By the other hand, taking a look at Fig. 5.3.e it can be seen that both spectroscopic instruments had absolutely the same behaviour, keeping a constant difference around 7 ppm_v for a WC lower than 20 ppm_v, which is an ordinary humidity range under optimal working conditions of drying plant.

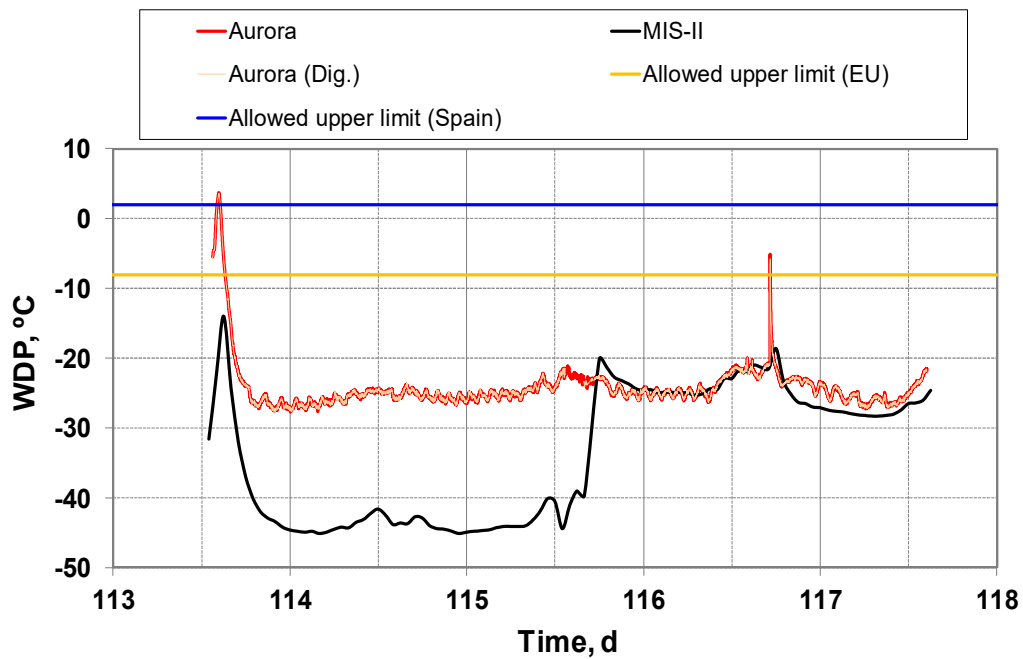


Fig. 5.3.f WDP readings collected during the 4th extraction time.

Another remarkable fact that was seen at the beginning of this period, was the quite difference between readings of both instruments, around 20 °C, despite showing the same behaviour. It was concluded that MIS-II probe could be affected by drift effects, very often in this kind of sensors, and for this reason was giving humidity levels so dry. For that, it was decided to substitute such probe for another spare the day 115 and, despite this new probe was out of calibration period, its readings were much more consistent with Aurora readings than the previously probe.

The detailed analysis of the three most important extraction periods is provided below. For each time, two figure will show the daily minima of WC and WDP with the corresponding uncertainty and lastly, a summary table that indicates the mean and standard deviation given by each instrument.

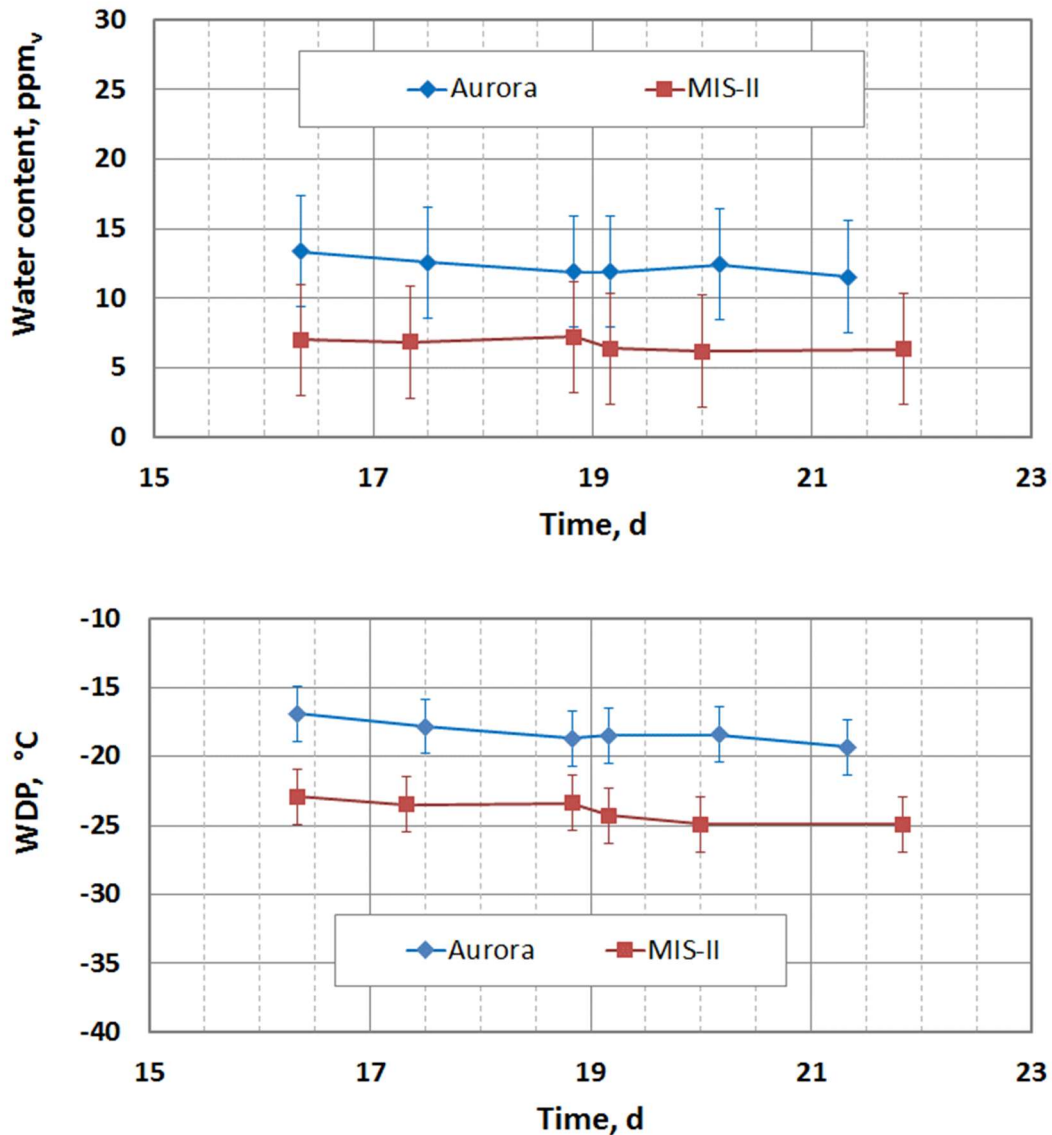
a) First extraction time

Fig. 5.3.g Daily minima of WC and WDP together with their assigned expanded uncertainty during the 1st extraction time.

Below a summary table demonstrates as all readings were pretty stable because the standard deviation of all humidity instruments were lower than their corresponding uncertainties than during the first injection time, so NG humidity was absolutely stable during the whole injection process studied in this thesis.

5. RESULTS

Table 5.3.c Summary of the mean and standard deviations of the readings of WC and WDP in the 1st extraction stage.

PARAMETER		INSTRUMENT		
		AURORA	TDL600	MIS-II
WC, ppm _v	Mean	12.3	---	6.7
	Std. Dev	0.6	---	0.4
WDP, °C	Mean	-18.3	---	-24.0
	Std. Dev	0.8	---	0.8

b) Third extraction time

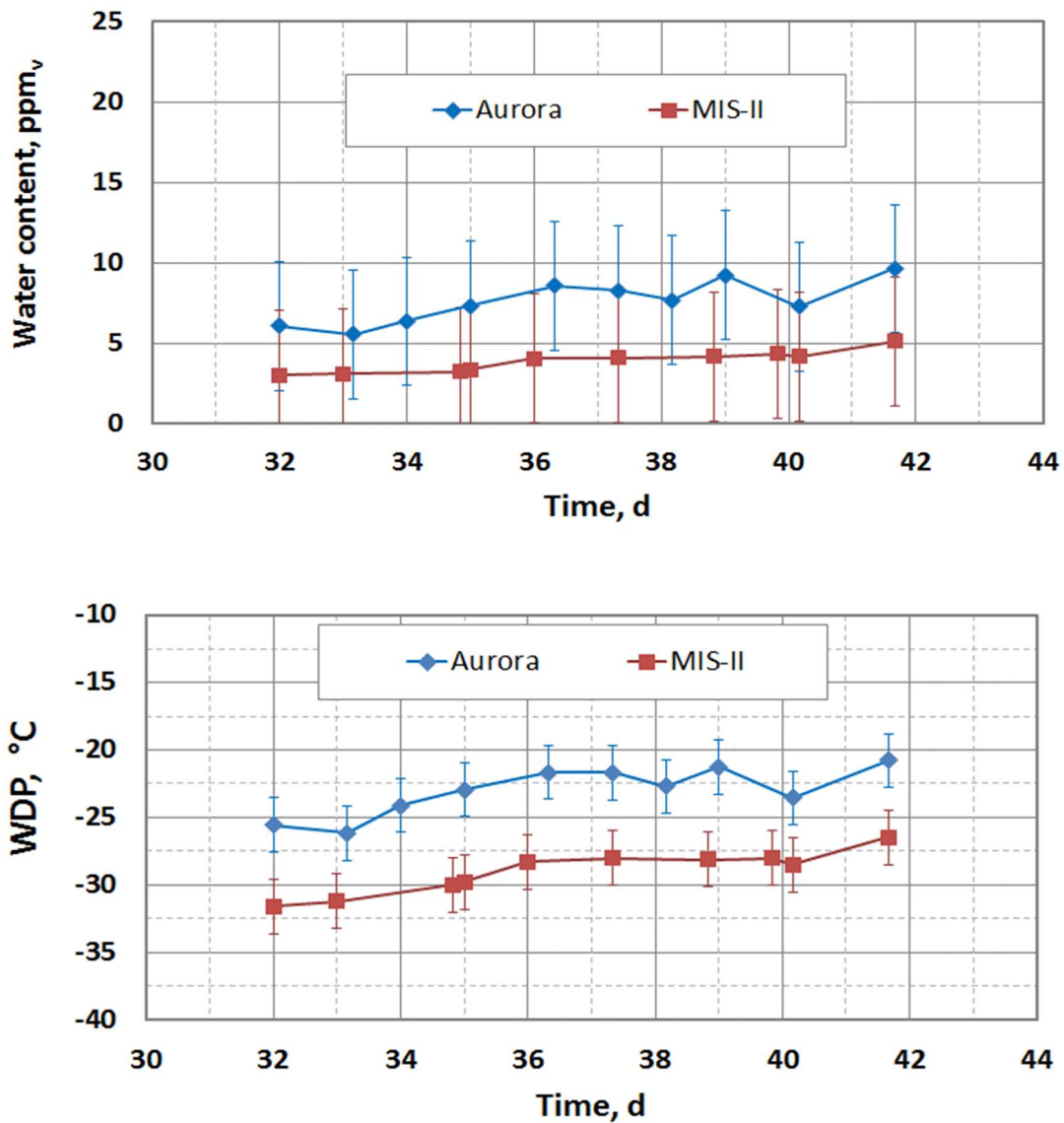


Fig. 5.3.h Daily minima of WC and WDP together with their assigned expanded uncertainty during the 3rd extraction time.

Table 5.3.d Summary of the mean and standard deviations of the readings of WC and WDP in the 3rd extraction stage.

PARAMETER	INSTRUMENT			
	AURORA	TDL600	MIS-II	
WC, ppm _v	Mean	7.6	---	3.9
	Std. Dev	1.3	---	0.7
WDP, °C	Mean	-23.0	---	-29.0
	Std. Dev	1.8	---	1.6

c) Fourth extraction time

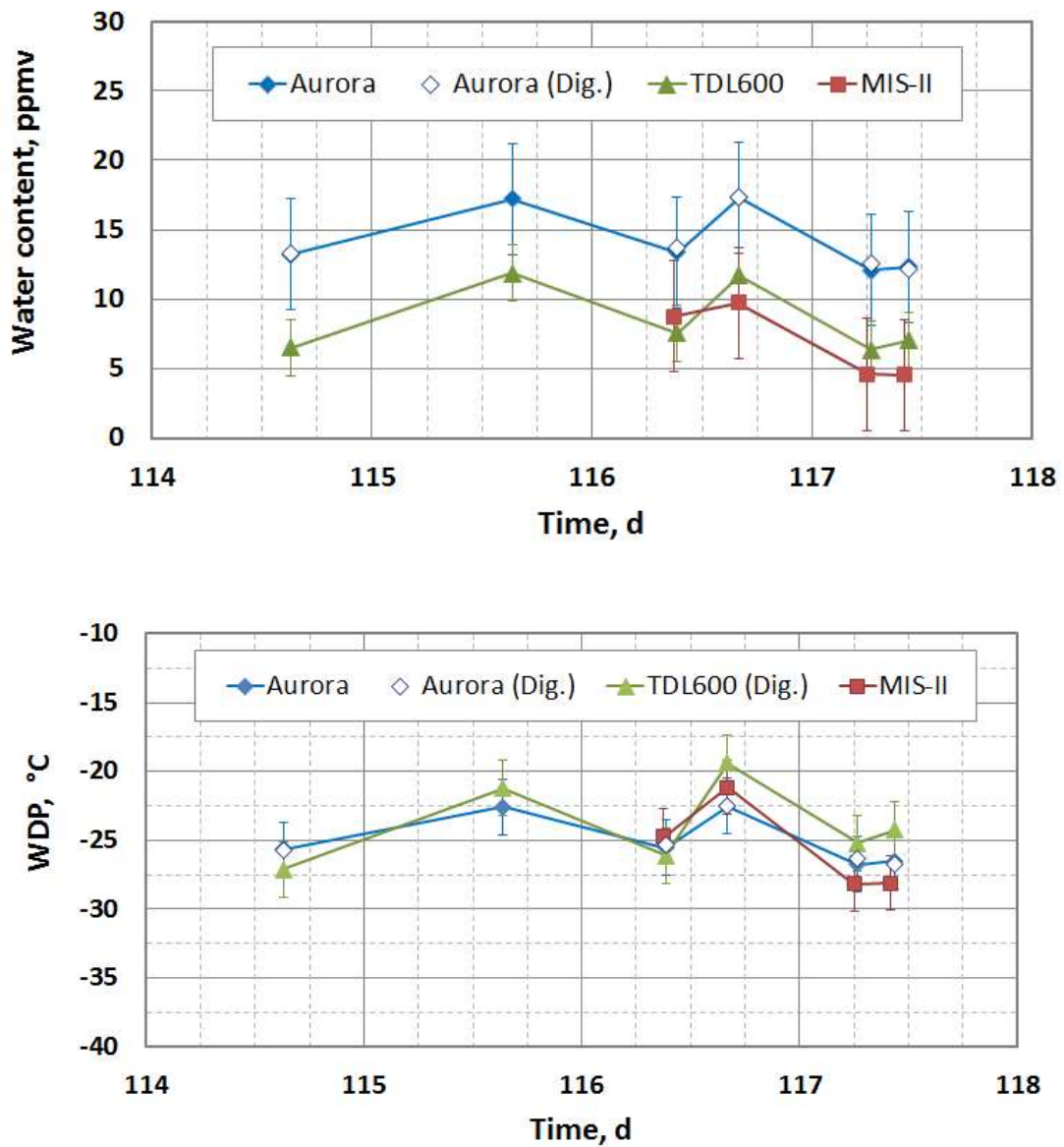


Fig. 5.3.i Daily minima of WC and WDP together with their assigned expanded uncertainty for the three instruments during the 4th extraction time.

As occurred in Fig. 5.3.e, digital and analogue signals of the Aurora are completely identical. The constant offset between the instruments is indicative of the high level of correlation within the measurement uncertainty. The readings of the MIS-II for the first two days were not shown in Fig. 5.3.i because the instrument were substituted for a spare probe and only the readings of the new sensor have been reported. Also, the instrument standard deviations shown in the three tables (Table 5.3.c, Table 5.3.d and Table 5.3.e) were almost identical, and in all cases within the instrument specifications, hence it can be consider right to say that the conditions during these studied periods were steady. It should be noted that at this point of the tests, WDP values for the spectroscopic analyzers had been obtained using a simulated line pressure because the pressure transducers had not been fitted yet.

Table 5.3.e Summary of the mean and standard deviations of the readings of WC and WDP of the three instruments in the 4th extraction stage

PARAMETER		INSTRUMENT		
		AURORA	TDL600	MIS-II
WC, ppm _v	Mean	14.3	8.5	6.9
	Std. Dev	2.4	2.6	2.7
WDP, °C	Mean	-24.9	-23.9	-25.5
	Std. Dev	1.9	3.0	3.3

5.3.2.2. Shutdown

In this section, it was done the same detailed review but in this case for the most important shutdown times. Firstly, in Table 5.3.f are shown all shutdown times recorded during this research.

Table 5.3.f Start and end data of all shutdown periods recorded.

TIME	START DATA		END DATA	
	Date	Time, d	Date	Time, d
First	28/12/2013 16:00:00	27.7	30/12/2013 12:30:00	29.5
Second	31/12/2013 12:30:00	30.5	02/01/2014 13:30:00	32.6
Third	12/01/2014 16:00:00	42.7	24/03/2014 13:30:00	113.6
Fourth	28/03/2014 14:30:00	117.6	29/04/2014 15:45:00	149.7

As the first two shutdown times were less than three days, they were not considered interesting from the point of view to get additional information of those extracted from the other two shutdown periods. For that and from this point on the report, it is going to talk only of two shutdown times.

Coming up next, it is going to show and explain all real readings gathered in both times and, finally it is going to study the relative behavior during the steadiest conditions.

a) Third shutdown time

Below figure depicts WC reading for the third shutdown period:

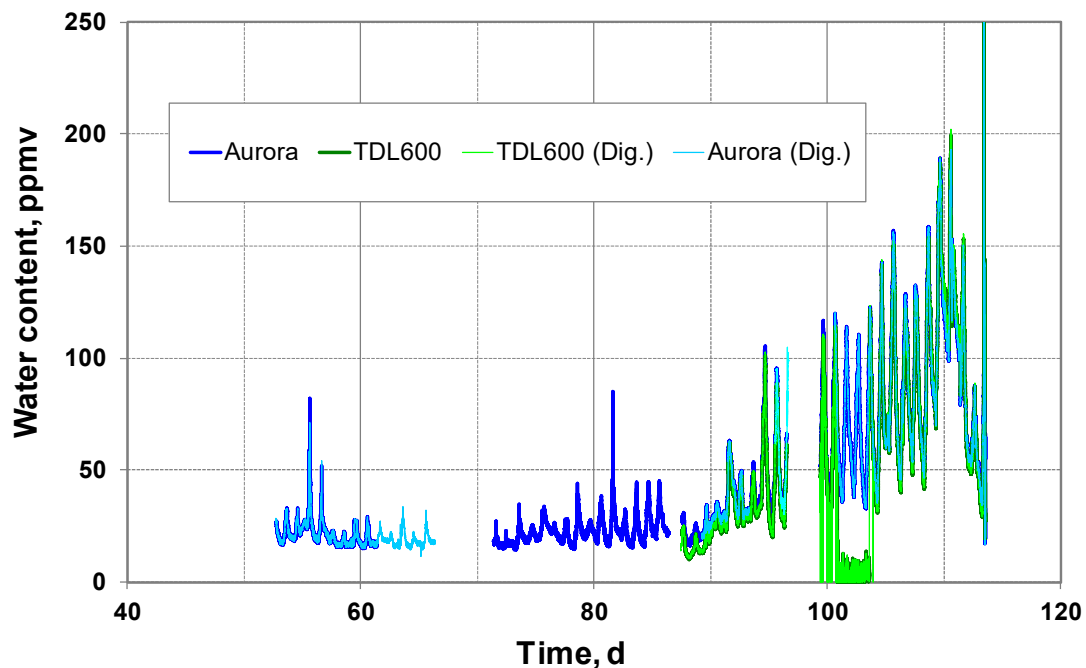


Fig. 5.3.j WC readings collected during the 3rd shutdown time analyzed.

As can be seen in figure above, in this case the amplitudes of daily oscillations were quite higher than for all extraction times, already analyzed above. This wave behaviour was uninterrupted and the amplitude of both signals were in fairly correlated with each other. Besides, it can be also noticed when the TDL600 was installed and turned on, 87 day, because from that day analogue and digital WC output were recorded.

By the other hand, another effect clearly identified in Fig. 5.3.j are the numerous discontinuities that Aurora' signals suffered. That was due to the micro-power cuts that happened in the plant, which reset the factory defaults for the RS-485 communication parameters, losing remote communication of the Aurora. This fact was a great problem that happened along the whole study, so logging and subsequent data analysis was really

5. RESULTS

complicated. This instrument, which was being already used in diverse applications in field distributed along several countries, does not really have shown this communication problems, because it is a basic requirement of any equipment installed outdoors and that should not be subject to a continuous maintenance and control. However, in this case the Aurora that provided GE was a demo that had not yet implemented this improvement. To solve this setback, staff of GE traveled a couple of times to install the latest version of the firmware of Aurora to solve this problem, however it was not possible to install it, so it remained until the end.

Other information extracted from the figure above was the great overlap between analogue and digital outputs for both spectroscopic instruments during the whole time an exception of 99 day to 105 day for the TDL600. The reason of such disagreement was set a lapse time of readings of 10 sec, because the initial software version, which was provided by Michell, was only able to work with lapse times longer than 1 min. For that, communication parameters failed and readings given during this time were exceptionally down and not real.

Following with the comparative between both spectroscopic instruments, it can be noticed that readings recorded by the Aurora were always slightly higher than those given by the TDL600, which was also confirmed in Table 5.3.g. In Fig. 5.3.k WDP readings collected for this period are shown.

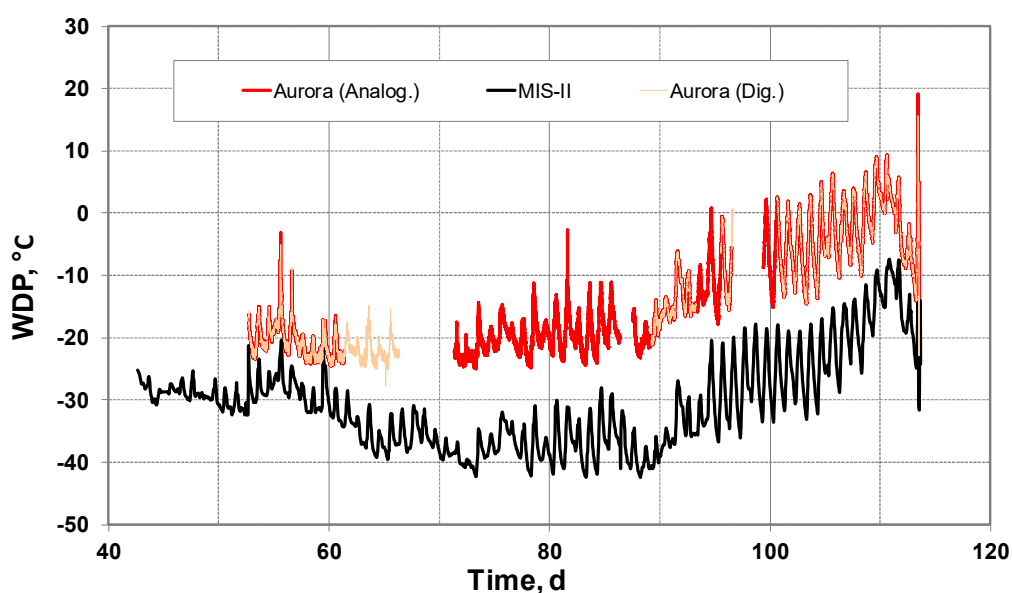


Fig. 5.3.k WDP readings collected during the 3rd shutdown time analyzed.

Figure above shows the same effects already mentioned for WC signals: bigger oscillations than during injection process and interrupted signals. Regarding the different cuts produced in the analogue signal of the Aurora, these were due to human faults of unknown origin when the Agilent registration software were used by the own staff of the plant, despite being a measurement system widely used by INTA and not give loss or stop data logging problems.

Another effect that can be seen in both figures was the progressive increase of the NG humidity levels that started to occur since 90 day and lasted until the end of the period.

b) Fourth shutdown time

Lastly, in Fig. 5.3.l and Fig. 5.3.m are shown all WC and WDP readings, respectively, logged during the last shutdown time.

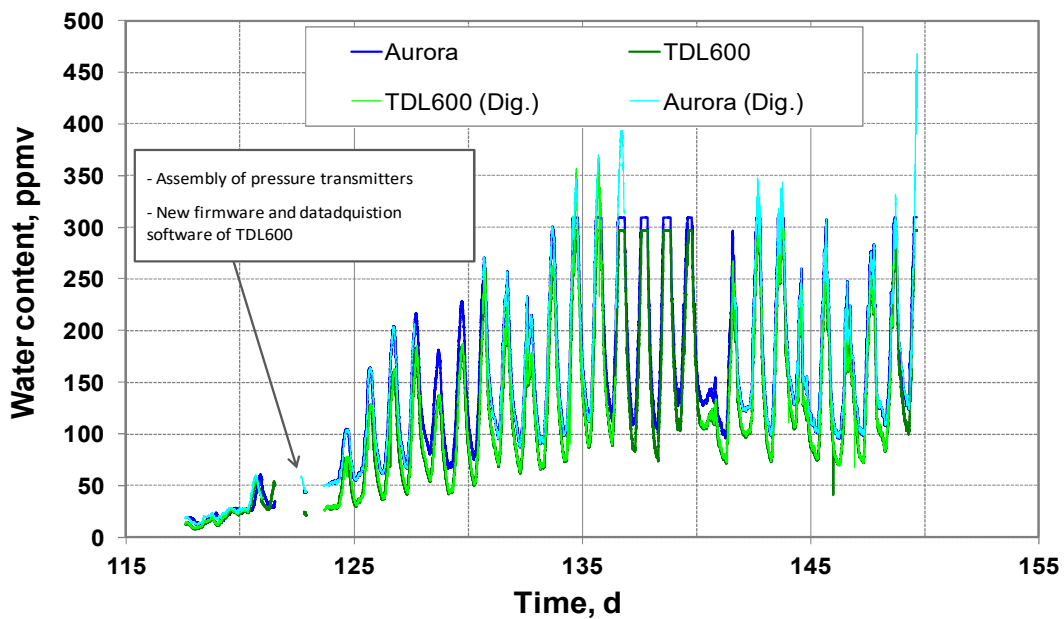


Fig. 5.3.l WC readings collected during the 4th shutdown time analyzed.

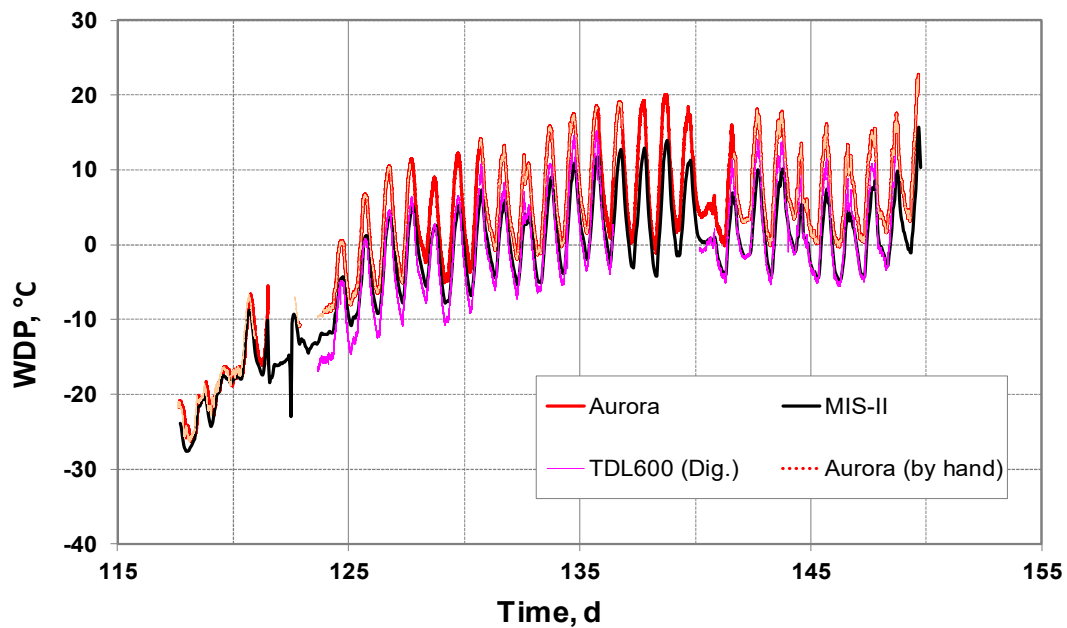


Fig. 5.3.m WDP readings collected during the 4th shutdown time analyzed.

Both graphs show as the daily maximum and minimum values increase progressively during the first 18 days from which they were stabilized.

In addition, it can be seen as the readings of TDL600 began to be around 20 ppmv lower than the other spectroscopic instrument, with which had been kept a great agreement in the previously times. This fact happened just later the pressure transmitter of Michell had been assembled to be able to measure the actual WDP readings and updating of the new firmware for this instrument. All tasks performed those days were carried out by us under directly on-site supervision by Michell staff who traveled from England to ensure the perfect yield of their humidity instrument. However, any activity performed those days would not be related to such both activities, so would not justified that difference between readings.

By the other hand, during this second shutdown time it can be seen a couple of failures with the Aurora connections during the days 127 to 131 and since 136 to 142.

Following, the same detailed analysis used for extraction times, using the analysis of daily minima of WC and WDP has been developed, including summary table that indicates the mean and standard deviation given by the three humidity sensors for both periods.

a) Third shutdown time

Due to the high oscillations, several interruptions signals and the stabilization times for all signals, to find a time slot really representative of steady conditions of the plant during this shutdown time was quite difficult. From the study of daily minima, which can be seen in the two graphs of

Fig. 5.3.n, the steadiest time occurred during the first two weeks, but the TDL600 had not been installed yet, and besides these values were presumably direct consequence from the extraction time. Thus, it was decided to consider the whole period to analyze the behaviour of the three humidity measurers.

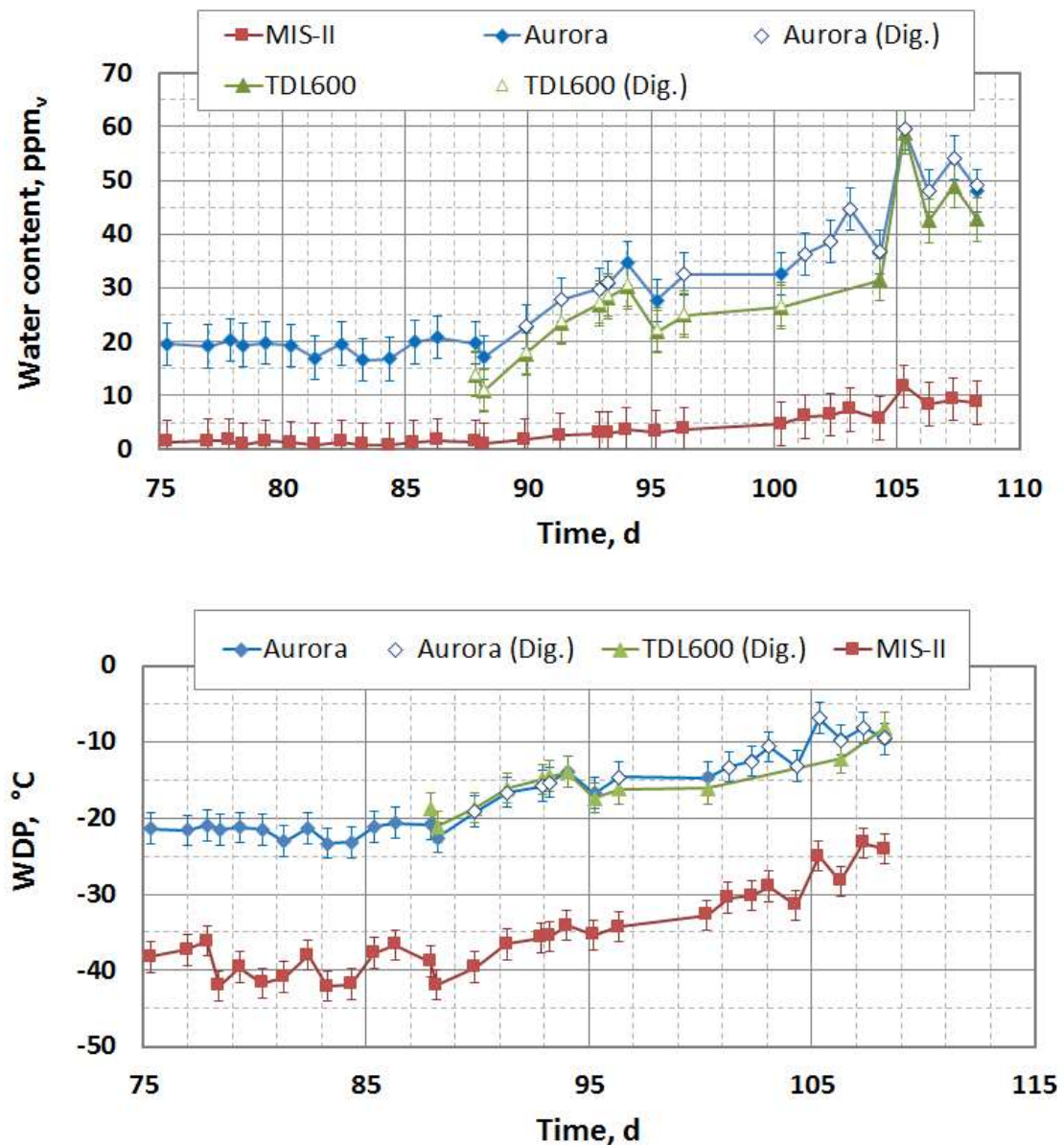


Fig. 5.3.n Daily minima of WC and WBP and assigned uncertainty for the third shutdown period.

5. RESULTS

As it was already explained from Fig. 5.3.j, since 99 day to 105 day the TDL600 had a failure and was recorded wrong data practically during all time. For this reason, there were only a couple of daily minima valid in those days.

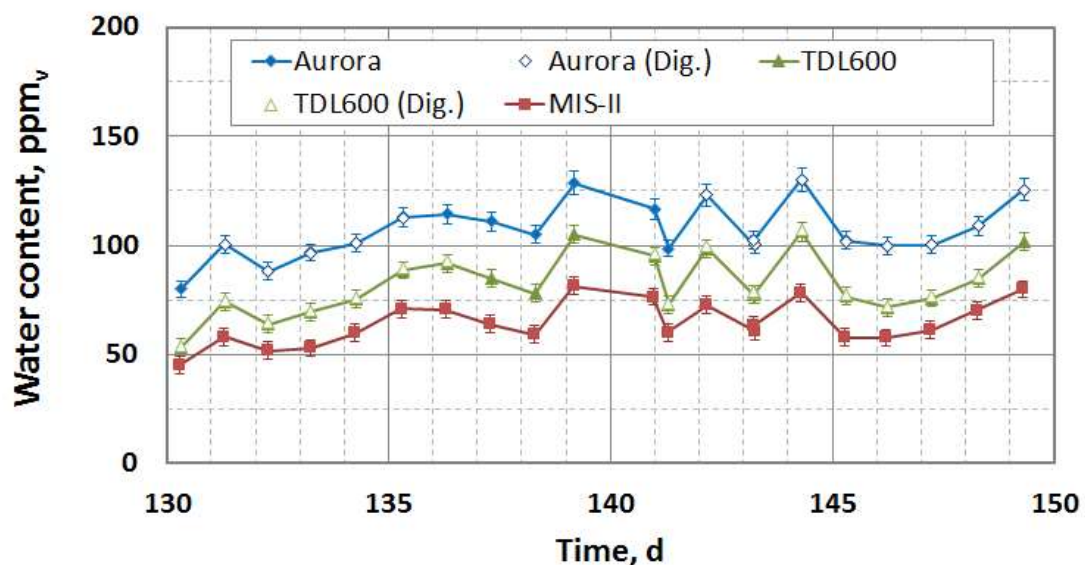
Table 5.3.g Means and standard deviations of the readings of WC and WDP for the three instruments during the 3rd shutdown period.

PARAMETER		INSTRUMENT		
		AURORA	TDL600	MIS-II
WC, ppm _v	Mean	29.0	29.9	3.6
	Std. Dev	12.2	13.2	3
WDP, °C	Mean	-17.2	-15.7	-35.3
	Std. Dev	5	3.4	5.5

As can be seen from Table 5.3.g, the standard deviations from this period were disproportionate regarding with any extraction time previously commented, so the instability of the period was more than evident.

b) Fourth shutdown time

Due to the same problems that the previously case: high oscillations, interruptions signals and big stabilization times; and watching Fig. 5.3.l or Fig. 5.3.m. For all of that, it was decided to analyze this period for the steadiest timeslot which corresponds between 130 and 150 day.



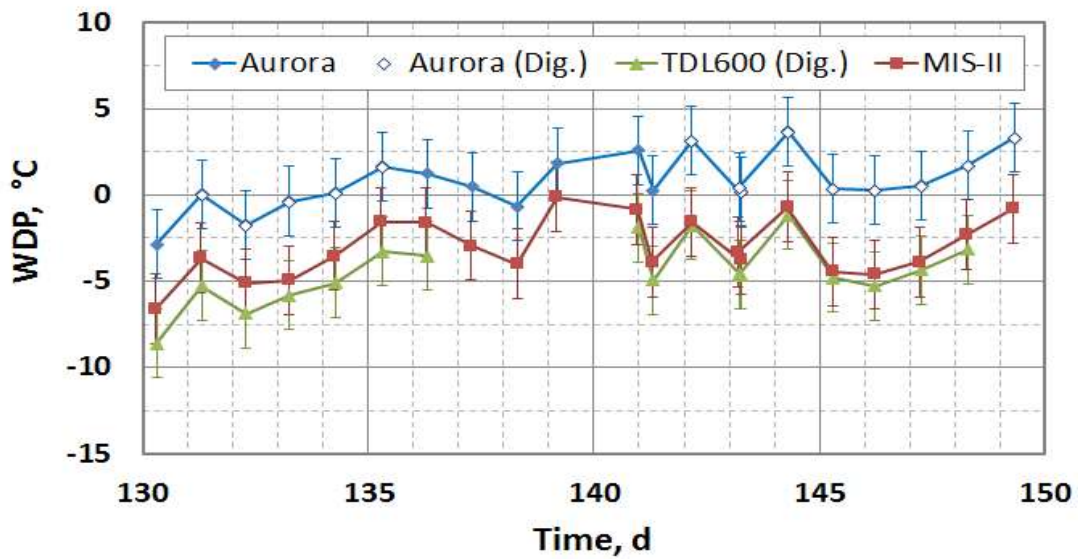


Fig. 5.3.o Daily minima of WC and WDP and assigned uncertainty for the 4th shutdown period.

As can be seen the measured WDP for the three instruments exhibit an identical behaviour with a constant offset, and identical standard deviations during the shutdown period. The trend in the series shows a gradual increase in humidity at a rate of approximately 0.5 °C/day. Although the assigned expanded uncertainty of the instruments is larger than the increase, it can be seen clearly that they all are capable of detecting the change in a similar fashion. This is indicative of an improved performance with respect to the manufacturers' specification for WDP above -10 °C. Following, the summary table shows the means and standard deviations obtained for the three instruments.

Table 5.3.h Means and standard deviations of the readings of WC and WDP for the three instruments during the 4th shutdown time.

PARAMETER		INSTRUMENT		
		AURORA	TDL600	MIS-II
WC, ppm _v	Mean	107	80.5	64.4
	Std. Dev	12.9	13.4	9.8
WDP, °C	Mean	0.8	-4.4	-3.1
	Std. Dev	1.6	1.9	1.7

As can be seen from the above table, the standard deviations of WC readings were really high for the three instruments, but nevertheless were quite acceptable for WDP readings. Therefore, the big deviations in WC readings did not seem to indicate a low performance of the hygrometers or a lack of stability of the plant, but a potential secondary effect due to the high humidity levels reached during long shutdown times and, very probably also drifted to the adsorption/desorption cycles.

Other of the great difference regarding with the injection times, and easily appreciable in figure depicted above, was the absence of stability in all signals collected during the two shutdown times analyzed. From the study of daily minima and comparing the summary standard deviation of all signals in the Table 5.3.g and Table 5.3.h with their corresponding for injection times, it can be notices as they were much higher than those values given during injection. That was the reason by which was considered appropriated to performing one more detail study about the behavior of humidity instrument during transitional conditions, which occurred before and later of shutdown times (Section 5.3.3).

5.3.2.3. Injection

The injection phase of 2014 season began on 29th of April at 15:45 (149 d) and continued until the end of this comparative study, that is, the 31st of July at 13:00 (242 d).

In the following charts (Fig. 5.3.p and Fig. 5.3.q) are depicted all WDP and WC readings during the three months in which the plant had been injecting GN to the UGS. As can be seen in both figures, humidity levels were very high during the first five days, but at the end of that week humidity values started to decline until reaching usual production values.

The fifth day a test was performed to verify that effectively, the spectroscopic moisture meters were really measuring the humidity of NG that was arriving to Serrablo facilities. This checking test is explained in detail in Section 5.3.4.

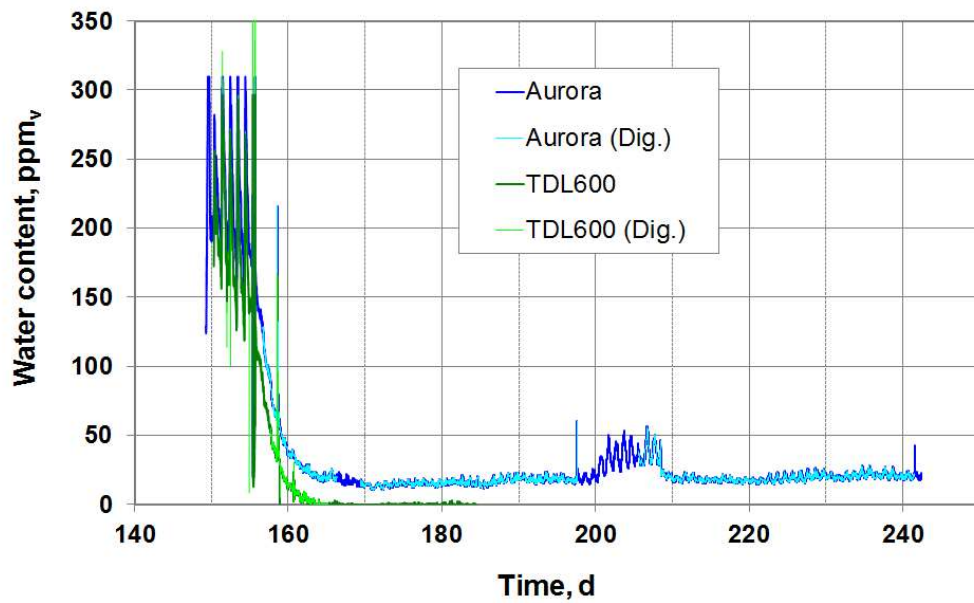


Fig. 5.3.p WC readings logged during the injection time.

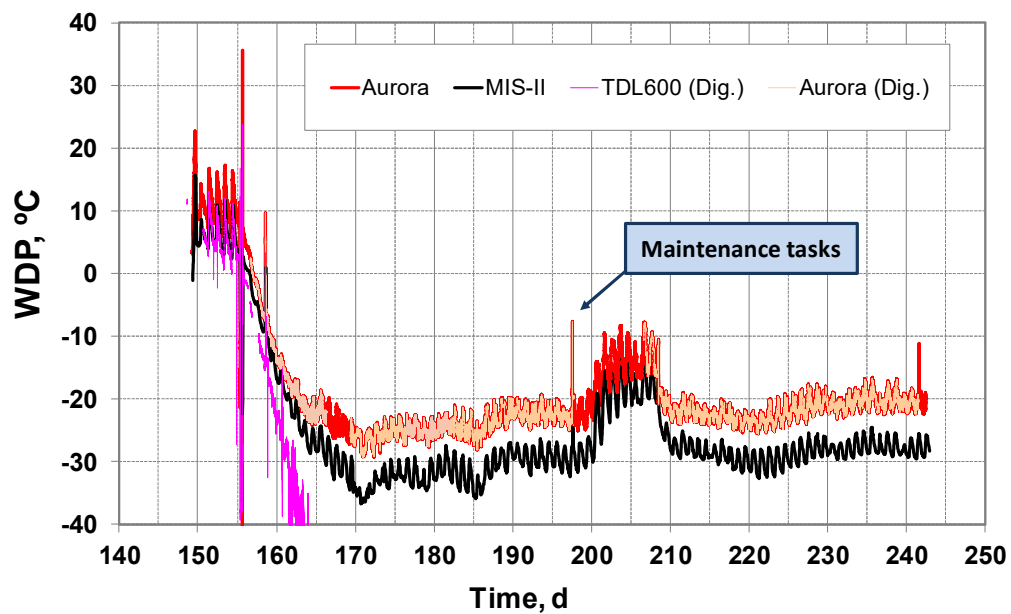


Fig. 5.3.q WDP reading collected during the injection time.

The low WC readings provided by the TDL600 with regard to the Aurora, which had already been appeared in the last final shutdown period, were still maintained during the injection phase. Once state conditions were reached during the injection process, the Aurora had a WC average of 17 ppm_v, whilst the TDL600 readings were zero or practically zero, so keeping the distance of approx. 20 ppm_v below the Aurora signal.

Initially, it was thought that the NG could actually arrived very dry to Serrablo (around 2 ppmv and 3 ppmv) and that could be within specifications of both instruments. However, thanks to the diagnostic files sent by INTA to Michell engineers, they found that their equipment was having some sort of problem and therefore had to be returned to the factory to identify and correct it. The 184 day, TDL600 was switched off, disassembled and packaged to be returned to the factory for checking. For this reason, the behaviour of TDL600 could not be analyzed in injection phase in this thesis.

There was a peak of humidity detected by both instruments the 197 day, and three days later there was an increase of humidity that lasted approximately one week more. This phenomenon was attributed to a periodic cleaning task performed in some point located upstream in national grid. This maintenance task consists of introducing inside the pipes a kind of pistons, called pigs, which are equipped with brushes and blades to remove potential hydrocarbon hydrates or condensates or they are also outfitted with monitoring systems to inspect the inside of the pipes [STA05].

As can be seen in Fig. 5.3.p Fig. 5.3.q, between the 200 and 210 days there were an increase of humidity, equally detected by both instruments and that was due to the maintenance tasks previously described. Because of these ten days were completely affected by such effect, they were not considered inside of injection time, therefore the following humidity data series from 210 day were analyzed as a new injection, carrying out a more detailed study during injection phase by means of the study of daily minima too.

a) First injection time

Fig. 5.3.r shows results obtained during the first injection phase by the MIS-II and the Aurora. As, it can be seen, both moisture instruments had a great stability for both humidity signals during the whole test time analyzed.

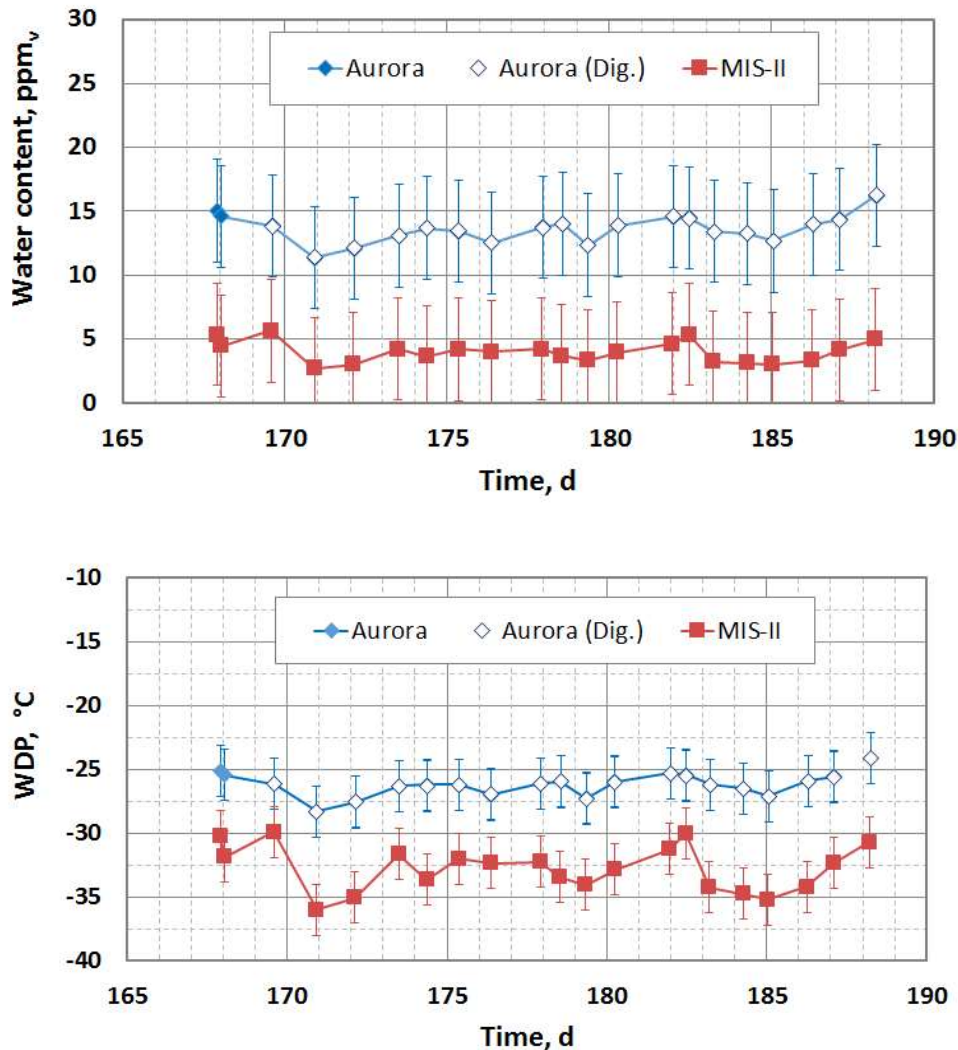


Fig. 5.3.r Daily minima of WC and WDP and their correspondent assigned uncertainty for the MIS-II (analogue signal) and Aurora (digital and analogue) during the first injection phase.

Table 5.3.i summarizes the means and deviations of WC and WDP signals for both humidity instruments. The great stability shown by all data series in the previously figures can be also appreciated glancing any standard deviations data, which were always lower than the uncertainty given by any instrument, thus humidity levels during this time can be considered quite stable.

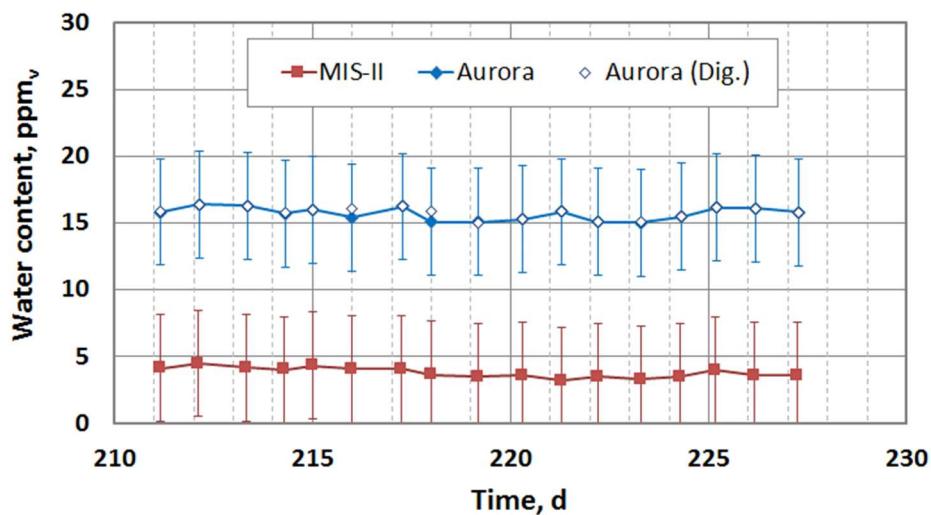
Table 5.3.i Means and standard deviations of the WDP readings for the MIS-II and Aurora analogue outputs during the 1st injection phase.

PARAMETER		INSTRUMENT		
		AURORA	TDL600	MIS-II
WC, ppm _v	Mean	13.9	---	4.1
	Std. Dev	1.4	---	0.9
WDP, °C	Mean	-25.9	---	-32.6
	Std. Dev	1.16	---	1.9

WDP values shown in Fig. 5.3.r had a virtually constant offset with the MIS-II reading drier. When the WC readings were analyzed, the same behaviour was found with an offset of 13 ppmv as is demonstrated in the table above.

b) Second injection time

Making the same study for the second injection time, the high stability of the two instruments both for WC and WDP data series is more than evident according with Fig. 5.3.s.



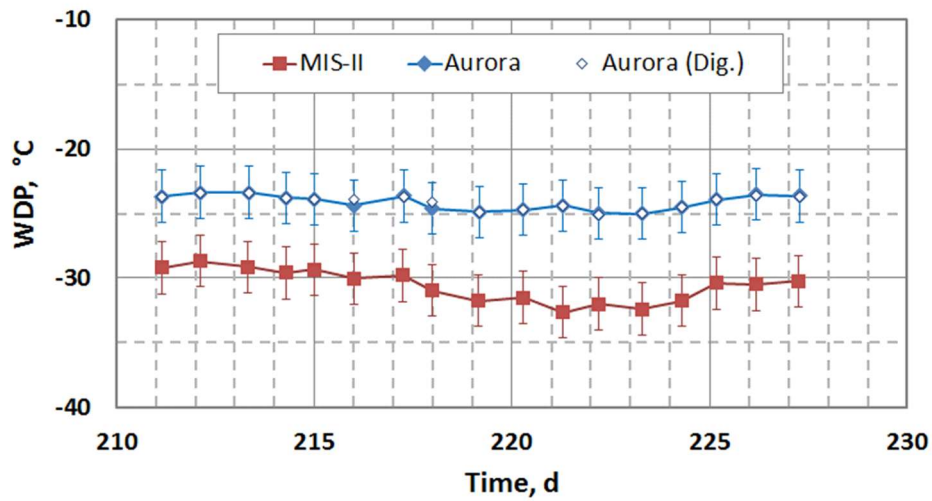


Fig. 5.3.s Daily minima of WC and WDP and their correspondent assigned uncertainty for the MIS-II (analogue signal) and Aurora (digital and analogue) during the second injection phase.

Making the same summary table performed in the previously periods, it can be demonstrated as all readings were even more stable than during the first injection time, so NG humidity was absolutely stable during the whole injection process studied in this thesis.

Table 5.3.j Means and standard deviations of the WDP readings for the MIS-II and Aurora analogue outputs during the 2nd injection phase.

PARAMETER		INSTRUMENT		
		AURORA	TDL600	MIS-II
WC, ppm _v	Mean	15.7	---	3.8
	Std. Dev	0.5	---	0.4
WDP, °C	Mean	-24.1	---	-30.6
	Std. Dev	0.6	---	1.2

5.3.2.4. Summary and discussion

To compare the three instruments and to be able to determine the correlation level among them, the acceptance criterion given by Eq. 5.3.c was used. It is based on calculating the maximum permissible limits from the readings given by the instrument used as reference. After that, if the readings from the instrument under study were within the range given by these limits, both instrument were considered correlated. The accepted range was calculated from the expanded uncertainty of measurement, obtained from the

root square summation of the individual standard uncertainties, multiplied by a coverage factor, $k = 2$, for a confidence level of approximately 95 %.

$$x_{instr} = x_{ref} \pm 2 \cdot \sqrt{u_{instr}^2 + u_{ref}^2 + u_{calc}^2} \quad \text{Eq. 5.3.c}$$

where x is the measured quantity (WC or WDP), u , is the *standard uncertainty* of x , and the subscripts *ref* and *instr* refer to the instrument used as reference or the instrument under study, respectively. Finally, the last term inside the root, u_{calc} , is the standard uncertainty due to the equivalence between WC and WDP and vice versa, calculated according to the model used by GERG [O&A01]. In such reference, the budget uncertainty of WC was expressed in $\text{mg}\cdot\text{Nm}^{-3}$ units, however in this thesis the WC has been always referred as ppm_v units. For that, the original equations were divided by 1.245, which is the conversion factor at standard conditions (101325 Pa and 273.15 K). Thus, the resulting final equations, using the WC as ppm_v , for the standard uncertainty because of the conversion between WC and WDP, u_{calc} , are summarized in Eq. 5.3.d and Eq. 5.3.e, depending on the humidity range:

- If WC is lower than $100 \text{ mg}\cdot\text{Nm}^{-3}$ (80.3 ppm_v) then:

$$U_{calc}(\text{ppm}_v) = \pm (2.7 + 0.134 \cdot WC) \quad \text{Eq. 5.3.d}$$

- By contrast, if $WC \geq 100 \text{ mg}\cdot\text{Nm}^{-3}$

$$U_{calc}(\text{ppm}_v) = \pm (14.4 + 0.017 \cdot WC) \quad \text{Eq. 5.3.e}$$

For the case of the uncertainty calculation of WDP the following was applied:

$$U_{calc}(^{\circ}\text{C}) = \pm 2.0 \quad \text{Eq. 5.3.f}$$

As can be seen the uncertainty assessment performed here is the same described in the first experimental section, but deleting the uncertainty due to the humidity generation system, $u_{generation}$, because in this case there were not such system. In this case, it was possible to carry out a simple uncertainty budget because the number of hygrometers was much lower, and the complex uncertainty component due to unit conversion, u_{calc} , was fairly simplified.

The study was performed for both WC and WDP readings given by the humidity analyzers. The instruments used as reference were two: the MIS-II, because it was the only Al₂O₃ capacitive sensor; and the TDL600 because it was the latest instrument added at this work. Table 5.3.k summarizes the acceptance criteria obtained for WC in each process phase.

For the case of WDP the acceptance criterion was 5.7 °C along the whole range, except during the 4th extraction time, because the TDL600 was only reading in WC and these values had to be converted to WDP, hence the criterion increased up to 7 °C.

Table 5.3.k Summary of acceptance criteria for the comparison of the readings of WC in the production stages reported.

WC, ppm _v	EXTRACTION			SHUT DOWN		INJECTION	
	1 st	3 rd	4 th	3 rd	4 th	1 st	2 nd
$ x_{\text{Aurora}} - x_{\text{MIS-II}} \leq$	13	13	14	12 up to 14	21 up to 35	13	15
$ x_{\text{TDL600}} - x_{\text{MIS-II}} \leq$	---	---	12	12 up to 14	21 up to 35	---	---
$ x_{\text{Aurora}} - x_{\text{TDL600}} \leq$	---	---	12	11	12 up to 14	---	---

As mentioned previously, the TDL600 was only compared in the last extraction period as it coincided with its installation. It was not evaluated during the two injection stages as it had been returned to the factory to implement the latest updates developed.

The previous sections have illustrated examples of results obtained during the three phases (extraction, shutdown and injection). Below, Table 5.3.l summarizes the level of agreement among the readings of the three instruments, according with the criteria described, both WC and WDP values.

5. RESULTS

Table 5.3.1 Summary of the correlation level both WC and WDP for the three instruments during the extraction, shutdown and injection phases.

	WATER CONTENT, ppm _v			WATER DEW POINT, °C		
	Mean	Std. Dev.	% accepted values	Mean	Std. Dev.	% accepted values
EXTRACTION						
First time						
χ Aurora - χ MIS-II	5.6	0.6	100	5.7	0.6	50
Third time						
χ Aurora - χ MIS-II	3.7	0.8	100	6.0	0.7	40
Fourth time						
χ Aurora - χ MIS-II	6.9	1.5	100	0.2	1.5	100
χ TDL600 - χ MIS-II	1.3	1.7	100	1.8	2.3	100
χ Aurora - χ TDL600	5.7	0.5	100	1.1	1.7	100
SHUTDOWN						
Third time						
χ Aurora - χ MIS-II	25.4	9.2	0	18.1	1.7	0
χ TDL600 - χ MIS-II	19.6	5.4	20	19.6	1.6	0
χ Aurora - χ TDL600	4.9	1.7	100	0.1	1.4	100
Fourth time						
χ Aurora - χ MIS-II	42.6	4.4	0	3.8	0.7	100
χ TDL600 - χ MIS-II	17.7	4.8	100	-1.1	0.6	100
χ Aurora - χ TDL600	24.2	1.5	0	4.3	1.7	95
INJECTION						
First time						
χ Aurora - χ MIS-II	9.8	0.9	100	6.6	1.2	22
Second time						
χ Aurora - χ MIS-II	11.9	0.4	100	6.5	0.8	18

The results obtained in Table 5.3.1 are discussed as follows for the three production phases.

a) Extraction

During the first and third extraction periods, 100 % of the WC readings given by the Aurora and the MIS-II met the established acceptance criteria. However, the percentage of agreement in WDP readings was almost the half, despite of the means of

the differences between the Aurora and the MIS-II was practically the same than the acceptance criterion, 5.7 °C. This fact, which happened during the first three periods for WDP readings, can be attributed to the following factors:

- The line pressure used to the Aurora to do the conversion was a fixed simulated value, so it could differ from the actual value measured by the MIS-II installed at the full line pressure. This was corroborated by recalculating the data using the MIS-II pressure values. In subsequent measurements this was not a problem because each manufacturer provided pressure sensors and the instruments were reconfigured to use the actual pressure readings.
- The first MIS-II probe that had been recording during the first three extraction periods had undergone an excessive drift, thus it was reading too dry in comparison with the Aurora. When this probe was substituted for other spare, the correlation among all instrument was practically perfect, as can be seen in the fourth period.

During the fourth extraction period, the performance of the spectroscopic analyzers at the humidity levels achieved during the extraction phase (4 ppm_v to 20 ppm_v, and -29 °C to -19 °C) exhibit an identical behaviour and agreement for 100 % of values. At the same time, Al₂O₃ capacitive prove (MIS-II) was completely correlated with both spectroscopic instruments.

According with all of this, during this extraction period the degree of confidence regarding with the NG humidity level that was being supplied to the national grid was very high, so the safety and quality of the NG was guaranteed at all time.

b) Shutdown

During both shutdown periods, the percentage of acceptable values was more variable due to, among other factors, the large fluctuations. Fact corroborated by the high standard deviations of the differences between the three instruments.

Looking at Fig. 5.3.j and comparing it with Table 5.3.1, it can deduce that the level of agreement between the spectroscopic instruments was excellent, achieving the acceptance criteria in 100 % of the cases (no taking into account the time during which TDL600 was reading exceptionally dry due to a small failure in recording software).

By contrast in the fourth period and hereinafter, the TDL600 had only very good level of agreement with the MIS-II, instead of showing the same behaviour that the other spectroscopic instruments. That inflection point happened starting with the software update and assembling of the pressure transmitter for TDL600. Whether these facts are directly related or not, we could confirm. But certainly, since that moment TDL600 gave readings suspiciously dry (see Fig. 5.3.1). When the manufacturer beard out malfunction of its instrument, TDL600 was shipped to the factory to check and solve the problem.

c) Injection

As it has been already explained, the TDL600 was not during production phase, so we could only compare the other two hygrometers.

During the injection times the percentage of acceptable values was 100 % for WC readings, so their behaviour of the Aurora and MIS-II was absolutely identical. However, the agreement of WDP readings was not higher than 22 %. These values were pretty similar in the two injection periods that was quite coherent because both periods really belonged to the same step.

By the other hand, that difference of agreement depending on the humidity quantity was evaluated could be linked with the uncertainty term which must be added to the total budget uncertainty because of the unit conversion of WDP reading from the MIS-II. This could have led to more restrictive acceptance criterion for WDP than for WC readings, especially for low humidity levels where the sensitive coefficient to convert WC to WDP is especially large. That explanation would justify partially, the low percentage of accepted values during the first and third extraction times.

5.3.3. BEHAVIOUR DURING TRANSITIONAL CONDITIONS

Because of the great oscillations and variations of daily minimum values both of WC and WDP signals, very especially during both shutdown times (see last days of Fig. 5.3.k and first days of Fig. 5.3.l), it was concluded that would be very interesting to know the dynamic behaviour of humidity measurement instruments upon resuming operation of the facility after shutdowns of the plant, or vice versa.

By the other hand, such knowledge would be very useful to Enagás staff because they could predict potential troubles or even hazardous situations such as, hydrates formation, because of the excessive humidity increase of the NG confined inside the plant

during long shutdown times, which could come to exceed the legal limits to be commercialized.

To assess the dynamic behavior of the plant and humidity analyzers were used the the variation of the cumulative average of those properties defined to sinusoidal signals, namely, the amplitude and period of the daily minima of WC and WDP during the time required to achieve a new stable condition. The study the cumulative average of both quantities would allow to know the overall behavior of the instruments, minimizing individual daily perturbations that any hygrometer can suffer because of particular events.

The *cumulative average of the amplitude* allows to determine the time required by the analyzers to reach more or less stable daily cyclical measurements, that is to say, indicates when the plant has reached a steady state situation, namely, when the difference between the corresponding daily maxima and minima keeps constant. This property would be essential to detect potential differences such as signal delays or even drift effects. However, from the point of view of the analyzers, this tool must not be used to find the final values measured by the analyzers, only to know the relative behavior between the maxima and minima reached by the humidity analyzers.

On the other hand, *the cumulative average of the period* allows to verify if the cycles actually have a daily behavior or not.

Two representative examples have been chosen: (a) when the plant was extracting and then was stopped, and (b) when NG began to be injected into the wells. This way, the behavior of WC and WDP readings during the three production processes were evaluated and the second production stage lasted long enough to reach really steady conditions in both cases. Firstly, the cumulative average of the amplitude for both WC and WDP will be analyzed, and later the period.

5.3.3.1. Amplitude study

Below are shown two graphs that summarize the behavior of the three instruments for the two selected cases.

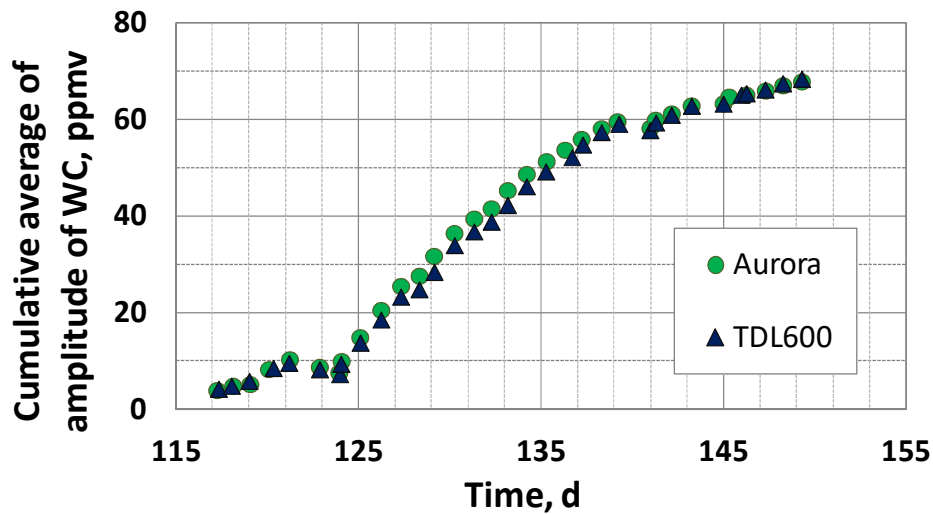


Fig. 5.3.t The cumulative average of the amplitude from the 4th extraction time to the 4th shut-down time for WC readings.

Fig. 5.3.t does not show data series of MIS-II because its readings of WDP had to be converted to WC using the international standard ISO 18453:2004 [ISO04], so we would be added more uncertainty at this instrument regarding the rest.

Looking at Fig. 5.3.t it can be said that both spectroscopic instruments had a completely identical behaviour since the beginning of the change until when the stability of the process was achieved. No kind of drift or delated was shown by any equipment.

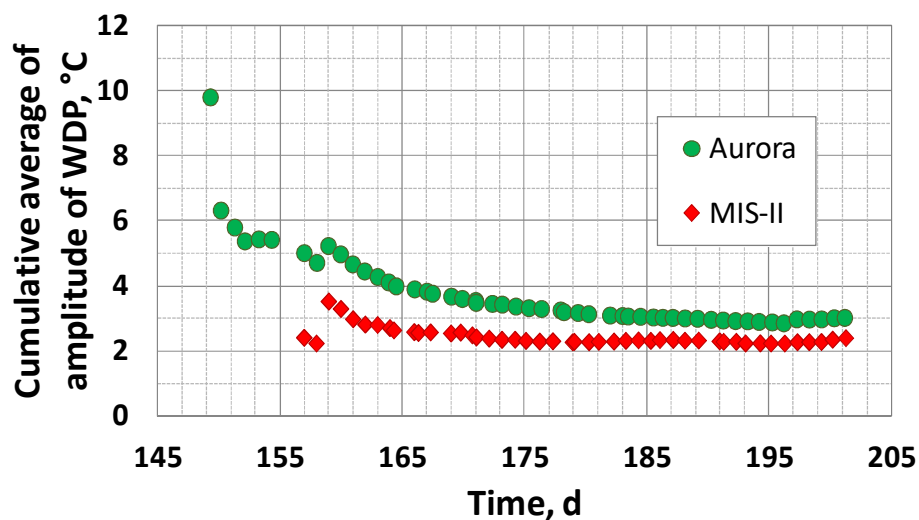


Fig. 5.3.u The cumulative average of the amplitude from the 4th shutdown time to the 1st injection time for WDP readings.

Whilst watching Fig. 5.3.u we can see that the Al_2O_3 probe gave smaller amplitudes in all the periods studied. This can be justified by the fact that the maxima recorded by this sensor were always lower than the other instruments, especially at higher humidity values.

By the other hand, when in the initial state NG was drier than in the second, as happened in Fig. 5.3.t, a noticeable variation in NG humidity trend happened after the first week approximately. This fact could mean which was the required time by the NG confined in the plant to start being moisturized by desorption effect from the inner walls of any component of plant in contact with the gas. In other words, it would be an interesting effect of the dynamic behavior of the plant which must be taken into account to avoid excessive increasing of the NG humidity during the shutdown times.

5.3.3.2. Period study

As well as the previously section, below are shown two graphs that summarize the behavior of the three instruments for the same cases.

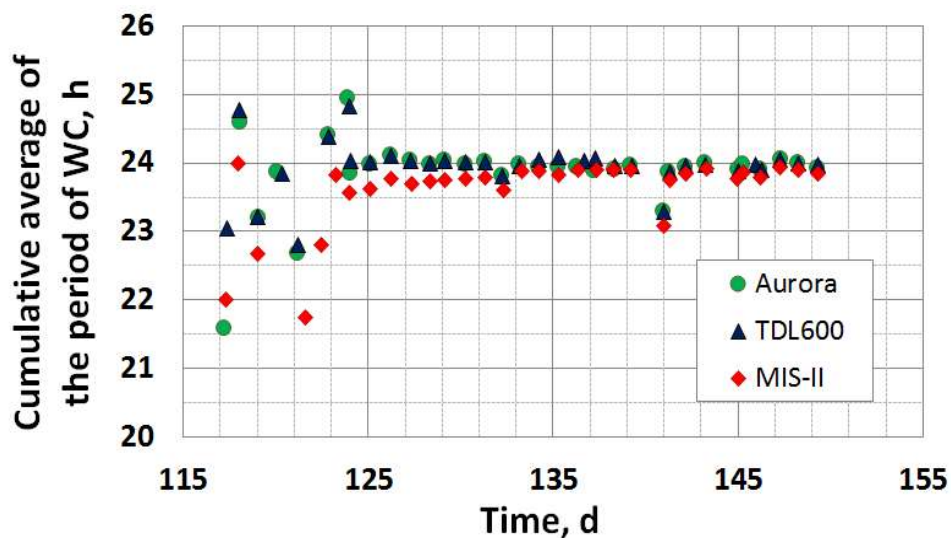


Fig. 5.3.v Cumulative average of the period from extraction from the 4th extraction time to the 4th shutdown time for WC readings.

In this case, although Fig. 5.3.v shows the WC readings, the behavior of the MIS-II can be shown despite having directly read in WDP, because the time required to reach the maximum and minimum is independent of the humidity quantity in which the period is expressed.

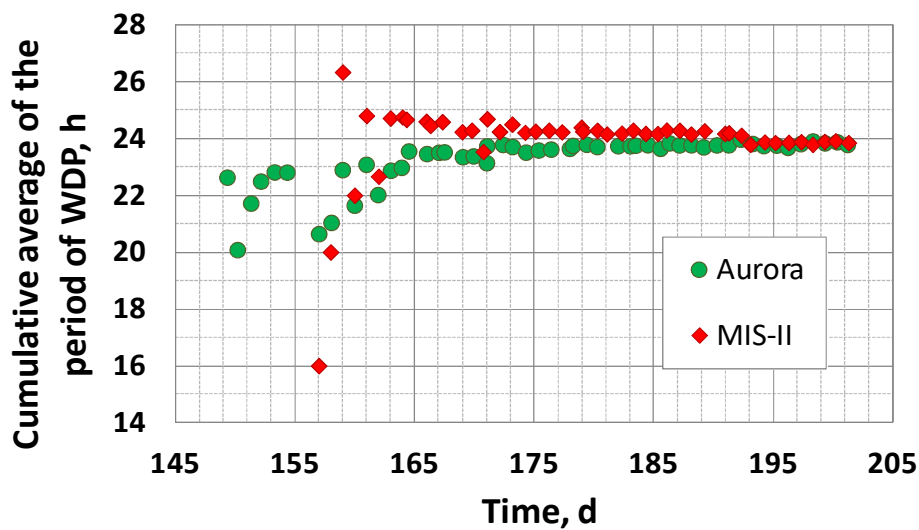


Fig. 5.3.w Cumulative average of the period from the 4th shutdown time to the 1st injection time for WDP readings.

The results depicted in Fig. 5.3.v and Fig. 5.3.w show that in all cases and regardless of the process change, the cumulative average of the period tends to the same normal time constant equal to 24 h, coinciding with the day/night thermal cycles. When the outside temperature raised, especially a couple of hours after noon, all components which constitute the drying plant of Serrablo were heated, so finally this temperature increase will raise the temperature of the NG leading to decreased water vapor adsorption by the internal walls of the all pipelines and instruments of the facility, with the consequent increase in WC and WDP. By contrast, when the outside temperature falls, especially during the last hours of the night, the NG humidity will be lower for the same reason. Evidences of this effect were also reported by Løkken in laboratory environments in which all hygrometers followed a daily cycle synchronized with the ambient temperature variations during the day and night [Løk12b], similar to our findings.

This study was also performed using of the daily maxima but no extra or different conclusion were reached. For that, the choice to use the daily minimum values throughout the thesis like the most important and representative point of the day, looks quite acceptable.

By the other hand, it was corroborated the capability of both sensing technologies to detect increases and decreases of the gas humidity.

5.3.4. INTERMEDIATE CHECK WITH STANDARD SAMPLE

During the third shutdown time, the three hygrometers were having a significant constant offset. Because of this, knowing which of them was giving the most correct reading to be able to use as a reference was essential for the project.

For this reason, and before started the last extraction time the 24th of March of 2014, Enagás staff of Zaragoza traveled to Serrablo to checking the readings of the meters and to evaluate their corrections and relative differences between them. Previously, a standard sample of N₂ / H₂O with a water concentration of 24 ppm_v ± 4 ppm_v was sent for use as a reference.

Before to carry on the check test, it was necessary a purging and drying process of the sampling system shared by all hygrometers. In this sense, initially the NG supply was closed for the entire plant section in which the moisture meters were located; later N₂ at 5 MPa was pumped to dry it; and finally, the inlet pressure of N₂ was then reduced to 0.5 MPa to facilitate drying of the line. All this purging process together with the own checking test performed on the humidity instruments has been depicted in Fig. 5.3.x.

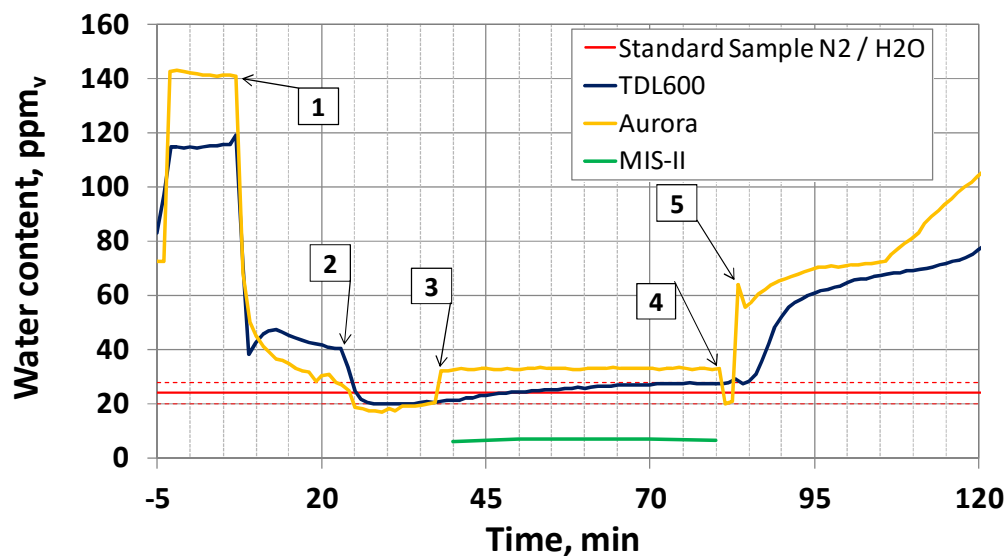


Fig. 5.3.x Readings given by the three instruments studied before and during the intermediate check of their performance, flowing N₂/H₂O with a concentration of 24 ppm_v.

Once the wet gas started to reach stable values, the dry N₂ gas cylinder was substituted for one containing a nominal water vapour concentration of 24 ppm_v. At first the standard sample was supplied at a pressure of 1.7 MPa [1], but later was increased to

5.9 MPa, the pressure simulated by the spectroscopic instruments was set in [2]. Then the configuration of the Aurora was changed to read N₂ mode, hence the change observed in [3]. Once stable readings period was completed, the cylinder that contained the standard sample was removed from the sampling system [4] and lastly, the recording mode of the Aurora was switched to NG [5].

Fig. 5.3.y shows the readings of the three instruments during the measurement of the standard sample with N₂, points [3] and [4] of the Fig. 5.3.x. The colored area represents the range generated from the expanded uncertainty of water concentration multiplied by a coverage factor, $k = 2$, for a confidence level of approximately 95 %.

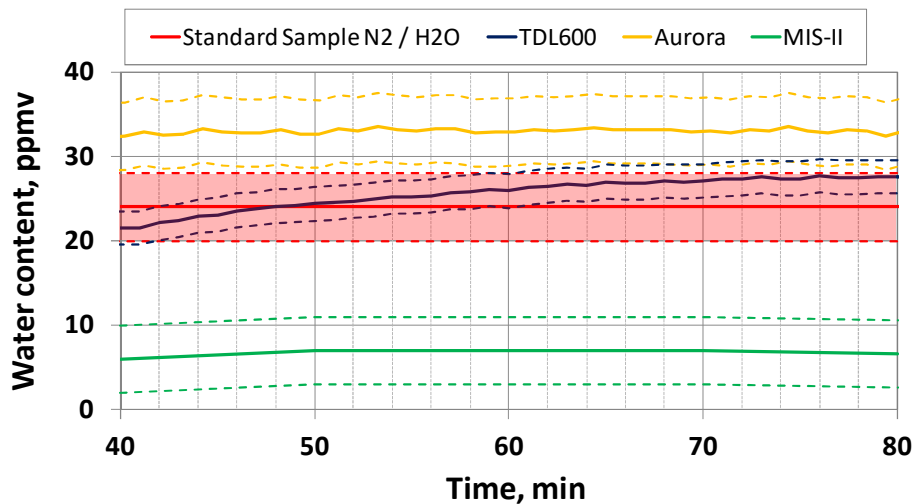


Fig. 5.3.y Readings given by the three instruments studied while the standard sample of N₂/H₂O with a concentration of 24 ppm_v ± 4 ppm_v (shaded region) was applied.

First information can be extracted is that both the Aurora and MIS-II had already obtained stable humidity values, whilst the TDL600 took nearly another 30 min to achieve a stable signal. Besides, it can be seen that the MIS-II was providing extremely dry values, despite having been recently re-calibrated.

On the other hand, we can notice that the spectroscopic instruments follow each other very closely in relation to the final stable value measured. However, despite needing more time to reach stable values, the TDL600 was the only instrument to meet specifications when compared with the reference gas, although the version of instrument used here had not been equipped with the nitrogen test gas mode, which was already included in its commercial version, and could be already used in spot-checks

and/or field verification. Thereby, the performance of TDL600 may be supposed even better than shown here.

Regarding the Aurora, it must be noted that the obtained values were consistent with the standard sample, although it had not been recalibrated since it was supplied two years before, so it can be affirmed that its performance was under specifications.

5.3.5. LONG-TERM STABILITY STUDY

The difference between the readings of the MIS-II equipped with Al_2O_3 probe and the Aurora spectroscopic analyzer as a function of time can be seen in Fig. 5.3.z together with the line pressure as indicated by the pressure transducers of both instruments. The Aurora WC measurements in ppm_v were converted to WDP using the equations contained in GERG [O&A01], based on line pressure measured by the Aurora and the gas composition measured by the chromatograph. The series starts with a transition to injection mode from a shutdown period on day 149 (see Section 5.3.2.3) and the measurements take approximately two weeks to stabilize that is the normal time for the plant to reach a stable condition after a prolonged shutdown period. This is consistent with the analysis of the cumulative average of the amplitude shown on Section 5.3.3. On day 196, maintenance tasks were performed upstream of the pipeline in which scrapers were introduced in the line between Serrablo and Zaragoza. That produced an increase in the WDP that was finally detected three days later as the pipeline inner surfaces adsorbed water vapour and finally reached the Serrablo facility. The increased WDP lasted approximately 8 days before the readings stabilized again as can be seen in the next figure.

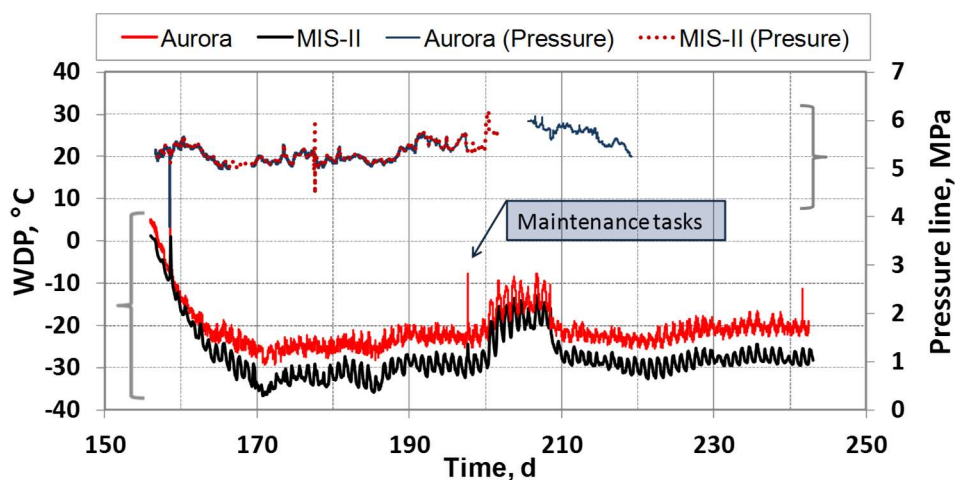


Fig. 5.3.z WDP signals of MIS-II and Aurora as a function of time and line pressure recorded by both instruments.

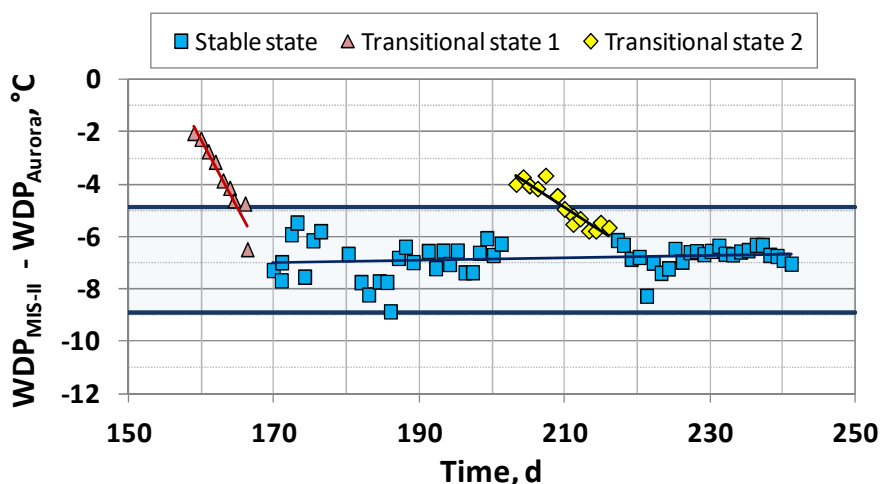


Fig. 5.3.aa Long-term stability of difference in WDP of the MIS-II versus Aurora in stable and transition periods. The shaded region represents the expected reproducibility of the MIS-II sensor (± 2 °C).

Fig. 5.3.aa shows the results of the difference between the MIS-II and Aurora WDP in °C as a function of time during the same period. The shaded area represents the expected reproducibility of the Al_2O_3 probe. The red triangles are the reading in the first transitional state in which the MIS-II WDP signal converges towards the Aurora readings at a rate of approximately -0.52 °C/day, meeting the expected reproducibility 17 days after the commencement of injection. The yellow rhombi are the readings after the maintenance task and take 8 days to meet the expected reproducibility limit, converging to the Aurora readings at a nominal rate of -0.18 °C/day, much lower than that observed in the first transitional state.

The blue squares represent the two stable periods, where, the mean differences between the instrument readings were maintained with a small positive relative drift over 85 days with a nominal drift rate of 0.14 °C/month, within the manufacturer's specification for the MIS-II for the typical annual recalibration period. However, this was different to what had been observed previously in the tests performed under laboratory conditions on other Al_2O_3 sensors, where in general the drift had been to drier readings (See Section 5.1). If we analyse the data of both the stable periods as one series, the standard deviation of the difference was 0.64 °C. During the first stable region the standard deviation was somewhat higher after the prolonged shutdown with a maximum interval of ± 1.7 °C, whereas in the second stable period this was reduced to ± 1.1 °C,

consistent with the values for the individual instruments given in Table 5.3.i. and Table 5.3.j, and the expected reproducibility of the Al_2O_3 sensor.

5.3.6. INFLUENCE OF METHANOL

Below figure shows the results obtained on the possible influence of methanol on the humidity indications of this two technologies. The marker at $t = 0$ indicates the start of methanol injection.

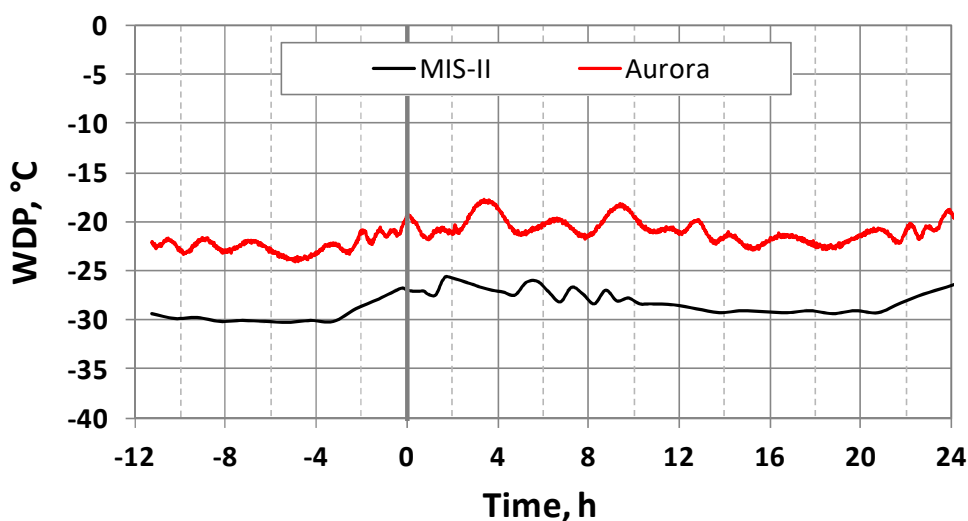


Fig. 5.3.bb WDP readings during the test to determine the influence the methanol on the analyzers.

From the results obtained in the previous figure we can interpret that methanol at the concentration applied ($7 \mu\text{mol/mol}$) does not influence the measurements of the spectroscopic instruments, as claimed by the manufacturers.

Similarly, the MIS-II based on Al_2O_3 sensor was not affected by the presence of methanol. However, such methanol concentration was slightly lower than the study previously performed by Løkken [Løk12b] where it was evaluated more extensively the effects for methanol concentration in the range from $750 \mu\text{mol/mol}$ to $10 \mu\text{mol/mol}$ and they detected appreciable changes in only one of the two Al_2O_3 sensors studied.

6 CONCLUSIONS

A thorough study was carried out on the behaviour of different moisture measurement technologies, verifying their performance in NG and in real industrial conditions.

A total of 14 sensors, based on 6 different measurement technologies were studied. Techniques traditionally used, such as: condensation hygrometers, electrolytic and capacitive sensors based on metal oxides; were compared to novel and promising measuring technologies, which constitute the state of the art in the world of hygrometry, such as: microwave resonators, absorption spectroscopy and polymeric capacitive sensors.

For this, a complex test rig was designed and built to work under laboratory conditions, capable of comparing all equipment simultaneously, controlling the pressure up to 5.8 MPa, adjusting flow rates and controlling the WC of the NG by means of a flow mixer, which allowed generating a useful range for the gas industry, from 13 ppm_v to 250 ppm_v.

Measurement protocols were developed and various properties of the equipment were evaluated, thus validating relative performance of the different technologies with each other. Characteristics of the dynamic behaviour of the equipment (response times to changes in humidity and variations due to changes in pressure), as well as studies of short-term drift, hysteresis and linearity, were performed.

In addition, it participated in the development and validation phase of the quasi-spherical microwave resonator by evaluating its performance with real NG, for a WC range between 25 ppm_v and 100 ppm_v, and at a pressure of 0.75 MPa, was quite satisfactory showing itself as a promising technologies in The field of hygrometry, but with issues yet to be developed for real industrial applications.

In spite of the differences exhibited by certain equipment, due to factors and inconveniences already commented, the consistency exhibited by the results demonstrates the validity of the experimental and analysis methods used; Demonstrating the utility of all technologies for the requirements of the gas industry, with particular aspects in all cases.

On the other hand, a complete NG sampling system was built prior to the measurement of humidity, specifically designed for industrial applications in the field, outdoors, under extreme weather conditions, and within explosive areas. This system was capable of servicing 3 humidity meters simultaneously, in addition to a complete chromatographic analysis system, which meant a great advance and modernization of the underground gas storage and drying plant of Serrablo (Enagás), in addition to an increase in reliability and accuracy over moisture control at all stages of processing.

All conclusions obtained in this thesis are the result of analysing a large amount of data collected for almost 280 days of tests. During all that time the good performance of the spectroscopic analyzers was demonstrated even in real and extreme industrial conditions, and during all stages of production, which allowed to have a greater knowledge of the gas quality at all times. As proof of this, Enagás acquired one of these instruments to be installed in key points of its national distribution network. This was a clear outcome of the metrological support of this thesis to the industrial sector, as well as in the development of new and better measurement technologies, both of which are key aspects in the last European roadmaps for humidity.

Finally, the question of traceability and the lack of reproducibility between the conditions of calibration and use of the instruments was a problem always present in this thesis. However, many national metrology institutes (NMI) are currently developing new equipment and facilities capable of replicating these industrial conditions. As a sample of the first steps taken in this regard is the calibration performed by the NPL of some hygrometers used in this thesis, and how the ranges, and the measurement and calibration capabilities (CMC) of various NMIs in the EU have been improved in order to provide the metrological infrastructure that satisfies the industrial needs. The work performed in this thesis contributes to a better understanding of the influence quantities that affect the uncertainty of measurement in the conditions of use that can sometimes be significantly larger than those in the ideal conditions found in the laboratory during formal calibration and are fundamental for ensuring the quality of industrial measurement in the strategic NG industry.

7 REFERENCES

- [Act98] A. Actis, S. A. Bell, R. Benyon, B. Cretinon, M. De Groot, M. Heinonen, G. Scholz, A. Steiner. (1998). The use of a humid air generator as a reference method for measuring humidity Papers and Abstracts from the Third International Symposium on Humidity and Moisture, National Physical Laboratory, UK, 10-19.
- [Aki06] O. Akin-Ojo, A. Harvey, K. Szalewicz. (2006). Methane-water cross second virial coefficient with quantum corrections from an ab initio potential. *J. Chem. Phys.* **125**, 014314.
- [ALP04] Alpha Moisture Systems. Dew TEC DS200 – User’s Manual. Printed in 2004. Document No. 1125.
- [Anb12] M. Anbia, S. E. Moosavi Fard, K. Shafiei, M. A. Hassanzadeh, A. Mayahipour. (2012). Humidity Sensing Properties of the Sensor Based on V-Doped Nanoporous $Ti_{0.9}Sn_{0.1}O_2$ Thin Film. *Chinese Journal of Chemistry*. **30**, 842–846.
- [Any14] C. I. C. Anyadiegwu, A. Kerunwa, P. Oviawe. (2014). Natural gas dehydration using triethylene glycol (TEG). *Petroleum & Coal*. **56** (4), 407-417.
- [Arg10] *Argonne National Laboratory. U.S. Department of Energy laboratory.* GREET, The greenhouse gases, regulated emissions, and energy use in transportation model. (August 26, 2010). GREET 1.8d.1. Appendix A. Available from: <http://greet.es.anl.gov/> Last Access: 14th March 2016.
- [AST95] ASTM designation D1142-95, Standard Test Method for Water Vapor Content of Gaseous Fuels by Measurement of Dew-Point Temperature. *American Society for Testing and Materials, Philadelphia, USA.* (1995)
- [Ati12] M. Atilhan, S. Aparicio, F. Benyahia, E. Deniz (2012). Advances in Natural Gas Technology. Chapter 7: Natural Gas Hydrates. Edited by Dr. Hamid Al-Megren. *InTech*. ISBN: 978-953-51-0507-7. Available from: http://www.intechopen.com/books/advances-in-natural-gas-technology/natural_gas_hydrates
Last Access: 26th April 2016.
- [Avi99] S. Ávila. (1999). Curvas de rocío de gases naturales sintéticos y de sus mezclas con agua y metanol. Determinación experimental y predicciones teóricas. *Doctoral dissertation*. Spanish ed., University of Zaragoza, España.

-
- [A&E96] O. A. Alduchov, R. E. Eskridge. (1996). Improved Magnus Form Approximation of Saturation Vapor Pressure. *Journal of Applied Meteorology*. **35**, pp. 601-609.
- [Bag09] V. S. Bagad. (2009). Microwave Engineering. Technical Publications Pune.
- [Bapt07] J. M. M. Baptista. (2007). Análise da formação de hidratos em atividades de perfuração de campos petrolíferos. Universidade Tecnológica Federal do Paraná, Curitiba (Brazil). Available from:
<http://www.ppgem.ct.utfpr.edu.br> Last Access: 19th April 2016.
- [Bel04] S. Bell, T. Gardiner, R. M. Gee, M. Stevens, K. Waterfield, A. Woolley. (2004). An evaluation of performance of trace moisture measurement methods. *Proceedings of the 9th International Symposium on Temperature and Thermal Measurements in Industry and Science*. Edited by D. Zvizdic, L.G. Bermanec, T. Stasic and T. Veliki. LFM/PSB Zagreb, pp. 663-668.
- [Bel08] S. Bell, R. Benyon, N. Böse, M. Heinonen. (2008). A roadmap for humidity and moisture measurement. *Int. J. Thermophysics*. **29** (5), pp. 1537-1543.
- [Bel13] S. Bell. (May 2013). Test on metal oxide sensors (and others) in methane and gas mixtures. *Presentation of NPL in EMRP ENG01 GAS Final Project Meeting*.
- [Bel98] S. Bell. (1998). Validation of the NPL gravimetric hygrometer. *Doctoral dissertation*. City University London, England.
- [Ben07] R. Benyon, H. Mitter. (2007). The new INTA high-range standard humidity generator and its comparison with the Austrian national humidity standard maintained at BEV/E+E. *10th International Symposium on Temperature and Thermal Measurements in Industry and Science (TEMPMEKO 2007)*. Lake Louise (Canada), del 21 al 25 de mayo de 2007. *Int. Journal of Thermophysics* (2008). **29** (5), 1623-1631.
- [Ben10] A. Benton. (2010). Dew Point Measurements in Natural Gas. MICHELL Instruments. *53rd Technical Seminar. ABNT-CB-09 – Comitê Brasileiro de Gases Combustíveis*. Natal, Brazil.
- [Ben98] R. Benyon, P. Huang. (1998). A comparison of INTA and NIST humidity standard generators, Papers and Abstracts from the Third International Symposium on Humidity and Moisture, National Physical Laboratory, UK. 28-36.
- [BIPM] Bureau International des Poids et Mesures. Available from: www.bipm.org Last Access: 17th April 2017.

-
- [BOE00] Real Decreto Ley 6/2000, de 23 de junio, de Medidas Urgentes de Intensificación de la Competencia en Mercados de Bienes y Servicios. Available from:
www.boe.es/boe/dias/2000/06/24/pdfs/A22440-22458.pdf
Last Access: 12th February 2016.
- [BOE01] Real Decreto 346/2001, de 4 de abril, por el que se declaran al Laboratorio Central Oficial de Electrotecnia, al Departamento de Metrología y Ensayos del Taller de Precisión y Centro Electrotécnico de Artillería, y al Laboratorio de Temperatura y Humedad del Instituto Nacional de Técnica Aeroespacial, como laboratorios asociados al Centro Español de Metrología y depositarios de los patrones nacionales de las unidades derivadas de intervalo de alta tensión eléctrica (superior a 1.000 V), de atenuación en alta frecuencia y de humedad, respectivamente.
Available from: https://www.boe.es/diario_boe/txt.php?id=BOE-A-2001-7669
Last Access: 1st May 2017.
- [BOE03] Real Decreto 681/2003, de 12 de junio, por el que se dicta las disposiciones de aplicación de la Directiva del Parlamento Europeo y del Consejo 1999/92/EC, relativa a las disposiciones mínimas para la mejora de la protección de la salud y la seguridad de los trabajadores expuestos a los riesgos derivados de atmósferas explosivas. Available from:
<https://www.boe.es/boe/dias/2003/06/18/pdfs/A23341-23345.pdf>
Last Access: 18th January 2016
- [BOE04] Real Decreto 250/2004, de 6 de febrero, por el que se declara al Centro Nacional de Sanidad Ambiental del Instituto de Salud "Carlos III" y al Laboratorio de Radiofrecuencia y Microondas del Instituto Nacional de Técnica Aeroespacial "Esteban Terradas" como laboratorios asociados al Centro Español de Metrología, y depositarios de los patrones nacionales de ozono, y de potencia, ruido e impedancia en alta frecuencia, respectivamente. Available from:
https://www.boe.es/diario_boe/txt.php?id=BOE-A-2004-4513
Last Access: 1st May 2017.
- [BOE06] ORDEN ITC/2581/2006, de 28 de julio (BOE 186/2006, de 5 de agosto), por la que se definen los patrones nacionales de las unidades derivadas, del sistema internacional de unidades, de capacidad eléctrica, concentración de ozono en aire, flujo luminoso, impedancia en alta frecuencia, par de torsión, potencia en alta frecuencia, resistencia

eléctrica, ruido electromagnético en alta frecuencia, tensión eléctrica, actividad (de un radionucleido), kerma (rayos x y γ), dosis absorbida, ángulo plano, densidad de sólidos, fuerza, presión, volumen, atenuación en alta frecuencia, humedad e intervalo de medida de alta tensión eléctrica (superior a 1000 V). Available from: <https://www.boe.es/boe/dias/2006/08/05/pdfs/A29521-29524.pdf>

Last Access: 1st May 2017.

[BOE11] Ley 14/2011, de 1 de junio, de la Ciencia, la Tecnología y la Innovación. Available from: <https://www.boe.es/buscar/pdf/2011/BOE-A-2011-9617-consolidado.pdf>

Last Access: 1st May 2017.

[BOE12] Resolución, de 26 de julio de 2012, de la Comisión Nacional de Energía, sobre la solicitud de certificación de ENAGAS como gestor de la red de transporte de gas. Available from:

www.boe.es/boe/dias/2012/08/17/pdfs/BOE-A-2012-10969.pdf

Last Access: 14th February 2016.

[BOE14] Real Decreto 925/2015, de 16 de octubre, por el que se aprueba el Estatuto del Instituto Nacional de Técnica Aeroespacial «Esteban Terradas».

<https://www.boe.es/boe/dias/2015/10/17/pdfs/BOE-A-2015-11162.pdf>

Last Access: 10th May 2017.

[BOE72] Decreto 623/1972, de 24 de marzo de 1972, por el que se crea la Empresa Nacional de Gas S. A. Page 5268. Available from:

www.boe.es/boe/dias/1972/03/24/pdfs/A05268-05268.pdf

Last Access: 12th February 2016.

[BOE14b] Ley 32/2014, de 22 de diciembre, de Metrología.

<https://www.boe.es/boe/dias/2014/12/23/pdfs/BOE-A-2014-13359.pdf>

Last Access: 10th May 2017.

[BOE16] Real Decreto 244/2016, de 3 de junio, por el que se desarrolla la Ley 32/2014, de 22 de diciembre, de Metrología.

<https://www.boe.es/boe/dias/2016/06/07/pdfs/BOE-A-2016-5530.pdf>

Last Access: 10th May 2017.

[BOE85] Real Decreto 415/1985, de 27 de marzo, por el que se reestructura el Ministerio de la Presidencia. Available from:

-
- https://www.boe.es/diario_boe/txt.php?id=BOE-A-1985-5216
Last Access: 30th April 2017.
- [BOE86] Ley 13/1986, de 14 de abril, de Fomento y Coordinación General de la Investigación Científica y Técnica. Available from:
<https://www.boe.es/boe/dias/1986/04/18/pdfs/A13767-13771.pdf>
Last Access: 1st May 2017.
- [BOE90] Ley 31/1990, de 27 de diciembre, de Presupuestos Generales del Estado para 1991. Available from:
https://www.boe.es/diario_boe/txt.php?id=BOE-A-1990-31180
Last Access: 30th April 2017.
- [BOE94] Real Decreto 648/1994, de 15 de abril, por el que se declaran los patrones nacionales de medida de las unidades básicas del Sistema Internacional de Unidades (BOE núm. 103, de 30 de abril de 1994). Available from:
<https://www.boe.es/buscar/pdf/1994/BOE-A-1994-9802-consolidado.pdf>
Last Access: 1st May 2017.
- [BOE96] Real Decreto 400/1996, de 1 de marzo, por el que se dicta las disposiciones de aplicación de la Directiva del Parlamento Europeo y del Consejo 94/9/CE, relativo a los aparatos y sistemas de protección para uso en atmósferas potencialmente explosivas. Available from:
<http://www.boe.es/boe/dias/1996/04/08/pdfs/A12903-12916.pdf>
Last Access: 17th December 2015
- [Boyle] B. Boyle. Humidity generation and humidity measurement. The complete guide. *Owlstone Nanotech Inc.* Available in:
<http://info.owlstonenanotech.com/rs/owlstone/images/Humidity%20Generation%20and%20Humidity%20Measurement.pdf>
Accessed March 29, 2017.
- [BP15] BP p.l.c. (June 2015). BP statistical review of world energy. 64th edition. Available from: www.bp.com/statisticalreview
Last Access: 23rd February 2016
- [Brow09] A. S. Brown, M. J. T. Milton, G. M. Vargha, R. Mounce, C. J. Cowper, A. M. V. Stokes, A. J. Benton, D. F. Lander, A. Ridge, A. P. Laughton. (February 2009). Measurement of the hydrocarbon dew point of real and synthetic natural gas mixtures by direct and indirect methods. *Energy and*

Fuels, published by *American Chemical Society*. DOI: 10.1021/ef8009469.

- [Bru87] E. B. Brucart. (1987). Gas Natural. Características, distribución y aplicaciones industriales. *Editores técnicos asociados, S.A.* Barcelona, (Spain). ISBN: 84-7146-241-9.
- [Buc81] L. Buck. (1981). New equations for comparing vapor pressure and enhancement factor. *Journal of Applied Meteorology*. **20**, 1527-1532.
- [Buk55] R. F. Bukacek. (1955). Equilibrium Moisture Content of Natural Gases. *Institute of Gas Technology, Research Bulletin 8*.
- [Bul11] J. A. Bullin, C. Fitz, T. Dustman. (2011). Practical hydrocarbon dew point specification for natural gas transmission lines. Available from: www.bre.com/portals/0/technicalarticles/hydrocarbon_dew_point_specification.pdf
Last Access: 1st April 2016.
- [B&B01] S. A. Bell, S. J. Boyes. (2001). An assessment of experimental data that underpin formulae for water vapour enhancement factor. *National Physical Laboratory (NPL)*.
- [B&C02] J. J. O'Brien, H. Cao. (2002). Absorption spectra and absorption coefficients for methane in the 750 – 940 nm region obtained by intracavity laser spectroscopy. *Journal of Quantitative Spectroscopy & Radiative Transfer*. **75** (3), 323-350. Available online in: <http://vpl.astro.washington.edu/spectra/ch4obrienvisible.htm>
Accessed April 14, 2017.
- [B&C52] G. Birnbaum, S. K. Chatterjee. (1952). The dielectric constant of water vapor in the microwave region. *J. Appl. Phys.* **23** (2), 220.
- [B&H12] R. Benyon, P. Hernández. (2012). Comparative study of humidity analyzers in nitrogen below 1 $\mu\text{mol/mol}$. *Int. J. Thermophysics*. **33**, 1441-1443.
- [Cañ13] I. Cañas, R. Benyon, T. Vicente, C. Porras, F. Mazarrón. (2013). Establishing a methodology for the characterization of the temperature and humidity in underground wine cellars. Universidad Politécnica de Madrid E.T.S.I Agrónomos. *Oral session IN TEMPMEKO 2013, XII International Symposium on Temperature and thermal Measurements in Industry and Science, Madeira (Portugal)*.
- [Car03] J. J. Carroll. (2003). Problem is the results of industry's move to use higher pressures. *Pipeline & Gas Journal*. **230**

-
- [Car09] J. J. Carroll. (2009). Natural gas hydrates: a guide for engineers. *Second edition. Elsevier*. ISBN: 978-0-7506-8490-3
- [Car13a] P. A. Carroll, S. A. Bell, M. Stevens. (2013). Multi-gas and multi-pressure humidity calibration facility. *Int. J. Thermophysics*. Paper presented at TEMPMEKO 2013, XII International Symposium on Temperature and thermal Measurements in Industry and Science, Madeira (Portugal).
- [Car13b] P. A. Carroll. (May 2013). Private communication during the last stage and after the end of the EMRP ENG01 GAS.
- [Cha04] A. Chapoy. (November 2004). Phase behaviour in water/hydrocarbon mixtures involved in gas production systems. *Doctoral dissertation* directed by D. Richon. English ed. L' Ecole des Mines de Paris. France).
- [Cha09] T. H. Chao, S. R. Davis, S. D. Rommel, G. Farca, B. Luey, A. Martin., M. H. Anderson. (2009). Compact liquid crystal waveguide based Fourier transform spectrometer for in-situ and remote gas and chemical sensing *Proceeding article. SPIE 7508*. International Conference on Optical Instruments and Technology: Advanced Sensor Technologies and Applications, 75080K (November 23, 2009)
- Accessed April 14, 2017.
- [Chow87] S. C. Pangtay. (1987). *Petroquímica y sociedad. La ciencia desde México*. Fondo de Cultura Económica (México).
- [CEM] Centro Español de Metrología. Available from: www.cem.es Last Access: 17th April 2017.
- [CLA09] Elaborated by Comisión de Laboratorios Asociado. (24 Sept. 2009). Reconocimiento, designación y seguimiento de laboratorios asociados y laboratorios colaboradores del CEM. Approved by Plenario del Consejo Superior de Metrología. Available from:
- http://www.cem.es/sites/default/files/reconocimiento20designacion20seguimiento20llaa_llcc.pdf
- Last Access: 3rd February 2016
- [Cla37] R. Clausius. (1867). The mechanical theory of heat with its applications to the steam engine and to physical properties of bodies. *London: J. v. Voorst*. 14-69.
- [CNMC16] Informe de supervisión de la gestión técnica del sistema gasista del tercer trimestre de 2015. Comisión Nacional de los Mercados y la Competencia (CNMC). Expediente IS/DE/005/15. (21 de enero de 2016).
- Available from: www.cnmc.es Last Access: 17th February 2016.

-
- [Coc] D. Cockman. Temperature/Humidity sensors. Available in:
http://teaching.csse.uwa.edu.au/units/CITS4419/lectures/wk2.submissions/cockmd01/Temperature_humidity_sensors_final.docx
Accessed March 27, 2016. Figure taken from:
http://images.machinedesign.com/images/archive/sensorsense0100_00000031561.jpg
- [COD14] CODATA. (2014) CODATA Value: electric constant. *Committee on Data for Science and Technology (CODATA)*.
- [Col59] L. G. Cole, M. Czuha, R. W. Mosley, D. T. Sawyer. (1959). Continuous coulometric determination of parts per million of moisture in organic liquids. *Analytical Chemistry*. **31** (12), 2048-2050.
- [Cuc12] R. Cuccaro, R. M. Gavioso, G. Benedetto, D. Madonna Ripa, V. Fericola, C. Guianvarc'h. (2012). Microwave determination of water mole fraction in humid gas mixtures. *Int. J. Thermophys.* **33**, 1352-1362.
- [Cur07] M. R. Mc Curdy, Y. Bakhirkin, G. Wysocki, F. K. Tittel, (2007). *J. Biomed. Opt.* **12**, 034034.
- [CVS10] Instruction manual. Dew Point tester. *CVS Controls Ltd.* Calgary, Canada. (2010). Available in: www.cvs-controls.com Accessed April 15, 2015.
- [C&D59] J. K. Crawshawb, F. G. Davidson. (1959). Electrolytic hygrometers for measurements in gases down to a few parts per million. *Journal of Scientific Instruments*. **3**, 121.
- [C&G13] S. Corbellini, R. M. Gavioso. (2013). A low-cost instrument for the accurate measurement of resonances in microwaves cavities. *IEEE Transactions on Instrumentation and Measurement*. **62** (5), 1259-1266.
- [C&L07] W.Y. Chen, J. Liu. (2007). Mathcad Modules for Supercritical Fluid Extraction Based on Mixing Rules Appendix A – Mixing Rules. *Department of Chemical Engineering, University of Mississippi, (USA)*.
- [Delg13] J. G. Delgado L. (2013). Hidratos del gas. *Laboratorio de formulación, interfases, reología y procesos (FIRP), Engineering Faculty, Chemical Engineering School., University of the Andes. Merida, Venezuela*.
- [EAS05] EASEE - gas. (2005). Common Business Practice document CBP-2005-01/02 “Harmonization of Natural Gas Quality”. Available from:
http://easee-gas.eu/media/4085/cbp%202005-001-02%20_3.pdf.
Accessed 15 October 2014.
Last Access: accessed 15th October 2014.

-
- [Ena10] Enagás, 2010. Underground storage of natural gas in Serrablo. Spanish version. Available from: <http://www.enagas.es>
Last Access: 15th July 2015.
- [ENAC] Available from: www.enac.es Last Access: 30th April 2017.
- [ENG] *Enagás S.A.* Available from: www.enagas.es Last Access: 9th March 2016.
- [ENG01] Joint Research Project Protocol Annex Ia. ENG01-Gas. Characterization of Energy Gases. (2009). Running under the European Metrology Research Program (EMRP).
- [EPR09a] Regulation (EC) No. 715/2009 of the European Parliament and of the Council of 13 July 2009 on conditions for access to the natural gas transmission networks and repealing Regulation (EC) No. 1775/2005. Available from:
<https://www.boe.es/doue/2009/211/L00094-00136.pdf>
(Spanish version) Last Access: 16th February 2016.
- [EPR09b] Directive 2009/73/EC of the European Parliament and of the Council of 13 de Julio de 2009, concerning common rules for the internal market in natural gas and repealing Directive 2003/55/EC. Available from:
<https://www.boe.es/doue/2009/211/L00094-00136.pdf>
(Spanish version) Last Access: 11th April 2016.
- [Ert04] K. Ertel. (2004). Application and development of water vapor DIAL systems. *Doctoral dissertation*. English ed., Max Planck Institute for Meteorology, University of Hamburg, Germany.
- [Esl00] M. B. Esler, D. W. T. Griffith, S. R. Wilson, L. P. Steele. (2000). *Anal. Chem.* **72** (1), pp 206–215.
- [EUD94] Directive 94/9/EC of the European Parliament and the Council of 23 March 1994 on the approximation of the laws of the Member States concerning equipment and protective systems intended for use in potentially explosive atmospheres.
The fourth edition of the Guidelines on the application of Directive 94/9/EC, available from:
http://ec.europa.eu/growth/sectors/mechanical-engineering/atex/index_en.htm
Last Access: 17th December 2014
- [EUD99] Directive 1999/92/EC of the European Parliament and the Council of 16 December 1999 on minimum requirements for improving the safety and

health protection of workers potentially at risk from explosive atmospheres (15th individual Directive within the meaning of Article 16(1) of Directive 89/391/EEC). Available from: <http://eur-lex.europa.eu>
Last Access: 18th January 2015

- [Fat07] K. Fattah. (2007). A Prediction of Water content in Sour Natural Gas. *Research Report no. 28/426, College of Engineering, King Saud University*.
- [Gal15] J. G. Gallegos, R. Benyon, S. Avila, A. Benito, R. M. Gavioso, H. Mitter, S. Bell, M. Stevens, N. Böse, V. Ebert, M. Heinonen, H. Sairanen, A. Peruzzi, R. Bosma, M. Val'ková. (2015). An investigation of the comparative performance of diverse humidity sensing techniques in natural gas. *Journal of Natural Gas Science & Engineering (JNGSE)*. **23**, 407-416.
- [Gal16] J. G. Gallegos, S. Avila, R. Benyon, G. McKeogh, A. Stokes. (March 2016). Experimental evaluation of the performance of humidity analyzers in natural gas under industrial conditions. *Journal of Natural Gas Science & Engineering (JNGSE)*. **31**, 293-304.
- [Gam14] A. L. M. Gama, G. Niemietz, M. C. Rodrigues, S. G. S. Coelho. (2014). Hydrate formation. Temperature transition on up-start and shut-in of offshore pipelines affecting hydrate formation. *Norwegian University of Science and Technology (NTNU), Trondheim (Norway)*.
- [Gav14] R. M. Gavioso, D. Madonna Ripa, R. Benyon, J. G. Gallegos, F. Perez-Sanz, S. Corbellini, S. Avila & A. M. Benito. (March 2014). Measuring Humidity in Methane and Natural Gas with a Microwave Technique. *Int. J. Thermophys.* **35** (3-4), 748-766.
- [Geo05] D. L. George, A. M. Barajas, R. C. Burkey. (2005). The need for accurate hydrocarbon dew point determination. *Pipeline & Gas Journal*. **232** (9), 32-36.
- [GE-2] General Electric Company: Measurement & Control Solutions. MIS Probe 2 Specifications. – User's Manual. 920-545A.
- [GE07] General Electric Company: Sensing. HygroPro Moisture Transmitter – User's Guide. 916-099B1. (June 2007).
- [GE11] General Electric Company: Measurement & Control Solutions. Aurora H2O – User's Manual. 910-284 Rev. D. (October 2011).
- [GND] *Gas Natural Distribución SDG. S.A.* Available from: www.gasnaturaldistribucion.com Last Access: 9th March 2016.

-
- [Gof49] J. A. Goff. (1949). Standardization of thermodynamic properties of moist air. *A.S.H.V.E. Journal Section, Heating, Piping, Air Conditioning*. **21**, 118.
- [Goo96] A. R. H. Goodwin, J. B. Mehl, M. R. Moldover. (1996). Resonators for accurate dielectric measurements in conducting liquids. *Rev. Sci. Instrum.* **67**, 4294.
- [GUM08] Evaluation of measurement data – Guide to the expression of uncertainty in measurement. *JCGM 100:2008. GUM 1995 with minor corrections*.
- [G&B08] L. George, R. C. Burkey. (January 2008). Test of instrument for measuring hydrocarbon dew points in natural gas streams, phase 1. *Gas Processors Association (GPA)*. Research Report RR-196.
- [G&B14] M. M. Ghiasi, A. Bahadori. (2014). A new correlation for accurate estimation of natural gases water content. *Petroleum & Coal*. **56** (5) 582-594.
- [G&G45] J. A. Goff, S. Gratch. (1945). Thermodynamic Properties of Moist Air. *Transactions of the American Society of Heating and Ventilating Engineers*. **51**, pp. 125-164.
- [Hal13] S. Hale. (2013). Hydrocarbon dew point measurement using gas chromatographs. *Pipeline & Gas Journal*. 240, 2.
- [Ham39] E. G. Hammerschmidt. (May, 1939). Gas Hydrate Formations: A Further Study on Their Prevention and Elimination from Natural Gas Pipe Lines. *GAS*, pp. 30-35.
- [Har02] G. E. Harper. (2002). Manual de instalaciones electromecánicas en casas y edificios. Hidráulicas, sanitarias, aire acondicionado, gas, eléctricas y alumbrado. *Ed. Limusa*. ISBN 9789681858742.
- [Har98] B. Hardy. (1998). ITS-90 formulations for vapour pressure, frost point temperature, dew point temperature, and enhancement factors in the range $-100\text{ }^{\circ}\text{C}$ to $100\text{ }^{\circ}\text{C}$. *The Proceedings of the Third International Symposium on Humidity & Moisture, Teddington, London (England)*.
- [He10] Y. He, T. Zhang, W. Zheng, R. Wang, X. Liu, Y. Xia and J. Zhao. (2010). Humidity Sensing Properties of BaTiO₃ Nanofiber Prepared via Electrospinning. *Sens. Actuators B Chem.* **146**, 98–102.
- [Her11] J. Herring. (October 2011). Measuring hydrocarbon dew point. The economic impact. 19th *Symposium of the industrial application of gas turbines committee (IAGT)*. 11-IAGT-105. Banff, Alberta (Canada).
- [Hir54] J. O. Hirshfelder, C. F Curtiss R. B. Bird. (1954). The Molecular Theory of Gases and Liquids. *John Wiley & Sons, Inc.*, New York.

-
- [HITRAN] The HITRAN molecular spectroscopy database. Homepage <http://www.cfa.harvard.edu/hitran/> Accessed April 4, 2017.
- [HIT04] The HITRAN molecular spectroscopy database. Version 2004. Available online in: <http://vpl.astro.washington.edu/spectra/h2o.htm> Accessed April 14, 2017.
- [Hsu15] J. W. Hsu. (30th October 2015). Hopes for ‘Golden Age of Gas’ Evaporate. Slumping prices and weak Chinese demand for gas casts a pall over the LNG industry. *The Wall Street Journal*. Available from: www.wsj.com Last Access: 9th March 2016.
- [Hua06] P. H. Huang, D. C. Ripple, M. R. Moldover, G. E. Scace. (2006). A reference standard for measuring humidity of air using a re-entrant radio frequency resonator, *Presented at the 5th international symposium on humidity and moisture*. Rio de Janeiro, Brazil.
- [Hyl75] R.W. Hyland. (1975). A correlation for the second interaction virial coefficients and enhancement factors for Moist Air. *Journal of Research of the National Bureau of Standards – A. Physics and Chemistry*. **79** A(4), 551-560.
- [H&H07] A. H. Harvey, P. H. Huang (2007). First-principles calculation of the air–water second virial coefficient. *Int. J. Thermophys.* **28**, 556-565.
- [H&L05] A. H. Harvey, E. W. Lemmon. (2005). Method for estimating the dielectric constant of natural gas mixtures. *Int. J. Thermophys.* **26** (1), 31.
- [H&T13] J. Hodgkinson, R. P. Tatam. (2013). Optical gas sensing: a review. *Meas. Sci. Technol.* **24** (2013) 012004 (59pp).
- [H&W73] R.W. Hyland, A. Wexler. (1973). The Second Interaction (Cross) Virial Coefficient for Moist Air. *J. Res. NBS.* **77** A(1), 133-147.
- [IEA11] *International Energy Agency*. World energy outlook 2011. Are we entering a golden age of gas? Special report. (2011).. Available from: www.worldenergyoutlook.org/goldenageofgas/ Last Access: 14th March 2016.
- [IEA12] *International Energy Agency*. Gas Medium-Term Market Report. (2012). Available from: www.iea.org Last Access: 12th March 2016.
- [IEA15a] *International Energy Agency*. World energy outlook 2015. (November 2015). Available from: www.worldenergyoutlook.org Last Access: 11th March 2016.
- [IEA15b] *International Energy Agency*. Gas Medium-Term Market Report. Executive summary. (2015). Available from: www.iea.org Last Access: 12th March 2016.

-
- [Igl09] E. P. Iglesias. (October 2009). *Petróleo y gas natural: industria, mercados y precios*. Ediciones AKAL. Madrid (Spain).
- [INN] *Innergy Soluciones Energéticas* (Chile). Available from: www.innergy.cl/ Last Access: 3rd March 2016.
- [INTA] Available from: www.inta.es Last Access: 30th April 2017.
- [IPE] Why are gas hydrates important? *Institute of Petroleum engineering, Heriot-Watt University*, Edinburg (Scottish). Available from: http://www.pet.hw.ac.uk/research/hydrate/hydrates_why.cfm
Last Access: 20th April 2016.
- [ISA84] ANSI/ISA-S5.1. (1984). Instrumentation symbols and identification. *The International Society of Automation*. Re-approved by American National Standard (2009).
- [ISO01] ISO 6570:2001. Natural gas - Determination of potential hydrocarbon liquid content – Gravimetric methods.
- [ISO03] EN ISO 6974:2003 Natural gas - Determination of composition and associated uncertainty by gas chromatography - Part 1: General guidelines and calculation of composition. Part 2: Uncertainty calculations
- [ISO04] EN ISO 18453:2004. Natural gas - Correlation between water content and water dew point. English version. Approved by European Committee for Standardization (CEN).
- [ISO05] ISO/IEC 17025:2005 General requirements for the competence of calibration and testing laboratories.
- [ISO05b] EN ISO 6976:2005. Natural gas - Calculation of calorific values, relative density and Wobbe index from composition.
- [ISO06] EN ISO 15403:2006. Natural gas – Designation of the quality of natural gas for use as a compressed fuel for vehicles.
- [ISO93] ISO 10101:1993. Natural gas - Determination of water by Karl-Fisher method.
- [ISO97a] EN ISO 10715:1997. Natural gas – Sampling guidelines.
- [ISO97b] EN ISO 11541:1997. Determination of water content at high pressure.
- [JMA] Chapter 3: Measurement of humidity. Japan Metrology Agency. Available in: <http://www.jma.go.jp/jma/indexe.html> Accessed April 20, 2015.
- [KCDB] BIPM. The BIPM key comparison database. Available from: <http://kcdb.bipm.org> Last update: 30th April 2017.

-
- [Kei95] F. A. Keidel. (1959). Determination of water by direct amperometric measurement. *Anal. Chem.* **31** (12), 2043-2048.
- [K&K40] D. L. Katz, F. Kurata. (June 1940). Retrograde condensation. *Ind. & Eng. Chem.* **32** (6), 817.
- [K&P] R. Kolass, C. Parker. Moisture measurement in natural gas. *Michell Instruments Ltd.* Technical article.
- [K&R85] A. L. Kohl, F. C. Riesenfeld. (1985). *Gas Purification. Fourth edition.* Gulf Publishing Company, Houston, TX.
- [K&S11] G. Mc Keogh, K. Soleyn. A comparison of moisture measurement technologies for natural gas. *6th International Gas Analysis Symposium & Exhibition – GAS2011*, Rotterdam (Netherland).
<http://www.ge-mcs.com/download/moisture-humidity/GAS-2011-white-paper-moisture-measurement-natural-gas.pdf>
Accessed April 20, 2015.
- [Laj08] J. M. Langridge, S. M. Ball, A. J. L. Shillings, R. L. Jones. (2008). A broadband absorption spectrometer using light emitting diodes for ultrasensitive, in situ trace gas detection. *Review of Scientific Instruments.* **79**, 123110.
- [Laj09] P. Laj *et al.* (2009). Measuring atmospheric composition change. *Atmospheric Environment.* Publisher. Elsevier. **43** (33), 5351–5414.
- [Li12] Y. Li. (2002). A Novel Highly Reversible Humidity Sensor Based on poly(2-Propyn-2-Furoate), *Sens. Actuators B Chem.* **86**, 155–159.
- [Løk12] T. V. Løkken. (2012) Comparison of hygrometers for monitoring of water vapour in natural gas. *Journal of Natural Gas Science and Engineering.* **6**, 24-36.
- [Løk12b] T. V. Løkken (2012). Water vapour monitoring in natural gas in the presence of methanol. *Journal of Natural Gas Science and Engineering.* **7**, 7-15.
- [Løk13] T. V. Løkken (2013). Water vapour monitoring in natural gas in the presence of ethylene glycol. *Journal of Natural Gas Science and Engineering.* **12**, 13-21.
- [Lov09] J.W. Lovell-Smith. 2009. The propagation of uncertainty for humidity calculations. *Metrologia.* **46**, 607–615.
- [Mac98] P. Mackrodt, R. Benyon, G. Scholz G. (1998). State-of-the-art calibration of high-range chilled-mirror hygrometers and their use in the intercomparison of humidity standard generators. *Papers and Abstracts*

from the Third International Symposium on Humidity and Moisture, National Physical Laboratory, UK, Vol.1 159-166.

- [May03] E. F. May, T. J. Edwards, A. G. Mann, C. Edwards. (2003). Dew point, liquid volume, and dielectric constant measurements in a vapor mixture of methane + propane using a microwave apparatus. *Int. J. Thermophys.* **24** (6), 1509-1525.
- [May08] E. F. May, M. R. Moldover, J. W. Schmidt. (2008). Electric and magnetic susceptibilities of gaseous oxygen: Present data and modern theory compared. *Physical Review A.* **78**, 032522.
- [MEE05] Meeco Inc. Technical specifications of the Accupoint LP 2. Micro-Processor based low pressure transmitter. Printed in 2005.
- [Meh09] J. B. Mehl. (2009). Second-order electromagnetic eigenfrequencies of a triaxial ellipsoid. *Metrologia.* **46**, 554–559.
- [Mey10] C. W. Meyer, J. T. Hodges, R. W. Hyland, G. E. Scace, J. Valencia-Rodriguez, J. R. Whetstone. (2010). The second-generation NIST standard hygrometer. *Metrologia.* **47**, 192-207.
- [MIC11] Michell Instruments. Condumax II User’s Manual. 97081 Issue No. 24.2. (V3.02) (December 2011)
- [MIC12a] Michell Instruments. Easidew Transmitter. Dew-Point Transmitter. Issue No. 97166_V3_UK_1112
- [MIC12b] Michell Instruments. Easidew PRO I.S. Intrinsically safe Dew-Point Transmitter. Issue No. 97208_V5_UK_0312
- [MIC15] Michell Instruments. OptiPEAK TDL600. Moisture in Natural Gas Analyzer. Issue No. 97470_V2_UK_0215 (2015).
- [MMA] La Guía MetAs. Acuerdos de Reconocimiento Mutuo (MRA) en Metrología. (2009). MetAs & Metrólogos Asociados. Available in: <http://www.metas.com.mx> Last Access: 30th April 2017.
- [Moh09] A. S. B. Mohamad. (April, 2009). Natural Gas Dehydration using Triethylene Glycol (TEG). *Faculty of Chemical & Natural Resources Engineering University of Malaysia Pahang.*
- [Mok06] S. Mokhatab, W. Poe, J. Speight. (2006). Handbook of natural gas transmission and processing. *Elsevier.* ISBN: 978-0-7506-7776-7
- [Mok12] S. A. Mokdad. (2012). Contribution à la détermination de la courbe de pression de vapeur saturante de l’eau pure dans la plage de –80 °C à +100 °C, avec une très haute exactitude. *Doctoral dissertation.* France ed., University of CNAM (Conservatoire National des Arts et Metiers), France.

-
- [MRA99] CIPM Mutual Recognition Arrangement (CIPM-MRA). Mutual recognition of national measurement standards and of calibration and measurement certificates issued by national metrology institutes. (October 1999). Technical Supplement revised in October 2003.
- Available from: <http://www.bipm.org/en/cipm-mra/>. Last update: 30th April 2017.
- [Myc02] B. J. Mychajliw. (2002). Determination of water vapor and hydrocarbon dew point in gas. *77th International School of Hydrocarbon Measurement*.
- [M&C83] P.M. Mathias, T.W. Copeman. (1983). Extension of the Peng-Robinson Equation of State to Complex Mixtures: Evaluation of the Various Forms of the Local Composition Concept. *Fluid Phase Equilib.* **13**, 91-108.
- [M&M02] E. F. May, R. C. Miller. (2002). Dielectric constants and molar polarizabilities for vapor mixtures of methane + propane and methane + propane + hexane obtained with a radio frequency reentrant cavity. *J. Chem. Eng. Data.* **47** (1), 102-105.
- [M&R08] H. Mohammadi & D. Richon. (2008). Determination of water content of natural gases: state of the art. Chapter 2 in Natural gas research progress. Editors: Nathan David and Theo Michel. *Nova Science Publishers, Inc.* ISBN: 978-1-60456-700-7.
- [Nasr05] K. Nasrifar, O. Bolland, M. Moshfeghian. (2005). Predicting natural gas dew points from 15 equations of state. *Energy Fuels.* **19**, 561–572.
- [Nie03] J. Nielsen, J. Lovell-Smith, M. de Groot, S. Bell. (2003). Uncertainty in the generation of humidity. Technical Report CCT/03-20.
- [Noë95] O. Le Noë, L. Schieppati, B. Viglietti, L. Oellrich, K. Althaus F. Pot., L. Van der Meulen, H. Kaesler, G. Moncó, G. Wismann. (1995). Development of a mathematical correlation between water content and water dewpoint. *International Gas Research Conference (IGRC)*. **1**, 25-34.
- [Nwa14] J. A. Nwaboh, O. Werhahn, V. Ebert. (2014). Line strength and collisional broadening coefficients of H₂O at 2.7 μ m for natural gas quality assurance applications. *Molecular Physics: An International Journal at the Interface Between Chemistry and Physics.* **112** (18) 2451–2461.
- [N&D12] M. Netušil, P. Dítl. (2012). Natural Gas Dehydration. *Czech Technical University in Prague, Faculty of Mechanical Engineering, Department of Process Engineering, Prague, (Czech Republic)*.
- [Onn02] H. K. Onnes. (1902). Expression of the equation of state of gases and liquids by means of series. *Huygens Institute - Royal Netherlands*

-
- Academy of Arts and Sciences (KNAW)*. Proceedings, 4. Amsterdam, 1902, pp. 125-147.
- [Ort08] E. L. Ortiz, P. Lawrence, C. C. Pantelides, C. S. Adjiman, C. D. Immanuel. (2008). An Integrate Framework for Model-Based Flow Assurance in Deep-Water Oil and Gas Production. *Chemical Engineering. 18th European Symposium on Computer Aided Process Engineering*. London.
- [O&A01] L.R. Oellrich, K. Althaus. (2001). Relationship between water content and water dew point keeping in consideration the gas composition in the field of natural gas. GERG Technical Monograph TM 14.D.
- [O&S98] H. Orbey, S. I. Sandler. (1998). Modeling Vapor-Liquid Equilibria: Cubic Equations of State and Their Mixing Rules. *Cambridge University Press*. Cambridge (U.K.).
- [Pan09] H. J. Panneman. (October 2009). On-line water dew point measurements in natural gas at Gasunie. Lecture at Workshop “Water in Natural Gas”. *Van Swinden Laboratory (VSL)*, Delft (Netherlands).
- [Per03] R. H. Perry, D. W. Green. O. O’ Maloney. (2003). Manual del Ingeniero Químico. 3rd Spanish Edition. *Mc. Graw Hill*. (Madrid).
- [Pol09] L. Polák. (May, 2009). Modelling Absorption drying of natural gas. *Department of Petroleum Engineering and Applied Geophysics of Norwegian University of Science and Technology (Norwegian: Norges Teknisk-Naturvitenskapelige Universitei (NTNU))*. Trondheim, Norway.
- [PREN15] PREN 16726:2015. Gas infrastructure – Quality of gas – Group H. European Standard. Section 3: Requirements. *CEN (European Committee for Standardization)*.
- [PRTR-S] *Registro Estatal de Emisiones y Fuentes Contaminantes*. In English: *Spanish Pollutant Release and Transfer Register (PRTR)*. Available from: www.prtr-es.es Last Access: 2nd March 2016.
- [P&A86] T. Pichery, P. Ancel. (1986). Monitoring of condensate content of natural gas in pipelines. Gas quality; Proceedings of the Congress of “Gas Quality – specifications and measurement of physical and chemical properties of natural gas”. Groningen (The Netherlands). *Eselvier Science Publisehers*. 273-288.
- [P&R76] D. Y. Peng, D. B. Robinson. (1976). A New two Constant Equation of State. *Ind. Eng. Chem. Fundam.* **15**, 59-64.
- [Rou00] J. F. Rouleau, J. Goyette, T. K. Bose, M. F. Fréchette. (2000). Performance of a microwave sensor for the precise measurement of water vapor in gases. *IEEE Trans. Dielectr. Electr. Insul.* **7**, 825–831.

-
- [R&Z12] J. Rajzinger, L. Zálezková. (2012). Calculation of maximum water content in gas phase for selected natural gases. *Institute of Thermal Power Engineering, Faculty of Mechanical Engineering of Bratislava* (Slovakia).
- [Sat46] F. E. Satterthwaite. (1946). An Approximate Distribution of Estimates of Variance Components. *Biometrics Bulletin*. **2** (6), pp. 110–114.
- [Sch07] J. W. Schmidt, R. M. Gavioso, E. F. May, M. R. Moldover. (2007). Polarizability of Helium and Gas Metrology. *Phys. Rev. Lett.* **98**, 245504.
- [Sch93] H. I. Schiff, G. I. Mackay, J. Bechara. (1994). The use of tunable diode laser absorption spectroscopy for atmospheric measurements. *Res. Chem. Intermed.* **20**, 3/4/5, pp. 525-556.
- [SEDI] *Asociación española del Gas. SEDIGAS*. Available from: www.sedigas.es Last Access: 2nd March 2016.
- [SEDIb] *Asociación española del Gas. SEDIGAS*. (2015). El gas en España. Informe anual 2015. Available from: www.sedigas.es Last Access: 2nd March 2016.
- [SEDIc] *Asociación española del Gas. SEDIGAS*. (2013). El gas en España. Informe anual 2013. Available from: www.sedigas.es Last Access: 2nd March 2016.
- [SGTC08] Subdirección General de Tecnología y Centros. (2008). Boletín de Observación Tecnológica en Defensa nº 21. 4th trimestre 2008.
- [SHAW1] Shaw Moisture Meters. Specifications sheet of Dewpoint Transmitter Model SDT. SP_SD3 [1110].
- [SHAW2] Shaw Moisture Meters. Specifications sheet of Superdew 3 Hygrometer. SDT_Specification_0907
- [Slo10] E. D. Sloan, C. A. Koh, A. K. Sum. (2010). Natural gas in flow assurance. *Gulf Professional Publishing*. Published by *Elsevier Inc.* ISBN: 978-1-85617-945-4.
- [Smi97] J. M. Smith, H.C. Van Ness, M. M. Abbott. (1997). Introducción a la Termodinámica en Ingeniería Química. 5th *Spanish Edition*. *Mc. Graw Hill* pp. 97-100.
- [Soa72] G. Soave. (1972). Equilibrium constants from a modified Redlich-Kwong equation of state. *Chemical Engineering Science*. **4** (27), 1197-1203.
- [Sol09] K. Soley. (2009). The war against water. *GE Measurement & Control*. Available in: www.ge-mcs.com Last Access: 25th April 2016.

-
- [Son02] S. Son. (2002). Polymeric Humidity Sensor Using Phosphonium Salt-Containing Polymers. *Sens. Actuators B Chem.* **86**, 168–173.
- [Son90] D. Sonntag. (1990). Important new values of the physical constants of 1986, vapor pressure formulations based on ITS-90, and psychrometer formulae. *Z. Meteorol.* **70**, pp. 340-344.
- [Sot99] G. Sotelo. (1999). Hidráulica General. *Edit. Limusa*. ISBN 978-968-18-0503-6.
- [Spa00] R. Span, E.W. Lemmon, R.T. Jacobsen, W. Wagner & A. Yokozeki. (2000). A reference equation of state for the thermodynamic properties of nitrogen for temperature from 63.151 to 1000 K and pressures to 2200 MPa. *J. Phys. Chem. Ref. Data.* **29**, 1361.
- [STA05] Natural Gas STAR (2005). Efficient pigging of gathering lines. *Processors Technology Transfer Workshop Gas Processors Association, Devon Energy*. Available in: <http://slideplayer.com/slide/4902861/> Last access 15 October 2014.
- [S&H14a] H. Sairanen, M. Heinonen. (2014). Validation of new apparatus measuring water vapour enhancement factors up to 6 MPa. *Meas. Sci. Technol.* **25**, 035301.
- [S&H14b] H. Sairanen, M. Heinonen. (2014). Enhancement factor for water vapor pressure correction in humid methane. *Int. J. Thermophys.* **35**, 1280-1289.
- [S&M03] J. W. Schmidt, M. R. Moldover. (2003). Dielectric permittivity of eight gases measured with cross capacitors. *International Journal of Thermophysics.* **24** (2), 375-403.
- [S&W87] A. Saul, W. Wagner. (1987) International Equations for the Saturation Properties of Ordinary water Substance. *J. Phys. Chem. Ref.* **16** (4), 893-901.
- [S&W91] U. Setzmann, W. Wagner. (1991). A new equation of state and tables of thermodynamic properties for methane covering the range from the melting line to 625 K at pressure up to 1000 MPa. *J. Phys. Chem. Ref. Data.* **20** (6), 1061-1155.
- [T&Y08] M. J. Thorpe, J. Ye. (2008). Cavity-enhanced direct frequency comb spectroscopy. *Appl. Phys. B. Lasers and Optics.* **91**, 397–414
- [Und12] R. J. Underwood, R. Cuccaro, S. Bell, R. M. Gavioso, M. Stevens, M. de Podesta. (2012). A microwave resonance dew-point hygrometer. *Meas. Sci. Tech.* **23**, 085905.
- [UNION] *UNIONGAS. An Enbridge Company*. Chemical composition of natural gas. Available from:

<https://www.uniongas.com/about-us/about-natural-gas/chemical-composition-of-natural-gas>

Last Access: 20th April 2017.

- [Veg12] D. Vega Maza, W. W. Miller, D. C. Ripple, G. E. Scace. (2012). A humidity generator for temperatures up to 200 °C and pressures up to 1.6 MPa. *Int. J. Thermophys.* **33** (8-9), 1477-1487.
- [Vic13] T. Vicente, J. G. Gallegos, R. Benyon. (2013). Los patrones nacionales de humedad en el marco de la hoja de ruta de EURAMET en el campo de la medida de humedad. 5th Spanish national metrology meeting, Madrid (Spain). 12th to 14th June.
- [VIM12] International vocabulary of metrology – Basic and general concepts and associated terms (VIM). *JCGM 200:2012. 3rd edition. 2008 version with minor corrections.*
- [Vish] Vishay Precision Group. Available online in:
<http://www.vishaypg.com/docs/63014/vpf3vpf4.pdf>
Last access 18 May 2016.
- [Wag94] W. Wagner, A. Saul, A. Pruß (1994). International equations for the pressure along the melting and along the sublimation curve of ordinary water substance. *J. Phys. Chem. Ref. Data.* **23** (3), pp. 515-525.
- [Wan09] W. Wang, Z. Li, L. Liu, H. Zhang, W. Zheng, Y. Wang, H. Huang, Z. Wang, C. Wang. (2009). Humidity Sensor Based on LiCl-Doped ZnO Electrospun Nanofibers. *Sens. Actuators B Chem.* **141**, 404–409.
- [Weg12] M. S. Węglowski. (2012). Monitoring of Arc Welding Process Based on Arc Light Emission. *Welding Processes* book edited by Dr. R. Kovacevic, publisher: InTech. DOI: 10.5772/49987.
Available from:
<https://www.intechopen.com/books/welding-processes/monitoring-of-arc-welding-process-based-on-arc-light-emission>
Accessed April 13, 2017.
- [Wel08] S. Welzel, G. Lombardi, P. B. Davies, R. Engeln, D. C. Schram, and J. Röpcke. (2008). Trace gas measurements using optically resonant cavities and quantum cascade lasers operating at room temperature. *Journal of Applied Physics.* **104**, 093115.
- [Wel47] B. L. Welch. (1947). The generalization of "student's" problem when several different population variances are involved. *Biometrika.* **34** (1/2), pp. 28–35.

-
- [Wex77] A. Wexler. (1977). Vapor pressure formulation for ice. *J. Res. Natl. Bur. Stand. A, Phys. Chem.* **81A**, pp. 5-20.
- [W&G71] A. Wexler, L. Greenspan. (1971). Vapor Pressure Equation for Water in the Range 0 to 100 °C. *Journal of Research of the National Bureau of Standards- A. Physics and Chemistry.* **75A** (3), pp. 213-245.
- [W&G76] A. Wexler, L. Greenspan. (1976) L., Vapor pressure formulation for water in range 0 to 100 degrees C. A revision. *Journal of research of NBS* **80A**, pp. 775-785.
- [W&H83] A. Wexler, R. W. Hyland. (1983). Formulations for the thermodynamic properties of dry air from 173.15 K to 473.15 K, and of saturated moist air from 173.15 K to 372.15 K, at pressures to 5 MPa, *In Thermodynamic properties of dry air, moist air and water and SI psychrometric charts.* Edited by Wexler A., Hyland R.W. and Stewart R., resulting from ASHRAE Project RP-216, ASHRAE, New York, 150-303.
- [W&P02] W. Wagner, A. Pruß. (2002). The IAPWS Formulation 1995 for the Thermodynamic Properties of Ordinary Water Substance for General and Scientific Use. *J. Phys. Chem. Ref. Data.* **31**, 387-535.
- [W&P93] W. Wagne, A. Pruß (1993). International Equations for the Saturation Properties of Ordinary Water Substance. Revised According to the International Temperature Scale of 1990. *J. Phys. Chem. Ref. Data.* **22** (3), 783-787.
- [W&S09] C. Wang, P. Sahay. (2009). Breath analysis using laser spectroscopic techniques: breath biomarkers, spectral fingerprints, and detection limits. *Sensors.* **9**, pp. 8230-8262.
- [Zam10] J. V. Zamora. Estudio del comportamiento interfacial de sistemas acuosos de alcanolaminas y sustancias térmicamente estables. (July 2010). *Departamento de Ingeniería Química y Alimentos Universidad de las Américas Puebla.* (México). Available from:
http://catarina.udlap.mx/u_dl_a/tales/documentos/lpro/vega_z_j/
Last Access: 4th March 2016.

8 ANNEXES

8.1 DRIFT SHORT-TERM

8.1.1 ELECTROLYTIC INSTRUMENT USED AS A REFERENCE

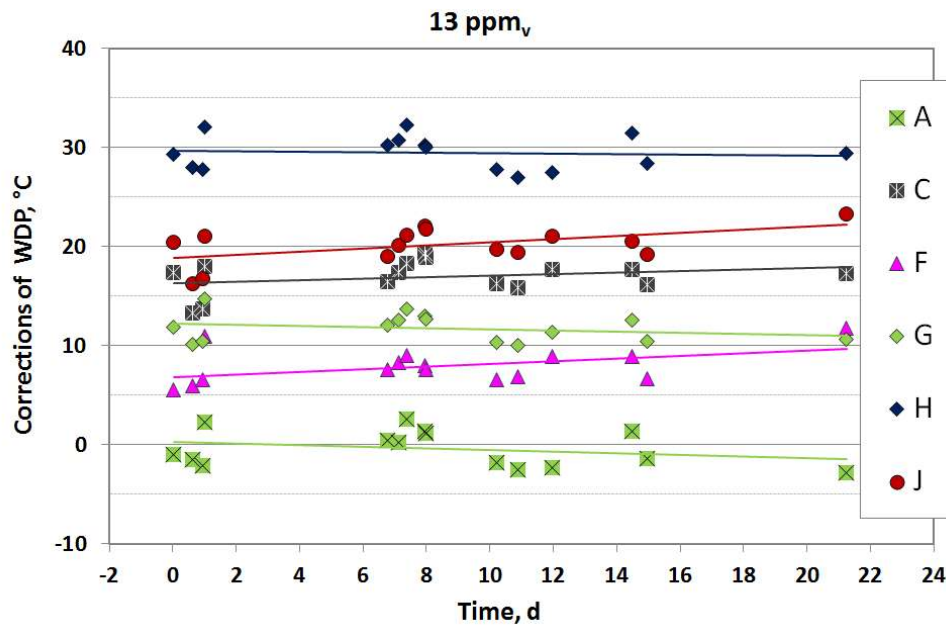


Fig. 8.1.a Short-term relative drift at nominal water content of 13 ppm_v, using electrolytic instrument as reference.

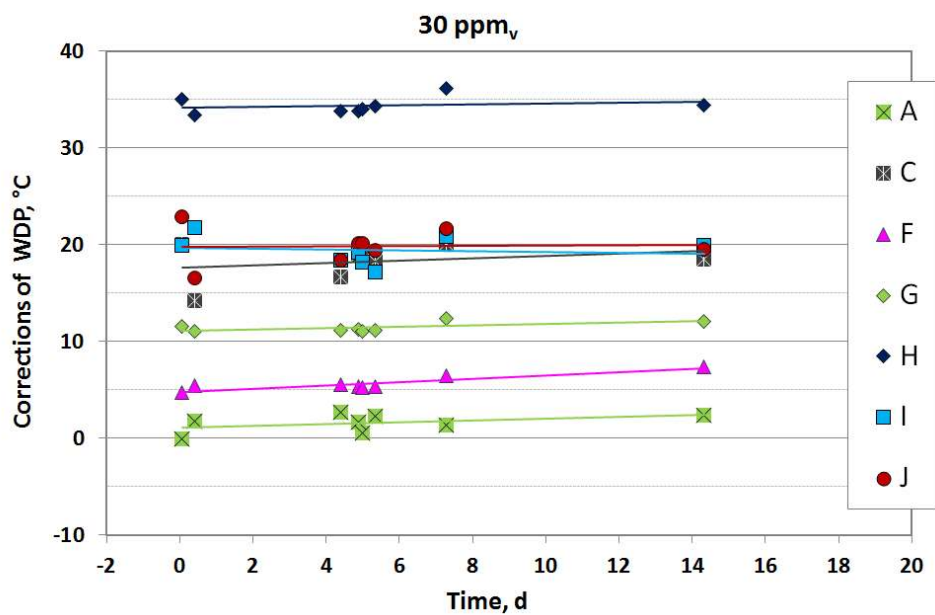


Fig. 8.1.b Short-term relative drift at nominal water content of 30 ppm_v, using electrolytic instrument as reference.

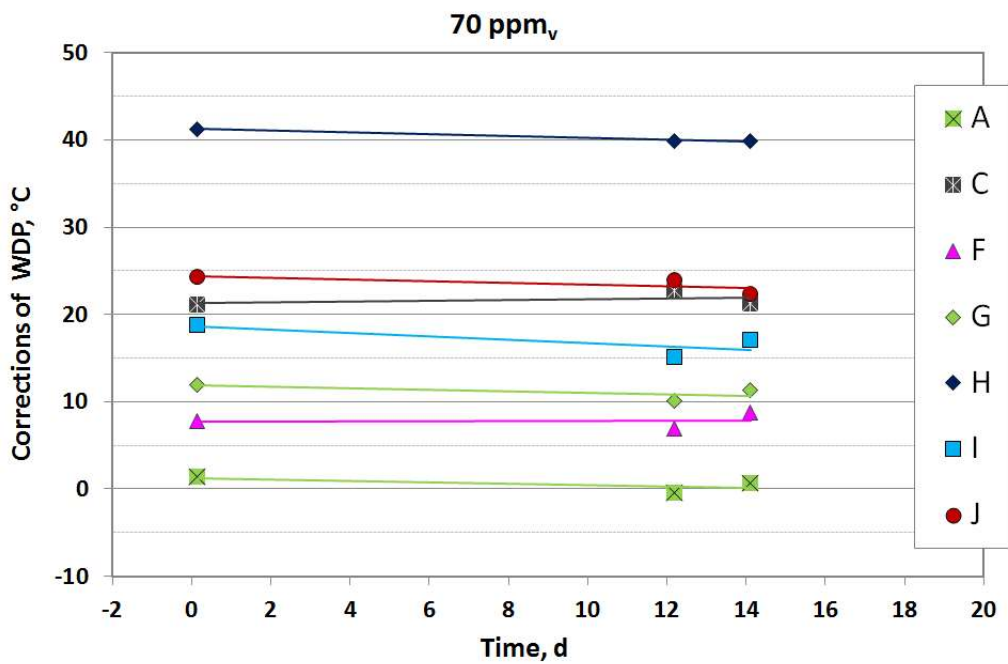


Fig. 8.1.c Short-term relative drift at nominal water content of 70 ppm_v, using electrolytic instrument as reference.

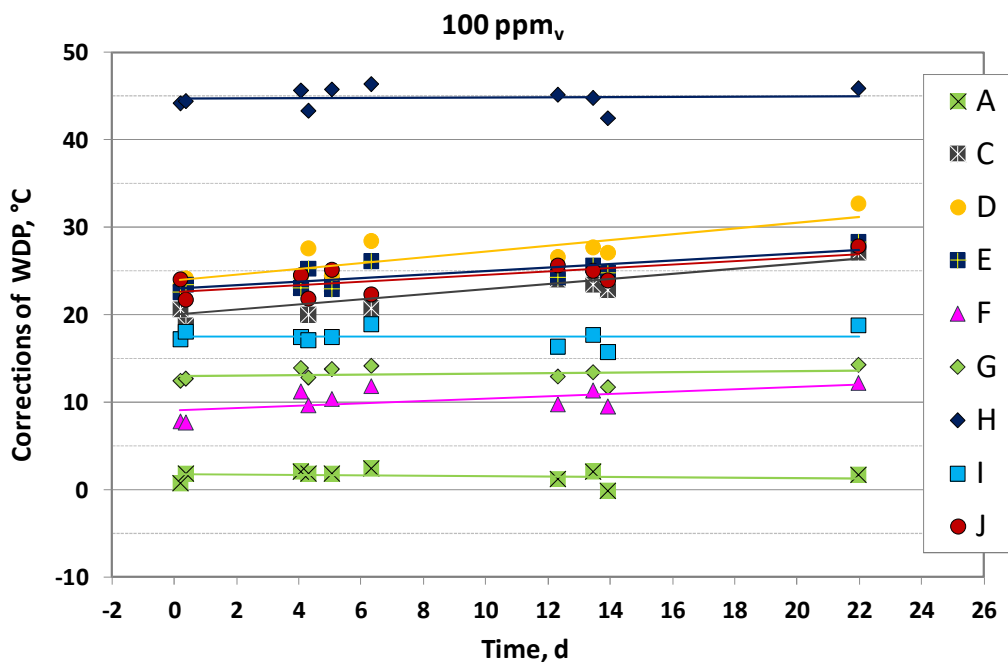


Fig. 8.1.d Short-term relative drift at nominal water content of 100 ppm_v, using electrolytic instrument as reference.

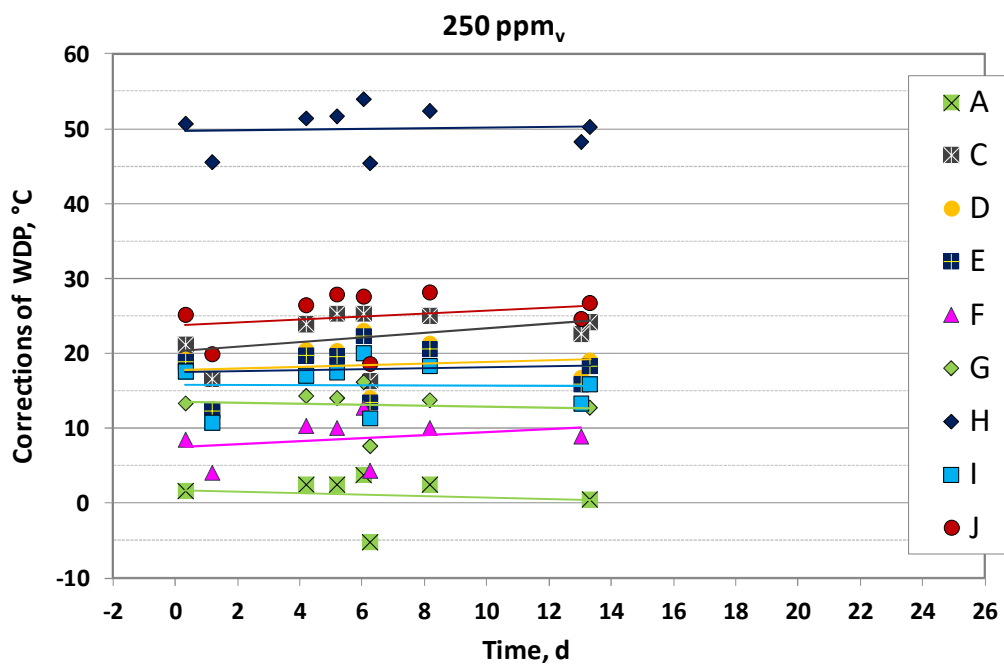


Fig. 8.1.e Short-term relative drift at nominal water content of 250 ppm_v, using electrolytic instrument as reference.

8.1.2 ELECTRICAL IMPEDANCE INSTRUMENT USED AS A REFERENCE

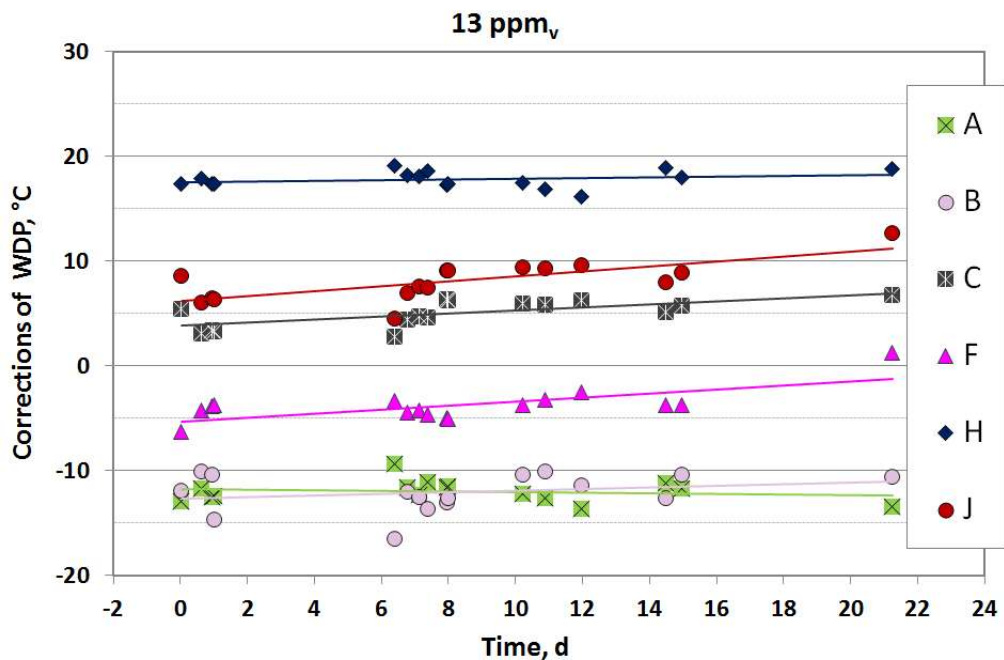


Fig. 8.1.f Short-term relative drift at nominal water content of 13 ppm_v, using an electrical impedance instrument as reference.

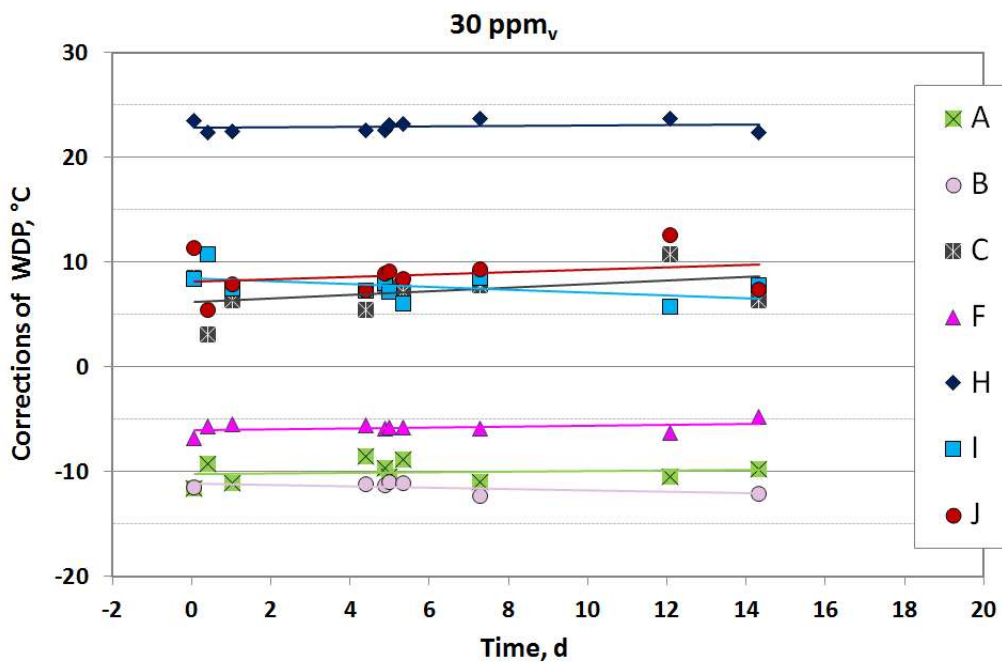


Fig. 8.1.g Short-term relative drift at nominal water content of 30 ppm_v, using an electrical impedance instrument as reference.

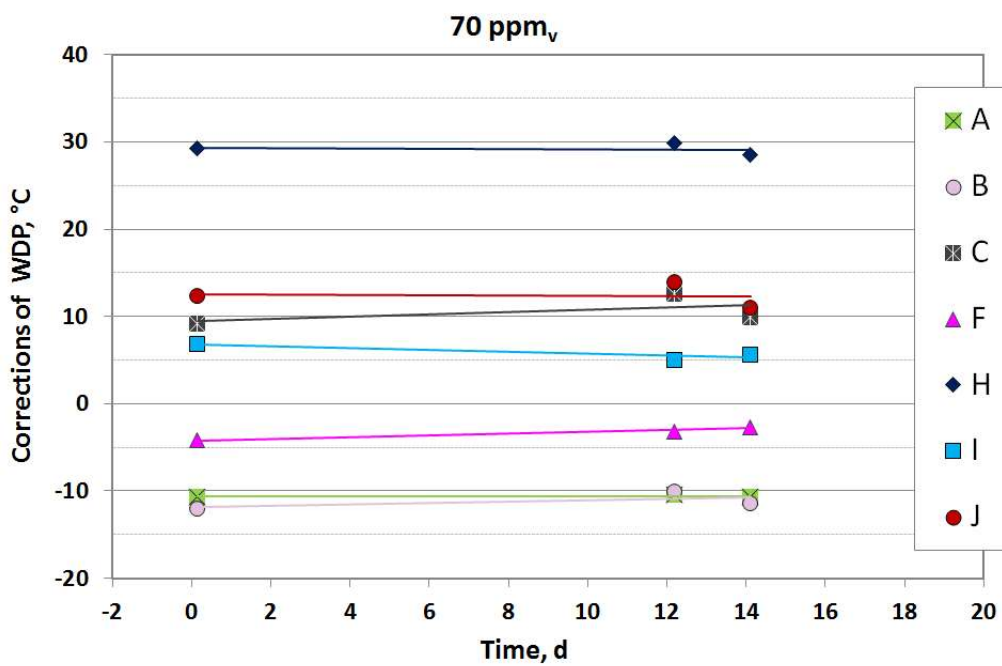


Fig. 8.1.h Short-term relative drift at nominal water content of 70 ppm_v, using an electrical impedance instrument as reference.

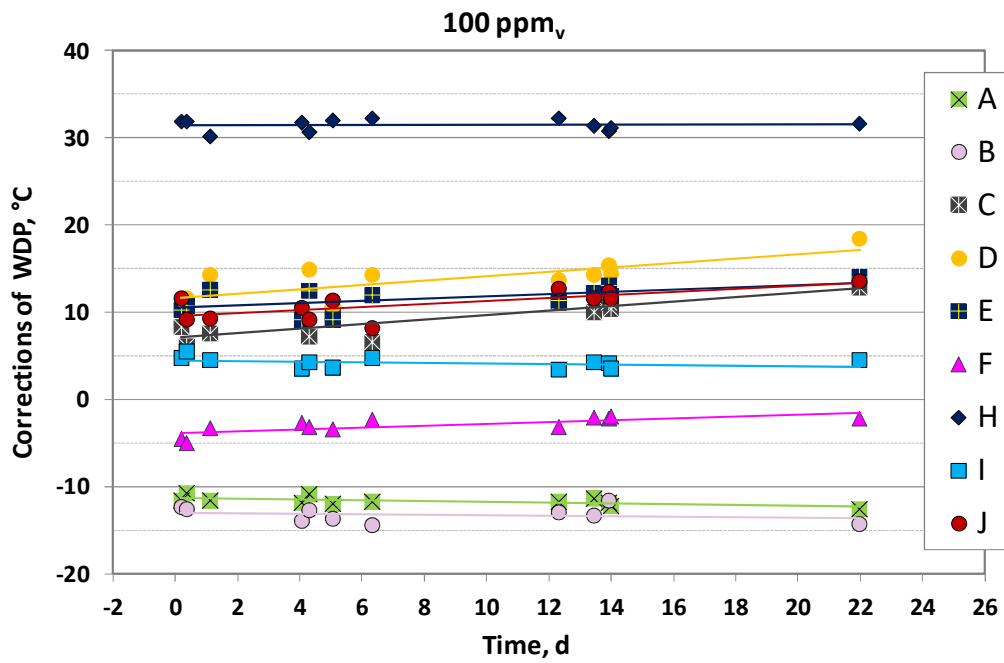


Fig. 8.1.i Short-term relative drift at nominal water content of 100 ppm_v, using an electrical impedance instrument as reference.

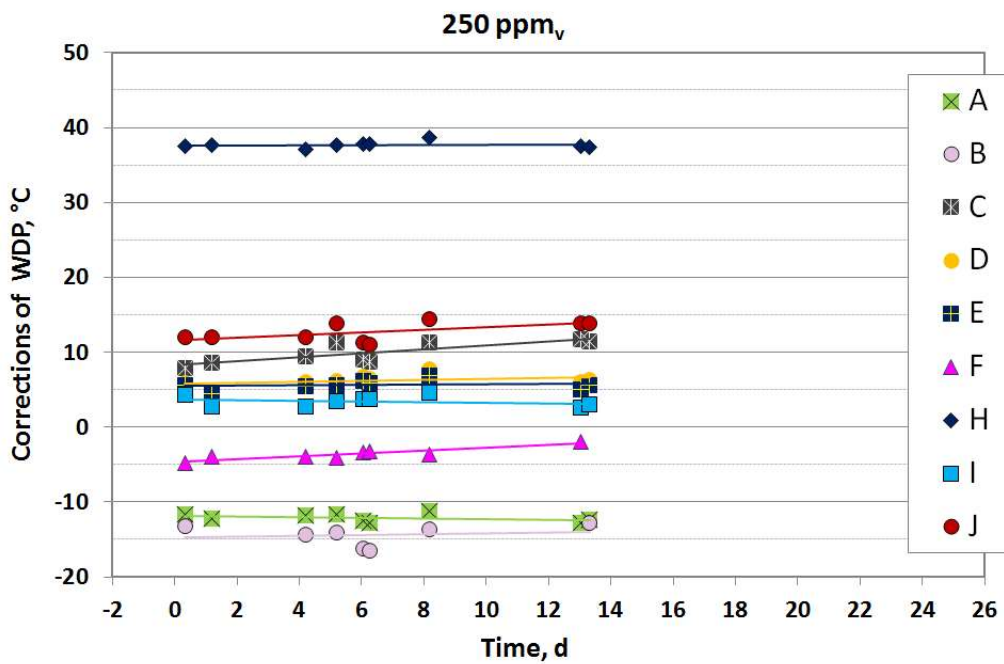


Fig. 8.1.j Short-term relative drift at nominal water content of 250 ppm_v, using an electrical impedance instrument as reference.

8.2 PUBLICATIONS

8.2.1 MEASURING HUMIDITY IN METHANE AND NATURAL GAS WITH A MICROWAVE TECHNIQUE

Int J Thermophys (2014) 35:748–766
DOI 10.1007/s10765-014-1566-8

Measuring Humidity in Methane and Natural Gas with a Microwave Technique

R. M. Gavioso · D. Madonna Ripa · R. Benyon · J. G. Gallegos · F. Perez-Sanz · S. Corbellini · S. Avila · A. M. Benito

Received: 23 July 2013 / Accepted: 30 January 2014 / Published online: 1 March 2014
© Springer Science+Business Media New York 2014

Abstract The results of microwave measurements with a quasi-spherical resonator in humid methane samples realized under laboratory conditions at the Istituto Nazionale di Ricerca Metrologica (INRiM) and under industrial conditions in a natural gas sample made available at the facilities of the Technical Manager of the Spanish Gas System and main supplier of natural gas in Spain (ENAGAS) are reported. Measurements at INRiM included vapor phase and condensation tests on methane samples prepared with amount fractions of water between 600 ppm and 5000 ppm at temperatures between 273 K and 295 K and pressures between 150 kPa and 1 MPa. ENAGAS measurements were performed at ambient temperature, 750 kPa on natural gas sampled from the pipeline and successively humidified at amount fractions of water between 140 ppm and 250 ppm for completeness of the comparison with several humidity sensors and instrumentation based on different technologies. To enhance the sensitivity of the microwave method at low humidity, an experimental procedure based on the relative comparison of the dielectric permittivity of the humid gas sample before and after

R. M. Gavioso (✉) · D. Madonna Ripa
Thermodynamics Division, Istituto Nazionale di Ricerca Metrologica, Strada delle Cacce 91,
Torino 10135, Italy
e-mail: r.gavioso@inrim.it

R. Benyon · J. G. Gallegos
Instituto Nacional de Técnica Aeroespacial, Torrejón de Ardoz, Spain

F. Perez-Sanz
Universidad de Valladolid, Valladolid, Spain

S. Corbellini
Politecnico di Torino, Torino, Italy

S. Avila · A. M. Benito
ENAGAS, SA, Zaragoza, Spain

8.2.2 AN INVESTIGATION OF THE COMPARATIVE PERFORMANCE OF DIVERSE HUMIDITY SENSING TECHNIQUES IN NATURAL GAS



An investigation of the comparative performance of diverse humidity sensing techniques in natural gas



J.G. Gallegos^{a,*}, R. Benyon^a, S. Avila^b, A. Benito^b, R.M. Gavioso^c, H. Mitter^d, S. Bell^e, M. Stevens^f, N. Böse^g, V. Ebert^g, M. Heinonen^h, H. Sairanen^h, A. Peruzziⁱ, R. Bosmaⁱ, M. Val'ková^j

^a INTA – Instituto Nacional de Técnica Aeroespacial, Madrid, Spain

^b ENAGÁS, S.A., Zaragoza, Spain

^c INRIM – Istituto Nazionale di Ricerca Metrologica, Torino, Italy

^d E+E – E+E Elektronik, Engerwitzdorf, Austria

^e NPL – National Physical Laboratory, Teddington, United Kingdom

^f UKAS – United Kingdom Accreditation Service, Feltham, United Kingdom

^g PTB – Physikalisch-Technische Bundesanstalt, Braunschweig, Germany

^h MIKES – Mittatekniikan Keskus, Espoo, Finland

ⁱ VSL – Van Swinderen Laboratory, Delft, Netherlands

^j SMU – Slovenský Metrologický Ústav, Bratislava, Slovakia

ARTICLE INFO

Article history:

Received 7 November 2014

Accepted 18 February 2015

Available online

Keywords:

Comparison

Hygrometer

Natural gas

Dew point

Humidity

Pressure

ABSTRACT

Moisture content is a key factor regardless of the activity carried out inside the natural gas industry (production, processing, transmission, etc.). Not only does the efficiency of the final product, known as heating value, decrease when the water content is high, but it can also trigger potentially dangerous conditions due to the formation of hydrates, that can block pipelines and damage pumping devices and produce other negative effects. For these reasons, accurate measurement and control of humidity is absolutely essential. However, current practice for such moisture measurements is for the devices to be calibrated at atmospheric pressure and in nitrogen or air as the matrix gas, conditions that vary significantly from those present in the actual industrial process. For that, eleven hygrometers based on different measurement principles (chilled-mirror, electrolytic sensor, a spectroscopic analyzer, polymeric and metal oxide humidity sensors) have been compared at facilities of the main carrier of natural gas in Spain, using natural gas at absolute pressures between 0.1 MPa and 6 MPa, and for a range of water content from 13 ppm_v to 250 ppm_v. Their relative performance is described in terms of the response times, long term stability, hysteresis and behaviour under large pressure changes. Most instruments, exceptions are detailed in the article, show good behaviour regarding response time, hysteresis and under sudden pressure changes. In contrast, drift can be identified in most of the aluminium oxide probes tested.

© 2015 Elsevier B.V. All rights reserved.

8.2.3 EXPERIMENTAL EVALUATION OF THE PERFORMANCE OF HUMIDITY ANALYZERS IN NATURAL GAS UNDER INDUSTRIAL CONDITIONS.

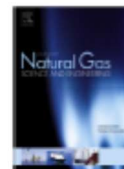
Journal of Natural Gas Science and Engineering 31 (2016) 293–304



Contents lists available at ScienceDirect

Journal of Natural Gas Science and Engineering

journal homepage: www.elsevier.com/locate/jngse



Experimental evaluation of the performance of humidity analyzers in natural gas under industrial conditions



J.G. Gallegos ^{a,*}, S. Avila ^b, R. Benyon ^a, G. McKeogh ^c, A. Stokes ^d

^a INTA – Instituto Nacional de Técnica Aeroespacial, Madrid, Spain

^b Enagás, S.A., Zaragoza, Spain

^c General Electric Company, USA

^d Michell Instruments Ltd, United Kingdom

ARTICLE INFO

Article history:

Received 4 January 2016

Received in revised form

26 February 2016

Accepted 1 March 2016

Available online 3 March 2016

Keywords:

Hygrometer

Natural gas

Humidity

Comparison

Absorption spectroscopy

Drying plant

ABSTRACT

The work reported is the continuation of the extensive comparison performed in controlled laboratory conditions using natural gas from the Spanish grid, as part of the European Metrology Research Project (EMRP) “Characterisation of Energy Gases” (ENG01-Gas, 2009). One of the outcomes of the project was the good performance of a laser absorption spectrometer with respect to other measurement technologies, in particular the absence of appreciable drift effects, exhibited by aluminium oxide (Al_2O_3) sensors that are traditionally used in the natural gas industry. The investigation was performed over a wide range of humidity content (13 ppm_v to 250 ppm_v) in ambient conditions of $23 \text{ }^\circ\text{C} \pm 3 \text{ }^\circ\text{C}$, at Enagás central laboratory in Zaragoza, Spain (Gallegos et al., 2015).

We report the subsequent comparison of two laser absorption analyzers, from different manufacturers, and a conventional Al_2O_3 installed on site in real industrial conditions, at an underground gas storage (UGS) and drying plant of Enagás in Serrablo, Spain. The performance of sensors is reported and discussed for all production stages of the plant (extraction, injection and shutdown), during which extreme ambient temperature values took place (from $-15 \text{ }^\circ\text{C}$ up to $40 \text{ }^\circ\text{C}$) and at line pressures up to 6.7 MPa. A purpose built sampling system was designed and constructed to accommodate the different instrumentation requirements and ensure an optimum metrological analysis.

The new results are compared with those previously obtained under more ideal laboratory conditions in the context assuring compliance with the contractual specifications that are to be met in Europe (EASEE-gas, 2005).

© 2016 Elsevier B.V. All rights reserved.



Universidad de Valladolid

ESCUELA DE INGENIERÍAS INDUSTRIALES

DPTO. INGENIERÍA ENERGÉTICA Y FLUIDOMECÁNICA

TESIS DOCTORAL:

**ESTUDIO COMPARATIVO DE LAS NUEVAS Y
TRADICIONALES TÉCNICAS DE MEDIDA DE HUMEDAD
EN GAS NATURAL**

Presentada por
JAIME GARCÍA GALLEGOS

Para optar al grado de doctor por la Universidad de Valladolid

Dirigida por:
Dr. JOSÉ JUAN SEGOVIA PURAS
Dr. ROBERT BENYON PUIG

Valladolid, Mayo 2017

AGRADECIMIENTOS

En primer lugar, quiero dar las gracias a mi tutor, el Dr. Robert Benyon Puig, por la oportunidad de empezar a trabajar en el mundo de la metrología, y por el enorme tiempo y esfuerzo que me ha dedicado.

Mi más sincero agradecimiento también a mi tutor Dr. José Juan Segovia Puras, por su completa disposición, paciencia y apoyo, y por su siempre sabio y útil consejo durante la orientación y redacción de la tesis.

Por supuesto, absolutamente gracias a todos mis compañeros de LabTH. Por su acogida, apoyo y enseñanzas en todos a todos los niveles, su colaboración en diversos aspectos de la tesis y por su paciencia y esfuerzo extra para permitirme dedicar tiempo suficiente a la tesis.

A todo el personal de Enagás en Zaragoza: Ángel María, Jorge y Eva. Pero especialmente a la Dra. Susana Ávila, persona clave en la estrecha colaboración mantenida con el INTA, permitiendo el acceso y uso de las instalaciones de Enagás, y ayudándome técnicamente tanto en la fase experimental como en el procesamiento e interpretación de los datos. Gracias también a Alberto Martínez y M^a. Pilar por el acceso a la planta de Almacenamiento Subterráneo de Serrablo y por haber facilitado nuestro trabajo en todo momento.

Gracias al Dr. Roberto Gavioso y al resto del personal de INRiM no sólo por las dos publicaciones conjuntas resultantes de la gran colaboración realizada en Zaragoza, sino por los buenos momentos que pasamos en la mejor compañía.

Doy las gracias al Dr. Volker Ebert por permitirme hacer mi estancia en el extranjero en su departamento en el PTB, dándome todas las facilidades para llevarlo a cabo. Así como al Dr. Norbert Bosse por su gran amabilidad y apoyo allí.

Quiero expresar mi gratitud al INTA y al Ministerio de Defensa de España por llevar a cabo programas de acceso a jóvenes investigadores, como son las becas FPI, oportunidad única para nuestro futuro al mismo tiempo que un elemento clave para asegurar el futuro de Ciencia en nuestro país.

Agradecimientos también a todo el personal de Michell Ltd., representada por Andy Benton, Andrew Stokes y Michael Summers; y de GE, representado por César Muñoz y Gerard Mc Keogh. Gracias por la estrecha comunicación y por el interés que mostraron

al final de la primera parte de esta tesis porque fue esencial para continuar la investigación un paso más allá.

Y, finalmente, pero de manera muy especial, gracias a mi familia. Porque siempre estaré eternamente agradecido a mis padres, porque todo lo que he sido, soy y seré se lo debo a ellos y a su esfuerzo. Gracias.

TABLA DE CONTENIDOS

1	INTRODUCCIÓN	3
2	OBJETIVOS.....	7
3	TECNOLOGÍAS DE MEDIDA DE HUMEDAD	9
4	MONTAJE EXPERIMENTAL Y PROCEDIMIENTOS	11
	4.1 CONDICIONES SEMI-INDUSTRIALES	11
	4.2 RESONADOR DE MICROONDAS	16
	4.3 CONDICIONES INDUSTRIALES.....	20
5	RESULTADOS	27
	5.1 RESULTADOS CONDICIONES SEMI-INDUSTRIALES.....	27
	5.2 RESULTADOS DEL RESONADOR DE MICROONDAS.....	35
	5.3. RESULTDOS CONDICIONES INDUSTRIALES	37
6	CONCLUSIONES.....	45

1 INTRODUCCIÓN

El Centro de Metrología y Calibración (CMyC) del Instituto Nacional de Técnica Aeroespacial (INTA), y más concretamente en el Laboratorio de Temperatura y Humedad (LabTH), es el Instituto Designado (DI) por el Centro Español de Metrología (CEM), como depositario de los patrones nacionales para la magnitud de la humedad.

Entre las muchas funciones que los DIs deben realizar se encuentran desarrollar y mantener dichos patrones, participar y promover la participación en proyectos de I+D, asegurar la calidad y la trazabilidad metrológica, y ofrecer soluciones, o al menos facilitar los conocimientos necesarios, para superar los grandes retos de la actualidad.

De acuerdo con las últimas hojas de ruta europeas de la humedad definidas para el primer cuarto de siglo XXI, algunos de los objetivos claves fueron: desarrollar y validar nuevas tecnologías de medidas y modelos predictivos capaces de determinar con mayor precisión ampliando los rangos de temperatura y presión y para gases no-convencionales, reproduciendo durante la calibración de los higrómetros las condiciones reales de medida, desarrollando la infraestructura metrológica necesaria para dar servicio a los grandes retos de la industria.

En este sentido, el LabTH participó en diversos proyectos de investigación entre los cuales destaca el proyecto de investigación conjunta titulado *Characterization of Energy Gases "ENG01-Gas"*, el cual está gestionado por el European Metrology Research Programme (EMRP). Por este motivo y en estas condiciones, se desarrolló parte del trabajo de esta tesis, por lo que la mayoría de los objetivos fijados en los paquetes de trabajo en los que el LabTH tenía tareas asignadas a este proyecto son compartidos en este trabajo.

Entre los muchos objetivos planteados en dicho proyecto, el INTA participó principalmente en el estudio comparativo de las diferentes tecnologías de medida de la humedad sobre gas natural (GN) en condiciones reales de trabajo, aportando soluciones metrológicas a los grandes problemas y retos derivados de la humedad en la industria gasista. Éstas fueron las condiciones en las que se desarrolló la tesis aquí presentada.

El gas natural es un combustible fósil constituido por una mezcla compleja de hidrocarburos ligeros y trazas de pesados (C_{6+}), además de CO_2 , N_2 , H_2O e incluso azufre. Es una fuente de energía no renovable, pero que cuenta con una buena opinión pública

debido las bajas emisiones de CO₂, NO_x and SO_x, que generan problemas medioambientales mundiales como: el efecto invernadero, la lluvia ácida y el calentamiento global de la Tierra. Por todo ello, es considerado más limpio y respetuoso con el medio ambiente y los seres vivos. Lo cual unido a una alta capacidad energética y un manejo relativamente seguro, lo convierten en una fuente energética con grandes perspectivas de futuro en detrimento de otros combustibles fósiles, como el carbón.

Sus aplicaciones se extienden principalmente a la generación energética, al sector doméstico (como fuente de luz y calor, y para cocinar), sector industrial (tanto como materia prima propiamente, como fuente de energía), y como medio de transporte. Por todo ello, ciertas predicciones lo sitúan como la segunda fuente energética mundial para el 2035, con una aportación del 25 %.

Una de las características principales de cualquier fuente de energía es su eficiencia energética, en el caso concreto de los combustibles fósiles se mide a partir del *poder o la capacidad calorífica*. Es éste punto uno de los grandes problemas de la presencia de agua en el gas, ya que disminuye su eficiencia afectando, en último lugar, al rendimiento de cualquier proceso en el que esté involucrado.

La presencia de agua en fase líquida puede dar lugar a multitud de efectos secundarios indeseados como: la rotura de elementos móviles en compresores y turbinas y formación de sustancias ácidas y corrosivas. Todo ello reduciría la esperanza de vida de multitud de materiales e instrumentos, por lo que aumentarían los costes y tiempos empleados en las tareas de reparación, mantenimiento y limpieza de las instalaciones.

Además, la presencia de agua líquida combinada con altas p y bajas T , puede dar lugar a la formación de hidratos, que aumentarán la pérdida de carga del gas durante su transporte y, por ende, los costes de bombeo. Incluso podrían llegar a acumularse hasta provocar el bloqueo de tuberías, llegando incluso a producir situaciones de alto riesgo, como son las explosiones. Por tanto, controlar adecuadamente el contenido en agua (WC) del GN es esencial para asegurar las propiedades finales del gas comercializado, pero también durante su procesamiento y distribución.

Por otro lado, la humedad modifica los comportamientos de condensación del gas, pudiendo dar lugar a la condensación de hidrocarburos, (*hydrocarbon dew point* –HCDP), agua (*water dew point* –WDP) o una mezcla de ambos, dependiendo de las condiciones

de p y T y la composición del gas. Todo ello estaría relacionado con la posición relativa de la curva de la *envolvente de fases* del GN y la curva de saturación del agua pura.

El proceso de secado del gas es una etapa clave, ya que permite conocer y controlar de forma precisa y fiable la humedad del gas durante todas las etapas de su procesamiento y distribución. Se estima que hasta un 15 % de los costes de procesamiento del GN son derivados de procesos de secado y prevención de hidratos.

En España, Enagás se encarga del desarrollo y mantenimiento de la infraestructura gasista nacional y de la operación y gestión de toda la compleja red principal. Está certificada por la Comisión Europea como Transmission System Operator (TSO), garantizando así su independencia frente a productores, consumidores y comerciantes. Enagás es además responsable de la optimización de la eficiencia energética en todas las etapas de procesamiento del gas, y participa de forma activa en proyectos nacionales e internacionales de I+D, por lo que fue un colaborador clave para el INTA en el EMRP previamente mencionado y esencial para el desarrollo total de esta tesis.

HC y WDP pueden ser obtenidos de dos formas: empíricamente utilizando los instrumentos de medida adecuados y mediante el cálculo de modelos teóricos predictivos. Por tanto, existen dos líneas de investigación con impacto directo sobre la industria del GN: desarrollar modelos termodinámicos capaces de describir el comportamiento de fases; o desarrollar nuevas tecnologías de medida de humedad o evolucionar las existentes.

Existen infinidad de trabajos publicados para describir las propiedades termodinámicas y equilibrios de fases de mezclas complejas, pero demostradas para ciertas condiciones de p , T y la composición, que no siempre se dan en la industria. En esos casos se deben realizar extrapolaciones, que bien pueden derivar en errores de WDP de hasta 10 °C, inaceptables para la industria gasista donde una precisión inferior al 3 °C es reclamada. Además, no existen suficientes trabajos centrados en el desarrollo de las propias tecnologías de medida. Por todo ello, esta tesis se centró en esa segunda línea de investigación.

Tradicionalmente, dos son las técnicas utilizadas en la industria gasista para medir la humedad del gas: los higrómetros de condensación de espejo enfriado y los sensores capacitivos. Sin embargo, ambas tecnologías presentan una serie de inconvenientes que pueden derivar en la obtención de medidas erróneas y, por tanto, de un mal control de la

humedad y consecuentemente todos sus problemas derivados. Los primeros requieren de un sistema previo de despresurización del gas hasta niveles atmosféricos, pudiendo modificar enormemente el comportamiento de condensación del gas, mientras que los segundos sufren fuertes fenómenos de deriva, demostrado en la literatura, dando lugar a lecturas más secas del gas.

Por otro lado, las condiciones de calibración de estos sensores (bajas presiones y con nitrógeno u aire) distan mucho de las condiciones de trabajo en las que son utilizados, por lo que su rendimiento en GN puede ser muy diferente. Por último, es necesario establecer unos criterios para definir unos patrones de transferencia aceptados por fabricantes, distribuidores y consumidores, que permitan determinar de forma precisa y fiable la humedad del GN, asegurando por tanto su calidad.

En resumen, la metrología juega un rol esencial como elemento clave para superar los grandes retos del sector energético, maximizando el rendimiento de sus procesos, especialmente de las fuentes de energía no renovables. Por ello, esta tesis se centró en la medida de la humedad mediante el uso directo de las diferentes tecnologías disponibles en la actualidad, tanto aquellas tradicionalmente utilizadas como las más novedosas, además de proporcionar el apoyo metrológico necesario con el fin de desarrollar y validar nuevos métodos de medida altamente precisos que cumplan con los requerimientos de la industria gasista mundial.

2 OBJETIVOS

Por lo tanto, teniendo en cuenta que el LabTH del INTA es el DI español en el campo de la humedad; su participación en proyectos nacionales e internacionales de investigación, como el "ENG01-Gas. Characterization of Energy Gases "como parte del Programa Europeo de Investigación Metrológica (EMRP); y los objetivos marcados en las hojas de ruta europea de la humedad para el primer cuarto de siglo XXI. Como resultado de todas estas condiciones de contorno, el objetivo inherente de esta tesis fue proporcionar el soporte metrológico requerido por la industria del gas natural en el campo de la higrometría, con el fin de superar los grandes retos de la actualidad.

En esta línea, los objetivos específicos de esta tesis son los siguientes:

- Desarrollar y validar nuevos métodos de medición altamente precisos para lograr la incertidumbre requerida por la European Association for the Streamlining of Energy Exchange – Gas (EASEE-gas) [EAS05] para las medidas de humedad del GN que es introducido en la red europea de suministro. Esto incluye participar en el desarrollo de prototipos de medida de humedad basados en nuevas y prometedoras tecnologías de detección como la resonancia por microondas y la espectroscopía de absorción.
- Elaborar nuevos métodos y protocolos de medida para comparar la mayoría de los sensores de humedad comúnmente utilizados en las condiciones industriales de monitorización del gas natural, frente a las nuevas tecnologías de detección previamente desarrolladas aquí.
- Diseñar y construir las instalaciones necesarias para obtener nuevos datos empíricos que permitan comparar el comportamiento de las diferentes tecnologías de medida de humedad en GN y bajo condiciones industriales reales.
- Evaluar el comportamiento dinámico de las tecnologías de detección de humedad estudiadas, caracterizando su respuesta frente a variaciones de algunas de las variables de proceso, como por ejemplo: presión de línea, contenido de agua y composición de gas natural, debido a las interacciones entre agua y otras moléculas de gas.
- Dar soporte técnico para mejorar la validez y fiabilidad durante el muestreo de las medidas de la humedad, y desarrollar métodos para armonizar los procesos de calibración

industrial. Aumentando de esta manera, el control preciso de la humedad en la industria del gas natural.

- Validar el rendimiento de todas las técnicas de detección de humedad disponibles, durante su uso en diversas etapas del proceso de gas natural, por medio de la validación de higrómetros representativos para cada clase.

- Lastly and as a part of development of the European metrology infrastructure, it should be given traceability to humidity sensors studied, through the new humidity standards for high temperatures and pressures in non-air gases and steam, whose development was carried out by other NMIs inside of EMRP "ENG01-Gas" project, during the course of this thesis.

- Por último y como parte del desarrollo de la infraestructura metrológica europea, se debe dar trazabilidad a los sensores de humedad estudiados, a través de nuevos patrones de humedad para altas temperaturas y presiones y sobre gases no convencionales y vapores, los cuales fueron desarrollados por otros NMIs también dentro del proyecto EMRP "ENG01-Gas", simultáneamente al desarrollo de esta tesis.

3 TECNOLOGÍAS DE MEDIDA DE HUMEDAD

A lo largo de la historia muchas técnicas han sido desarrolladas para la medida de la humedad en gases, las cuales están basadas en diferentes principios de medida. En esta tesis las técnicas de medidas evaluadas han sido divididas en dos grandes grupos: aquellas tradicionalmente utilizadas en el mundo de la higrometría, y las nuevas técnicas desarrolladas actualmente.

Dentro de las técnicas tradicionalmente utilizadas, las tecnologías de medida estudiadas aquí fueron: los sensores de impedancia eléctrica basados en óxidos metálicos, los electrolíticos y los higrómetros de condensación. Mientras que las nuevas tecnologías cuyo rendimiento fue evaluado fueron: sensores capacitivos basados en materiales poliméricos, la espectroscopía de absorción y la resonancia por microondas.

Todas las tecnologías estudiadas son descritas atendiendo a los principios de medida, a su descripción física, a los diferentes tipos y clasificaciones que existen, y a sus principales características.

A lo largo de toda la tesis se comparó el rendimiento de 16 medidores de humedad, basados en 6 tecnologías de medida diferentes. Debido a la gran heterogeneidad de instrumentos analizados, todos ellos fueron ampliamente descritos previamente, ya que sus especificaciones técnicas y características eran claves a la hora de diseñar los montajes y procedimientos experimentales que serían llevados a cabo.

Existen numerosas formas de expresar la humedad, en parte debido a la gran diversidad de métodos de medida utilizados. En la industria del GN las dos formas más utilizadas son: el contenido en agua (WC), medido como la relación de volúmenes en partes por millón, *ppm_v*; y la temperatura de rocío (WDP) que indica la temperatura a la cual empieza a producirse la condensación del agua. Debido a que ambas expresiones son utilizadas indiferentemente y dependiendo del tipo de higrómetro se dan de una forma u otra. Se utilizó la Norma Internacional ISO 18453:2005, desarrollada por el European Gas Research Group (GERG) y basada en el modelo de Peng Robinson, para convertir las medidas a la misma expresión y comparar adecuadamente las tecnologías.

Tabla 8.2.a Lista de todos los medidores de humedad estudiados, especificando el modelo, el fabricante, la tecnología de medida, el número de equipos disponibles y las instalaciones en las que fueron implementados: Zaragoza y Serrablo (*). Los códigos de los equipos son utilizados durante la sección semi-industrial para hacer referencia a cada equipo/tecnología con mayor facilidad.

Fabricante	Modelo	Tecnología	Cantidad	Código
Michell	Condumax II HCDP/WDP	Condensación / Al ₂ O ₃	1	L1/L2
	Easidew Transmitter	Al ₂ O ₃	2	D,E
	Easidew Pro I.S.	Al ₂ O ₃	1	F
	TDL600	TDLAS	1(*)	
GE	HygroPro	Al ₂ O ₃	1	G
	Aurora	TDLAS	2 (1*)	A
	MISII	Al ₂ O ₃	1 (*)	
Alpha	DS2000	Al ₂ O ₃	1	C
Shaw	SDT DP Transmitter	Al ₂ O ₃	1	H
	Superdew 3	Al ₂ O ₃	1	J
Meeco	Accupoint 2 LP	P ₂ O ₅	1	B
E+E	EE371	Polimérico	1	I
MBW	DP3D	Condensación	1	K
INRiM	QSR	Resonador de MW	1	

4 MONTAJE EXPERIMENTAL Y PROCEDIMIENTOS

Esta tesis, eminentemente experimental, está dividida en dos grandes bloques. El primero, denominado “condiciones semi-industriales” y el segundo “condiciones industriales”. Esta diferencia se debe a que en el primero se modifican diversas variables de las que depende la medida de la humedad, con el fin de hacer un estudio más exhaustivo mientras que, en el segundo, los equipos son probados en condiciones industriales reales y extremas, y en todos los modos de procesamiento de la planta.

Además, debido a la gran peculiaridad del resonador de microondas (prototipo en fase de desarrollo) basado en una tecnología completamente novedosa en el campo de la higrometría, con su sistema propio de acondicionamiento previo de la muestra y una complejidad inherente en su manipulación y análisis posterior de los datos. Por todo ello, esta tecnología de medida fue analizada de forma particular en secciones individuales.

4.1 CONDICIONES SEMI-INDUSTRIALES

Este bloque experimental se desarrolló en las instalaciones de Enagás de Zaragoza, concretamente en su Centro de I+D, donde se encontraba su antiguo laboratorio de higrometría. Enagás fue un colaborador clave durante todo el desarrollo de la tesis, permitiendo tener acceso a sus instalaciones, al gas natural y gracias a todos sus conocimientos en la materia.

Estas instalaciones se encuentran en un punto estratégico de la red principal nacional, ya que pueden recibir gas de diversos orígenes como, por ejemplo: gas regasificado (LNG) procedente de los barcos metaneros que desembarcan en la costa catalana, GN procedente de centro Europa mediante las conexiones con Francia y GN extraído de almacenamientos subterráneos. Por este motivo, las propiedades del gas podrían ser muy diferentes dependiendo de la procedencia del mismo.

Además, dichas instalaciones contaban con las máximas medidas de seguridad durante el manejo del gas, como: detectores, sistemas de corte eléctrico y de suministro de gas automáticos, sistemas de protección y lucha antincendios y sistema de ventilación.

El banco de pruebas fue diseñado de acuerdo con las normativas, guías y recomendaciones para instalaciones de gas presurizadas y muestreo del GN.

La primera norma para diseñar el montaje experimental de esta sección fue agrupar a los 14 equipos analizados en función de sus rangos de presión. De esta forma, se clasificaron en función de tres valores nominales: el nivel máximo dado por el muestreo directo a la red principal (aprox. 5.8 MPa), un nivel intermedio cercano a los valores típicos de *cricondentherm* (2.8 MPa) y un nivel inferior ajustado a 0.55 MPa para aquellos equipos que no soportaban altas presiones. Una vez organizados los equipos por sus rangos de presión, fueron divididos en función de sus rangos de caudal, colocando en las mismas líneas de muestreo a aquellos que tuvieran los mismos rangos. Además de estos criterios, la instalación debía permitir medir todos los equipos a la vez y tener control sobre las siguientes variables del proceso: presión, caudal y humedad del gas.

El diagrama de bloques mostrado abajo, indica las diferentes secciones de la instalación y cuáles fueron sus funciones principales. La primera etapa consistía en monitorizar y registrar las condiciones del gas de entrada: presión, HCDP y WDP. Esta función fue llevada a cabo por el único equipo capaz de medir dichas variables a la vez, el Condumax II, por lo que quedó fuera de la comparativa con respecto al resto de higrómetros.

La segunda etapa se encargaba de la adecuación de las propiedades del gas (humectación, filtrado y ajuste de presión). La tercera etapa era el propio proceso de medida de todos los equipos estudiados, atendiendo a las características individuales propias de cada equipo de medida. Y en la cuarta, se ajustaban los caudales que pasaban a través de los medidores y finalmente se despresurizaban todas las líneas para su posterior venteo.

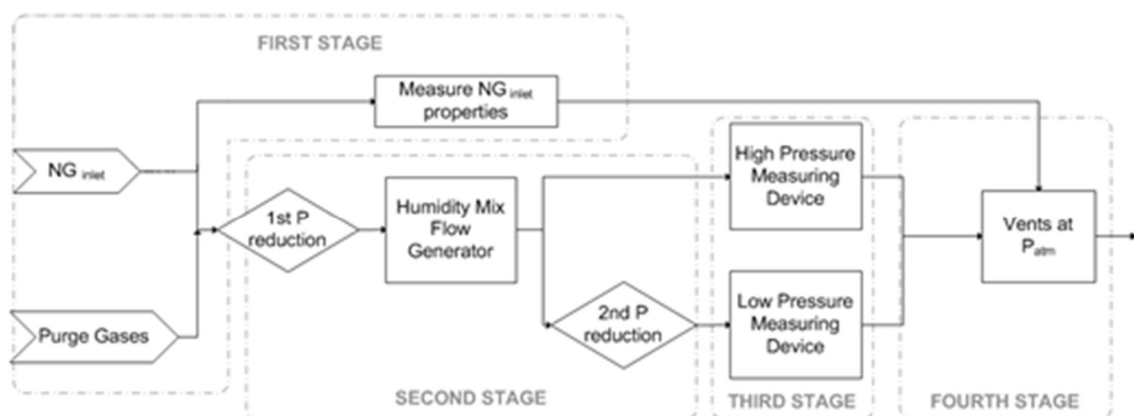


Fig. 4.1.a Esquema de las diferentes etapas del montaje experimental construido para estudiar el rendimiento de numerosas tecnologías de medida en condiciones semi-industriales.

4. MONTAJE EXPERIMENTAL Y PROCEDIMIENTOS

El resonador de microondas fue instalado en el grupo de equipos de alta presión, pero completamente en paralelo al resto de instrumentos. De esta forma se podría trabajar independientemente con toda su compleja instalación auxiliar sin necesidad de influir en el resto del montaje.

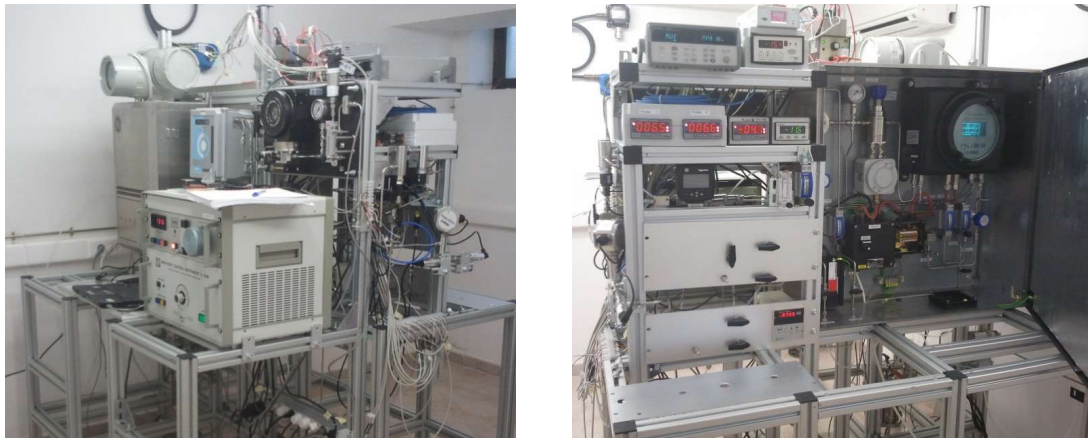


Fig. 4.1.b Imágenes reales del banco de ensayos utilizado durante el primer bloque experimental de esta tesis. Toda la instalación asociada al resonador de MW no está incluida en estas fotos.

Fig. 4.1.j muestra el diagrama P&I de la instalación donde se indica todo el montaje y la instrumentación asociada. En ella se pueden ver los diferentes reguladores de presión, con sus correspondientes indicadores y transmisores. La sección de humectación del gas protagonizada por el generador de humedad (S-01), las tres secciones de equipos (baja y alta presión, y el resonador de MW) y su posición en las diferentes líneas de muestreo.

El generador de humedad era un elemento clave de la instalación, ya que era esencial para comprobar el rendimiento de los equipos en un rango útil para la industria, puesto que el gas proveniente de la red principal estaba extremadamente seco (aprox. 6 ppm_v), muy próximo a los límites de detección de la mayoría de los equipos estudiados.

Se decidió utilizar un generador de tipo de mezcla de flujo cuyo elemento principal era el saturador, cedido por Enagás y utilizado previamente para fines similares. El generador fue caracterizado a partir de la relación de caudales entre la línea seca, que evita el saturador, y la línea húmeda que atravesaba el saturador. De esta forma se definieron los diferentes valores nominales de WC que iban desde 13 ppm_v, hasta 250 ppm_v.

Durante las medidas en condiciones semi-industriales se registraron las condiciones ambientales a las cuales estaban sometidos los equipos durante las pruebas, con el fin de

detectar posibles efectos de deriva, o cambios de comportamiento y rendimiento. Se registraron los valores de la presión atmosférica, la temperatura y la humedad del laboratorio. Fig. 4.1.o muestra el aspecto de la sección de humidificación de la planta.

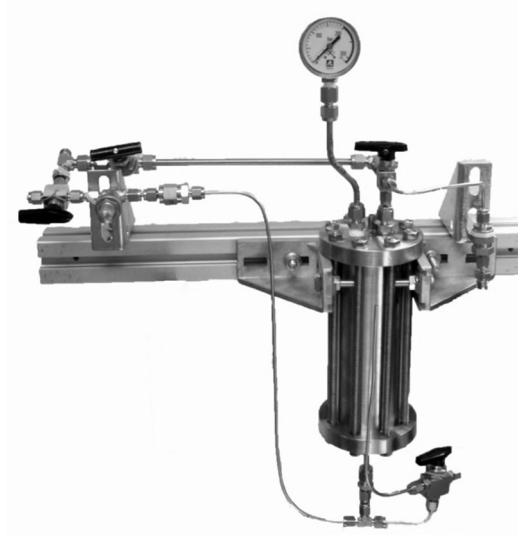


Fig. 4.1.c Imagen real del generador de humedad de mezcla de flujos construido.

Toda la información procedente tanto de las lecturas de los equipos, como de las variables de proceso y magnitudes medidas fueron registradas para su posterior análisis. Se registraron tanto las salidas analógicas como las digitales de todos los equipos disponibles.

4. MONTAJE EXPERIMENTAL Y PROCEDIMIENTOS

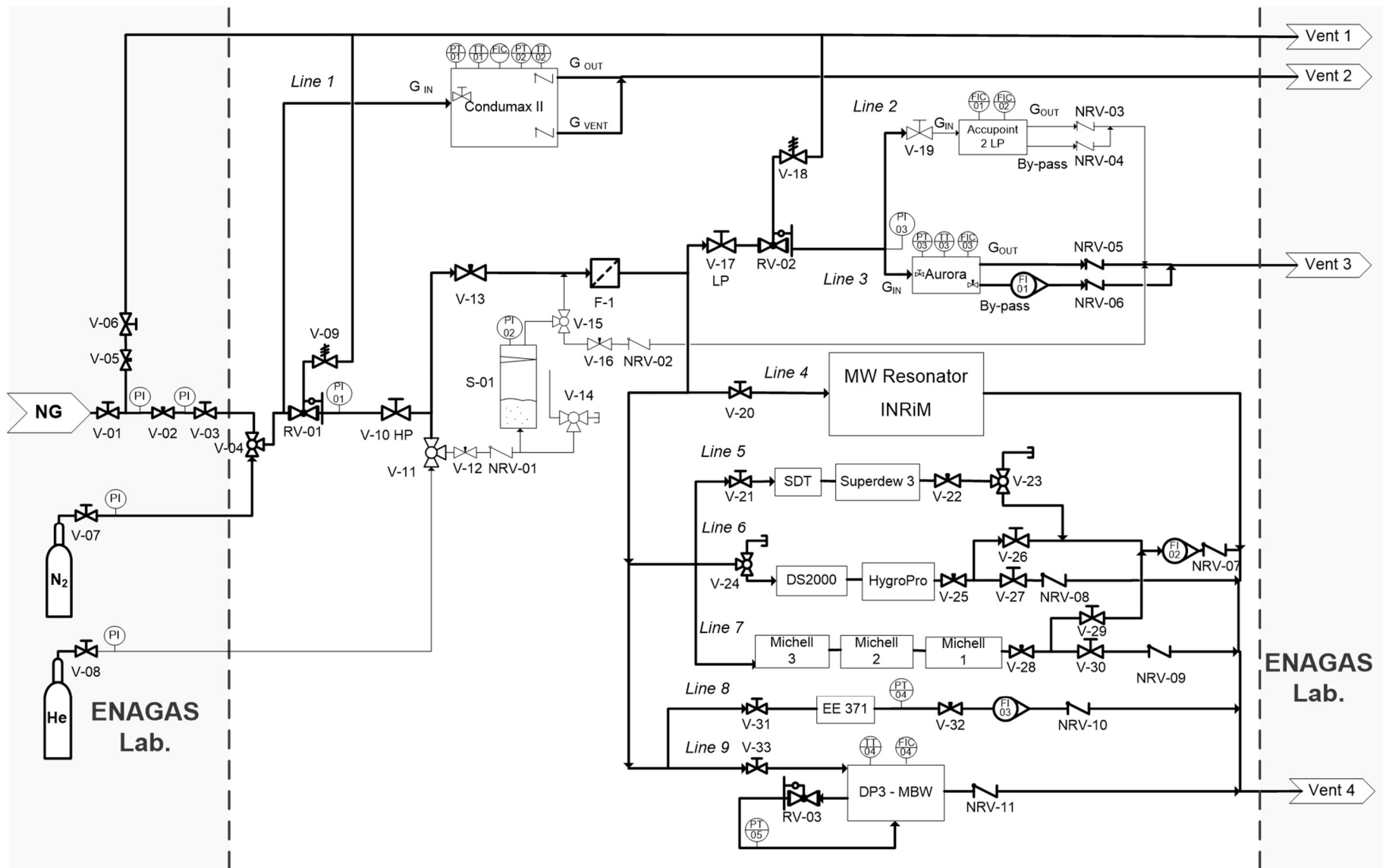


Fig. 4.1.d Diagrama P&I de la instalación completa construida en Zaragoza para llevar a cabo el estudio del comportamiento de los sensores bajo condiciones semi-industriales.

Dos fueron los tipos de pruebas realizados en estas instalaciones: pruebas a humedad variable y prueba de cambios de presión a humedad constante. Dentro del primer grupo de pruebas se generaron en numerosas ocasiones hasta 11 valores hominales diferentes de humedad dentro del rango previamente indicado. De esta forma se pudieron analizar las siguientes propiedades: tiempos de respuesta (y comparación entre salidas analógicas y digitales en el caso de haberlas), efectos de histéresis y análisis de deriva.

En el estudio de los equipos ante cambios de presión, se evaluó su comportamiento sólo para un valor nominal de humedad intermedio dentro del margen estudiado (100 ppm_v) cuando existe un fuerte cambio de presión en la línea del gas. El cambio de presión fue entre los niveles medio y superior antes explicados y sólo se realizó con aquellos equipos capaces de soportar el valor máximo de presión (5.8 MPa).

Debido a que a lo largo de toda esta comparativa no se disponía de un patrón, puesto que era uno de los grandes retos de la industria gasista ya comentado en la introducción. Por ello, la mayoría de las propiedades evaluadas tienen un carácter relativo respecto al equipo considerado como referencia en cada caso. Se evaluaron varios equipos de diferentes tecnologías y en función a varios criterios para considerar los mejores equipos como referencia y eliminar cualquier posible malinterpretación de los resultados derivado de este problema.

Durante toda la fase previa al montaje, se elaboraron todos los protocolos relacionados con la realización de las diferentes pruebas experimentales, de puesta en marcha y apagado de la instalación, ajuste de las magnitudes fijadas, tareas de limpieza y mantenimiento, pruebas de fugas, protocolos de seguridad, etc.

4.2 RESONADOR DE MICROONDAS

En este apartado se explica el fundamento teórico de esta tecnología de medida de humedad, completamente innovadora y en desarrollo, una descripción rápida de su instalación asociada y las pruebas previamente realizadas sobre mezclas binarias antes de dar el salto a medidas en GN.

El fundamento teórico de esta tecnología se basa en la tendencia de un material a ser polarizado por un campo eléctrico, reduciendo al mismo tiempo el propio campo eléctrico. La *permisividad eléctrica*, ϵ , de un material es la propiedad física que describe

4. MONTAJE EXPERIMENTAL Y PROCEDIMIENTOS

como un campo eléctrico afecta y es afectado por un material. Se puede definir la permisividad eléctrica de una mezcla, suponiendo que no está constituida por ningún componente magnético, como:

$$\epsilon_{\text{mix}} = \left(\frac{f_0}{f_p} \right)^2 \quad \text{Eq. 4.2.a}$$

donde f_0 and f_p son las frecuencias de resonancia obtenidas experimentalmente de la cavidad vacía y llena con la mezcla a la misma presión y temperatura.

La permisividad eléctrica también puede ser medida a partir de la *polaridad molar*, \wp , y la densidad de la mezcla a partir de la siguiente expresión:

$$\epsilon_{\text{mix}} = \frac{2 \rho_{\text{mix}} \wp_{\text{mix}} + 1}{1 - \rho_{\text{mix}} \wp_{\text{mix}}} \quad \text{Eq. 4.2.b}$$

La densidad de la mezcla puede ser definida como: $\rho_{\text{mix}} = \rho_0 / (1 + B_{\text{mix}} \rho_0)$ donde

$\rho_0 = p/RT$. B_{mix} es el segundo coeficiente del virial, que es función de la fracción mola de agua y para una mezcla binaria se define como:

$$B_{\text{mix}} = x_w^2 B_{ww} + x_2^2 B_{22} + 2x_w x_2 B_{w2}$$

A partir de estas dos expresiones es posible averiguar la fracción molar de agua de la mezcla. Existe un método para obtener el WC para mezclas binarias, sin embargo, dicho método no es válido para mezclas multi-componentes como el GN.

Por ello, a lo largo de esta tesis se desarrolló y validó un nuevo método de medida para mezclas complejas. Este método se basa en los modos de propagación de la resonancia electromagnética: modo magnético transversal (TM modo) y eléctrico transversal (TE modo). Cada uno de estos modos aparecen como tripletes, es decir, tres picos de resonancia, los cuales se observan cuando la cavidad resonante no es perfectamente esférica. El grupo de investigación del INRiM liderado por Roberto Gavioso definió la siguiente expresión para obtener la permisividad eléctrica relativa de cualquier gas puro o mezcla:

$$\epsilon_r = \frac{1}{\mu_r} \left(\frac{\langle f_{ln}^\sigma + g_{ln}^\sigma \rangle_0}{\langle f_{ln}^\sigma + g_{ln}^\sigma \rangle_p (1 - k_T^p / 3)} \right)^2 \quad \text{Eq. 4.2.c}$$

donde: $\langle f \rangle$ es el promedio de la frecuencia, $\langle g \rangle$ es el promedio de la mitad del ancho del triplete degenerado medido a la misma temperatura T tanto

en el vacío (subíndice 0) como a presión, p ; μ_r es la *permeabilidad magnética relativa*; k_T es el *factor de compresibilidad isotérmica* del metal del resonador; σ , subíndice que describe el tipo de modo.

Gavioso *et al.* definieron las siguiente ecuaciones para determinar x_w :

$$\varepsilon_{mix}(p, T) = \varepsilon_{dry}(p, T) \left(\frac{f_{dry}(p, T)}{f_{mix}(p, T)} \right)^2 \quad \text{Eq. 4.2.d}$$

Los subíndices *dry* y *mix* indican las frecuencias de resonancia (obtenidas experimentalmente) y la permeabilidad magnética (a partir de la Eq. 4.2.a) tanto cuando fluye a través del resonador el gas completamente seco como húmedo, respectivamente.

A partir de las densidades y polaridades de la fracción seca y húmeda del gas objetivo y mediante diversas operaciones se obtiene la ecuación definitiva para obtener el WC de cualquier sustancia gaseosa:

$$x_w = \frac{\left(\frac{\varepsilon_{mix} - 1}{\varepsilon_{mix} + 2} \frac{\varepsilon_{dry} + 2}{\varepsilon_{dry} - 1} \right) - 1}{\rho_w / \rho_{dry} - 1} \quad \text{Eq. 4.2.e}$$

El montaje asociado al resonador debía ser capaz de controlar las siguientes variables: presión, temperatura y flujo. Además, debido al nuevo método de cálculo debía incluir una unidad de secado del gas, para poder calcular la permisividad de la mezcla seca, ε_{dry} .

En la Fig. 4.2.a se muestra toda la instalación asociada al resonador de MW. Tanto el burbujeador, utilizado de la misma manera que el generado antes explicado, como el sistema de bombeo, sólo fueron utilizados en las pruebas de caracterización previas a comprobar su rendimiento sobre GN.

Durante el desarrollo de esta tecnología dentro del mundo de la higrometría, el INRiM desarrollo también un instrumento de medida y registro de las frecuencias de microondas. Este equipo fue desarrollado como alternativa a los complejos y muy caros analizadores comercializados, que además suelen ser muy grandes y poco útiles para aplicaciones en campo. El rendimiento de este prototipo fue comparado con un VNA, modelo *HP8510C*.

4. MONTAJE EXPERIMENTAL Y PROCEDIMIENTOS

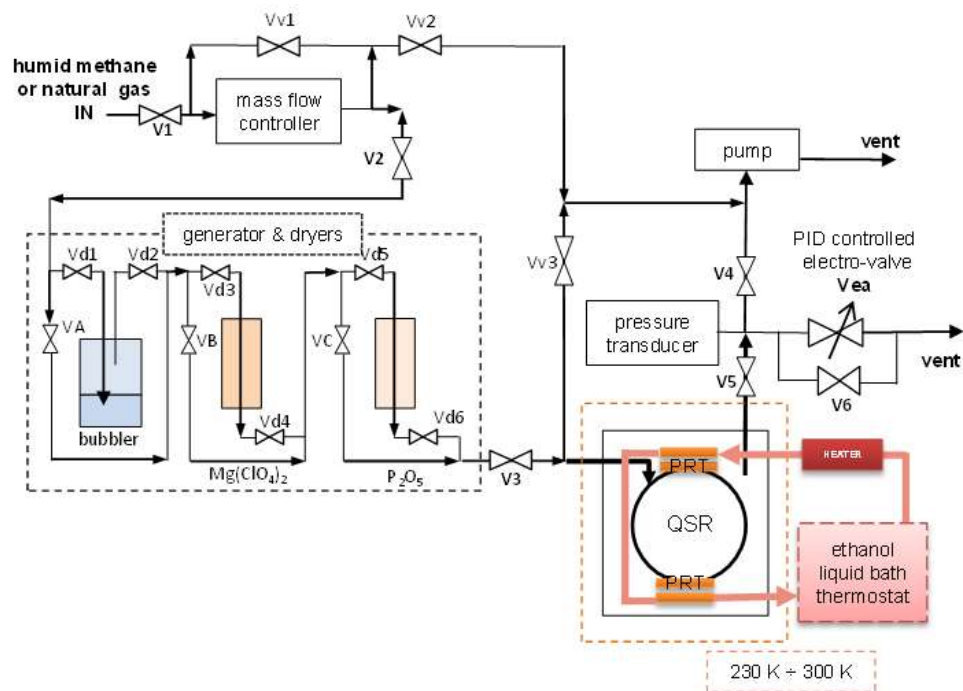


Fig. 4.2.a Diagrama esquemático de la instalación asociada al resonador de MW para las pruebas de medida de humedad en metano y GN.

Se realizaron una serie de pruebas antes de comprar el rendimiento del resonador sobre GN. Primero se caracterizó dimensionalmente el resonador: definiendo la frecuencia de resonancia en el vacío, f_0 , y su variación con respecto a la temperatura; y el factor de compresibilidad isotérmica, k_T , con pruebas con helio.

A continuación, se comprobó el rendimiento del resonador, determinado la permisividad relativa, ϵ_r , del nitrógeno y metano puro para los cuatro tripletes (TM_{11} a TE_{12}). Se comprobó que había muy buena correlación de los resultados independientemente del modo de frecuencia resonante seleccionado, reduciendo así el volumen de datos analizado en el futuro para uno o dos modos, o incluso su relación.

El siguiente paso fue comprobar su rendimiento sobre metano húmedo a diferentes niveles de humedad. Este tipo de tecnología puede operar de dos maneras: midiendo directamente la fracción molar de agua, x_w , en la fase vapor; y la segunda, utilizando el método de condensación, que consiste en reducir la temperatura del resonador hasta detectar un cambio en las frecuencias resonantes recogidas, momento en el cual se obtiene la temperatura de rocío (WDP).

El último paso fue comprobar su rendimiento sobre GN en condiciones semi-industriales, es decir, composición del gas variable. Se probó hasta una presión máxima de 750 kPa, registrando únicamente el modo de resonancia TM_{11} con el prototipo de bajo coste cuyo rendimiento ya había sido comprobado en las pruebas anteriores.

La prueba consistió en suministrar un nivel de humedad nominal intermedio durante el tiempo suficiente para estabilizar y controlar todas las variables de proceso. Una vez esto se sucediera, se el generador de humedad sorteado y el GN circularía por el sistema de secado asociado al resonador de MW. De esta forma se dejaría circular por el resonador el GN completamente seco el tiempo suficiente para obtener una medida precisa de f_{dry} , la cual será cesaría para el cálculo final de la humedad. Después de esto, se volvería a pasar a la posición inicial generando el mismo nivel de humedad nominal, y se registrarían las lecturas de TM_{11} durante más de una hora, obteniendo así f_{mix} . Ahora ya se podría determinar la humedad del gas mediante uno de los dos métodos descritos anteriormente. El rendimiento del resonador fue comparado con otros cuatro equipos, basados en diferentes tecnologías de medida.

4.3 CONDICIONES INDUSTRIALES

Esta sección fue continuación del gran estudio desarrollado en Zaragoza y en condiciones semi-industriales. Dentro del proyecto de EMRP "Characterization of Energy Gases", se realizó una pequeña tarea inicial, pero debido a los buenos resultados, al interés mostrado por todas las partes implicadas (fabricantes de equipos, Enagás y el LabTH), y a algunos problemas que tuvo Enagás al inicio de la nueva temporada de extracción. Por todo ello, se decidió profundizar y ampliar más el estudio del rendimiento y el comportamiento de ciertas tecnologías de medida, pero esta vez en condiciones industriales completamente reales.

En este bloque, la instalación elegida para tal fin fue el almacenamiento subterráneo y planta de secado de Enagás en Serrablo (Huesca). La misión de este tipo de instalaciones es doble: como reserva estratégica nacional y para cubrir los picos de demanda puntuales. El gas almacenado en los pozos se encuentra a presiones próximas a los 19 MPa, mientras que la red de distribución trabaja a unas presiones máximas alrededor de 7 MPa. Por ello, una estación de bombeo y despresurización debe estar siempre asociada. Además el gas cuando se extrae de los pozos, debido al enfriamiento asociado a la despresurización, está

4. MONTAJE EXPERIMENTAL Y PROCEDIMIENTOS

completamente saturado de agua, por lo que debe asociarse también a una planta de secado del gas, que en este caso específico incluía una etapa previa de separación física mediante decantadores y, finalmente, un proceso de deshidratación químico mediante trietilenglicol (TEG).

Como ya se ha comentado, el proceso de secado es clave para controlar la humedad del gas en el resto de la red nacional de distribución. Por ello, el emplazamiento de estas instalaciones en condiciones climatológicas extremas aportaba un gran valor añadido al estudio del rendimiento de tecnologías de medidas de humedad en condiciones industriales completamente reales, sin ninguna variable manipulada.

Inicialmente, como parte del proyecto de EMRP, se realizó un estudio muy básico para comprobar el rendimiento de un analizador espectroscópico en campo. Para ello, se instaló en el mismo punto de muestreo que el sensor capacitivo utilizado por Enagás, modificando lo mínimo posible las instalaciones de la planta de sacado. Este equipo estuvo leyendo durante la fase de inyección de gas a los pozos, momento en el que la planta de secado no está trabajando, ya que el gas viene seco de la red principal y en el interior de los pozos se va a saturar de nuevo.

Debido al interés de todas las partes involucradas en comprobar el rendimiento de los analizadores espectroscópicos en todas las fases de la planta de secado, especialmente durante la extracción. Además, debido a un fallo importante en el sistema de muestreo originario de Enagás, el cual se inundó completamente al inicio de la nueva temporada de extracción, era esencial corregir este gran problema ya que se tenían una medida incorrecta de la humedad final del gas al finalizar el proceso de secado.

Por ello, se decidió construir un nuevo sistema de muestreo más avanzado, que diera servicio a la sección de higrometría y cromatografía de la planta, y que garantizase la imperturbabilidad de la humedad y la composición del gas, teniendo una fiabilidad mayor en la medida y control de ambas propiedades durante cualquier etapa de proceso de la planta, asegurando la completa seguridad de los analizadores y de los operarios, y facilitando todas las labores de limpieza y mantenimiento requeridas. El sistema fue diseñado de acuerdo con las guías, recomendaciones y normas para las buenas prácticas en el muestreo de GN a presión para medidas de humedad.

Todo el equipamiento y la instrumentación asociada al nuevo sistema de muestreo instalado a lo largo de esta fase experimental, cumplían con todas las especificaciones para ser instalados en campo, a intemperie, soportar las condiciones climáticas de la zona, y tener certificaciones para ser instalados en atmosferas explosivas como, por ejemplo, certificación ATEX/IEC y protecciones Ex.

Este sistema de muestreo diseñado y construido a lo largo de esta tesis, formaría parte de las instalaciones de Enagás a la conclusión del estudio, como agradecimiento y recompensa a toda su colaboración.

En la Tabla 3.1.a ya se indicaron los 3 equipos estudiados, 2 espectroscópicos debido a los buenos resultados mostrados en condiciones semi-industriales y un capacitivo de Al_2O_3 , por ser el sensor utilizado por Enagás y el tipo de tecnología más utilizado por la industria gasista mundial. En la Fig. 4.3.1 se puede ver un esquema del nuevo sistema de muestreo y todos los equipos asociados a él.

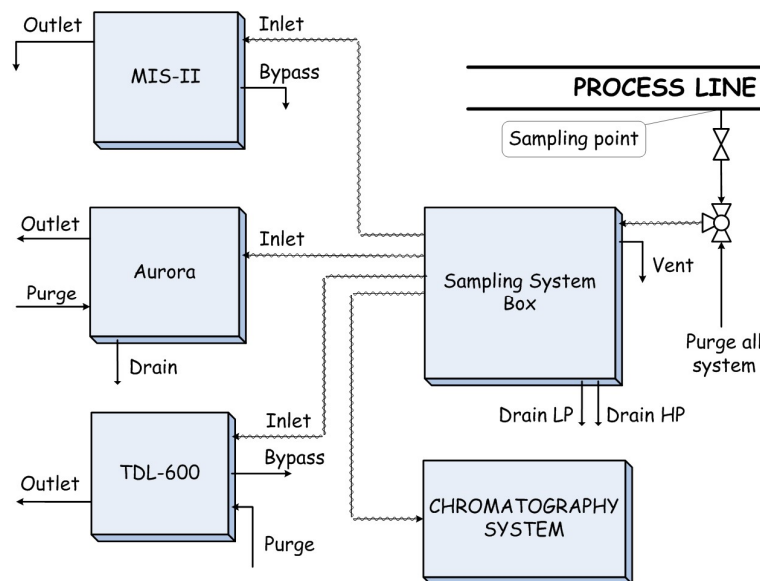


Fig. 4.3.a Diagrama completo de toda la instalación asociada al nuevo sistema de muestreo. Todas las líneas de entradas estaban equipadas con sistema de calefacción por traceado eléctrico, para evitar cualquier problema de condensación previo a las celdas de medida.

Las variables de medida y control de esta instalación son las mismas que en las secciones experimentales anteriores, es decir: la presión, la temperatura, el caudal y la composición. El sistema diseñado era capaz de trabajar a dos niveles de presión de línea (HP) o baja presión (LP). Este sistema era clave para poder conectar el Aurora y la sección de cromatografía de la planta, los cuales no eran capaces de soportar altas presiones. Para

4. MONTAJE EXPERIMENTAL Y PROCEDIMIENTOS

ello, había diferentes reguladores de presión, además de válvulas de alivio en las líneas de baja presión. La presión además de ser controlada, debía ser registrada para poder realizar la conversión de unidades, por lo que cada analizador espectroscópico acabó incluyéndolo en su sistema de muestreo. La temperatura fue otra magnitud medida y registrada por los propios sistemas de muestreo de los medidores espectroscópicos. El caudal era ajustado en cada una de las líneas de muestreo y la composición diaria del gas era facilitada por Enagás a través del propio sistema cromatográfico asociado a esta instalación. A continuación, en la Fig. 4.3.p, se puede ver el diagrama detallado de P&I del propio sistema de muestreo.

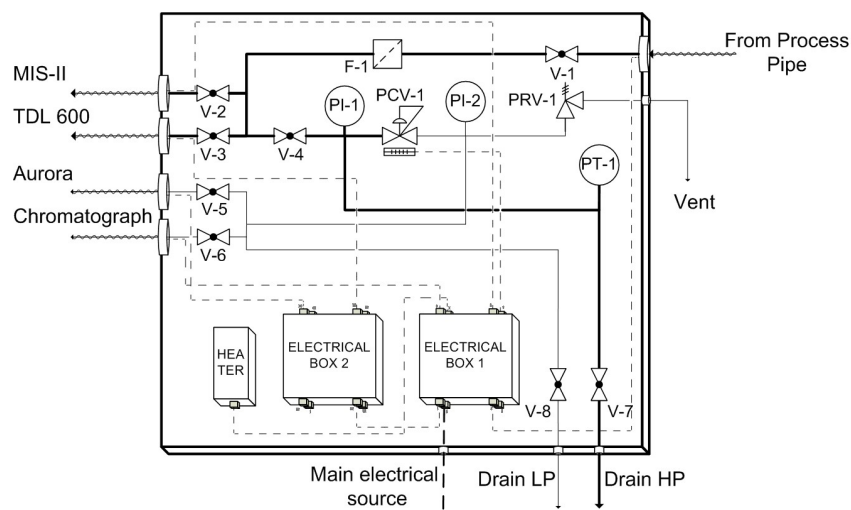


Fig. 4.3.b Diagrama P&I del moderno sistema de muestreo diseñado y fabricado para llevar a cabo esta comparación y renovar el antiguo sistema de la planta de secado de Serrablo.

A continuación, se muestra el aspecto final de toda la instalación fabricada para la realización de esta fase experimental.



Fig. 4.3.c Aspecto final de la instalación completa construida en la planta de almacenamiento subterráneo de Serrablo, para llevar a cabo el estudio comparativo de 3 instrumentos en condiciones industriales reales.

Como se ha ido comentando, el objetivo principal de esta sección experimental fue comprobar el rendimiento de la prometedor tecnología de medida de humedad basada en la espectroscopía de absorción, frente a la tecnología comúnmente utilizada en el mundo gasista, como son las sondas capacitivas de Al_2O_3 , en condiciones industriales reales. En estas instalaciones industriales concretas, se deseaba conocer su comportamiento durante los tres posibles estados de producción de la planta: inyección, extracción y parada.

Para ello, se llevó a cabo un registro online e ininterrumpido de las medidas de humedad dadas por los tres equipos analizados, además de otras variables relacionadas y también medidas como la presión, la temperatura y la composición del gas. De esta forma, se podría tener un mayor conocimiento no sólo acerca del comportamiento de los equipos durante los periodos estables de producción y de su comportamiento dinámico durante los cambios de etapas, sino también de la propia planta de secado.

Debido a que las condiciones iniciales de los equipos fueron muy dispares y, al igual que en las pruebas semi-industriales, no había un instrumento patrón sobre el que realizar las correcciones oportunas. Por todo ello, todo el estudio realizado aquí también será de carácter relativo. Sin embargo, se llevó a cabo una prueba para comprobar el rendimiento de los equipos con una mezcla patrón de N_2 y H_2O con una concentración de $24 \text{ ppm}_v \pm 4 \text{ ppm}_v$.

4. MONTAJE EXPERIMENTAL Y PROCEDIMIENTOS

Por otro lado, se realizó una sencilla prueba para comprobar si el rendimiento de ambas tecnologías se veía alterado por la presencia de sustancias típicamente empleadas en la industria gasista como aditivos del gas. En este caso se evaluó la influencia del metanol, utilizado como anticongelante del gas, para evitar la formación de hidratos.

Por supuesto, además de los protocolos asociados a las medidas de los equipos, también se desarrollaron todos los protocolos asociados con cualquier actividad que implicase el manejo de la nueva instalación, es decir: protocolos de inicio y apagado, de pruebas de fugas, tareas de mantenimiento y limpieza y cualquier aspecto relacionado con la seguridad durante su manejo.

5 RESULTADOS

5.1 RESULTADOS CONDICIONES SEMI-INDUSTRIALES

El bloque más importante de pruebas, fueron aquellas integradas dentro del grupo denominado pruebas de “humedad variable”. Durante estas pruebas diversas características de los equipos y, por tanto, de sus tecnologías de medida, fueron evaluadas mediante la generación repetida de once valores nominales de humedad: (13, 30, 45, 55, 70, 85, 100, 125, 160, 200 and 250) ppm_v.

Tiempos de respuesta

La primera característica estudiada fueron los tiempos de respuesta de los equipos. Para ello, se evaluó su comportamiento frente a los cambios de humedad en diversas situaciones: los más pequeños realizados en el margen superior e inferior del rango de humedades antes descrito, entre el máximo y el mínimo de todo el rango, y para cambios intermedios. Todos los cambios de humedad fueron repetidos tanto en sentido ascendente como descendente de humedad. En la Fig. 5.1.r se muestra un ejemplo de los datos sin tratar recogidos por todos los equipos analizados.

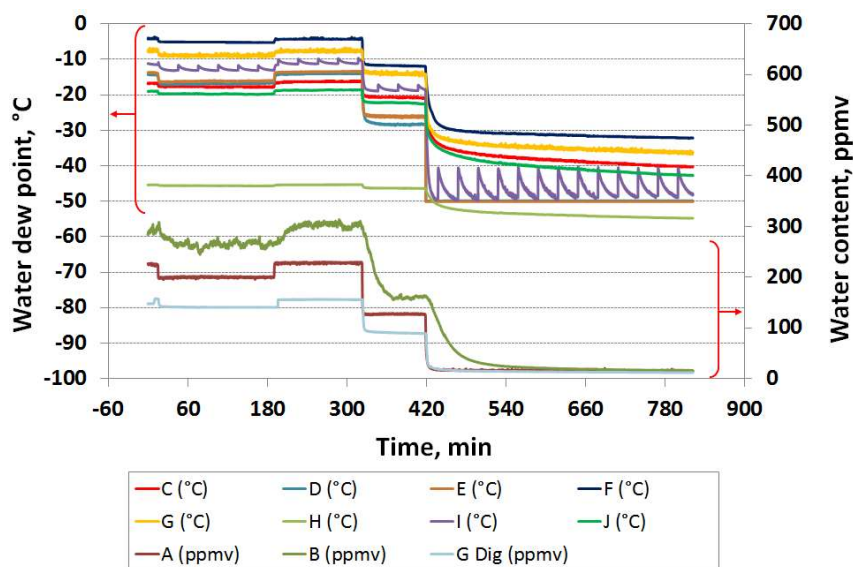


Fig. 5.1.a Ejemplo de las lecturas registradas durante las pruebas de humedad variable.

A continuación, cada uno de los cambios de humedad fueron analizados individualmente, mediante la normalización de la señal entre los puntos inicial y final, una vez alcanzada la estabilidad de ambos. De esta manera el porcentaje del valor

normalizado la humedad en función del tiempo se calculó a partir de la siguiente ecuación:

$$H \% (t) = \frac{(H_t - H_0)}{(H_F - H_0)} \cdot 100 \quad \text{Eq. 5.1.a}$$

donde H_F , era la humedad final alcanzada, H_0 la humedad del punto de partida y H_t la humedad en cada instante.

Los valores iniciales y finales estables de cada salto y, extrapolando, de toda la tesis fueron obtenidos mediante una herramienta de cálculo, denominada *Ptramos* y desarrollada por el LabTH, la cual es capaz de determinar el valor medio más estable entre un rango de valores previamente determinado.

Para este tipo de pruebas se escogió al instrumento espectroscópico como equipo de referencia, porque era uno de los más rápidos en detectar cualquier cambio de humedad. Por tanto, era el que determinaba el $t = 0$ en cada salto, herramienta utilizada a la hora de graficar todas las lecturas de los equipos. Sin embargo, el tiempo requerido por cada equipo para alcanzar la lectura final estable era calculado de forma individual.

En los siguientes gráficos se muestran un ejemplo de las señales de los equipos (analógicas y digitales) normalizadas y con el mismo origen de referencia temporal.

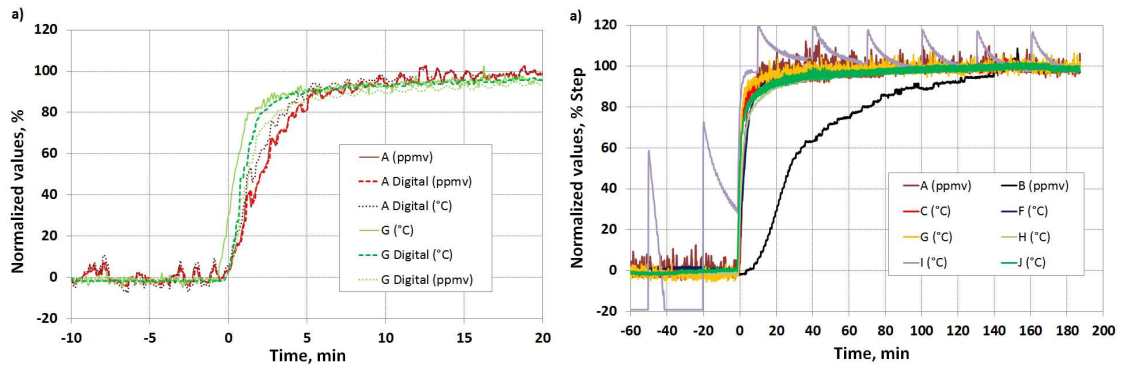


Fig. 5.1.b Estudio de tiempos de respuesta para al cambio de humedad de (13 a 30) ppmv. Izq.) Comparación de las salidas analógicas y digitales del instrumento A y G. Derecha) Respuestas analógicas de todos los equipos.

El tiempo de respuesta se evaluó como el tiempo requerido por cada equipo para alcanzar el 63.2 % y 90 % del valor final, para todos los saltos y en ambos sentidos.

A raíz de la gran cantidad de resultados obtenidos se puede decir que el analizador electrolítico, B, fue el más lento, mientras que los sensores de óxido de aluminio D, E y

G fueron los más rápidos para la mayoría de los saltos evaluados. El espectroscópico, polimérico y el resto de sensores de Al_2O_3 mostraron comportamientos muy similares pero ligeramente más lentos que los citados anteriormente.

Por otro lado, es destacable la gran lentitud de los sensores de Al_2O_3 (excepto el D y el E) para el mayor salto de secado, es decir, desde 250 ppm_v hasta 13 ppm_v. Éste comportamiento podría indicar que dichos sensores se saturaron y necesitaron más tiempo para regenerar su parte activa y ser capaz de detectar cambios de humedad de nuevo.

Otro efecto que puede ser observado, es que los sensores de Al_2O_3 tienen un comportamiento más heterogéneo para situaciones de humedad decreciente. Mientras que, para humedades crecientes tienen un rendimiento muy similar todos.

Estudio de histéresis

Para comprobar si algún instrumento sufría este tipo de efecto, y si podría asociarse a alguna de las tecnologías, este estudio fue realizado. Para ello, se realizó un ciclo ascendente y otro descendente para ocho niveles de humedad nominales a la misma presión de línea. Los niveles de humedad generados fueron: (13, 30, 55, 70, 85, 100, 160 y 250) ppm_v.

En primer lugar, se tuvo que elegir el instrumento de referencia sobre el que calcular las medidas corregidas del resto de equipos. Para ello, se comprobó que el instrumento espectroscópico A, no sufría ningún tipo de histéresis respecto a los valores nominales generados, que además demostraba la buena respetabilidad del sistema de generación de humedad fabricado. Los resultados del estudio de histéresis, respecto al equipo A, se muestran en la Fig. 5.1.mm.

Los instrumentos D y E exhibieron un comportamiento claramente diferente respecto al resto de equipos, pero similar entre ellos. Instrumentos C y J también mostraron un comportamiento similar, lo cual era predecible ya que era el mismo sensor pero con diferente electrónica implementada por cada fabricante.

Se puede decir que, para el margen de humedades estudiado, la mayoría de los equipos no mostraron histéresis asociada a su tecnología, con excepción del electrolítico, B, y de las sondas de óxido de aluminio C y J, que mostraron una histéresis importante para WDP inferiores a -12 °C.

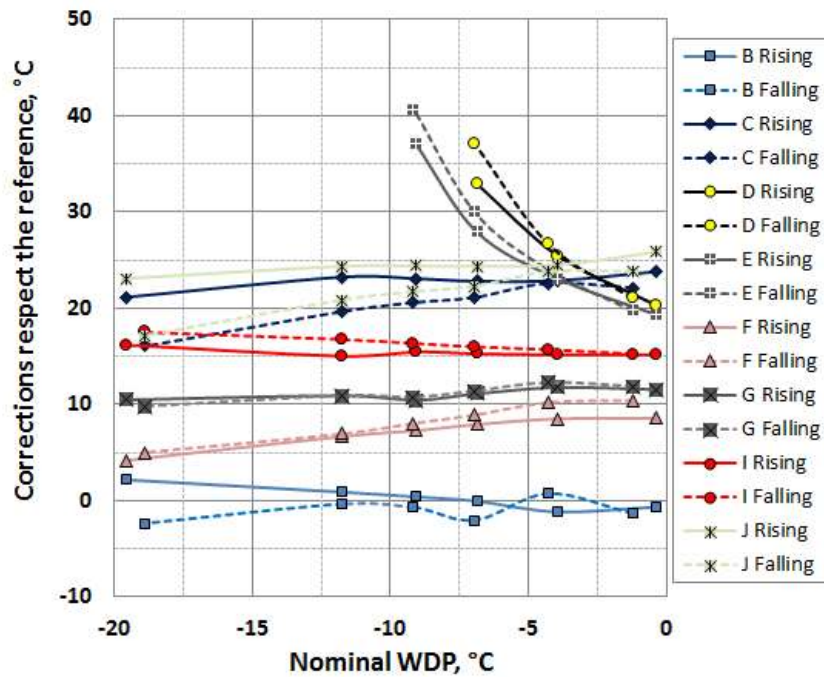


Fig. 5.1.c Histeresis de los instrumentos corregida respecto al analizador espectroscópico, A. Las líneas continuas muestran los ciclos ascendentes y las discontinuas los descendentes.

Estudio de deriva

Fue realizado para seis niveles de humedad (13, 30, 70, 100, 200 and 250) ppm_v, representativos de todo el rango estudiado.

Debido al problema explicado anteriormente relativo a la falta de un patrón o equipo de referencia. Tres equipos (A, B y G), basados en diferentes tecnologías de medida, fueron considerados como tal para analizar las correcciones relativas del resto de equipos con respecto a dichas referencias.

La estabilidad, o deriva a corto plazo, fue evaluada a partir de la evolución de las lecturas corregidas respecto al tiempo. La corrección, c , para cada lectura, j , fue obtenida a partir de la siguiente ecuación:

$$c(j) = r(j) - i(j) \quad \text{Eq. 5.1.b}$$

donde r e i fueron las lecturas del instrumento de referencia y de cada uno del resto de equipos, respectivamente. Por lo tanto, una corrección positiva indica que el instrumento está leyendo más seco que la referencia. Analizando los tres equipos seleccionados como referencia, se comprobó que los resultados y, por tanto, las

conclusiones eran similares. Por lo que se simplificó su estudio únicamente para el sensor espectroscópico.

A continuación, se muestra un ejemplo del estudio de deriva realizado para el valor nominal de 100 ppm_v.

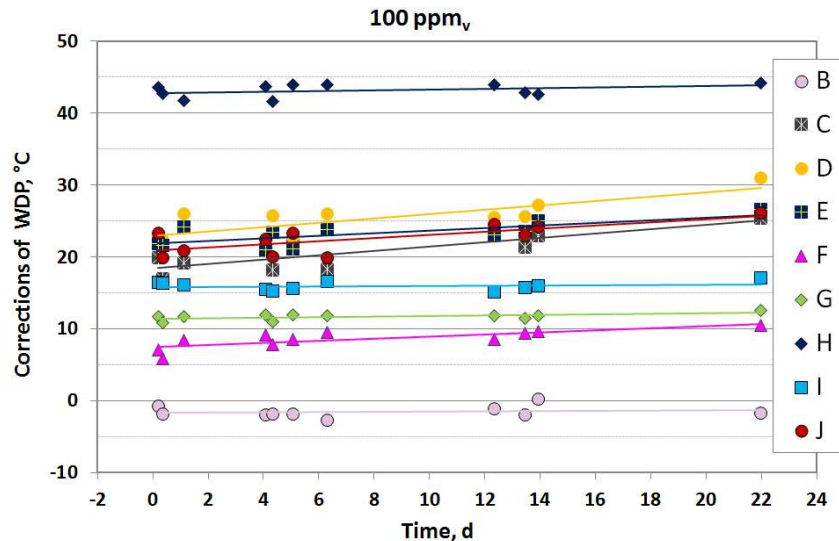


Fig. 5.1.d Short-term relative drift at nominal water content of 100 ppm_v, using spectroscopy instrument as reference.

Este tipo de gráfico se realizó para los otros niveles nominales de humedad comentados. A partir de estos gráficos se obtienen las siguientes conclusiones:

- Como ocurrió en el estudio de las anteriores propiedades, los pares de series de D/E y C/J tuvieron un comportamiento muy similar en todos los niveles, dado que eran el mismo sensor.
- Un fenómeno claramente observable durante todas las pruebas fue la gran dispersión mostrada entre todos los medidores, como queda reflejada en la dispersión de su corrección.
- En cuanto a la dispersión entre las lecturas de una misma serie y para un mismo nivel de humedad. Se observa como dicho efecto es del mismo nivel que la reproducibilidad de los instrumentos, excepto para D/E y C/J. Esto podría indicar que la reproducibilidad del sistema de generación de humedad es bastante aceptable para los objetivos marcados en esta tesis.

Si el tipo de gráfico anterior es resumido en uno sólo para todos los niveles de humedad, se podría evaluar si la deriva del instrumento está relacionada con el rango de humedad medido o no. La Fig. 5.1.ii muestra el resultado de este estudio.

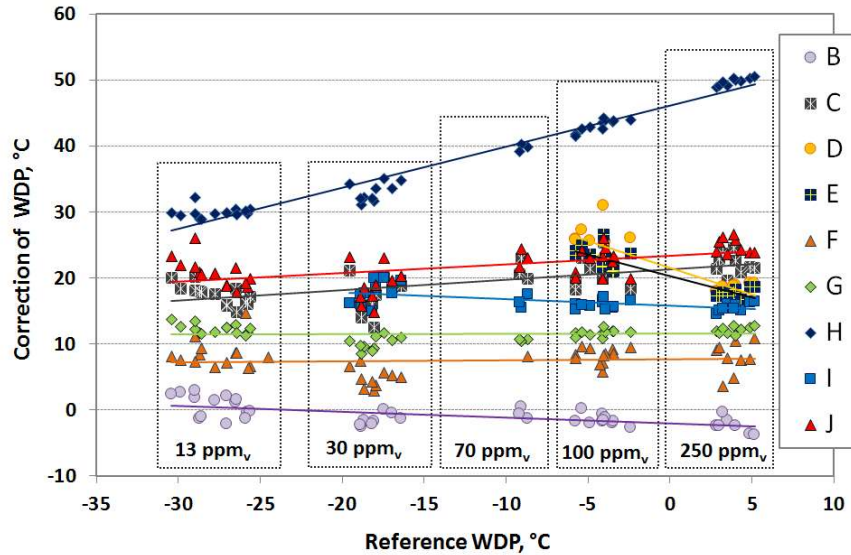


Fig. 5.1.e Relative corrections of humidity sensors regarding with spectroscopic instrument for five humidity levels generated.

A través de este tipo de gráficos se observan dos tipos de comportamientos: el mismo comportamiento de deriva independientemente del rango de humedad, mostrado por aquellas series de datos que tienen un comportamiento más o menos horizontal; y un segundo comportamiento, en el que claramente el efecto de deriva está íntimamente relacionado con el nivel de humedad del gas, como es el caso de los sensores capacitivos de Al₂O₃ D/E, C/J y, especialmente, el equipo H, y del tipo polimérico I.

Los instrumentos A, B, F, G, and C/J representativos de las diferentes tecnologías de medida, excepto la de condensación y la polimérica, mostraron un comportamiento de deriva similar para concentraciones inferiores a 100 ppm_v, es decir, dentro del margen útil para la industria. Los valores de deriva diaria iban desde -0.33 °C hasta valores despreciables de ±0.05 °C, holgadamente cubierto por la reproducibilidad del sistema.

También se puede concluir que los sensores de Al₂O₃, excepto el G, mostraron una deriva positiva durante casi todo el rango estudiado, tendiendo a leer cada vez más seco. Efecto bien conocido por este tipo de sensores y demostrado en la literatura sobre gases convencionales, como el nitrógeno.

Respecto al segundo tipo de pruebas realizadas, es decir, conocer el comportamiento de las tecnologías ante cambios bruscos de presión, manteniendo la humedad constante de 100 ppm_v. Inicialmente, el gas fue ajustado a 2.8 MPa. Cuando se obtuvieron lecturas estables, la presión del gas se incrementó hasta 5.8 MPa, y se mantuvo así durante cuatro días. Después se volvió a las condiciones de presión iniciales y se dejó estabilizar las lecturas. El posible efecto de la presión se calculó como la diferencia entre las lecturas corregidas de los equipos antes y después de someterse al incremento de presión.

El resultado fue que todos los sensores evaluados leyeron más secos tras el incremento de presión, pero dentro de las especificaciones del equipo a excepción de los sensores D/E, cuyo modelo parece que sí experimentó un cambio debido a los cambios de presión.

La mayoría de los equipos electrolíticos basados en óxidos metálicos antes de ser evaluados aquí fueron previamente calibrados por el NPL en metano hasta 3 MPa. Estas condiciones se aproximaban bastante bien a las que en esta sección de la tesis se realizaron (GN y 2.8 MPa). Cuando esta sección experimental terminó, los equipos fueron devueltos al NPL para recalibrar y de esta forma comprobar si alguno de ellos había sufrido cambios en su comportamiento o efectos de deriva.

La heterogeneidad de las correcciones mostrada sobre las pruebas en GN, también quedó patente en las calibraciones sobre metano, con correcciones entre 4 °C y 20 °C, y siempre dando lecturas más secas. Hecho que sugiere que dicha dispersión no se debe a las lecturas en NG sino a las diferentes condiciones en las cuales los sensores fueron prestados para este estudio.

Respecto a la tecnología de medida de los higrómetros de condensación, ésta suponía uno de los grandes retos de esta sección experimental, debido a la dificultad de obtener medidas de WDP con certeza sobre la naturaleza del condensado. Por ello, solo dos simples pruebas pudieron ser realizadas:

- Evaluar el rendimiento del DP3D a diferentes valores de humedad generados y para el valor de presión fijo de 2.8 MPa, cerca de los valores típicos de cricondentherm.
- Comparar aquellas lecturas obtenidas del HCDP y WDP del GN de entrada a la instalación, que fueron registradas por el Condumax II; con las lecturas del WDP dadas

por el DP3D durante los cuatro días en los que el gas estuvo fluyendo a la máxima presión de línea como parte de la prueba de los cambios de presión, y que por tanto no sufrió ninguna humectación añadida.

El número de resultados experimentales de WDP mostrados en esta tesis fue bastante reducido, debido a la dificultad de tener una alta seguridad en la naturaleza del condensado, y que sólo se mostraron aquellos cuya naturaleza fue contrastada con respecto a los valores de HCDP registrados por el monitor. Por esta razón, valores de humedad por debajo de 70 ppm_v fueron realmente pocos.

A pesar de ello, la dispersión mostrada por la respetabilidad de las medidas fue inferior a ± 2 °C, por lo que su comportamiento parece bastante aceptable para los requerimientos de la industria gasista. Sin embargo, este tipo de tecnología requiere de un gran conocimiento tanto de la misma como del mundo del GN, por lo que nuevas mejoras basadas en la tecnología de *dark spot*, utilizada en el Condumax II, o un moderno equipamiento de detección óptica automática, permitirían obtener medidas precisas y fiables tanto del WDP como del HCDP.

Respecto al análisis de incertidumbre de las medidas realizadas en esta sección. Debido a la complejidad inherente dada por la ausencia de un equipo con características de patrón; y dado que el objetivo principal de esta sección no era realizar un estudio amplio del cálculo de incertidumbres asociado a este proceso, sino evaluar el rendimiento y la utilidad de las diferentes tecnologías de medida en la industria del GN. Debido a todo ello, únicamente se planteó, de forma cualitativa, como debería de realizarse el cálculo de incertidumbres, y cuáles deberían ser las componentes más importantes a tener en cuenta.

Para este caso particular, la estimación de la incertidumbre de la medida de cualquier higrómetro evaluado fue la combinación de tres incertidumbres típicas debido a: la generación del valor nominal de la humedad, $u_{generation}$; y aquellas relacionadas con los instrumentos de medida utilizados, tanto el de referencia como el instrumento a analizar, u_{ref} y u_{inst} respectivamente. La estimación de la incertidumbre se realizó de acuerdo a la ley de propagación de incertidumbres (ver Eq. 5.1.e), puesto que es el método más aceptado en el campo de la metrología.

$$u_c(WDP) = \sqrt{\sum_{i=1}^n u_i^2(x_i) \cdot c_i^2} = \sqrt{u_{generation}^2 + u_{ref.}^2 + u_{instr.}^2} \quad \text{Eq. 5.1.c}$$

Cada una de las tres componentes estaba a su vez formada por diferentes componentes. Un listado de los factores más importantes de cada una de ellas, y de cómo debían de ser evaluadas fue realizado.

5.2 RESULTADOS DEL RESONADOR DE MICROONDAS

En primer lugar, en esta tesis se indicaron algunos de los resultados realizados por el INRiM, como elementos claves para entender el funcionamiento y el comportamiento de esta nueva técnica de medida de humedad.

Se comprobó la veracidad del segundo método de cálculo para conocer la humedad de mezclas complejas, mediante la determinación de diferentes mezclas de metano húmedo, determinando, ε_{dry} , a partir del f_{dry} , y después determinando el f_{mix} , para obtener el ε_{mix} de cada mezcla.

Una vez confirmado que la relación TM_{11}/TE_{11} era realmente estable y repetible. Se comprobó también la validez del modo de condensación para determinar el WDP de cualquier gas (ver Fig. 5.2.b) mediante el cambio en dicha relación.

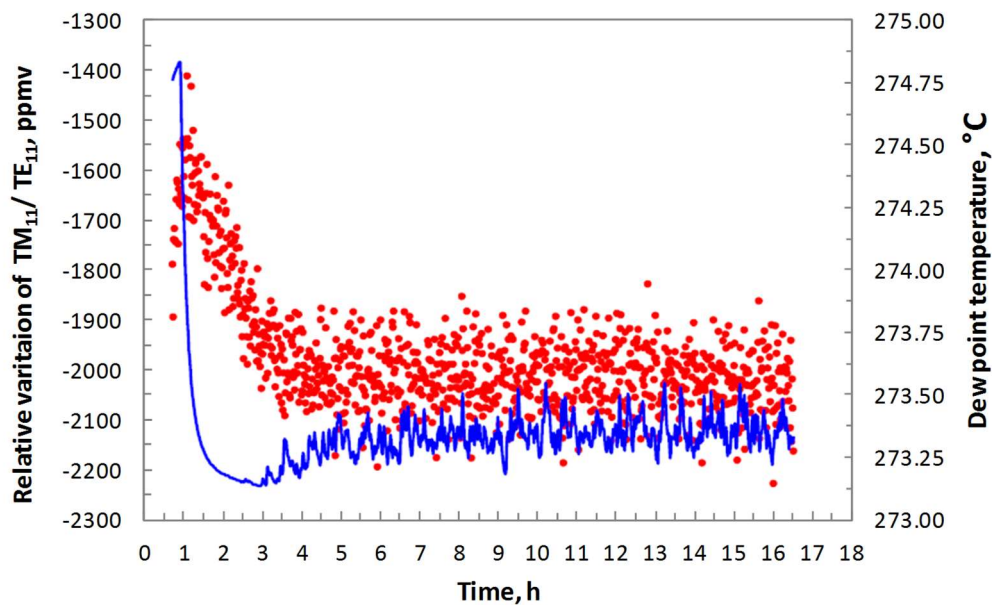


Fig. 5.2.a Condensation tests for humid methane at 750 kPa.

Respecto a las pruebas realizadas finalmente sobre GN, la cavidad resonante se mantuvo estable a (297.00 ± 0.01) K, (752.00 ± 0.01) kPa y un caudal de $0.1 \text{ L} \cdot \text{min}^{-1}$. Se registró el modo de resonancia TM_{11} cada 70 s, y su variación durante la primera prueba para dos niveles de humedad, se mostró en la Fig. 5.2.e, donde también se puede ver el valor establecido como referencia durante el proceso de secado total del gas.

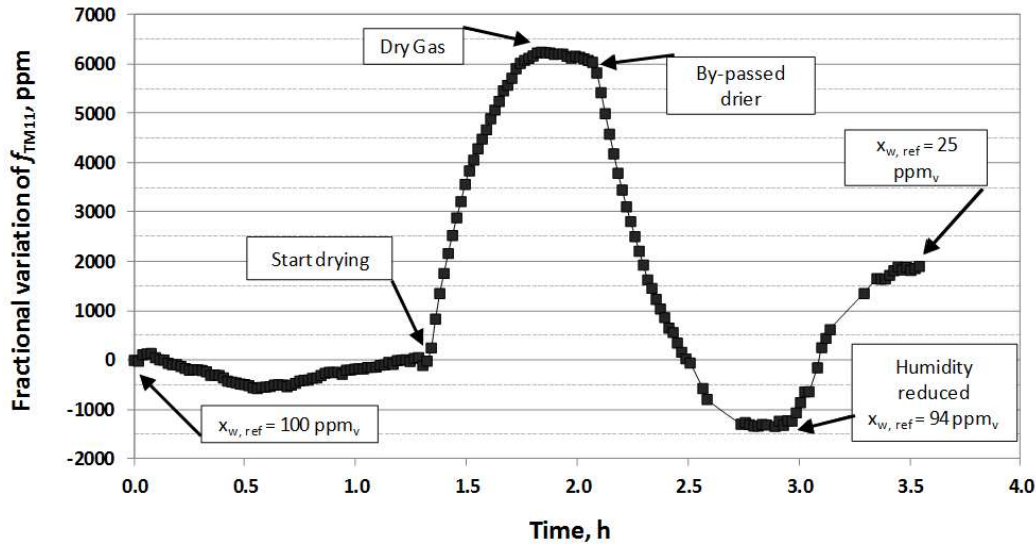


Fig. 5.2.b Relative frequency change recorded for mode TM_{11} during the different phases of the test to determine the water fraction in a NG stream.

El valor de f_{dry} se obtuvo para un promedio de 20 lecturas consecutivas relativamente estables, y su valor fue $f_{dry} = 5138.4790 \pm 0.0005$ MHz. Luego corrigiendo el valor de $f_0(T)$ para la temperatura de la prueba, la permisividad de la mezcla seca será $\epsilon_{dry} = 1.006478$. Ahora, conociendo f_{dry} and ϵ_{dry} , y mediante el registro de la f_{mix} a lo largo del tiempo (figura anterior), aplicando al Eq. 4.2.h se puede conocer la variación de ϵ_{mix} a lo largo del tiempo y, finalmente, mediante la Eq. 4.2.m. conocer la humedad del GN, x_w .

Las lecturas del WC del gas obtenidas por el resonador de MW fueron comparadas con las lecturas de otros cuatro equipos basados en tecnologías diferentes. En este caso se utilizó como referencia el EE371 y los valores de humedad generados fueron de 100 ppm_v y 25 ppm_v, respectivamente.

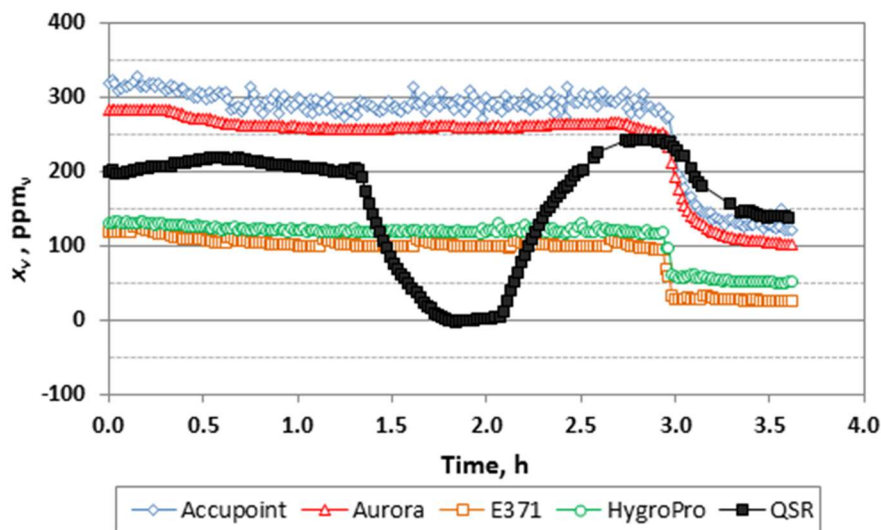


Fig. 5.2.c Comparación de las lecturas del contenido en agua del gasnatural dadas por el resonador de MW y por otros cuatro equipos de medida diferentes, basados todo en tecnologías distintas.

La dispersión entre las lecturas mostradas por los diferentes equipos, fue un fenómeno que se mantuvo a lo largo de todo el estudio experimental. Se observa como el comportamiento dinámico del resonador se asemejaba más al del sensor electrolítico y espectroscópico, que a los otros dos equipos.

Se realizó un estudio de la incertidumbre para cada una de las magnitudes evaluadas con esta tecnología de medida, y para lo resultados los enhancement factors obtenidos para el metano, y los cálculos de humedad realizados sobre GN.

5.4. RESULTDOS CONDICIONES INDUSTRIALES

Las lecturas de los tres instrumentos fueron registradas a lo largo de las diferentes etapas de producción de la planta (inyección y extracción) alternadas por diversos periodos de parada.

A lo largo de los más de ocho meses de lectura hubo diversas situaciones en las que por multitud de motivos algunos equipos dieron lecturas incorrectas o perdieron su comunicación con el sistema de registro de datos, ya sea por: versiones pre-comerciales del firmware o del software de registro, fallo o reinicio de las comunicaciones digitales debido a micro-cortes del suministro eléctrico, sondas e incluso instrumentos enviados a recalibrar, etc. La mayoría de estos problemas fueron corregidos a lo largo del proyecto, o ayudaron a corregir las versiones definitivas comerciales de los equipos. Sin embargo,

el estudio comparativo de los tres equipos no siempre pudo ser llevado a cabo debido a estos factores indeseados y no siempre evitables.

Una de las propiedades exhibidas por los tres equipos a lo largo de toda esta sección experimental, fue el comportamiento cíclico exhibido por los tres medidores de humedad independientemente del estado de producción de la planta y de la magnitud medida (WC o WDP). Este tipo de comportamiento es bien conocido en instalaciones no aisladas, ni termostatizadas instaladas a intemperie debido a efectos de absorción y desorción de las moléculas de agua entre el gas y la propia instalación.

Por este motivo, las señales fueron analizadas de acuerdo a dos parámetros típicos para este tipo de señal, tales como: la amplitud y el periodo. Se desarrolló una herramienta de cálculo que permitía detectar los máximos y mínimos diarios, calcular el tiempo entre máximos y mínimos diarios consecutivos y su amplitud.

Se eligieron los valores mínimos para estudiar el comportamiento de los equipos por varios motivos: primero, porque coincidían con las temperaturas mínimas ambientales, momento más crítico para que se produzcan riesgos de condensación; segundo, porque las diferencias entre lecturas son mayores en sus mínimos, luego si se alcanza una buena correlación en estos puntos, mejor será durante el resto del tiempo; y, por último, los valores mínimos son más interesantes desde el punto de vista de los rangos utilizados en la industria del GN.

Los rendimientos de los analizadores se comprobaron una vez alcanzadas unas condiciones relativamente estables, para los tres modos de la planta: extracción, inyección y parada.

Este estudio se realizó para los periodos más importantes de todos ellos, en primer lugar, mostrando todos los datos recogidos sin tratar (ver Fig. 5.3.e).

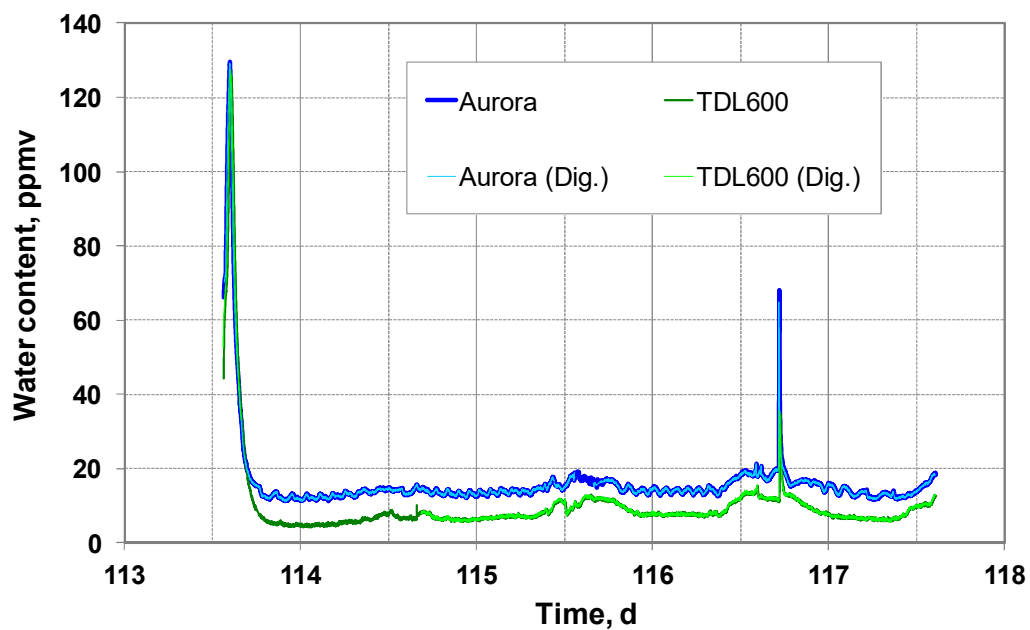


Fig. 5.4.a Lecturas del WC dadas por los dos analizadores espectroscópicos durante el último periodo de extracción de la planta.

A continuación, se evaluó su comportamiento a partir del estudio de mínimos diarios (ver Fig. 5.4.b y Fig. 5.3.s), todo ello tanto para el WC como el WDP.

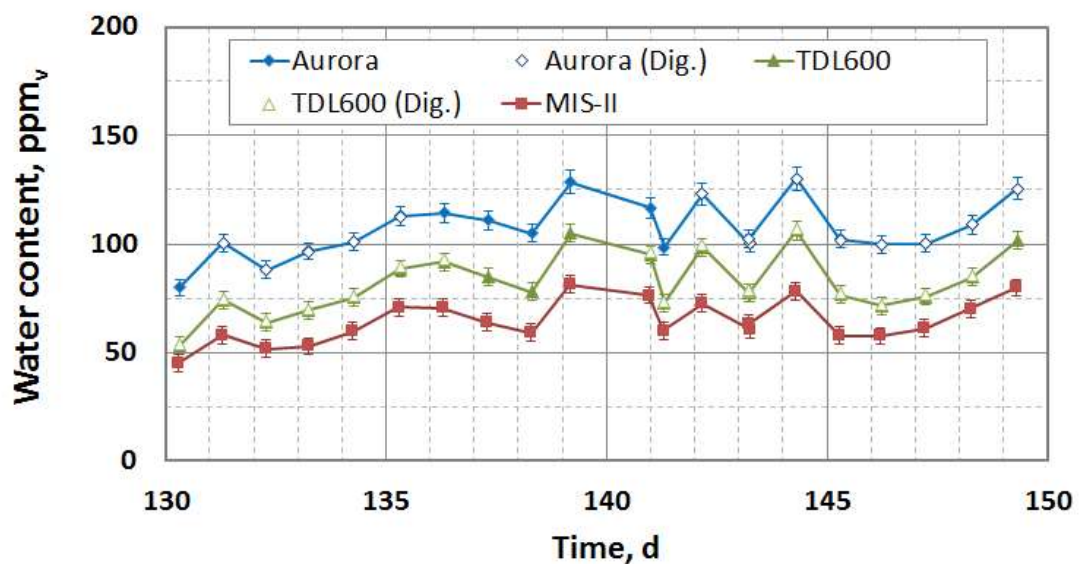


Fig. 5.4.b Evolución de los mínimos diarios de WC para los tres analizadores estudiados durante el 4º periodo de para de la planta.

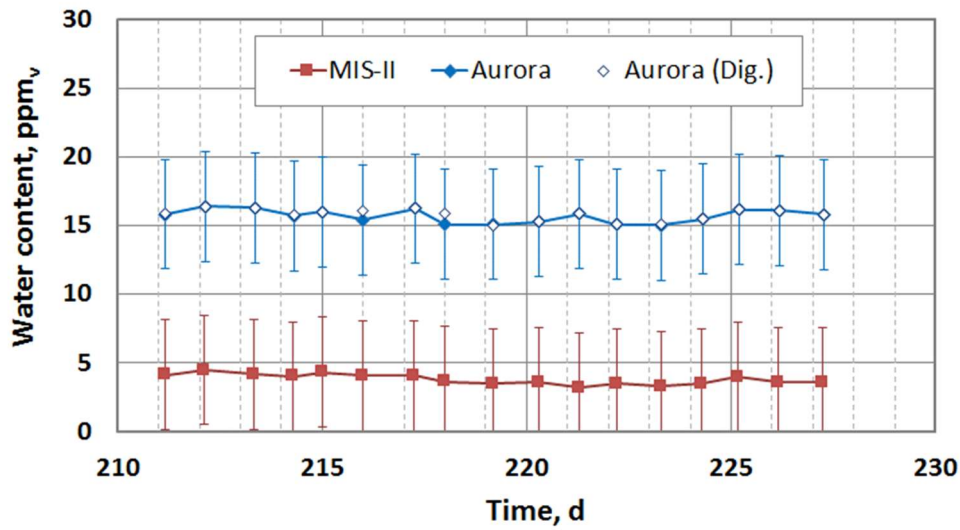


Fig. 5.4.c Evolución de los mínimos diarios de WC para dos de los higrómetros estudiados durante la segunda fase de inyección.

Por último, a raíz de este tipo de gráficos se determinaron los criterios de aceptación para establecer el grado de correlación entre los instrumentos de medida de humedad comparados. El criterio fue dado por la Eq. 5.3.c, la cual está basada en el cálculo de los límites permisibles máximos a partir de la lectura dada por el instrumento considerado como referencia. El rango fue calculado para una incertidumbre expandida para un factor de cobertura de $k = 2$, para un nivel de confianza de aproximadamente el 95 %.

$$x_{instr} = x_{ref} \pm 2 \cdot \sqrt{u_{instr}^2 + u_{ref}^2 + u_{calc}^2} \quad \text{Eq. 5.3.c}$$

Como se puede ver, las componentes individuales de la incertidumbre son las mismas que en la Sección 5.1, pero en este caso eliminando la componente asociada a la generación del valor nominal de humedad. Este estudio fue realizado para el WDP y el WC, para la primera forma de expresar la humedad fue de 5.7 °C mientras que, los criterios de aceptación del WC fueron resumidos en la siguiente tabla:

Table 5.4.a Resumen de los criterios de aceptación para la comparación de las lecturas del WC en todas las etapas de producción analizadas.

WC, ppm _v	EXTRACCIÓN			PARADA		INYECCIÓN	
	1 st	3 rd	4 th	3 rd	4 th	1 st	2 nd
$ \mathcal{X}_{Aurora} - \mathcal{X}_{MIS-II} \leq$	13	13	14	12 hasta 14	21 hasta 35	13	15
$ \mathcal{X}_{TDL600} - \mathcal{X}_{MIS-II} \leq$	---	---	12	12 hasta 14	21 hasta 35	---	---
$ \mathcal{X}_{Aurora} - \mathcal{X}_{TDL600} \leq$	---	---	12	11	12 hasta 14	---	---

A raíz del estudio realizado para todos los estados de producción de la planta. Se obtuvieron las siguientes conclusiones

Durante los periodos de extracción existió muy buena correlación entre las lecturas del MIS-II y el Aurora para las lecturas de WC. Sin embargo, su correlación para las medidas de WDP fue bastante menor. Esto podría deberse a varios factores: el transmisor de presión del medidor espectroscópico no había sido instalado aún, luego puede que el valor de presión simulado para realizar la conversión no fuese el adecuado; la primera sonda del MIS-II habría sufrido una excesiva deriva a lecturas más secas, y cuando fue sustituida por una de repuesto su correlación fue prácticamente perfecta con el Aurora.

Durante el último periodo de extracción, primero en el que estuvieran los tres equipos instalados, la correlación de los dos instrumentos espectroscópicos fue absoluta, del 100 %, y con respecto al sensor capacitivo de Al₂O₃ fue prácticamente completa para ambos. Todo ello, justifica que la confianza de que los niveles de humedad final del GN que abandona la planta de secado hacía la red nacional, cumplían con completa seguridad los criterios de calidad establecidos.

Durante los periodos de parada, los porcentajes de valores que cumplen los criterios de aceptación fueron más variables, debido principalmente a las mayores fluctuaciones en la humedad del gas, hecho demostrado por la gran desviación pica mostrada por los mínimos diarios. Sin embargo, el nivel de correlación entre los equipos espectroscópicos continuó siendo absoluto.

Durante la inyección, el porcentaje de valores que cumplen el criterio es del 100 % para las lecturas del WC, por lo que se puede decir que tuvieron un comportamiento idéntico.

Si el estudio se amplía a los periodos de transición de la planta, entre un estado de producción y otro, se podría conocer y entender mucho mejor el comportamiento dinámico de los higrómetros. Conocimiento que, por otro lado, sería muy útil para Enagás, ya que podría prevenir el tiempo requerido por la planta para alcanzar niveles de humedad tan elevados que pudieran derivar en situaciones problemáticas e incluso de riesgo, derivadas de la formación de hidratos, situación especialmente delicada durante los largos periodos de parada de la planta.

Para evaluar dicho comportamiento dinámico, tanto de la planta como de los analizadores de humedad, se utilizó la variación del promedio acumulado de las propiedades de una señal sinusoidal utilizadas anteriormente, es decir, la amplitud y el periodo entre los mínimos diarios consecutivos del WC y WDP.

El periodo acumulado y la amplitud permitía determinar el tiempo necesario para alcanzar medidas cíclicas más o menos estables, es decir, el tiempo requerido por la planta para alcanzar un grado de estabilidad elevado. Además, esta propiedad podría detectar efectos de deriva o retardos en las señales de los equipos.

Por otro lado, el promedio acumulado del periodo permitió verificar si realmente estos ciclos tenían un comportamiento diario o no. Hecho que quedó demostrado ya que esta propiedad tendía siempre a 24 h independientemente del cambio de etapas que se analizara. Éste estudio también se realizó a partir de máximos diarios, pero se confirmaron las mismas conclusiones.

Por otro lado, quedó de sobra comprobada la capacidad de ambas tecnologías para detectar cualquier incremento o disminución de la humedad en el GN.

Se realizó una comprobación intermedia del rendimiento de los analizadores con una mezcla patrón de N_2 / H_2O de $24 \text{ ppm}_v \pm 4 \text{ ppm}_v$, con el fin de determinar qué equipo estaba dando lecturas más correctas y poder corregir el valor de offset que había habido entre ellas a lo largo de todas las pruebas.

Esta prueba demostró, que el TDL600 fue el único que realmente cumplía las especificaciones, a pesar de que el modo de lectura sobre N_2 aún no había sido instalado en aquella versión del equipo. Sin embargo, el Aurora obtenía valores consistentes con la concentración de agua de la mezcla y, puesto que no había sido recalibrado durante 2 años se puede decir que también estaba dentro de las especificaciones del fabricante.

5. RESULTADOS

Se estudió la influencia del metanol sobre ambas tecnologías, demostrando que ninguna de ellas mostraba una aparente variación por la presencia de dicho compuesto usualmente utilizado en la industria gasista.

6 CONCLUSIONES

Se realizó un estudio exhaustivo sobre el comportamiento de diferentes tecnologías de medida de humedad, verificando su desempeño en GN y en condiciones industriales reales.

Un total de 14 sensores, basados en 6 tecnologías de medida diferentes, fueron estudiados. Se compararon técnicas tradicionalmente utilizadas, tales como: higrómetros de condensación, sensores electrolíticos y capacitivos basados en óxidos metálicos; fueron comparados frente a novedosas y prometedoras tecnologías de medida, que constituyen el estado del arte en el mundo de la higrometría, tales como resonadores de microondas, espectroscopia de absorción y sensores poliméricos de tipo capacitivo.

Para ello, se diseñó y construyó un complejo banco de ensayos para trabajar en condiciones de laboratorio, capaz de comparar todos los equipos simultáneamente, controlar la presión hasta 5,8 MPa, ajustar los caudales y controlar el WC del GN mediante un generador de flujo de mezcla que permitía generar dentro de un rango útil para la industria del gas, de 13 ppm_v a 250 ppm_v.

Se desarrollaron protocolos de medida y se evaluaron diversas propiedades de los equipos, validando así el rendimiento relativo de las diferentes tecnologías entre sí. Se realizaron estudios para caracterizar el comportamiento dinámico de los equipos (tiempos de respuesta frente a variaciones de humedad y variaciones debidas a cambios de presión), así como estudios de deriva a corto plazo, histéresis y linealidad.

Además, se participó en la fase de desarrollo y validación del QSR por MW, evaluando su rendimiento con GN real, para un rango de WC entre (25; 100) ppm_v y con una presión de 0.75 MPa. Demostró un rendimiento bastante satisfactorio mostrándose como una tecnología prometedora en el campo de la higrometría, pero con cuestiones aún por desarrollar para aplicaciones industriales reales.

A pesar de las diferencias exhibidas por ciertos equipos, debido a factores e inconvenientes ya comentados, la consistencia mostrada por los resultados demuestra la validez de los métodos experimentales y de análisis utilizados. Demostrando a su vez, la utilidad de todas las tecnologías para los diferentes requerimientos de la industria del gas, pero con peculiaridades en todos los casos.

Por otro lado, un completo sistema de muestreo NG, previo a la medida de la humedad, fue construido. Fue específicamente diseñado para aplicaciones industriales en campo, al aire libre, bajo condiciones climáticas extremas y dentro de áreas explosivas. Este sistema era capaz de dar servicio a 3 medidores de humedad simultáneamente, además de un completo sistema de análisis cromatográfico, lo que significó un gran avance y modernización de la UGS y la planta de secado de Serrablo (Enagás), además de un aumento en la fiabilidad y precisión sobre el control de la humedad en todas las etapas de procesamiento de la planta.

Todas las conclusiones obtenidas en esta tesis son el resultado de analizar una enorme cantidad de datos recogidos durante casi 280 días de pruebas. El buen rendimiento de los analizadores espectroscópicos se demostró incluso en condiciones industriales reales y extremas, y en todas las etapas de producción, lo que permitió tener un mayor conocimiento de la calidad del gas en todo momento. Como prueba de ello, Enagás adquirió uno de estos instrumentos para ser instalado en puntos clave de su red de distribución nacional. Esto fue un resultado claro del apoyo metrológico de esta tesis al sector industrial, así como en el desarrollo de nuevas y mejores tecnologías de medida, siendo ambos aspectos clave en la hoja de ruta europea de la humedad [Bel08, Fer12].

Finally, the question of traceability and the lack of reproducibility between the conditions of calibration and use of the instruments was a problem always present in this thesis. However, many NMIs are currently developing new equipment and facilities capable of replicating these industrial conditions. As a sample of the first steps taken in this regard is the calibration performed by the NPL of some hygrometers used in this thesis, and how the ranges and CMCs of various NMIs in the EU have been improved in order to provide the metrological infrastructure that satisfies the industrial needs. The work performed in this thesis contributes to a better understanding of the influence quantities that affect the uncertainty of measurement in the conditions of use that can sometimes be significantly larger than those in the ideal conditions found in the laboratory during formal calibration and are fundamental for ensuring the quality of industrial measurement in the strategic NG industry.

Finalmente, la cuestión de la trazabilidad y la falta de reproducibilidad entre las condiciones de calibración y uso de los instrumentos fue un problema siempre presente en esta tesis. Sin embargo, muchos NMIs están desarrollando actualmente nuevos equipos

6. CONCLUSIONES

e instalaciones capaces de reproducir las condiciones industriales. Como muestra de las primeras medidas tomadas a este respecto se encuentra la calibración realizada por el NPL de algunos higrómetros utilizados en esta tesis y cómo se han mejorado los rangos y CMCs de varios NMIs de la UE para proporcionar la infraestructura metrológica que satisfaga las necesidades industriales. El trabajo realizado en esta tesis contribuye a una mejor comprensión de las magnitudes de influencia que afectan la incertidumbre de medida en las condiciones de uso, que a veces pueden ser significativamente mayores que en las condiciones ideales encontradas en el laboratorio durante la calibración formal y que son fundamentales para asegurar la calidad de las medidas en la industria del GN.